Adekunle M. Adesina

Tarik Tihan

Christine E. Fuller

Tina Young Poussaint

Editors

Atlas of Pediatric Brain Tumors

Atlas of Pediatric Brain Tumors

Adekunle M. Adesina • Tarik Tihan
Christine E. Fuller • Tina Young Poussaint
Editors

Atlas of Pediatric Brain Tumors

Editors

Adekunle M. Adesina
Baylor College of Medicine
Houston, TX
USA
aadesina@bmc.tmc.edu

Tarik Tihan
University of California
San Francisco, CA
USA
tarik.tihan@ucsf.edu

Christine E. Fuller
Medical College of Virginia/Virginia
Commonwealth University
Richmond, VA
USA
cfuller@mcvh-vcu.edu

Tina Young Poussaint
Children's Hospital
Boston, MA
USA
Tina.Poussaint@childrens.harvard.edu

Preface

In the presentation of this atlas of pediatric brain tumors, we have followed the 2007 World Health Organization (WHO) classification of brain tumors. We do recognize that there are some tumor types that do not fit nicely into this classification. It is also critically important to recognize that pediatric tumors within the same histological category are significantly different from those occurring in adults. For example, a rare but increasingly recognized group of malignant glioneuronal tumors with prominent epithelioid morphology is discussed separately in Chap. 22 under the presumptive category of "malignant epithelioid glioneuronal tumors." We believe that this group of neoplasms has histologic characteristics distinctly different from anaplastic ganglio-gliomas, epithelioid glioblastoma or primitive neuroectodermal tumors. We expect that, as more cases are reported, this group of malignant tumors may be recognized as a distinct entity or group of entities in future WHO classification schemes.

In compiling the chapters, we have distilled only the important diagnostic information including clinical, neuroimaging, and histologic features with an emphasis on the recognized variants and their differential diagnoses. A section on molecular pathology and electron microscopy is also included for each tumor category. A list of classic reviews and landmark articles on each of the tumor entities are provided as suggested reading at the end of each chapter. The last chapter represents a list of interesting and unusual cases for a diagnostic exercise by the reader.

In contrast to the more limited pathologic variations associated with adult brain tumors, most pathologists are often aware of the extreme diversity and florid phenotypic variation associated with pediatric brain tumors. The rarity of some of these phenotypic variants often makes the definitive diagnosis of each of these entities a diagnostic challenge even for the experienced pediatric pathologist. Those who have limited experience in pediatric neuropathology are acutely aware of the fact that the ultimate definition of each specific tumor is not without therapeutic and/or prognostic implications. This atlas is born out of the need to fill a "void" in the practice of pediatric neuropathology. It is designed to provide a practical and well-illustrated "beside-the-microscope" resource for the diagnostic pathologist who is called upon to make critical decisions on sometimes tiny and often very "taxing" specimens.

As in every field of diagnostic pathology, a picture is worth a thousand words. We hope that the bullet format used for its text will make for easy identification of relevant information that will aid in the evaluation of clinical cases at the microscope. We have also included a significant number of neuroradiological images that provide the critical correlations that are crucial for recognizing some of the entities. We anticipate that the format and the illustrations will allow easy use as a practical text for practitioners and trainees in neuropathology, neuroradiology, neurooncology, and general surgical pathology.

This book is dedicated to all the children with brain tumors who are the inspiration for our work. Their challenging tumors have shaped our practice experiences and their courageous struggle for survival has given us encouragement. To them, we remain forever indebted.

Houston, TX   Adekunle M. Adesina
Richmond, VA   Christine E. Fuller
San Francisco, CA   Tarik Tihan
Boston, MA   Tina Young Poussaint

Contents

Contributors

Adekunle M. Adesina, M.D., Ph.D.
Professor of Pathology, Medical Director, Section of Neuropathology and Molecular Neuropathology Laboratory, Department of Pathology, Texas Children's Hospital, Baylor College of Medicine, Houston, TX, USA

Christine E. Fuller, M.D.
Professor of Pathology, Director of Neuropathology, Department of Pathology, Virginia Commonwealth University, Richmond, VA, USA

Jill V. Hunter, M.B., B.S.
Associate Professor of Radiology, Department of Radiology, Texas Children's Hospital, Baylor College of Medicine, Houston, TX, USA

Anna Illner, M.D.
Assistant Professor of Radiology, Department of Radiology, Texas Children's Hospital, Baylor College of Medicine, Houston, TX, USA

Abir Mukherjee, M.D.
Neuropathology Fellow, Department of Pathology, The Methodist Hospital, Houston, TX, USA

Sonie Narendra, M.D.
Resident, Department of Pathology, SUNY Upstate Medical University, Syracuse, NY, USA

Brian Pavlovitz, M.D.
Resident, Department of Pathology, SUNY Upstate Medical University, Syracuse, NY, USA

Tina Young Poussaint, M.D.
Associate Professor of Radiology, Harvard Medical School, Director, PBTC Neuroimaging Center, Children's Hospital, Boston, MA, USA

Ronald A. Rauch, M.D.
Associate Professor of Radiology, Department of Radiology, Texas Children's Hospital, Baylor College of Medicine, Houston, TX, USA

Andy Rivera, M.D.
Assistant Professor, Department of Pathology, Ohio State University, Columbus, OH, USA

Marie Rivera-Zengotita, M.D.
Assistant Professor, Department of Pathology, University of Puerto Rico School of Medicine, San Juan, PR, USA

Lucy B. Rorke-Adams, M.D.
Clinical Professor, Department of Pathology, The Children's Hospital of Philadelphia, Philadelphia, PA, USA

Hiroyoshi Suzuki, M.D.
Department of Pathology, Sendai Medical Center Hospital, Sendai, Miyagi, Japan

Hidehiro Takei, M.D.
Assistant Professor, Department of Pathology, Weil Cornell Medical College
and Baylor College of Medicine, The Methodist Hospital, Houston, TX, USA

Tarik Tihan, M.D., Ph.D.
Professor of Pathology, Department of Pathology, Neuropathology Unit,
San Francisco, CA, USA

Ioana Tolocica, M.D.
Resident, Department of Pathology, SUNY Upstate Medical University,
Syracuse, NY, USA

Introduction and Overview of Brain Tumors

Adekunle M. Adesina

0.1 CLASSIFICATION OF BRAIN TUMORS

- In this issue of the *Atlas of Pediatric Brain Tumors*, we have classified the tumor types based on the 2007 WHO classification of brain tumors (Table 0.1).
- This classification assumes that the pattern of differentiation reflects the cell of origin.
- The longstanding concept suggesting that brain tumors arise as a result of "degeneration" of mature cell types has been questioned.
- Current concepts suggest that all tumors arise from cancer stem cells, which share some common characteristics with neural progenitor stem cells in the central nervous system (CNS), including:
  - the ability for self-renewal and
  - the ability for divergent differentiation
- The extent or pattern of differentiation reflects the nature of activation and deregulation of specific signaling pathways:
  - Deregulation is often directed at genes that control nodal points where cell growth, proliferation and differentiation converge, with the upregulation of genes involved in organismal survival and deregulation of cell cycle control.

0.2 TUMOR GRADING

- The WHO grading system is a four-tier grade system with each increasing grade implying lesser degrees of differentiation, increasing anaplasia, increasing proliferative potential, and mitotic activity.
- There is an acquisition of aggressive characteristics in the higher grade tumors that in the astrocytomas include vascular proliferation and necrosis.
- The proportion of tumor cells in the cancer stem cell pool is lowest in the lower grade tumors and highest in the higher grade tumors, and correlates with the proliferation indices of these tumors.
- In the astrocytomas, tumors with a discrete growth pattern rather than an infiltrative growth pattern are often amenable to surgical treatment with good survival and are often graded as Grade I, e.g., pilocytic astrocytoma.
- Increasing anaplasia is associated with the clonal evolution of a subpopulation of cells that have acquired additional genetic events, e.g., *myc* amplification resulting in the transformation of classic medulloblastomas to anaplastic/large-cell medulloblastomas.

0.3 UTILITY OF NEUROIMAGING FINDINGS IN THE INTERPRETATION OF TISSUE BIOPSIES

- Although a tissue-based diagnosis must be made and must stand by itself independent of neuroradiologic findings, it is very reassuring if there is a concordance/correlation between the surgical pathology impression and the neuroradiologic differential diagnoses.
- Notable neuroradiologic "rules" suggest that:
  - Contrast-enhancing lesions exhibiting a diffuse pattern of growth are probably high grade/malignant lesions
  - Discrete enhancing and non-enhancing lesions are suggestive of low grade or benign tumors
  - Cystic mass lesions with enhancing mural nodules are probably low grade lesions, especially when located in the temporal lobe or cerebellum
  - Diffusion restriction is consistent with a highly cellular tumor and raises the differential diagnoses of atypical teratoid rhabdoid tumor or primitive neuroectodermal tumor/medulloblastoma or anaplastic ependymoma, etc. and
  - Increased perfusion (correlates with contrast enhancement) is usually associated with higher grade tumors with the exception of pilocytic astrocytoma, which, in spite of its increased perfusion, is a low-grade tumor

0.4 ANALYSIS OF CNS TUMORS

- Intraoperative consultation is an integral part of the management of brain tumors in most centers.
- The goal of a gross examination is to determine how the tissue differs from the normal.
  - Firm to rubbery consistency often suggests a low-grade glial tumor.
  - Soft, necrotic and hemorrhagic tissue is more characteristic of high-grade malignant tumors.
- When histologic sections are available for review, the following determination has to be made: (1) Is the tissue representative and diagnostic? (2) Is the lesion neoplastic or not? (3) If it is neoplastic, is it primary or secondary? (4) If primary, is it low grade or high grade? (5) Is the putative differential diagnosis corroborated by the clinical history and the pre-operative neuroradiologic findings?
- The ultimate final diagnosis often has prognostic implications and must, therefore, be unambiguous because upon such a diagnosis rests the important decisions regarding the utility or otherwise of further attempts at surgical resection, as well as the appropriate use of chemotherapy and/or radiotherapy for tumor control.

Table 0.1 Classification of tumors of the nervous system.

Astrocytic Tumors

    Pilocytic astrocyoma

    Pilomyxoid astrocytoma

    Pleomorphic xanthoastrocytoma

    Diffuse astrocytoma

    Anaplastic astrocytoma

    Glioblastoma

    Giant-cell glioblastoma

    Gliosarcoma

    Gliomatosis cerebri

Oligodendroglial Tumors

    Oligodendroglioma

    Anaplastic oligodendroglioma

    Oligoastrocytoma

    Anaplastic oligoastrocytoma

Ependymal Tumors

    Ependymoma

    Anaplastic ependymoma

    Myxopapillary ependymoma

    Subependymoma

Choroid Plexus Tumors

    Choroid plexus Papilloma

    Atypical choroid plexus papilloma

    Choroid plexus carcinoma

Other Neuroepithelial Tumors

    Astroblastoma

    Chordoid glioma of the third ventricle

    Angiocentric glioma

Neuronal and Mixed Neuronal-Glial Tumors

    Ganglioglioma and gangliocytoma

    Desmoplastic infantile astrocytoma and ganglioglioma

    Central neurocytoma and extraventricular neurocytoma

    Cerebellar liponeurocytoma

    Papillary glioneuronal tumor (PGNT)

    Rosette-forming glioneuronal tumor of the 4th ventricle (RGNT)

    Paraganglioma (spinal)

Tumors of the Pineal Region

    Pineocytoma

    Pineal parenchymal tumor of intermediate differentiation

    Pineoblastoma

    Papillary tumor of the pineal region

Embryonal Tumors

    Medulloblastoma

    CNS primitive neuroectodermal tumor (PNET)

    Medulloepithelioma

    Ependymoblastoma

    Atypical teratoid/rhabdoid tumor

Tumors of the Cranial Nerves

    Schwannoma

    Neurofibroma

    Perineurioma

    Malignant peripheral nerve sheath tumor (MPNST)

Meningeal Tumors

    Meningiomas

    Mesenchymal, non-meningothelial tumors

    Hemangiopericytoma

    Melanocytic lesions

    Hemangioblastoma

Tumors of the Hematopoietic System

    Malignant lymphomas

    Histiocytic tumors

Germ Cell Tumors

    CNS germ cell tumors

Familial Tumor Syndrome

    Neurofibromatosis type 1

    Neurofibromatosis type 2

    Schwannomatosis

    Von Hippel–Lindau disease and haemangioblastoma

    Tuberous sclerosis complex and subependymal giant cell astrocytoma

    Li–Fraumeni syndrome and TP53 germline mutations

    Cowden disease and dysplastic gangliocytoma of the cerebellum/

    Lhermitte-Duclos Disease

    Turcot syndrome

    Naevoid basal cell carcinoma syndrome

    Rhabdoid tumor predisposition syndrome

Tumors of the Sellar Region

    Pituitary adenoma

    Craniopharyngioma

    Granular cell tumor of the neurohypophysis

    Pituicytoma

    Spindle cell oncocytoma of the adenohypophysis

Metastatic Tumors of the CNS

- A multidisciplinary approach to treatment decisions provides the best framework for optimal patient care.
- There is an emerging and growing list of molecular tumor markers with potential diagnostic and prognostic utility. The availability of such data can only enhance the quality of treatment decisions; they are particularly critical for counseling in the setting of familial tumor syndromes.

SUGGESTED READING

Silber J, Lim DA, Petritsch C, Persson AI, Maunakea AK, Yu M, Vandenberg SR, Ginzinger DG, James CD, Costello JF, Bergers G, Weiss WA, Alvarez-Buylla A, Hodgson JG (2008) miR-124 and miR-137 inhibit proliferation of glioblastoma multiforme cells and induce differentiation of brain tumor stem cells. BMC Med 6:14

Dirks PB (2008) Brain tumor stem cells: bringing order to the chaos of brain cancer. J Clin Oncol 26(17):2916–24 Review

Fan X, Eberhart CG (2008) Medulloblastoma stem cells. J Clin Oncol 26(17):2821–7 Review

Pérez Castillo A, Aguilar-Morante D, Morales-García JA, Dorado J (2008) Cancer stem cells and brain tumors. Clin Transl Oncol 10(5):262–7

Ben-Porath I, Thomson MW, Carey VJ, Ge R, Bell GW, Regev A, Weinberg RA (2008) An embryonic stem cell-like gene expression signature in poorly differentiated aggressive human tumors. Nat Genet 40(5):499–507

Hambardzumyan D, Becher OJ, Holland EC (2008a) Cancer stem cells and survival pathways. Cell Cycle 7(10):1371–8

Rebetz J, Tian D, Persson A, Widegren B, Salford LG, Englund E, Gisselsson D, Fan X (2008) Glial progenitor-like phenotype in low-grade glioma and enhanced CD133-expression and neuronal lineage differentiation potential in high-grade glioma. PLoS One 3(4):e1936

Kong DS, Kim MH, Park WY, Suh YL, Lee JI, Park K, Kim JH, Nam DH (2008) The progression of gliomas is associated with cancer stem cell phenotype. Oncol Rep 19(3):639–43

Hambardzumyan D, Becher OJ, Rosenblum MK, Pandolfi PP, Manova-Todorova K, Holland EC (2008b) PI3K pathway regulates survival of cancer stem cells residing in the perivascular niche following radiation in medulloblastoma in vivo. Genes Dev 22(4):436–48

Ailles LE, Weissman IL (2007) Cancer stem cells in solid tumors. Curr Opin Biotechnol 18(5):460–6 Review

Section A: Glial Tumors

Christine E. Fuller, Sonia Narendra and Ioana Tolicica

Abstract Section A addresses glial tumors that arise in the pediatric population. The first subsections cover astrocytic tumors, including invasive/infiltrative astrocytomas of low (diffuse astrocytoma), intermediate (anaplastic astrocytoma), and high grade (glioblastoma and variants), as well as the "solid" astrocytic lesions, pilocytic astrocytoma and pleomorphic xanthoastrocytoma. Also highlighted are the recently recognized monomorphous pilomyxoid astrocytoma and the concept of gliomatosis cerebri. The next subsection deals with oligodendroglial tumors including oligodendroglioma, mixed oligoastrocytoma, and their corresponding anaplastic counterparts. The final subsection covers ependymomas; the various histologic subtypes, including anaplastic ependymoma, are presented. Specific emphasis will be placed on the classic neuroimaging and pathologic characteristics of each of these entities, with careful consideration of differential diagnosis in each instance.

Pilocytic Astrocytoma and Pilomyxoid Astrocytoma

Christine Fuller and Sonia Narendra

1.1 OVERVIEW

- **Pilocytic astrocytoma (PA)**
  - Circumscribed, slow-growing, and often cystic astrocytic neoplasm, typically with a biphasic compact and loose architecture by histology and corresponding to WHO grade I.
  - Though most are sporadic, there is a well-established association of pilocytic astrocytoma and Neurofibromatosis Type 1 with germline mutations of the NF1 (neurofibromin) gene; optic nerve involvement, particularly bilateral, is the most common CNS finding.
  - Has been referred to as "optic nerve glioma", "cerebellar astrocytoma", "dorsal exophytic brain stem glioma."
- **Pilomyxoid astrocytoma (PMA)**
  - A recent addition to the 2007 WHO classification of tumors of the CNS, this lesion shares some histologic features of PA, though tends to occur in younger children and exhibits a more aggressive clinical behavior. It is correspondingly given a WHO grade II designation.
  - Sporadic in nature, only a single example reported arising in the context of NF1.
  - Though its histogenesis remains uncertain, theories include the following:
    - The term "tanycytoma" has been proposed by some authors in reference to the fact that PMA have been shown to exhibit ultrastructural characteristics similar to those of "tanycytes," precursor cells found within circumventricular organs and floor of the third ventricle.
    - Others have proposed that PMA represents some variant of glioneuronal neoplasm in reference to immunohistochemical and ultrastructural features outlined elsewhere.
    - PMAs may represent an "immature pilocytic astrocytoma" as there have been several documented cases in which recurrent lesions have shown features of classic PA.

1.2 CLINICAL FEATURES

- **Pilocytic astrocytoma**
  - Pilocytic astrocytoma is the most frequent glioma of childhood and accounts for the vast majority of cerebellar astrocytomas; it likewise represents the most common pediatric brain tumor.
  - Occasionally occurring in adulthood, most lesions come to clinical attention within the first two decades of life. There is no particular gender predilection.
  - Clinical presentation of PAs varies depending on their localization, with the corresponding signs / symptoms of a slowly evolving process:
    - Optic pathways lesions produce visual compromise.
    - Endocrinopathies often accompany hypothalamic / third ventricular lesions.
    - Posterior fossa lesions often present with signs of CSF obstruction / increase in intracranial pressure, clumsiness, or specific signs of brainstem dysfunction.
    - Cord lesions produce localizing signs and symptoms related to mass growth and nerve root impingement.
- **Pilomyxoid astrocytoma**
  - PMA is much less common than PA, though the true incidence is unclear given that it has only recently been well-characterized from a diagnostic perspective.
  - Mean age at diagnosis is 18 months (versus 5 years for PA); only rarely presents in adults. There is no gender predilection.
  - Patients may present with failure to thrive, developmental delays, diplopia, and signs / symptoms related to increased intracranial pressure / hydrocephalus.

1.3 NEUROIMAGING

- **Pilocytic astrocytoma**
  - Though they may arise anywhere within the CNS, the cerebellum and brainstem are the most common sites of localization in the pediatric population, followed by the hypothalamus / optic chiasm and optic nerve. Less common sites include the thalamus, basal ganglia, cerebrum, and spinal cord.
  - Intracranial lesions are frequently periventricular.
  - Cerebral lesions tend to occur in an older cohort of patients.
  - Several imaging patterns have been described:
    - Many show a cyst / mural nodule configuration (typically with strongly enhancing mural nodule; cyst wall may or may not enhance) (Fig. 1.1a-b)
    - Less frequently encountered is a predominantly solid mass. (Fig. 1.1c-f) Rarely may present as a necrotic mass with central non-enhancing zone. (Fig. 1.1g)
    - The cyst / mural nodule configuration is typical of cerebellar or cerebral tumors, while hypothalamic tumors form discrete well-circumscribed masses. Brainstem lesions typically manifesting as a dorsally-exophytic mass. (Fig. 1.1h)

– Optic nerve gliomas tend to grow as fusiform enlargements secondary to confinement by dura sheath.
– They are hypointense on T1-w and hyperintense on T2-w and FLAIR MR imaging (Fig. 1.1c-e, respectively).
– The characteristic strong contrast enhancement post-contrast is helpful in differentiating these tumors from low grade infiltrative gliomas which typically do not enhance.
– Rarely are they multifocal, and intralesional hemorrhage, calcifications, peritumoral edema, and CSF dissemination are quite uncommon.
– By MR spectroscopy, they most frequently show elevated choline (Cho) and decreased Creatine (Cr) and N-acetyl aspartate (NAA).

- **Pilomyxoid astrocytoma**
  – Characteristically arises within the hypothalamic / chiasmatic area; rare examples have been documented within the thalamus, temporal lobe, posterior fossa structures, and spinal cord.
  – By MR imaging, they are solid, sometimes with cystic or necrotic areas. Typically they are hypointense to isointense on T1 and hyperintense on T2-weighted images, with T2 signal abnormalities frequently extending out into surrounding parenchyma.
  – Homogeneous contrast enhancement is a consistent finding. (Fig. 1.2)
  – They may show infiltration or encasement of adjacent structures, including the circle of Willis. CSF dissemination may also be present.
  – CT Scan - hypodense on non-enhanced and heterogeneous on contrast enhanced images.
  – One study showed high Cho/Cr ratio in peritumoral regions of PMA, possibly reflecting the more aggressive and infiltrative behavior of this lesion. Short echo MRS showed a much higher Cho/Cr ratio for PMA compared with PA, as well as a lower Myo/Cr ratio.

1.4 PATHOLOGY

- *Gross pathology*: Pilocytic astrocytomas tend to be well-circumscribed and often cystic, whereas PMA are usually solid and may show areas of hemorrhage.
- *Intraoperative cytologic imprints / smears*:
  – **Pilocytic astrocytoma** smear preparations contain a variably myxoid background harboring cells with fine elongated cell processes and bland nuclei. (Fig. 1.3a-b) Rosenthal fibers and eosinophilic granular bodies (EGBs) are helpful findings when present (Fig. 1.3c and d)
  – Nuclear pleomorphism, microcalcifications, perivascular pseudorosettes, and hemosiderin-laden macrophages are infrequently present.
  – Smear preparations of **PMA** may closely resemble those of pilocytic astrocytoma, (Fig. 1.3e-f) although they are usually entirely lacking in Rosenthal fibers and EGBs.
- *Histology*
- **Pilocytic astrocytoma (WHO grade I):** Although well-known for their histologic heterogeneity (see below), the classic pilocytic astrocytoma exhibits a biphasic histopathology in which compact arrangements of astrocytes with elongated hair-like "piloid" processes alternate with loose,

hypocellular microcystic zones containing cells with a more stellate multipolar appearance.(Fig. 1.4a-d)
– Rosenthal fibers (brightly eosinophilic corkscrew-shaped structures), (Fig. 1.5a) eosinophilic granular bodies (EGBs), (Fig. 1.5b) and hyaline droplets may be plentiful or rare, but are a consistent finding in pilocytic astrocytomas.
– Spread often occurs along perivascular Virchow-Robin and subarachnoid spaces, (Fig. 1.6) the latter frequently accompanied by a rich reticulin network.
– Large multinucleated cells ("pennies on a plate"), nuclear pleomorphism, (Fig. 1.7a and b) and complex glomeruloid vascular structures (Fig. 1.7c) may be encountered, and are of no prognostic significance. Infarct-like necrosis may also be seen.
– Though discrete-appearing grossly, over 50% will exhibit microscopically infiltrative margins (so-called "creeping substitution").
– Examples that are extensively infiltrative are referred to as the "diffuse" pattern, though they share the same favorable prognosis as the typical pilocytic astrocytomas; these most often arise in the cerebellar hemispheres.
– Other diagnostically problematic patterns to consider:
  – Extracellular myxoid material and perinuclear halos can be extensive, mimicking oligodendroglioma. (Fig. 1.8a)
  – Vascular hyalinization and telangiectasias or angiomatous features are occasionally prominent enough to suggest a diagnosis of vascular malformation.
  – Perivascular pseudorosettes (mimicking ependymoma) and "spongioblastoma-like" rhythmic palisades may be encountered. (Fig. 1.8b-c)
– Anaplastic / malignant progression is extremely rare, often associated with prior radiation therapy.
  – Though not yet clearly defined, these lesions should display some degree of hypercellularity, brisk mitotic activity, endothelial proliferation and palisading necrosis.

- **Pilomyxoid astrocytoma (WHO grade II):** Its name accurately portrays its histologic findings, containing a monomorphous population of bipolar cells with delicate elongated "piloid" processes bathed by an abundant myxoid matrix. These cell processes frequently radiate from vessels in a pseudorosette fashion. (Fig. 1.9a-d)
- Rosenthal fibers and EGBs are absent, as is the characteristic biphasic compact and loose architecture of classic PA.
- Focal areas of necrosis, hemorrhage, or vascular proliferation may be seen, and mitotic figures range from few to quite frequent.

1.5 ELECTRON MICROSCOPY

- **Pilocytic astrocytoma** Ultrastructurally, the individual cells contain abundant cytoplasmic intermediate filaments, and Rosenthal fibers correspond to intracellular amorphous electron-dense masses surrounded by intermediate filaments.
  – **Pilomyxoid astrocytoma**
    – Tumor cells are typically bipolar, extending elongated thin cell processes to rest upon the basal lamina of bloods vessels in pseudorosette-like formations. (Fig. 1.10a)

- Some cells contain abundant intermediate (glial) filaments.
- Apical surfaces may display microvilli, blebs, and occasional cilia.
- Vesicles and coated pits, as well as dense core granules (Fig. 1.10b) and "synaptoid" complexes have all been described.

1.6 IMMUNOHISTOCHEMISTRY

- **Pilocytic astrocytoma**
  - As with other astrocytic lesions, GFAP positivity can be demonstrated by immunohistochemistry, typically most prominent in the compact zones. (Fig. 1.11a)
  - Ki67 / Mib-1 proliferation index is low, though is not helpful in differentiating PA from low grade infiltrative astrocytomas.
  - Absence of intratumoral anti-neurofilament positive processes indicative of a solid growth pattern is helpful in differentiating PA from more diffusely infiltrative astrocytomas. (Fig. 1.11b)
  - A recent study has found frequent immunopositivity for oligodendroglial differentiation markers including myelin basic protein (MBP), PDGFR-alpha, Olig-1 and Olig-2. An inverse correlation was found between MBP expression and proliferative index, while PDGFR-alpha expression held a positive correlation with both proliferation and shortened progression-free survival.
- **Pilomyxoid astrocytoma**
  - Lesional cells are characteristically diffusely positive for GFAP, S100, and vimentin. (Fig. 1.11c)
  - Synaptophysin may be positive, (Fig. 1.11d) though other neuronal markers (chromogranin and neurofilament) are negative. Neurofilament may on occasion stain overrun neuritic processes, indicating infiltrative tumor.
  - Ki67 / Mib-1 labeling may range from 2 to 20%.

1.7 MOLECULAR PATHOLOGY

- **Pilocytic astrocytoma**
  - In addition to the aforementioned association of PA with NF1, recent studies suggest focal gains of chromosome 7q34 and BRAF gene mutation or rearrangement (tandem duplication) resulting in aberrantly increased BRAF-MEK-ERK signaling are common findings in sporadic PAs.
  - PAs have been found to lack genetic changes commonly seen in diffuse astrocytomas, including alterations of p53, p16, EGFR, RB, and PTEN.
- **Pilomyxoid astrocytoma**
  - No defining genetic signature has thus far been elucidated, though rarely PMA has been found in the context of NF1.

1.8 DIFFERENTIAL DIAGNOSIS

- **Pilocytic astrocytoma-** Because it may display a variety of histologic patterns, PA may be confused with a variety of neoplastic (and non-neoplastic) processes.
  - The compact areas of pilocytic astrocytoma may be indistinguishable from areas of "piloid gliosis" containing abundant Rosenthal fibers. Correlation with radio-

graphic and surgical findings will frequently aid in this differentiation.
  - PA may resemble low grade infiltrative astrocytoma (or sometimes oligodendroglioma as noted above), particularly on limited biopsies.
  - Diffuse PAs, by definition, tend to be more infiltrative, so this alone cannot be used as a differentiating feature.
    - Rosenthal fibers and EGBs are however reliable clues to the diagnosis of PA in these settings. Please note that Rosenthal fibers and EGBs are not limited to PAs, and may be encountered in ganglion cell tumors and PXAs as noted elsewhere.
  - Architectural patterns such as ependymoma-like perivascular pseudorosettes and rhythmic "spongioblastic" palisades should always prompt a careful search for other more classic features of PA.
  - Care should be taken in the assessment of small biopsies from presumed optic nerve PAs as one may encounter significant meningothelial hyperplasia which could be misinterpreted as meningioma.
- **PMA**
  - Though it may closely resemble PA, the absence of Rosenthal fibers, EGBs, biphasic architecture, and presence of abundant myxoid background and angiocentric arrangements help differentiate PMA from pilocytic astrocytoma.
  - The perivascular pseudorosettes of PMA may lead one to consider ependymoma, however the latter does not tend to bear an abundant myxoid background, nor does it typically show positivity for synaptophysin. Ependymomas may uncommonly involve the hypothalamic/chiasmatic region, as is typical of PMA.

1.9 PROGNOSIS

- **Pilocytic astrocytoma**
  - Prognosis is excellent overall, with mean progression-free and overall survival times of 13 and 20 years, respectively. Unfortunately, tumors arising in unfavorable locations may occasionally result in significant morbidity and mortality despite slow growth. In these cases, chemotherapy and gamma knife radiosurgery may be helpful in disease stabilization.
  - Recurrence is more common in chiasmatic/hypothalamic lesions, these tumors being particularly difficult to completely excise given the high morbidity/mortality rates associated with surgery in this region. Chemotherapy is therefore the primary treatment in these cases, with surgery reserved for post-therapy relapses.
- **PMA**
  - PMA behaves more aggressively than pilocytic astrocytomas, experiencing a higher rate of recurrence as well as shortened progression-free and overall survivals.
  - On occasion, these tumors are rapidly fatal, and may show CSF dissemination.
- A recent gene expression profiling study found decreased levels of aldehyde dehydrogenase 1 family member L1 (ALDH1L1) in clinically aggressive compared to typical PAs, in PAs with increased cellularity and necrosis, and in the majority of PMAs, indicating that ALDH1L1 underexpression is associated with aggressive histology and/or biologic behavior in these neoplasms with pilocytic morphology.

SUGGESTED READING

Li J, Perry A, James CD, Gutmann DH. (2001) Cancer-related gene expression profiles in NF1-associated pilocytic astrocytomas. Neurology 56:885–890

Cheng Y, Pang JC, Ng HK, Ding M, Zhang SF, Zheng J et al. (2000) Pilocytic astrocytomas do not show most of the genetic changes commonly seen in diffuse astrocytomas. Histopathology 37(5):437–444

Fuller CE, Frankel A, Smith M, Rodziewitz G, Landas SK, Caruso R et al. (2001) Suprasellar monomorphous pilomyxoid neoplasm: an ultrastructural analysis. Clin Neuropathol 20(6):256–62

Tihan T, Fisher PG, Kepner JL, Godfraind C, McComb RD, Goldthwaite PT et al. (1999) Pediatric astrocytomas with monomorphous pilomyxoid features and a less favorable outcome. J Neuropathol Exp Neurol 58(10):1061–1068

Fernandez C, Figarella-Branger D, Girard N, Bouvier-Labit C, Gouvernet J, Peredes A et al. (2003) Pilocytic astrocytomas in children: prognostic factors- a retrospective study of 80 cases. Neurosurgery 53:544–555

Komotar RJ, Burger PC, Carson BS, Brem H, Olivi A, Goldthwaite PT et al. (2004) Pilocytic and pilomyxoid hypothalamic / chiasmatic astrocytomas. Neurosurgery 54:72–80

Ceppa EP, Bouffet E, Griebel R, Robinson C, Tihan T. (2007) The pilomyxoid astrocytoma and its relationship to pilocytic astrocytoma: report of a case and a critical review of the entity. J Neurooncol 81(2):191–196

Bar EE, Lin A, Tihan T, Burger PC, Eberhart CG. (2008) Frequent gains at chromosome 7q34 involving BRAF in pilocytic astrocytoma. J Neuropathol Exp Neurol 67(9):878–887

de Chadarevian JP, Halligan GE, Reddy G, Bertrand L, Pascasio JM, Faerber EN et al. (2006) Glioneuronal phenotype in a diencephalic pilomyxoid astrocytoma. Pediatr Dev Pathol 9:480–487

Morales H, Kwock L, Castillo M. (2007) Magnetic resonance imaging and spectroscopy of pilomyxoid astrocytomas: case reports and comparison with pilocytic astrocytomas. J Comput Assist Tomogr 31:682–687

Chikai K, Ohnishi A, Kato T, Ikeda J, Sawamura Y, Iwasaki Y et al. (2004) Clinico-pathological features of pilomyxoid astrocytoma of the optic pathway. Acta Neuropathol (Berl) 108:109–114

Arslanoglu A, Cirak B, Horska A, Okoh J, Tihan T, Aronson L et al. (2003) MR imaging characteristics of pilomyxoid astrocytomas. AJNR Am J Neuroradiol 24:1906–1908

Lieberman KA, Wasenko JJ, Schelper R, Chang JK, Rodziewicz GS. (2008) Tanycytomas: a newly characterized hypothalamic-suprasellar and ventricular tumor. AJNR Am J Neuroradiol 24:1999–2004

Rodriguez FJ, Giannini C, Asmann Y, Sharma MK, Perry A, Tibbetts KM et al. (2008) Gene expression profiling of NF-1-associated and sporadic pilocytic astrocytoma identifies aldehyde dehydrogenase 1 family member L1 (ALDH1L1) as an underexpressed candidate biomarker in aggressive subtypes. J Neuropathol Exp Neurol 67(12):1194–1204

Teo JG, Ng HK. (1998) Cytodiagnosis of pilocytic astrocytoma in smear preparations. Acta Cytol 42(3):673–678

Takei H, Yogeswaren ST, Wong KK, Mehta V, Chintagumpala M, Dauser RC, Adesina AM. (2008) Expression of oligodendroglial differentiation markers in pilocytic astrocytomas identifies two clinical subsets and shows a significant correlation with proliferation index and progression free survival. J Neurooncol 86(2):183–190

Komotar RJ, Mocco J, Carson BS, Zacharia BE, Sisti AC, Canoll PD et al. (2004) Pilomyxoid astrocytoma: a review. Med Gen Med 6(4):42
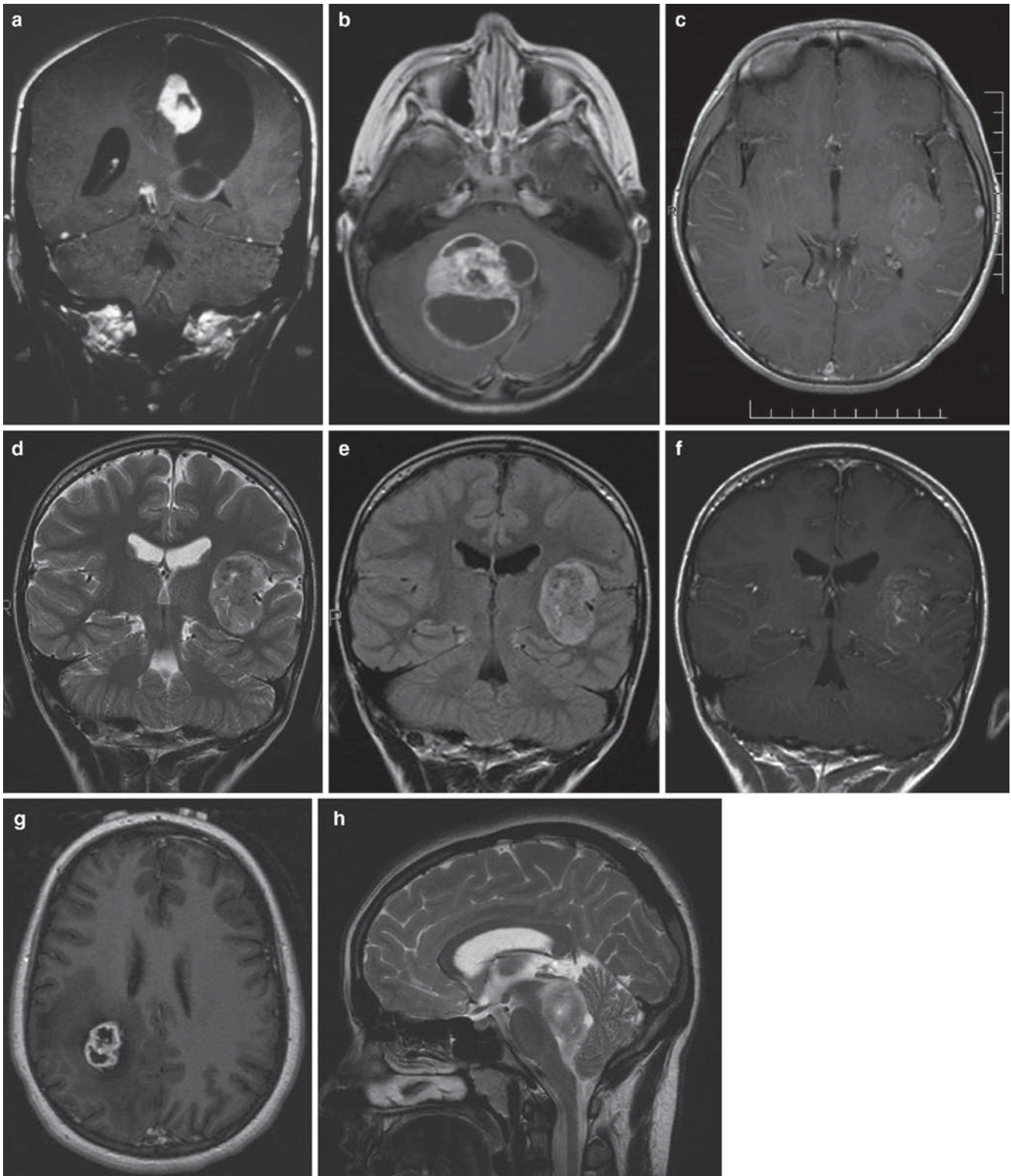
Fig. 1.1. (**a**) Coronal T1-w post-Gd MR image of cerebral pilocytic astrocytoma showing characteristic cyst with enhancing mural nodule. Some lesions are multicystic, as is this cerebellar example (**b**, axial T1-w post-Gd). Note the variability of cyst wall enhancement in these two images. Images **c** through **f** demonstrate a predominantly solid PA, with unusual localization in the insular region. The lesion is hypointense on T1 (**c**), hyperintense of T2 and FLAIR (**d** and **e** respectively), and show only slight contrast enhancement (**f**). Rarely, PA can present as a ring-enhancing lesion with central necrosis as seen in (**g**); this tumor likewise has surrounding edema, and closely mimicked glioblastoma from a radiographic perspective. (**h**) Sagittal T2-w MR image of a dorsally exophytic brain stem pilocytic astrocytoma. (Fig. 1**b-g** courtesy of Dr Gary Tye, Virginia Commonwealth University, Richmond, VA)

Fig. 1.2. (**a**) Axial T1-w post-Gd MR image of a pilomyxoid astrocytoma showing a large suprasellar lesion with strong contrast enhancement.
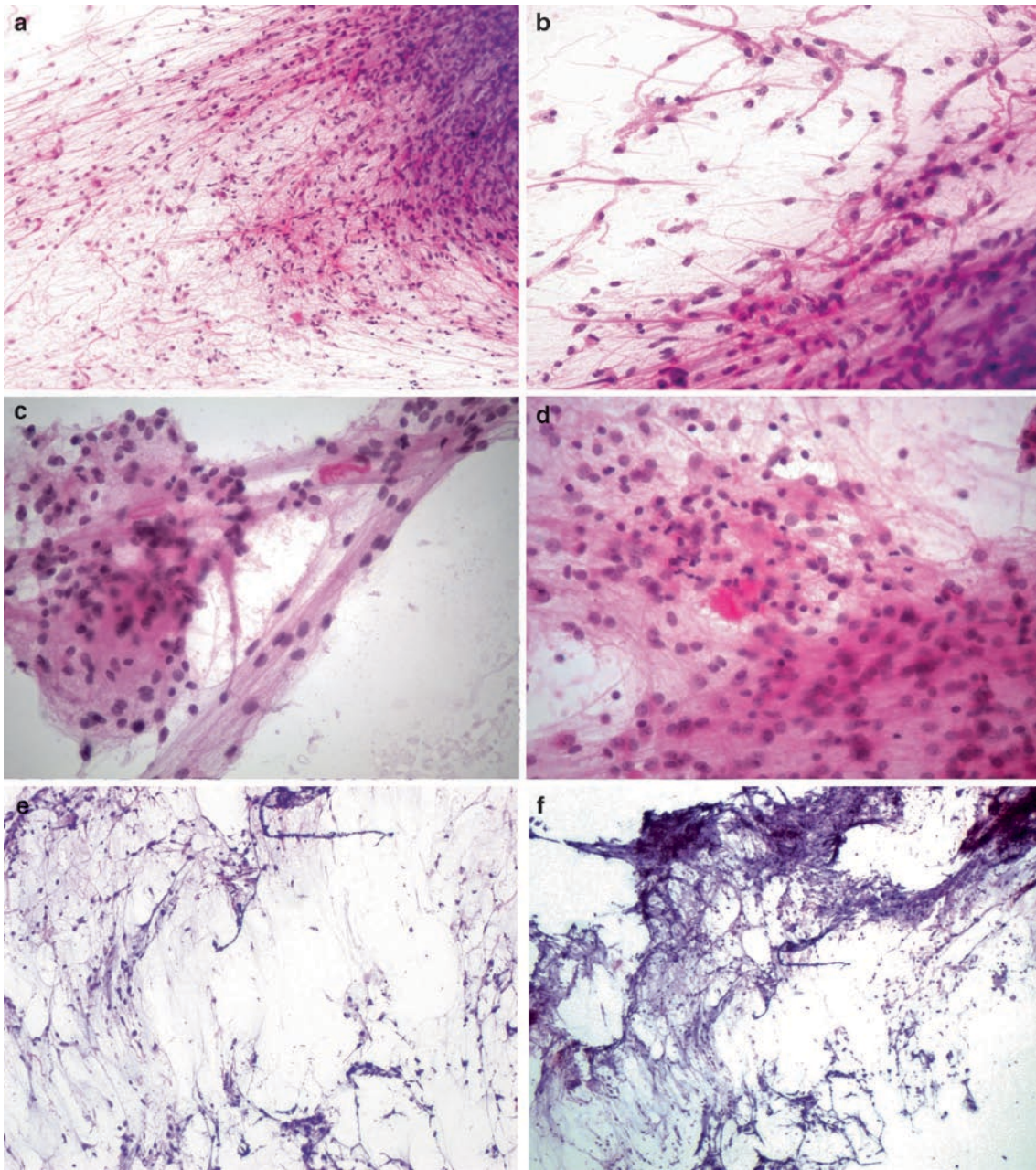
Fig. 1.3. Smear preparations of pilocytic astrocytoma at low (**a**) and high (**b**) magnification showing bipolar cells with elongated hair-like processes. Rosenthal fibers (**c**) and eosinophilic granular bodies (**d**) are a helpful diagnostic feature when present. Cytologic preparations of pilomyxoid astrocytoma (**e-f**) show similar features to pilocytic astrocytoma, though have notably more myxoid background material.
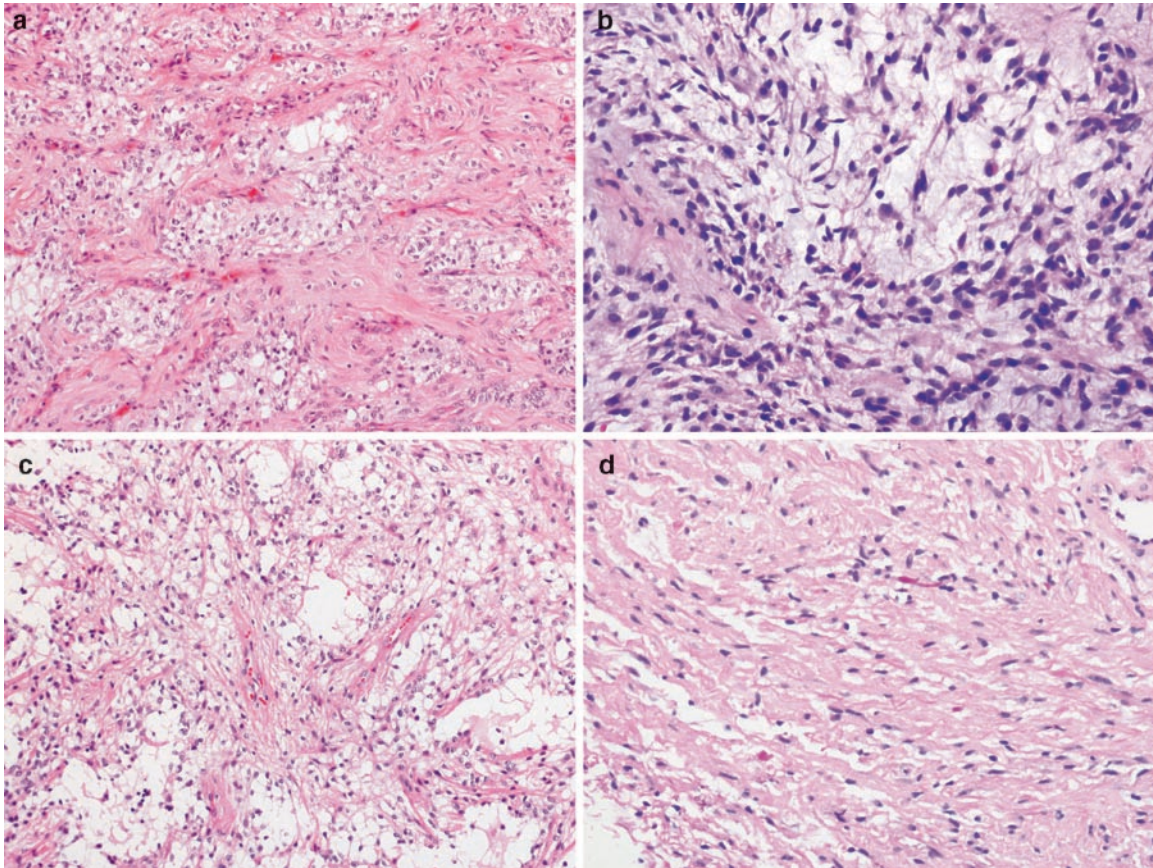
Fig. 1.4. (**a**) Classic biphasic appearance of pilocytic astrocytoma with alternating compact and loose architectures. (**b** and **c**) Within the looser microcystic areas, myxoid material is often present, and cells may take on either a bipolar or stellate appearance, bearing elongated delicate processes. (**d**) In more compact areas, cells tend to be elongated and their delicate nature less obvious; often Rosenthal fibers are seen in these areas.
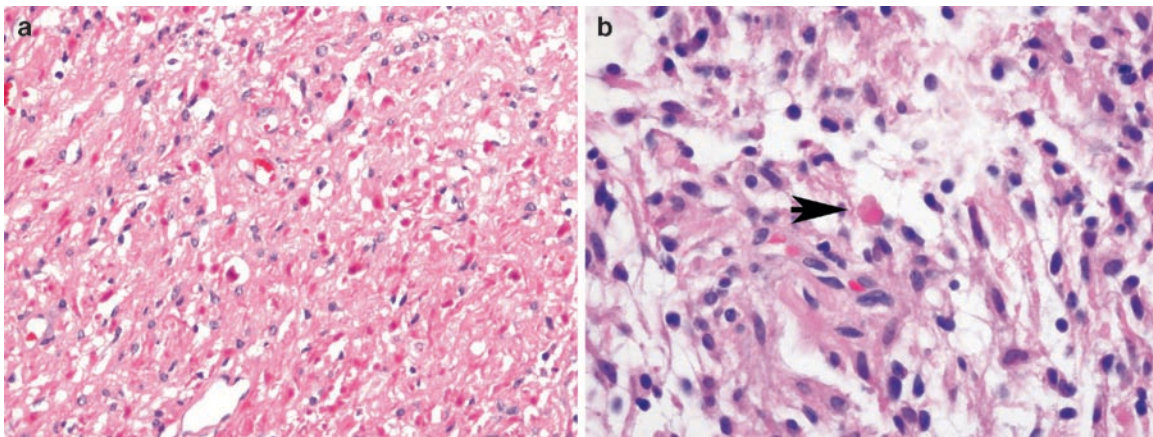
Fig. 1.5. (**a**) Rosenthal fibers may on occasion be excessive, obscuring the underlying neoplasm. (**b**) Eosinophilic granular bodies (EGBs) are typically present in the less compact / microcystic areas of pilocytic astrocytoma.
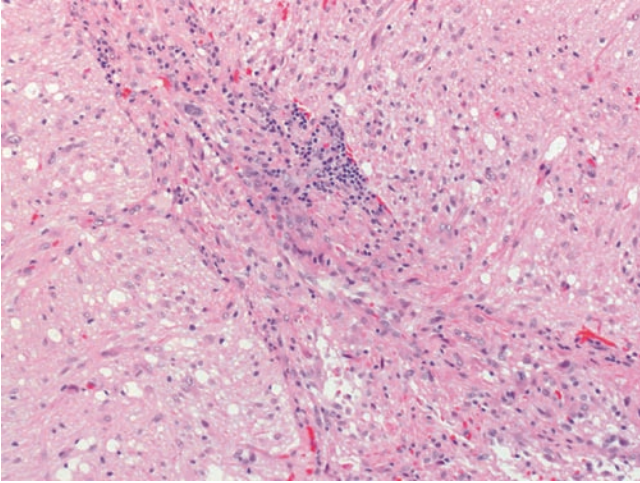
Fig. 1.6. Leptomeningeal extension by pilocytic astrocytoma is not unusual, and is of no prognostic significance.
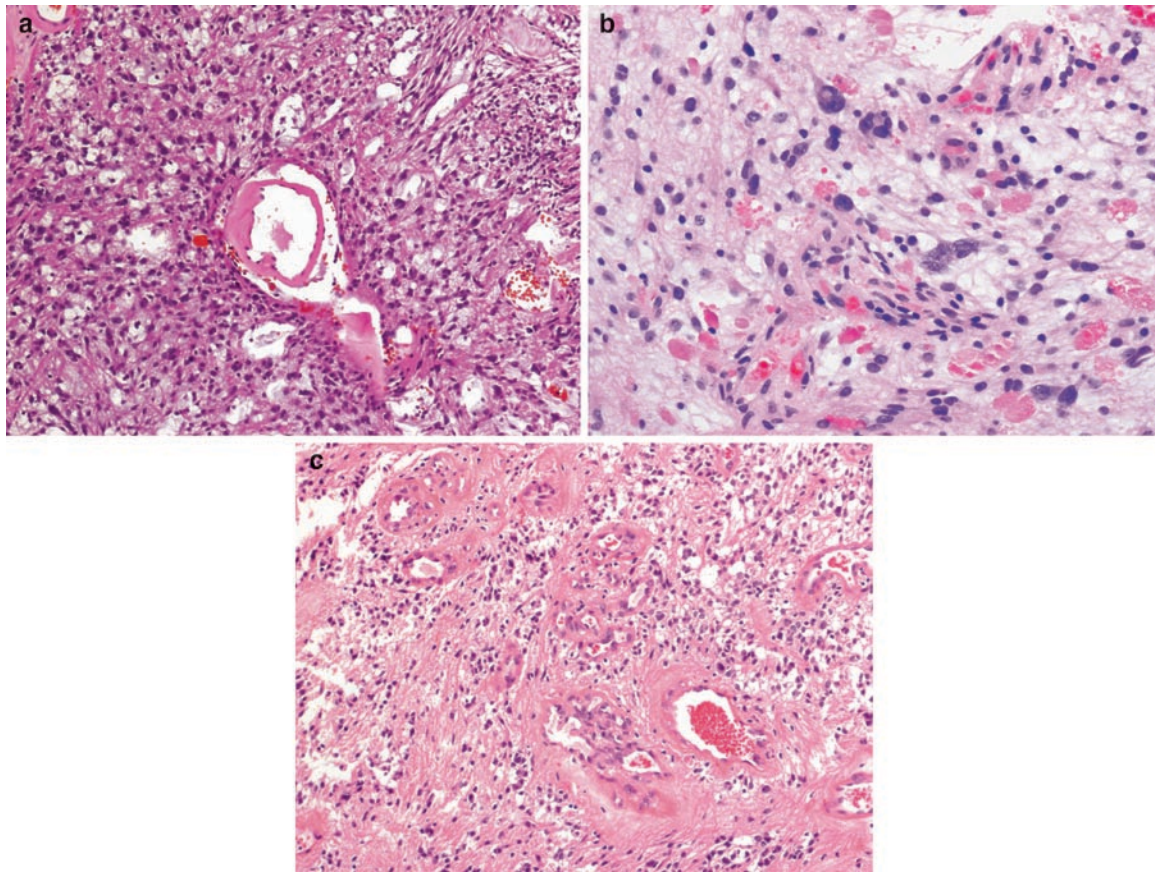
Fig. 1.7. (**a** and **b**) Degenerative-type nuclear pleomorphism and multinucleated tumor giant cells are not infrequent in pilocytic astrocytoma, and again are not prognostically relevant. Numerous EGBs are seen in 7B. (**c**) Glomeruloid vascular structures may likewise be present and do not connote malignant degeneration.
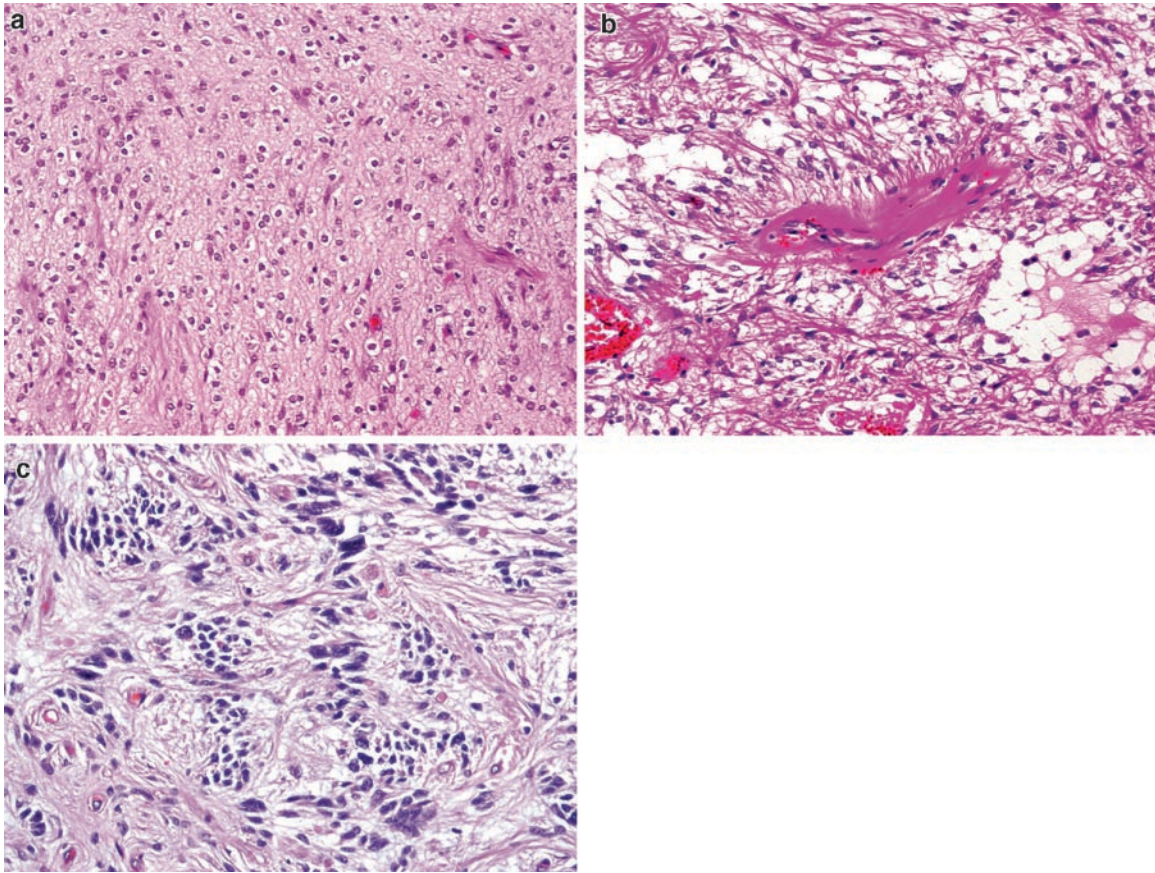
Fig. 1.8. As one of the great mimickers, pilocytic astrocytomas may harbor areas resembling oligodendroglioma (**a**) with clear zones/ cytoplasm surrounding rounded nuclei. (**b**) Perivascular pseudorosettes similar to those of ependymomas are seen on occasion. (**c**) Rhythmic "spongioblastic" palisades may rarely be encountered. All of these elements should prompt a careful search for more typical histologic features of pilocytic astrocytoma.
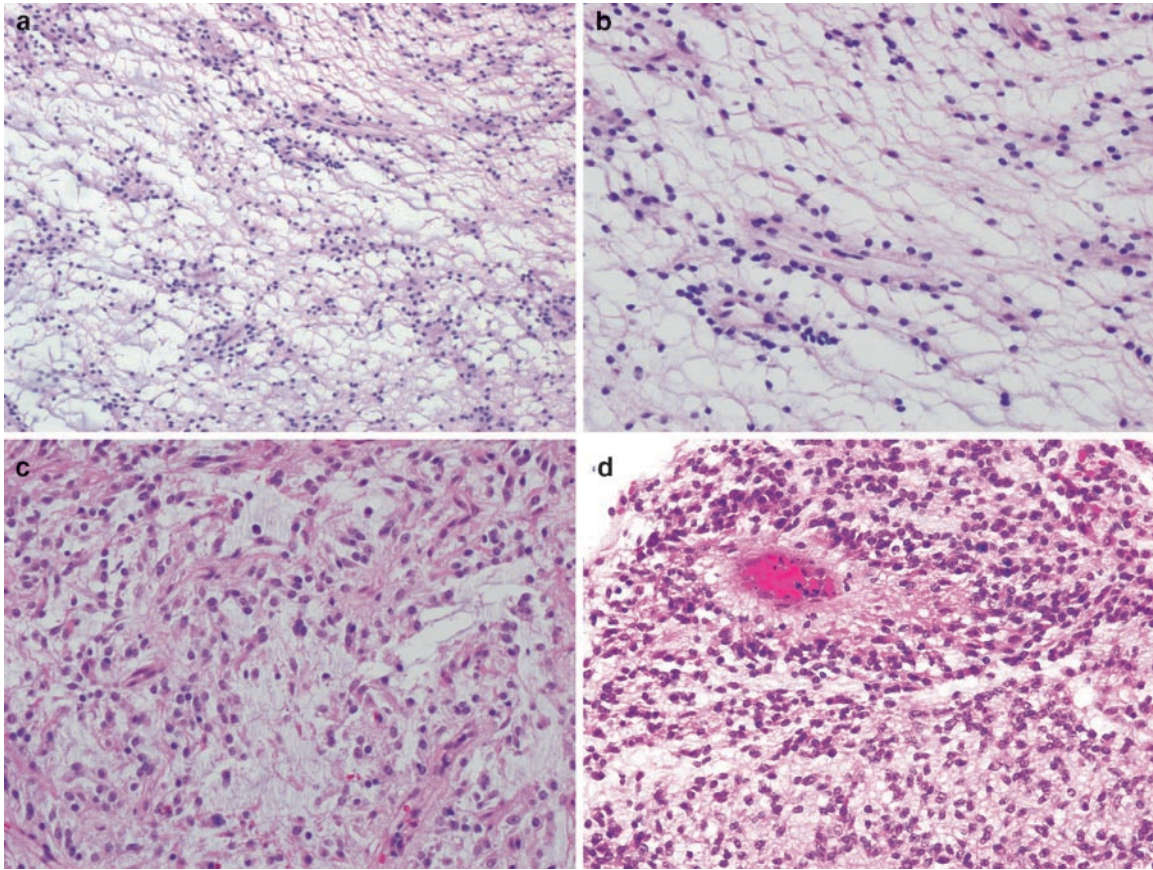
Fig. 1.9. (**a** and **b**) Pilomyxoid astrocytomas are characterized by a monotonous population of cells with bland nuclei and elongated cell processes scattered amongst a background of abundant myxoid material. These lesions may be of low to moderate cellularity (**c** and **d**), though always lack Rosenthal fibers and EGBs unlike pilocytic astrocytomas. Perivascular pseudorosettes are a frequent finding (**a**, **b**, and **d**).(Fig. 9d courtesy of Dr Arie Perry, Washington University School of Medicine, St Louis, MO)
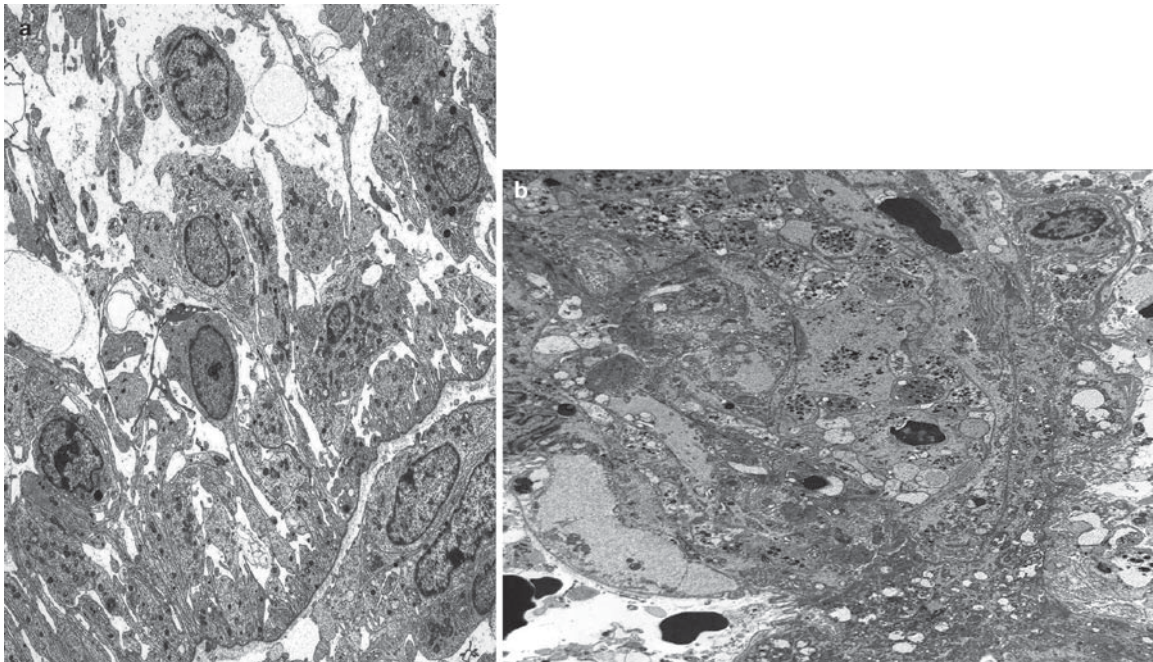
Fig. 1.10. (**a**) Ultrastructurally, pilomyxoid astrocytomas contain cells with a bipolar morphology, with elongated thin cell processes extending to rest upon the basal lamina of blood vessels (corresponding to perivascular pseudorosettes by histology). (**b**) Dense core granules may be seen in some cases.
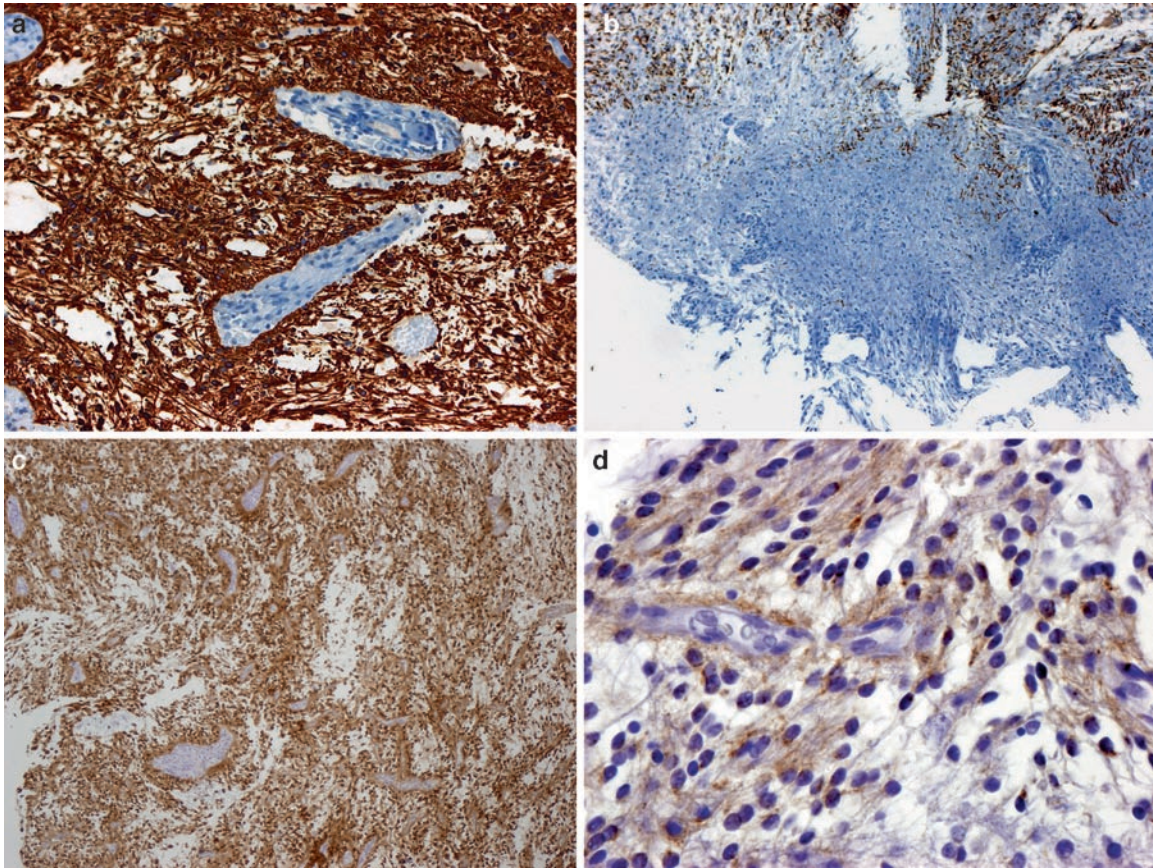
Fig. 1.11. (**a**) Pilocytic astrocytomas are diffusedly positive for GFAP. (**b**) Neurofilament staining may be helpful in showing the solid growth pattern of pilocytic astrocytoma, here seen as a lack of neurofilament stained processes in the central portion of this photomicrograph. Pilomyxoid astrocytoma is similarly diffusely positive for GFAP (**a**), though may be similarly positive for synaptophysin (**b**).

Pleomorphic Xanthoastrocytoma

Christine E. Fuller

2.1 OVERVIEW

- Pleomorphic xanthoastrocytoma (PXA) is an uncommon astrocytic lesion that despite its significant histologic pleomorphism, generally behaves in a less aggressive fashion than similarly pleomorphic infiltrative gliomas; the latter affords it a WHO grade II designation.
- The vast majority are sporadic, with only rare examples described in association with neurofibromatosis type I (NF1).
- Previously referred to as fibroxanthoma and xanthosarcoma, they have also been misclassified as forms of giant cell glioblastoma or monstrocellular sarcoma.
- Postulated to originate from subpial astrocytes, multipotential neuroectodermal precursor cells, or pre-existing hamartomatous lesions, PXAs represent distinctive astrocytic neoplasms with a variable degree of neuronal differentiation demonstrable by immunohistochemistry and electron microscopy.

2.2 CLINICAL FEATURES

- Representing <1% of all astrocytic tumors, PXAs most frequently arise within the first three decades of life. No gender predilection is apparent, and occasional cases have been reported in the elderly.
- Given their superficial "meningo-cerebral" localization, patients typically present with a history of seizures, often of a longstanding nature.
- Headaches may also occur.

2.3 NEUROIMAGING

- PXAs are almost always supratentorial and superficially-situated within the cerebral hemispheres (most commonly the temporal or parietal lobe) with involvement of the leptomeninges.
- Rare sites include the cerebellum, spinal cord, thalamus, and cerebellopontine angle.
- 70% arise as a cyst with solid mural nodule, the remainder being predominantly solid with variable small cystic areas.
- Their solid component is iso to hypodense on CT, isointense on T1-weighted MR imaging, mildly hyperintense on T2-weighted imaging, and strongly enhances following gadolinium administration (Fig. 2.1a and b).
- Intratumoral hemorrhage or calcifications are uncommon; peritumoral edema may be present, but is typically minimal.
- They may rarely show multifocality or leptomeningeal dissemination.

2.4 PATHOLOGY

- *Gross pathology*: Operative sampling of PXAs yield solid firm tissue (+/- cystic component) with variable coloration ranging from tan to yellow, the latter areas corresponding to xanthomatous histology.
- Leptomeninges are usually present in the sample, incorporated into the solid portion of the tumor.
- *Intraoperative cytologic imprints / smears*: Cytologic samples are polymorphous, containing cells with quite variable cytomorphology; fibrillary astrocytic, spindled, and giant pleomorphic forms with abundant sometimes vacuolated cytoplasm may all be present. (Fig. 2.2a and b).
- Eosinophilic granular bodies and scattered lymphocytes are often identifiable.
- *Histology*:
  - PXAs as a group are quite heterogeneous in their histologic appearance, however several key features are consistently present in all:
  - They are composed of spindle cells arranged in fascicles, intersecting bundles, or a storiform pattern, together with an admixture of variably pleomorphic giant cells, the nuclei of which may be singular, multilobated, or multiple. Nuclear hyperchromasia is typical, and intranuclear cytoplasmic invaginations are often present. (Fig. 2.3a and b)
  - Large xanthomatous cells with abundant intracytoplasmic lipid droplets are a helpful diagnostic feature when present, (Fig. 2.3c) though these may be quite inconspicuous in some cases.
  - A rich reticulin network surrounds individual cells and small cell nests. (Fig. 2.3d)
  - Though not a diagnostic requirement, eosinophilic granular bodies (EGBs) are almost always present. (Fig. 2.3c).
  - Perivascular and intratumoral collections of small lymphocytes are also frequent. (Fig. 2.3e)
  - Similar to pilocytic astrocytoma and ganglion cell tumors, PXAs display a solid growth pattern, particularly those examples situated predominantly in the subarachnoid space.
  - The interface with underlying / surrounding brain parenchyma is however variable, and infiltrative areas resembling diffuse astrocytoma may be encountered.
  - Typical PXAs have a negligible mitotic rate and are devoid of necrosis and vascular proliferation.
  - The term "PXA with anaplastic features" is reserved for those tumors with ≥ 5 mitoses/10 high power fields, and/ or necrosis. (Fig. 2.3f)

– Composite PXA/ganglioglioma, replete with identifiable ganglion cell component, may be occasionally encountered, and PXAs with clear cell change, pigmentation, and papillary structures have been reported.
– Features of cortical dysplasia may be seen in cortex adjacent to PXA in some cases.

2.5 IMMUNOHISTOCHEMISTRY

- PXAs are notable for their biphenotypic glial and neuronal staining pattern.
  – They are consistently positive for S-100 and GFAP, though the latter may be patchy. (Fig. 2.4a)
  – Expression of neuronal markers, including synaptophysin, neurofilament, MAP2, and Class III β-tubulin, may be detected in individual pleomorphic cells; (Fig. 2.4b) these markers will also highlight any true ganglion cell component.
  – CD34 expression is also frequently encountered.

2.6 ELECTRON MICROSCOPY

- Ultrastructural features include cells containing numerous intermediate filaments, lipid droplets, and lysosomes.
- Neuronal features present in some cells include microtubules, dense core granules and/or clear vesicles.
- Intercellular basement membrane and aggregates of secondary lysosomes (corresponding to EGBs) are common.

2.7 MOLECULAR PATHOLOGY

- PXAs appear to be molecularly distinct from infiltrative astrocytomas, exhibiting a low incidence of p53 mutations.
- Amplifications of EGFR, CDK4, and MDM2 have not been detected.
- Multiple chromosomal abnormalities have been documented via cytogenetics and comparative genomic hybridization, though only chromosome 9p loss with coincident homozygous deletion involving CDKN2A/p14[ARF]/CDKN2B loci has been encountered with significant frequency in 50% of cases.

2.8 DIFFERENTIAL DIAGNOSIS

- For PXA, the main alternate diagnostic consideration is glioblastoma, especially the giant cell variant; both of these cellular gliomas contain variable numbers of pleomorphic astrocytes, though have significantly different therapeutic and prognostic implications.
- Radioimaging findings of a cyst with enhancing mural nodule strongly favors PXA, as do the histologic findings of xanthomatous change, EGBs, a paucity of mitoses, and lack of necrosis and vascular proliferation.
- Immunohistochemistry may be of assistance in demonstrating positivity for neuronal markers and CD34, both of which would be unexpected in glioblastoma.
- Immunopositivity for S-100 and GFAP effectively differentiates PXA from the occasional pleomorphic leptomeningeal-based sarcoma such as malignant fibrous histiocytoma.

- Ganglioglioma and pilocytic astrocytoma are two other entities that arise in the young and may present as a cyst with mural nodule on radioimaging studies.
  – The former contains abundant dysmorphic ganglion cells and lacks the prominent pleomorphism and lipidized cells of PXA.
  – Pilocytic astrocytomas also tend not to display the extent of pleomorphism or reticulin network found in PXA, and are usually less compact in their architecture, frequently exhibiting loose microcystic areas containing cells with typical piloid processes.

2.9 PROGNOSIS

- Although PXAs afford a relatively favorable prognosis, with 5 year recurrence-free and overall survival rates of 70 and 80% respectively, a significant proportion will recur, undergo anaplastic progression, or both.
- Completeness of initial resection and low mitotic rate are both independent predictors of prolonged recurrence-free survival, whereas elevated mitotic rate (>5 mitoses / 10 HPF) and necrosis are significantly associated with poor overall survival.

SUGGESTED READING

Hirose T, Ishizawa K, Sugiyama K, Kageji T, Ueki K, Kannuki S. (2008) Pleomorphic xanthoastrocytoma: a comparative pathological study between conventional and anaplastic types. Histopathology 52:183–193

Crespo-Rodriguez AM, Smirniotopoulos JG, Rushing EJ. (2007) MR and CT imaging of 24 pleomorphic xanthoastrocytomas (PXA) and a review of the literature. Neuroradiology 49:307–315

Weber RG, Hoischen A, Ehrler M, Zipper P, Kaulich K, Blaschke B et al. (2007) Frequent loss of chromosome 9, homozygous CDKN2A/p14(ARF)/CDKN2B deletion and low TSC1 mRNA expression in pleomorphic xanthoastrocytoma. Oncogene 26(7):1088–1097

Hirose T, Giannini C, Scheithauer BW. (2001) Ultrastructural features of pleomorphic xanthoastrocytoma: a comparative study with glioblastoma multiforme. Ultrastruct Pathol 25(6): 469–478

Kepes JJ, Rubinstein LJ, Eng LF. (1979) Pleomorphic xanthoastrocytoma: a distinctive meningocereberal glioma of young subjects with relatively favorable prognosis. A study of 12 cases. Cancer 44:1839–1852

Tien RD, Cardenas CA, Rajagopalan S. (1992) Pleomorphic xanthoastrocytoma of the brain: MR findings in six patients. AJR Am J Roentgenol 159(6):1287–1290

Davies KG, Maxwell RE, Seljeskog E, Sung JH. (1994) Pleomorphic xanthoastrocytoma: report of four cases, with MRI scan appearances and literature review. Br J Neurosurg 8(6):681–689

Fouladi M, Jenkins JJ, Burger PC, Langston J, Merchant T, Heideman R et al. (2001) Pleomorphic xanthoastrocytoma: favorable outcome after complete surgical resection. Neuro-oncol 3(3):184–192

Giannini C, Hebrink D, Scheithauer BW, Dei Tos AP, James CD. (2001) Analysis of p53 mutation and expression in pleomorphic xanthoastrocytoma. Neurogenetics 3(3):159–162

Giannini C, Scheithauer BW, Lopes MB, Hirose T, Kros JM, VandenBerg SR. (2002) Immunophenotype of pleomorphic xanthoastrocytoma. Am J Surg Pathol 26(4):479–485

Bucciero A, De Caro M, De Stefano V, Tedeschi E, Monticelli A, Siciliano A et al. (1997) Pleomorphic xanthoastrocytoma: clinical, imaging and pathological features of four cases. Clin Neurol Neurosurg 99:40–45

Giannini C, Scheithauer BW, Burger PC, Brat D, Wollan PC, Lach B et al. (1999) Pleomorphic xanthoastrocytoma. Cancer 85:2033–2045
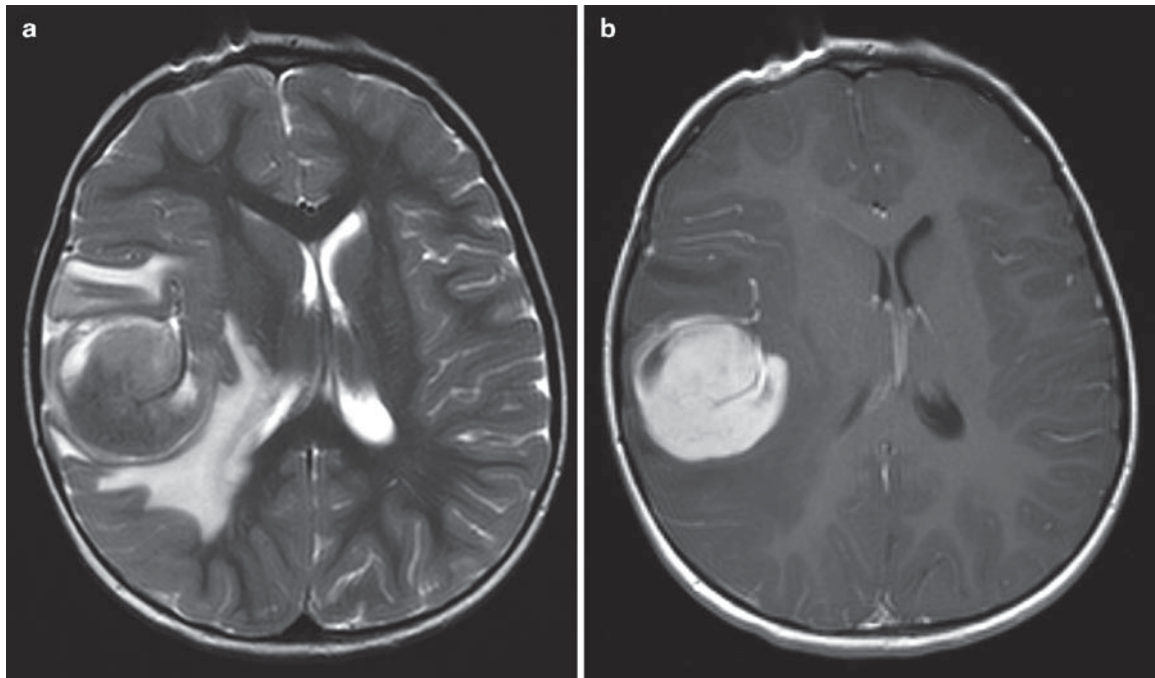
Fig. 2.1. Axial MR imaging (a) T2-w showing a large solid mildly hyperintense well-circumscribed nodule with associated fluid-filled cyst arising within the outer aspects of the right temporoparietal region. Peritumoral edema is fairly prominent in this case, and there is noticeable mass effect. (**b**) Axial TI-w post-Gd imaging shows intense homogeneous enhancement of the solid nodule with rim enhancement of the cyst wall.
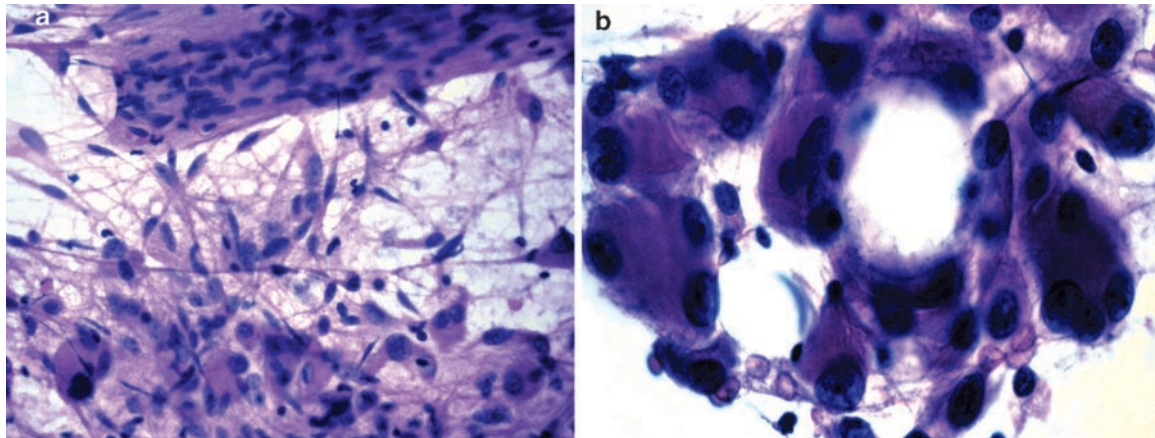
Fig. 2.2. Intraoperative cytologic smear preparations are quite polymorphous, containing a mixture of cells with (**a**) fibrillary astrocytic, spindled, and (**b**) giant pleomorphic morphologies.
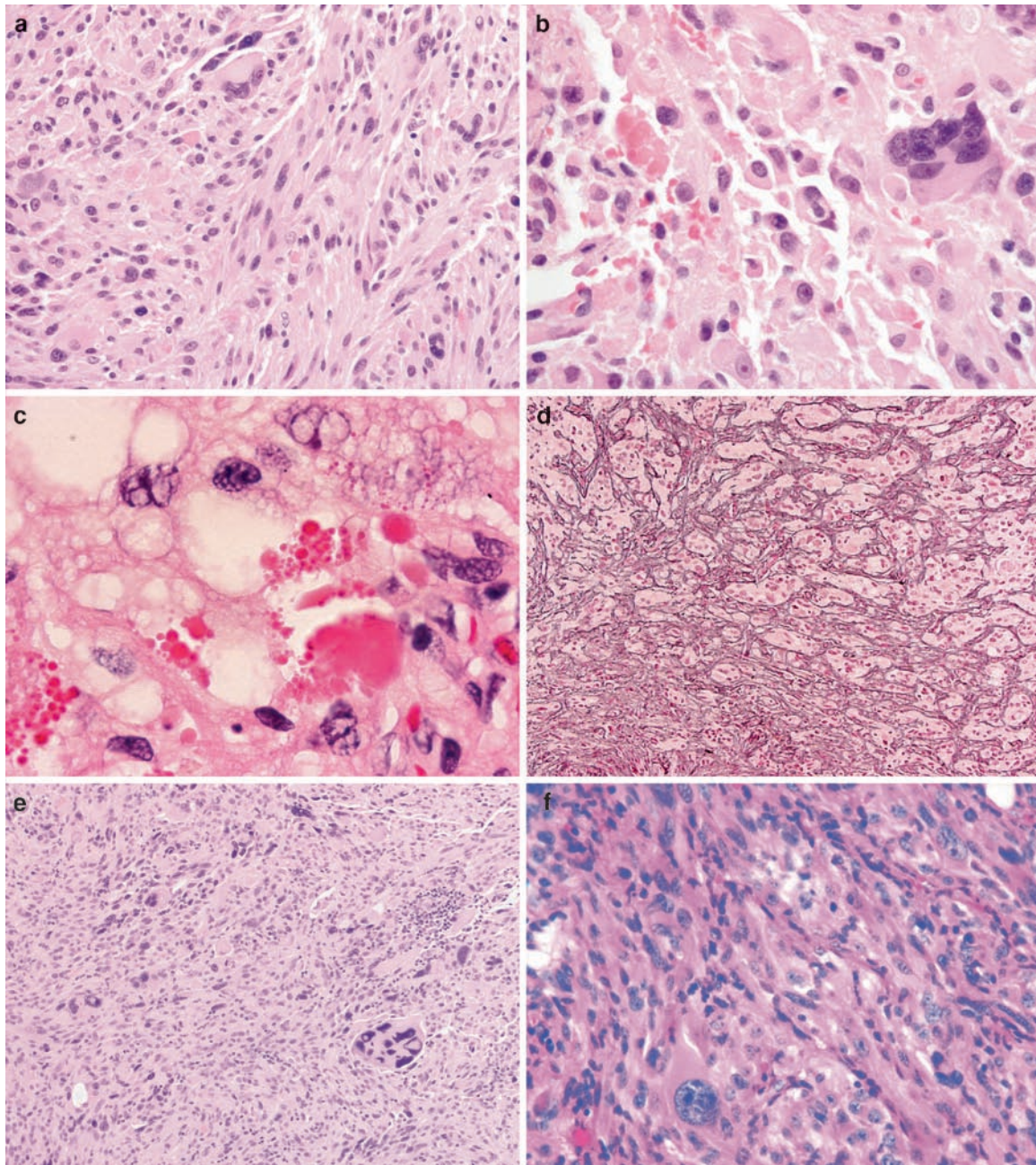
Fig. 2.3. (**a** and **b**) PXAs, though notable for their heterogeneous histologic appearance, fairly consistently contain spindle cells arranged in fascicles or intersecting bundles, together with an admixture of pleomorphic giant cells, the nuclei of which may be singular, multilobated, or multiple. Nuclei are often hyperchromatic, though some cells may exhibit nuclear features similar to those seen in ganglion cells, containing more open chromatin and singular prominent nucleoli (**b**). Eosinophilic granular bodies are another consistent feature (**a-c**). Cytoplasmic vacuolization may be extensive as in this example (**c**), though in some PXAs may be exceedingly difficult to identify. (**d**) Verification of a rich reticulin network is helpful in differentiating PXA from higher grade gliomas. (**e**) Similar to gangliogliomas, PXAs also frequently contain interspersed collections of lymphocytes. (**f**) This PXA with anaplastic features was notable for brisk mitotic activity; necrosis was present elsewhere in the tumor.
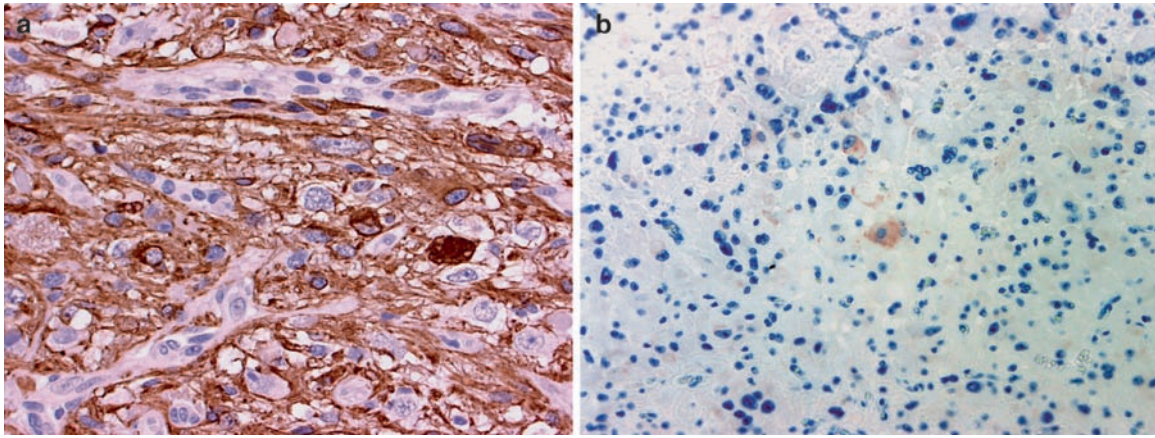
Fig. 2.4. (a) GFAP is likewise consistently positive in PXAs. (b) Not uncommonly, scattered individual tumor cells will express neuronal markers, such as synaptophysin shown here.

Infiltrative Astrocytomas (Diffuse Astrocytoma, Anaplastic Astrocytoma, Glioblastoma)

Christine E. Fuller

3.1 OVERVIEW

- Infiltrative astrocytomas represent a diverse group of glial tumors of variable degree of malignancy that share in common the qualities of astrocytic differentiation and an inherent ability to diffusely invade CNS parenchyma.
- The WHO 2007 classification divides infiltrative astrocytomas into three grades as follows:
  - *Diffuse astrocytoma* (also known as well-differentiated or low grade astrocytoma) – WHO grade II.
  - *Anaplastic astrocytoma* – WHO grade III.
  - *Glioblastoma* (also know as glioblastoma multiforme) WHO grade IV.
- As a group, infiltrative astrocytomas represent the most frequent glial tumors afflicting adults, with glioblastoma accounting for the largest percentage of all malignant CNS tumors.
  - They are second to pilocytic astrocytoma in terms of frequency in the pediatric age group.
  - Approximately 10% of all glioblastomas occur within the first two decades of life.
- The vast majority are sporadic. Epidemiological studies have shown that previously irradiated patients are at increased risk of subsequent astrocytoma development.
- A minority are encountered in the context of various tumor syndromes, including Li-Fraumeni syndrome (p53), Turcot syndrome (APC), Tuberous sclerosis (TSC1 and 2), Neurofibromatosis Type I (NF1), and multiple enchondromatosis (Ollier's disease).
- *Gliomatosis* – represents an aggressive diffusely infiltrative glioma that involves broad regions of the CNS, typically more than two lobes with or without bilateral hemispheric involvement or extension into the posterior fossa and the spinal cord.

3.2 CLINICAL FEATURES

- Symptoms/signs are related to tumor location and/or secondary mass effect, and many times are nonlocalizing.
- Cerebral hemispheric lesions may result in seizures or focal motor deficits, whereas endocrinopathies can result from hypothalamic lesions.
- Pontine gliomas may present with cranial nerve deficits, while spinal cord lesions may cause pain, weakness, paresthesias, or gait disturbance.
- Symptoms/signs associated with high grade lesions are usually of short duration prior to tumor detection.
- There is no particular gender predilection with the exception of supratentorial diffuse astrocytomas where afflicted males outnumber females 2:1.
- The vast majority of glioblastomas in children arise de novo (i.e., primary glioblastoma) with malignant transformation from an underlying low grade astrocytoma to glioblastoma (i.e., secondary glioblastoma) being extremely rare in this age group.
  - Approximately <10% of low grade astrocytomas undergo malignant transformation in children compared with over 90% in adult patients.
- Pontine high grade astrocytomas occur at a younger age (mean = 8 years) compared with high grade astrocytomas of other sites.
- Gliomatosis is rare in adults and children, with neurologic signs/symptoms generally nonlocalizing.

3.3 NEUROIMAGING

- Though they do occur in the cerebral white matter, pediatric grade II astrocytomas more often arise in deep brain midline structures (especially thalami) with rare occurrence in the cerebellum and the spinal cord (Fig. 3.1a, b).
- Pediatric glioblastomas may arise within cerebral white matter, often extending into deep gray structures or across the midline (Fig. 3.1c).
  - Unlike their adult counterparts, pediatric glioblastoma additionally represents the most frequent tumor of the brainstem, particularly the pons.
  - Rarely do they arise in the cerebellum or spinal cord.
- Localization of pediatric anaplastic astrocytoma is overlapping at same sites noted for grade II and IV lesions.
- Both grade II and grade III lesions tend to be ill-defined, being low density masses on CT studies.
  - Calcification or cystic changes may be seen.
  - Anaplastic astrocytoma often shows at least focal enhancement.
- Glioblastoma characteristically presents as a ring-enhancing lesion (Fig. 3.1c).
- Enhancement may be more heterogeneous in brainstem lesions.
- Grade II lesions are poorly-marginated, hypointense on T1 and hyperintense on T2 (Fig. 3.1a) and FLAIR MR images.
  - Contrast enhancement is not a feature (Fig. 3.1b), but when contrast enhancement appears on follow-up imaging studies, it heralds the occurrence of malignant progression or transformation.

- High grade lesions are similar in their MR characteristics to grade II astrocytoma; however, they frequently have surrounding bright areas on T2-w imaging due to peritumoral edema, as well as contrast enhancement (Fig. 3.1d–f).
- Giant cell glioblastoma and gliosarcoma tend to be more demarcated than other glioblastomas.
- Brain stem gliomas may take the form of
  - "Pontine glioma" – markedly expanded pons, often with encroachment/engulfment of the basilar artery.
    - Signal characteristic are variable, dependent upon grade of tumor present.
    - Ring enhancement of glioblastoma may be encountered (Fig. 3.2a–c).
  - "Tectal glioma" – these lesions are limited to the periaqueductal region and are isointense on T1 and hyperintense on T2-weighted MR imaging, and they seldom show enhancement.
- Brainstem dorsally exophytic gliomas – These are usually pilocytic astrocytomas (see pilocytic astrocytoma section for more details)
- Gliomatosis – At least three cerebral lobes are typically involved, and they are usually bilateral and extend into deep gray structures.
  - Gliomatosis may extend to involve the posterior fossa elements or even the spinal cord.
  - Lesions are characteristically hyperintense on T2 and FLAIR MR imaging (Fig. 3.3).

3.4 PATHOLOGY

- *Gross pathology*:
  - Diffuse astrocytoma is frequently ill-defined grossly, distorting the involved anatomical region and blurring gray-white matter demarcations.
    - These lesions do not show tissue destruction, merely infiltration.
    - Cystic areas or calcifications may be present, though the gray-tan color and firm texture are otherwise homogeneous (Fig. 3.4a).
  - High grade astrocytomas, particularly glioblastomas, tend to have a much more heterogeneous appearance, forming grossly-obvious masses, often containing areas of hemorrhage and/or necrosis. Because of this, they typically have a mottled tan, red, and brown coloration with alternating firm and softened zones (Fig. 3.4b).
    - Gliosarcomas may be quite firm in consistency, due to the particular sarcomatous component present.
- *Intraoperative cytologic imprints/smears*:
  - Smear/squash preparations of infiltrative astrocytomas contain cells with oval to irregular-shaped hyperchromatic nuclei and elongated fibrillary cytoplasmic processes. These processes are most evident at the periphery of sheets of tumor cells (Fig. 3.5a).
    - Cells with gemistocytic morphology may be plentiful (Fig. 3.5b).
  - High grade lesions, not surprisingly, are obviously hypercellular, often times with mitotic figures identifiable on cytology preparations.
    - Vascular proliferation and a "dirty" necrotic background are features supportive of glioblastoma (Fig. 3.5c,d).

- *Histology*: Four histologic criteria are utilized in the grading of infiltrative astrocytomas:
  - Nuclear atypia
  - Mitosis
  - Necrosis and/or
  - Microvascular proliferation.
  - Tumor grade is established based on the area of greatest anaplasia.
  - *Diffuse/low-grade astrocytoma (WHO grade II)*: moderately cellular astrocytomas that fulfill only one of the listed criteria (nuclear atypia). Mitotic figures should be exceeding difficult to find, and vascular proliferation and necrosis are absent (Fig. 3.6a–c).
  - *Anaplastic astrocytoma (WHO grade III)*: hypercellular astrocytomas that in addition to nuclear atypia, have increased mitotic activity.
    - Vascular proliferation and necrosis are absent.
    - Cells with large pleomorphic or multiple nuclei may be present (Fig. 3.6d,e).
  - Neuropil-rich islands that are surrounded by oligodendroglial-like cells may be encountered in rare infiltrative astrocytomas (grades II and III). These areas are characteristically positive for neural markers synaptophysin and Neu-N.
  - A note of caution in grading:
    - "Few mitoses are acceptable in a large sample of otherwise typical grade II astrocytoma, whereas detection of even a single mitotic figure within a tiny needle core biopsy would be grounds for upgrading to high grade astrocytoma" (at least anaplastic astrocytoma).
  - *Glioblastoma (WHO grade IV)*: In addition to findings as listed for anaplastic astrocytoma, glioblastomas display necrosis (typically pseudopalisading necrosis) or microvascular proliferation.
    - Frequently both of the latter features are demonstrable.
    - Individual tumor cells may range from small to bipolar to huge cells with markedly pleomorphic nuclei or multinucleation (see below).
    - Atypical mitotic figures may be present (Fig. 3.7a–d).
  - Microvascular proliferation may take the form of large glomeruloid tufts (Fig. 3.7c) to linear capillaries with intraluminal multilayered endothelial proliferation (Fig. 3.7d); both should show mitotic activity.
  - Secondary structures (subpial accumulation of tumor cells, perineuronal and perivascular satellitosis) are more common in high grade astrocytomas than grade II astrocytoma), though this growth pattern is also common in oligodendroglial tumors and gliomatosis (Fig. 3.8a–c).
  - Multiple morphologic variants described:
    - Fibrillary – this is by far the most frequently encountered morphology, which despite its name is typified by cells bearing only minimal discernible cytoplasm (naked nuclei). This morphology may be present in both low (grade II) and high grade (III and IV) lesions (Figs. 3.6a–e, 3.7a–d).
    - Gemistocytic – cells with plump eosinophilic cytoplasmic "bellies", often with some extensions of stout cytoplasmic processes at their periphery, and

eccentric nuclei. Again, this morphology may be seen in both low and high grade lesions. At least 20% of all cells in a given tumor must harbor this morphology to warrant the designation of "gemisto-cytic astrocytoma", a variant known to be more prone to malignant progression, at least in the adult population; whether this propensity for progression holds true in children is not clear (Fig. 3.9a–b).

- Protoplasmic-neoplastic astrocytes showing small cell bodies and few thin processes. *Protoplasmic astrocytoma*, solely bearing this morphology, is exceeding rare, though cells with similar morphology may be seen in other forms of astrocytoma, particularly within the loose areas of pilocytic astrocytoma.
- Giant cell – though some multinucleated tumor giant cells are not uncommon in high grade astrocytomas, glioblastoma populated nearly exclusively by large, bizarre multinucleated giant cells are termed *giant cell glioblastoma* (Fig. 3.10a–b).
    - They tend to be more circumscribed on radioimaging studies, subcortical in location, and sometimes contain prominent reticulin networks.
    - These are positive for GFAP, S100, and vimentin, though negative for neural markers (unlike PXA). This variant has been found to have a slightly better prognosis, due in part to less invasiveness compared with other forms of glioblastoma.

Small cell – may be encountered in high grade astrocytomas, individual tumor cells bearing round to slightly oval nuclei with minimal to imperceptible cytoplasm.

- *Small cell glioblastoma* (predominance of cells with this morphology) has been well recognized in adults, typically showing a high proliferation rate and little GFAP staining; many will have EGFR mutation/amplification, and positive staining by immunohistochemistry. The incidence of this lesion in children is unknown (Fig. 3.10c–f – represents an example of small cell glioblastoma in an adult, while g and h are a pediatric example).
- Uncommon cell morphologies include
    - Lipidized cells.
    - Carcinoma/epithelial-like cells – components resembling adenocarcinoma, including signet ring cells, and even a squamous appearance have been encountered.
        - Chordoid areas may be seen (Fig. 3.11a).
    - Granular cell – PAS and often CD68-positive cells with abundant cytoplasm and oval hyperchromatic nuclei.
        - These are more often encountered in high grade lesions and unfortunately are often GFAP negative (Fig. 3.11b).
    - Rhabdoid – cells resembling rhabdoid cells of AT/RT may be present, replete with polyphenotypia by immunohistochemistry. Unlike AT/RT, these cells retain nuclear positivity for INI1 (BAF47) (Fig. 3.11c).
    - Metaplastic components – benign stromal elements (muscle, cartilage, bone) have been described, though their incidence is far rarer than the sarcomatous elements of gliosarcoma.

- *Gliosarcoma (WHO grade IV)* – a biphasic high grade glioma with both malignant astrocytic (glioblastoma) and sarcomatous components. The sarcomatous portion is frequently fibrosarcoma, though may include malignant fibrous histiocytoma, chondrosarcoma, osteosarcoma, leiomyosarcoma, rhabdomyosarcoma, or even liposarcoma. Trichrome and reticulin stains are frequently positive (Fig. 3.12a–f).
- *Gliofibroma* – very rare tumor, though more common in children than adults. This biphasic tumor is similar to gliosarcoma; however, the fibroblastic component is nonsarcomatous. Grade is dependent upon the astrocytic component though it is typically low grade and thus carries a relatively favorable prognosis.
- *Gliomatosis* – most frequently astrocytic, though infrequently may contain oligodendroglial elements. Nuclei tend to be elongated and hyperchromatic, and pleomorphic forms are not uncommon. Secondary structures are frequently present. Mitotic activity is variable. Areas akin to glioblastoma may be present in some cases (Fig. 3.13a–d).

3.5 IMMUNOHISTOCHEMISTRY

- Glial fibrillary acidic protein (GFAP) expression reflects the extent of cytoplasmic development and is similarly present in the intervening fibrillary matrix of these lesions (Fig. 3.14a).
- S100 shows diffuse nuclear and cytoplasmic positivity, and Vimentin is similarly positive.
- Ki-67 is variably positive, reflecting the low (grade II) to brisk (grades III and IV) proliferative activity of the respective lesions.
- Neurofilament staining of intratumoral neuritic processes provides evidence of the infiltrative pattern of these neoplasms (Fig. 3.14b).
- Pancytokeratin is often positive at least focally in higher grade lesion, showing cross reactivity with glial intermediate filaments. More specific cytokeratin antibodies are usually negative.
- Sarcomatous portions of gliosarcoma, though not positive for GFAP, are consistently vimentin positive and tend to take on the staining properties of the particular sarcoma element present (muscle, fat, cartilage, etc.).
- Gliomatosis is variably positive for GFAP and S100.

3.6 ELECTRON MICROSCOPY

The finding of abundant intermediate filaments by ultrastructural analysis is characteristic.

3.7 MOLECULAR PATHOLOGY

There are both similarities and differences between adult and pediatric infiltrative astrocytomas from a molecular standpoint.

- EGFR amplification is found in a significant proportion of primary glioblastomas in adults, particularly the small cell variant; in contradistinction, EGFR amplification is uncommon in pediatric glioblastomas.

- Occasional p53 mutations have been encountered in pediatric astrocytomas, mainly in high grade tumors arising in children >3 years old, whereas similar mutations may be found in over 60% of grade II and III astrocytomas in adults.
- Alterations of cell cycle regulatory genes including p16/CDKN2A, RB, and PTEN have been encountered in both adult and pediatric astrocytomas; in the latter, some authors have found a correlation between the presence of PTEN mutation and poor prognosis in high grade astrocytomas.

3.8 DIFFERENTIAL DIAGNOSIS

- *Diffuse astrocytoma versus reactive astrocytosis* – even in astrocytomas of low cellularity, the distribution of cells is irregular, nuclear hyperchromasia is evident, and typical "star-like" elongated processes of reactive astrocytes are absent.
  - Neoplastic gemistocytes, similarly, will have stubby processes, and not the elongated processes of reactive astrocytes.
- *Infiltrative astrocytomas versus other gliomas* – diffuse astrocytomas can be differentiated from oligodendroglial tumors by paying close attention to nuclear morphology; astrocytic tumors have oval to irregular-shaped nuclei, whereas oligodendroglial tumors have round nuclei, with perinuclear halo. Diffuse astrocytomas should not contain Rosenthal fibers and eosinophilic granular bodies that are usually present in pilocytic astrocytomas; radiographic finding are dissimilar as well.
- *Small cell glioblastoma may closely resemble PNET*, though typically has at least some positivity for GFAP, neuronal stains should be negative, and EGFR positive staining should be present.
  - Again, the incidence of small cell glioblastoma in children is not known, and therefore it is not clear whether these findings typical of small cell glioblastoma arising in an adult will hold true for a pediatric example.
- *High grade astrocytoma with unusual cell types* – rhabdoid cells present in a glioblastoma can be problematic, raising the differential diagnosis of AT/RT, but retained nuclear positivity for INI1/BAF47 in the former will clinch the correct diagnosis.
  - When epithelioid elements make up the bulk of a glioblastoma, these can easily be confused with metastatic carcinoma; cytokeratin expression is a common finding too in this situation, though GFAP positivity helps rule out carcinoma. Happily, metastatic carcinomas are extremely rare in the pediatric population, though differentiation from choroid plexus carcinoma may be problematic.

3.9 PROGNOSIS

- Although the majority of grade II astroctyomas arising in adults will undergo malignant transformation, only a small percentage (<10%) of pediatric low grade astrocytomas (LGA) are destined to that fate. The remainder can expect prolonged progression-free survival (mean approximately 10 years). This is particularly true of LGA arising in the cerebrum with 10 year progression-free and overall-survival rates of approximately 80 and over 90%, respectively.
- The median progression-free and overall survival for high grade astrocytomas is 0.5 years and 1 year, respectively. Tumor grade and extent of resection are significant prognostic factors for high grade lesions arising outside the pons, whereas radiation and chemotherapy appear to provide minimal survival benefit irrespective of tumor localization.
- Glioblastomas overall have a slightly longer survival times in children in comparison with adults, though in both age groups the prognosis is grim.
- Brainstem gliomas are variable in their biologic potential. Dorsally exophytic and some tectal gliomas are in fact pilocytic astrocytomas (see elsewhere), though even nonpilocytic tectal gliomas rarely display invasive/aggressive clinical behavior and should be managed conservatively, with radio- or chemotherapy reserved for clinical progression. In contradistinction, brain stem gliomas carrying a poor prognosis are those in which there is abducens palsy or short duration of symptoms prior to presentation, pontine location (diffusely infiltrative pontine astrocytoma), or engulfment of the basilar artery. Though radiation therapy frequently results in significant neurologic improvement in these patients, the one year overall survival rate for these patients still borders on only 25%.
- Infiltrative astrocytomas of the spinal cord carry a variable prognosis depending on tumor grade. In all cases, complete surgical resection is difficult as a distinct interface between normal tissue and tumor is typically absent. Radiation therapy often affords prolonged survival for grade II lesions (5 year overall survival up to 70%) whereas patients with high grade spinal astrocytomas rapidly succumb to their disease (within months) despite radiation or chemotherapy.
- Few studies have shown a significant association between overexpression of p53 (Fig. 3.14c) and shortened progression free survival in high grade pediatric astrocytomas, while loss of PTEN expression may be associated with shortened overall survival.
- With gliomatosis, better survival is afforded by younger age and lower histologic grade.

SUGGESTED READING

Fisher PG, Breiter SN, Carson BS, Wharam MD, Weingart JD, Foer DR et al (2000) A clinicopathologic reappraisal of brain stem tumor classification. Cancer 89:1569–1576

Raffel C, Frederick L, O'Fallon JR, Atherton-Skaff P, Perry A, Jenkins RB et al (1999) Analysis of oncogene and tumor suppressor gene alterations in pediatric malignant astrocytomas reveals reduced survival for patients with PTEN mutations. Clin Cancer Res 5:4085–4090

Sung T, Miller DC, Hayes RL, Alonso M, Yee H, Newcomb EW (2000) Preferential inactivation of the p53 tumor suppressor pathway and lack of EGFR amplification distinguish de novo high grade pediatric astrocytomas from de novo adult astrocytomas. Brain Pathol 10(2):249–259

Giannini C, Scheithauer BW (1997) Classification and grading of low-grade astrocytic tumors in children. Brain Pathol 7:785–798

Pollack IF, Claassen D, al-Shboul Q, Janosky JE, Deutsch M (1995a) Low-grade gliomas of the cerebral hemispheres in children: an analysis of 71 cases. J Neurosurg 82(4):536–547

Sure U, Ruedi D, Tachibana O, Yonekawa Y, Ohgaki H, Kleihues P et al (1997) Determination of p53 mutations, EGFR overexpression, and loss of p16 expression in pediatric glioblastomas. J Neuropathol Exp Neurol 56(7):782–789

Pollack IF, Finkelstein SD, Woods J, Burnham J, Holmes EJ, Hamilton RL et al (2002) Expression of p53 and prognosis in children with malignant gliomas. N Engl J Med 346:420–427

Pollack IF, Finkelstein SD, Burnham J, Holmes EJ, Hamilton RL, Yates AJ et al (2001) Age and TP53 mutation frequency in childhood malignant gliomas: results in a multi-institutional cohort. Cancer Res 61:7404–7407

Felix CA, Slave I, Dunn M, Strauss EA, Phillips PC, Rorke LB et al (1995) p53 gene mutations in pediatric brain tumors. Med Pediatr Oncol 25(6):431–436

Broniscer A, Baker SJ, West AN, Fraser MM, Proko E, Kocak M et al (2007) Clinical and molecular characterization of malignant transformation of low-grade glioma in children. J Clin Oncol 25(6):682–689

Louis DN, Ohgaki H, Wiestler OD, Cavenee WK (2007) WHO classification of tumours of the central nervous system, 4th edn. IARC, Lyon

Nakamura M, Shimada K, Ishida E, Higuchi T, Nakase H, Sakaki T et al (2007) Molecular pathogenesis of pediatric astrocytic tumors. Neurooncol 9:113–123

Wolff JE, Classen CF, Wagner S, Kortmann RD, Palla SL, Pietsch T et al (2008) Subpopulation of malignant gliomas in pediatric patients: analysis of the HIT-GLIOBLASTOMA database. J Neurooncol 87(2):155–164

Thorarinsdottir HR, Santi M, McCarter R, Rushing EJ, Cornelison R, Jales A et al (2008) Protein expression of platelet-derived growth factor receptor correlates with malignant histology and PTEN with survival in childhood gliomas. Clin Cancer Res 14(11):3386–3394

Daglioglu E, Cataltepe O, Akalan N (2003) Tectal gliomas in children: the implications for natural history and management strategy. Pediatr Neurosurg 38(5):223–231

Pollack IF, Claassen D, al-Shboul Q, Janosky JE, Deutsch M (1995b) Low-grade gliomas of the cerebral hemispheres in children: an analysis of 71 cases. J Neurosurg 82(4):536–547

Bowers DC, Georgiades C, Aronson LJ, Carson BS, Weingart JD, Wharam MD et al (2000) Tectal gliomas: natural history of an indolent lesion in pediatric patients. Pediatr Neurosurg 32(1):24–29
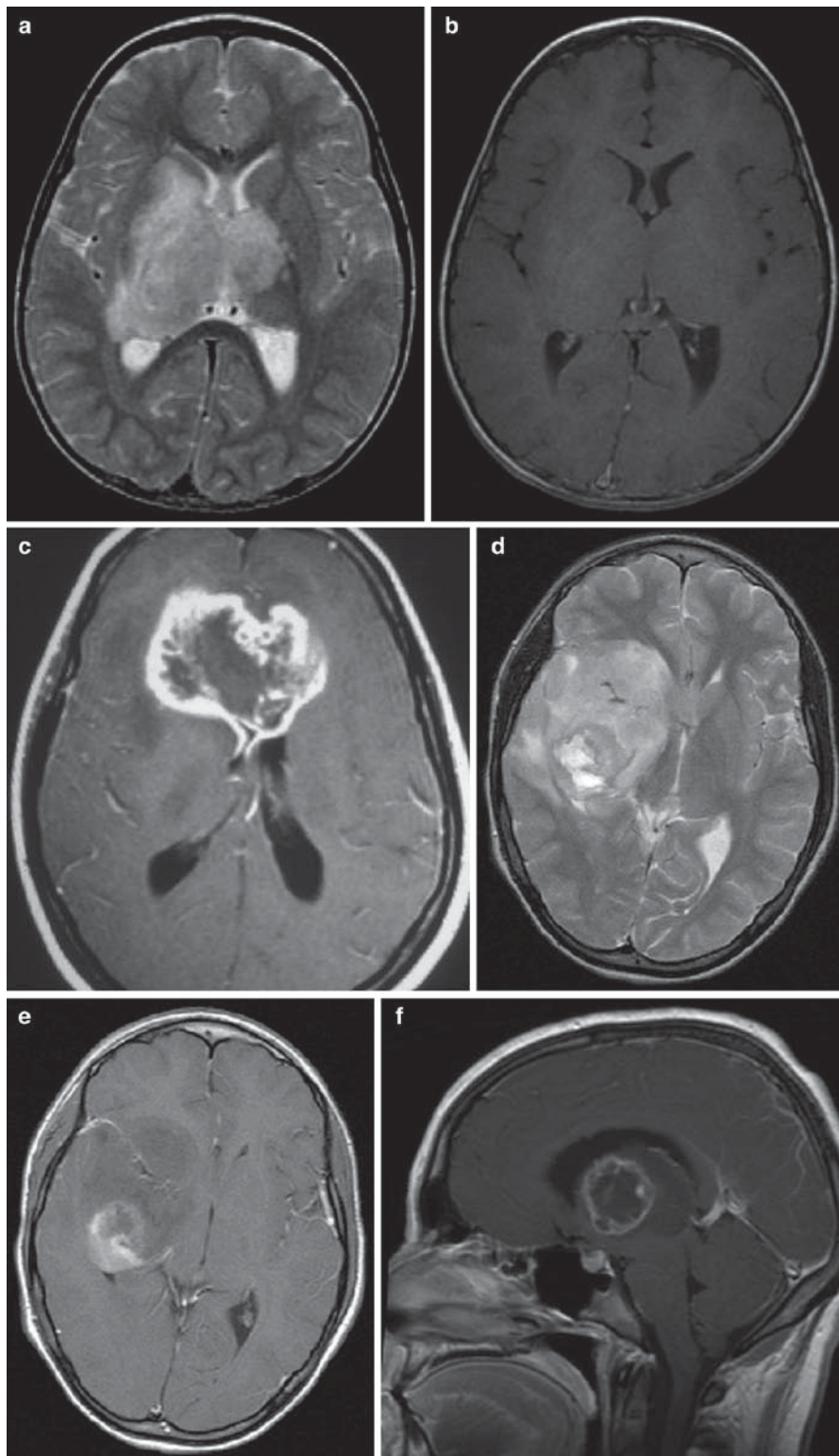
Fig. 3.1. (**a**) Axial T2-w and (**b**) T1-w post contrast MR images showing a deep-situated low grade astrocytoma with bithalamic involvement; note the lesion is hyperintense on T2, though it is difficult to appreciate on the T1-w image as there is no evidence of enhancement. (**c**) Postcontrast computer tomography (CT) scan of a "butterfly" glioblastoma, crossing the midline through the corpus callosum and showing strong ring enhancement. (Courtesy Dr Murat Gokden, University of Arkansas, Little Rock, AK, USA) Axial T2-w (**d**) and T1-w postcontrast (**e**) MR images of a deep-seated glioblastoma. The former shows extensive T2 hyperintense peritumoral edema surrounding a lesion with heterogeneous signal intensity, while the latter shows an irregular ring of enhancement with surrounding zone of hypointensity. (**f**) This thalamic glioblastoma likewise shows characteristic ring enhancement, seen here on sagittal T1-w postcontrast MR imaging (Courtesy Dr Gary Tye, Virginia Commonwealth University, Richmond, VA, USA).
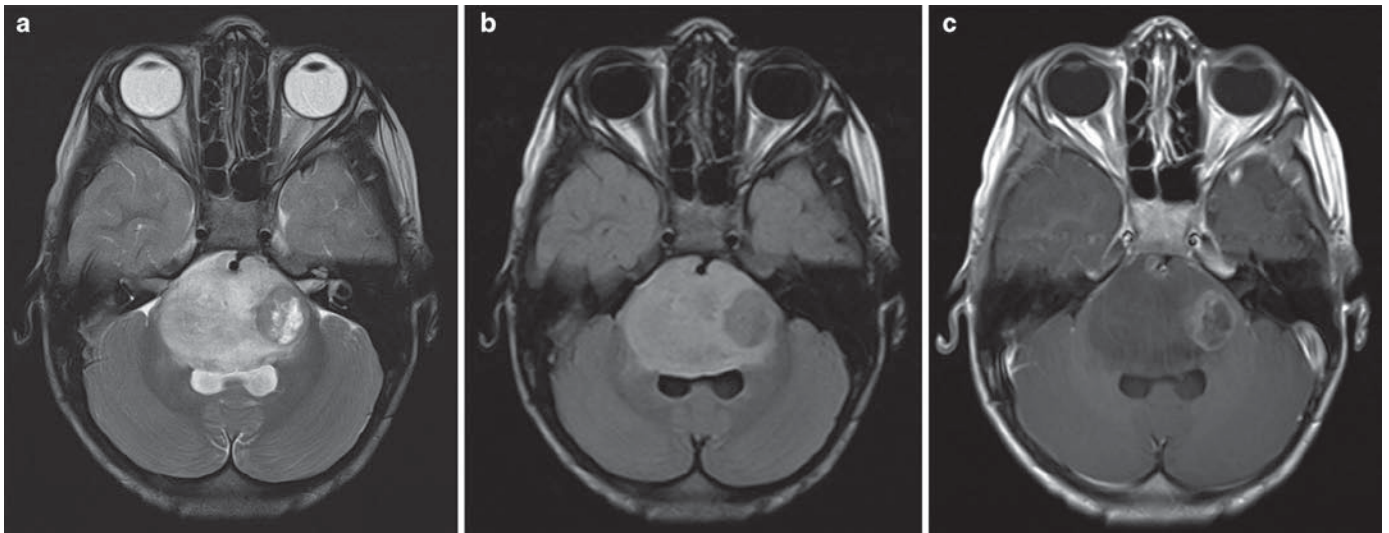
Fig. 3.2. Axial T2-w (**a**), FLAIR (**b**), and (**c**) T1-w postcontrast images of a pontine diffuse astrocytoma showing markedly expanded pons with encasement of the adjacent basilar artery. The lesion is hyperintense on both T2 and FLAIR while hypointense on T1, whereas the small round focus with central necrosis and surrounding ring contrast enhancement indicates glioblastoma component.
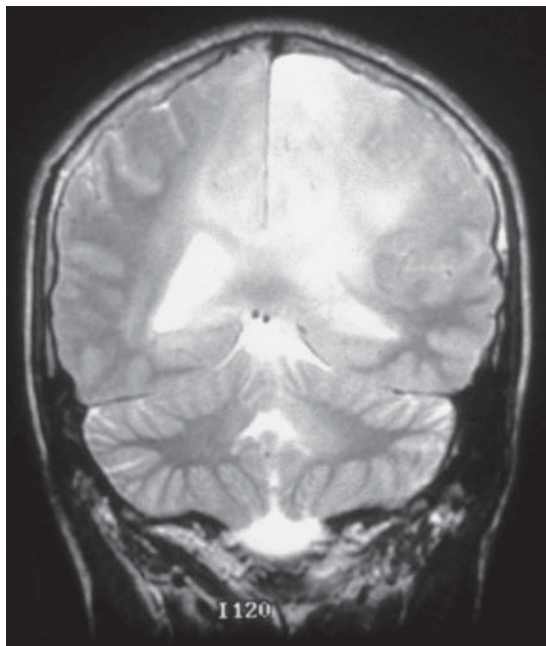
Fig. 3.3. This coronal T2-w MR image depicts an example of gliomatosis, showing bright signal present in cerebral hemispheres, bilaterally, as well as within the cerebellum around the 4th ventricle.
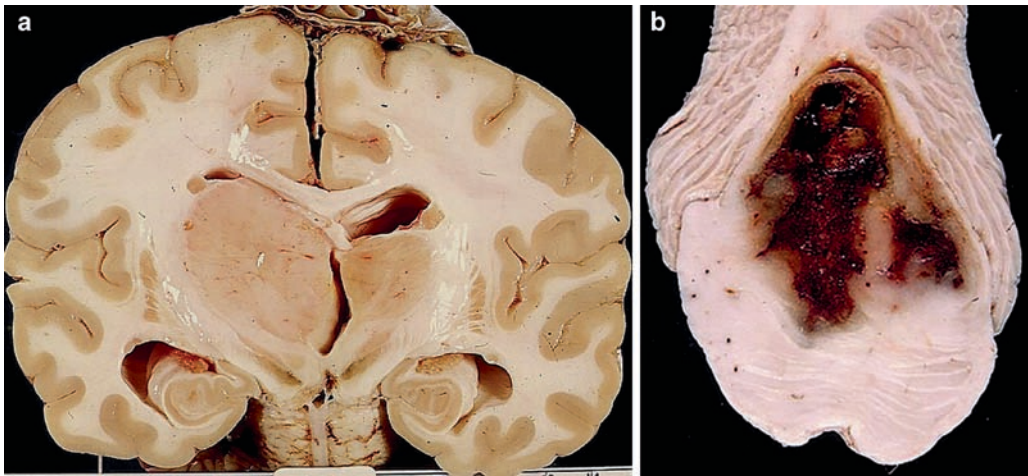
Fig. 3.4. (**a**) Coronal brain section showing a large right thalamic diffuse astrocytoma with homogeneous consistency that markedly expands this region and blurs the underlying architecture. (**b**) This pontine glioblastoma has a heterogeneous red and tan mottled appearance with areas of hemorrhage and destructive necrosis.
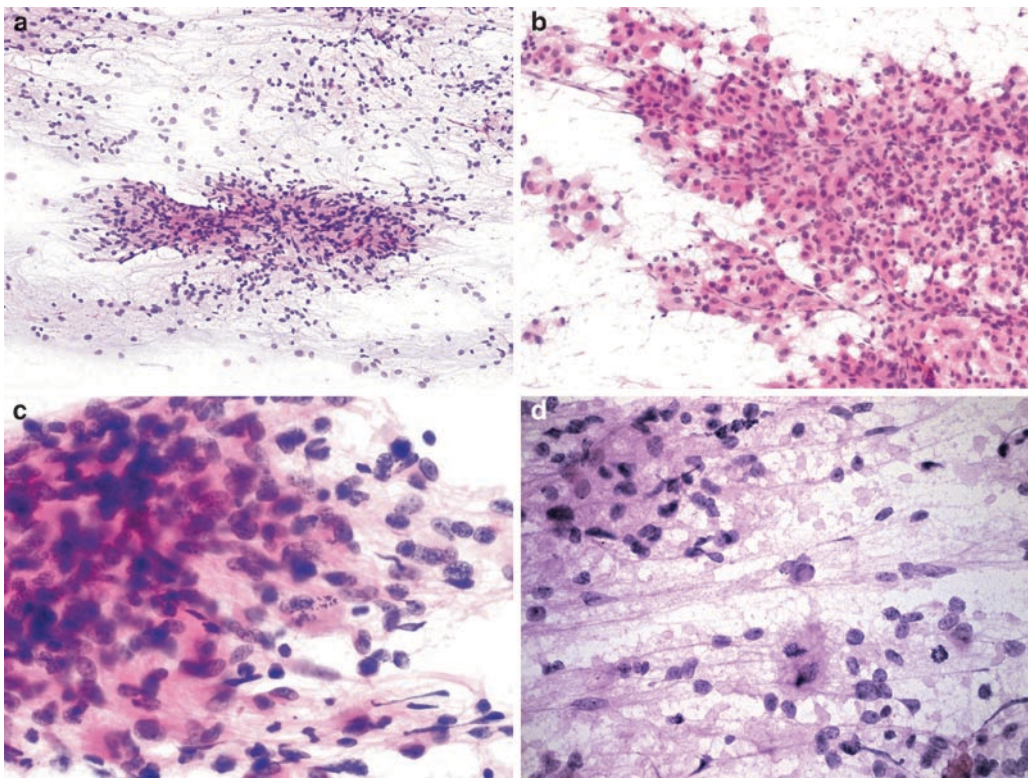
Fig. 3.5. (**a**) Smear preparation of a diffuse astrocytoma containing moderately cellular fragments of tissue and cells with oval hyperchromatic nuclei and elongated fibrillar cytoplasmic processes. (**b**) This smear preparation of diffuse astrocytoma demonstrates the gemistocytic morphology, the tumor cells having plump cytoplasmic "bellies", some with discernible short processes, and eccentric round to oval nuclei. (**c** and **d**) Cytologic preparations of high grade astrocytomas are much more hypercellular with cell crowding and overlap and atypical nuclei. Elongated fibrillary process typical of astrocytomas should still be present. Mitotic figures may be seen, and a "dirty" background indicative of necrosis (**d**) is often seen in smears of glioblastoma.
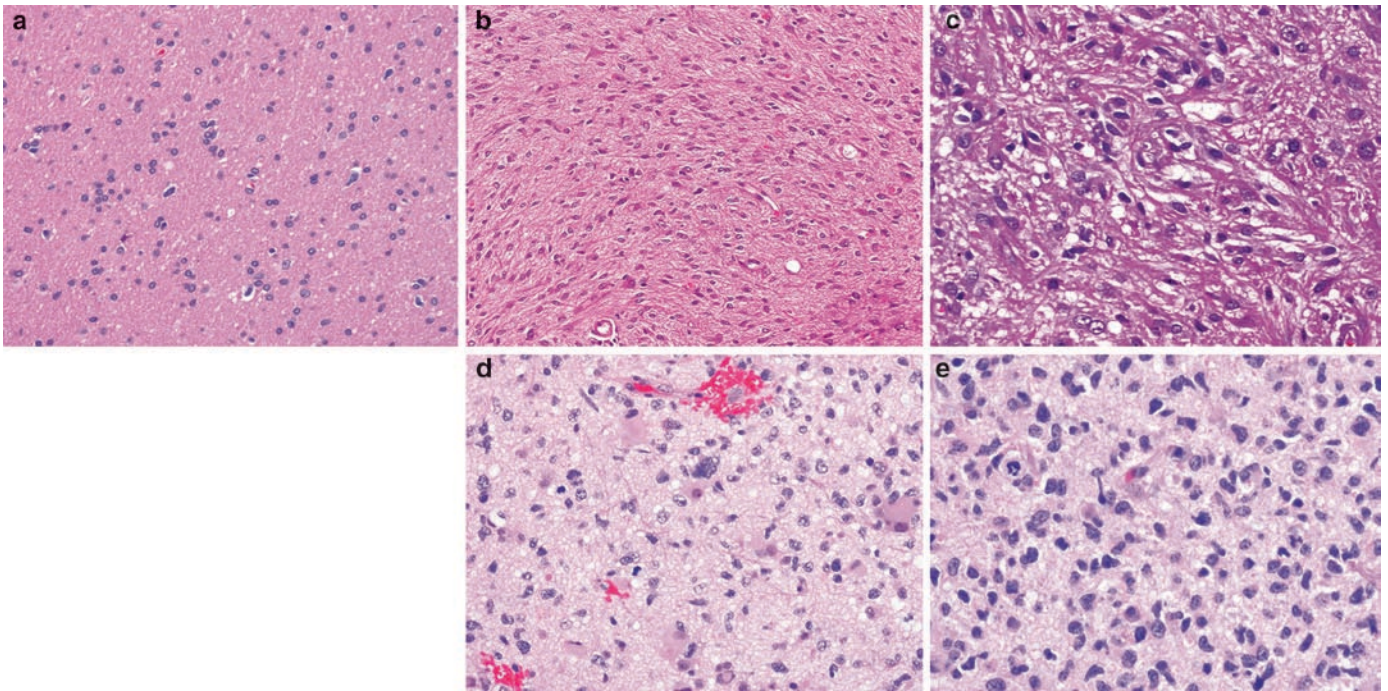
Fig. 3.6. Diffuse/low grade astrocytomas are quite variable in their cellularity, ranging from mildly (**a**) to moderately (**b**) hypercellular. Features helpful in discriminating grade II astrocytoma from reactive gliosis include the presence of atypical, usually hyperchromatic nuclei and irregular cell distribution in the former. In these fibrillary astrocytomas (**a–c**), the oval to irregular shaped nuclei have little in the way of discernible cytoplasm ("naked nuclei"), though fibrillary processes are seen within the background tissue. (**d**, **e**) Anaplastic astrocytomas (WHO grade III) are notably more cellular, often with significant nuclear atypia, and with the additional feature of increased mitotic activity.
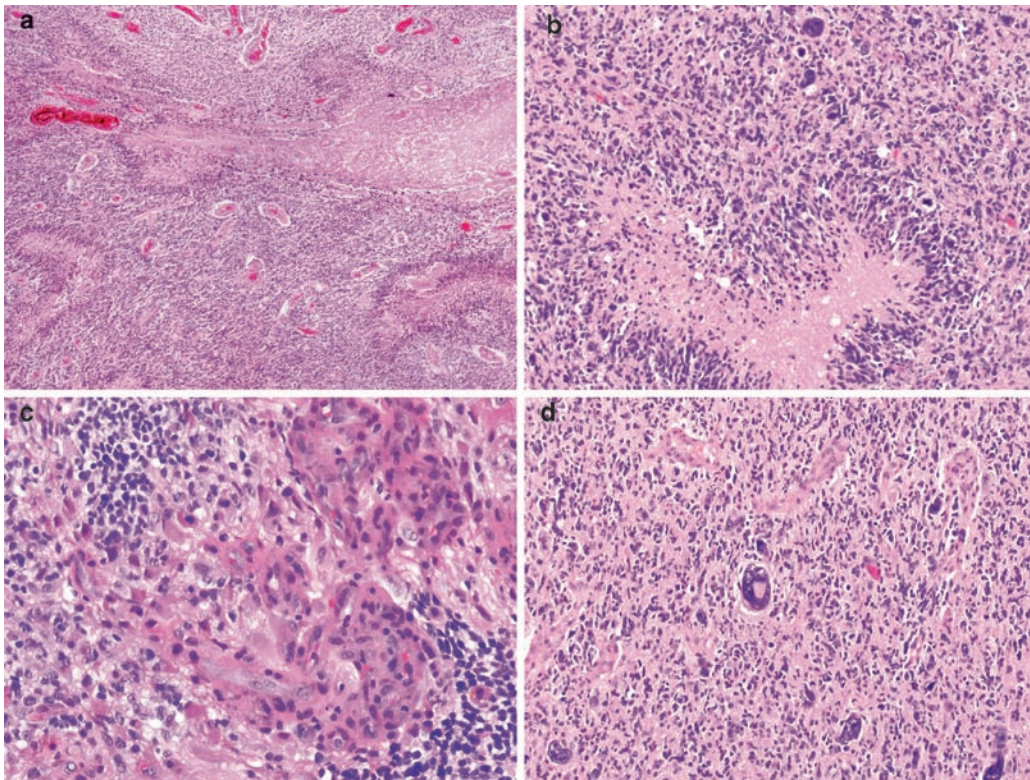
Fig. 3.7. (**a**) At low power, glioblastoma appears as a highly cellular neoplasm, this case showing the characteristic serpiginous zones of pseudopalisading necrosis. (**b**) Individual tumor cells are quite variable in their morphology and may range from small and bipolar to giant and pleomorphic; mitotic figures should be easy to find. Microvascular proliferation may take the form of (**c**) large glomeruloid capillary tufts or (**d**) more linear-appearing capillaries with multilayered proliferating endothelial lining. Striking nuclear pleomorphism is also seen in multiple cells in (**d**).
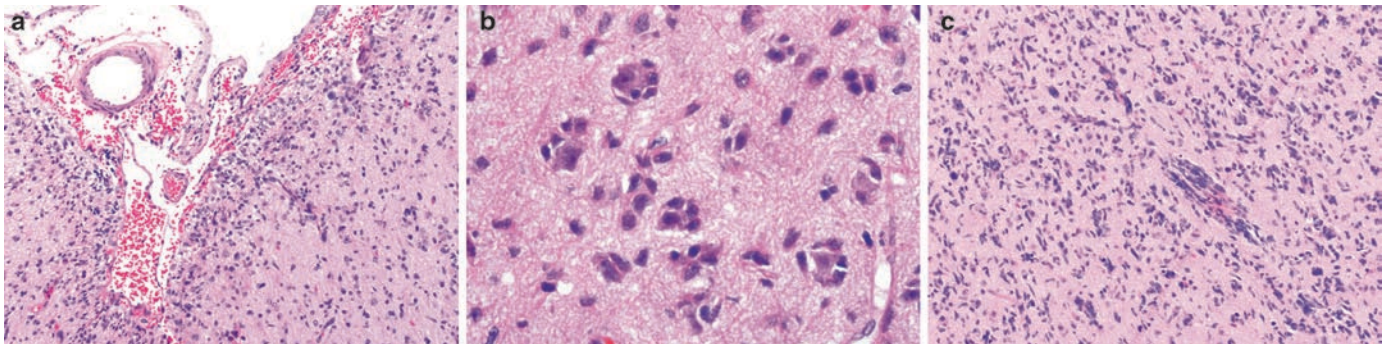
Fig. 3.8. Secondary structure formation is frequently encountered at the less cellular infiltrative edges of high grade astrocytomas. These include subpial accumulation of tumor cells (**a**), perineuronal satellitosis (**b**), and perivascular satellitosis (**c**).
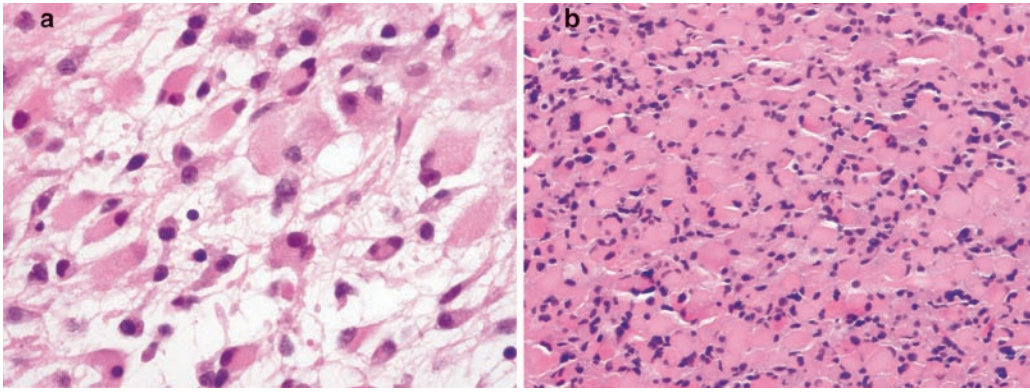
Fig. 3.9. (**a**) The gemistocytic morphology is characterized by cells with large eosinophilic cytoplasmic "bellies" and eccentric hyperchromatic, often irregular shaped nuclei. When they represent a significant proportion of an infiltrative astrocytoma (**b**), the term "gemistocytic astrocytoma" is appropriate.
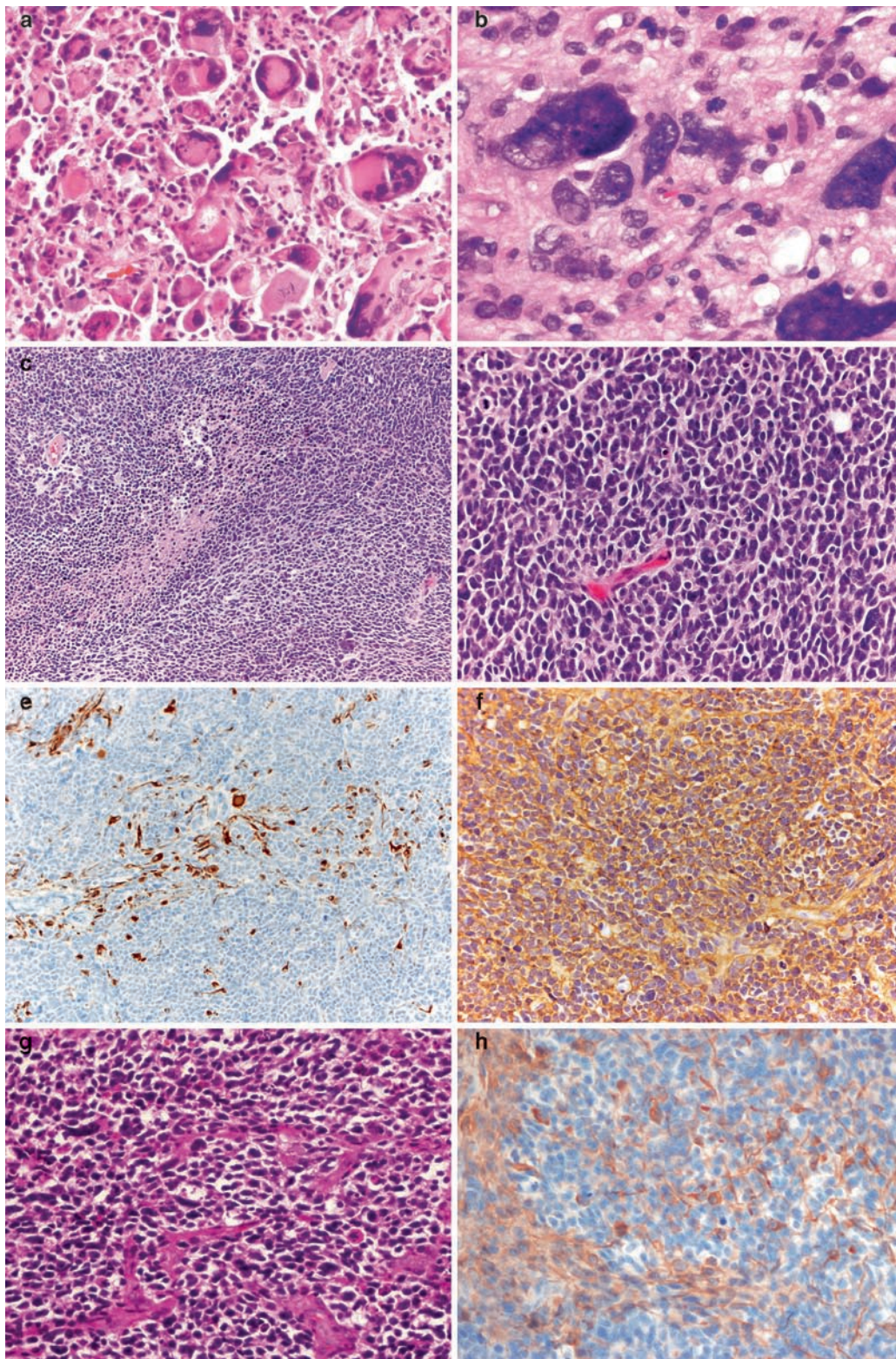
Fig. 3.10. (**a** and **b**) Giant cell glioblastoma, as its name implies, contains a preponderance of giant cells, including those with large bizarre or multilobated nuclei as well as multinucleated forms. Smaller malignant astrocytic cells are intermixed. Figures c–f depict an example of a small cell glioblastoma that arose in an adult patient. Note the marked hypercellularity and paucity of cellular cytoplasm (**c**, **d**) causing superficial resemblance to PNET. A small subpopulation of tumor cells are immunopositive for GFAP (**e**), while there is strong diffuse membrane staining for EGFR (**f**). Neuronal markers were negative and Ki67 indicated a brisk proliferation index (not shown). (**g**) and (**h**) represent a small cell glioblastoma from a child; note scattered cells staining positive for GFAP in h.
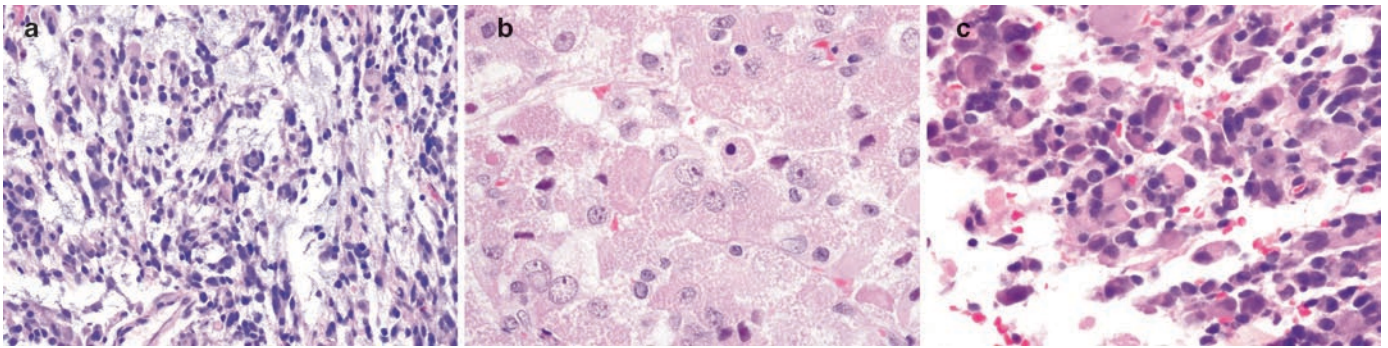
Fig. 3.11. Unusual components of glioblastoma include (**a**) chordoid areas containing cells with an epithelioid morphology in a myxoid background, (**b**) granular cells, and (**c**) cells with a rhabdoid appearance (note the cellular dyscohesion, eccentric nuclei including some with vesicular chromatin and prominent nucleoli, and eosinophilic rounded cytoplasmic "bellies").
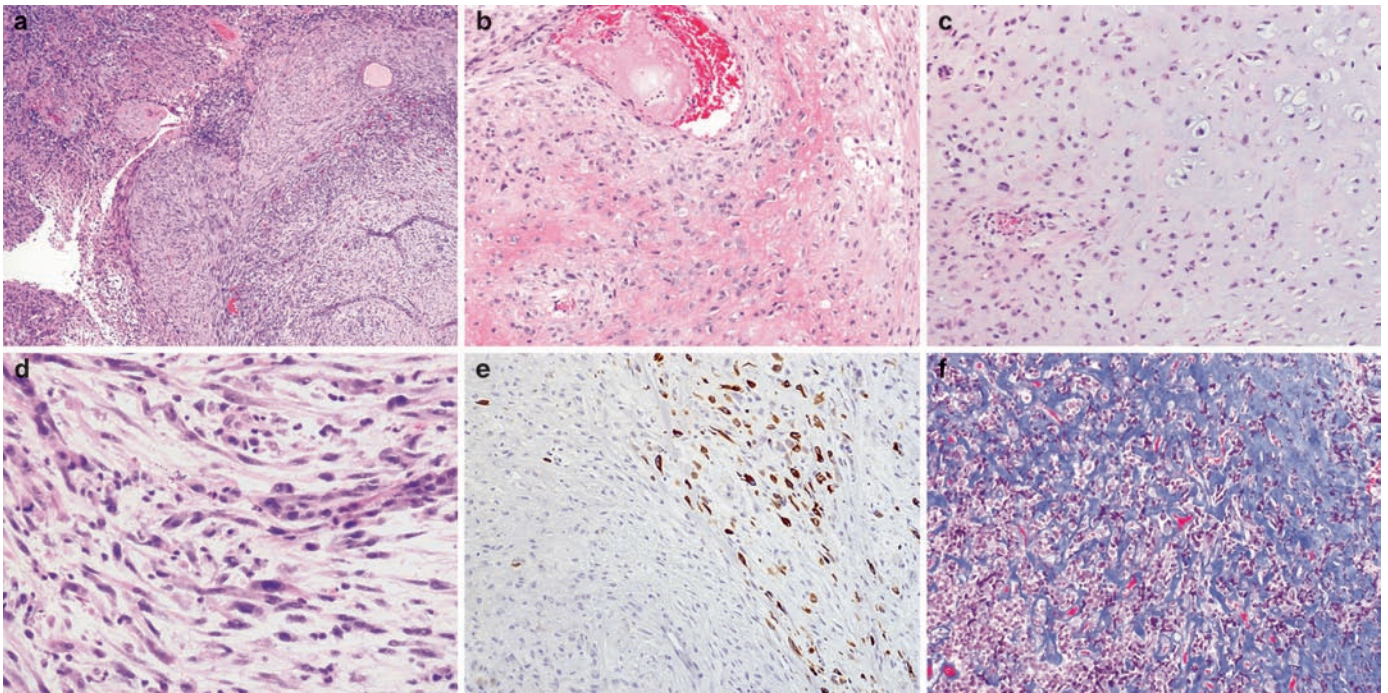
Fig. 3.12. Gliosarcoma is a biphasic tumor that in addition to a malignant glial (typically astrocytic) component includes a sarcomatous component. These may include fibrosarcoma (**a**-most common), (**b**) osteosarcoma, (**c**) chondrosarcoma, (**d**) rhabdomyosarcoma, and others. The malignant astrocytic component can more easily be identified by its GFAP positivity (**e**), and trichrome stain (**f**) highlights abundant collagen within fibrosarcomatous components.
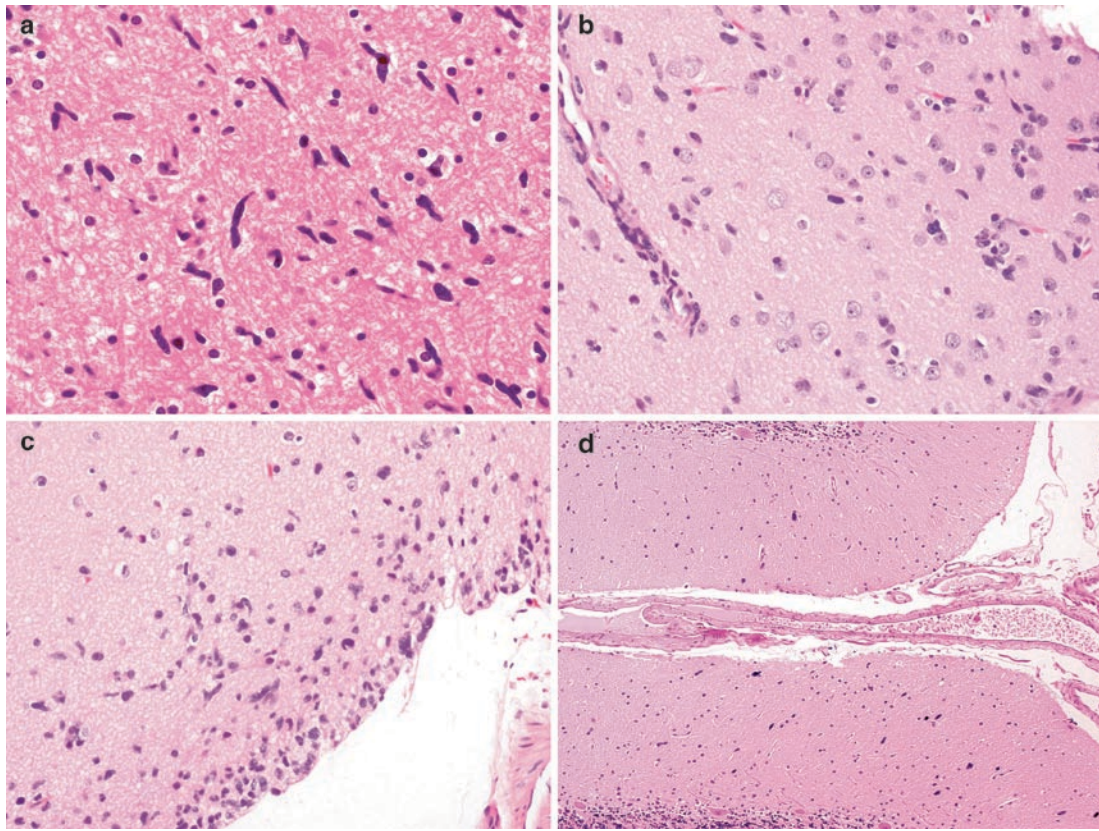
Fig. 3.13. (**a** and **b**) Gliomatosis represents the most widely infiltrative of all gliomas, often presenting as hyperchromatic elongated "naked nuclei" percolating widely through brain parenchyma. Not surprisingly, there is a tendency for developing secondary structures (**c**). Tumor cells may even extend into posterior fossa area as shown in this section of cerebellum (**d**) or even the brainstem and spinal cord.
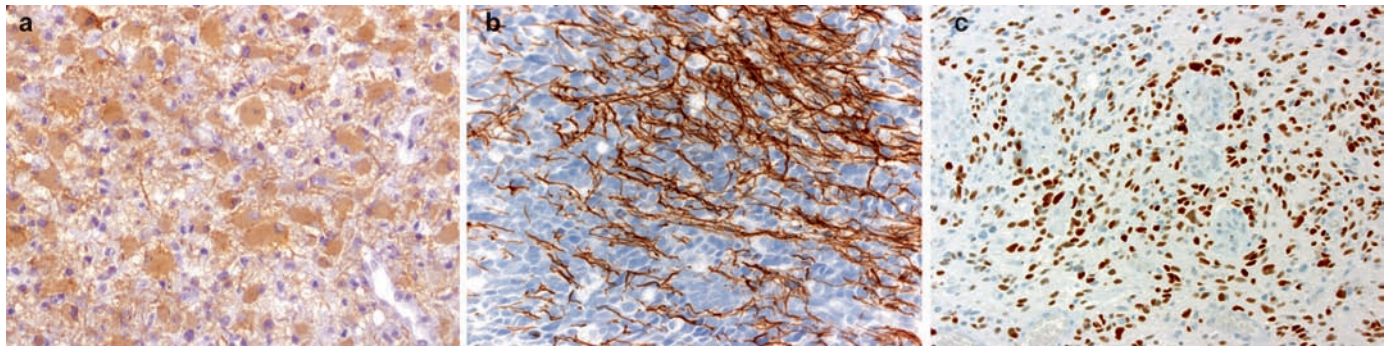
Fig. 3.14. (**a**) GFAP is characteristically positive in astrocytoma, though may be quite variable, depending upon the amount of cytoplasm present and degree of differentiation. (**b**) Neurofilament is helpful in documenting the infiltrative quality of these tumors as it decorates native neuritic processes that have been overrun by invasive tumor. (**c**) Nuclear positivity for p53 may be encountered in some pediatric cases, though it is less frequent than similar positivity in astrocytomas arising in adults.

Oligodendroglial Tumors

Christine E. Fuller

4.1 OVERVIEW

- Oligodendroglial tumors represent diffusely infiltrative gliomas composed of cells morphologically resembling oligodendroglia. This group includes oligodendroglioma (WHO grade II) and anaplastic oligodendroglioma (WHO grade III), as well as tumors bearing a mixture of cells with astrocytic and oligodendroglial morphologies: mixed oligoastrocytoma (WHO grade II) and anaplastic mixed oligoastrocytoma (WHO grade III).
- The vast majority are sporadic tumors, only rarely presenting as radiation-induced gliomas or, in the context of heritable cancer family syndromes, similar to those listed for astrocytomas.
- Overall, this group of tumors accounts for approximately 5% of glial tumors, being far less common than astrocytomas in adults, and even more infrequent in children. However, the incidence of these tumors has increased in recent years, due mainly to an expanded histomorphologic definition.

4.2 CLINICAL FEATURES

- The majority of oligodendroglial lesions occur in adults in their fourth decade of life; they are uncommon in children, accounting for less than 3% of primary central nervous system (CNS) tumors in this age group. There is no significant gender predilection.
- Given the tendency of these tumors to diffusely infiltrate the cerebral cortex, many patients will present with seizures, regardless of age. Headache, focal neurologic deficits, and signs/symptoms related to increased intracranial pressure may also occur.

4.3 NEUROIMAGING

- Oligodendrogliomas and mixed oligoastrocytomas (MOAs) arise within the cerebral hemispheres, involving the cortex and subcortical white matter.
  - Frontal and temporal lobes are most frequent sites of tumor origin, with parietal and occipital origination less common.
  - Multilobe involvement can occur, and rare cases showing bilateral hemispheric tumor or localization within the deep grey structures, posterior fossa, spinal cord, or leptomeninges have been reported.

- Computerized tomography (CT) scans typically show a well-demarcated hypo- to isodense lesion within the cerebral cortex and subcortical white matter (Fig. 4.1a).
- Calcifications are encountered much more frequently in oligodendroglial tumors than in infiltrating astrocytomas.
- Oligodendroglial tumors are hypointense on T1, hyperintense on T2 and fluid-attenuated inversion recovery (FLAIR) images, and again are well demarcated with generally minimal surrounding vasogenic edema (Fig. 4.1b–f).
- Areas of cystic change, hemorrhage, or calcification may be seen on occasion.
- Anaplastic (WHO grade III) lesions generally show contrast enhancement and have a more heterogeneous appearance on most image sequences given their variable content of intratumoral hypercellularity, vascular proliferation, hemorrhage, and necrosis.
  - Ring enhancement akin to that typical for glioblastoma correlates with particularly poor prognosis.

4.4 PATHOLOGY

- *Gross pathology*: Tissue from oligodendroglial tumors is typically soft and grey-tan, sometimes with mucoid or hemorrhagic areas or flecks of calcification. Necrosis is limited to higher grade tumors.
  - At autopsy, these lesions appear as well-defined grey soft masses involving the cortex and underlying white matter. They tend to expand the involved gyri and cause blurring of the grey–white junction.
- *Intraoperative cytologic imprints/smears*:
  - Cytological squash/smear preparations of oligodendroglial tumors contain cells with small, round nuclei typically lacking fine fibrillary processes, and a fine capillary network (Fig 4.2a). Minigemistocytes may be present (Fig. 4.2b).
  - MOAs additionally contain a neoplastic astrocytic component, identifiable as cells with oval to irregular-shaped nuclei and fibrillary cytoplasmic processes.
  - High-grade lesions tend to be more hypercellular with substantial nuclear atypia and proliferating vasculature, with or without necrosis.
- *Histology*: The classification and grading of oligodendroglial tumors is less reproducible than it is for astrocytic tumors, due in part to definitional shifts in the accepted morphologic spectrum of what is considered evidence of "oligodendroglioma" or an "oligodendroglial component."
  - Apart from the classic "fried egg" morphology (Fig. 4.3a) as described below, any of these oligodendroglial tumors

may contain tumor cells resembling small gemistocytes with small round nuclei (termed micro- or minigemistocytes) or cells with limited glial fibrillary acidic protein (GFAP) positive process formation (gliofibrillary oligodendrocytes) (Fig. 4.3b and c).

- *Oligodendroglioma (WHO grade II)* can display a spectrum of histomorphologies, though classically they contain the following:
  - A monomorphous population of infiltrative tumor cells with uniformly round nuclei and surrounding perinuclear clearing/"halo," imparting a "fried egg" appearance. This helpful diagnostic feature is artifactual, secondary to formalin fixation and unfortunately lacking in frozen section, smears, and rapidly fixed specimens (Figs. 4.3a and 4.4a).
  - A fine network of branching capillaries resembling "chicken wire" may be present.
  - Microcalcifications and microcysts containing mucoid material are common findings (Fig. 4.4b).
  - Tumor cells have a tendency to accumulate in subpial zones and form secondary structures such as perineuronal and perivascular satellitosis; this feature is not, however, limited to oligodendroglial tumors, and may be seen in other highly infiltrative glial tumors, particularly high-grade astrocytomas and gliomatosis (Fig. 4.4c, d).
  - Occasional mitotic figures and scattered atypical nuclei are also still compatible with a WHO grade II designation.
  - Uncommon though notable findings in otherwise typical oligodendroglioma include cells with granular eosinophilic cytoplasm or signet ring morphology, and rhythmic cellular palisading akin to a polar spongioblastoma-like pattern.
- *Anaplastic Oligodendroglioma (WHO grade III)*: In addition to the features noted above, anaplastic oligodendroglioma is notably hypercellular with numerous mitotic figures, nuclear atypia, and microvascular proliferation (Fig. 4.5a–c). Necrosis is sometimes present, often with pseudopalisading of surrounding tumor cells.
  - Hypercellular nodules with nuclear atypia and increased proliferation may be encountered in otherwise typical grade II oligodendroglioma. These areas may well represent early outgrowth of more malignant tumor clones; however, a grade III designation should not be applied in the absence of other and more diffuse features of anaplasia. A note of this "focal anaplasia" in the pathology report will alert the treating clinician of the potential for near-term anaplastic progression and the need for close follow-up.
- *Mixed Oligoastrocytoma (WHO grade II)*: These contain an admixture of two neoplastic cell types: oligodendroglial and astrocytic.
  - Biphasic (compact) and intermingled (diffuse) patterns occur, the former with separate discrete areas of oligodendroglioma and astrocytoma, while the latter has an admixture of cell types. The diffuse variant is far more frequently encountered (Fig. 4.6a–c).
  - Neoplastic cells with features intermediate between those of classic oligodendroglioma and classic astrocytomas may be present.
- *Anaplastic Mixed Oligoastrocytoma (WHO grade III)*: Similar to anaplastic oligodendrogliomas, grade III MOAs

are hypercellular, have endothelial proliferation, and are more mitotically active with a brisk Ki67 proliferation index (Fig. 4.6d, e).
  - The terms "grade IV MOA" or "GBM with oligodendroglial component" (preferred) may apply for cases with severe atypia, prominent angulated cellular component, and the additional finding of pseudopalisading necrosis.

4.5 IMMUNOHISTOCHEMISTRY

- To date, there is unfortunately no immunohistochemical marker that reliably distinguishes oligodendroglial from astrocytic tumors.
  - Similar to other neuroectodermally derived lesions, oligodendroglial tumors are positive for S100 protein.
  - Whereas GFAP decorates minigemistocytes, gliofibrillary oligodendrocytes (Fig. 4.3c), and cells of the astrocytic component of MOAs, the "fried egg" cells are typically not stained (Fig. 4.7).
  - Vimentin may be positive, and pancytokeratin may show focal false-positive staining due to cross-reactivity with glial intermediate filaments (similar to observations in astrocytic tumors). They are negative for epithelial membrane antigen (EMA).
  - They are positive for MAP2, Olig1, and Olig2, though all of these may be expressed in other glial tumors
- Synaptophysin may be positive in neuropil overrun by tumor; however, the tumor cells themselves are typically not positive (apart from few rare cases showing focal neural differentiation with rosettes).

4.6 ELECTRON MICROSCOPY

- Ultrastructural examination is often nonspecific, though concentric arrays of membranes (membrane lamination or whorls) may be encountered. Minigemistocytes contain tight bundles of intermediate filaments in their cytoplasm. Neural features have also been documented, including occasional synapse-like structures and neurosecretory granules.

4.7 MOLECULAR PATHOLOGY

- Unbalanced translocation of chromosomes 1 and 19 results in the characteristic codeletion of 1p and 19q, a frequent finding in oligodendrogliomas, anaplastic oligodendrogliomas, and a smaller subpopulation of MOAs in adults. In pediatric oligodendroglial tumors, this is an uncommon molecular finding, limited mainly to oligodendrogliomas arising in children >10 years old.
- Deletion of p16, an alteration also shared with adult oligodendroglial tumors, is similarly more frequent in older children.
- Multiple studies have established 1p/19q deletion as a "molecular signature" for classic oligodendroglioma morphology in the adult population, and this association is similarly true in pediatric oligodendroglial tumors, with deletions limited to oligodendrogliomas and not detected in MOAs.
- Also similar to adult oligodendroglial tumors, some tumors arising in children may show overexpression of p53 by

immunohistochemistry or deletion involving phosphatase and tensin homolog (PTEN).

- Rare epidermal growth factor receptor (EGFR) amplifications may be encountered in high-grade examples.

4.8 DIFFERENTIAL DIAGNOSIS

- Pediatric oligodendroglial tumors are diagnostically more problematic than their adult counterparts due to a number of histologically similar tumors common to this age group.
- Differentiation from infiltrative astrocytomas requires careful histologic inspection for classic oligodendroglial morphologies, including minigemistocytes and gliofibrillary oligodendrocytes.
- Clear cell ependymoma may closely mimic oligodendroglial tumors, though the former will typically demonstrate, at least focally, identifiable perivascular pseudorosettes, and should have a dot-like positivity for EMA. Ultrastructural features of ependymoma can also be confirmed, if necessary.
- Pilocytic astrocytomas may have areas resembling oligodendroglioma, but should also contain more classic features including biphasic architecture, Rosenthal fibers, and eosinophilic granular bodies.
- Dysembryoplastic neuroepithelial tumor (DNT) typically contains oligodendroglial-like cells and may even have areas of classic oligodendroglioma in the context of a "complex DNT." It should also, however, contain the characteristic "patterned mucin rich nodules" and specific glioneuronal unit with "floating neurons" within pools of mucin, all features that are lacking in oligodendrogliomas. Radiographic features are likewise not overlapping, as described elsewhere.
- Neurocytoma, be it central or otherwise, may simulate an oligodendroglial tumor by virtue of round regular nuclei. The diagnosis of the former is confirmed via identification of diffuse cellular staining for neuronal markers, particularly synaptophysin, or by ultrastructural means.
- Lastly, clear cell meningioma may enter the differential diagnosis; this dural-based tumor should be GFAP negative, EMA positive, with PAS-positive glycogen-rich cytoplasm, and often contains areas of more easily identifiable meningioma morphology. Ultrastructural review will likewise disclose interdigitating cell membranes and junctions.

4.9 PROGNOSIS

In general, oligodendroglial tumors tend to be slower growing and afford prolonged survival relative to their grade-matched astrocytoma counterparts. Time to recurrence and malignant progression are likewise prolonged in comparison.

- In series of pediatric oligodendroglial tumors, gross total resection and low tumor grade have been shown to be strongly associated with improved progression-free survival (PFS) and overall survival (OS).
- The presence of p53 overexpression as detected by immunohistochemistry and *PTEN* deletion both have been found significantly associated with shorter OS in pediatric patients.
- Deletions of 1p/19q in pediatric oligodendroglial tumors, unlike similar alterations in their adult counterparts, do not afford a favorable outcome.
- Nevertheless, 5-year PFS and OS rates of 81 and 84%, respectively, have been reported. Deep/central tumors are an exception, fairing far worse (median survival less than 2 years) than their cerebral-centered counterparts.

SUGGESTED READING

Peters O, Gnekow A, Rating D, Wolff JE (2004) Impact of location on outcome in children with low-grade oligodendroglioma. Pediatr Blood Cancer 43(3):250–256

Kreiger PA, Okada Y, Simon S, Rorke LB, Louis DN, Golden JA (2005) Losses of chromosomes 1p and 19q are rare in pediatric oligodendrogliomas. Acta Neuropathol (Berl) 109:387–392

Fallon KB, Palmer CA, Roth KA, Nabors B, Wang W, Carpenter M et al (2004) Prognostic value of 1p, 19q, 9p, 10q, and EGFR-FISH analyses in recurrent oligodendrogliomas. J Neuropathol Exp Neurol 63(4):314–322

Tice H, Barnes PD, Goumnerova LC, Scott RM, Tarbell NJ (1993) Pediatric and adolescent oligodendrogliomas. AJNR Am J Neuroradiol 14(6):1293–1300

Razack N, Baumgartner J, Bruner J (1998) Pediatric oligodendrogliomas. Pediatr Neurosurg 28(3):121–129

Raghavan R, Balani J, Perry A, Margraf L, Vono MB, Cai DX et al (2003) Pediatric oligodendrogliomas: a study of molecular alterations on 1p and 19q using fluorescence in situ hybridization. J Neuropathol Exp Neurol 62(5):530–537

Pollack IF, Finkelstein SD, Burnham J, Hamilton RL, Yates AJ, Holmes EJ et al (2003) Association between chromosome 1p and 19q loss and outcome in pediatric malignant gliomas: results from the CCG-945 cohort. Pediatr Neurosurg 39:114–121

Fuller C, Dalton J, Baker S, Gajjar A, Kun L, Broniscer A (2006) Molecular characterization of pediatric gliomas. Brain Pathol 16(S1):S84

Mitsuhashi T, Shimizu Y, Ban X, Ogawa F, Matsutani M, Shimizu M et al (2007) Anaplastic oligodendroglioma: a case report with characteristic cytologic features, including minigemistocytes. Acta Cytol 51(4):657–660

Inagawa H, Ishizawa K, Hirose T (2007) Qualitative and quantitative analysis of cytologic assessment of astrocytoma, oligodendroglioma and oligoastrocytoma. Acta Cytols 51(6):900–906

Liberski PP (1996) The ultrastructure of oligodendroglioma: personal experience and the review of the literature. Folia Neuropathol 34(4):206–211
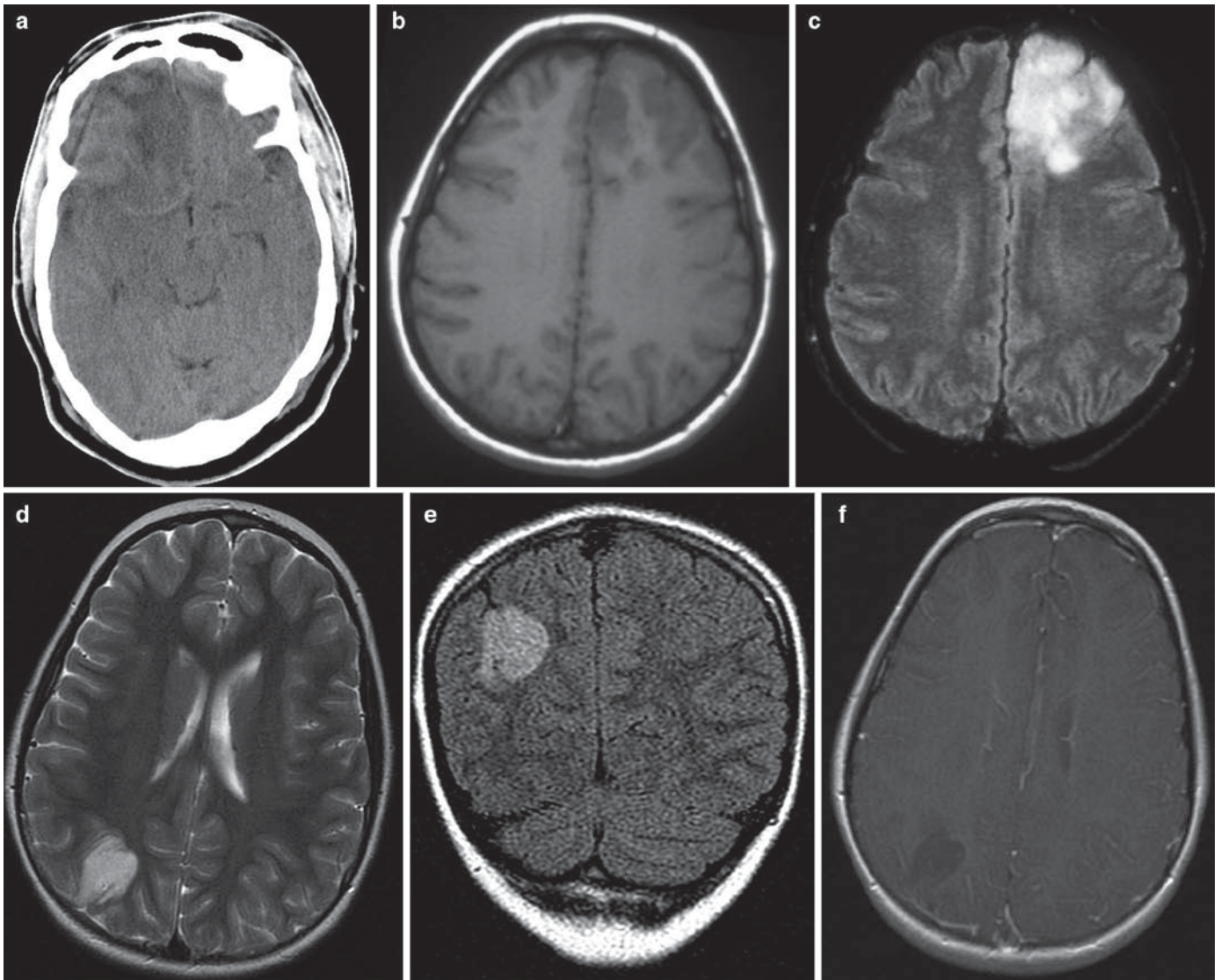
Fig 4.1 (**a**) CT scan showing a right frontal oligodendroglioma that is hypodense and involves cortical grey and subcortical white matter. Axial T1-w (**b**) and T2-w (**c**) MR images of a left frontal oligodendroglioma with gyral expansion. The tumor is rather ill defined and variably hypo- to isointense on T1, while it appears much more well delineated on T2. (Courtesy of Dr Murat Gokden, University of Arkansas, Little Rock, AR, USA) Fig. 4.1d–f are from a child with oligodendroglioma of the left occipital lobe; note that the lesion is hyperintense on both T2-w (**d**) and FLAIR (**e**), and is hypointense and without enhancement on this T1-w post contrast image (**f**).
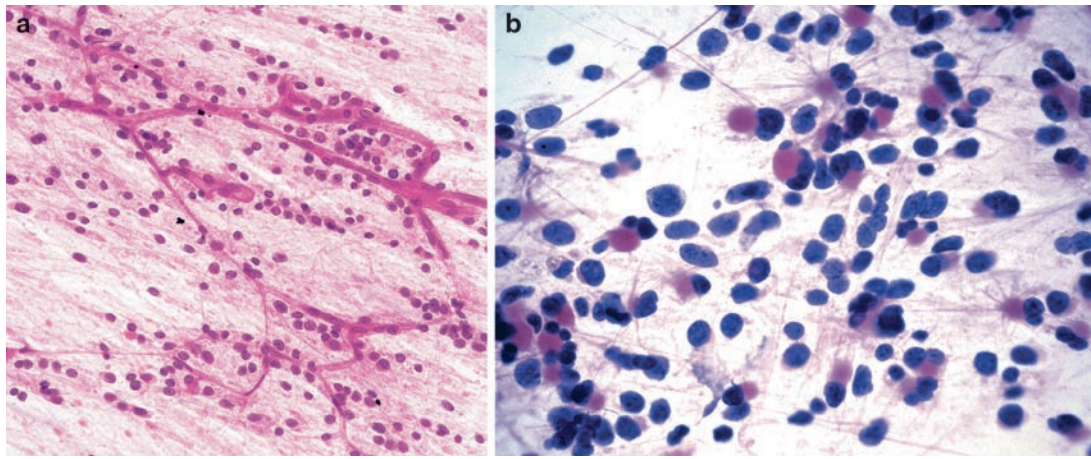
Fig 4.2 (**a**) Hematoxylin and eosin-stained cytologic smear preparation of oligodendroglioma showing a delicate capillary network, tumor cells with round regular nuclei without accompanying fibrillary cell processes. (Courtesy of Dr Arie Perry, Washington University, St Louis, MO, USA) (**b**) Minigemistocytes with their eccentric rounded cytoplasmic bellies and stubby processes are seen in occasional smears.
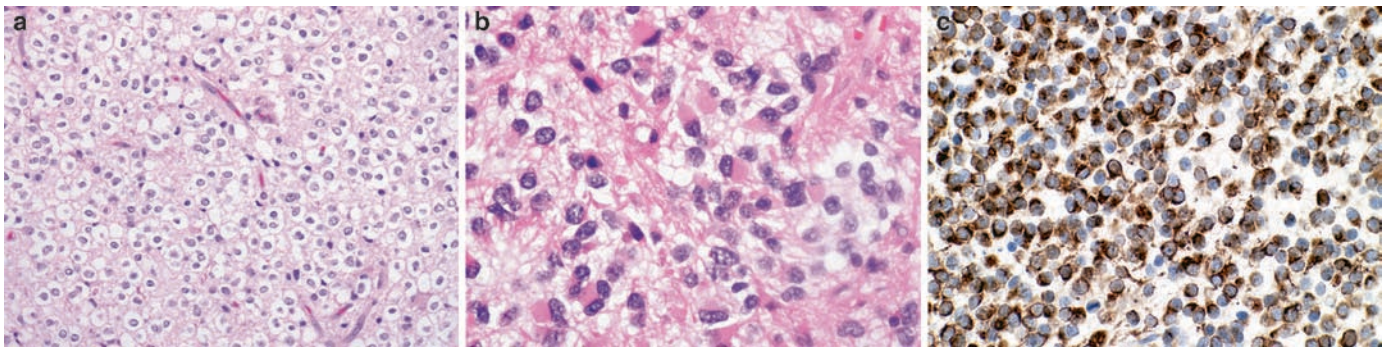
Fig 4.3 (**a**) The classical appearance of oligodendroglioma is that of a tumor composed of cells with monotonously round nuclei with surrounding perinuclear halo/clear zone ("fried egg" appearance) and intervening delicate capillary network. Minigemistocytes with their small eosinophilic cytoplasmic bellies (**b**) and gliofibrillary oligodendrodrocytes (**c**) with their GFAP-positive perinuclear rim are other cell types that are seen in oligodendroglial tumors and should not be equated with astrocytic differentiation (3c courtesy of Dr Arie Perry).
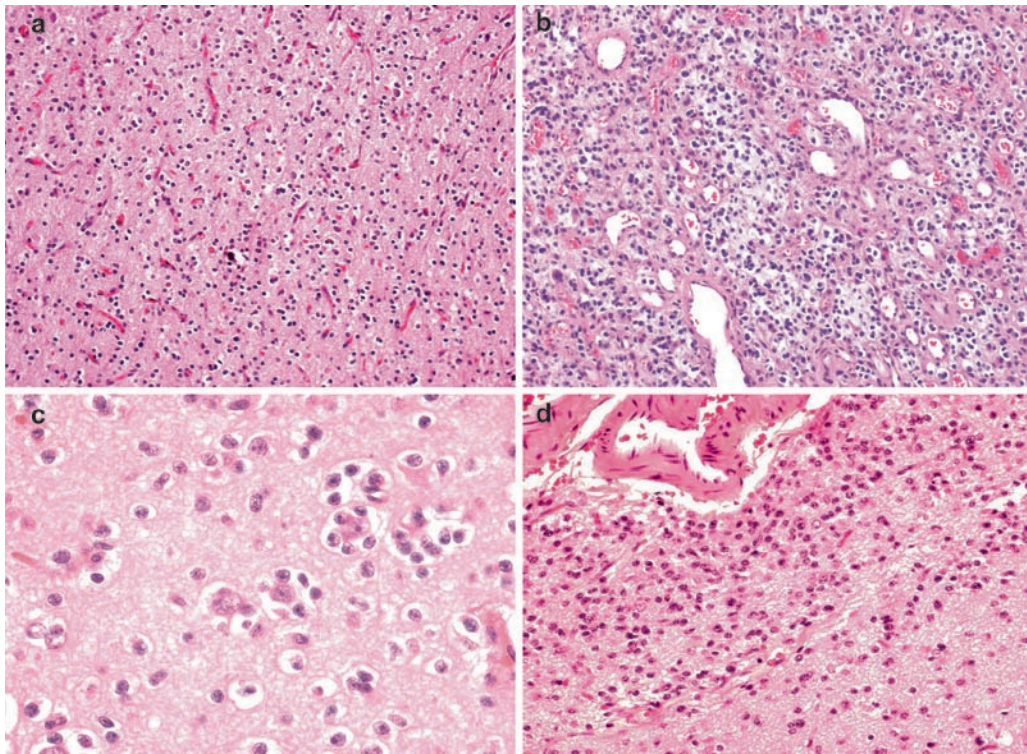
Fig 4.4 (**a**) Low-power view of grade II oligodendroglioma with characteristic "fried egg" cells, delicate capillary network, and rare microcalcification. (**b**) Microcystic areas are often present in oligodendroglial tumors. Secondary structures including perineuronal and perivascular satellitosis (**c**) and subpial accumulation of tumor cells (**d**) are quite common in oligodendroglial tumors, confirming their infiltrative properties.
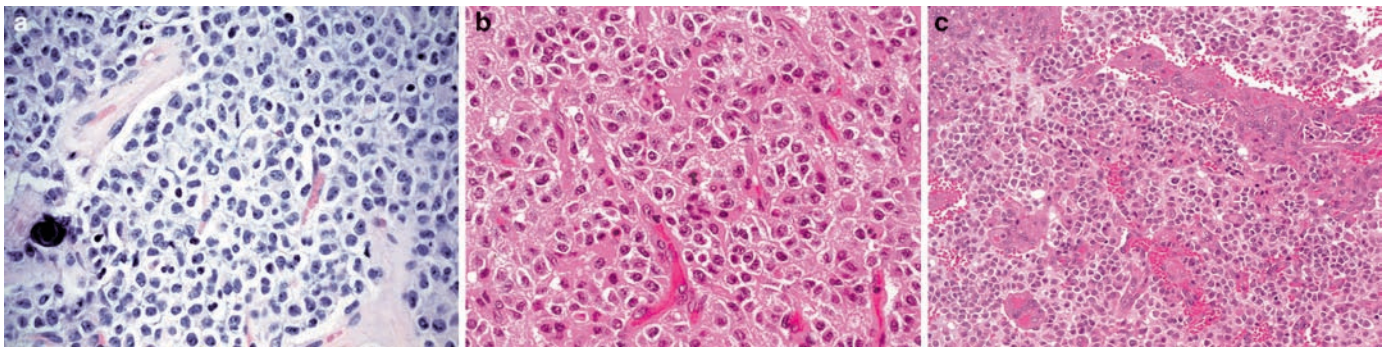
Fig 4.5 In anaplastic oligodendroglioma (WHO grade III), (**a**) perinuclear halos and delicate capillary network are often retained, though tumor nuclei are often more atypical and less uniformly rounded than in grade II lesions. Microcalcifications may also be present. Frequent mitotic figures (**b**) and vascular proliferation (**c**) are also often present in these high-grade tumors.
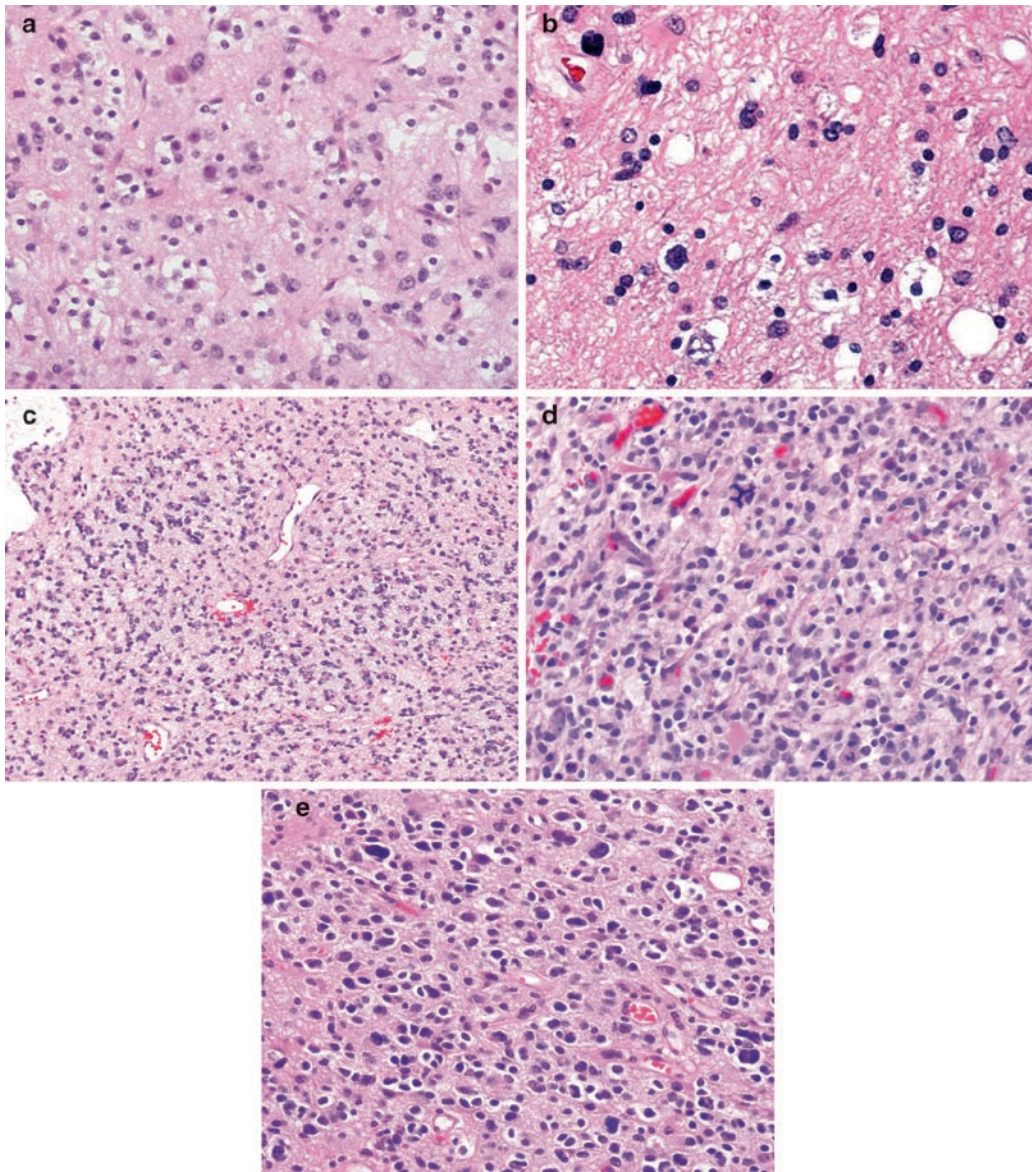
Fig 4.6 (**a** and **b**) Mixed oligoastrocytomas are composed of an admixture of cells with oligodendroglial features (round regular nuclei +/− perinuclear halo) and astrocytic features (oval to irregular-shaped hyperchromatic nuclei, sometimes with discernible fibrillary cytoplasm). Similar to oligodendrogliomas, delicate branched capillaries may be present, as seen in 6a. (**c**) Minigemistocytes with their eosinophilic cytoplasmic "bellies" may represent the bulk of the oligodendroglial component as in this MOA, which additionally displays an unusual clustering of tumor cells. Note the larger astrocytic nuclei, best seen toward the center of the field. Anaplastic MOAs are more hypercellular with numerous mitotic figures (**d** and **e**). Though not illustrated here, vascular proliferation is often present.
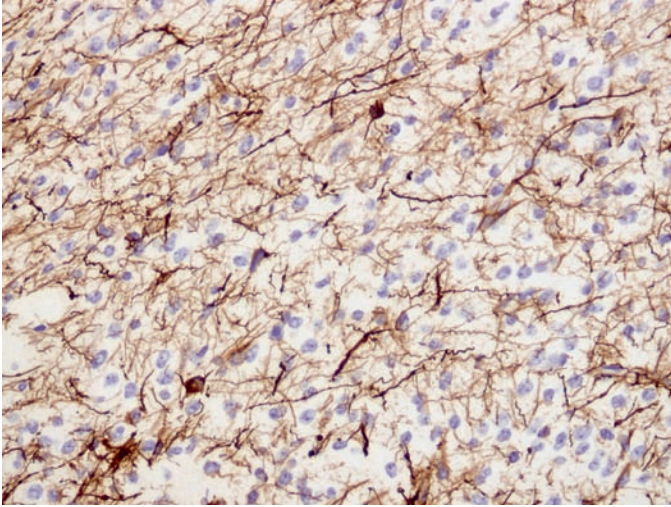
Fig 4.7 The round nuclei and perinuclear halos of cells with a classic oligodendroglial morphology stand out as negative against the intermingled GFAP-positive background glial processes and intratumoral reactive astrocytes.

Ependymal Tumors

Christine E. Fuller, Sonia Narendra and Ioana Tolicica

5.1 OVERVIEW

- A group of glial tumors exhibiting ependymal differentiation including subependymoma (WHO grade I), myxopapillary ependymoma (WHO grade I), ependymoma (WHO grade II; variants including cellular, tanycytic, papillary, and clear cell), and anaplastic ependymoma (WHO grade III).
- Most are sporadic; ependymomas may be seen as part of neurofibromatosis type 2, a hereditary cancer predisposition syndrome with germline mutation of NF2/Merlin gene.
- Recent evidence supports radial glia as the candidate cell of origin for ependymomas; subependymomas appear to derive from subependymal glial precursors.

5.2 CLINICAL FEATURES

- Though much less common than infiltrative gliomas, ependymomas are the most common tumor of the spinal cord (particularly in adult patients), and the third most common pediatric central nervous system (CNS) tumor, representing up to 30% of intracranial tumors in those under 3 years old.
- Infratentorial tumors have their peak age of occurrence in the first decade, while spinal tumors tend to peak from age 30–40.
- They have an equal gender distribution, though they are nearly twice as frequent in Caucasians compared to African-Americans.
- Intracranial ependymomas typically result in blockage of cerebrospinal fluid (CSF) pathways, causing signs and symptoms related to hydrocephalus and increased intracranial pressure.
- Spinal ependymomas, including myxopapillary ependymoma, may cause back pain and motor and/or sensory deficits, depending on their specific anatomic involvement.
- Anaplastic ependymomas are far more frequent in the pediatric age group, presenting as intracranial tumors, more frequently supratentorial.
  - Clinical signs and symptoms are similar to those for WHO grade II ependymoma, albeit they tend to develop in an accelerated fashion.

- Approximately 20% of myxopapillary ependymomas present in children with a 2:1 male to female bias; in this age group they exhibit a higher rate of dissemination through the CSF pathways.
- Subependymomas are often incidental autopsy findings in the brains of older adults; they are symptomatic when they obstruct CSF flow.
  - They are quite rare in children.

5.3 NEUROIMAGING

- The vast majority of pediatric ependymomas (90%) are intracranial, favoring the fourth ventricle followed by supratentorial locations;
  - In adults the distribution is approximately 60% spinal/40% intracranial, the latter mostly supratentorial.
- Supratentorial tumors (including ependymomas and subependymomas) more frequently involve the lateral ventricles compared to the third ventricle.
- Uncommonly, they arise remote from the ventricles, especially in intraparenchymal supratentorial locations in children.
- Rare extraneural sites include the ovaries, mediastinum, and sacrococcygeum.
- They may arise at any spinal cord level, though certain histologic subtypes have preferred locations:
  - Tanycytic ependymoma – thoracic/cervico-thoracic cord
  - Myxopapillary ependymomas – conus medullaris/filum terminale/cauda equina region
  - Subependymoma – cervical cord
- Myxopapillary ependymomas are the most common intramedullary neoplasm arising in the conus medullaris/cauda equina/filum terminale region; infrequent sites of origin include other cord levels, intracranial sites (both intraventricular and intraparenchymal), and subcutaneous sarcococcygeal areas.
- MRI/CT imaging findings:
  - Ependymomas and anaplastic ependymomas.
    - Spinal lesions typically involve several spinal segments and grow as centrally situated intramedullary tumors, hyperintense on T2-weighted MR images, with sharp tumor margins, and the majority with uniform contrast enhancement (Fig. 5.1a).
    - Rostral and caudal cysts are common, being hypointense on T1 and hyperintense on T2-weighted images.

- Intracranial tumors are also sharply demarcated, arising within or near the ventricular system. They are at least partially cystic, isointense on T1, iso- to hyperintense on T2, and moderately hyperintense on fluid-attenuated inversion recovery (FLAIR) MR imaging, with variable enhancement post contrast (Fig. 5.1b–e).
  - Intratumoral hemorrhage and/or calcifications may be seen.
  - Ventricular dilatation is frequently encountered.
  - Occasional tumors show infiltration of surrounding parenchyma, making differentiation from other gliomas difficult.
- Myxopapillary ependymomas are characteristically well circumscribed, hyperintense on both T1 and T2 weighted MR imaging (Fig. 5.2a and b) (unlike conventional ependymomas which are typically hypointense on T1), and brightly enhance post contrast.
  - Cystic change (particularly in intracranial examples) or hemorrhage may be encountered.
- Subependymomas are sharply demarcated nodular lesions bulging into ventricles or arising eccentrically within the spinal cord.
  - They show variable signal characteristics on MR and CT imaging.
  - Uncommonly enhance, and may contain foci of calcium or hemorrhage (Fig. 5.2c).
- Patterns of metastasis:
  - Ependymomas (grades II and III) as well as myxopapillary ependymomas (grade I) have been reported to metastasize via subarachnoid spread to seed other spinal and intracranial locations.

5.4 PATHOLOGY

- *Gross pathology*:
  - Classic ependymomas are soft tan to grey masses with well-defined boarders. They may be partially cystic and/or contain areas of hemorrhage, necrosis, or calcification.
  - Anaplastic examples may show evidence of frank parenchymal invasion.
  - Myxopapillary ependymomas are lobulated, soft, grey to tan, and often encapsulated.
  - Subependymomas are firm multilobulated/nodular intraventricular masses; spinal examples nearly always show an eccentric location.
- *Intraoperative cytologic imprints/smears*:
  - Smear preparations of ependymomas contain cohesive clusters of cells with variable cytomorphology, ranging from epithelial-like to bipolar fibrillated cells.
    - Nuclei tend to be bland and round to oval.
    - Perivascular pseudorosettes may be seen (Fig. 5.3a and b).
  - Cytology preparations from the following subtypes may be particularly problematic:
    - Tanycytic – contain long processes and oval to spindle-shaped nuclei; perivascular pseudorosettes are uncommon, and the smear preparation findings may closely resemble pilocytic astrocytoma.
    - Papillary – often have a more epithelial consistency and may closely mimic choroid plexus tumors or metastatic carcinomas.

- Myxopapillary ependymoma – papillary structures with perivascular radially – arranged cells with delicate glial processes within abundant myxoid material (Fig. 5.3c).
- Subependymomas – bland nuclei in a fibrillary background, sometimes with discernable microcysts.
- *Histology*
- *Ependymoma (WHO grade II)*:
  - Ependymomas classically present as well-demarcated moderately cellular tumors with bland round to oval nuclei with fine chromatin pattern.
  - Key architectural features (Fig. 5.4a):
    - Perivascular pseudorosettes (anuclear zones formed by the elongated glial-like processes of tumor cells in their radial arrangement around blood vessels): seen in majority of cases (Fig. 5.4b). These may be poorly formed in hypocellular areas (Fig. 5.4c).
    - True ependymal rosettes and canals (cuboidal to columnal epithelial-like tumor cells surrounding a true central lumen): seen in the minority of cases (Fig. 5.4d).
    - Conversely, ependymal-type lining seen at the periphery of tissue fragments from an ependymoma sampling is not particularly uncommon, and is a helpful diagnostic aid (Fig. 5.4e).
    - On occasion, epithelial-type elements predominate, imparting a "tubular adenoma-like" (Fig. 5.4f) or organoid appearance (Fig. 5.4g).
  - Mitotic figures are uncommon; foci of necrosis are not infrequent, though pseudopalisading necrosis and endothelial proliferation are absent.
    - Degenerative changes are common and include myxoid degeneration, vascular hyalinization, hemorrhage, and calcification (Fig. 5.4g).
  - Cartilage, bone, lipomatous elements, neuropil-like islands, and cells with melanin, signet ring (Fig. 5.4h) or giant cell morphology, or eosinophilic intracytoplasmic inclusions have all been described.
  - Well-characterized histopathologic variants of ependymoma include the following:
  - *Cellular ependymomas* – variant with notable hypercellularity yet lacking an elevated mitotic rate, vascular endothelial proliferation, or pseudopalisading necrosis. Perivascular pseudorosettes may be inconspicuous, and true rosettes and canals are generally lacking (Fig. 5.5a).
  - *Tanycytic ependymoma* – typified by elongated, often thin, eosinophilic cell processes and inconspicuous perivascular pseudorosettes within an otherwise fascicular architecture; true ependymal rosettes are not seen. Nuclear pleomorphism may be prominent in some cases (Fig. 5.5b,c).
  - *Papillary ependymomas* – rare subtype in which single or multiple layers of cuboidal to columnar cells rest upon central finger-like projections of fibrillary glial material "stroma"; fibrovascular cores are not a feature, and the epithelial-like surfaces tend to be smooth in contour (Fig. 5.5d).
  - *Clear cell ependymomas* – contain sheets of cells with rounded nuclei and abundant surrounding clear cytoplasm; perivascular pseudorosettes are invariably present,

though true rosettes are absent. Branching thin-walled vessels may be present, and many cases show anaplastic features (including endothelial proliferation, hypercellularity, and frequent mitoses), necessitating a grade III designation (Fig. 5.5e,f).
– Both clear cell and papillary areas may be intermixed components with otherwise typical, cellular, or anaplastic ependymoma

- *Myxopapillary ependymoma (WHO grade I)*:
  – Characteristically shows a papillary architecture with cuboidal to elongated glial cells radially arranged around Alcian blue-positive myxoid stroma with central vascular structure. Occasional examples harbor more epithelioid-appearing cells (Fig. 5.6a–c).
  – Some lesions are not particularly papillary at all, instead taking on a reticular or microcystic pattern with intermixed mucin-rich microcysts and occasional perivascular pseudorosettes (Fig. 5.6d,e).
  – Collagen balls/balloons may be seen in some cases (Fig. 5.6f); these may be highlighted by trichrome or periodic acid Schiff's (PAS) stains.
  – Mitotic rate is low, and necrosis and endothelial/vascular proliferation are usually absent.
  – Degenerative changes, including vascular hyalinization or fibrosis, are occasionally prominent (Fig. 5.6g,h).
  – Rare anaplastic and giant cell variants have been described as case reports.

- *Subependymoma (WHO grade I)*:
  – Often having a nodular appearance at low power (Fig. 5.7a), subependymomas are composed of hypocellular collections of monotonously bland cells with round to oval nuclei set within a delicate glial matrix; cells have a tendency to cluster, and microcysts are commonly encountered (Fig. 5.7b–d).
  – Perivascular pseudorosettes are quite uncommon, and true rosettes are not encountered.
  – Hemorrhage and/or hemosiderin-laden macrophages, calcification (Fig. 5.7a), sclerotic vessels, and focal nuclear pleomorphism have all been described.
  – Approximately 20% of subependymomas will harbor areas of classic or even anaplastic ependymoma; in these instances, the lesions should be graded according to the highest grade component.

- *Anaplastic ependymoma (WHO grade III)*:
  – Grading of ependymomas has historically been a contentious issue. Studies aimed at identifying histopathologic parameters that can distinguish different prognostic groups of ependymomas found that ependymomas harboring at least two or more of the following features were strongly correlative of shortened event-free survival and were indicative of a WHO grade III designation:
    – Elevated/brisk mitotic index (>5 per 10 high-power fields – should be seen throughout the tumor, not just focally) (Fig. 5.8a);
    – Hypercellularity with nuclear hyperchromasia and/or pleomorphism with marked atypia (Fig. 5.8b,c);
    – Endothelial proliferation;
    – Palisading necrosis (Fig. 5.8d).
  – They retain many features of conventional ependymoma, including perivascular pseudorosettes which may contain normal vessels or proliferating vasculature (Fig. 5.8e).

– Unfortunately, there exists a subset of ependymomas containing only small areas of "focal anaplasia," the significance of which is unclear though may suggest a more aggressive biologic potential than that of WHO grade II ependymoma (Fig. 5.8f).

5.5 IMMUNOHISTOCHEMISTRY

- Ependymomas/anaplastic ependymomas are positive for S100, GFAP (Fig. 5.9a), and vimentin. Epithelial membrane antigen (EMA) often shows a characteristic punctuate, dot-like positivity (Fig. 5.9b); though more specific, ring-like EMA staining is less frequently encountered. CD99 is frequently positive, with varying membranous or dot-like staining. Stains for neural markers are generally negative except for NeuN which may show nuclear positivity in some anaplastic ependymomas.

- Myxopapillary ependymomas are positive for GFAP, S100, vimentin, and CD99. Occasional examples are immunopositive for p53. They are negative for cytokeratin and have a low Ki67 labeling index. Unlike other ependymomas, these are EMA negative.

- Subependymomas are positive for GFAP (Fig. 5.9c) and S100; they are also often weakly positive for low-specificity neuronal markers such as neural cell adhesion molecule (NCAM) and neuron-specific enolase (NSE). Ki67 labeling index is lower than all other types of ependymoma.

- Mib-1/Ki67 may be helpful in confirming brisk proliferation in areas of anaplasia, including examples of focal anaplasia (Fig. 5.9d).

5.6 ELECTRON MICROSCOPY (EM)

- Ependymomas and anaplastic ependymomas, including all of the listed variants above, share similar ultrastructural characteristics of ependymal differentiation, including intracellular intermediate filaments and intercellular junctional complexes including desmosomes, occasional cilia, and microvilli, the latter present both on cell surface and within microlumina (Fig. 5.10).

- Myxopapillary ependymomas, apart from features typical for ependymal differentiation (intermediate filaments, microvilli, cilia), exhibit interdigitating cell processes and microtubular aggregates bound by rough endoplasmic reticulum.

- Subependymomas show ultrastructural features typically associated with ependymal differentiation, including intermediate filaments, lumen-like structures, microvilli, and cilia.

5.7 MOLECULAR PATHOLOGY

- Comparative genomic hybridization (CGH) analyses have documented losses involving chromosomes 6q, 17p, and 22 and gains of 1q, 7q, and 9p as the more frequent alterations in pediatric intracranial ependymomas. Of interest, gain of 1q has been shown to be correlative with increased recurrence and shortened survival in several studies.

- Loss of chromosome 22q is frequently observed in adult ependymomas and is strongly associated with a spinal location.

Many of these spinal tumors harbor concomitant *NF2* mutation; this is not the case for intracranial ependymomas with 22q deletions. Loss of *4.1B* (formerly *DAL-1;* 18p11.3), a related structurally homologous Protein 4.1 family member, is more frequent in intracranial ependymomas. Losses of *4.1B* and related *4.1R* (1p32-33) are more frequent in pediatric, intracranial, and/or WHO grade III tumor subsets, and deletion of 4.1G (6q23) may portend a propensity for aggressive biologic behavior.

- ErbB2 and ErbB4 coexpression is quite frequent in pediatric ependymomas, and one investigation found strong positive correlation between elevated ErbB2/4 coexpression levels and high Ki67 proliferation index, as well as a clear trend towards worse clinical outcome.
- Clear cell ependymomas lack deletions of 1p, 19q, and NF2; one study indicated frequent loss of chromosome 18.
- Systematic molecular characterization of subependymomas and myxopapillary ependymomas has not been undertaken.

5.8 DIFFERENTIAL DIAGNOSIS

- Ependymomas in general may be differentiated from infiltrative gliomas by virtue of their generally solid growth pattern, lacking significant intratumoral neurofilament-positive processes.
- Highly cellular anaplastic ependymomas may resemble ependymoblastomas and other primitive neuroectodermal tumors (PNETs), though the former will be more diffusely positive for GFAP and will lack ependymoblastic rosettes and neuronal-type markers by immunohistochemistry (IHC).
- Ependymomas, especially the tanycytic variant, may closely resemble astrocytoma (particularly pilocytic astrocytoma), schwannoma, or meningioma. Ependymomas in general lack Rosenthal fibers and eosinophilic granular bodies of pilocytic astrocytomas, and are positive for GFAP unlike schwannomas and meningiomas. In some cases, however, definitive diagnosis relies heavily on ultrastructural findings of ependymal differentiation.
- Clear cell ependymoma needs to be differentiated from other primary CNS lesions containing clear cells (oligodendroglioma, neurocytoma, and hemangioblastoma) and metastatic clear cell carcinomas. Identification of perivascular pseudorosettes is the first clue to the diagnosis of clear cell ependymoma; immunohistochemistry (especially dot-like positivity for EMA), EM features of ependymal differentiation, and molecular findings (lack of 1p/19q deletion and – C18) help confirm the diagnosis.
- Papillary ependymoma may be confused with choroid plexus tumors, papillary meningiomas, or metastatic carcinomas. Strong positivity for GFAP and lack of diffuse cytokeratin staining are characteristic of the former, and EM confirmation is usually not necessary.
- Myxopapillary ependymoma may be differentiated from potential diagnostic mimics such as chordoma, renal cell carcinoma, myxoid chondrosarcoma and other myxoid soft tissue lesions, and paraganglioma by virtue of its immunohistochemical pattern (positive for vimentin, S100, GFAP;

cytokeratin negative) and characteristic ultrastructural finding of microtubular aggregates.

- Subependymomas may mimic other hypocellular glial tumors, including low-grade astrocytoma or pilocytic astrocytoma. Identification of a lobular architecture, cell clustering, microcysts, and lack of Rosenthal fibers or eosinophilic granular bodies is helpful is separating the former from these potential diagnostic pitfalls.

5.9 PROGNOSIS

- In general, children with ependymomas tend to fare far worse than their adult counterparts, due in part to the much higher incidence of intracranial/posterior fossa location and higher grade tumors arising in the pediatric age group.
  - Those affected during the first few years of life have particularly poor outcomes, especially given the difficulty in administering radiotherapy to these immature brains due to related morbidities.
  - Chemotherapy has been shown to be beneficial in these instances.
- Extent of tumor excision has consistently been shown as an important variable predictive of outcome.
  - In most instances, first recurrence is at the site of tumor resection bed, and recent evidence indicates that demonstration of tumor microinvasion on the original resection specimen correlates with poor overall and progression-free survival.
- Though most studies have found histologic grading (grade II vs. grade III) to be significantly predictive of overall and/or recurrence-free survival, a few observers have shown otherwise.
  - Specific diagnostic criteria for grade III designation have been proposed as outlined above, providing excellent prognostic correlation in those studies.
- Elevated Ki67 proliferation index correlates well with grade III status and with more aggressive biologic behavior.
- Clear cell ependymomas appear to constitute a more aggressive phenotype, often representing grade III tumors.
  - Local recurrence is quite common, and these tumors may infrequently show transdural invasion into venous sinuses or extracranial metastasis into soft tissue and lymph nodes.
- Myxopapillary ependymomas are generally slow growing tumors with a favorable 10-year overall survival rate (approximating 95%).
  - Despite their WHO grade I designation, up to 45% of patients may experience local recurrence, irrespective of adequate excision. Patients who succumb to their disease typically do so following a protracted course with multiple recurrences.
  - Tumor encapsulation (enabling gross excision) portends a lower rate of recurrence as compared to those tumors removed piecemeal/subtotally.
  - Adjuvant radiation therapy has been shown to aid in reducing the recurrence rate.
  - Neuroaxis metastasis, though uncommon overall, are more frequent in pediatric patients, thus emphasizing the

importance of complete neuroaxis screening both at the time of diagnosis and during follow-up.

- Subependymomas are benign neoplasms that grow slowly, a significant proportion remaining clinically silent through life, to be detected only incidentally at autopsy.
  - Surgical removal is usually curative; incomplete excision has been associated with rare recurrences.
  - In contradistinction, mixed lesions with subependymoma and ependymoma components exhibit biologic behavior akin to the higher grade component present in these tumors.

SUGGESTED READING

Dyer S, Prebble E, Davison V, Davies P, Ramani P, Ellison D, Grundy R (2002) Genomic imbalances in pediatric intracranial ependymomas define clinically relevant groups. Am J Pathol 161:2133–2141

Fassett DR, Pingree J, Kestle JR (2005) The high incidence of tumor dissemination in myxopapillary ependymoma in pediatric patients. Report of five cases and review of the literature. J Neurosurg 102:59–64

Figarella-Branger D, Civatte M, Bouvier-Labit C, Gouvernet J, Gambarelli D, Gentet J-C, Lena G, Choux M, Pellissier JF (2000) Prognostic factors in intracranial ependymomas in children. J Neurosurg 93:605–613

Fouladi M, Helton K, Dalton J, Gilger E, Gajjar A, Merchant T, Kun L, Newsham IF, Burger PC, Fuller CE (2003) Clear cell ependymoma: a clinicopathologic and radiographic analysis of 10 patients. Cancer 98:2232–2244

Grill J, Avet-Loiseau H, Lellouch-Tubiana A, Sevenet N, Terrier-Lacombe M-J, Venaut A-M, Doz F, Sainte-Rose C, Kalifa C, Vassal G (2002) Comparative genomic hybridization detects specific cytogenetic abnormalities in pediatric ependymomas and choroid plexus papillomas. Cancer Genet Cytogenet 136:121–125

Kramer DL, Parmiter AH, Rorke LB, Sutton LN, Biegel JA (1998) Molecular cytogenetic studies of pediatric ependymomas. J Neurooncol 37:25–33

Mendrzyk F, Korshunov A, Benner A, Toedt G, Pfister S, Radlwimmer B, Lichter P (2006) Identification of gains on 1q and epidermal growth factor receptor overexpression as independent prognostic markers in intracranial ependymoma. Clin Cancer Res 12:2070–2079

Merchant TE, Jenkins JJ, Burger PC, Sanford RA, Sherwood SH, Jones-Wallace D, Heideman RL, Thompson SJ, Helton KJ, Kun LE (2002) Influence of tumor grade on time to progression after irradiation for localized ependymoma in children. Int J Radiat Oncol Biol Phys 53:52–57

Perilongo G, Massimino M, Sotti G, Belfontali T, Masiero L, Rigobello L, Garre L, Carli M, Lombardi F, Solero C, Sainati L, Canale V, del Prever AB, Giangaspero F, Andreussi L, Mazza C, Madon E (1997) Analyses of prognostic factors in a retrospective review of 92 children with ependymoma: Italian Pediatric Neuro-Oncology Group. Med Pediatr Oncol 29:79–85

Reardon DA, Entrekin RE, Sublett J, Ragsdale S, Li H, Boyett J, Kepner JL, Look T (1999) Chromosome arm 6q loss is the most common recurrent autosomal alteration detected in primary pediatric ependymoma. Genes Chromosomes Cancer 24:230–237

Shu HK, Sall WF, Maity A, Tochner ZA, Janss AJ, Belasco JB, Rorke-Adams LB, Phillips PC, Sutton LN, Fisher MJ (2007) Childhood intracranial ependymoma: twenty-year experience from a single institution. Cancer 110:432–441

Snuderl M, Chi SN, De Santis SM, Stemmer-Rachamimov AO, Betensky RA, De Girolami U, Kieran MW (2008) Prognostic value of tumor microinvasion and metalloproteinases expression in intracranial pediatric ependymomas. J Neuropathol Exp Neurol 67:911–920

Taylor MD, Poppleton H, Fuller CE, Su X, Liu Y, Jensen P, Magdaleno S, Dalton J, Calabrese C, Board J, Macdonald T, Rutka J, Guha A, Gajjar A, Curran T, Gilbertson R (2005) Radial glia cells are candidate stem cells of ependymoma. Cancer Cell 8:323–335

Tihan T, Zhou T, Holmes E, Burger PC, Ozuysal S, Rushing EJ (2008) The prognostic value of histological grading of posterior fossa ependymomas in children: a Children's Oncology Group study and a review of prognostic factors. Mod Pathol 21:165–177

Ward S, Harding B, Wilkins P, Harkness W, Hayward R, Darling JL, Thomas DGT, Warr T (2001) Gain of 1q and loss of 22 are the most common changes detected by comparative genomic hybridization in paediatric ependymoma. Genes Chromosomes Cancer 32:59–66

Zamecnik J, Snuderl M, Eckschlager T, Chanova M, Hladikova M, Tichy M, Kodet R (2003) Pediatric intracranial ependymomas: prognostic relevance of histological, immunohistochemical, and flow cytometric factors. Mod Pathol 16:980–991
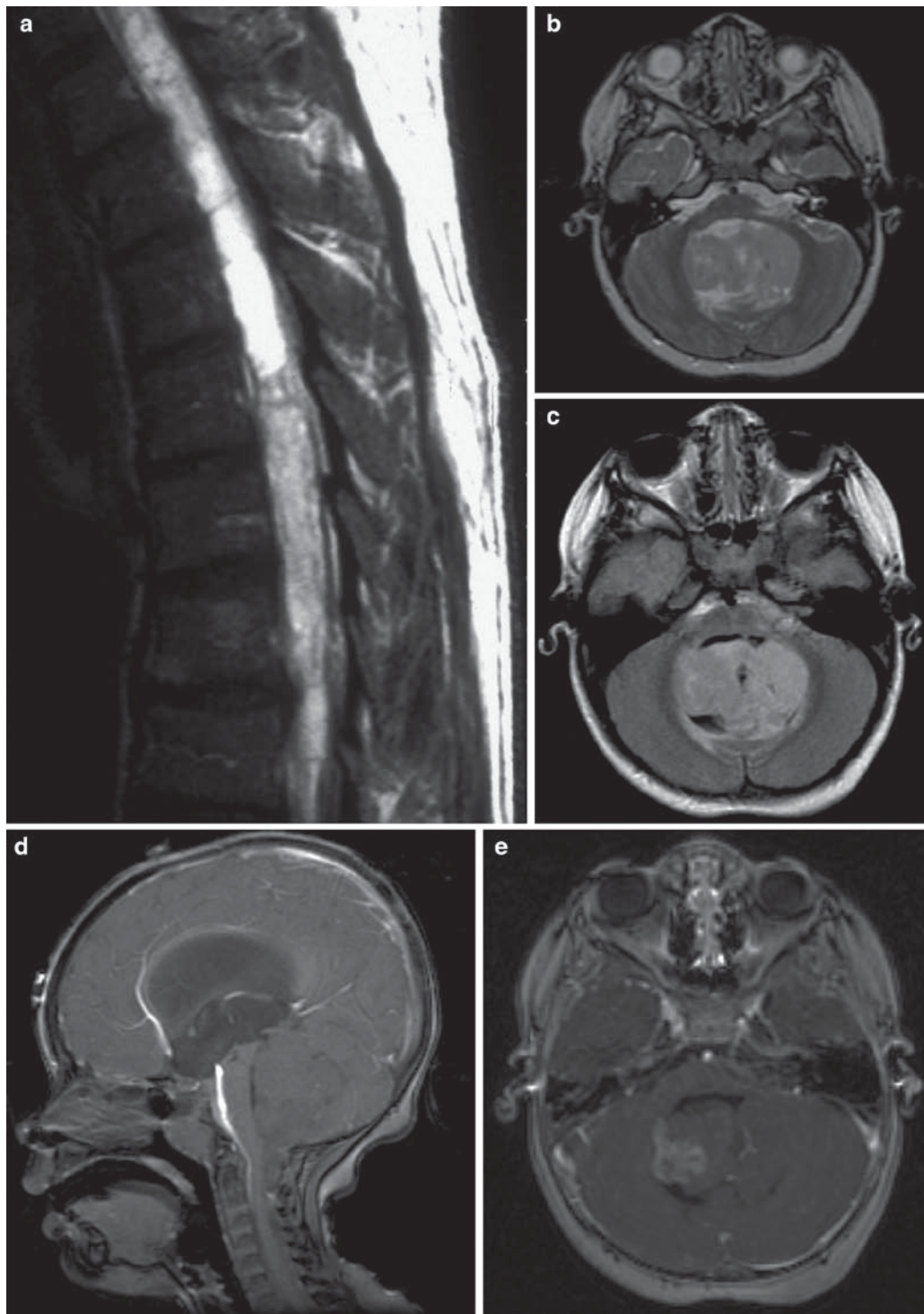
Fig. 5.1. (**a**) Sagittal TI-w post-Gd imaging of a well-demarcated spinal ependymoma with characteristic homogeneous post-contrast enhancement (Courtesy of Dr Murat Gokden, University of Arkansas, Little Rock, AK, USA). (**b**) Axial MR images of a fourth ventricular ependymoma show a predominantly solid, well-demarcated tumor that has heterogeneous signal characteristics, being iso- to hyperintense on T2-w and (**c**) hyperintense on FLAIR. (**d**) Sagittal and (**e**) axial T1-w post-Gd imaging shows this same lesion to be isointense with variable contrast enhancement. Hydrocephalus is prominent in this example.
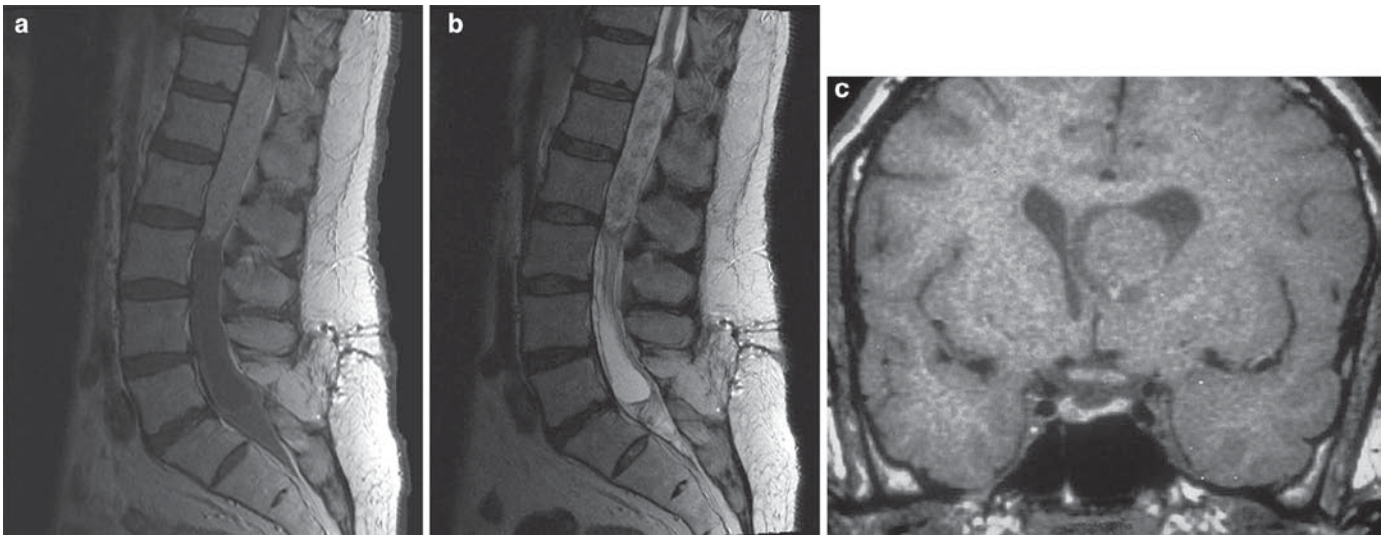
Fig. 5.2. Sagittal T1-w (**a**) and T2-w (**b**) images of a myxopapillary ependymoma showing a hyperintense lesion on both studies. (**c**) Subependymomas tend to be nodular, circumscribed intraventricular lesions, this example being isointense on coronal T1-w MR imaging.
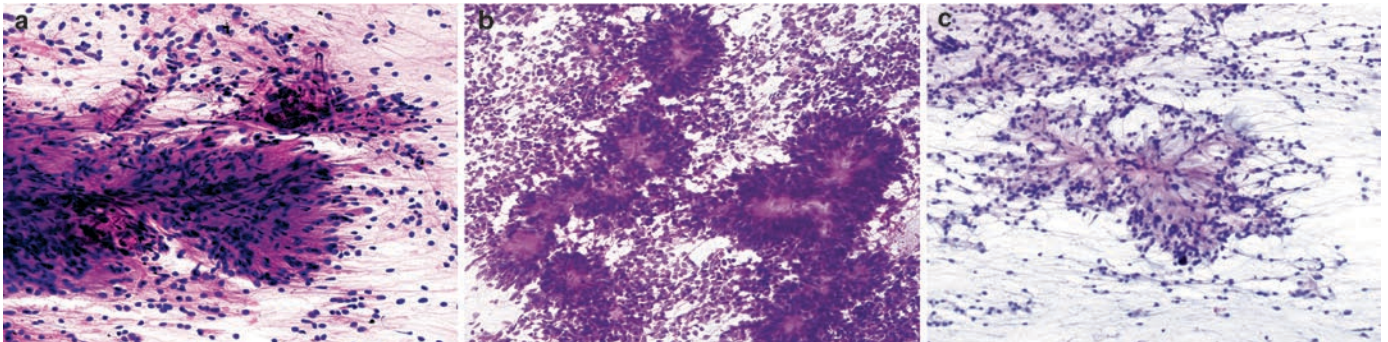
Fig. 5.3. (**a** and **b**) Cytologic preparations of ependymoma often show three-dimensional clusters of cells with elongated fibrillar glial processes; perivascular pseudorosettes may or may not be obvious. (**c**) Squash preparations of myxopapillary ependymoma are notable for papillary structures with perivascular radially arranged cell processes and abundant myxoid material.
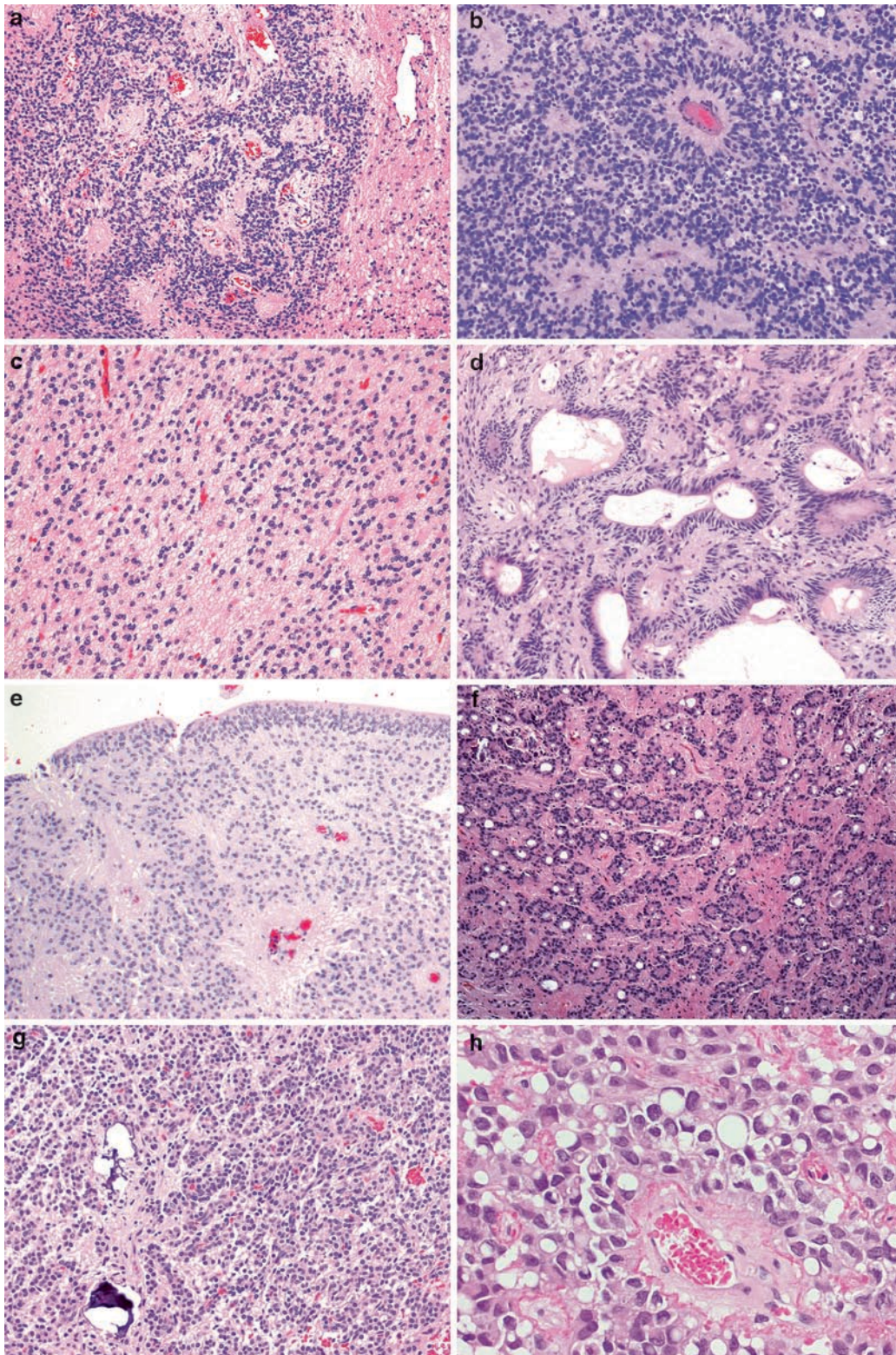
Fig. 5.4. (**a**) Conventional ependymomas exhibit a solid growth pattern with circumscription from surrounding parenchyma. (**b**) Perivascular pseudorosettes are a nearly universal finding, (**c**) though may be inconspicuous in hypocellular areas. (**d**) Ependymal canals and true rosettes are seen less frequently. (**e**) Identifying ependymal-type lining at the periphery of individual biopsy/resection tissue fragments is a helpful and not infrequent diagnostic finding indicative of ependymal neoplasm; this may be encountered even in the absence of canals or ependymal rosettes elsewhere in the sample. (**f**) Rarely, epithelial-type differentiation may predominate as in these "tubular adenoma-like" and (**g**) examples of organoid growth pattern. (**h**) Signet ring-like cells are an uncommon finding.
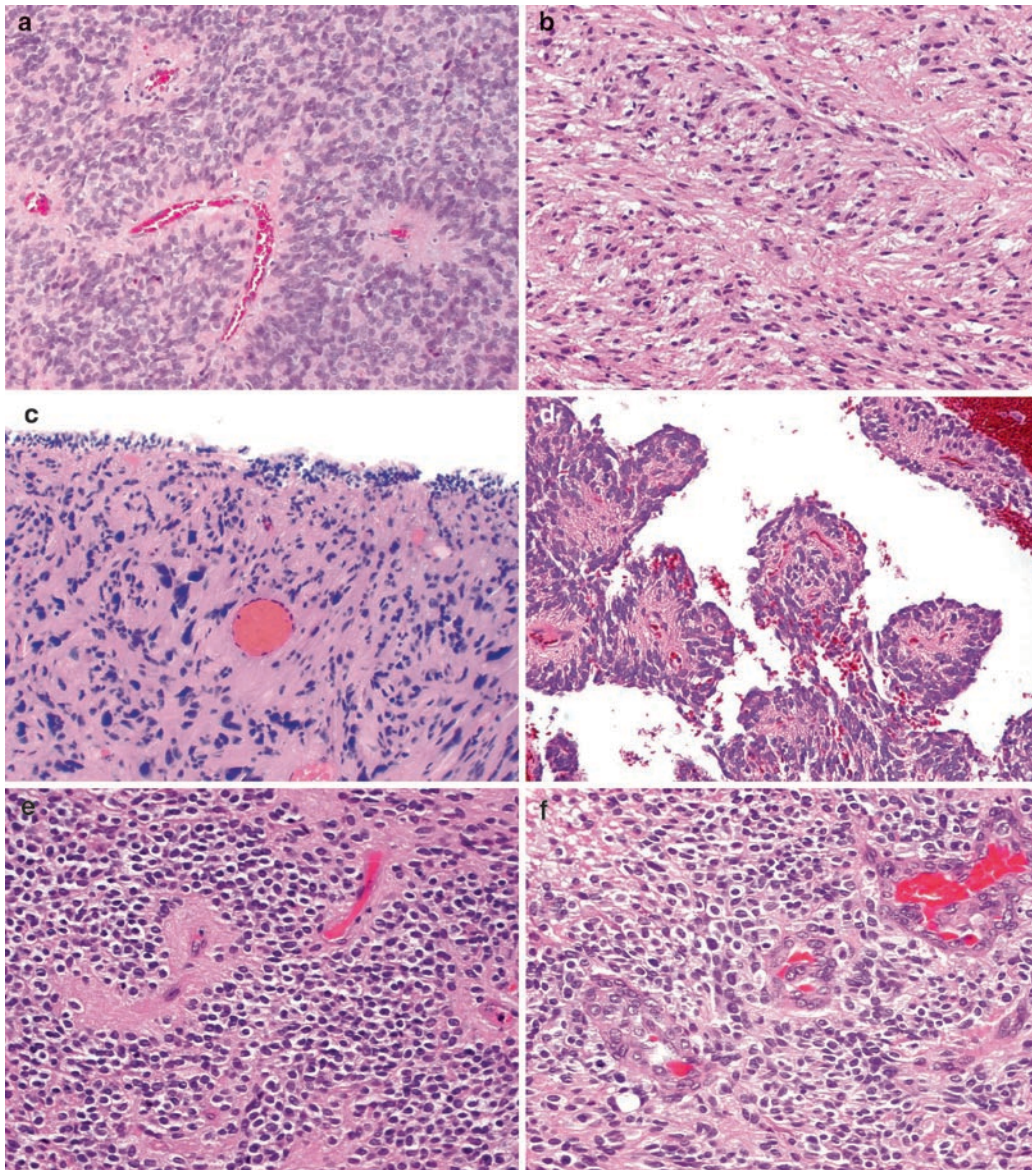
Fig. 5.5. (**a**) Cellular ependymomas are quite hypercellular, though they lack other histologic features of anaplastic ependymomas, including endothelial proliferation and increased mitoses. (**b**) The fascicular architecture of the tanycytic ependymoma renders perivascular pseudorosettes inconspicuous; (**c**) striking nuclear pleomorphism may be encountered in some cases. (**d**) Papillary ependymomas exhibit multiple (or single) layers of bland neoplastic ependymal cells resting upon papillary finger-like projections of fibrillary glial processes with central blood vessels. (**e**) Perivascular pseudorosettes are a helpful feature in differentiating clear cell ependymoma from other lesions with clear cell morphology. (**f**) Many clear cell ependymomas display high-grade features including endothelial proliferation.
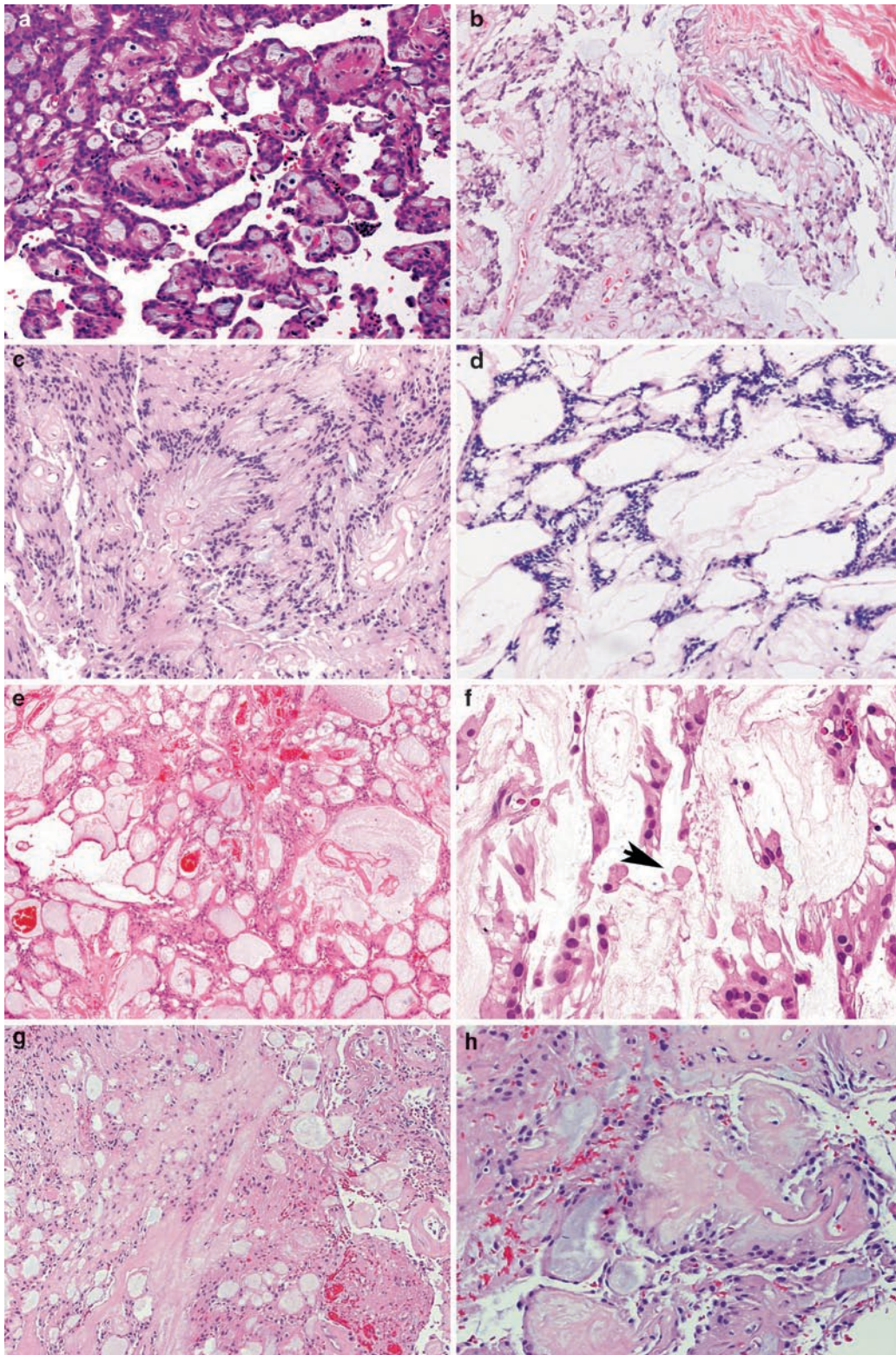
Fig. 5.6. (**a–c**) Myxopapillary ependymomas, similar to other ependymal tumors, contain ependymal cells with variable epithelial (**a**) to glial morphology with elongated eosinophilic processes (**b,c**); in this context, however, the perivascular pseudorosettes take the form of myxoid stroma-rich papillary structures. This papillary architecture may be inconspicuous in some cases, replaced instead by a more solid (**c**), reticular (**d**), or microcystic (**e**) pattern, again with characteristic myxoid material and scattered perivascular pseudorosettes. (**f**) Collagen "balloons" (arrow) and tumoral or vascular hyalinization (**g,h**) may be encountered.
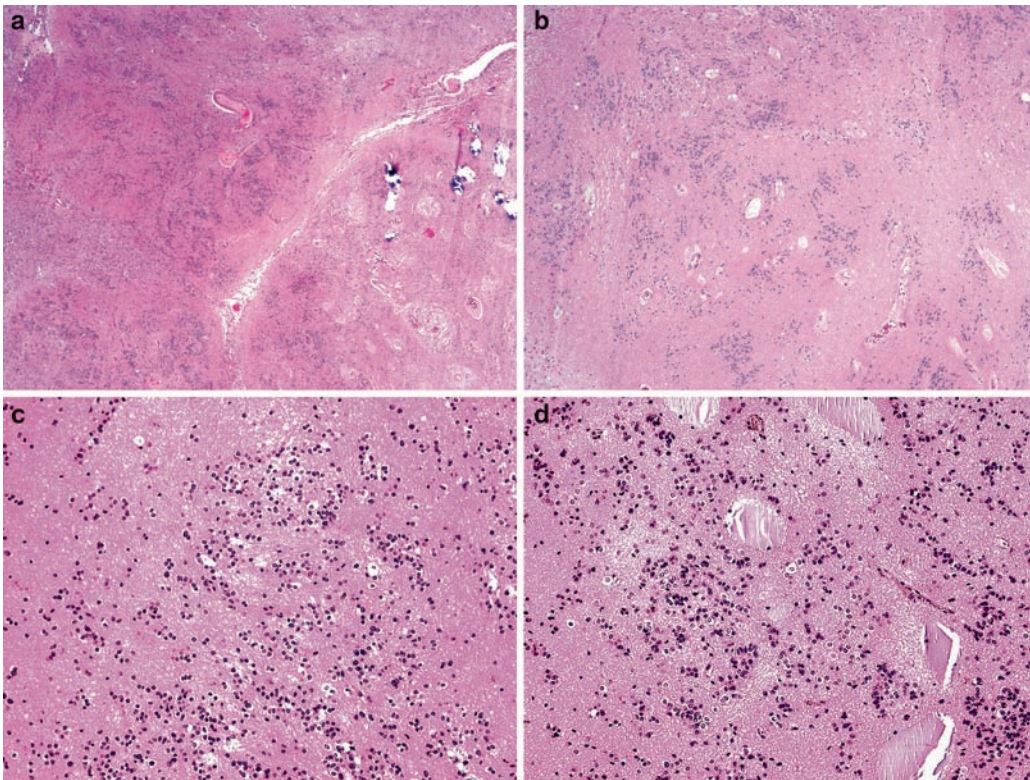
Fig. 5.7. (**a**) Subependymomas tend to be nodular on low-power microscopy and may show calcification; (**b**) they are hypocellular lesions containing abundant glial matrix interspersed with monotonously bland cells with rounded to oval nuclei. (**c**) Tumor cells have a tendency to cluster, and (**d**) microcysts are not infrequent.
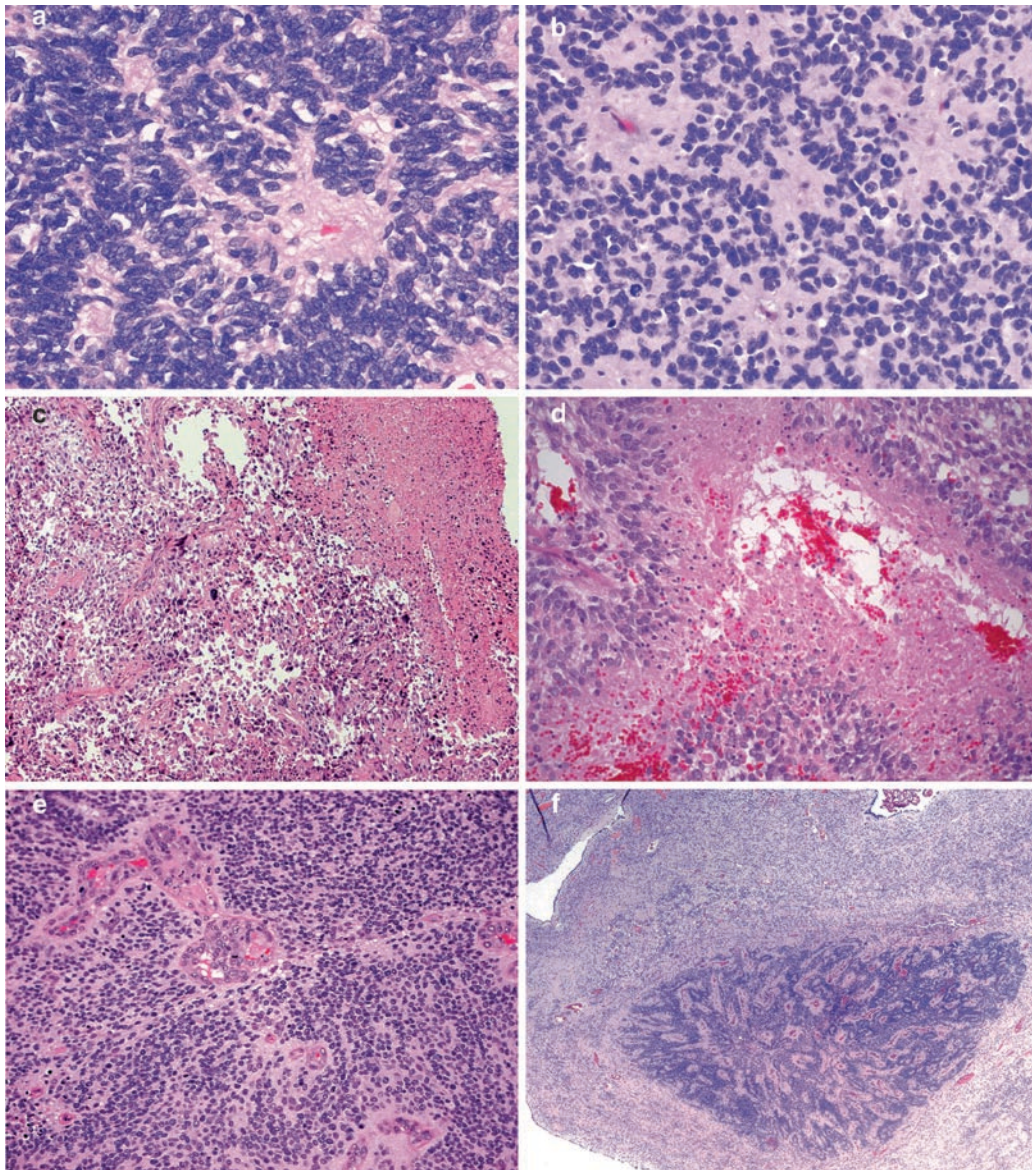
Fig. 5.8 (**a**) Anaplastic ependymomas are notably hypercellular, with elevated mitotic activity with (**b**) moderate to (**c**) significant nuclear pleomorphism. Extensive necrosis is common, often showing surrounding pseudopalisading of tumor cells (**d**). (**e**) Endothelial proliferation often residing within perivascular pseudorosettes is another typical feature; (**f**) Discrete foci of "focal anaplasia," replete with any or all of the features noted above, may be encountered in otherwise lower grade ependymoma variants, the significance of which is yet unclear.

Fig. 5.9. Junctional complexes and microlumina bearing numerous microvilli are ultrastructural features indicative of ependymal differentiation.
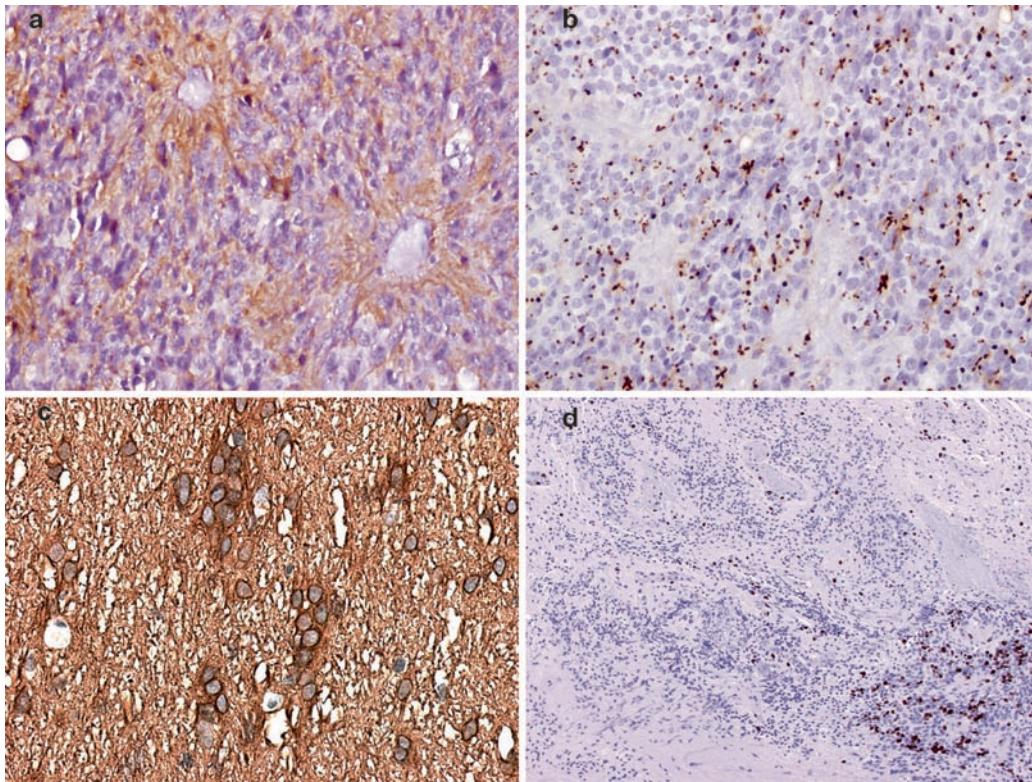
Fig. 5.10. Immunohistochemical stain for (**a**) GFAP highlights the elongated fine perivascular processes in ependymomas, where as (**b**) EMA staining tends to present in a punctate dot-like pattern. Subependymomas are similarly diffusely positive for (**c**) GFAP. (**d**) Ki67 labeling is markedly elevated within this focus of focal anaplasia.

Section B: Embryonal Neuroepithelial Tumors

Adekunle M. Adesina

Abstract Embryonal neuroepithelial tumors represent a significant group of pediatric brain tumors. They are characterized by "small blue cells" and exhibit a distinct pattern of divergent differentiation. Medulloepithelioma and supratentorial central nervous system primitive neuroectodermal tumors (PNETS) are presented together in the same chapter. Medulloblastoma represents a subset of "small blue cell" tumors that occur specifically in the cerebellum. These tumors are presented in a separate chapter followed by atypical teratoid rhabdoid tumors that are also presented in a separate chapter.

Central Nervous System Primitive Neuroectodermal Tumors and Medulloepithelioma

Adekunle M. Adesina, J. Hunter and L. Rorke-Adams

Keywords Primitive neuroectodermal tumors; Medullo-epithelioma; Cerebral neuroblastoma; Ganglioneuroblastoma; Ependymoblastoma

6.1 OVERVIEW

- Embryonal tumors at extracerebellar sites are composed of undifferentiated neuroepithelial cells with capacity for divergent differentiation, including neuronal, astrocytic, myoid, or melanocytic differentiation.
- Tumors may recapitulate the primitive neural tube (medulloepithelioma) or have ependymoblastomatous rosettes (ependymoblastoma) or have extensive neuronal differentiation (cerebral neuroblastoma) with ganglion cells (ganglioneuroblastoma).

6.2 CLINICAL FEATURES

- Most patients are below the age of 20 years, with only a minority occurring above this age.
- Medulloepitheliomas are often seen in children less than 2 years old and may rarely be congenital.
- Incidence is equal between males and females.
- Clinical presentation depends on location and corresponding localizing symptoms and signs, as well as the presence of raised intracranial pressure.
- May include headache, seizures, and progressive deterioration in level of consciousness.
- Localizing signs related to functional regions include motor weakness, hemiplegia, etc.
- Ependymoblastomas tend to occur in younger children and neonates.

6.3 NEUROIMAGING

- Typically presents as a cerebral hemispheric mass lesion. Brainstem, and spinal cord locations are less frequent.
- Characteristically, MRI shows a predominantly solid mass, hypo-intense or iso-intense with gray matter and moderate diffuse non-homogenous enhancement (Figs. 6.1 and 6.2), sometimes with a cystic and necrotic component (Fig. 6.3).
- Dense cellularity is often seen as restricted diffusion on ADC map (Fig. 6.2b).
- Intratumoral hemorrhage may occur.
- MR spectroscopy shows marked elevation of choline with little, if any, NAA peak (Fig. 6.4).
- Calcification may be appreciated on CT scans.
- Diffuse leptomeningeal enhancement and thecal sac drop metastases, when present, are consistent with CSF dissemination.

- Extra-CNS metastases to other organs, including the liver, bone, and cervical lymph nodes, may occur and may raise a diagnostic dilemma regarding whether the CNS tumor is primary or secondary.
- Presurgical MR angiography may show large feeding vessels that may require presurgical embolization.
- Periventricular and sacrococcygeal localization may be seen in ependymoblastomas.

6.4 PATHOLOGY

6.4.1 Gross

- Gross specimens from CNS PNETs vary from fragmented soft pink hemorrhagic tissue to large pieces of well-demarcated masses. Leptomeningeal invasion may induce desmoplasia and a slightly firm consistency.
- Grossly, *medulloepithelioma* is similar to other embryonal tumors of the CNS.
  - Whereas most PNETs have poorly-defined margins, medulloepitheliomas sometimes appear to be circumscribed.

6.4.2 Intraoperative Smears

- Characteristically, smears show diffuse sheets of relatively monotonous population of poorly differentiated "small blue cells" with hyperchromatic nuclei, micronucleoli and little amount of cytoplasm (Fig. 6.5).
- Rare Homer–Wright type rosettes may be seen.
- Anaplasia is demonstrated by varying degrees of nuclear pleomorphism, more prominent nucleoli, cell wrapping and frequent apoptosis.

6.4.3 Histology

- PNETs are typically composed of sheets of poorly differentiated small round blue cells with high nucleocytoplasmic ratio (Fig. 6.6).
- Neuroblastic differentiation with Homer–Wright rosettes is common. Flexner–Wintersteiner rosettes are rare and their presence is more frequent in PNETs originating in the pineal gland (*pineoblastoma*) (Fig. 6.7).
- Neuronal differentiation with a fibrillary neuropil stroma (Fig. 6.8) is associated with nuclear streaming (*cerebral neuroblastoma*) and ganglionic differentiation (*ganglioneuroblastoma*) (Fig. 6.9).
- Astrocytic differentiation may be focal, regional, or diffuse.

- Stromal fibrosis is common.
- Arrangement of cells in palisades mimicking polar spongioblastoma may be seen (Fig. 6.10a).
- Presence of stratified or multilayered rosettes with true lumina (Fig. 6.10b) (ependymoblastomatous rosettes) defines the *ependymoblastoma*.
- "*Embryonal tumor with abundant neuropil and true rosettes*" represents a variant closely resembling ependymoblastoma by its multilayered rosettes and also has unusually abundant differentiating neuropil within which isolated rosettes are seen (Fig. 6.11).
- Recapitulation of the features of the embryonic neural tube with the presence of a papillary, tubular or trabecular arrangement of neuroepithelial cells to form primitive neural tube-like structures along with sheets of undifferentiated neuroepithelial cells defines the *medulloepithelioma* (Fig. 6.12).
  - These primitive neural tube-like structures are distinguished from ependymoblastomatous rosettes by the presence of external and internal limiting membranes and have multilayered and pseudostratified cell layers. The external limiting membrane can be demonstrated by PAS stain or immunostain for collagen type IV (Fig. 6.13).
  - Tiny blebs may protrude along the inner surface of the cells, but cilia and blepharoplasts are absent.
  - Mitotic figures are typically found near the luminal margin.
  - Tubular structures may predominate or may be associated with fields of primitive neuroepithelial cells, which sometimes demonstrate differentiation along glial, neuronal, or ependymal lines.
  - Mesenchymal differentiation, including bone, cartilage and striated muscle may be present.
  - Melanin-bearing cells are also encountered occasionally.
  - Although the neoplastic cells generally exhibit an orderly appearance, they have the capacity to develop bizarre, anaplastic features (Fig. 6.14a–d).
  - Ependymoblastomatous rosettes are often present in medulloepitheliomas as well.
  - Divergent differentiation, including neuronal and glial, may be seen in association with the earlier described mesenchymal differentiation.

6.5 IMMUNOHISTOCHEMISTRY

- PNETs like medulloblastoma show immunoreactivity for neuronal markers, including synaptophysin, neurofilament protein (Fig. 6.15a and b), and class III β tubulin.
- Glial differentiation is associated with GFAP expression and must be distinguished from reactive astrocytes (Fig. 6.15c).
- Proliferation index with MIB1 or PCNA (Fig. 6.15d) immunolabelling is high, often ranging between 20% and 80% in all PNETs.
- Expression of cytokeratin and EMA may be seen in medulloepithelioma and ependymoblastoma.
- Immunopositivity for retinal S antigen may be rarely seen in pineoblastoma.
- In medulloepithelioma, cells forming the tubules express nestin, vimentin (Fig. 6.15e), microtubule-associated protein type 5, fibroblast growth factor and insulin-like growth factor 1 (IGF-1).
  - Expression of GFAP, NFP, and synaptophysin in intervening regions reflect the spectrum of differentiation that is present in the tumor, although tubular epithelium may occasionally express NFP (Fig. 6.15b).
  - Rarely, in addition to the presence of intracytoplasmic melanin pigments, melanocytic differentiation is demonstrable with the Masson's Fontana stain and/or by immunopositivity for the HMB45 antibody.
  - Ki-67 shows a very high proliferation index often in the 50–80% range with robust proliferative activity in the tubular structures of medulloepithelioma.

6.6 ELECTRON MICROSCOPY

- Neuronal differentiation is evidenced by the demonstration of cellular processes with microtubules, cytoplasmic dense core neurosecretory granules and synaptic type junctions.
- Intermediate filaments may be seen.
- In medulloepithelioma, the tubules are characterized by extensive zonulae adherentes similar to those found in the ependymal tumors, ATRTs and other epithelial tissues.
  - A distinct sometimes folded basal lamina is located on the outer surface of the epithelial cells.
  - Poorly differentiated cells with minimal cytoplasmic organelles or cells exhibiting characteristic features of glial cells containing intermediate filaments and/or neuronal cells with dense core neurosecretory vesicles may also be identified.
  - Ependymoblastomas may show rudimentary cilia and basal bodies.

6.7 MOLECULAR PATHOLOGY

- Although supratentorial PNETs share histologic features with cerebellar medulloblastoma, isochromosome 17q (a common event in medulloblastoma) is very rare in PNETs in general, although chromosome 17 alterations have been documented in some embryonal tumors with abundant neuropil and true rosettes.
  - No consistent pattern of genetic events has been reported.

6.8 DIFFERENTIAL DIAGNOSIS

- Ependymoblastomas are distinguished from anaplastic ependymomas by the presence of ependymoblastic rosettes.
  - Ependymal perivascular pseudorosettes show GFAP positivity in the acellular perivascular region of these pseudorosettes, while ependymal cells are positive for EMA.
  - Ependymoblastomas may show neuroepithelial components with immunoreactivity for neurofilament proteins.
- Medulloepitheliomas may be confused with immature teratoma, choroid plexus carcinoma or most frequently, primitive neuroectodermal tumor showing ependymal differentiation (ependymoblastoma).
  - Although medulloepitheliomas may have ependymoblastomatous-type rosettes (as seen in ependymoblastoma) they often show the presence of primitive neural tube-like structures with demonstrable external basal lamina by PAS or immunostain for collagen type IV.
  - The presence of trabecular, canalicular, and papillary configuration should elicit a search for characteristic neural tube-like structures.
- Immature teratoma may contain fields of tubular or canalicular structures.

- Presence of disparate tissue components, such as bone, cartilage, muscle, glands, *etc.*, allows recognition as a teratoma (Fig. 6.16a–f).
- Choroid plexus carcinoma is primarily an epithelial tumor that simply expresses epithelial antigens without a neural or glial component.

6.9 PROGNOSIS

- PNETs are high grade (WHO grade IV) tumors with high recurrence even after gross total resection and high potential for leptomeningeal extension and cerebrospinal fluid dissemination.
- Survival is poor and often less than 12 months for ependymoblastoma.
- PNETs with florid neuronal differentiation (cerebral neuroblastoma and ganglioneuroblastoma) are associated with better survival and up to 30% have chances of a 5-year survival.

SUGGESTED READING

Bennet JP Jr, Rubinstein LJ (1984) The biological behavior of primary cerebral neuroblastoma: a reappraisal of the clinical course in a series of 70 cases. Ann Neurol 16:21–27

Rubinstein LJ (1970) The definition of the ependymoblastoma. Arch Pathol 90:35–45

Cruz-Sanchez FF, Haustein J, Rossi M et al (1988) Ependymoblastoma: a histological, immunohistological and ultrastructural study of five cases. Histopathology 12:17–27

Rorke LB (1983) The cerebral medulloblastoma and its relationship to primitive neuroectodermal tumors. J Neuropathol Exp Neurol 42:1–15

Gould VE, Rorke LB, Jansson DS, Molenaar WM, Trojanowski JQ, Lee VM, Packer RJ, Franke WW (1990) Primitive neuroectodermal tumors of the central nervous system express neuroendocrine markers and may express all classes of intermediate filaments. Hum Pathol 21:245–252

Burnett ME, White EC, Sih S, von Haken MS, Cogen PH (1997) Chromosome 17p deletion analysis reveals molecular genetic heterogeneity in supratentorial and infratentorial primitive neuroectodermal tumors of the central nervous system. Cancer Genet Cytogenet 97:25–31

Karch SB, Urich H (1972) Medulloepithelioma: definition of an entity. J Neuropath Exp Neurol 31:27–53

Jellinger K (1972) Cerebral medulloepithelioma. Acta Neuropathol 22:95–101

Becker LE, Sharma MC, Rorke LB (2000) Medulloepithelioma. In: Kleihues P, Cavenee WK (eds) Pathology and genetics of tumours of the nervous system. IARC, Lyon, pp 124–126

Coccamo DV, Herman MM, Rubinstein LJ (1989) An immunohistochemical study of the primitive and maturing elements of human cerebral medulloepitheliomas. Acta Neuropathol 79:248–254

Auer RN, Becker LE (1983) Cerebral medulloepithelioma with bone, cartilage, and striated muscle. Light microscopic and immunohistochemical study. J Neuropathol Exp Neurol 42:256–267

Louis DN, Reifenberger G, Brat DJ, Ellison DW (2008) Tumours: introduction and neuroepithelial tumours. In: Love S, Louis DN, Ellison DW (eds) Greenfield's Neuropathology, 8th edn. Hodder Arnold, London, pp 1960–1961

Figeroa RE, el Gammal T, Brooks BS et al (1989) MR findings on primitive neuroectodermal tumors. J Comput Assist Tomogr 13:773–778
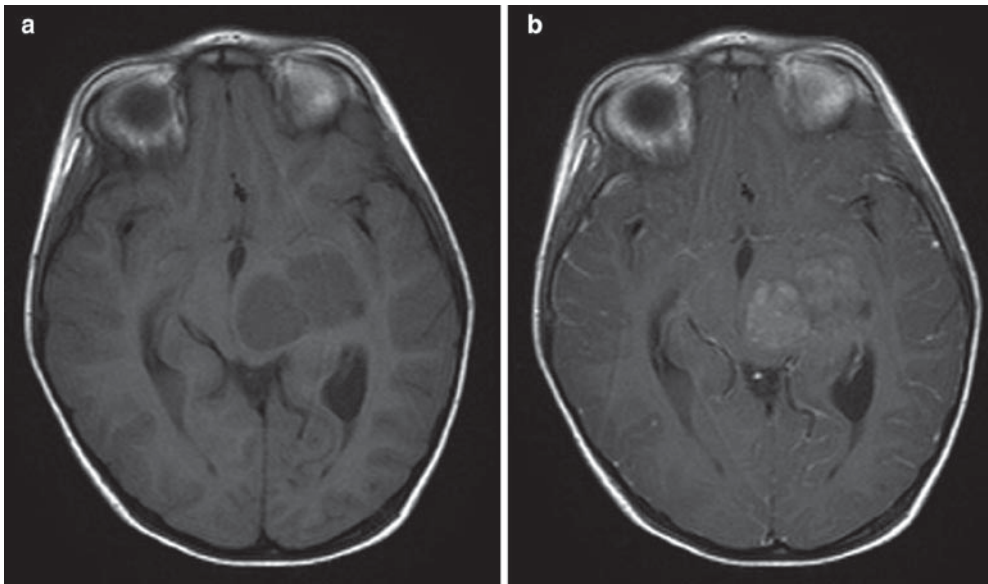
Fig. 6.1. (**a**) Axial T1-w and (**b**) axial T2-w post Gd images of a 17-month-old male with a large poorly enhancing predominantly iso-intense lesion in the left subcortical region causing mass effect and midline shift with ipsilateral hydrocephalus proven to be a supratentorial PNET.
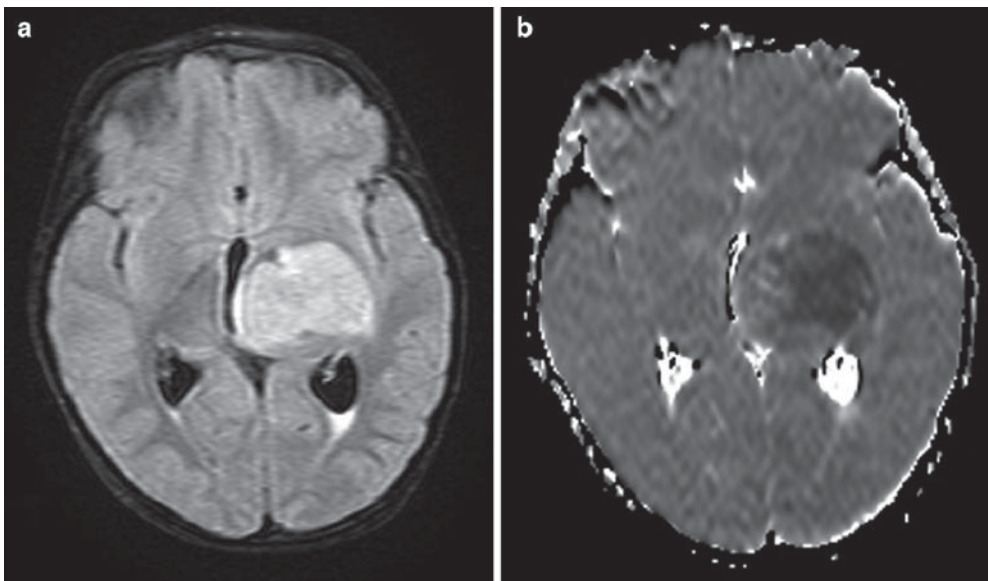
Fig. 6.2. (**a**) Axial FLAIR and (**b**) diffusion-weighted imaging demonstrating diffuse enhancement of the tumor and restricted diffusion abnormality on apparent diffusion coefficient (ADC) map.
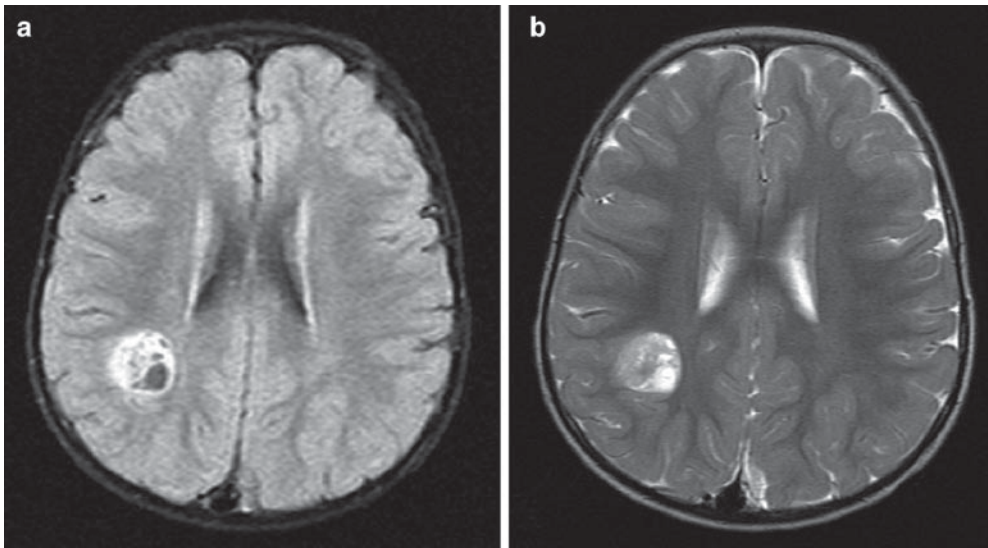
Fig. 6.3. (**a**) Axial FLAIR and (**b**) axial T1-w post gadolinium images demonstrating a contrast enhancing right parietal lobe supratentorial PNET with solid and cystic components.
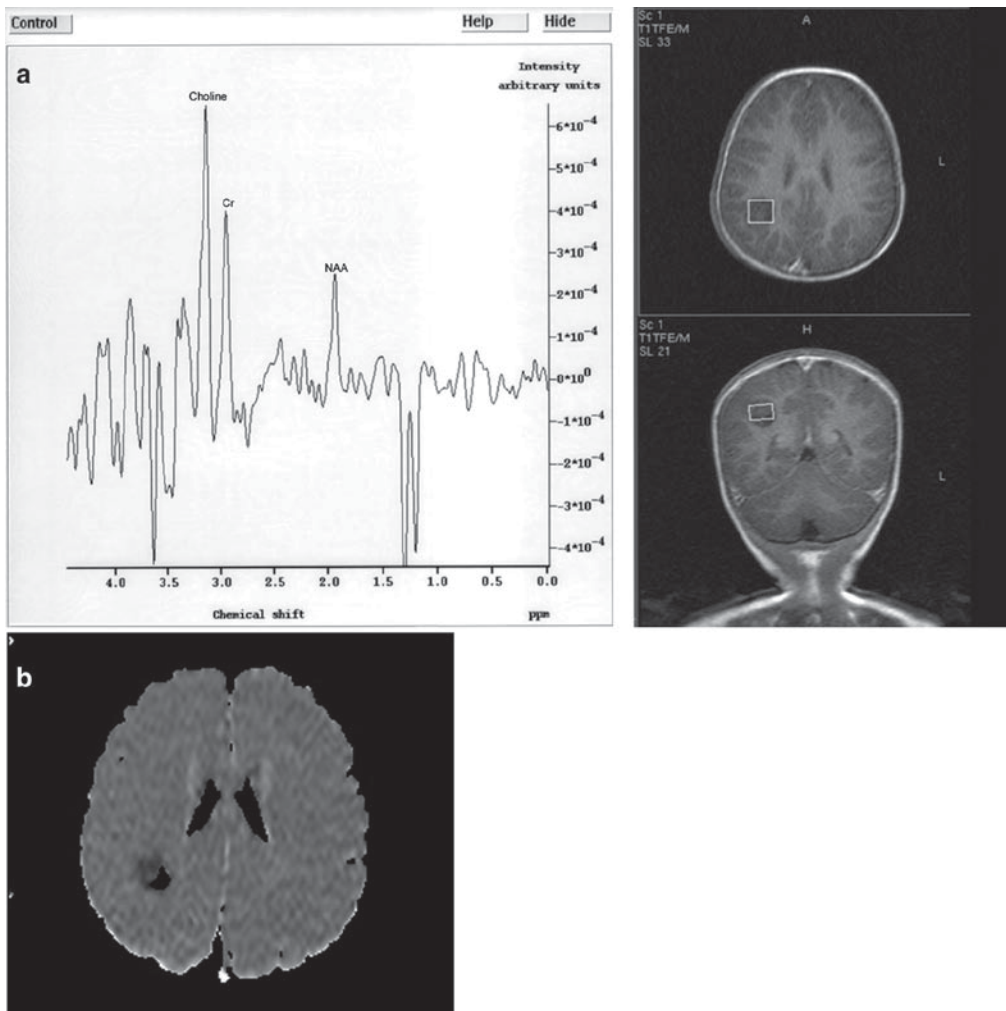
Fig. 6.4. (**a**) MR spectroscopy demonstrating elevation of the choline peak and a reduced NAA peak. The relative mildness of the elevation of the choline:NAA ratio first raised a differential diagnosis of a low-grade glial tumor. However, restricted diffusion on the ADC maps as in (**b**) suggested a cellular, more aggressive lesion, which was confirmed at histology to be a supratentorial PNET.
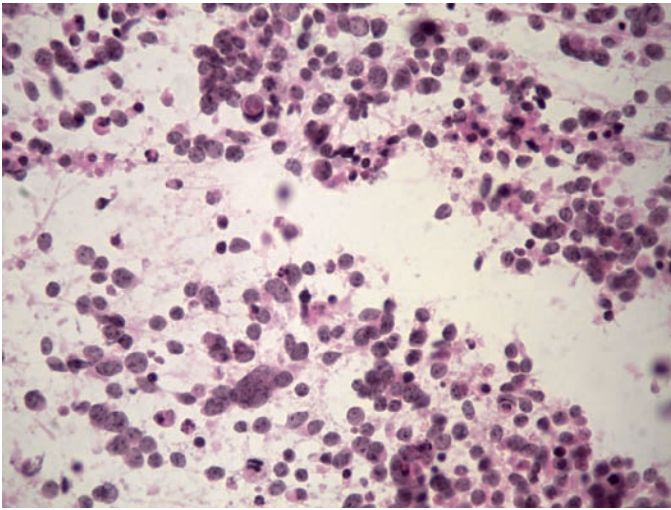
Fig. 6.5. Cytologic smear preparation showing a population of "small blue" cells with little or no cytoplasm, some nuclear pleomorphism, slightly vesicular nuclei with micronucleoli, occasional cell wrapping and few apoptotic bodies.
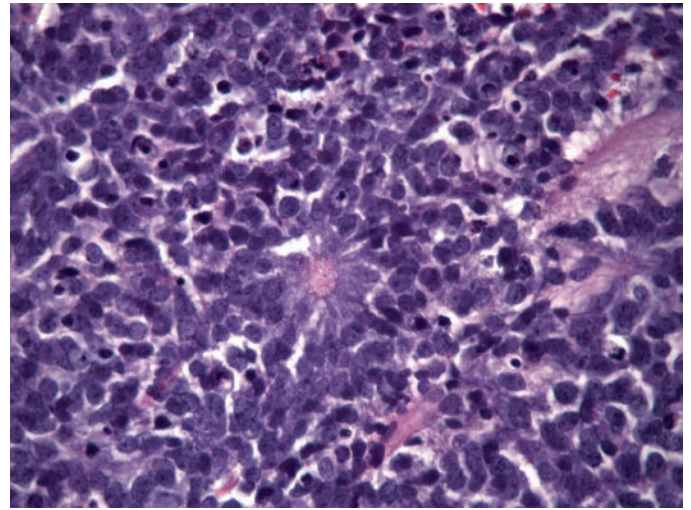
Fig. 6.7. Sheets of anaplastic tumor cells surrounding a centrally placed Flexner-Wintersteiner rosette.
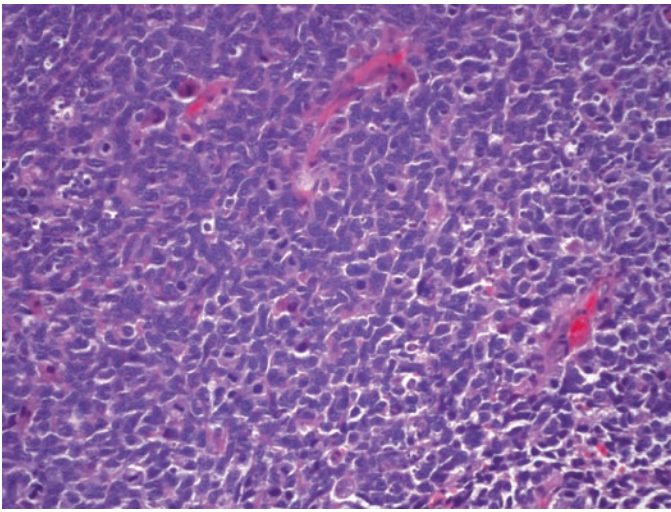
Fig. 6.6. Histologic section showing sheets of anaplastic "blue" cells with no demonstrable differentiation.
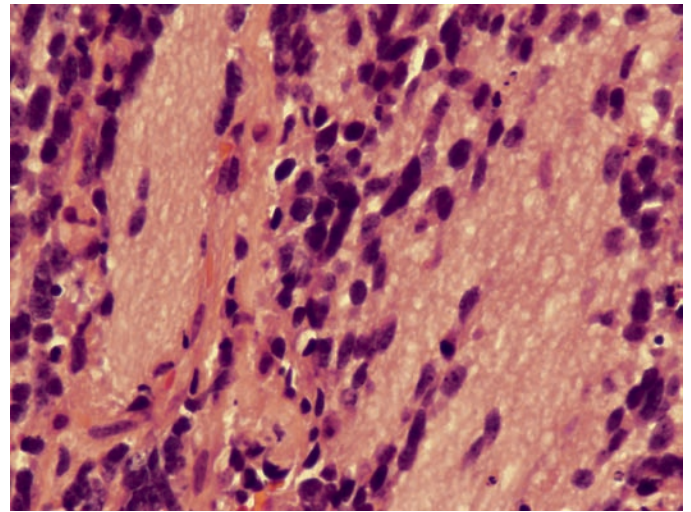
Fig. 6.8. Differentiating neuropil in a ganglioneuroblastoma.
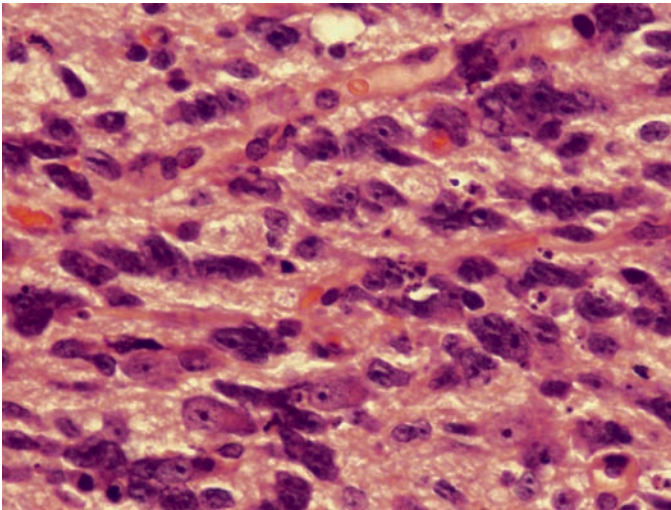
Fig. 6.9. Florid ganglionic differentiation in the same tumor illustrated in Figure 6.8.
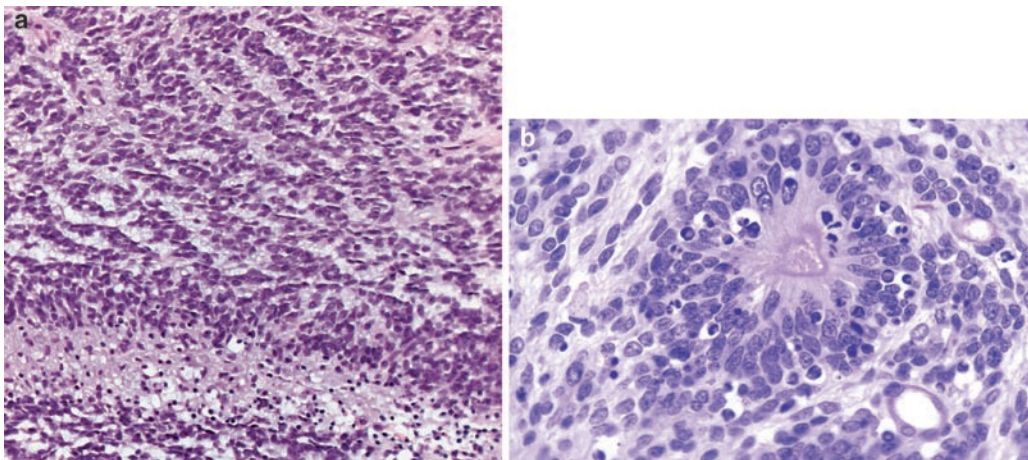
Fig. 6.10. (**a**) Rhythmic nuclear pallisades often referred to as a spongioblastomatous pattern. (**b**) Ependymoblastomatous canal/rosette showing resemblance to the primitive tubules seen in medulloepithelioma. Note the lack of an external limiting membrane, which is an important distinguishing feature. Mitotic figures are seen at the luminal border.
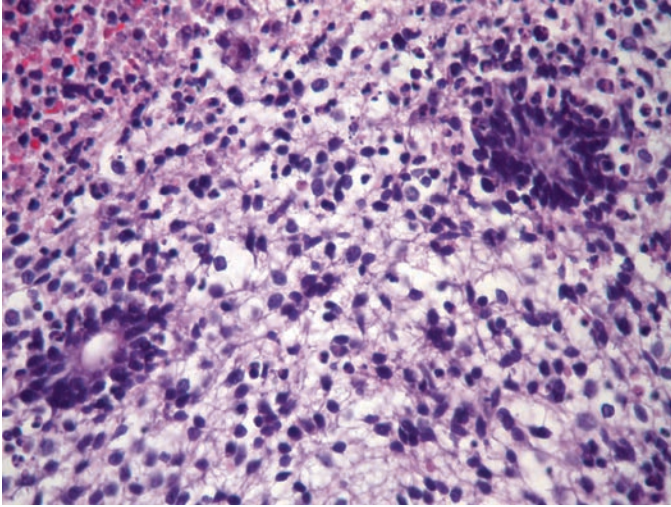
Fig. 6.11. Isolated ependymoblastic rosettes in an "embryonal tumor with abundant neuropil and true rosettes".
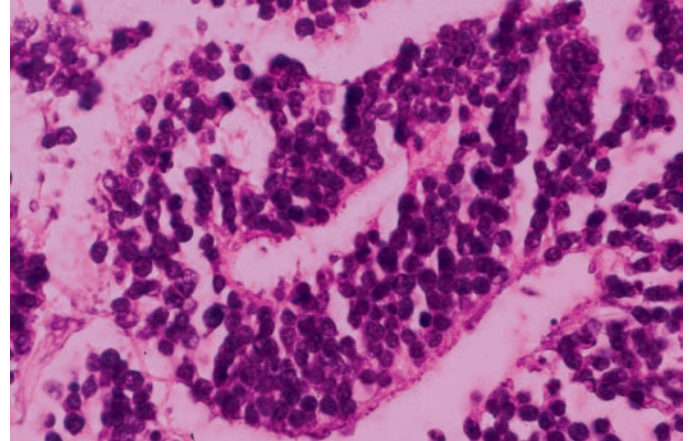
Fig. 6.13. Medulloepithelioma-type primitive tubule showing internal and external limiting membranes.
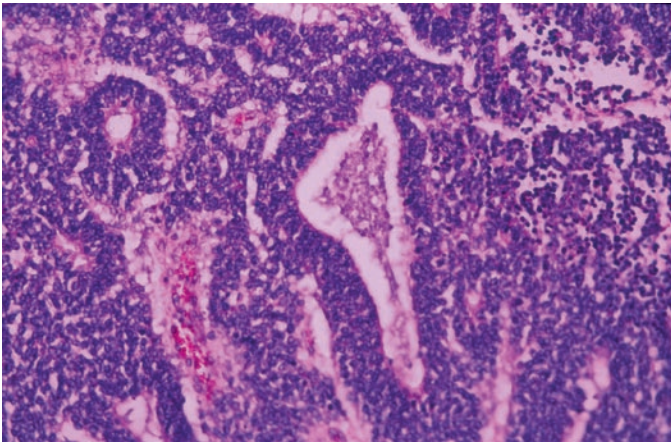
Fig. 6.12. Histology of a medulloepithelioma showing tubules of variable sizes and intervening primitive neuroepithelial cells.
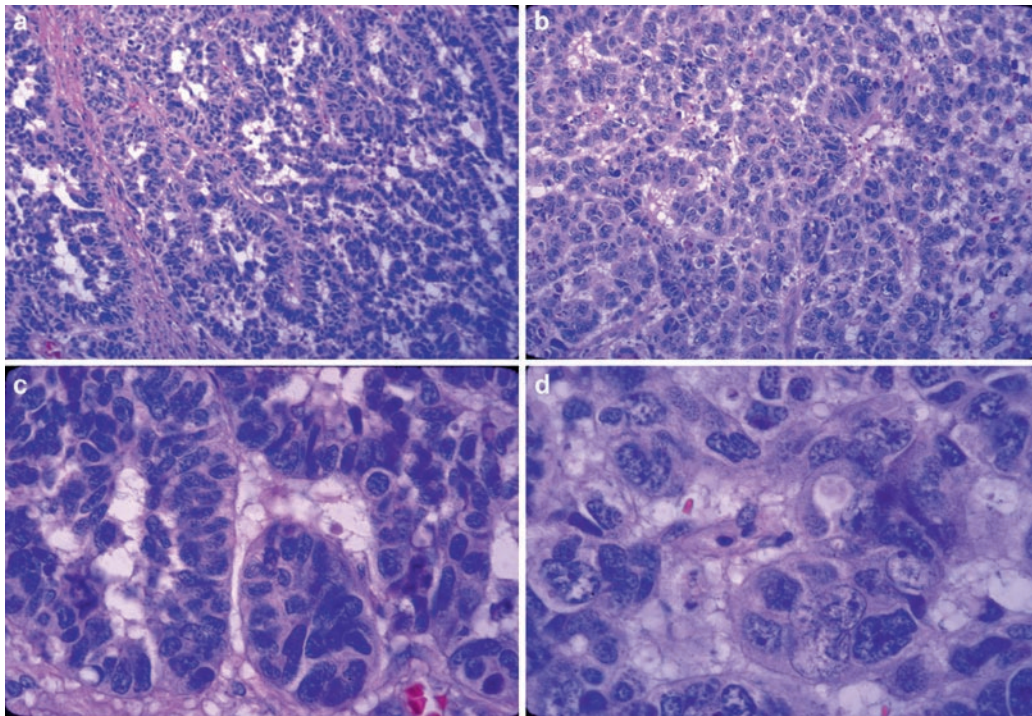
Fig. 6.14. Medulloepithelioma displaying variable histologic features and increasing anaplasia: (**a**) Region of tumor consisting of tubules. (**b**) Region of tumor composed of less well-differentiated tubules. (**c**) Tubules showing well-defined external limiting membranes. (**d**) Tubule composed of bizarre, anaplastic cells.
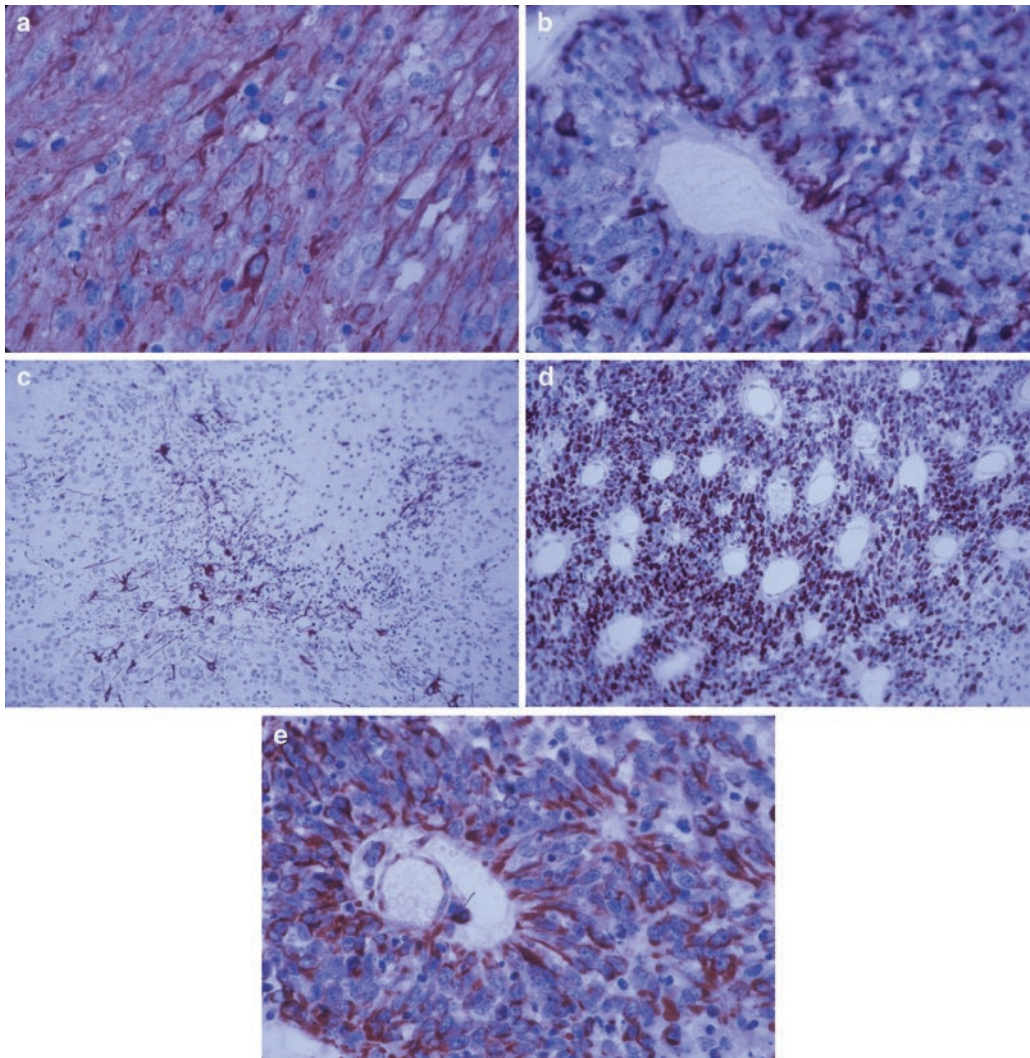
Fig. 6.15. Immunohistochemical analysis of medulloepithelioma showing: (**a**) NFP expression in differentiated region of medulloepithelioma. (**b**) NFP expression in a tubule-like structure. (**c**) GFAP expression in a differentiated region of medulloepithelioma. Some of the positive cells have features of reactive astrocytes. (**d**) Exuberant proliferative activity in tubules by PCNA immunohistochemistry. (**e**) Vimentin expression in tubules.
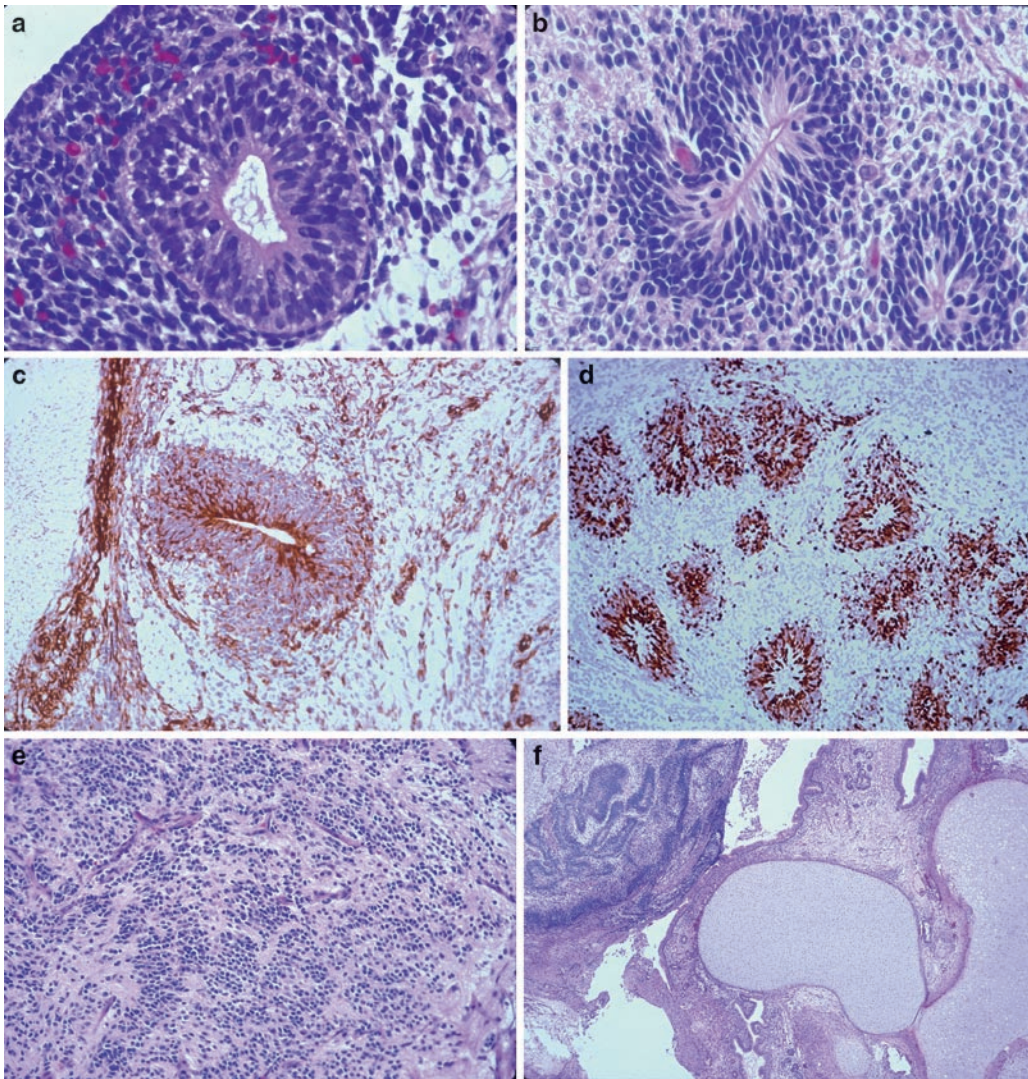
Fig. 6.16. Teratoma in parietal lobe of 3-month-old infant. (**a**) Neural tube-like structure. (**b**) Ependymomatous rosette/canal. (**c**) Vimentin expression in tubular structure. (**d**) Ki67 expression in tubular structures. (**e**) Region composed of primitive neuroepithelial cells in a background of differentiating neuropil. (**f**) Region of tumor containing cartilage, glandular epithelium, and primitive neural tissue.

Medulloblastoma

Adekunle M. Adesina and J. Hunter

Keywords Medulloblastoma; Large cell/anaplastic medullo-blastoma; Nodular/desmoplastic; Extensively nodular; Medullo-myoblastoma

7.1 OVERVIEW

- An invasive, high-grade (WHO grade IV) embryonal tumor defined both by histologic grade and location in the cerebellum.
- Even though this tumor shares histologic features with other central nervous system (CNS) primitive neuroectodermal tumors, it has been historically regarded as a distinct entity.
- Recent molecular studies including genomic and gene expression profiling, as well as signaling pathway dysregulation and biologic studies, have now justified its historic clinical definition as a distinct clinicopathologic entity with predominant occurrence in children.
- Most are sporadic.
- Less frequent occurrence in the setting of hereditary syndromes including Turcot's syndrome with germline mutation of the adenomatous polyposis coli (APC) gene and Gorlin's syndrome, the nevoid basal cell carcinoma syndrome with germ line mutation of the PTCH gene is seen in less than 2% of medulloblastomas.

7.2 CLINICAL FEATURES

- Accounts for 20% of malignant CNS tumors in childhood and is the second most common malignancy in childhood.
- Most tumors occur in children below the age of 20 with a peak between 5 and 8 years of age. A second but smaller peak is seen between 35 and 40 years. Rarely, it may be congenital.
- Patients present with symptoms and signs of cerebellar dysfunction including truncal and appendicular ataxia and raised intracranial pressure due to obstruction of the fourth ventricle and cerebrospinal fluid (CSF) flow with headache, vomiting, and progressive lethargy.

7.3 NEUROIMAGING

- Early onset of calcification of the falx cerebri, tentorium cerebelli, dura with bridging of the sella turcica due to calcification of the diaphragma sellae is seen with CT scans in 60–80% of patients with Gorlin's syndrome (Fig. 7.1).
- Typically it presents as midline vermian mass lesions in children or lateral cerebellar hemispheric tumors in adults.
- Characteristically, MRI shows a predominantly solid mass, hypointense or isointense with gray matter, with moderate diffuse nonhomogenous enhancement (Figs. 7.2–7.7).

- There is often associated restricted diffusion, consistent with a small cell and densely cellular tumor (Figs. 7.2 and 7.6).
- MR spectroscopy shows marked elevation of choline with little, if any, N-acetyl aspartate (NAA) peak (Fig. 7.8a).
  – Elevation of the taurine peak may also be seen in medulloblastoma.
- The extensively nodular variant often seen in young patients <1 year old may present with multiple grape-like enhancing nodular features (Fig. 7.8b).
- There is often evidence of mass effect including severe dilatation of the third and lateral ventricles, transependymal CSF flow, and brainstem compression (Figs. 7.10 and 7.12).
- Diffuse leptomeningeal enhancement and thecal sac drop metastases when present are consistent with CSF dissemination and poorer prognosis (Figs. 7.9–7.13).

7.4 PATHOLOGY

- Grossly, it presents as a midline vermian mass (Fig. 7.14).
- Resection specimens or intraoperative biopsies are often soft, gray-pink and appear necrotic. Extensively nodular/desmoplastic tumors may sometimes have a soft to slightly firm consistency with a lobulated appearance.
- *Intraoperative cytologic imprints or smears* show characteristic moderate cellularity. There is a good correlation between cytologic features and histologic classification as classic/nodular, anaplastic, or large cell medulloblastomas.
  – Classic and nodular medulloblastomas demonstrate monolayered sheets of relatively uniform round to oval, occasionally elongated or carrot-shaped molded nuclei with hyperchromasia and some chromatin clumping (Fig. 7.15a). Molded markedly atypical cells with high nucleocytoplasmic ratio in CSF cytospin are consistent with dissemination (Fig. 7.15b). Rosette-like arrangements representing Homer–Wright rosettes may be seen (Fig. 7.16).
  – Anaplastic medulloblastomas demonstrate a significant component of large pleomorphic cells with prominent chromatin clumping and visible nucleoli. Cell wrapping or "cannibalism" characterized by the nucleus of one cell wrapped around the nucleus of another, as well as apoptotic nuclei are frequent (Fig. 7.17). Occasional multinucleated cells may sometimes be seen.
  – Large cell medulloblastoma when present or predominant often shows a discohesive monotonous population of large cells with open chromatin and visible nucleoli sometimes mimicking the cytologic monotony of large cell lymphomas (Fig. 7.18).
  – Endothelial proliferation and mitosis may be present in all cytologic types.

– Rare evidence of cytologic differentiation with astrocytic, ganglionic, melanocytic differentiation (with melanin pigments) or rhabdomyoblastic differentiation may be seen.

7.4.1 Histology

Varied histologic features may be seen between and within tumors.
- *Classic* medulloblastomas are composed of monotonous sheets of small cells (Fig. 7.19).
  – Slight nuclear irregularity is often present.
  – Mitosis is present but often variable.
  – Necrosis with or without pseudopalisading may be present.
  – Apoptosis is often present.
  – Endothelial proliferation is present and can sometimes be florid.
  – Neuroblastic differentiation is seen as the Homer–Wright rosette (Fig. 7.20).
  – Mature neuronal differentiation as ganglion or "ganglioid" cells may be seen but must be distinguished from entrapped neurons.
  – A spindle or fascicular pattern when present is usually focal (Fig. 7.21).
  – Prominent nuclear irregularity with nucleoli and pleomorphism suggests the presence of anaplastic features which may be focal and a transition from classic to anaplastic may be appreciable (Fig. 7.22). Extensive anaplasia may justify designation as an anaplastic subtype.
  – Anaplasia may vary from slight to moderate to severe (Figs. 7.23 and 7.24).
- Regions with monomorphic discohesive large round cells with prominent nucleoli are suggestive of the presence of a large cell component (Fig. 7.25).
  – Predominance of large cells or severe anaplasia represents the *large cell/anaplastic* subtype and accounts for about 4% of medulloblastoma.
  – Severe anaplasia is often associated with increased apoptosis, increased frequency of mitotic activity, and "cell wrapping" or cannibalism.
- *Nodular (desmoplastic) medulloblastoma* is characterized by the presence of multiple reticulin-free pale nodules of neurocytic cells within a neuropil-like background, rarely mitotic with increased apoptosis (Figs. 7.26–7.28).
  – Leptomeningeal invasion with florid reactive desmoplasia (collagenous fibrosis) often demonstrating medium to large sized leptomeningeal vessels may occur but does not constitute a desmoplastic medulloblastoma (Fig. 7.29).
  – Internodular areas are reticulin-rich and are composed of cells similar to those of classic meduloblastoma.
- These areas tend to exhibit more brisk mitotic activity than seen within the pale nodules.
  – Internodular areas may sometimes show varying degrees of anaplasia (Fig. 7.23).
- The *extensively nodular medulloblastoma* (previously termed cerebellar neuroblastoma) is a variant showing florid nodularity and neurocytic differentiation with absent or minimal undifferentiated internodular component.
  – Cells are often arranged in a streaming pattern within a fibrillary matrix (Figs. 7.30 and 7.31).
  – Ganglion cell differentiation (forming cerebellar ganglioneuroblastoma) may be present as well (Fig. 7.32).
- Infrequent patterns of differentiation include:
  – Astrocytic differentiation which must be distinguished from entrapped reactive astrocytes (Figs. 7.33 and 7.34);
  – Skeletal muscle or rhabdomyoblastic differentiation, which may rarely be seen as strap cells with or without striations and constitute the *medullomyoblastoma* (Fig. 7.35a–c);
  – Melanocytic differentiation with melanin pigment production constituting the rare *melanotic medulloblastoma* (Fig. 7.36).
- Premelanosomes and melanosomes are demonstrable by electron microscopy.

7.5 IMMUNOHISTOCHEMISTRY

- Medulloblastomas show diffuse immunopositivity for synaptophysin (Fig. 7.37) and variable immunopositivity for chromogranin, neurofilament protein, and NeuN.
- Glial fibrillary acidic protein (GFAP) often highlights trapped reactive astrocytes. Rare positivity of tumor cells is seen (Figs. 7.33 and 7.34).
- Immunopositivity for retinal S-antigen and rhodopsin may be rarely seen in tumors with photoreceptor differentiation.
- Epithelial membrane antigen (EMA) is usually negative.
- *p53* immunopositivity is seen in a subset of medulloblastomas. Increased proportion of positive cells often correlates with increasing anaplasia and poorer survival (Fig. 7.38).
- MIB-1 (proliferation) index is variable, often very high and ranging between 30 and 80% (Fig. 7.39).

7.6 ELECTRON MICROSCOPY

- This shows tumor cells often paucicellular in organelles but with demonstrable neurosecretory granules.
- Cellular processes are frequent and contain microtubules.
- Synaptic type junctions may be seen.

7.7 MOLECULAR PATHOLOGY

- Medulloblastoma are presumed to arise from precursor stem cells in the external granular layer for lateral hemispheric nodular/desmoplastic medulloblastomas and dysplastic precursor cells arrested during migration for other vermian variants.
- 17p deletion with isochromosome 17q is the commonest cytogenetic abnormality in medulloblastoma, present in 30–40% of tumors (Fig. 7.40). Potential target genes in the 17p deletion include *HIC1* (17p13.3), frequently hypermethylated in medulloblastoma, and *REN* (17p13.2), a negative regulator of Hedgehog signaling pathway.
- Amplification of *MYCC* and less commonly *MYCN* is a common finding in large cell/anaplastic medulloblastoma (Figs. 7.41 and 7.42).
- Gains of *CDK6* (7q21), *hTERT* (5p15), *OTX2* (14q22), and *FoxG1* (14q12) have been reported
- Losses of 16q, 10q, and 11q are present in a subset of the tumors.
- *PTCH* gene loss of function mutation and the resulting activation of the hedgehog signaling pathway have been implicated in a subset of medulloblastomas
- Activation of *wnt* signaling pathway through mutation of the adenomatous polyposis coli *(APC)* gene has been associated with Turcot syndrome and only 3–4% of sporadic medulloblastoma.

- Increased activation of *Notch* signaling pathway, overexpression of *PAX5*, *PAX6*, and *SOX4*, and overexpression of repressors of neural differentiation *REST* and *FoxG1* have all been reported in medulloblastoma.

7.8 DIFFERENTIAL DIAGNOSIS

- Medulloblastomas may have areas with prominent perivascular pseudorosettes, thus raising anaplastic ependymoma as a major differential diagnosis.
  - However, ependymomas tend to show variation in cellularity including regions of well-differentiated ependymoma.
  - EMA is often positive in ependymomas and negative in medulloblastoma.
  - Synaptophysin is positive in perivascular pseudorosettes of medulloblastoma, while GFAP staining is more characteristic of ependymoma.
  - Nuclear positivity for NeuN is not helpful, as it may be positive in both tumor types.
- Atypical teratoid/rhabdoid tumor (ATRT) may have a prominent PNET-like small round cell component, while large cell/anaplastic medulloblastoma may mimic ATRT.
  - Fluorescent in situ hybridization (FISH) with INI-1 locus specific probe shows no demonstrable allelic deletion in medulloblastoma.
  - Similarly, immunostain with BAF-47 (anti-INI1) antibody shows positive nuclear staining in the neoplastic cells in medulloblastoma but negative staining is seen in ATRT.
- Medulloblastoma needs to also be differentiated from small cell glioblastoma.
  - The latter will characteristically show widespread GFAP positivity and lack evidence of neural differentiation (presence of Homer–Wright rosettes or neuronal immunohistochemical markers typical of medulloblastoma).
- Other small round blue cell tumors of children metastatic to the CNS, including rhabdomyosarcoma, Ewing/peripheral PNET, and leukemia/lymphoma, can all be effectively differentiated from medulloblastoma by immunohistochemistry.
  - Metastatic neuroblastoma may closely mimic medulloblastoma; however, it would be unlikely for neuroblastoma to present solely as a CNS metastasis without the primary peripheral lesion having been identified by imaging studies or from previous biopsy/ies.

7.9 PROGNOSIS

- The following clinical characteristics define high-risk patients:
  - Age < 3 years
  - Post resection residual tumor >1.5 cm
  - Metastatic disease at presentation with Chang stages M1–4
- Large cell and anaplastic histology are associated with poor survival.
- Poor prognostic molecular markers include amplification of *MYCC* or *MYCN* and overexpression of *c-erbB2* or *p53*.
- The nodular/desmoplastic and the extensively nodular phenotypes are associated with favorable outcome and better survival than the classic medulloblastoma.
- Expression of β catenin has been reported as a good prognostic marker.

SUGGESTED READING

Bailey P, Cushing H (1925) Medulloblastoma cerebelli: a common type of mid-cerebellar glioma of childhood. Arch Neurol Psychiatry 14: 192–224

Giangaspero F, Wellek S, Masuoka J, Gessi M, Kleihues P, Oghaki H (2006) Stratification on the basis of histopathologic grading. Acta Neuropathol 112:5–12

Giangaspero F, Perilongo G, Fondelli MP, Brisigotti M, Carollo C, Burnelli R, Burger PC, Garre ML (1999) Medulloblastoma with extensive nodularity: a variant with favorable prognosis. J Neurosurg 91:971–977

Giangaspero F, Rigobello L, Badiali M, Loda M, Andreini L, Basso G, Zorzi F, Montaldi A (1992) Large cell medulloblastoma. A distinct variant with highly aggressive behavior. Am J Surg pathol 16:687–693

Helton KJ, Fouladi M, Boop FA, Perry A, Dalton J, Kun L, Fuller C (2004) Medullomyoblastoma: a radiographic and clinicopathologic analysis of six cases and review of the literature. Cancer 101:1445–1454

Meyers SP, Kemp SS, Tarr RW (1992) MR imaging features of medulloblastomas. AJR American J Roentgenol 158:859–865

Panigrahy A, Krieger MD, Gonzalez-Gomez I et al (2006) Quantitative short echo time 1H-MR spectroscopy of untreated pediatric brain tumors: preoperative diagnosis and characterization. AJNR Am J Neuroradiol 27:560–572

Fig. 7.1. Axial CT examination of a patient with Gorlin (aka basal cell nevus) syndrome associated with medulloblastoma. Note the characteristic abnormal heavy calcification outlining the free edge of the tentorium as well as the falx in this young child.
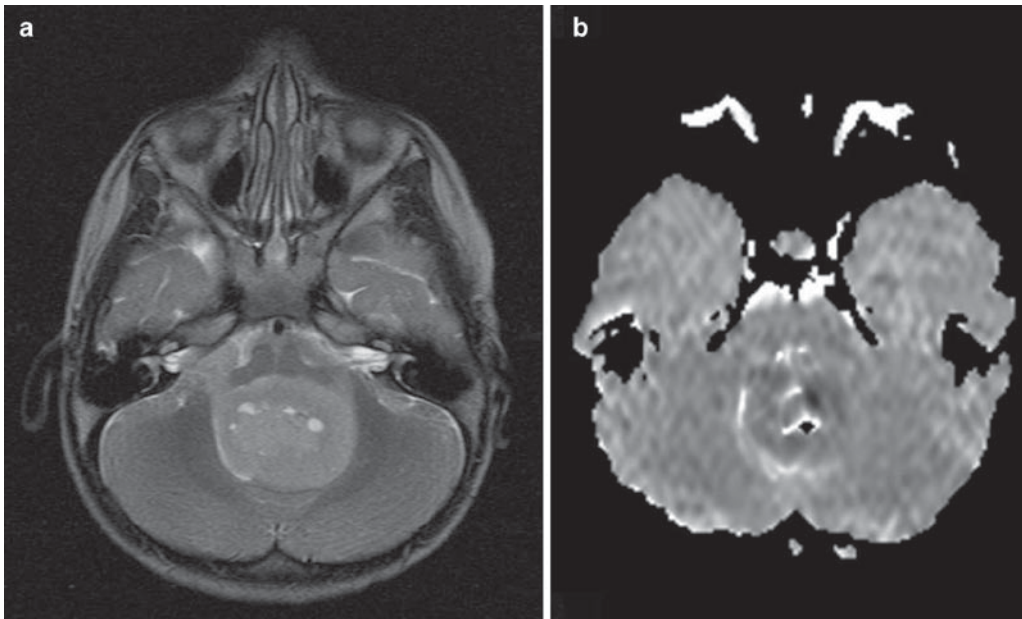
Fig. 7.2. (**a**) Axial T2-w and (**b**) apparent diffusion coefficient (ADC) maps demonstrating a heterogeneously hyperintense mass extending bilaterally to the CPAs, in a 27-month-old boy. There is restricted diffusion within the tumor which was confirmed to be a medulloblastoma on histology.
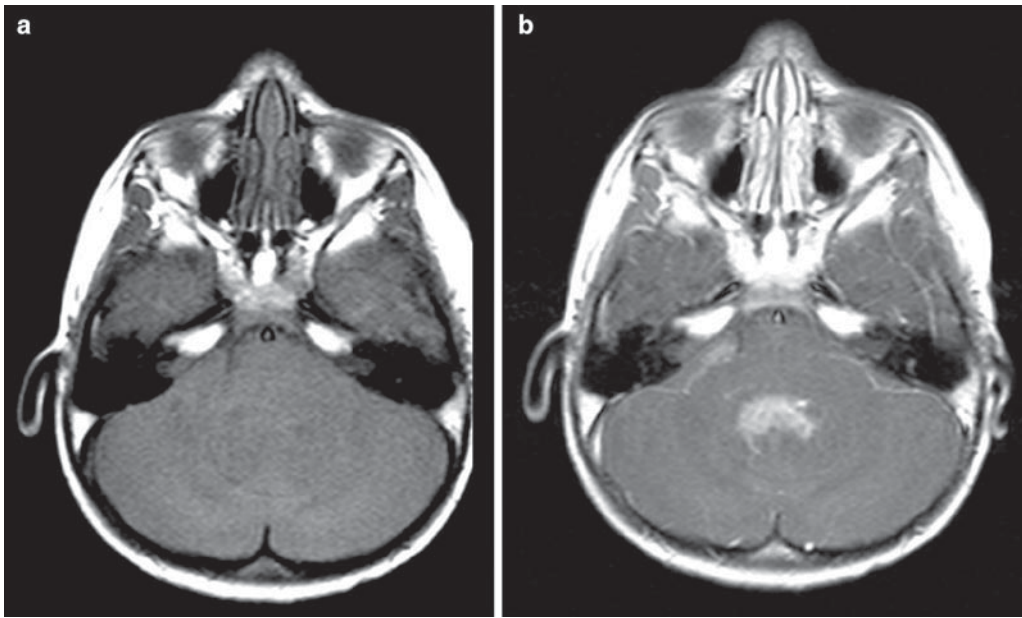
Fig. 7.3. Axial T1-w imaging (**a**) before and (**b**) after Gd demonstrates some central enhancement.

Fig. 7.4. Axial CT showing hyperdense centrally placed tumor within the posterior fossa consistent with a highly cellular tumor such as a medulloblastoma or ATRT.
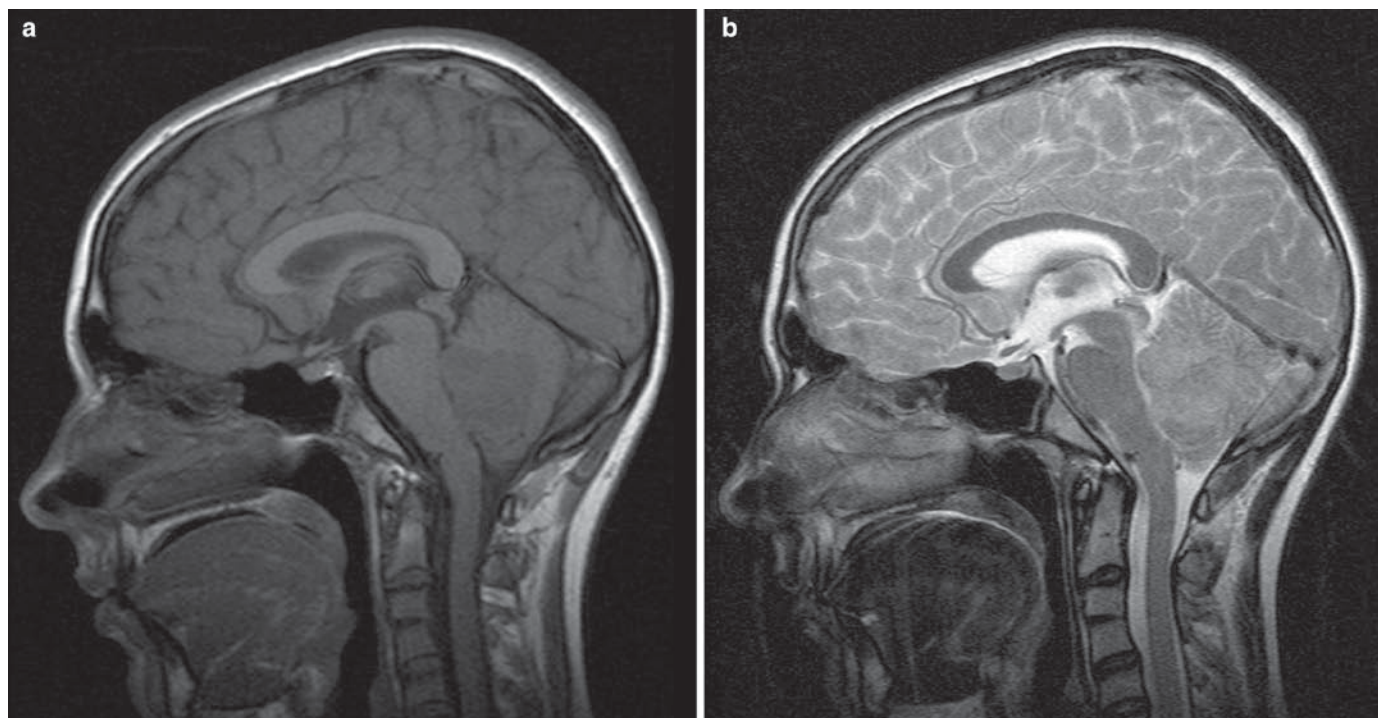
Fig. 7.5. Sagittal (**a**) T1-w and (**b**) T2-w imaging (same patient as in Fig. 7.4) demonstrates T1 hypointense and T2 hyperintense mass.
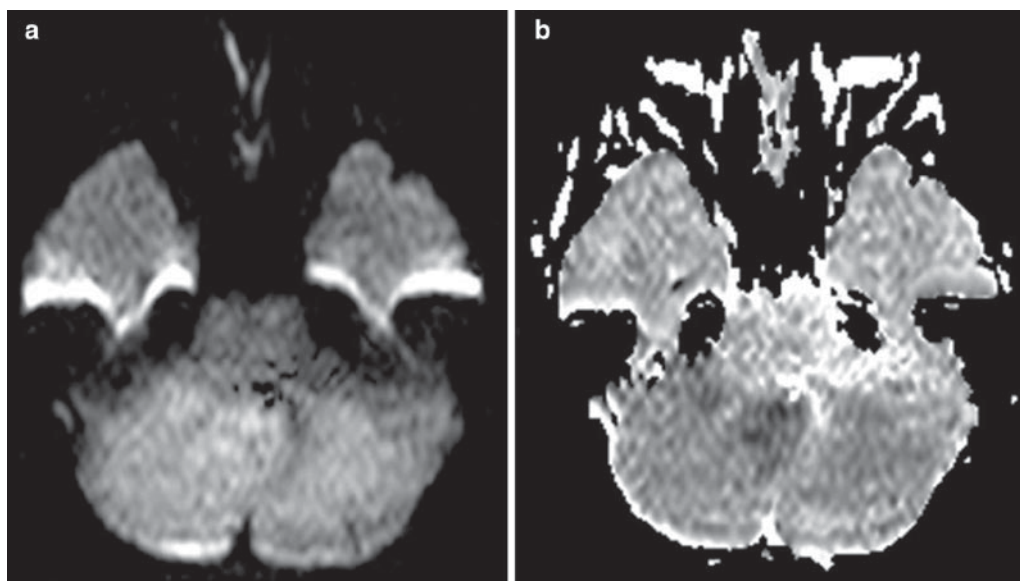
Fig. 7.6. (**a** and **b**) Diffusion weighted imaging (same patient as in Fig. 7.4) shows restriction as may be seen in a medulloblastoma, atypical teratoid rhabdoid tumor (ATRT), or anaplastic ependymoma. This case was histologically proven to be a medulloblastoma.
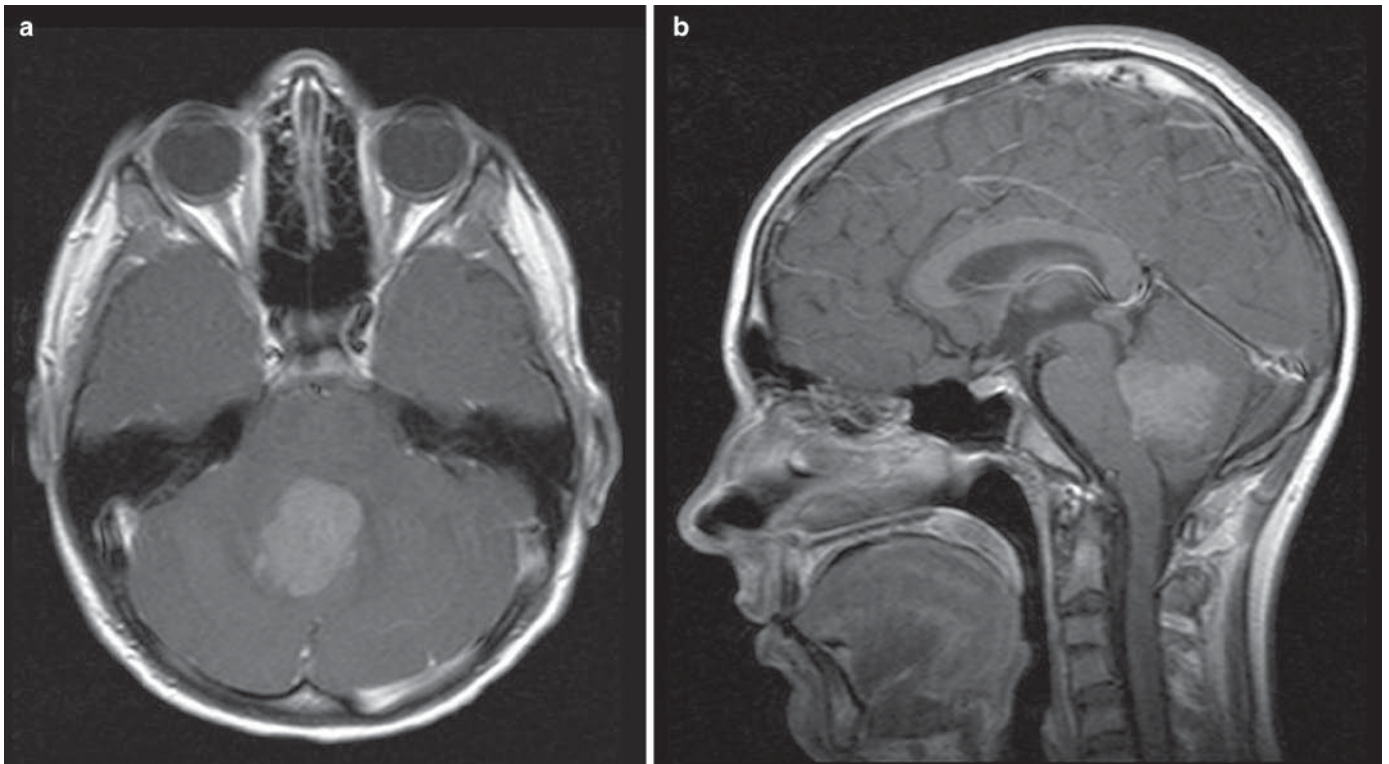
Fig. 7.7. (**a**) Axial and (**b**) sagittal T1-w images following Gd administration, showing moderate enhancement, much less than would be seen with a solid pilocytic astrocytoma.

Spectro Results

Metab	Position ppm	Area/Cr	SNR	Height/Cr	He
NAA?	2.025?	3.376?	1.9?	0.842?	
Cr	3.011	1.000	2.2	1.000	
Cho	3.220	5.712	6.7	3.046	2
Lac	1.326	9.236	3.8	1.710	1

Acquisition Parameters

Parameter	Value
Nucleus	1H
Freq	63.9
Te	136
Tr	2000
NSA	128
BW	1000
NP	4096
APsize	15
RLsize	15
FHsize	15
VOL	3375
VolSel	ECHO
ScnTyp	VS
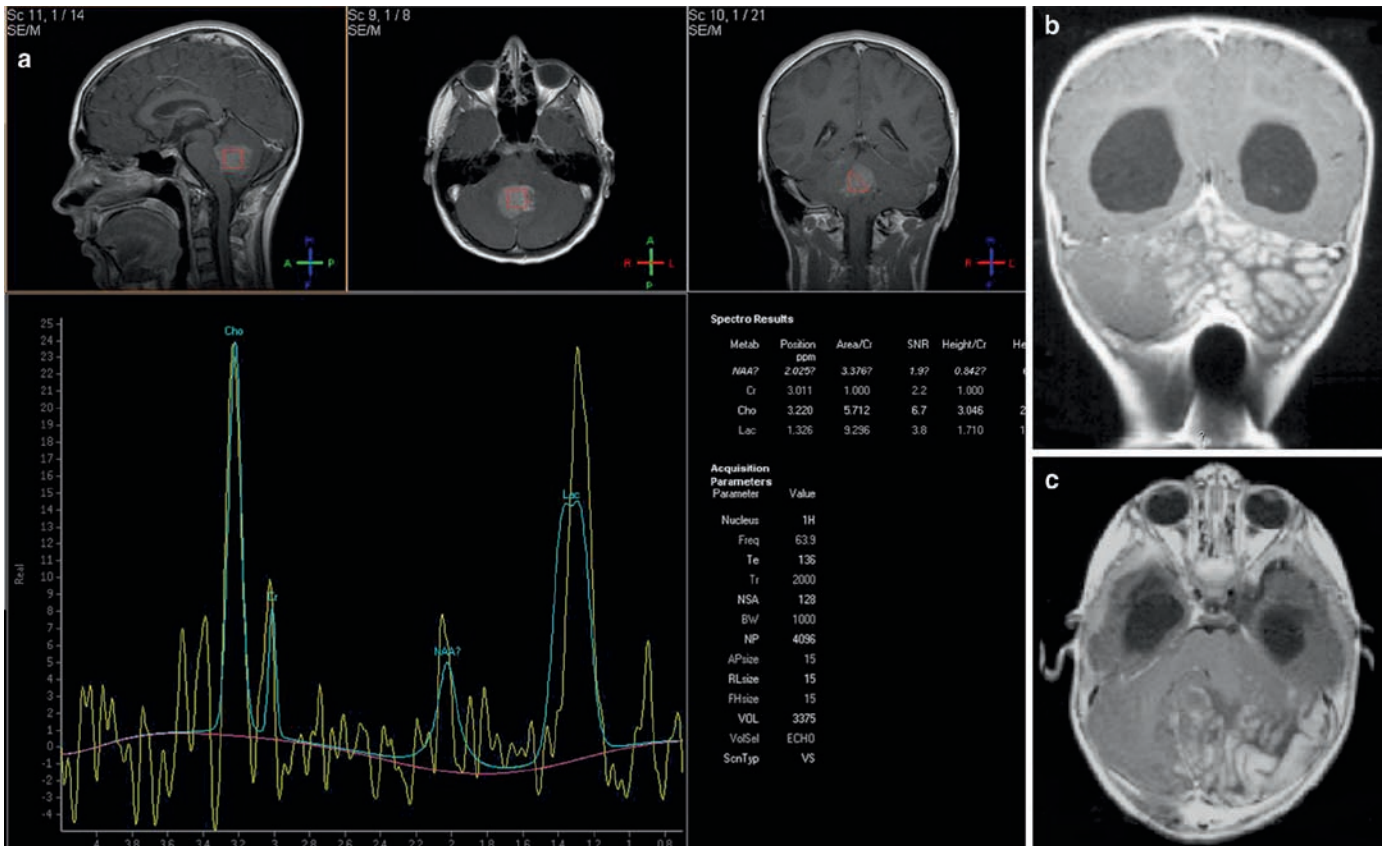
Fig. 7.8. (**a**) Typical appearances of MR spectroscopy utilizing a long TE in the same patient as in Fig. 7.7, demonstrating the presence of a marked decrease in *N*-acetyl aspartase (NAA), a marker of neuronal and axonal integrity, as well as a significant elevation in choline, a marker of cell membrane turnover. Also present is a lipid peak consistent with the presence of necrosis. (**b**) Coronal T1-w and (**c**) axial T1-w images post Gd showing cerebeller mass with grape-like nodules in a patient with an extensively nodular medulloblastoma.

Fig. 7.9. Sagittal T1-w post-Gd imaging of the lumbosacral spine in a patient with medulloblastoma, demonstrating evidence for abnormal leptomeningeal enhancement in the dorsal surface of the thoracic cord, as well as evidence for extensive drop metastases within the distal thecal sac.
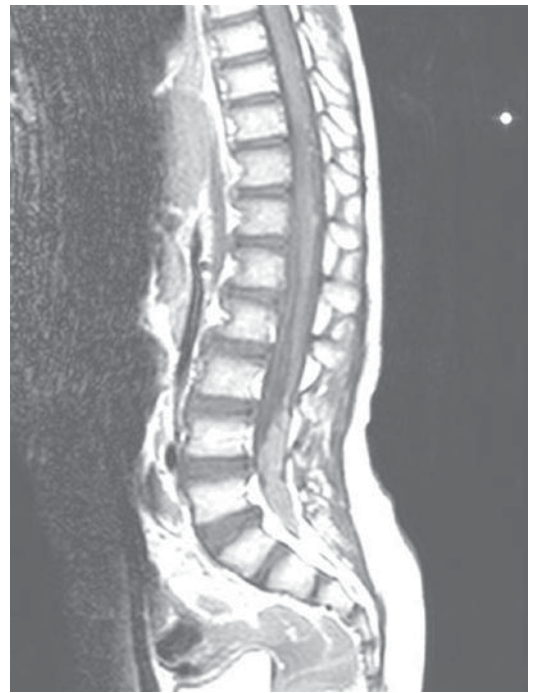
Fig. 7.10. Unenhanced axial CT demonstrating a mixed solid and cystic tumor arising in the posterior fossa and causing obstruction to the supratentorial ventricular system. The solid portion of the tumor appears hyperdense consistent with high cellularity. Note also the high density outlining the Sylvian fissures suspicious for disseminated tumor.
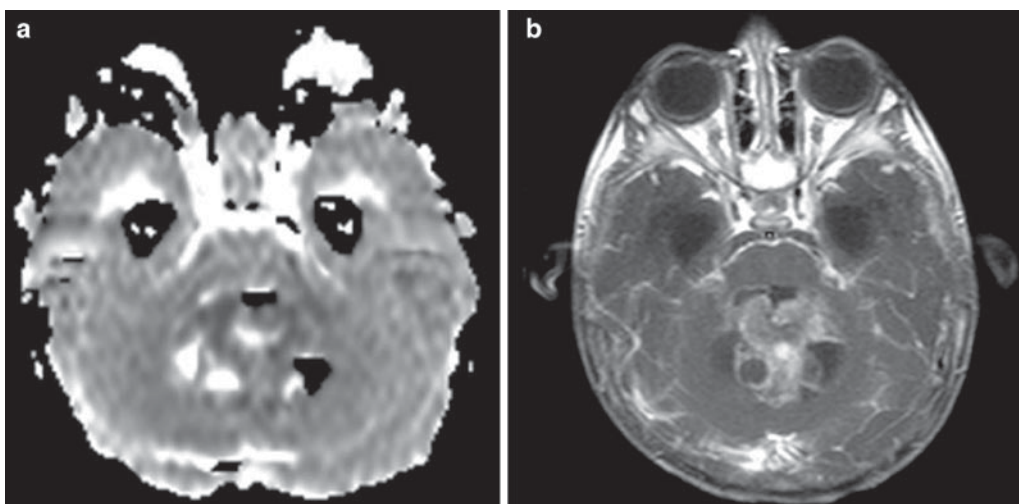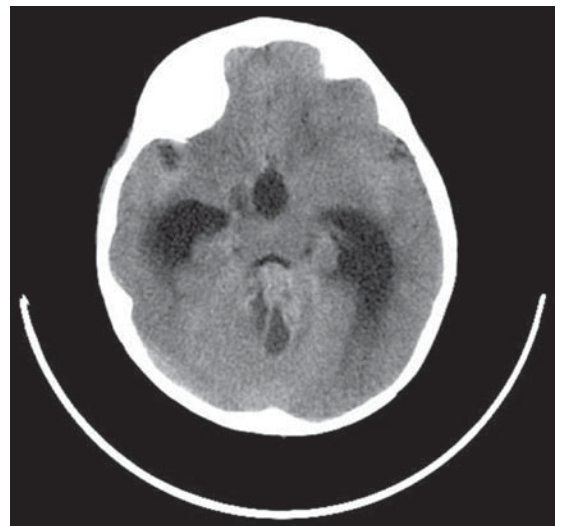
Fig. 7.11. (**a**) Restricted diffusion demonstrated within the enhancing solid portion of this tumor on the ADC map suggests a medulloblastoma, ATRT, or anaplastic ependymoma in the differential diagnosis. (**b**) Note the presence of abnormal leptomeningeal enhancement in the axial T1-w post-contrast image.
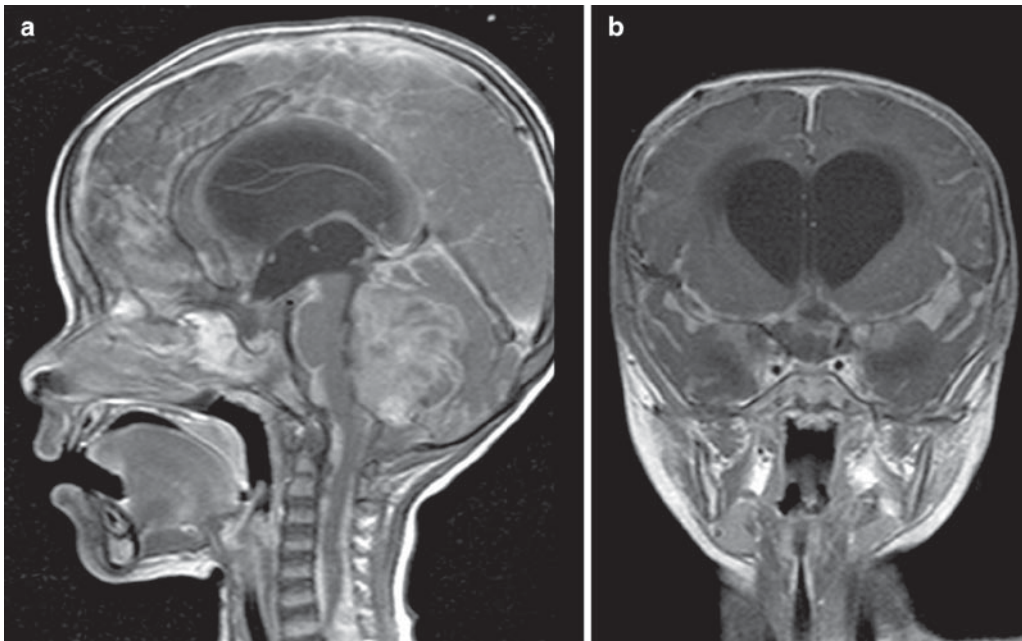
Fig. 7.12. Same patient as in Fig. 7.11 with (**a**) sagittal T1-w and (**b**) coronal T1-w images following the administration of Gd. Florid abnormal leptomeningeal enhancement is observed with hydrocephalus and extension of abnormal enhancement into the spinal canal. Histology revealed a medulloblastoma in this 15-month-old boy.
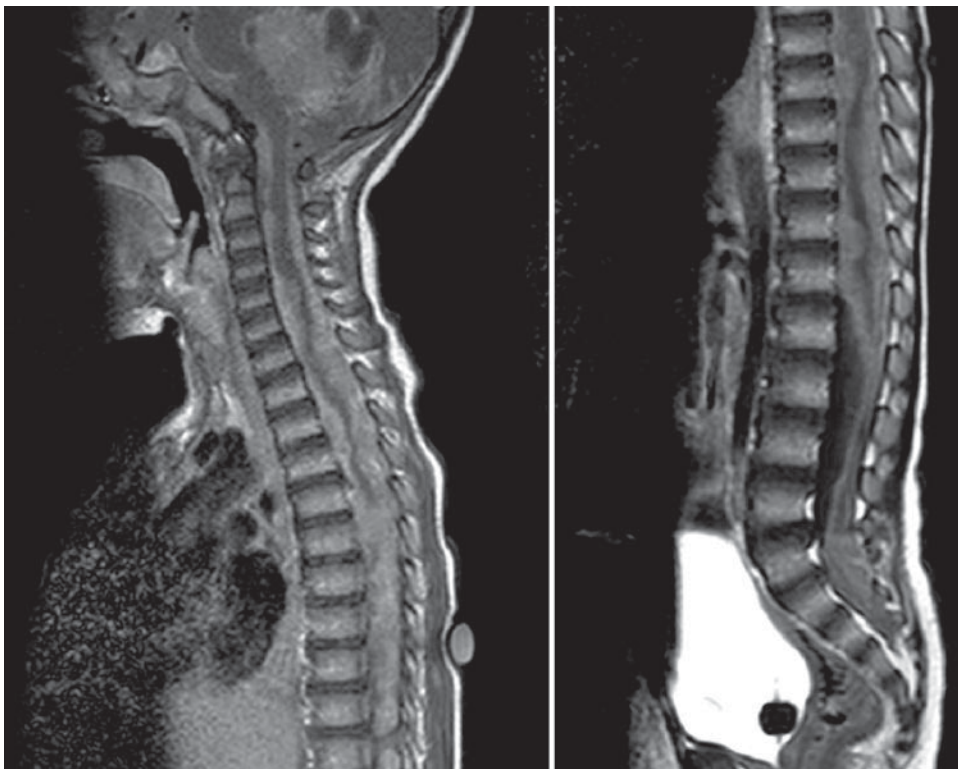
Fig. 7.13. (**a** and **b**) MR spine demonstrating extensive abnormal thick leptomeningeal enhancement surrounding the entire spinal cord at the time of presentation.

Fig. 7.14. Medulloblastoma arising in the vermis with associated necrosis and hemorrhage.
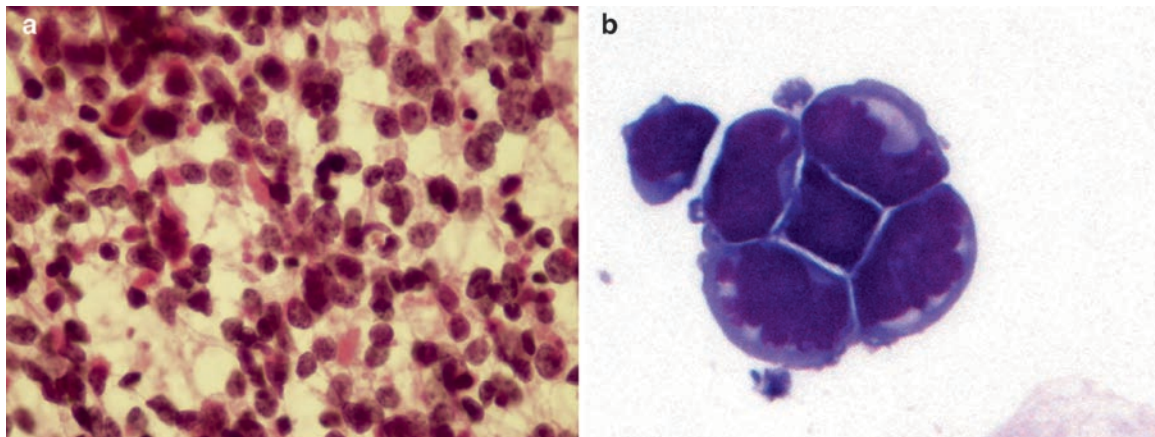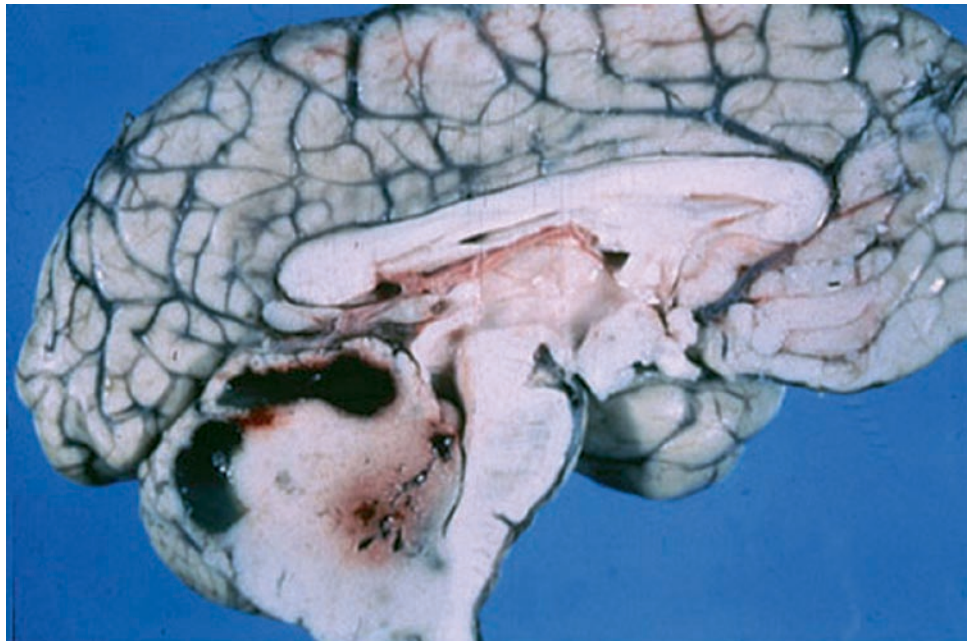
Fig. 7.15. Intraoperative cytology preparation of a classic medulloblastoma showing (**a**) "small blue" cells, with limited cytoplasm, moderate cellular pleomorphism, and nuclei with chromatin condensation and micronucleoli. Note the lack of a fibrillary background and an occasional apoptotic body. (**b**) Cluster of disseminated malignant cells in CSF in a patient with medulloblastoma showing cellular molding, irregular nuclear contour and high nucleocytoplasmic ratio.
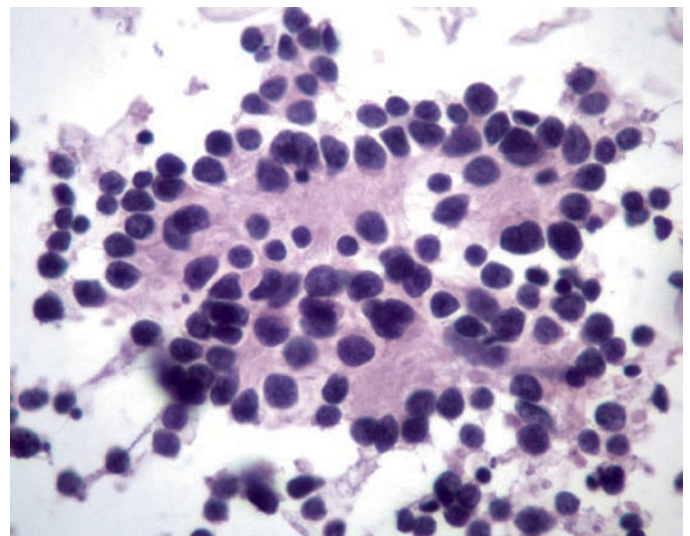
Fig. 7.16. Cytology preparation showing Homer–Wright rosettes.
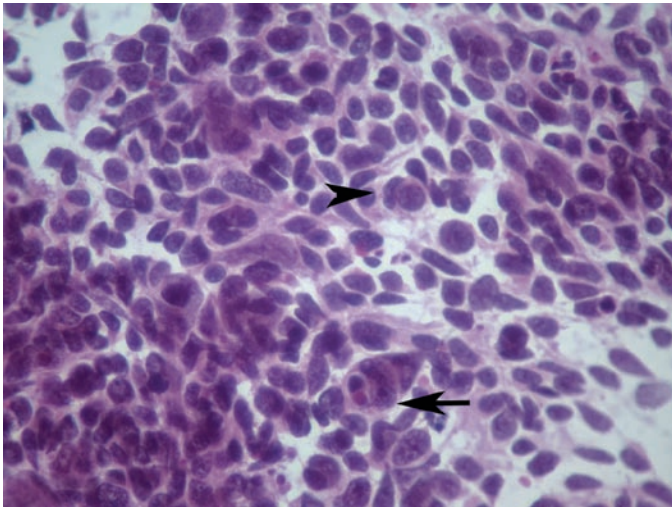
Fig. 7.17. Cytology preparation of an anaplastic medulloblastoma showing "carrot" shaped cells, moderate cellular pleomorphism, "cell wrapping" (*arrow head*), "cannibalism" (*arrow*), and hyperchromatic nuclei with chromatin condensation and micronucleoli.
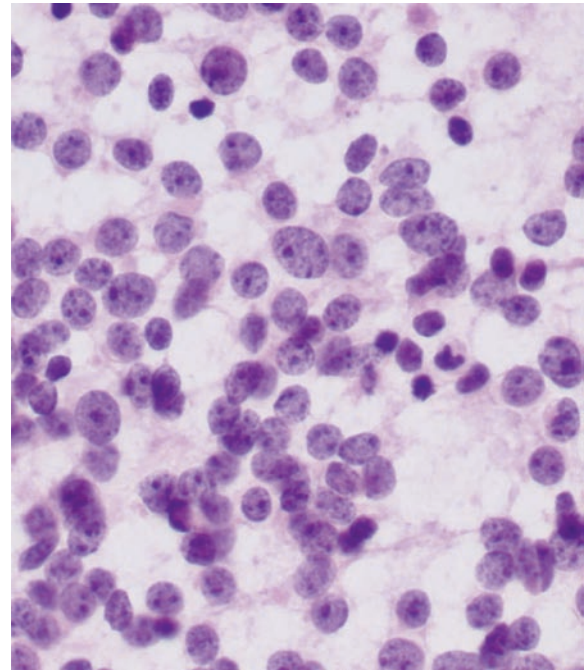
Fig. 7.18. Cytology preparation of a large cell medulloblastoma showing a monomorphic cytology, nuclei with open chromatin, and slightly prominent micronucleoli.
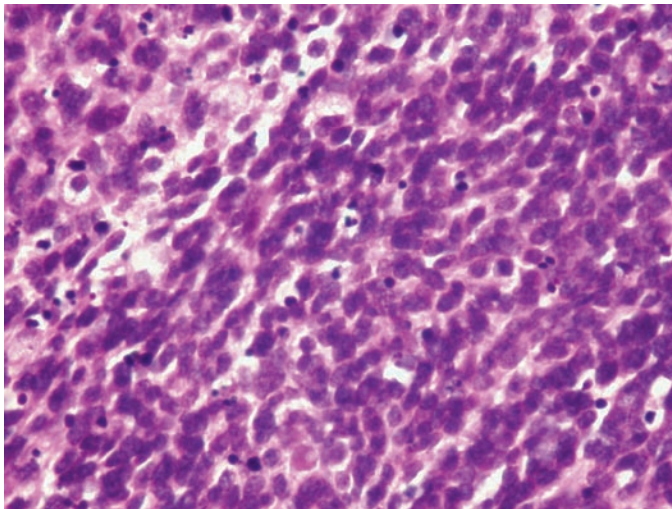
Fig. 7.19. Classic medulloblastoma with high cellularity, overlapping nuclei, some of which are "carrot" shaped. Few "dark" apoptotic bodies are present.
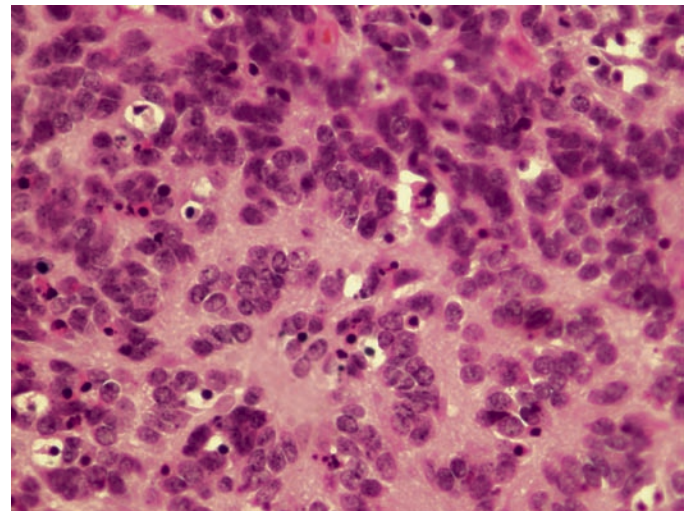
Fig. 7.20. Classic medulloblastoma with Homer–Wright rosettes.
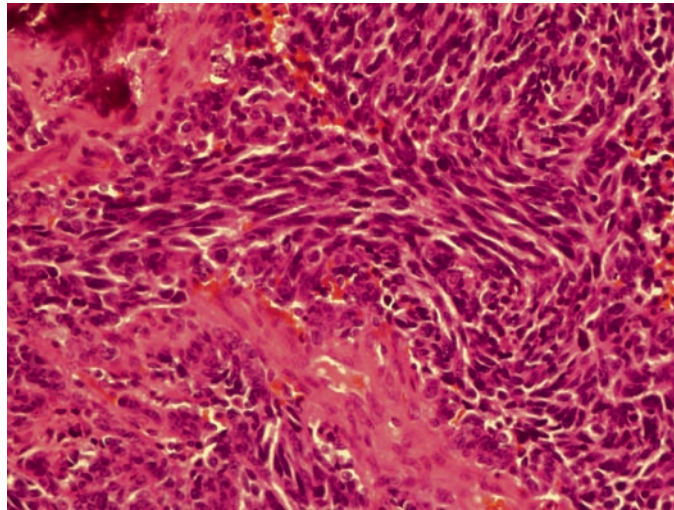
Fig. 7.21. Spindled and fascicular pattern of growth in a classic medulloblastoma.
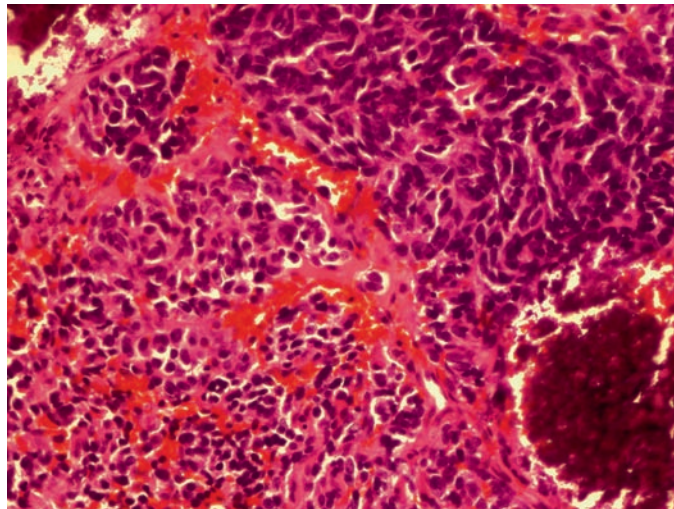
Fig. 7.22. Transition from classic medulloblastoma (*left bottom*) to low-grade anaplastic features (*right top*).
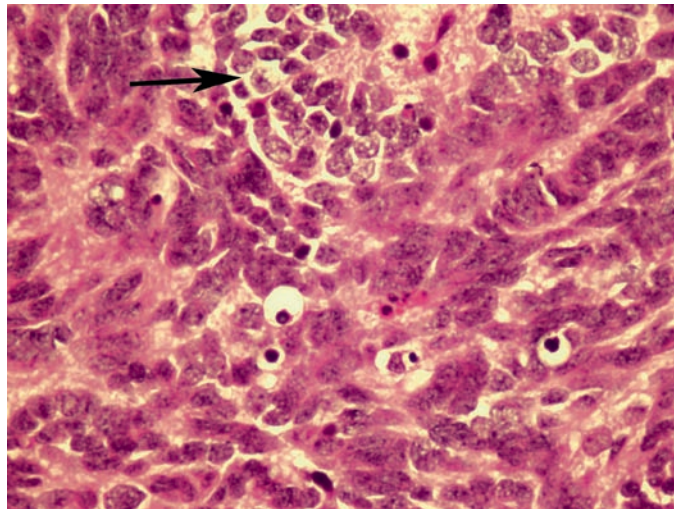
Fig. 7.23. Progressive transformation of internodular areas with increasing anaplasia is sometimes seen in desmoplastic medulloblastoma. Residual pale nodule area is shown partially at top of image (*arrow*).
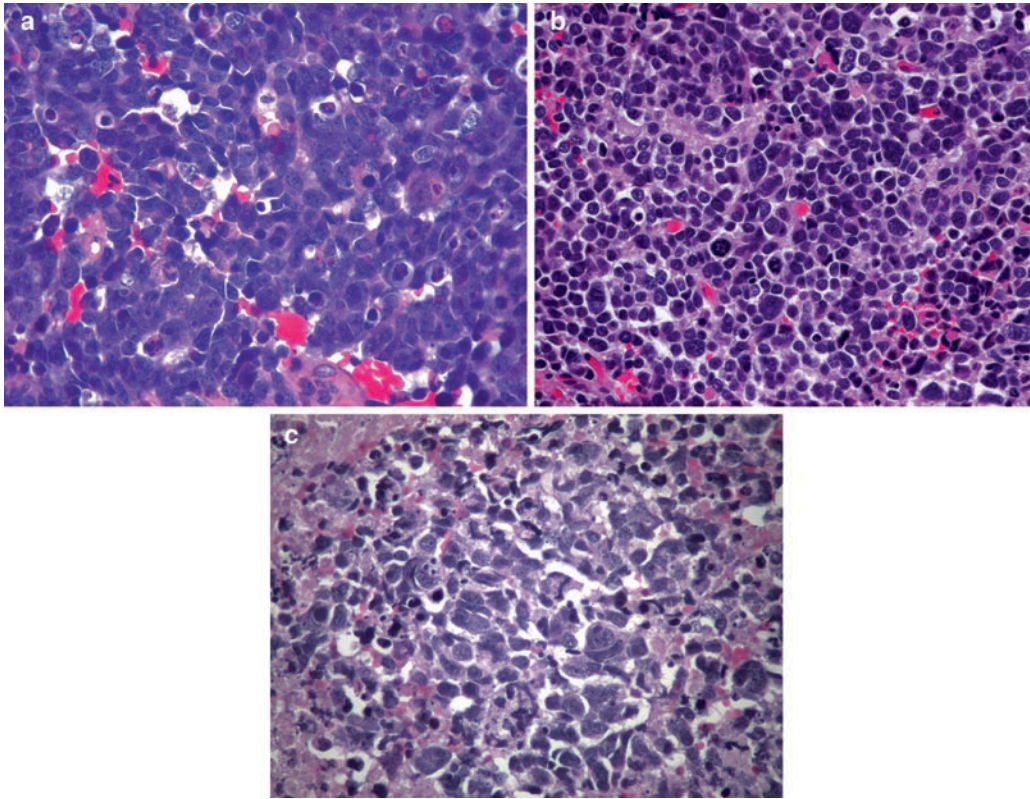
Fig. 7.24. (**a–c**) Anaplastic medulloblastoma with severe anaplasia. Note marked cellular pleomorphism, florid apoptosis, karyorrhexis, frequent "cell wrapping," and "cannibalism".
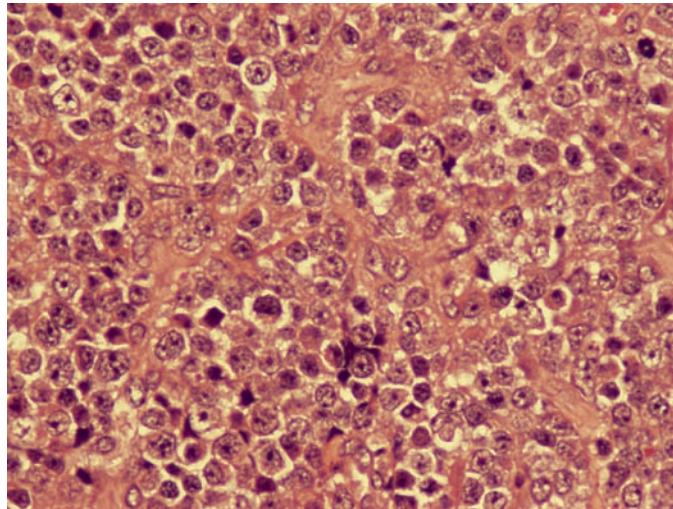
Fig. 7.25. Large cell medulloblastoma showing cellular monomorphism, vesicular nuclei, and distinct nucleoli. Note similarity of morphology to that of a diffuse large cell lymphoma.
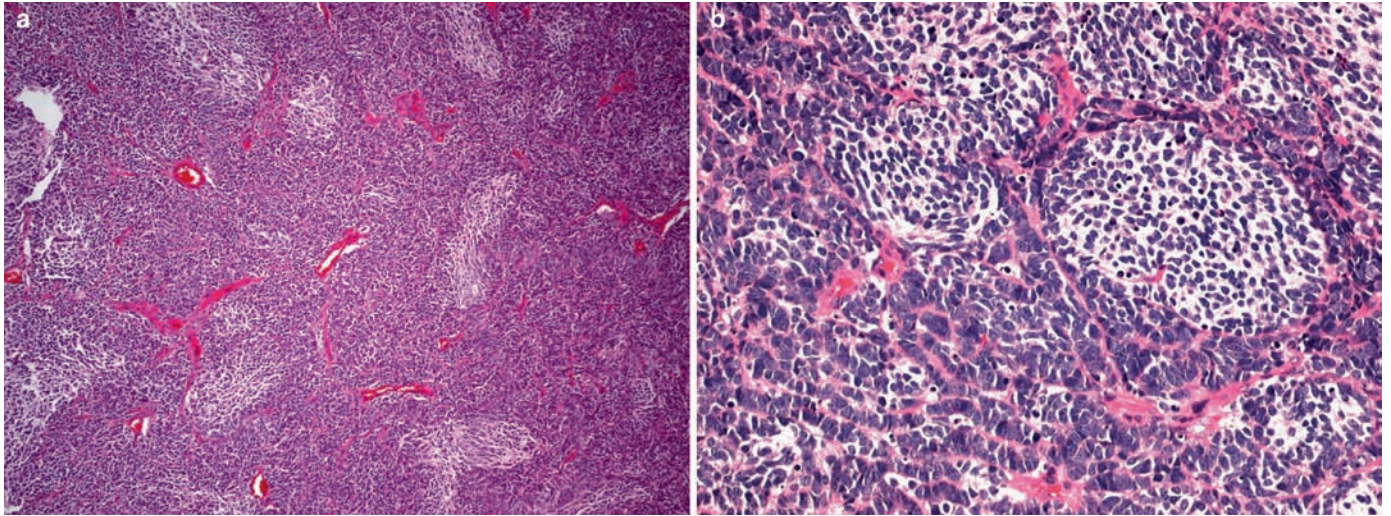
Fig. 7.26. (**a**) Low and (**b**) higher magnification of a desmoplastic (nodular) medulloblastoma showing the characteristic pale nodules.
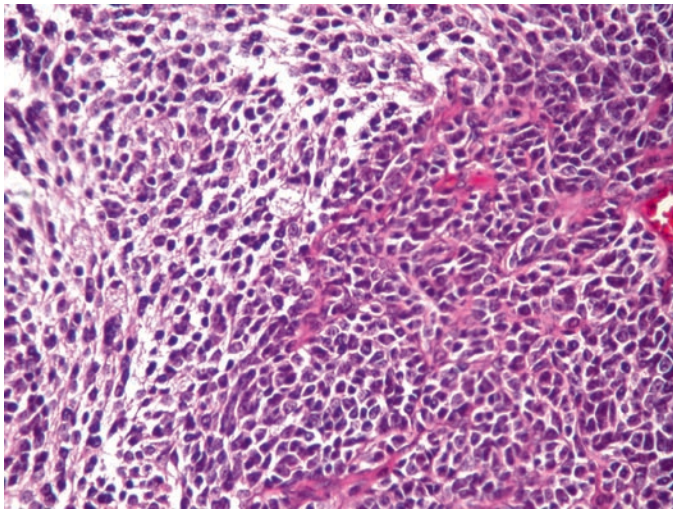
Fig. 7.27. Desmoplastic (nodular) medulloblastoma showing pale nodules (*left*) which are composed of neurocytes in a more differentiated fibrillary neuropil-like background. Contrast with the less differentiated neuroblastic internodular region (*right*).
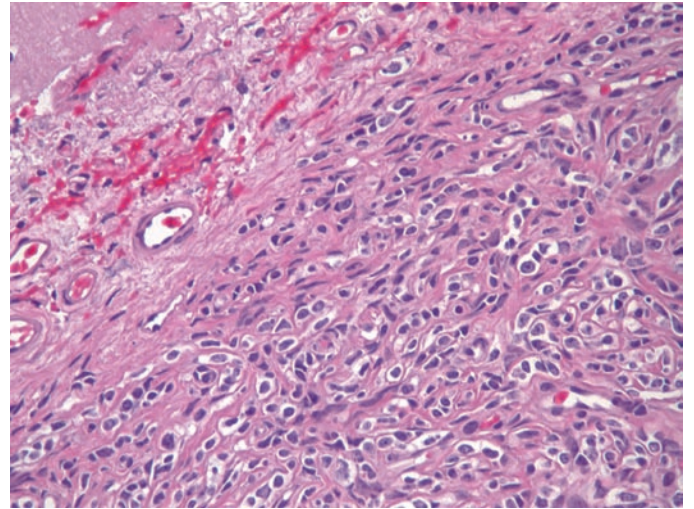
Fig. 7.29. Fibrosis following leptomeningeal invasion in a medulloblastoma. This should not be equated with a desmoplastic (nodular) medulloblastoma.
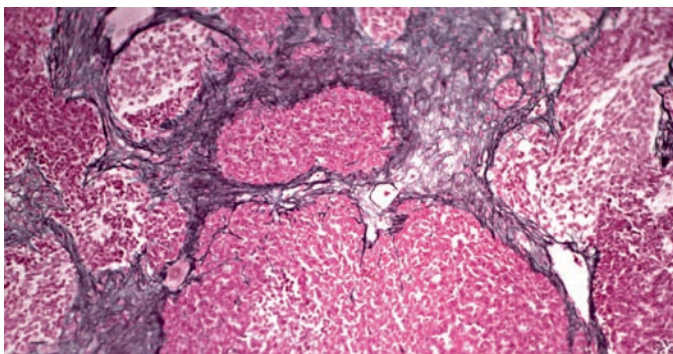
Fig. 7.28. Desmoplastic (nodular) medulloblastoma showing reticulin-free pale nodules and reticulin positive internodular areas.
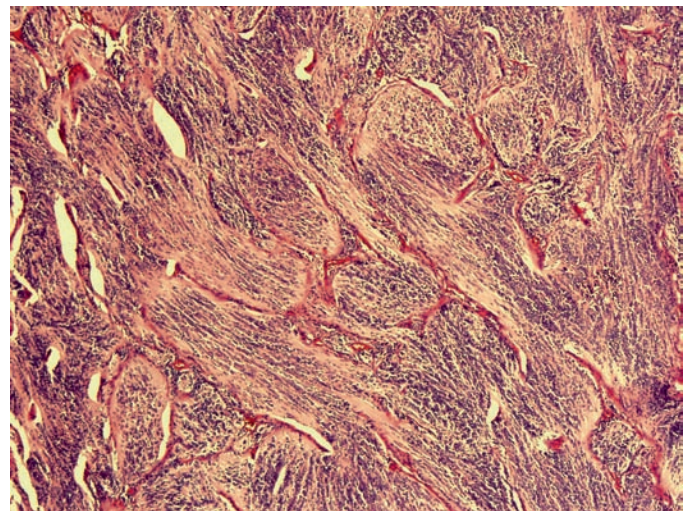
Fig. 7.30. Extensively nodular medulloblastoma composed of interlacing fascicles of differentiated neurocytes in a "fibrillary" neuropil-like matrix with limited internodular areas.
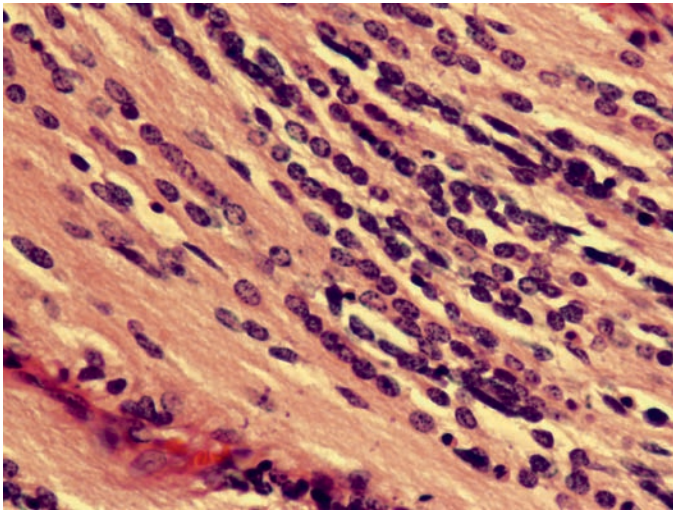
Fig. 7.31. Extensively nodular medulloblastoma with neurocytes arranged in rows reminiscent of an "indian file" pattern.

Fig. 7.32. Neuronal/ganglionic (*arrow*) differentiation in a medulloblastoma.

Fig. 7.33. Astrocytic differentiation in a medulloblastoma demonstrated by reactivity with antibody for GFAP in a subpopulation of tumor cells.
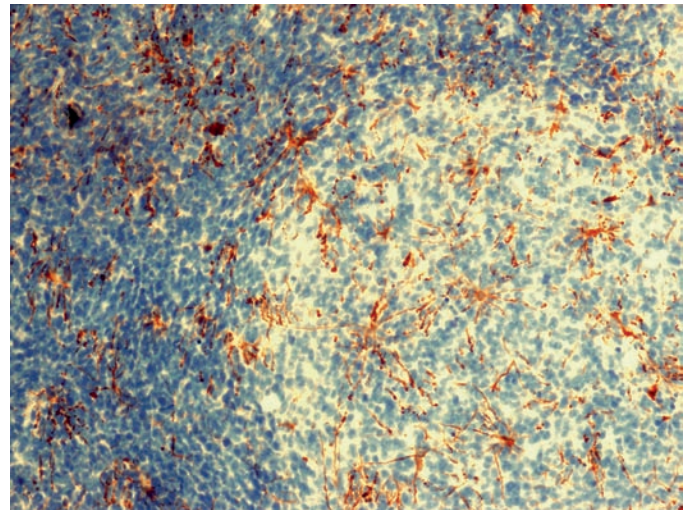
Fig. 7.34. Non-neoplastic reactive astrocytes within a medulloblastoma showing immunoreactivity for GFAP.
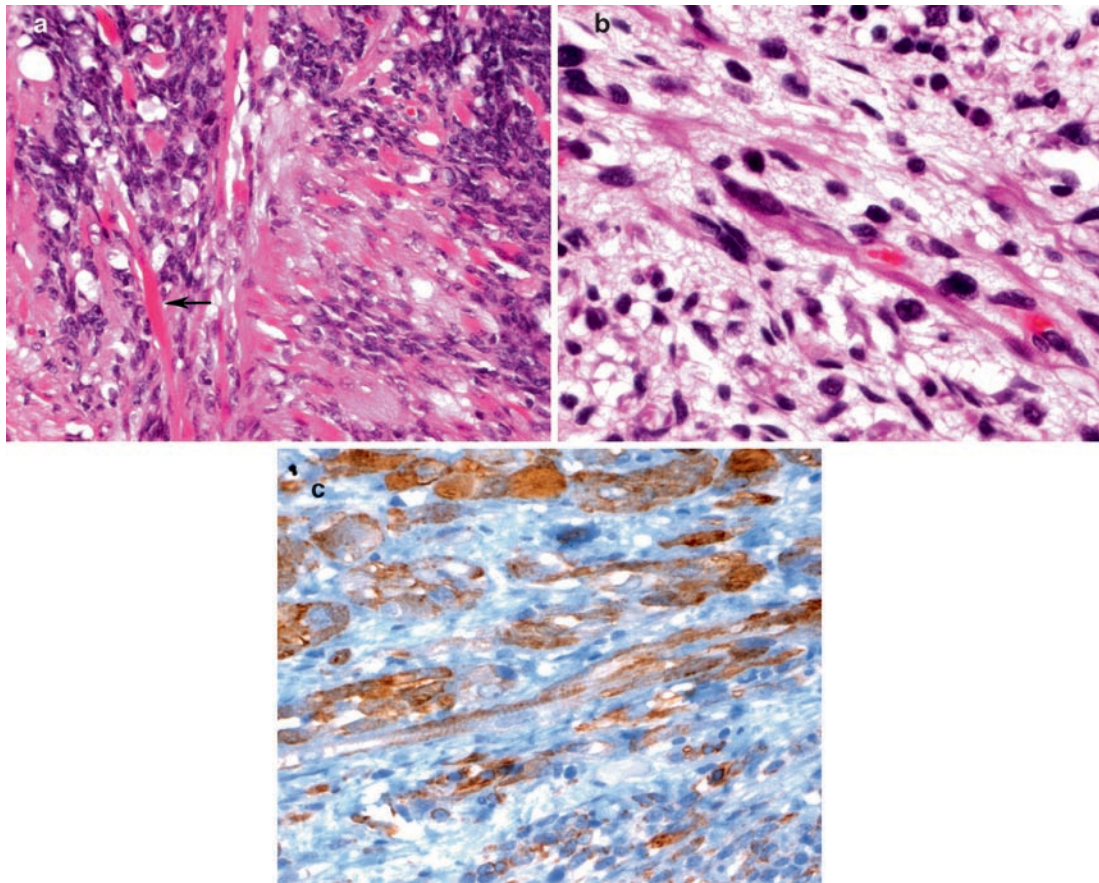
Fig. 7.35. (**a**) Medullomyoblastoma with florid skeletal muscle differentiation (*arrow*), (**b**) demonstrable strap cells with cross striations, and (**c**) desmin immunoreactivity in tumor cells.
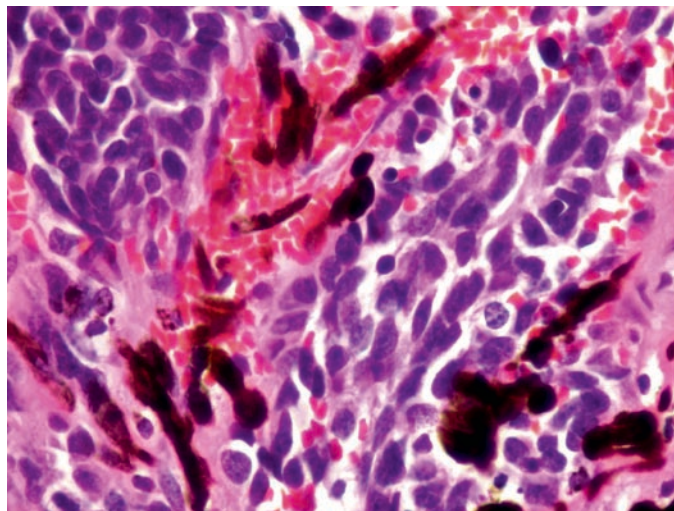
Fig. 7.36. Melanotic differentiation in a medulloblastoma.
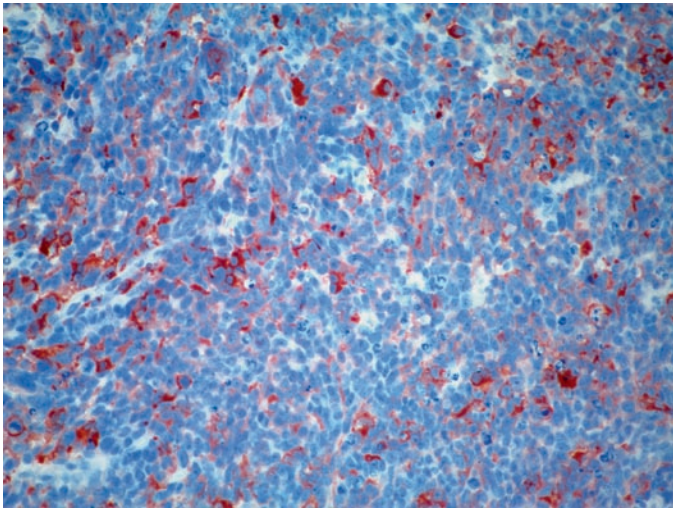
Fig. 7.37. Immunoreactivity for synaptophysin is consistent with neuroblastic differentiation in this poorly differentiated embryonal tumor.
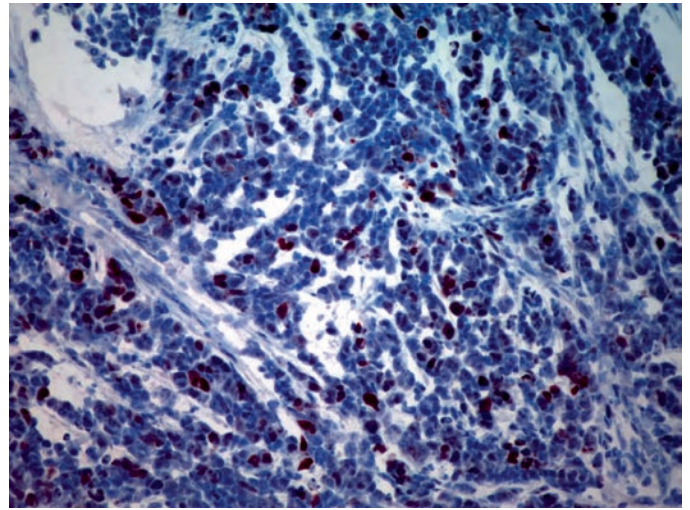
Fig. 7.38. A subpopulation of tumor cells exhibit immunoreactivity of p53 protein consistent with dysregulation of p53 in this tumor and implication for a poor prognosis.
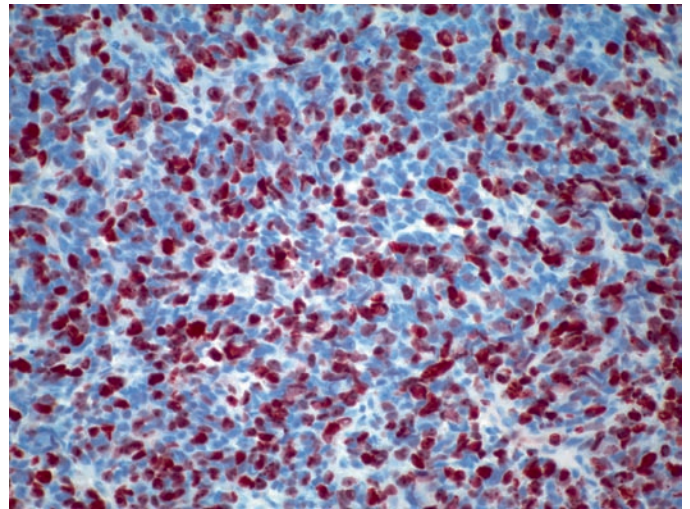
Fig. 7.39. Ki-67 immunoreactivity showing a high proliferation index.
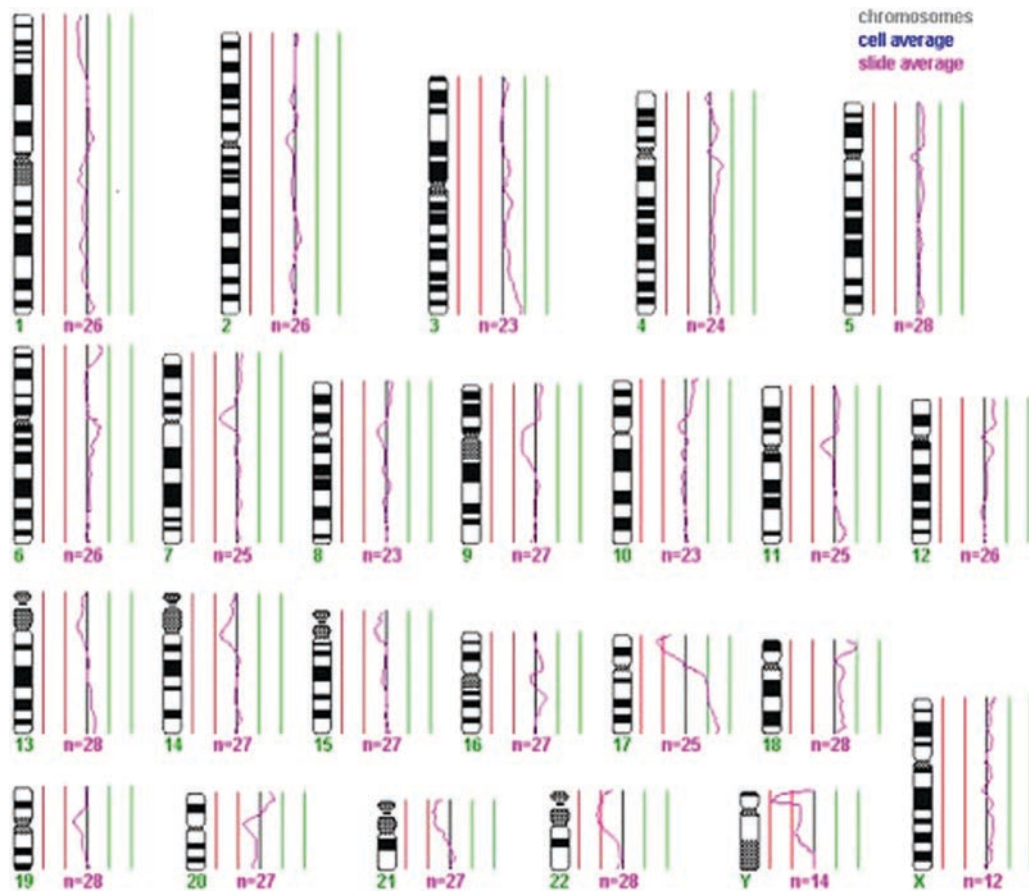
Fig. 7.40. Conventional comparative genomic hybridization (CGH) demonstrating loss of 17p and gain of 17q consistent with cytogenetic findings of isochromosome 17q.
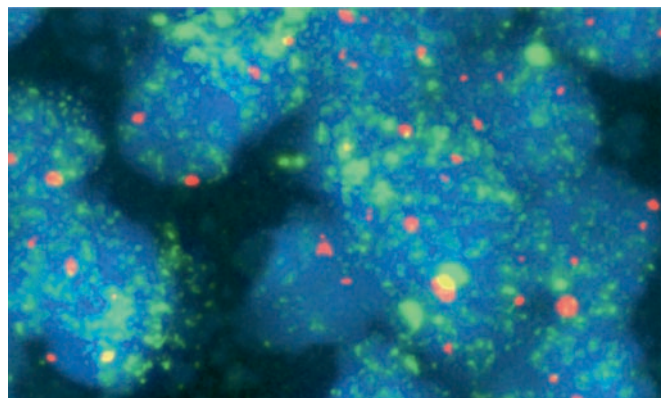
Fig. 7.41. FISH using an *N-myc*-specific probe demonstrates gene amplification (*green*) in an anaplastic medulloblastoma. Chromosome 2 centromeric reference probe is *red*.
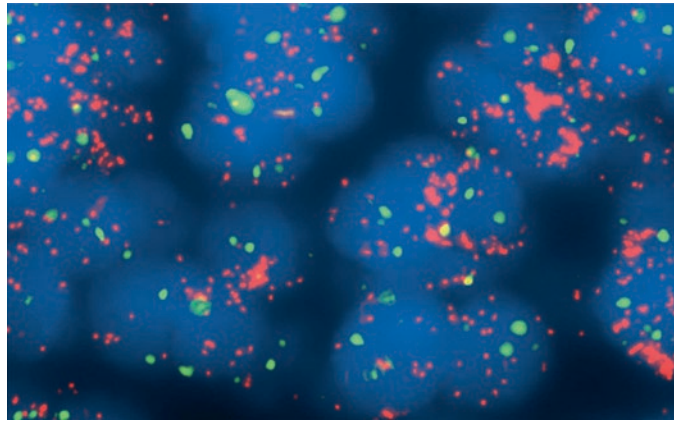
Fig. 7.42. FISH using a *c-myc*-specific probe demonstrates gene amplification (*red*) in an anaplastic medulloblastoma. Chromosome 8 centromeric reference probe is *green*.

Atypical Teratoid Rhabdoid Tumor

Adekunle M. Adesina, J. Hunter and L. Rorke-Adams

8.1 OVERVIEW

- Atypical teratoid/rhabdoid tumors are malignant high grade embryonal (WHO Grade IV) tumors seen in children often below the age of 3 years and rarely above the age of 6 years.
- Account for 10% of tumors in infants with slight male predominance, M:F ratio = 2:1
- Characteristically poorly differentiated, contain rhabdoid cells with divergent differentiation to form epithelial, mesenchymal, neuronal, and glial components and may be associated with a subpopulation of primitive neuroectodermal cells.

8.2 CLINICAL FEATURES

- Presenting symptoms are related to location that may include any of the following sites: cerebral hemispheres, suprasellar, pineal, cerebellar, cerebellopontine angle, or rarely spinal cord.
- Symptoms of raised intracranial pressure including vomiting and lethargy may occur.
- Cranial nerve palsy may be seen in cerebellopontine angle and brainstem lesions.
- Leptomeningeal dissemination is frequent and may be a presenting feature in a significant subset.
- Aggressive clinical course is typical.

8.3 NEUROIMAGING

- May present as a supratentorial mass (Figs. 8.1 and 8.2) or more commonly infratentorial mass (Fig. 8.3), classically involving the cerebellopontine angle (Figs. 8.4, 8.5–8.7).
- Though uncommon, it may also present as a spinal cord mass lesion (Fig. 8.8).
- Characteristically, MRI shows a predominantly solid mass which is hyperintense or isointense with gray matter with moderate diffuse heterogenous enhancement (Figs. 8.1, 8.2 and 8.9).
- Cystic areas and regions of necrosis may be present (Fig. 8.10a).
- There is typically associated restricted diffusion (Figs. 8.10b and 8.11a) consistent with a densely cellular tumor. The neuroimaging appearance can be radiographically indistinguishable from medulloblastoma.

- MR spectroscopy shows marked elevation of the choline peak with little, if any, NAA peak.
  - There may be an associated lipid/lactate peak within the tumor consistent with tumor necrosis.
- Diffuse leptomeningeal enhancement within the brain and spine is frequent and when present it is consistent with CSF dissemination.

8.4 PATHOLOGY

8.4.1 Gross

- Grossly tumors are variably sized, soft, variegated with pink-red hemorrhagic and sometimes necrotic appearance. In contrast to PNET, they more often contain foci of necrosis and hemorrhage.
- Significant mesenchymal component may confer a firm consistency. Uncommonly, they may contain small dense white foci reflecting a connective tissue component.

8.4.2 Intraoperative Smears

- Cytologic preparations are often cellular with cells arranged in predominantly cohesive clusters, in a necrotic background showing tumor diathesis. Rare or occasional pseudopapillary configuration (Fig. 8.12a) may be seen.
- The cells are poorly differentiated, often epithelioid and may consist of a variable component of typical rhabdoid cells with moderate size, pink cytoplasm and a round, eccentrically-placed nucleus having a prominent nucleolus (Fig. 8.12b inset).
- Poorly differentiated cells with hyperchromatic nuclei and little cytoplasm reminiscent of the "small blue" cells of a PNET may be present (Fig. 8.12b).
- Frequent mitosis, apoptosis, and cell wrapping can be seen.

8.4.3 Histology

- Histology is variable and complex. May be composed solely of sheets of rhabdoid cells (Fig. 8.13) or may consist primarily of primitive neuroectodermal cells (Fig. 8.14).
- Histology tends to be necrotic and hemorrhagic, and may contain foci of dystrophic calcification. Dilated, thrombosed blood vessels are sometimes seen as well.
- Rhabdoid cells are poorly differentiated with eccentric vesicular nuclei, prominent nucleoli, and eosinophilic (ground glass) cytoplasm containing distinct globular inclusions and with distinct cell borders (Fig. 8.15).

- Disparate tissues/cells are often recognizable without too much difficulty and may include spindled mesenchymal-type cells (Fig. 8.16a) or rare epithelium, which may be squamous (Fig. 8.16b) and/or adenomatous (Fig. 8.16c).
- Regional epithelial differentiation showing papillary, adenomatous, or cord-like pattern (Fig. 8.17) may be seen. More commonly, evidence of epithelial differentiation is only perceived by antigen expression.
- Regions of cells with prominent cytoplasmic vacuolation are frequent and should raise the differential diagnosis of ATRT (Fig. 8.18)
- Mesenchymal differentiation with desmoplastic spindle cell pattern or frank sarcomatous differentiation may be seen (Fig. 8.19).
- Mitotic activity is high, atypical mitoses can be readily identified, and cell wrapping may be seen.
- A regional component of primitive neuroectodermal cells is frequently seen but presence is not required to reach a diagnosis of ATRT. The fields of primitive neuroepithelial cells generally resembling the so called 'classical medulloblastoma' which may exhibit Homer Wright rosettes are seen in 60–70% of ATRTs.
- Rarely, a classical neurotubular structure, characteristic of medulloepithelioma, is encountered.
- The nodular architecture characteristic of desmoplastic or 'neuroblastic' medulloblastoma is not found in ATRTs, whereas distinguishing ATRT from anaplastic and large-cell medulloblastoma is challenging.
- Tumors that occur in more than one site may exhibit histological features that differ. For example, one may be composed entirely of rhabdoid cells, whereas another may be indistinguishable from a PNET/MB.

8.5 IMMUNOHISTOCHEMISTRY

- The rhabdoid cells typically show immunopositivity for EMA (Fig. 8.20a) and vimentin (Fig. 8.20b) with variable expression of SMA (Fig. 8.20c).
- Focal or regional positivity for Cytokeratin (Fig. 8.20d), GFAP (Fig. 8.20e) and neuronal markers such as synaptophysin (Fig. 8.20f) and neurofilament proteins (NFP) (Fig. 8.20g) may be seen.
- Immunostaining for SMARC1/INI1 protein is negative in tumor cell nuclei but present in endothelial cell nuclei which serve as internal control (Fig. 8.20h).
- Lack of expression of the INI1 antigen is most helpful in differentiating ATRT from look-alikes and is an indication of the rhabdoid nature of the cells.
- Ki-67 shows a high proliferation index often ranging between 25% and 85%.

8.6 ELECTRON MICROSCOPY

- The characteristic ultrastructural feature of rhabdoid cells is the presence of whorls of intermediate filaments in the perikaryon (Fig. 8.21a and b).

- Undifferentiated neuroepithelial cells have a small cell body, most of which is occupied by the nucleus with only a few organelles.
- Differentiated neuroepithelial cells show intermediate filaments, microtubules, and/or dense core vesicles.
- Epithelial cells exhibit desmosomes or longer junctions similar to zonulae adherentes, cilia, or other specific features of epithelial differentiation (Fig. 8.21c).

8.7 DIFFERENTIAL DIAGNOSIS

- Major differential diagnosis includes classic type of PNET/MB, anaplastic and large cell medulloblastoma, and choroid plexus carcinoma.
- The divergent histologic features and immunophenotype often raise the possibility of a germ cell tumor. However, the absence of differentiation into elements of the three germ layers can be helpful in distinction from germ cell tumors.
- ATRTs do not express desmin or germ cell markers such as AFP and beta HCG.
- Regions of cells with prominent cytoplasmic vacuolation may be a shared histologic feature with choroid plexus carcinoma and may be problematic with small biopsies. However, choroid plexus carcinoma shows nuclear positivity for INI1 protein.
- Interpretation of immunohistochemical findings may be complicated by the fact that PNET areas may express GFAP, NFP, vimentin, SMA, and, rarely, desmin. However, the primitive-appearing cells do not express EMA or keratin.
- Biopsies with PNET-like features and negative nuclear staining for INI11 should be regarded as representing PNET like region of an ATRT.
- The neoplastic mesenchymal component in ATRT may resemble a sarcoma. If this pattern predominates, it poses a major risk of misdiagnosis.
- Tumors that occur in more than one site may exhibit histological features that differ. For example, one may be composed entirely of rhabdoid cells, whereas another may be indistinguishable from a PNET/MB.
- Anaplastic/large cell medulloblastoma may mimic ATRT but can be easily differentiated by nuclear positivity for INI1.
- Rhabdoid meningioma shares the rhabdoid morphology with ATRT but unlike ATRT usually shows immunopositivity for INI1.

8.8 MOLECULAR PATHOLOGY

- Characteristic genetic event seen in 85% of ATRTs involves the deletion of the SMARC1/INI1 (hSNF5) locus at 22q11.2 and/or mutation of the INI gene (Fig. 8.20i).
- Biallelic (homozygous) deletion (Fig. 8.20j) or mutation of one allele followed by the loss of the second allele during homologous recombination represents mechanisms of inactivation of INI1 expression.

- Most of the mutations are nonsense or frameshift mutations leading to loss of expression of the INI1 protein.
- Loss of expression of INI1 protein without demonstrable gene mutation or hypermethylation of the INI1 gene promoter region has been described.
- Germline mutations involving the SMARC1/hSNF5/INI1 gene are associated with a novel autosomal dominant syndrome, the rhabdoid predisposition syndrome (RPS) with incomplete penetrance that predisposes to malignant posterior fossa brain tumors in infancy. Some of these cases represent recurrent, interstitial deletions mediated by low copy repeats in 22q11.2 with a predisposition to cancer.
- Spectrum of neoplasia that may be seen in RPS includes CNS ATRTs, central PNETS, medulloblastoma, choroid plexus carcinoma, as well as rhabdoid tumors in the kidneys and extrarenal tissues.
- Mechanism of action of the wild type INI protein in the prevention of neoplastic transformation is unclear.

8.9 PROGNOSIS

- Outcome in children less than 3 years is poor with survival ranging between 11 and 24 months.
- CSF dissemination is a frequent terminal event (Fig. 8.22).
- Long term survival has been observed in some of the patients with ATRTs in the setting of RPS.

SUGGESTED READING

Rorke LB, Packer RJ, Biegel JA (1996) Central nervous system atypical teratoid/rhabdoid tumors of infancy and childhood: definition of an entity. J Neurosurg 85:56–65

Burger PC, Yu IT, Tihan T, Friedman HS, Strother DR, Kepner JL, Duffner PK, Kun LE, Perlman EJ (1998) Atypical teratoid/rhabdoid tumor of the central nervous system: a highly malignant tumor of infancy and childhood frequently mistaken for medulloblastoma. Am J Surg Pathol 22:1083–1092

Manhoff DT, Rorke LB, Yachnis AT (1995) Primary intracranial atypical teratoid/rhabdoid tumor in a child with Canavan disease. Pediatr Neurosurg 22:214–222

Judkins AR, Mauger J, Rorke LB, Biegel JA (2004) Immunohistochemical analysis of hSNF5/INI 1 in pediatric CNS neoplasms. Am J Surg Pathol 28:644–650

Meyers SP, Khademian ZP, Biegel JA et al (2006) Primary intracranial atypical teratoid/rhabdoid tumors of infancy and childhood: MRI features and patient outcomes. AJNR Am J Neuroradiol 27:962–971

Giangaspero F, Rigobello L, Badiali M, Loda M, Andrieini L, Basso G, Zorzi F, Montaldi A (1992) Large cell medulloblastomas. A distinct variant with highly aggressive behavior. Am J Surg Pathol 16:687–693

Judkins AR, Burger PC, Hamilton RL, Kleinschmidt-DeMasters B, Perry A, Pomeroy SL, Rosenblum MK, Yachnis A, Zhou H, Rorke LB, Biegel JA (2005) INI 1 protein expression distinguishes atypical teratoid/rhabdoid tumor from choroid plexus carcinoma. J Neuropathol Exp Neurol 64:391–397

Sévenet N, Sheridan E, Amram D, Schneider P, Handgretinger R, Delattre O (1999) Constitutional mutations of the hSNF5/INI1 gene predispose to a variety of cancers. Am J Hum Genet 65(5):1342–8

Ammerlaan AC, Ararou A, Houben MP, Baas F, Tijssen CC, Teepen JL, Wesseling P, Hulsebos TJ (2008) Long-term survival and transmission of INI1-mutation via nonpenetrant males in a family with rhabdoid tumour predisposition syndrome. Br J Cancer 98(2):474–9

Jackson EM, Shaikh TH, Gururangan S, Jones MC, Malkin D, Nikkel SM, Zuppan CW, Wainwright LM, Zhang F, Biegel JA (2007) High-density single nucleotide polymorphism array analysis in patients with germline deletions of 22q11.2 and malignant rhabdoid tumor. Hum Genet 122(2):117–27
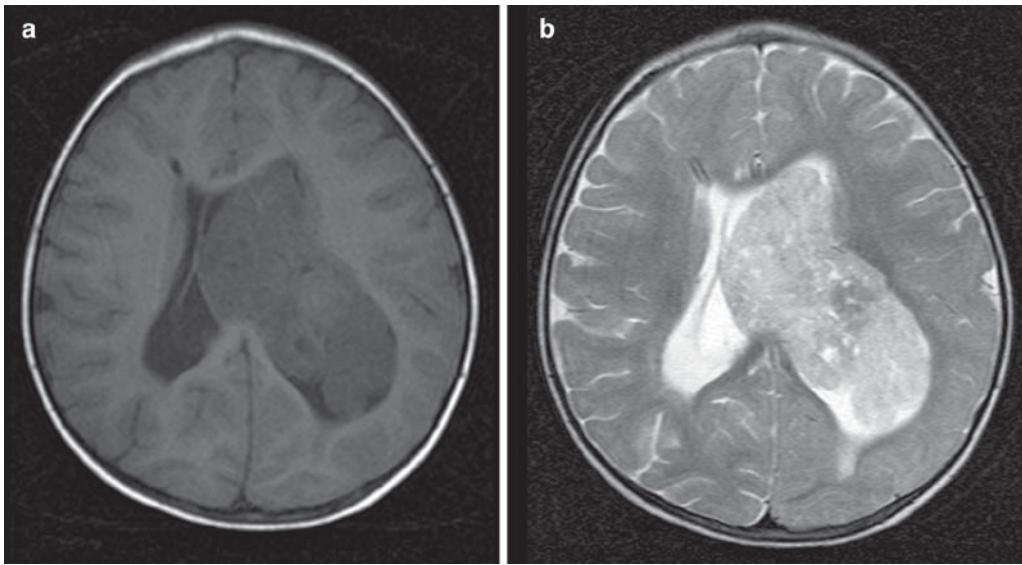
Fig. 8.1. (**a**) Axial T1- and (**b**) T2-w images in a 16-month-old boy demonstrating solid appearing heterogeneous mass occupying most of the body of the left lateral ventricle with bowing of the midline convex to the right in the presence of a dilated supratentorial ventricular system.
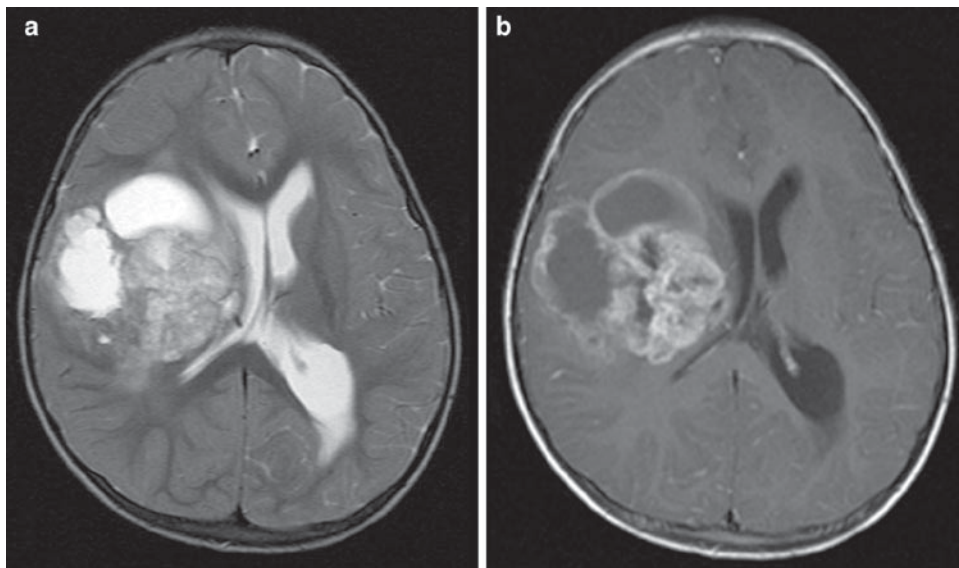
Fig. 8.2. (**a**) Axial T2- and (**b**) T1-w post Gd imaging in a 22-month-old girl, demonstrating a rim-enhancing mixed solid and cystic-appearing supratentorial tumor effacing the body of the right lateral ventricle and causing contralateral hydrocephalus with transependymal fluid spread on the left. Histopathology revealed an ATRT. Following a gross total resection and therapy this child survived for another 5 years.
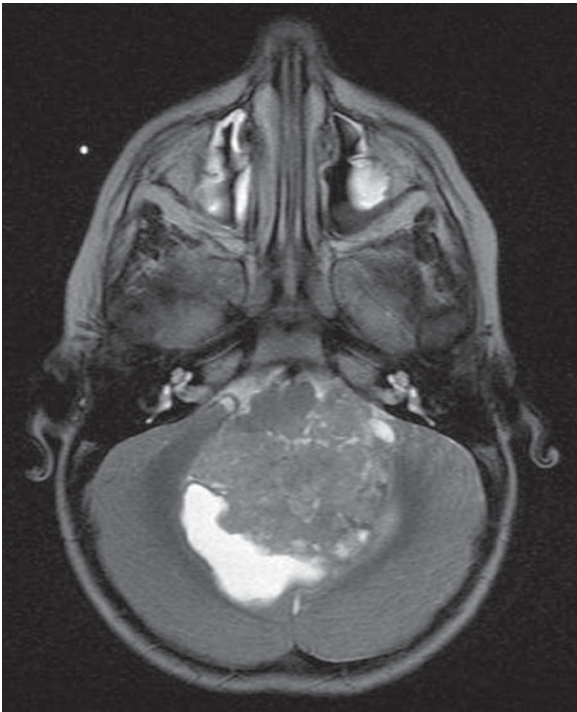
Fig. 8.3. Axial T2-w image through the posterior fossa in this 21-month-old male patient demonstrating heterogeneous mixed signal intensity mass with solid and more cystic-appearing components extending into the left cerebello-pontine angle (CPA), with non-visualization of the IVth ventricle.

Fig. 8.4. Unenhanced CT examination in an 18-month-old boy, presenting with hearing loss, which shows a hyperdense mass originating at the level of the left CPA. The hyperdensity suggests a highly cellular tumor, confirmed on MRI with restricted diffusion abnormality in the presence of altered blood and blood product. Bone windows on CT revealed some remodeling of the left internal auditory canal (IAC), in the presence of an otitis media. Despite resection that revealed an ATRT the child succumbed one month later.
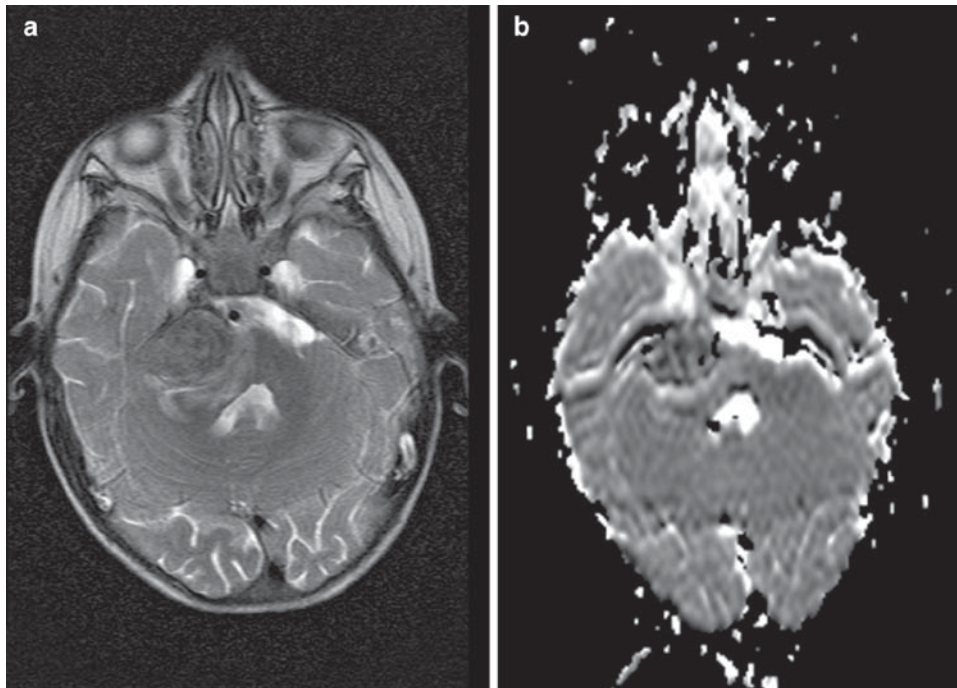
Fig. 8.5. (**a**) Axial T2-w image demonstrating a right CPA mass with (**b**) restricted diffusion abnormality on ADC map.
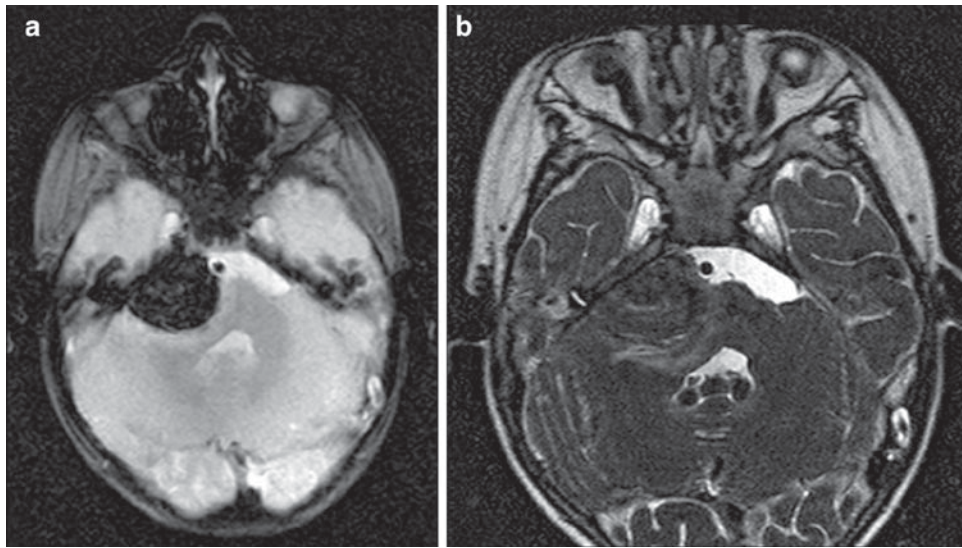
Fig. 8.6. Same patient in Fig. 8.5 revealing evidence for hemorrhage within the tumor on (**a**) gradient echo imaging with (**b**) fine cut heavily T2-w imaging demonstrating exophytic extension into the basal cistern.
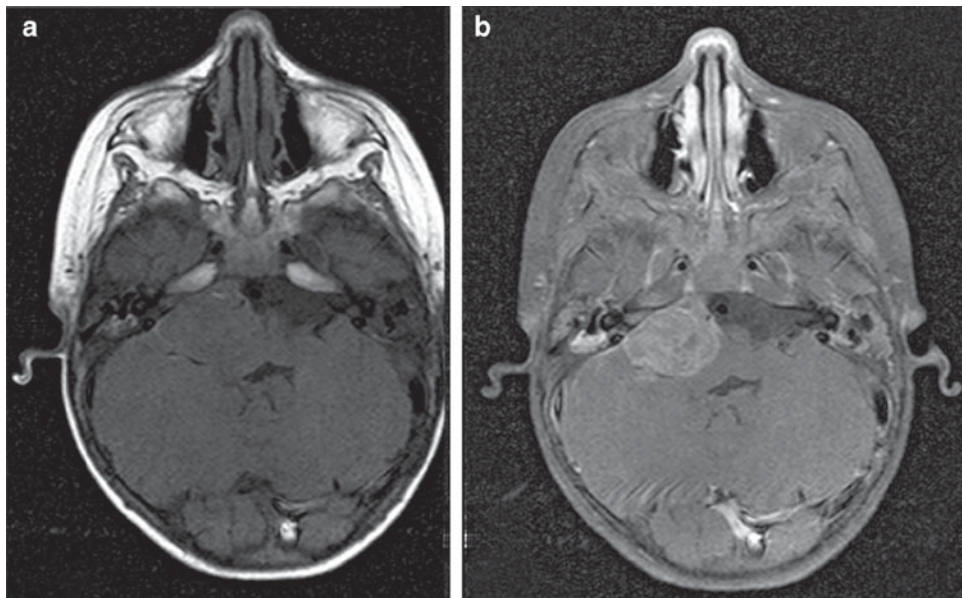
Fig. 8.7. (**a** and **b**) Fine cut T1-w imaging on the same patient in Fig. 8.5 shows the pattern of enhancement which extends into the pores of the right IAC. The patient survived for another 6 months despite resection and therapy.
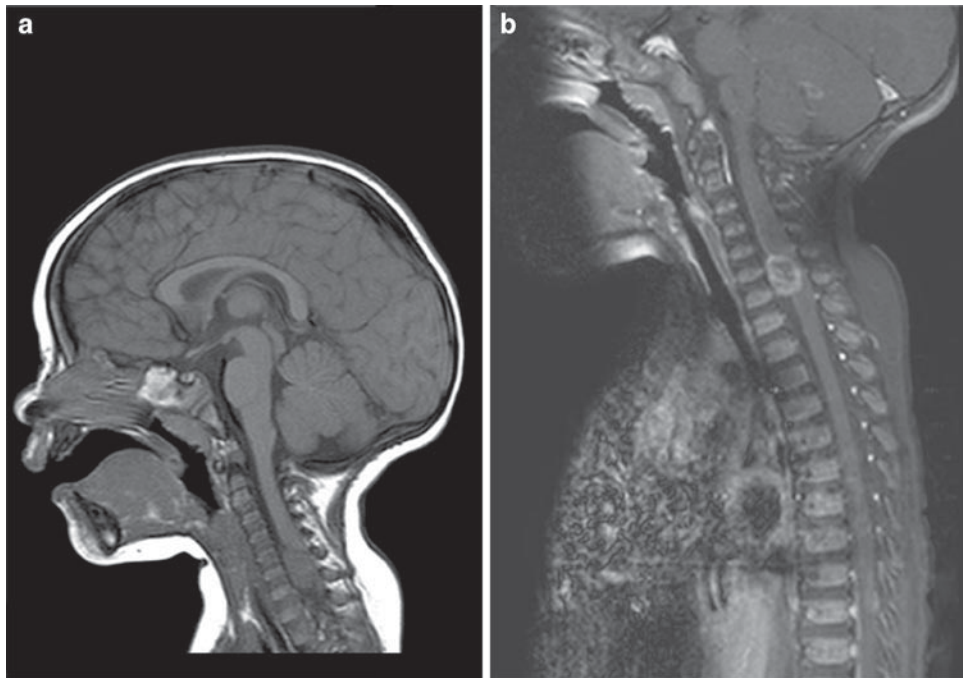
Fig. 8.8. Sagittal T1-w imaging of the (**a**) head and (**b**) neck, of a one year old girl presenting with left-sided weakness, before and after the administration of Gd showing an extradural mass lesion in the cervical spine with rim enhancement post-Gd. This proved to be a rhabdoid tumor with extension through the exit foramen into the soft tissues requiring more than one resection. This is a very unusual location for ATRT. She died from intracranial dissemination of tumor four months after first presentation.
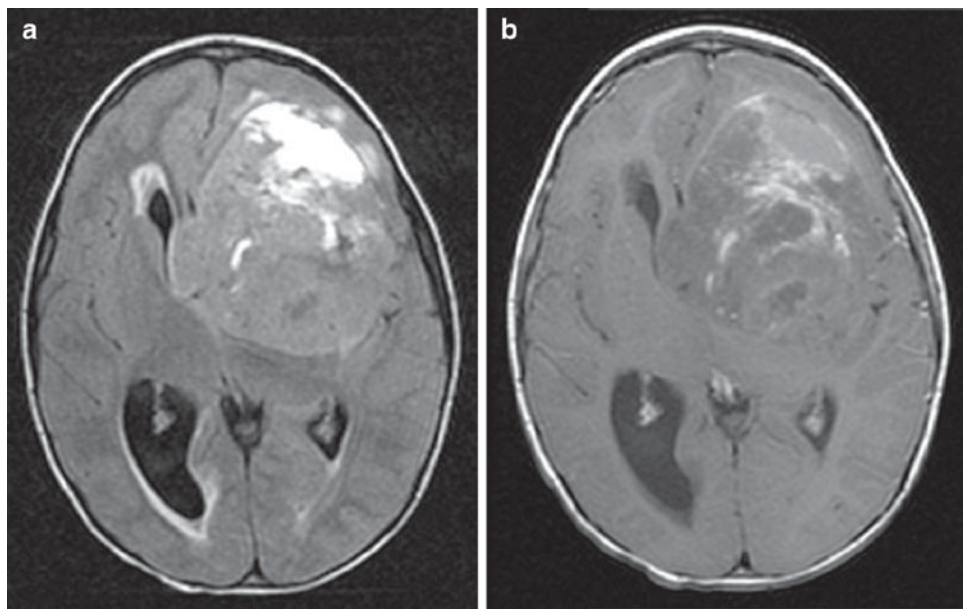
Fig. 8.9. (**a**) Axial T2-w and (**b**) T1-w post Gd images of a 17-month-old boy with a large poorly enhancing predominantly hyperintense lesion in the left frontal region causing mass effect and midline shift with contralateral hydrocephalus proven to be a supratentorial ATRT. He survived for another 5 months following removal.
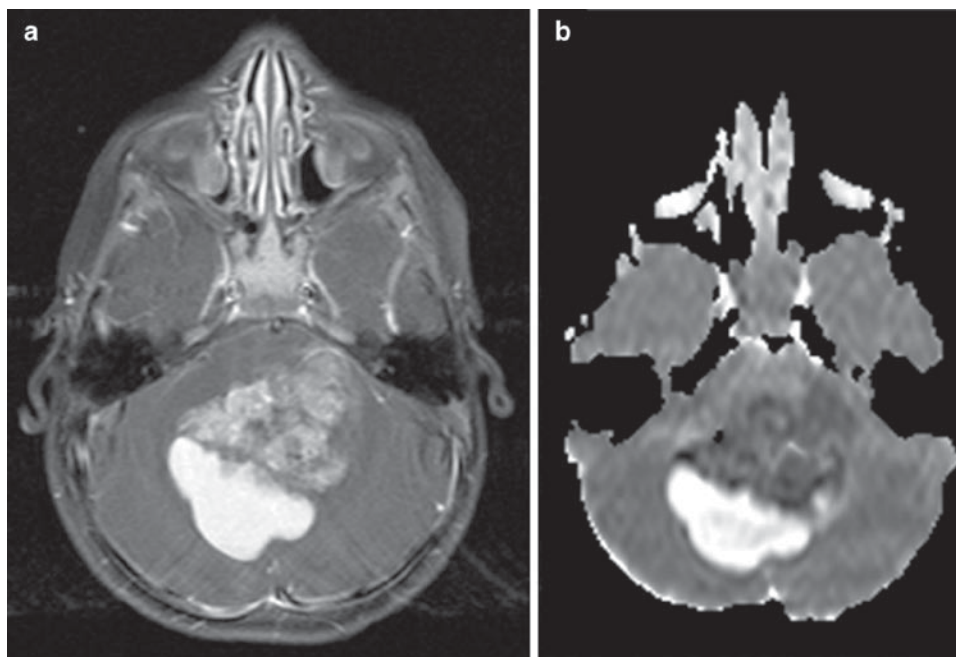
Fig. 8.10. (**a**) Axial T1-w imaging post-Gd and (**b**) axial diffusion-weighted imaging (DWI) in the same patient in Fig. 8.3 demonstrating diffuse enhancement of the solid appearing component of the tumor which shows restricted diffusion abnormality on apparent diffusion coefficient (ADC) map. The right posterior component of the tumor demonstrates unrestricted diffusion consistent with fluid filled cyst. Taking the morphology into account these appearances would be typical for an ATRT but differential diagnosis would include medulloblastoma and anaplastic ependymoma. This patient survived for another 5 years with treatment.
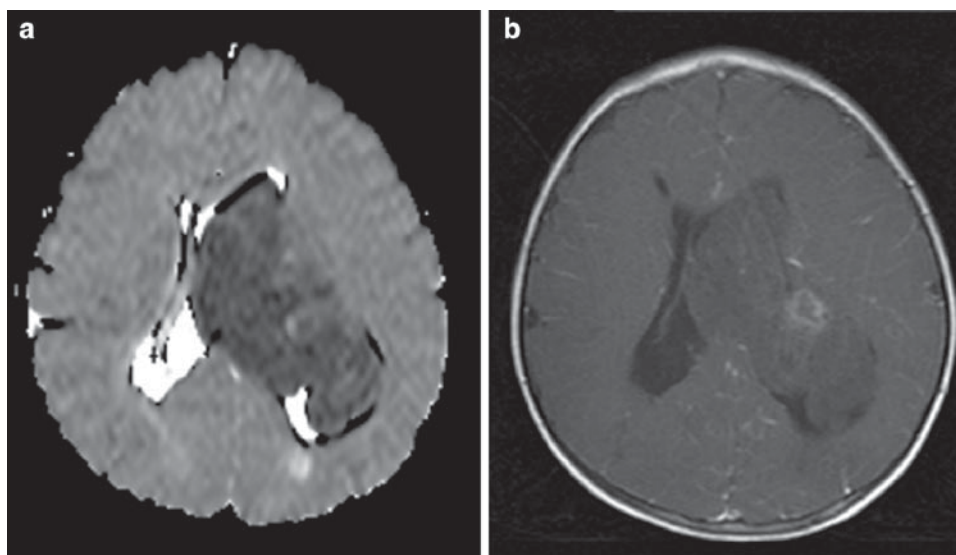
Fig. 8.11. (**a**) Axial ADC map and (**b**) T1-w post Gd imaging in the same patient in Fig. 8.5 demonstrating almost uniformly restricted diffusion abnormality in the poorly enhancing intraventricular mass which at surgery proved to be a supratentorial ATRT. Despite a gross total resection this patient survived only 2 months.
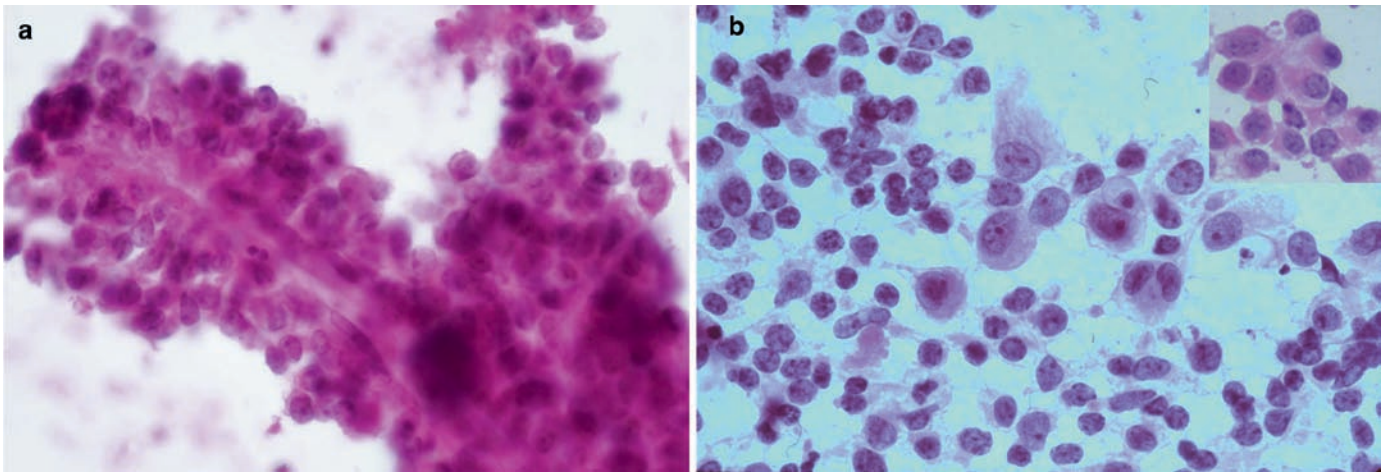
Fig. 8.12. Intraoperative cytologic preparations showing malignant poorly differentiated tumor cells arranged in (**a**) a pseudopapillary pattern, and a (**b**) smear of a rhadoid tumor with mixed population of primitive neuroepithelial cells and rhabdoid cells. Rhabdoid cells with vesicular nuclei and prominent nucleoli seen in the inset.
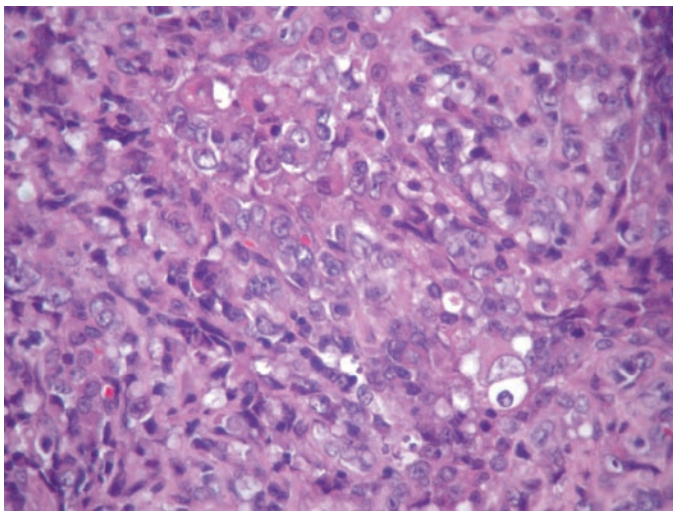
Fig. 8.13. Histology of ATRT showing sheets of epithelioid cells.
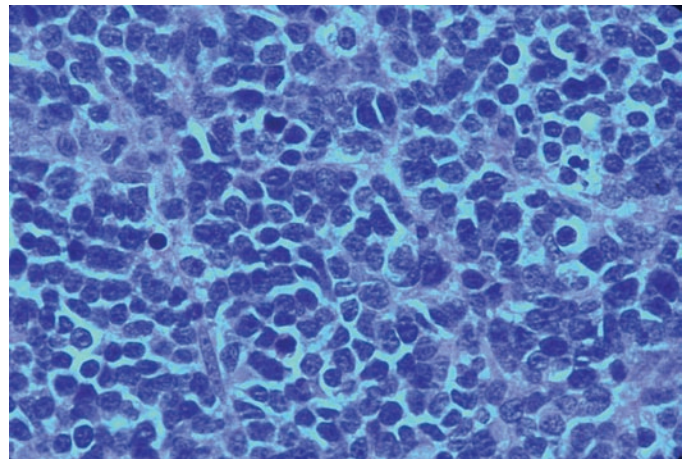
Fig. 8.14. Region in an ATRT showing poorly differentiated primitive neuroepithelial cells. or "small blue" cells consistent with a PNET component.
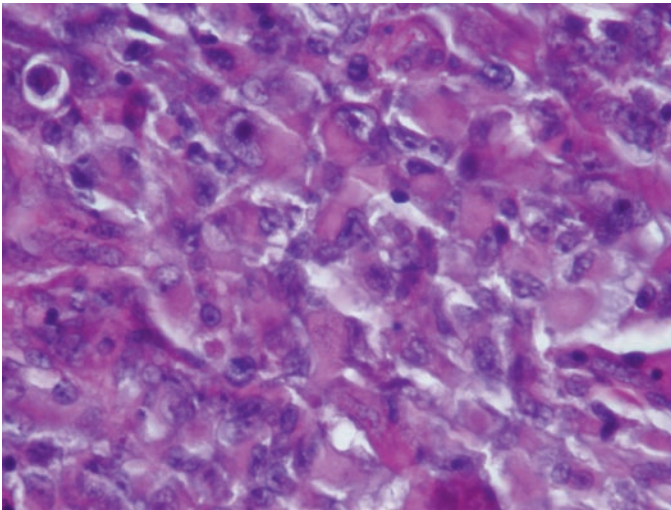
Fig. 8.15. Epithelioid (rhabdoid) cells with vesicular nuclei, prominent nucleoli and abundant, eccentric, eosinophilic cytoplasm.
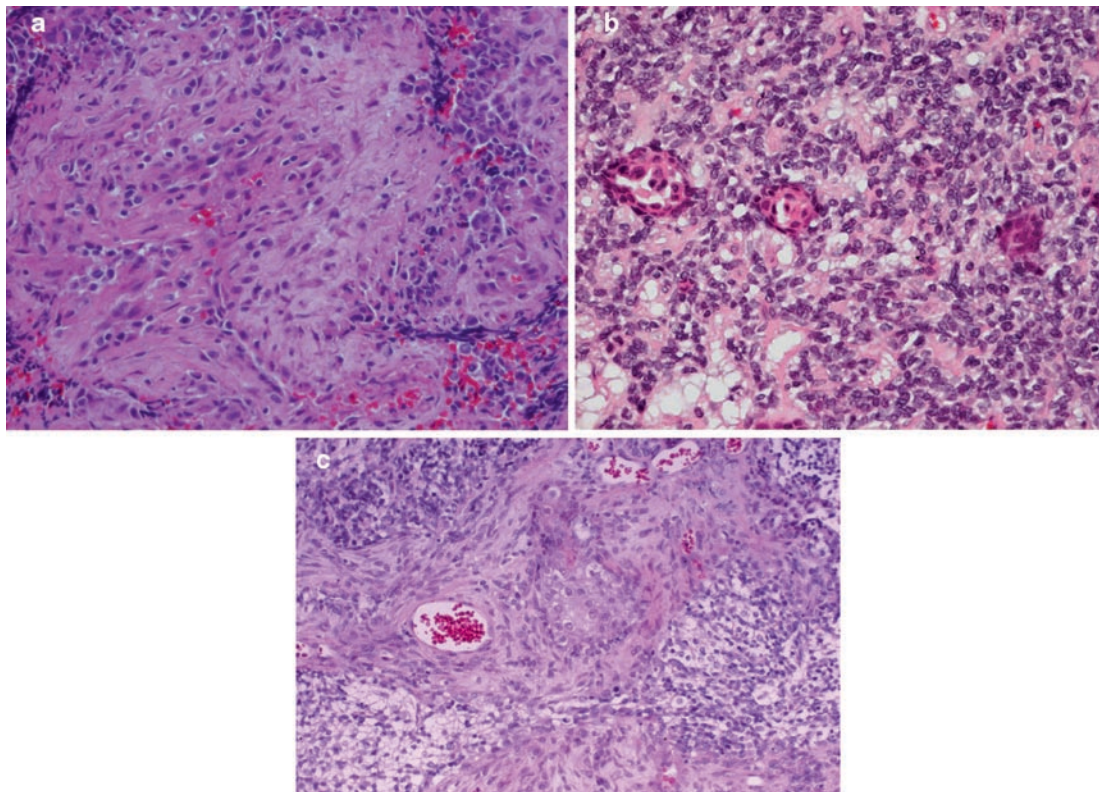
Fig. 8.16. Regional desmoplasia is a common finding in ATRT with (**a**) tissue culture type fibroblastic proliferation, (**b**) abrupt nests of squamous differentiation, and (**c**) field of ATRT containing nest of squamous and glandular epithelium in center, with a small amount of surrounding non-differentiating collagenous mesenchymal tissue and nests of primitive epithelial cells in the upper left and lower right regions.
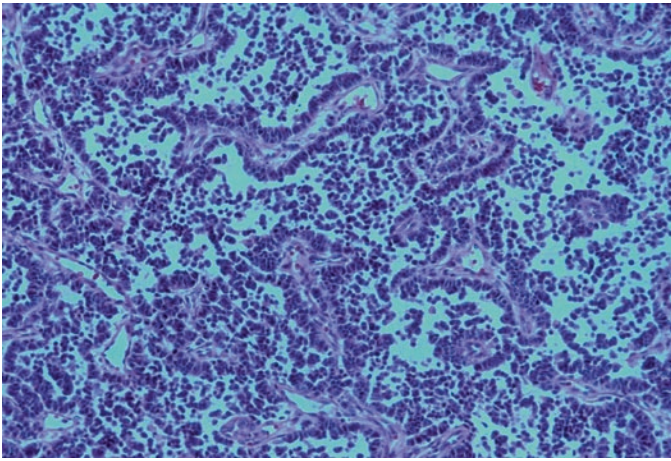
Fig. 8.17. Field of ATRT composed of papillary structures and primitive neuroepithelial cells.
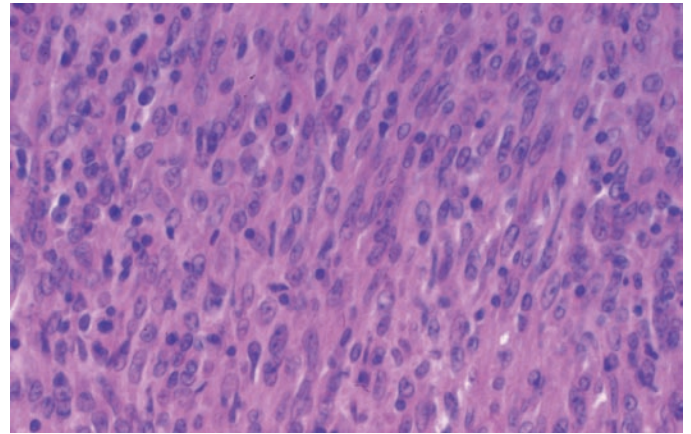
Fig. 8.19. Field consisting of elongated spindled cells resembling a sarcoma.
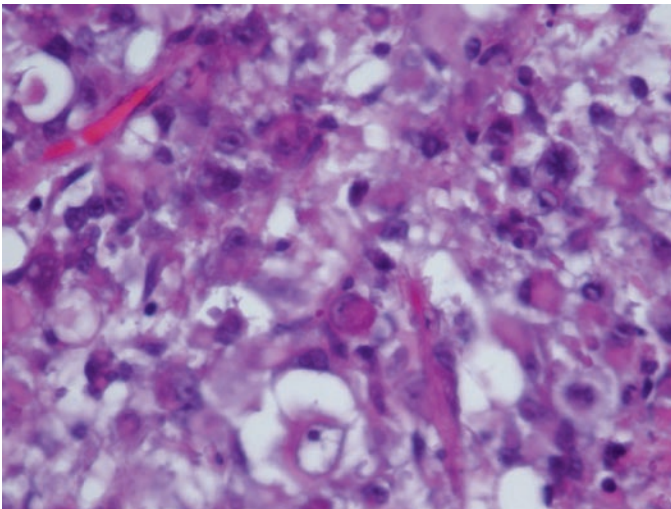
Fig. 8.18. Regional cytoplasmic vacuolation is common and may involve large regions of an ATRT.
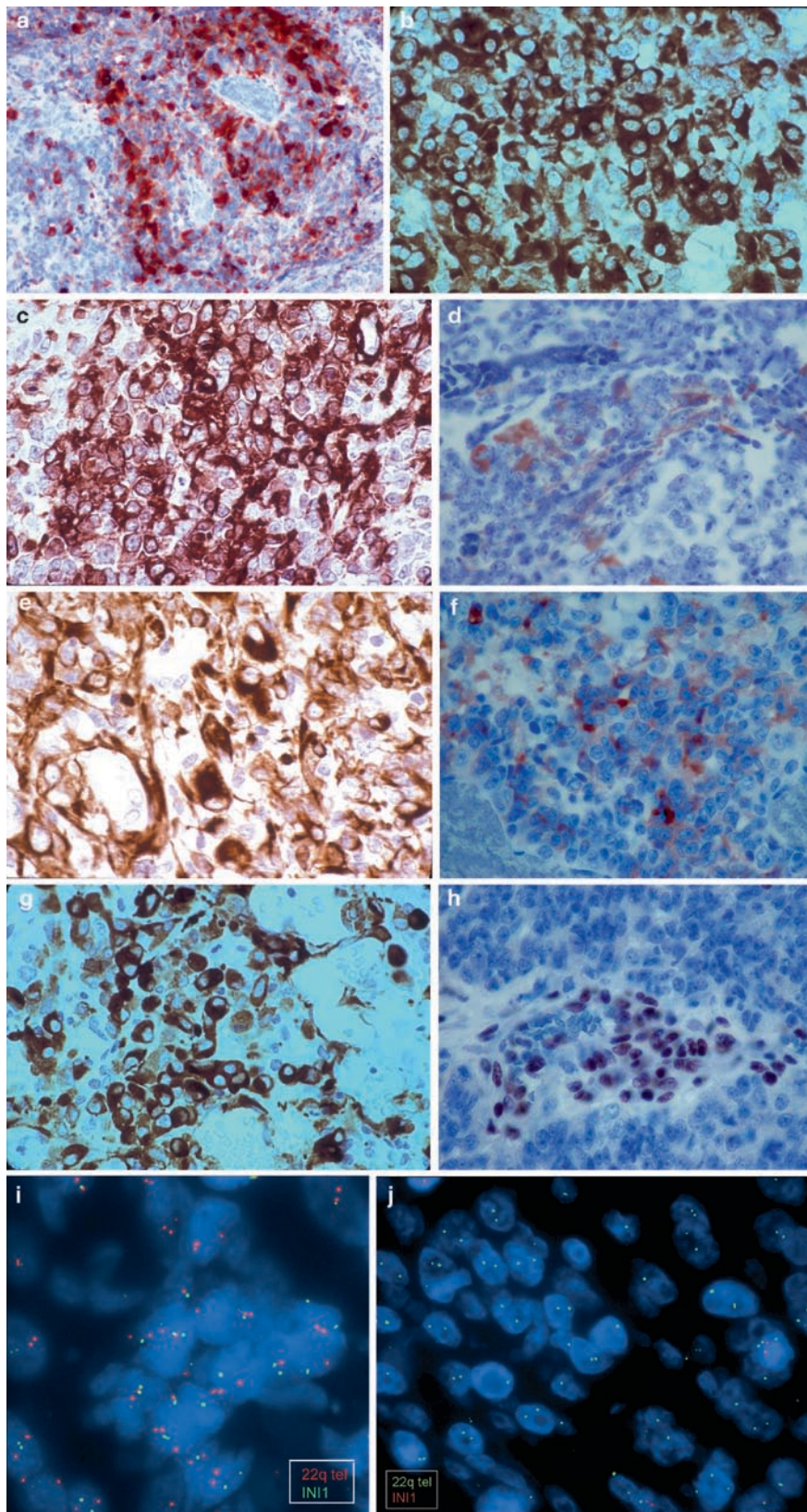
Fig. 8.20. Photomicrographs of ATRT demonstrating expression of various antigens. (**a**) EMA, (**b**) Vimentin, (**c**) SMA, (**d**) AE1-AE3 (Pan-cytokeratin) keratin, (**e**) GFAP, (**f**) Synaptophysin, (**g**) NFP, (**h**) INI1. Note positive immunostaining of the nuclei of endothelial cells and negative staining in tumor cells, (**i**) FISH analysis of ATRT showing heterozygous (allelic) deletion at the SMARC1/INI1 (hSNF5) locus at 22q11.2. The test probe (*green*)/reference probe (*red*) ratio is less than 0.8; (**j**) FISH analysis of AT/RT showing homozygous (biallelic) deletion at the SMARC1/INI1 (hSNF5) locus at 22q11.2. The test probe is red while the reference probe is green.
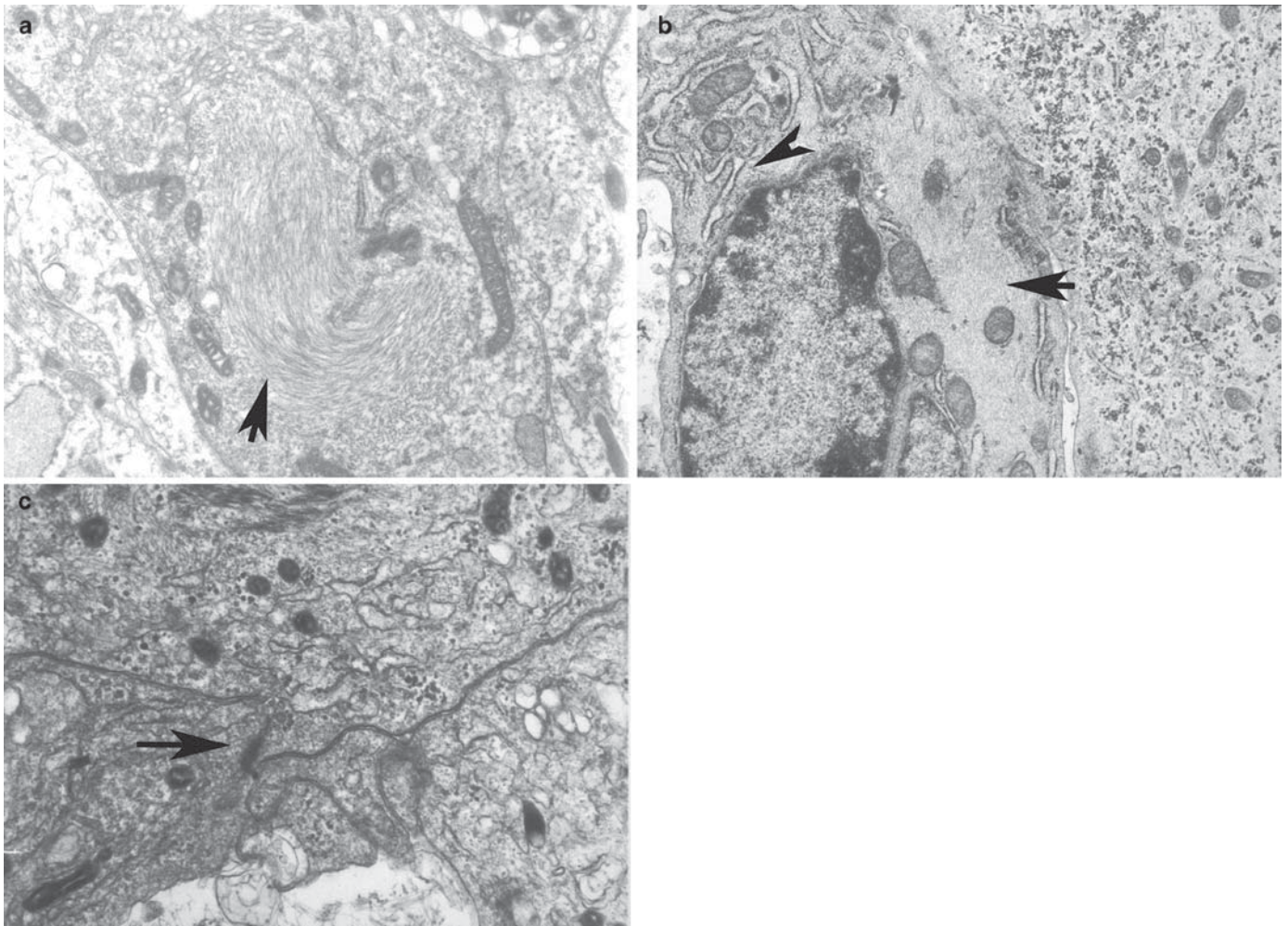
Fig. 8.21. Ultrastructural features of ATRT: (**a**) Large mass of intracytoplasmic whorls of intermediate filaments (*arrow*), (**b**) Intracytoplasmic filaments (*short arrow*) and dilated endoplasmic reticulum (*arrow head*), (**c**) Prominent cell junctions (*arrow*).
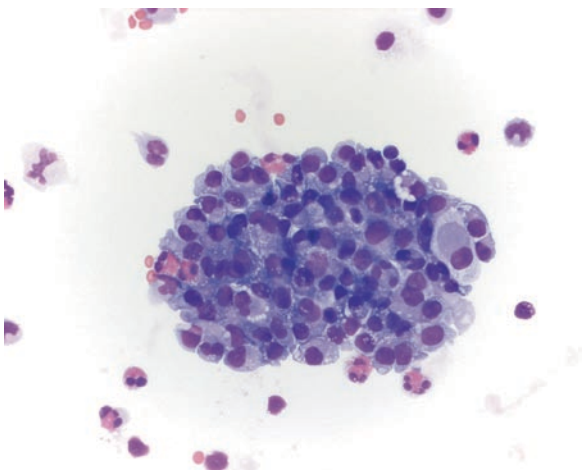
Fig. 8.22. Cluster of malignant cells in the CSF in a patient with disseminated ATRT.

Section C: Tumors of the Meninges

Christine E. Fuller and Brian Pavlovitz

Abstract Section C focuses on pediatric meningeal-based tumors. Meningiomas are presented first, with illustrative examples of the multiple histologic variants. Particular emphasis is given to histologies associated with WHO grades II and III, and the specific criteria set forth by the WHO for atypical and anaplastic meningioma are summarized. Non-meningothelial mesenchymal tumors, including hemangiopericytoma, are presented next, focusing primarily on those tumors that may arise in the pediatric age group. The third subsection addresses primary melanocytic lesions of the meninges, including diffuse melanocytosis, melanocytoma, and malignant melanoma and melanomatosis. Hemangioblastoma, a tumor of uncertain histogenesis, is presented in the final subsection. Specific emphasis will be placed on the classic neuroimaging and pathologic characteristics of each of these entities, with careful consideration of differential diagnosis in each instance.

Meningiomas

Christine Fuller and Brian Pavlovitz

Keywords Meningioma; Atypical meningioma; Anaplastic meningioma; Rhabdoid meningioma; Papillary meningioma; Chordoid meningioma; Clear cell meningioma

9.1 OVERVIEW

- Dural-based neoplasms derived from meningothelial (arachnoid) cells including a wide variety of histologic subtypes, ranging from benign WHO grade I variants to more biologically aggressive meningiomas encompassing WHO grades II and III.
- Many pediatric meningiomas are sporadic; however, a significant proportion arise in the context of a hereditary cancer predisposition syndrome, especially Neurofibromatosis type 2 (NF2).
- Multiplicity of meningiomas is not uncommon in NF2, and the pediatric onset of meningioma should prompt further evaluation for clinical and genetic findings diagnostic of NF2. Meningiomas are infrequently encountered with Gorlin syndrome.
- Exposure to radiotherapy for prior neoplasm is another significant predisposing factor in the development of meningiomas, particularly within the pediatric age group.

9.2 CLINICAL FEATURES

- Though they are quite common in adults, meningiomas infrequently arise in the pediatric population, accounting for less than 3% of all intracranial tumors in that age group.
- In contrast to observations among their adult counterparts, pediatric meningiomas are more common in males.
- Specific manifestations depend on tumor site and compression of adjacent structures.
- Signs and symptoms related to chronically elevated intracranial pressure (headaches, vomiting, papilledema), cranial nerve disorders and other focal neurologic deficits, and seizures have been reported in these children.

9.3 NEUROIMAGING

- In children, meningiomas typically arise at intracranial locations including over the cerebral convexities, parasagittal or parasellar regions, or the cerebellopontine angle (Fig. 9.1a, b).
- Absence of dural attachment (intraventricular and intraparenchymal locations) is more frequent in pediatric meningiomas, whereas spinal meningiomas are quite uncommon.
- By MR imaging, most meningiomas are iso- to hypointense to gray matter on T1, hyperintense on T2 and FLAIR, and are accentuated strongly postcontrast administration (Fig. 9.2a–e). The characteristic "dural tail" may be seen in over 50% of cases.
- Surrounding vasogenic edema frequently accompanies meningiomas; with angiomatous or higher-grade variants, this may be marked (Fig. 9.2b, c).
- Intratumoral calcifications, hemorrhage, necrosis, or cystic components are uncommon findings (Fig. 9.2a–e).
- Invasion of adjacent cranial bone may cause hyperostosis, readily identifiable on imaging studies (Fig. 9.2e).
- Angiography (typically performed when embolization is planned) shows a hypervascular tumor blush throughout the arterial phase of the middle meningeal artery injection, persisting into the late venous phase with slow washout (Fig. 9.2f).
- Tumor seeding along surgical trajectory, through CSF dissemination, or metastases outside the CNS is rarely encountered; though more frequent with higher grade tumors, histologically benign meningiomas have exhibited such behaviors.

9.4 PATHOLOGY

- *Gross pathology*: (Fig. 9.3)
  - Meningiomas are generally round or lobulated tan-yellow firm masses, frequently with dural attachment. Some tumors, usually the base of skull lesions, grow in a flat "en plaque" pattern. A granular appearance may indicate psammoma bodies.
  - Encasement of adjacent nerves or blood vessels, or invasion into bone or soft tissue may be encountered.
  - Atypical and anaplastic meningiomas are usually larger and may contain areas of micro- or macronecrosis.
- *Intraoperative cytologic imprints/smears*:
  - Cytologic smears/squash preparations show cohesive syncytial clusters of cells with oval to round nuclei.
  - Classic "whorl" formations, intranuclear cytoplasmic invaginations, and psammoma bodies are other helpful diagnostic features (Fig. 9.4a–f).
  - Squash: preparations from several meningioma variants may pose a significant diagnostic challenge.
    - The fibrous variant (Fig. 9.5a) with its elongated spindle cells may mimic glioma by cytology, whereas papillary (Fig. 9.5b) and rhabdoid (Fig. 9.5c) variants may be confused with carcinoma or AT/RT, respectively.
  - Nuclear anaplasia, macronucleoli, mitoses, and sheeting suggest a higher-grade lesion.
- *Histology*: A multitude of histologic variants have been recognized. In general, WHO grade I meningiomas carry a low risk of recurrence and behave in a benign fashion, whereas WHO grade II and III tumors carry an incrementally higher likelihood of recurrence and aggressive behavior.

- The higher-grade variants are notably more frequent in the pediatric population.
  - Note that pleomorphic nuclei may be encountered in any of the meningioma variants, most often connoting a degenerative atypia as opposed to higher tumor grade.
- *Meningothelial meningioma (WHO grade I)*:
  - Common variant with lobular architecture; these lobules contain syncytial arrays of cells with uniform oval nuclei, often containing intranuclear-cytoplasmic inclusions. Whorls and psammoma bodies are infrequent (Fig. 9.6a, b).
- *Fibrous meningioma (WHO grade I)*:
  - Contain spindle cells arranged in parallel fascicles with an interwoven collagen matrix, the latter on occasion may be quite dense.
  - Focal intranuclear cytoplasmic inclusions and psammoma bodies may be seen (Fig. 9.6c, d).
- *Transitional (mixed) meningioma (WHO grade I)*:
  - Perhaps the most recognizable variant, transitional meningiomas display a mixture of both meningothelial and fibrous patterns with numerous whorls and psammoma bodies (Fig. 9.6e–h).
- WHO grade I variants uncommon in children:
  - *Psammomatous meningioma*:
    - Contain more psammoma bodies than meningothelial tumor cells, the former often coalescing to form large calcified areas.
      - Whorl formations are common (Fig. 9.7a).
  - *Angiomatous meningioma*:
    - Typified by more vascular structures than tumor cells, harboring abundant small to medium caliber, often hyalinized blood vessels of variable wall thickness.
    - Degenerative nuclear atypia may be marked (Fig. 9.7b).
  - *Microcystic meningioma*:
    - Contain numerous intercellular microcystic spaces, sometimes containing eosinophilic mucinous secretions.
    - Similar to the angiomatous variant, nuclear pleomorphism may be a prominent feature (Fig. 9.7c).
  - *Secretory meningioma*:
    - Variant marked by the presence of focal epithelial differentiation consisting of intracellular lumens containing eosinophilic, PAS-positive secretions (pseudopsammoma bodies) (Fig. 9.7d, e).
    - These structures are CEA-positive (Fig. 9.7f).
    - Mast cells may be conspicuous.
  - *Lymphoplasmacyte-rich meningioma*:
    - Extremely rare variant with extensive chronic inflammatory cell infiltrate typically overshadowing the meningothelial cells.
  - *Metaplastic meningioma*:
    - Contain mesenchymal components in the form of bone, cartilage, lipid, or myxoid tissues. Xanthomatous areas may also be present (Fig. 9.7g).
- *Atypical meningioma (WHO grade II)*:
  - *By definition, a meningioma with increased mitotic rate (>4/10 hpf in the area of highest mitotic activity) or at least three of the following histologic findings*:
    - Hypercellularity

- Small cell change
- Prominent nucleoli
- Sheet-like growth
- Foci of spontaneous or geographic necrosis (i.e. not induced by therapeutic embolization) (Fig. 9.8a–d)
  - From a prognostic standpoint, meningiomas that are histologically benign (grade I) but show definite brain invasion, should also be considered WHO grade II as they have been documented as showing recurrence and mortality rates akin to other grade II meningiomas.
  - Brain-invasive meningiomas will show tongue-like projections of tumor infiltrating into the underlying brain parenchyma (Fig. 9.8e).
- *Chordoid meningioma (WHO grade II)*:
  - Composed of cords and trabeculae of eosinophilic cells, sometimes with cytoplasmic vacuolization, within a mucoid or myxoid background closely mimicking chordoma (Fig. 9.9a, b).
  - Most show mixing of this chordoid pattern with more typical meningioma morphology; pure examples are quite rare.
  - These tend to be large supratentorial tumors typified by a high rate of recurrence when not completely resected.
- *Clear cell meningioma (WHO grade II)*:
  - A rare aggressive meningioma variant, more common in children, containing cells with abundant clear glycogen-rich (PAS-positive) cytoplasm.
  - Dense "blocky" accumulations of collagen are a frequent finding (Fig. 9.10a, b).
  - Psammoma bodies and whorl formations are not typical features.
  - They show a tendency to involve the cerebellopontine angle and cauda equina region, frequently recur, and may even show CSF dissemination.
- *Anaplastic (malignant) meningioma (WHO grade III)*:
  - Contain obvious histologic malignant features, including:
    - Malignant cytology (may resemble carcinoma, sarcoma, or melanoma), and/or
    - Markedly elevated mitotic index, defined as >20 mitoses/10 hpf (Fig. 9.11a, b).
  - Scattered regions showing at least vaguely recognizable meningioma architecture can be found in most examples, though rarely these lesions prove formidable diagnostic dilemmas necessitating extensive immunohistochemical, ultrastructural, and even molecular workup.
  - Although brain invasion is frequently present (though not always), this feature alone is *not sufficient* to warrant a WHO grade III designation (see note above under atypical meningioma).
- *Papillary meningioma (WHO grade III)*:
  - Rare variant, more frequent in young patients, with prominent pseudopapillary pattern. (Fig. 9.12a, b)
- *Rhabdoid meningioma (WHO grade III):*
  - Uncommon variant, similarly more frequent in young patients, containing "rhabdoid cells" with eccentrically-situated vesicular nuclei that often contain prominent nucleoli, and abundant eosinophilic cytoplasmic "bellies," many showing obvious globular or whorled inclusions (Fig. 9.13a, b).

- The cells of this "rhabdoid phenotype" closely mimic those encountered in atypical teratoid/rhabdoid tumor and renal or extrarenal pure rhabdoid tumors, with definitive differentiation often requiring immunohistochemistry and/or molecular determination of INI1/BAF47 status (see below for differential diagnosis).
- A mixture of rhabdoid cells and papillary/pseudopapillary architecture may be encountered.
- Rhabdoid meningiomas frequently exhibit a high proliferative index and other aggressive histologic features.

9.5 IMMUNOHISTOCHEMISTRY

- Epithelial membrane antigen (EMA) and vimentin are positive in nearly all meningiomas (Fig. 9.14a); some variants, however, particularly fibroblastic and higher-grade meningiomas, may show only faint focal EMA staining.
- S-100 staining is variable.
- Strong staining for CEA is typical of the pseudopsammoma bodies of secretory meningioma (Fig. 9.7f).
- Claudin-1, a structural protein found in tight junctions, is detectable in up to 85% of meningiomas and may be especially useful in diagnostically equivocal cases in which EMA staining is weak.
- Ki-67, progesterone receptor (PR), and phosphohistone H3 (PHH3; a mitosis-specific antibody) staining may be useful from a prognostic standpoint (see below).

9.6 ELECTRON MICROSCOPY

- The majority of meningiomas contain intercellular complexes including desmosomes and interdigitation, as well as abundant intermediate filaments (Fig. 9.14c).
    - These features may be inconspicuous in the fibrous variant.
    - Microlumina, often with microvilli, are seen in secretory meningiomas.

9.7 MOLECULAR PATHOLOGY

- Alterations of various Protein 4.1 superfamily members are commonplace in meningiomas.
    - Inactivation of the neurofibromatosis 2 (*NF2*) gene on 22q12 and loss of its protein product merlin are detected in approximately half of sporadic and nearly all NF2-associated meningiomas.
    - NF2 alterations are infrequent in radiation-induced meningiomas (chromosome 1p deletions are more common in these) and are encountered in certain histologic variants (fibrous, transitional, and psammomatous) more frequently than in others (meningothelial).
    - Deletions involving Protein 4.1B (DAL-1 or "differentially expressed in adenocarcinoma of the lung") are seen at a similar frequency overall in meningiomas, including pediatric examples.
    - Though the above alterations have not been shown to have prognostic relevance independent of histologic grading, their detection may be helpful from a diagnostic standpoint in selected cases (see below).

- Multiplicity of the above abnormalities is more frequent in atypical and malignant meningiomas.
- Deletions of chromosomes 1p and 14q are frequent in pediatric and NF2-associated meningiomas, often accompanying other aggressive histologic features and tendency for recurrence.
- A variety of other molecular alterations have been documented in adult meningiomas [i.e., deletions of *p16 (CDKN2A* on 9p21), amplifications of *PS6K (*17q23)*, and LOH of several regions along chromosome 10]; however, the incidence and potential diagnostic/prognostic relevance of these changes in pediatric meningiomas are presently unknown.

9.8 DIFFERENTIAL DIAGNOSIS

- Spindle cell lesions such as schwannoma, solitary fibrous tumor, and hemangiopericytoma may resemble meningiomas, particularly the fibrous variant.
    - Unlike meningiomas, schwannomas are diffusely positive for S-00, and solitary fibrous tumors will be diffusely positive for CD34.
    - Hemangiopericytomas are more variable in their immunolabeling, possible staining including EMA, vimentin, CD34, and factor XIIIa, to a greater or lesser extent. They will, however, show the ultrastructural feature of pericellular basement membrane material (similar to schwannoma), a feature not present in meningiomas.
- Renal cell carcinoma may be distinguished from clear cell meningioma by virtue of its diffuse immunopositivity for cytokeratin; CD10 and RCC-marker antibody may likewise be helpful, though they are less-reliably positive in RCC.
    - Hemangioblastoma, another clear cell lesion, is EMA negative, and careful inspection should divulge characteristic bubbly stromal cells.
- Chordoid meningioma may closely mimic its namesake chordoma; however, the latter will show diffuse S-100 and cytokeratin positivity and contains typical physaliferous cells.
- Though meningiomas may be quite vascular, they differ from arteriovenous malformations and other vascular lesions in that they contain meningothelial cells.
- Grade III (anaplastic, rhabdoid, and papillary) meningiomas may frequently prove quite difficult to diagnose as they may show significant histologic and even immunohistochemical overlap with other high-grade neoplasms including sarcomas, hemangiopericytomas, high-grade gliomas, AT/RT, and choroid plexus carcinoma.
    - Detection of deletions of 22q (*NF2*), 18p (*Dal1*), 1p, or 14q by FISH analysis would provide additional support for classification as meningioma in these instances as these alterations are not expected in the other tumors noted earlier.
    - Immunohistochemical and/or molecular determination of INI1/BAF47 status is specifically helpful for differentiating rhabdoid meningioma from AT/RT, as in the latter INI1 should be lost, that is, not expressed. Immunohistochemistry has been found to be a more reliable method in this instance, as deletions involving 22q

are common to both tumor types, whereas INI1/BAF47 immunopositivity should be retained in rhabdoid meningiomas but not AT/RT (Fig. 9.14b).

- Melanocytoma and malignant melanoma may mimic benign and anaplastic/malignant meningiomas, respectively. Unlike the latter, both of these melanocytic tumors are characteristically positive for S-100, HMB-45, and MART1, while negative for EMA.
- Dural-based metastatic carcinomas, including choroid plexus carcinoma, may be effectively differentiated from meningiomas by virtue of their diffuse cytokeratin positivity.

9.9 PROGNOSIS

- Compared with meningiomas in adults, pediatric meningiomas have in general a poorer prognosis. The degree of initial tumor resection (dictated in part by tumor location), pathologic grade, and association with NF2 are the most important factors influencing prognosis in individual children.
- Recurrence-free survival time is significantly related to WHO grade; this does not appear to be the case for overall survival.
- WHO grade III meningiomas, including anaplastic, rhabdoid, and papillary meningiomas, are all notable for markedly aggressive biologic behavior, typified by frequent invasion of brain and other nearby tissue, higher rate of metastasis outside the CNS, and short recurrence-free and overall survival rates; median overall survival in the pediatric population has not been well established, though that in adults for this tumor cohort is typically less than 2 years.
- Similar to negative PR status and elevated Ki67 labeling index, a variety of molecular alteration have been reported as negative prognostic variables in meningiomas arising in adults, including deletions of 1p, 14q, and *p16*, LOH chromosome 10, and amplification of *PS6K*, as noted earlier. Whether or not these parameters will prove useful for

prognostication for pediatric meningiomas will need to be determined on adequately large cohorts of children.

SUGGESTED READING

Arivazhagan A, Devi BI, Kolluri SV, Abraham RG, Sampath S, Chandramouli BA (2008) Pediatric intracranial meningiomas- do they differ from their counterparts in adults? Pediatr Neurosurg 44(1):43–48

Cai DX, Banerjee R, Scheithauer BW, Lohse CM, Kleinschmidt-Demasters BK, Perry A (2001) Chromosome 1p and 14 q FISH analysis in clinicopathologic subsets of meningioma: diagnostic and prognostic implications. J Neuropathol Exp Neurol 60(6):628–636

Erdincler P, Lena G, Sarioglu AC, Kuday C, Choux M (1998) Intracranial meningiomas in children: review of 29 cases. Surg Neurol 49(2):136–140

Gasparetto EL, Leite Cda C, Lucato LT, Barros CV, Marie SK, Santana P et al (2007) Intracranial meningiomas: magnetic resonance imaging findings in 78 cases. Arq Neuropsiquiatr 65(3A):610–614

Lanzafame S, Torrisi A, Barbagallo G, Emmanuele C, Alberio N, Albanese B (2000) Correlation between histologic grade, MIB-1, p53, and recurrence in 69 completely resected primary intracranial meningiomas with a 6 year mean follow-up. Pathol Res Pract 196(7):483–488

Liu Y, Li F, Zhu S, Liu M, Wu C (2008) Clinical features and treatment of meningiomas in children: report of 12 cases and literature review. Pediatr Neurosurg 44(2):112–117

Perry A, Stafford SL, Scheithauer BW, Suman VL, Lohse CM (1997) Meningioma grading; an analysis of histologic parameters. Am J Surg Pathol 21(12):1455–1465

Perry A, Scheithauer BW, Stafford SL, Lohse CM, Wollan PC (1999) "Malignancy" in meningiomas: a clinicopathologic study of 116 patients, with grading implications. Cancer 85:2046–2056

Perry A, Giannini C, Raghavan R, Scheithauer BW, Banerjee R, Margraf L et al (2001) Aggressive phenotypic and genotypic features in pediatric and NF2-associated meningiomas: a clinicopathologic study of 53 cases. J Neuropathol Exp Neurol 60(10):994–1003

Rushing EJ, Olsen C, Mena H, Rueda ME, Lee YS, Keating RF et al (2005) Central nervous system meningiomas in the first two decades of life: a clinicopathological analysis of 87 patients. J Neurosurg 103(6 suppl):489–495

Siddiqui MT, Mahon BM, Cochran E, Garruso P (2008) Cytologic features of meningiomas on crush preparations: a review. Diagn Cytopathol 36(4):202–206

Takei H, Bhattacharjee MB, Rivera A, Dancer Y, Powell SZ (2007) New immunohistochemical markers in the evaluation of central nervous system tumors. A review of 7 selected adult and pediatric brain tumors. Arch Pathol Lab Med 131:234–241

Zwerdling T, Dothage J (2002) Meningiomas in children and adolescents. J Pediatr Hematol Oncol 24(3):199–204
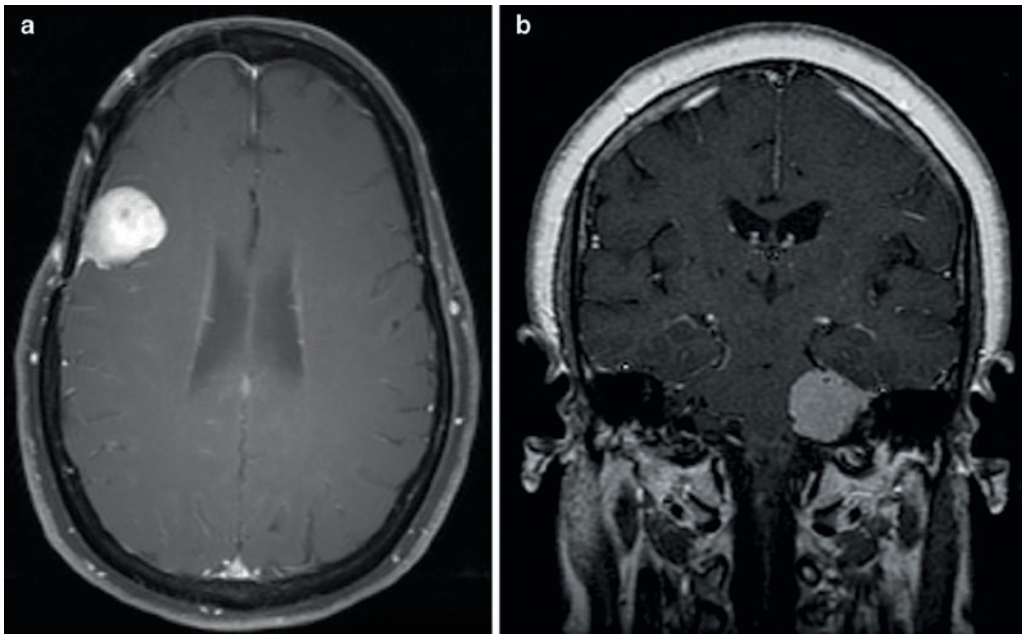
Fig. 9.1. T1-weighted postgadolinium axial (**a**) and coronal (**b**) MR images showing homogeneously enhancing pediatric meningiomas arising over the cerebral convexities and within the cerebellopontine angle, respectively. Note the characteristic "dural tail" in both images.
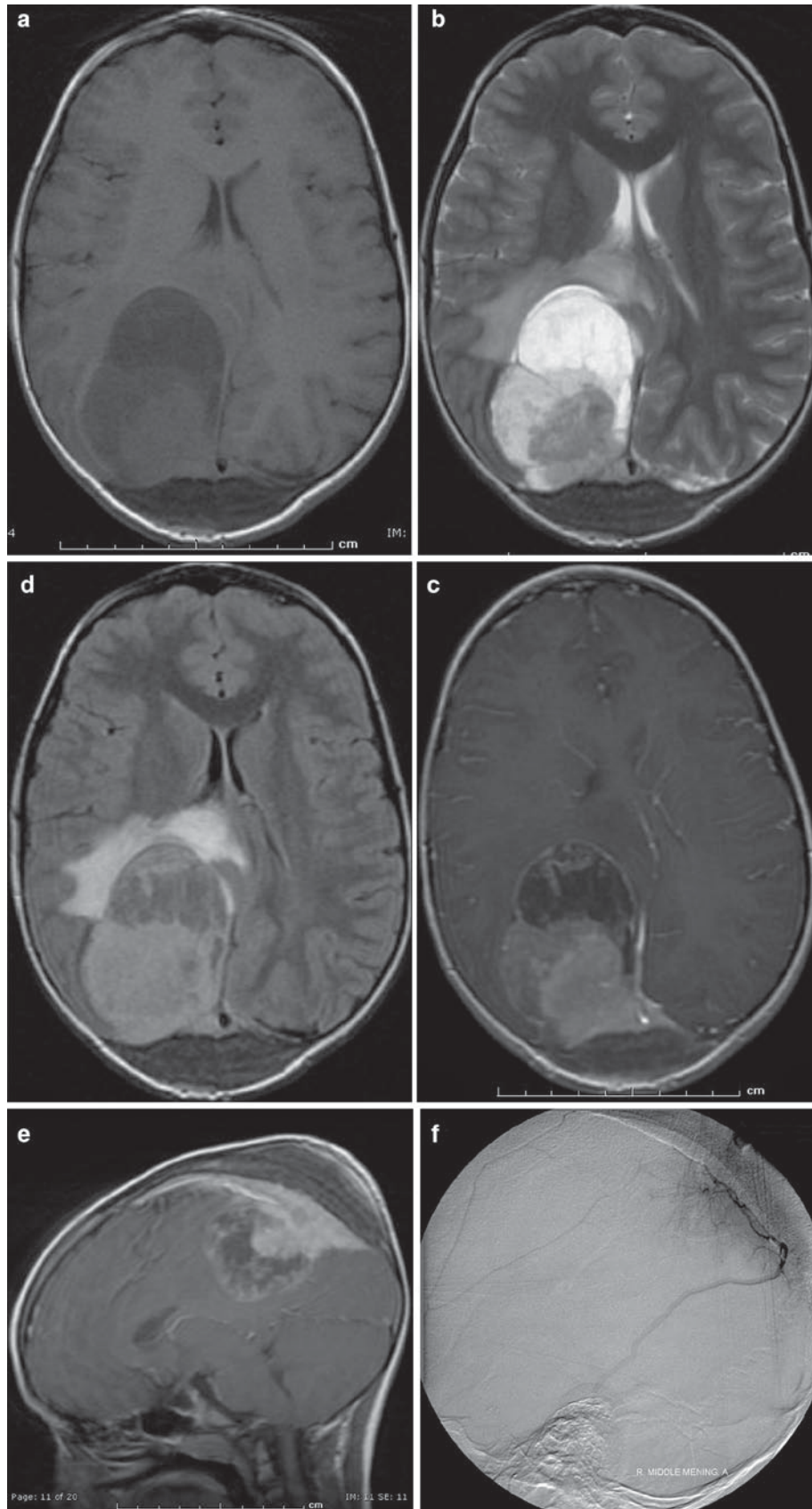
Fig. 9.2. This 8-year-old boy had a quite large parasagittal multilobulated dural-based mass with solid and cystic components in the right posterior parietal lobe; the solid component showed heterogeneous signal intensity, being iso- to hypointense to cortex on T1-weighted (**a**), hyperintense on T2-weighted (**b**) and FLAIR (**c**), and showing heterogeneous enhancement on T1-weighted post-Gd (**d**) axial MR images. Note the accompanying peritumoral edema and midline shift, seen best in **b** and **c**. Sagittal T1-weighted post-Gd image (**e**) shows thickening/hyperostosis of the overlying calvarial bone and scalp edema. Angiography (**f**) shows prominent tumor blush, with feeding vasculature arising from the right middle meningeal artery.

Fig. 9.3. Typical macroscopic appearance of meningioma, arising from the dura as a well-circumscribed firm mass.
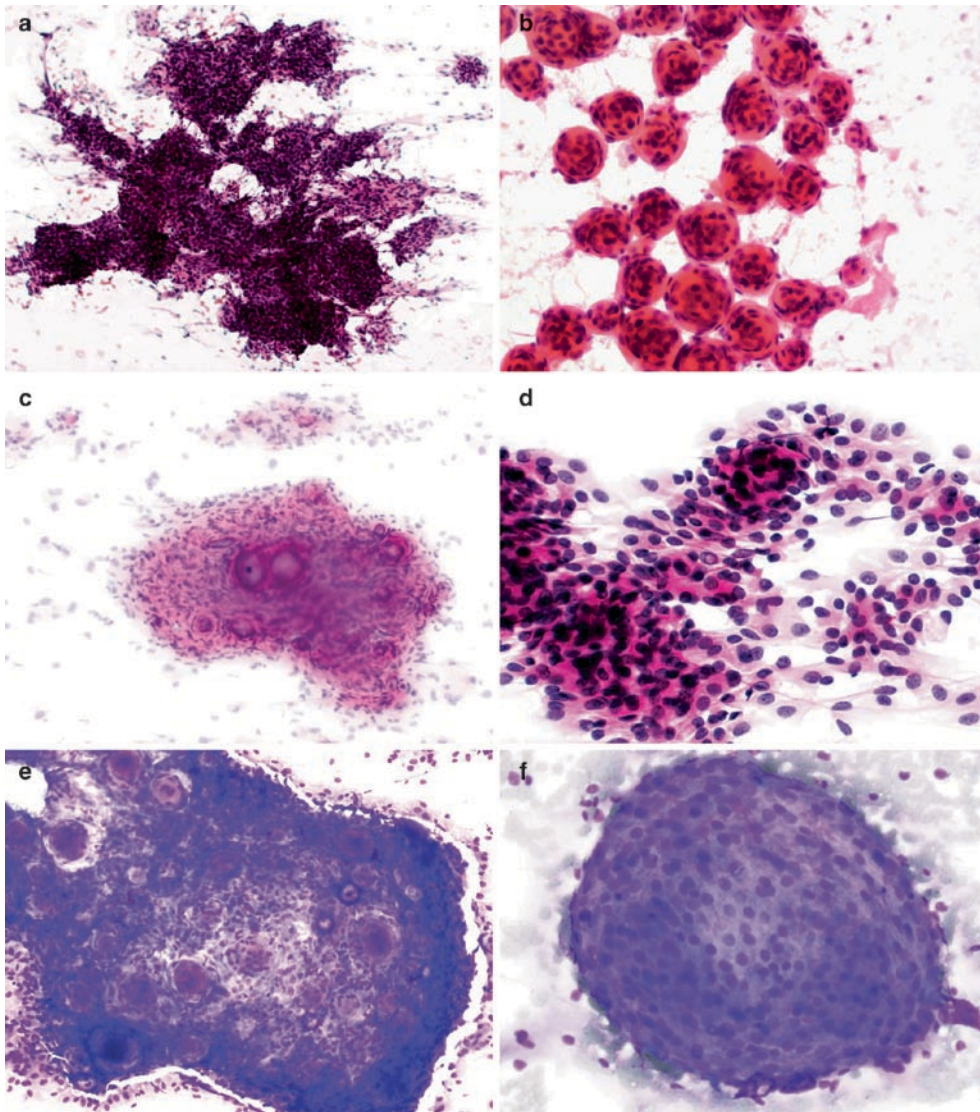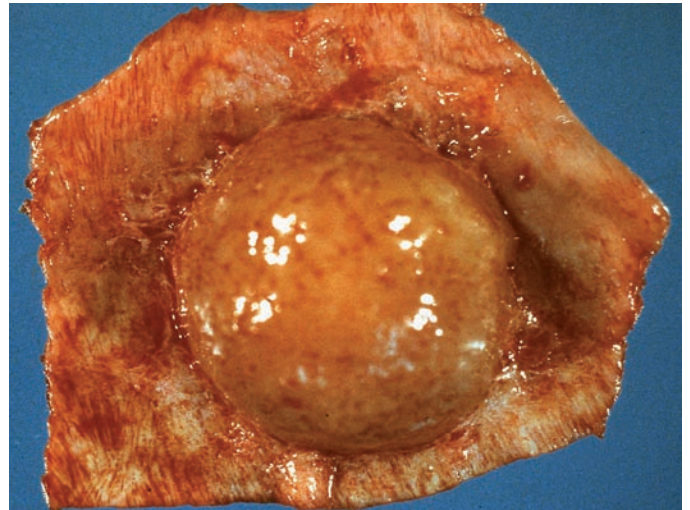
Fig. 9.4. Helpful cytologic features that may be encountered on crush/squash preparations of meningioma include the findings of cohesive syncytial clusters (**a**), whorls (**b**), and psammoma bodies (**c**). Careful inspection often reveals intranuclear cytoplasmic invaginations/pseudoinclusions, as seen here centrally (**d**). Similar findings are demonstrable on both conventional H&E (**a–d**) and Diff-Quik stained preparations (**e,f**).
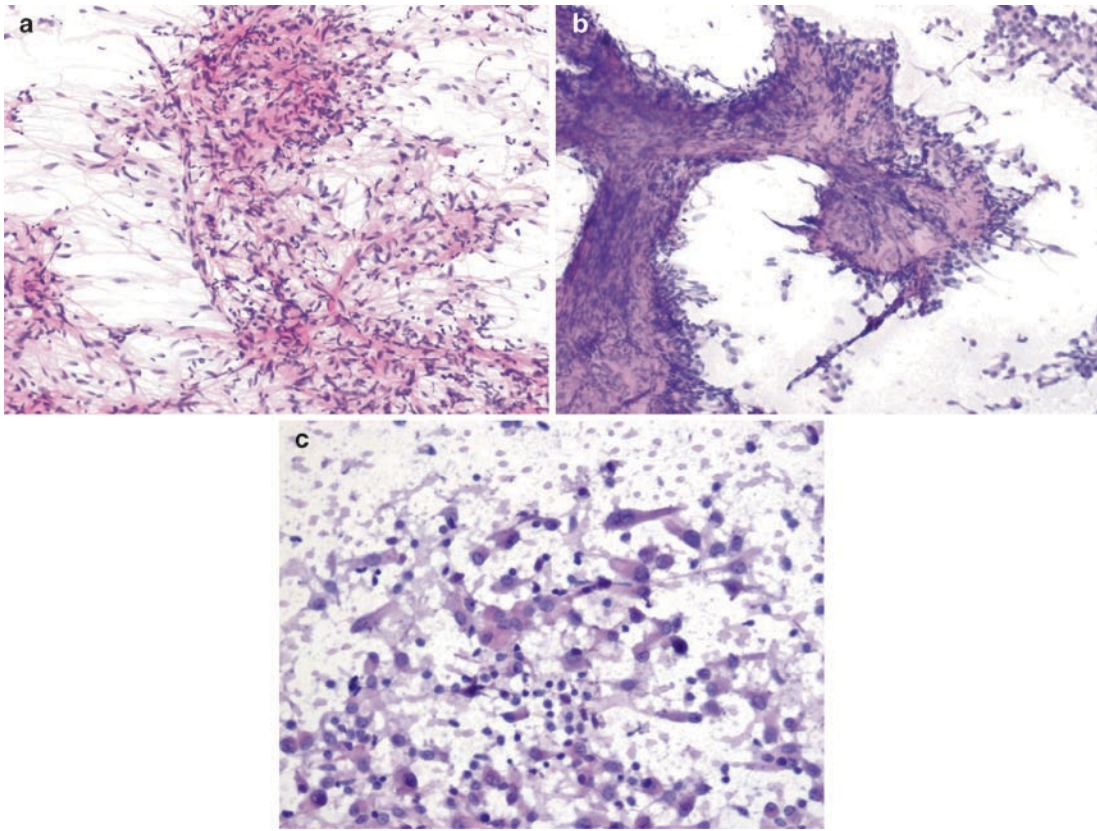
Fig. 9.5. (**a**) Squash preparation of a fibrous meningioma showing elongated spindled cells. (**b**) Papillary structures with multilayered covering of epithelioid cells may be seen in cytologic preparations of papillary meningioma. (**c**) Squash preparation of rhabdoid meningioma containing discohesive cells with eccentrically-situated nuclei and eosinophilic cytoplasmic "bellies," reminiscent of AT/RT.
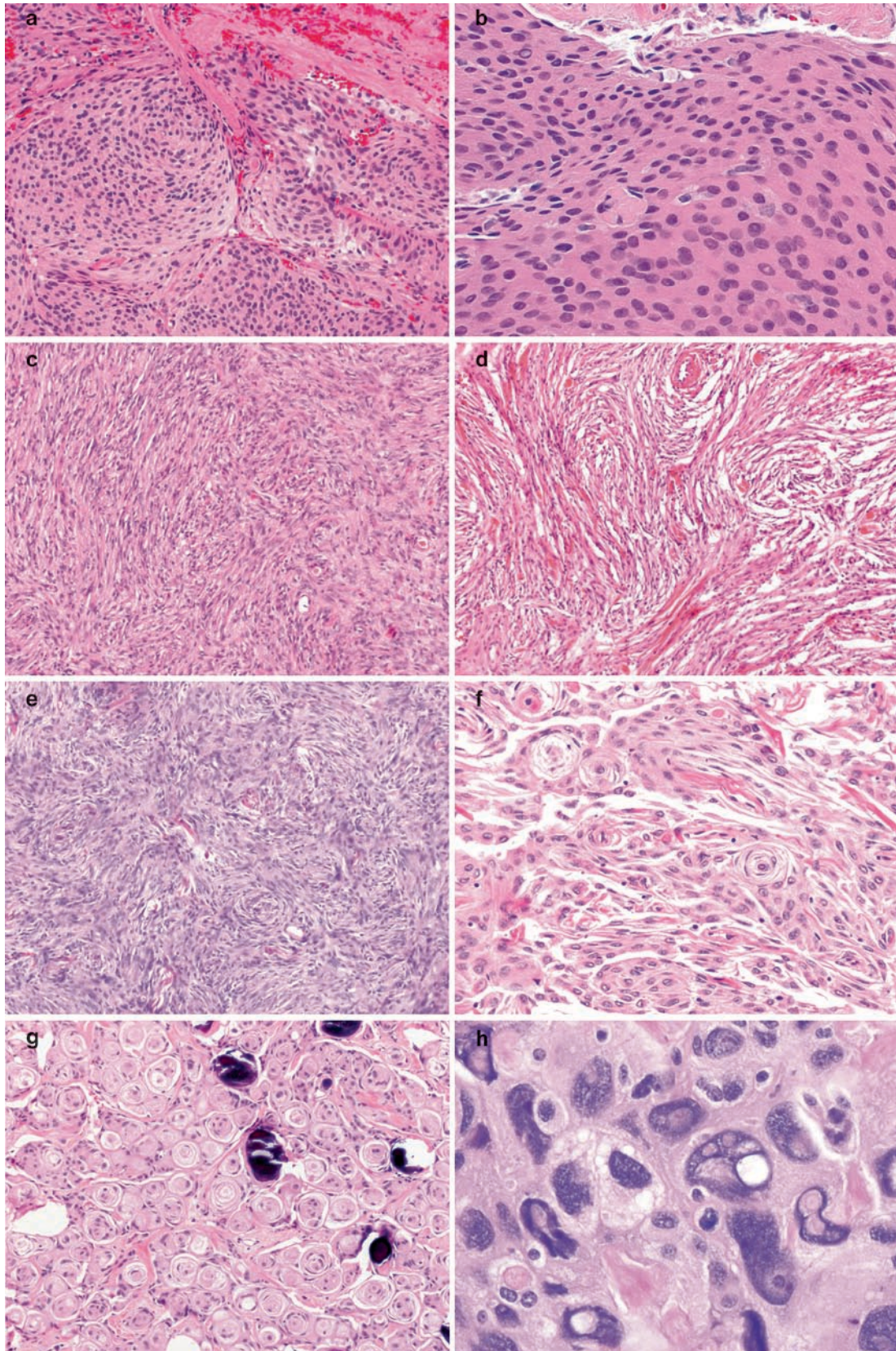
Fig. 9.6. Common WHO grade I variants. The meningothelial variant of meningioma is multilobular (**a**), containing syncytial arrays of cells with imperceptible cell boarders and uniform oval nuclei, often containing intranuclear-cytoplasmic inclusions (**b**). Whorls are uncommon and poorly-formed, and psammoma bodies are uncommon. Fibrous meningioma contains interwoven broad fascicles of bland spindle cells (**c** and **d**); often there are multiple clear clefts amongst these fascicles (**d**), and collagen content is variable. Transitional meningioma shows features of both fibrous and meningothelial variants (**e**), typically containing numerous tight whorl formations (**f**) and numerous psammoma bodies (**g**). Striking nuclear pleomorphism may be encountered in any meningioma (**h**), though in the absence of other histologic features indicative of grade II or III designation, these should be viewed as degenerative in nature.
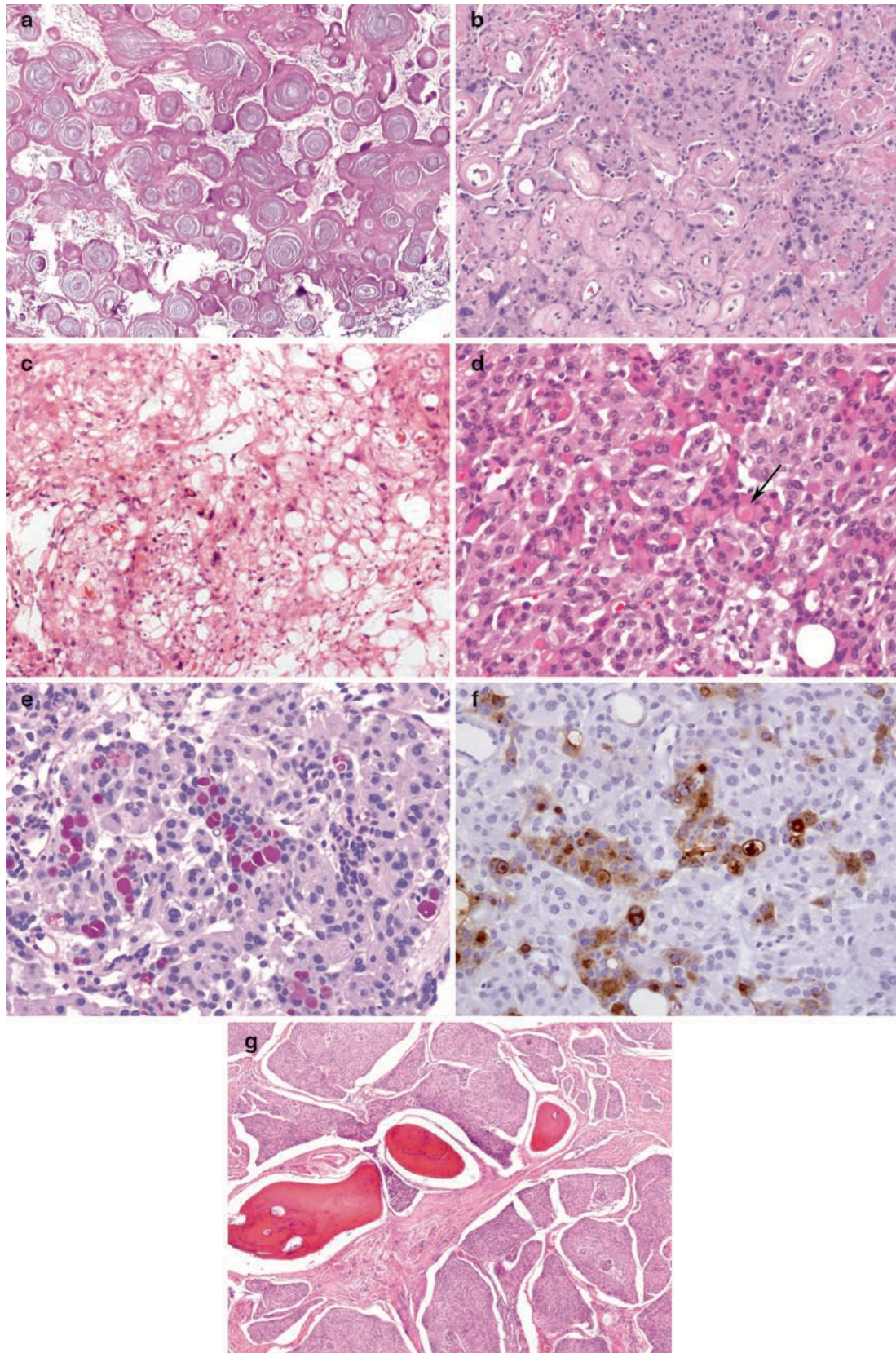
Fig. 9.7. Other WHO grade I variants. (**a**) In psammomatous meningioma, psammoma bodies may be so numerous as to make identification of the neoplastic meningothelium difficult. (**b**) Angiomatous meningioma contains numerous variably-sized blood vessels, sometimes hyalinized, and a tendency for nuclear pleomorphism. (**c**) In addition to the numerous microcystic spaces, easily-recognizable meningothelial cells are seen in this microcystic meningioma. Secretory meningiomas contain islands of obvious epithelial differentiation (**d**) as well as PAS and CEA-positive pseudopsammoma bodies (**e** and **f**, respectively). (**g**) Metaplastic changes may also be seen in meningioma, here showing an example with metaplastic bone formation.
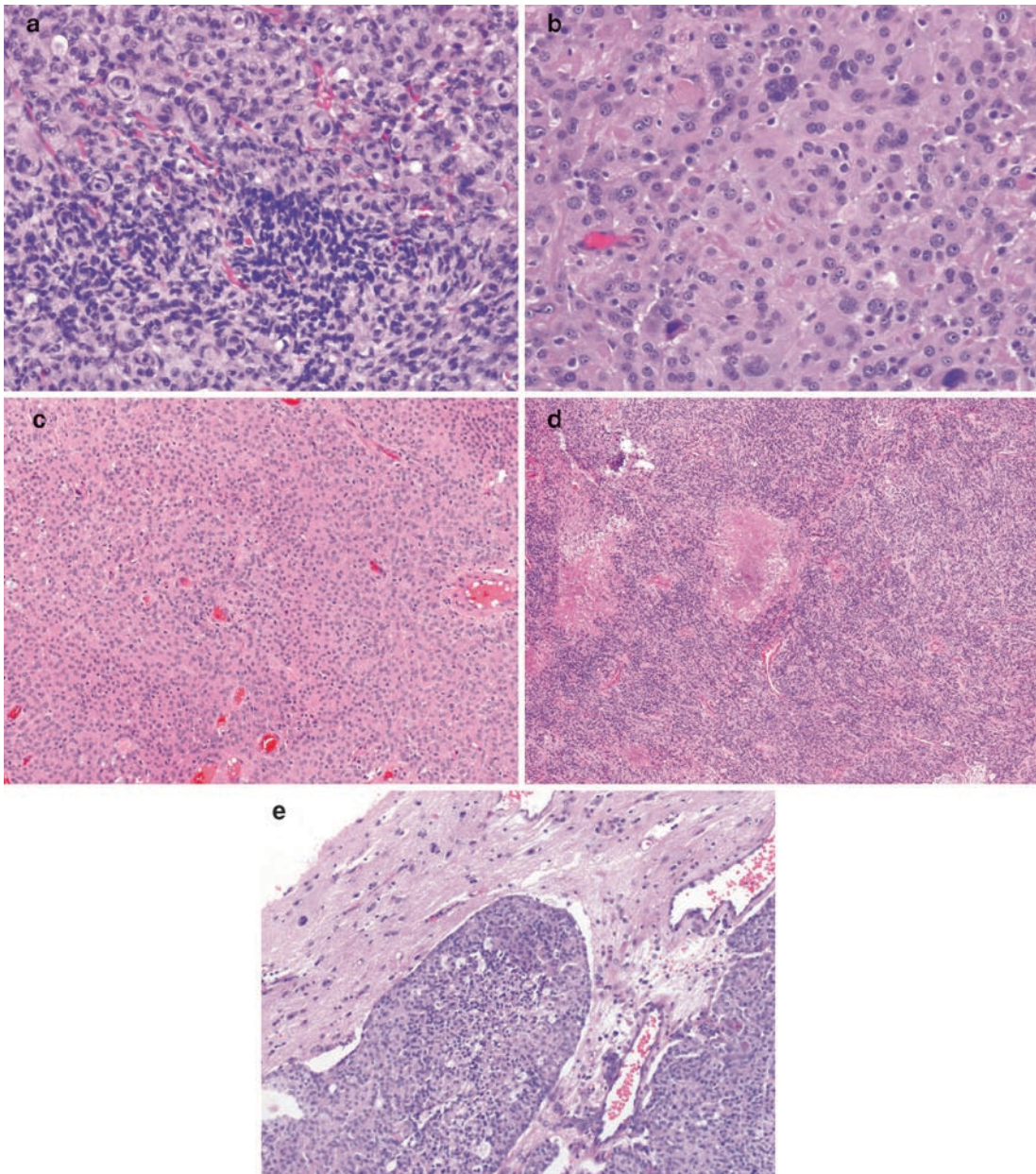
Fig. 9.8. Microscopic features of atypical meningioma (WHO grade II) may include elevated mitotic rate and/or three or more of the following features: hypercellularity, small cell change (**a**), prominent nucleoli (**b**), sheeting architecture (**c**), and foci of spontaneous necrosis (**d**). Brain invasive meningiomas (**e**) have a rate of recurrence similar to atypical meningioma.
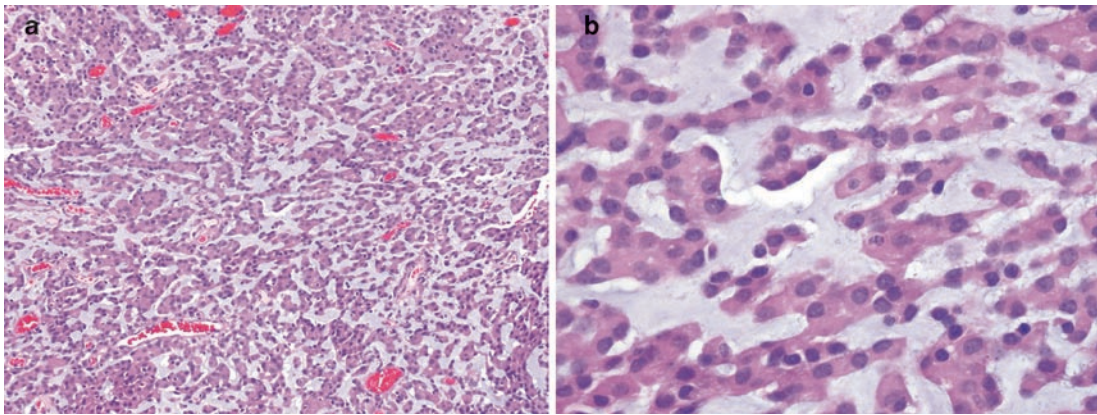
Fig. 9.9. With its distinctive cord-like architecture (**a**), chordoid meningioma (WHO grade II) superficially resembles chordoma, though closer inspection reveals that it lacks the bubbly physaliferous cells of that entity (**b**).
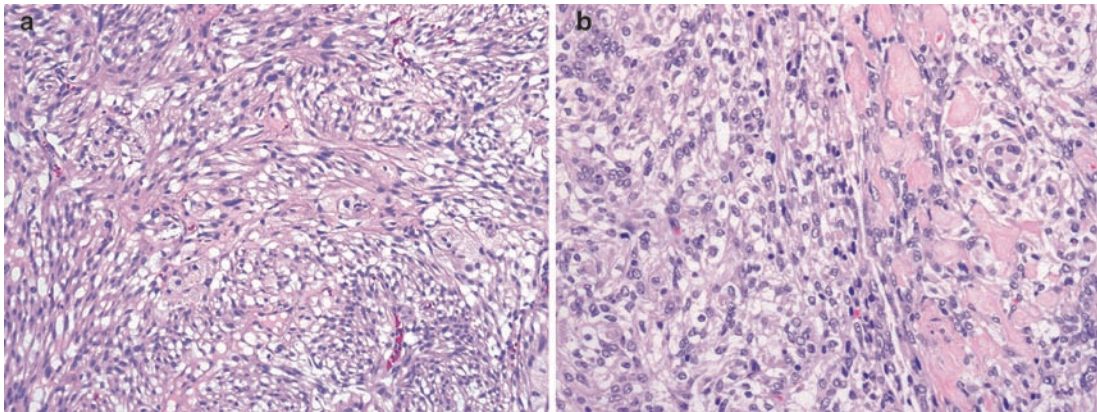
Fig. 9.10. A fascicular architecture with occasional vague whorls is seen in clear cell meningioma, WHO grade II (**a**). Dense collagen blocks are a helpful diagnostic clue seen in most cases (**b**).
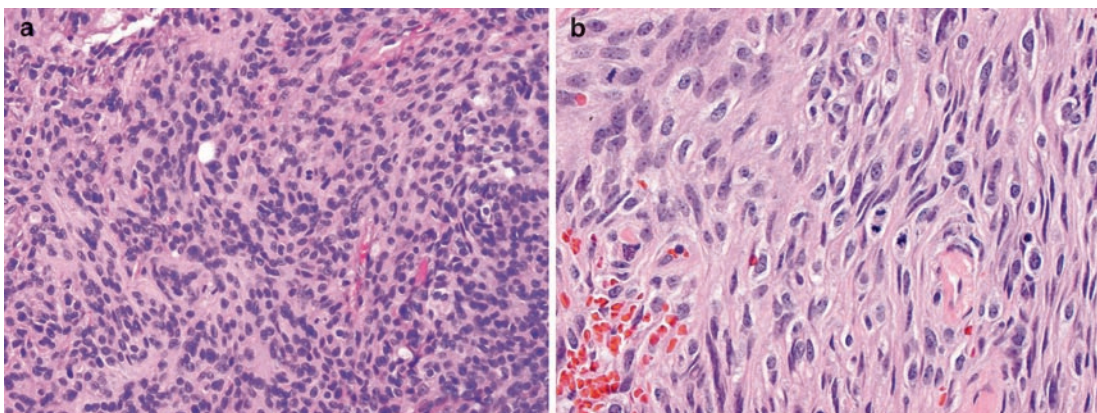
Fig. 9.11. Often barely recognizable as meningioma, anaplastic meningioma (WHO grade III) may resemble sarcoma, carcinoma, or melanoma (**a**) and have a brisk mitotic index (**b**).
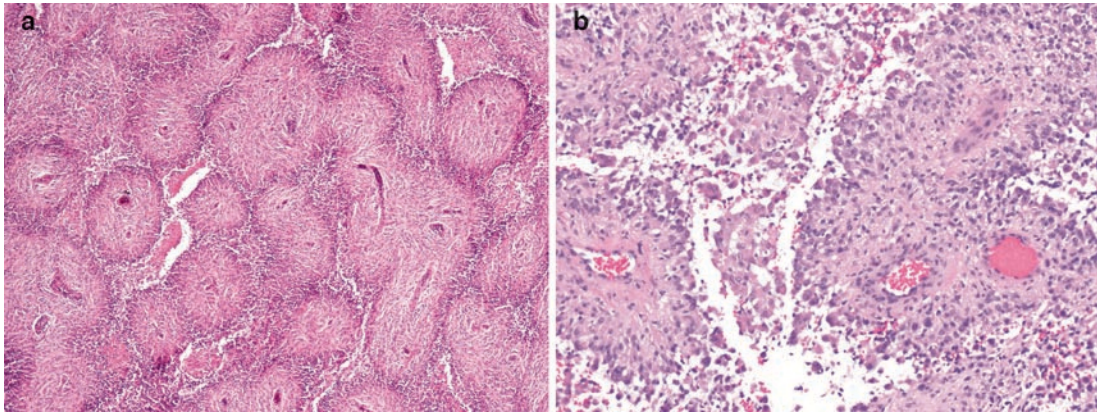
Fig. 9.12. Papillary meningioma (WHO grade III) contains broad fibrovascular cores covered by neoplastic meningothelium (**a** and **b**). A careful search of tissue from these tumors should reveal at least few foci recognizable as meningioma.
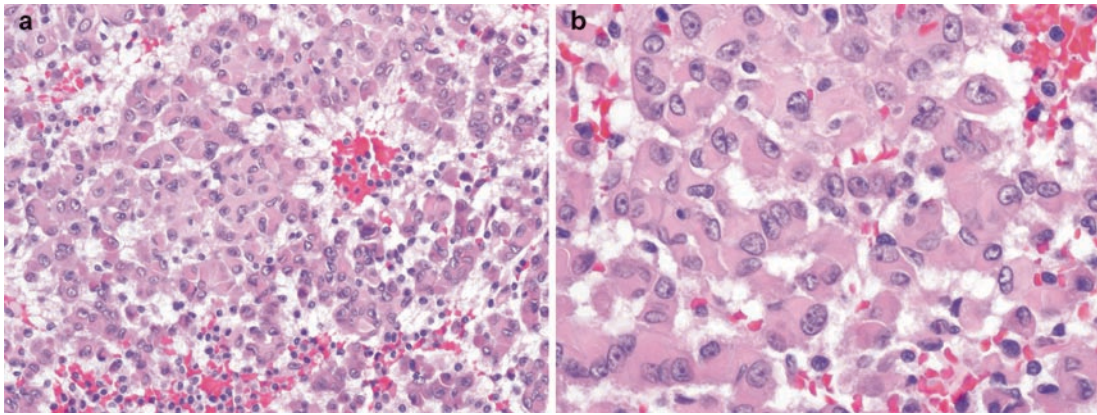
Fig. 9.13. Rhabdoid meningioma (WHO grade III) characteristically contains discohesive nests of cells with eccentric nuclei, often with vesicular chromatin pattern and prominent nucleoli, in addition to eosinophilic cytoplasmic "bellies" (**a** and **b**). Areas more recognizable as meningioma are usually identifiable elsewhere within these tumors, though this rhabdoid morphology may be the predominant morphology in some cases.
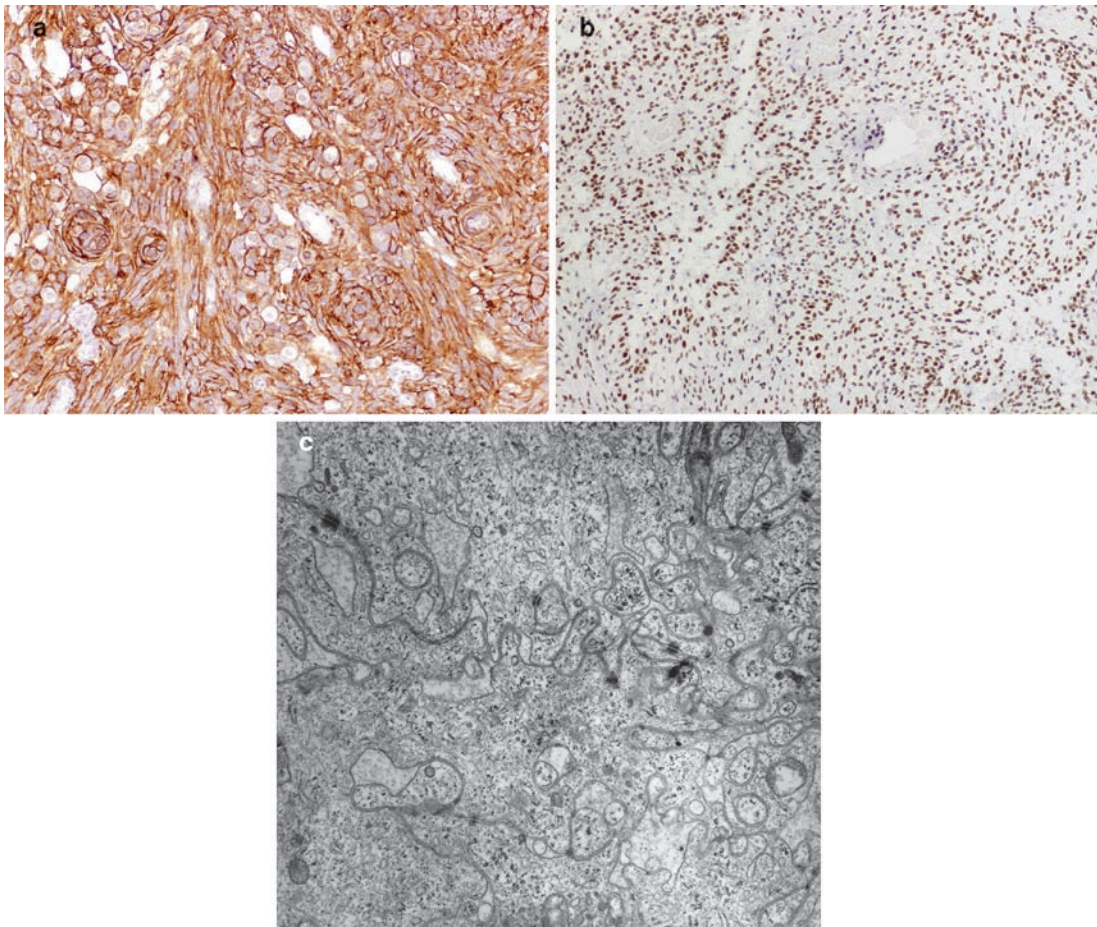
Fig. 9.14. (**a**) Meningiomas are consistently immunopositive for Epithelial Membrane Antigen (EMA). (**b**) Rhabdoid meningioma shows retained nuclear staining for INI1/BAF47 by immunohistochemistry; in true rhabdoid tumor or AT/RT, this nuclear staining is lost. (**c**) Meningioma ultra-structural findings include intercellular interdigitations and desmosomes.

Hemangiopericytoma and Other Mesenchymal Tumors

Christine E. Fuller

10.1 OVERVIEW

- Meningeal hemangiopericytomas are highly cellular mesenchymal tumors exhibiting characteristic "staghorn" vasculature, akin to their soft tissue counterparts.
- Their definite cell of origin is uncertain, though it has been suggested that they may be close relatives to solitary fibrous tumor.
  - At this point in time, however, the WHO recognizes hemangiopericytomas (grade II) and anaplastic hemangiopericytomas (grade III) as distinct from solitary fibrous tumors given their markedly different biologic behaviors.
- In older terminology, hemangiopericytomas were considered a variant of angioblastic meningioma.
- A variety of mesenchymal tumors, both benign and malignant, may occur within the CNS, many arising from the dura/meninges.
- These lesions all are histologically identical to their non-CNS soft tissue or bony counterparts, and should be named accordingly.
- Sarcomas may arise de novo or following cranial irradiation or previous trauma.
- The antiquated term "meningeal sarcoma" should be avoided as this term had previously been used to describe a wide array of lesions including true sarcomas, as well as anaplastic/malignant meningiomas.

10.2 CLINICAL FEATURES

- Hemangiopericytomas (HPC)
  - Are quite uncommon in all age groups, representing <1% of all CNS tumors, and <3% of dural-based lesions.
  - Have a peak age range within the third and fourth decades, less frequently arising in the elderly and pediatric age groups. Rare congenital lesions have been described.
  - There is a slight male predominance.
- Mesenchymal tumors may occur at any age and show no gender bias.
- Rhabdomyosarcoma and Ewing/PNET occur predominantly in children.
- The spectrum of clinical signs and symptoms mirrors that described for meningiomas as these tumors present as dural-based lesions, and is dependent largely on lesion localization.
- HPC may rarely present with acute intratumoral hemorrhage.

10.3 NEUROIMAGING

- Hemangiopericytomas
  - Are most commonly located intracranially, attached to dura in parasagittal and falcine regions; less frequently, they involve spinal dura.
  - Rare intraparenchymal, intraventricular, and optic nerve sheath tumors have been reported.
  - Unlike meningiomas, they are almost always solitary, do not contain calcifications, and there is an increased predilection for proximity to venous sinuses. They may be solid or have cystic components.
  - Skull base tumors may mimic aggressive primary bone tumors such as Ewing sarcoma, showing lytic destruction as opposed to the typical hyperostosis characteristic of meningioma.
  - Neuroimaging studies (both CT and MRI) show them to be sharply demarcated dural-attached tumors with intense enhancement following contrast administration (Fig. 10.1a, b). They are iso- to hyperintense on T1 and iso- to hypointense on T2-weighted imaging (Fig. 10.1b, c).
  - Angiography typically reveals extensive tumoral vascularity, often with dual cortical and meningeal supply, and sometime corkscrew-shaped feeding vessels (Fig. 10.1d).
- Lipomas are the most common of the benign mesenchymal lesions, showing both intracranial (midline) and spinal localization, whereas most sarcomas are supratentorial with the exception of rhabdomyosarcomas, which are often infratentorial.
- Chondrosarcomas tend to arise in the region of the base of skull.
- Whereas the neuroimaging appearance of dural mesenchymal lesions is nonspecific (Fig. 10.1e), lipomas appear as circumscribed lesions with high-signal intensity of T1-weighted MR images.

10.4 PATHOLOGY

- *Gross pathology:*
  - Resection specimens of HPC and other sarcomas are usually composed of firm, fleshy to overtly hemorrhagic tissue and/or necrotic tissue, HPC often showing grossly visible vascular spaces. Brain invasion may be seen in some. Lipomas are bright yellow and lobulated.
- *Intraoperative cytologic imprints/smears:*
  - Hemangiopericytomas are notable for cells with oval to spindled nuclear profiles, inconspicuous nucleoli, and a "ferning out" of blood vessels (Fig. 10.2a).

- Sarcomas are quite variable in their cytomorphologic appearance, though most often contain variably pleomorphic spindled cells, sometimes with identifiable mitoses, and a necrotic and/or hemorrhagic background. Smear preps of lipomas show only mature adipocytes.
- *Histology:*
  - Meningeal hemangiopericytomas resemble their non-CNS counterparts, and are typified by
    - A monomorphous population of randomly oriented oval to spindle-shaped cells with scant cytoplasm, indistinct cell borders, and lacking nuclear pseudoinclusions or nucleoli (Fig. 10.2b, d).
    - Numerous thin-walled gaping vascular spaces in a characteristic staghorn configuration (Fig. 10.2b, c), and
    - A rich reticulin network, with reticulin fibers surrounding individual tumor cells (Fig. 10.2e).
    - Anaplastic hemangiopericytoma (WHO grade III) harbors necrosis and/or elevated mitotic rate (>5 mitoses per 10 high power fields) and at least two of the following features-hemorrhage, nuclear atypia, and hypercellularity (Fig. 10.3a, b).
    - Areas of hypercellularity may be interrupted by more sparsely cellular regions with fibrosis, imparting a biphasic pattern.
    - Infiltration of adjacent bone or brain parenchyma is common; necrosis is uncommon and calcifications are not seen.
    - The spectrum of mesenchymal tumors particularly arising in the pediatric age group is broad and includes benign lesions such as fibrous histiocytoma and lipoma, fibromatosis, and a wide range of sarcomas including rhabdomyosarcoma, leiomyosarcoma, synovial sarcoma, Ewing/PNET, epithelioid sarcoma, fibrosarcoma, mesenchymal chondrosarcoma, osteosarcoma, myxofibrosarcoma, and pleomorphic sarcoma. All of these CNS examples are histologically identical to their counterparts arising elsewhere in the body (Figs. 10.4a-f).

10.5 IMMUNOHISTOCHEMISTRY

- Meningeal hemangiopericytoma has an identical immunohistochemical profile as its soft tissue counterpart, showing diffuse positivity for vimentin, CD99, and bcl-2, and more variable positivity for Leu-7, CD34, and factor XIIIa in individual tumor cells.
- CD34 positivity is generally patchy as opposed to the diffuse positivity typical of solitary fibrous tumor (Fig. 10.5a-c).
- Unlike the strong diffuse positivity for EMA and claudin-1 displayed by meningiomas, staining is typically patchy and weak for these antibodies in hemangiopericytoma.
- They are negative for S-100, CD31, and progesterone receptor; actin, desmin, and cytokeratin (CAM5.2) staining is rare.
- The immunoprofile of other mesenchymal lesions likewise mirrors their non-CNS counterparts.

10.6 ELECTRON MICROSCOPY

- Similarly, the ultrastructural findings of meningeal hemangiopericytoma are like those of hemangiopericytomas originating elsewhere in the body.

- Characteristic features include tightly packed spindled cells, each surrounded by basement membrane-like material.
- Junctional complexes, including desmosomes, are lacking.

10.7 MOLECULAR PATHOLOGY

- No consistent molecular alterations have been detected in meningeal hemangiopericytoma, though abnormalities of chromosomes 3, 6p, 7p, 12q, 19q and homozygous deletions of *p16* have been reported in adult series.
- They lack deletions of 14q and protein 4.1b typical of meningioma, and similarly deletions of 1p and *NF2* are extremely uncommon in HPC.
- EWS and FOXO1-related translocations are characteristic of Ewing/PNET and alveolar rhabdomyosarcoma, respectively.

10.8 DIFFERENTIAL DIAGNOSIS

- Schwannoma may resemble hemangiopericytoma, though the latter will lack S-100 positivity.
- Solitary fibrous tumor, particularly the more hypercellular examples, will closely mimic hemangiopericytoma, including the staghorn vasculature.
- Though they do overlap in their immunohistochemical staining pattern, solitary fibrous tumors are typically more diffusely positive for CD34, contain frequent and diffuse areas of hyalinization and collagen deposition, have only rare mitoses, and have a sparse pattern of reticulin staining with positivity around clusters of cells in contrast to the fine intercellular network typical of hemangiopericytoma.
- Meningiomas also entered into the differential diagnosis of HPC and other mesenchymal tumors.
- Hemangiopericytomas, as noted above, can most effectively be differentiated by demonstration of strong staining for bcl-2 and CD99; they likewise lack strong staining for EMA and claudin as is most typical for meningioma.
- They will likewise show the ultrastructural feature of pericellular basement membrane-like material (correlating with the rich reticulin network), a feature not present in meningiomas. In contradistinction, detection of deletions of 14q or protein 4.1b will also effectively rule out hemangiopericytoma.

10.9 PROGNOSIS

- Given the rarity of HPCs in children, the corresponding survival statistics have not yet been worked out. In adults, the following have been described:
  - Local recurrence is encountered in over 80% of cases and after a mean period of 3 years after surgery, seemingly irrespective of adequacy of initial resection.
  - Effective control of recurrence may be afforded by additional excision, radiotherapy, or gamma knife radiosurgery.
  - Extraneural metastasis may be seen up to 50% of patients, common sites of metastasis include bone, lung, liver, abdominal cavity, and elsewhere within the CNS.
  - Histology is predictive of survival time and rate of recurrence, patients with anaplastic tumors living half as long as those with differentiated tumors and with a much higher rate of recurrence.

- Whereas benign mesenchymal CNS lesions are curable surgically, sarcomas are quite aggressive and associated with poor outcomes. Local recurrence and distant metastases, including outside the CNS, are common.

SUGGESTED READING

Akiyama M, Sakai H, Onoue H, Miyazaki Y, Abe T (2004) Imaging intracranial haemangiopericytomas: study of seven cases. Neuroradiology 46(3):194–197

Aouad N, Vital C, Rivel J, Ramsoubramanian K, Santosh S, Chowdry O (1991) Giant supratentorial meningeal haemangioperictoma in a newborn. Acta Neurochir (Wien) 112(3–4):154–156

Bassiouni H, Asgari S, Hubschen U, Konig HJ, Stolke D (2007) Intracranial hemangiopericytoma: treatment outcomes in a consecutive series. Zentralbl Neurochir 68(3):111–118

Blank W, Spring A, Giesen H, Argmann H (1988) Intracranial hemangiopericytoma in a child. Klin Padiatr 200(5):422–425

Bunai Y, Akaza K, Tsujinaka M, Nakamura I, Nagai A, Jiang WX et al (2008) Sudden death due to undiagnosed intracranial hemangiopericytoma. Am J Forensic Med Pathol 29(2):170–172

Cavalheiro S, Sparapani FV, Moron AF, da Silva MC, Stavale JN (2002) Fetal meningeal hemangiopericytoma. Case report. J Neurosurg 97(5):1217–1270

Chiechi MV, Smirniotopoulos JG, Mena H (1996) Intracranial hemangiopericytomas: MR and CT features. AJNR Am J Neuroradiol 17:1365–1371

D'Amore ES, Manivel JC, Sung JH (1990) Soft-tissue and meningeal hemangiopericytomas: an immunohistochemical and ultrastructural study. Hum Pathol 21(4):14–423

Demirtas E, Ersahin Y, Yilmaz F, Mutluer S, Veral A (2000) Intracranial meningeal tumours in childhood: a clinicopathologic study including MIB-1 immunohistochemistry. Pathol Res Pract 196(3):151–158

Gill SS, Bharadwaj R (2007) Cytomorphologic findings of hemangiopericytoma of the meninges: a case report. Indian J Pathol Microbiol 50(2):422–425

Huisman TA, Brandner S, Niggli F, Kacl G, Willi UV, Martin E (2000) Meningeal hemangiopericytoma in childhood. Eur Radiol 10(7):1073–1075

Louis DN, Ohgaki H, Wiestler OD, Cavenee WK (2007) WHO classification of tumours of the central nervous system, 4th edn. IARC, Lyon

Mena H, Ribas JL, Pezeshkpour GH, Cowan DN, Parisi JE (1991) Hemangiopericytoma of the central nervous system: a review of 94 cases. Hum Pathol 22(1):84–91

Nakamura Y, Becker LE (1985) Meningeal tumors of infancy and childhood. Pediatr Pathol 3(2–4):341–358

Ono Y, Ueki K, Joseph JT, Louis DN (1996) Homozygous deletions of the CDKN2/p16 gene in dural hemangiopericytomas. Acta Neuropathol (Berl) 91(3):221–225

Rajaram V, Brat D, Perry A (2004) Anaplastic meningioma vs. meningeal hemangiopericytoma: Immunohistochemical and genetic markers. Hum Pathol 35:1413–1418

Schwent BJ, Wojno TH, Grossniklaus HE (2007) Hemangiopericytoma of the optic nerve sheath. Am J Ophthalmol 143(5):904–906

Sobel G, Halasz J, Bogdanyi K, Szabo I, Borka K, Molnar P et al (2006) Prenatal diagnosis of a giant congenital primary cerebral hemangiopericytoma. Pathol Oncol Res 12(1):46–49

Soyuer S, Chang EL, Selek U, McCutcheon IE, Maor MH (2004) Intracranial meningeal hemangiopericytoma: the role of radiotherapy: report of 29 cases and review of the literature. Cancer 100(7):1491–1497

Tihan T, Viglione M, Rosenblum MK, Olivi A, Burger PC (2003) Solitary fibrous tumors in the central nervous system. A clinicopathologic review of 18 cases and comparison to meningeal hemangiopericytomas. Arch Pathol Lab Med 127:432–439
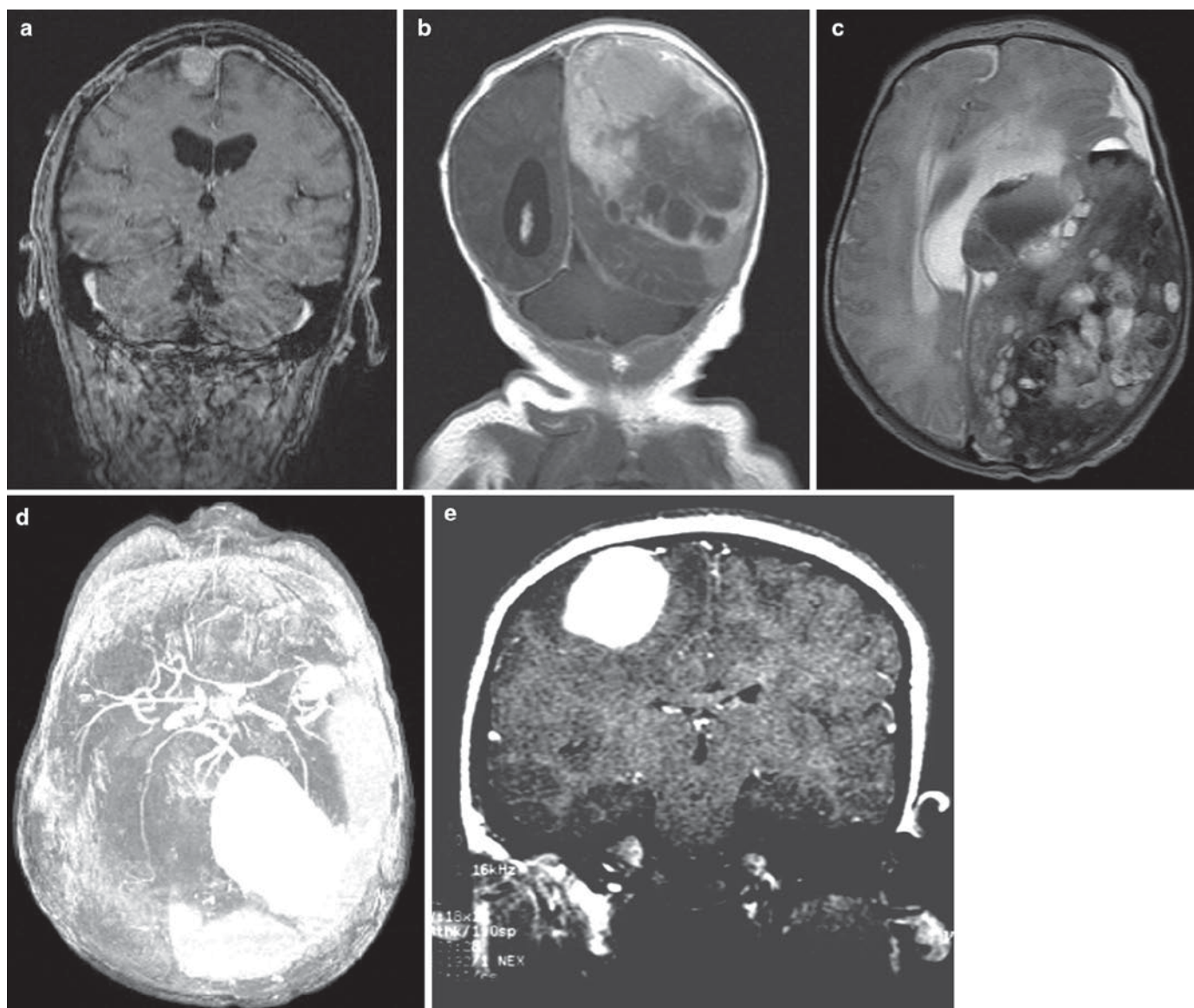
Fig. 10.1. (**a**) Coronal T1-w post-Gd MR image of a small parasagittal hemangiopericytoma showing homogeneous contrast enhancement of this dural-based nodule. (**b**) Coronal T1-w post-Gd MR image of a huge hemangiopericytoma with solid and cystic areas and heterogeneous contrast enhancement. (**c**) Axial T2-w imaging from this same tumor show heterogeneous signal intensity and multiple cysts, and angiography (**d**-venous phase) highlights tortuous feeder vessels entering this highly vascular lesion. (**e**) Coronal T1-w post-Gd MR image of a solitary fibrous tumor, arising as homogeneously enhancing dural-based nodule (Fig. 10.1e courtesy of Dr Mural Gokden, University of Arkansas, Little Rock, AK, USA).
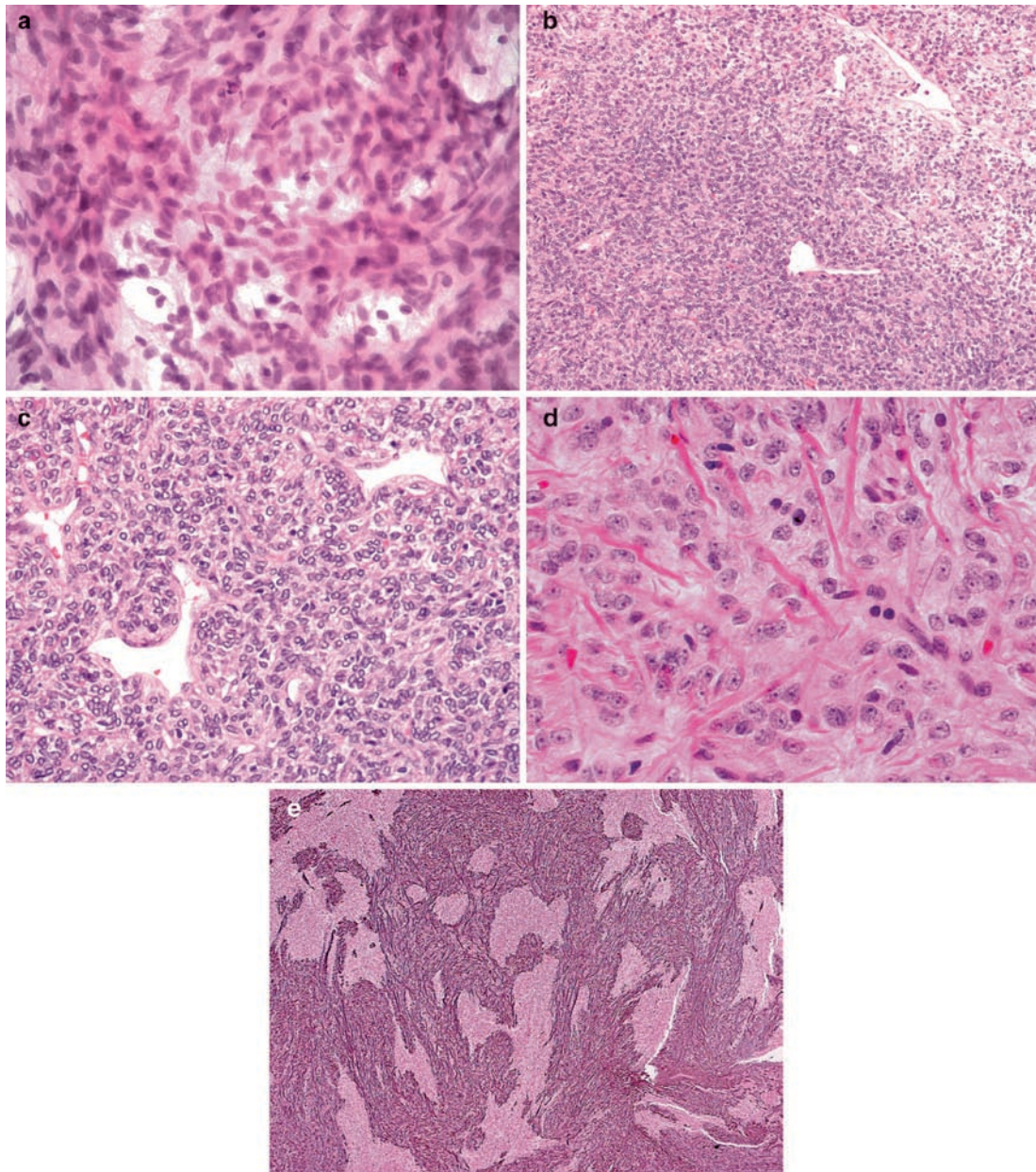
Fig. 10.2. (**a**) Cytologic smear preparation of hemangiopericytoma showing patternless sheets of spindled cells; whorls and intranuclear cytoplasmic invaginations (pseudoinclusions) are not present. (**b**, **c**); Typical histologic appearance of hemangiopericytoma showing randomly oriented spindled cells with scant cytoplasm and indistinct cell borders, and the characteristic "staghorn" gaping vasculature. (**d**) Nuclei are fairly monotonous with indistinct tiny nucleoli and lacking of nuclear pseudoinclusions. (**e**) Abundant reticulin is present, including investments around individual tumor cells.
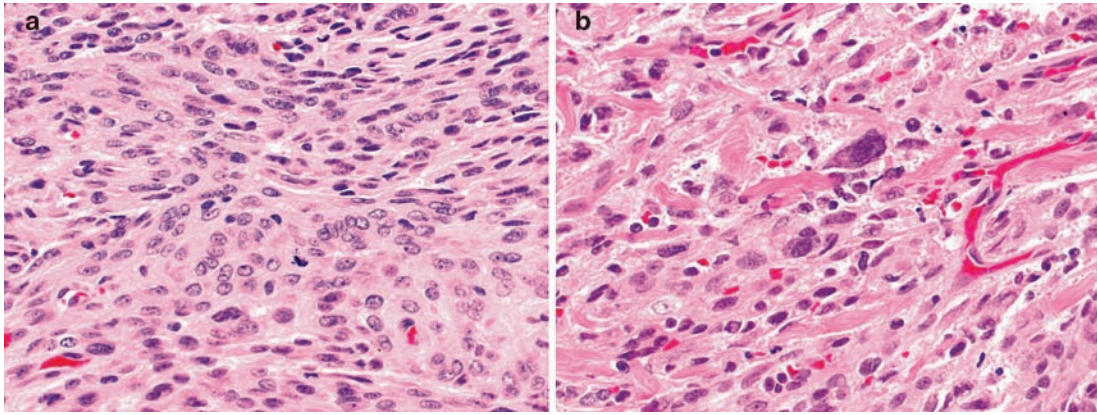
Fig. 10.3. Anaplastic hemangiopericytomas have increased mitotic activity (**a**) and may have notable nuclear pleomorphism (**b**).
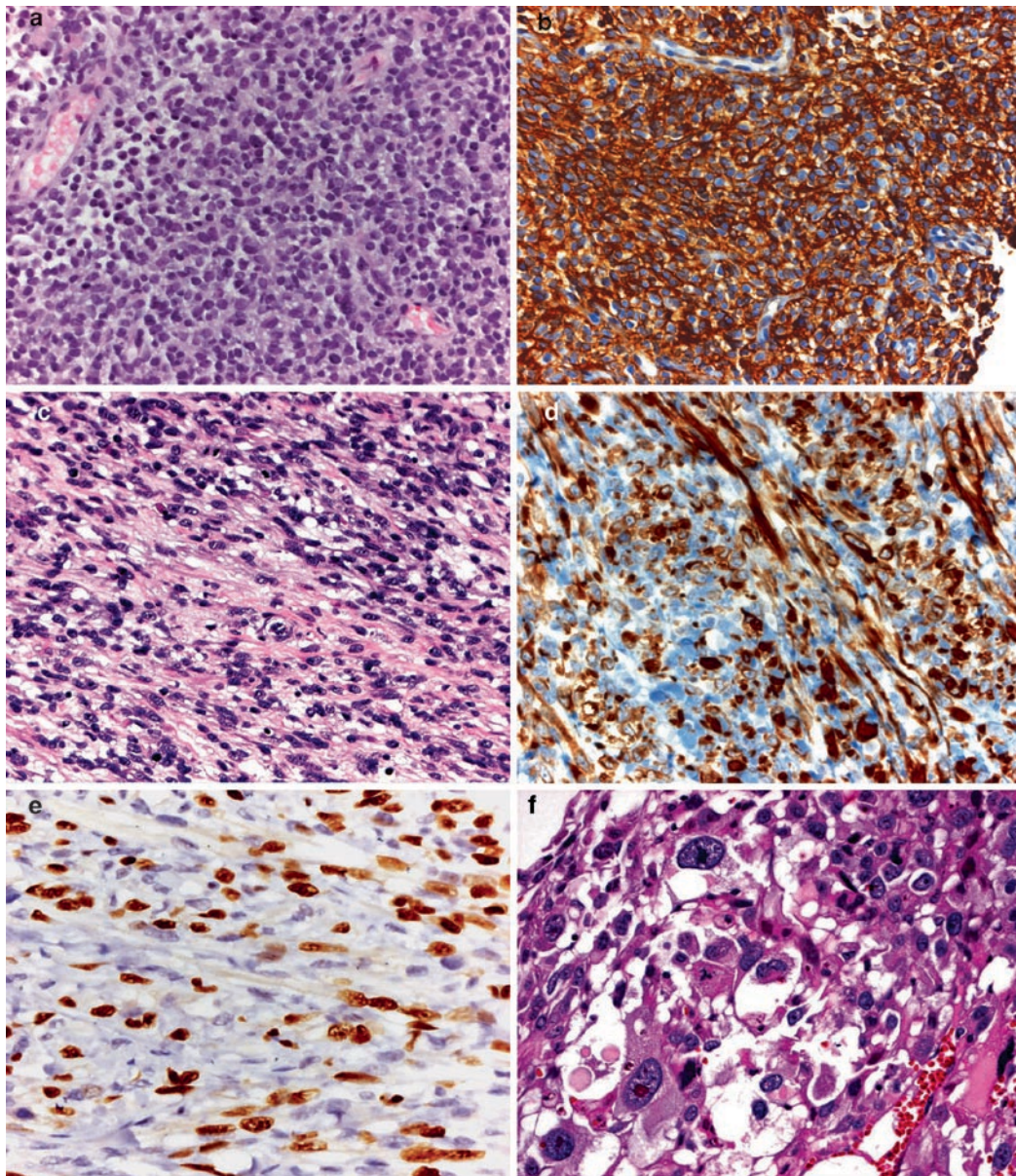
Fig. 10.4. (**a**) Ewing/PNET with monotonous sheets of small round blue cells, showing strong membranous positivity for CD99. (**b**) Rhabdomyosarcoma with scattered characteristic strap cells (**c**) by immunohistochemistry, this tumor showed strong positivity for both desmin (**d**) and myogenin (**e**). Fig. (**f**) depicts a pleomorphic sarcoma with numerous bizarre nuclei, several with prominent nucleoli.
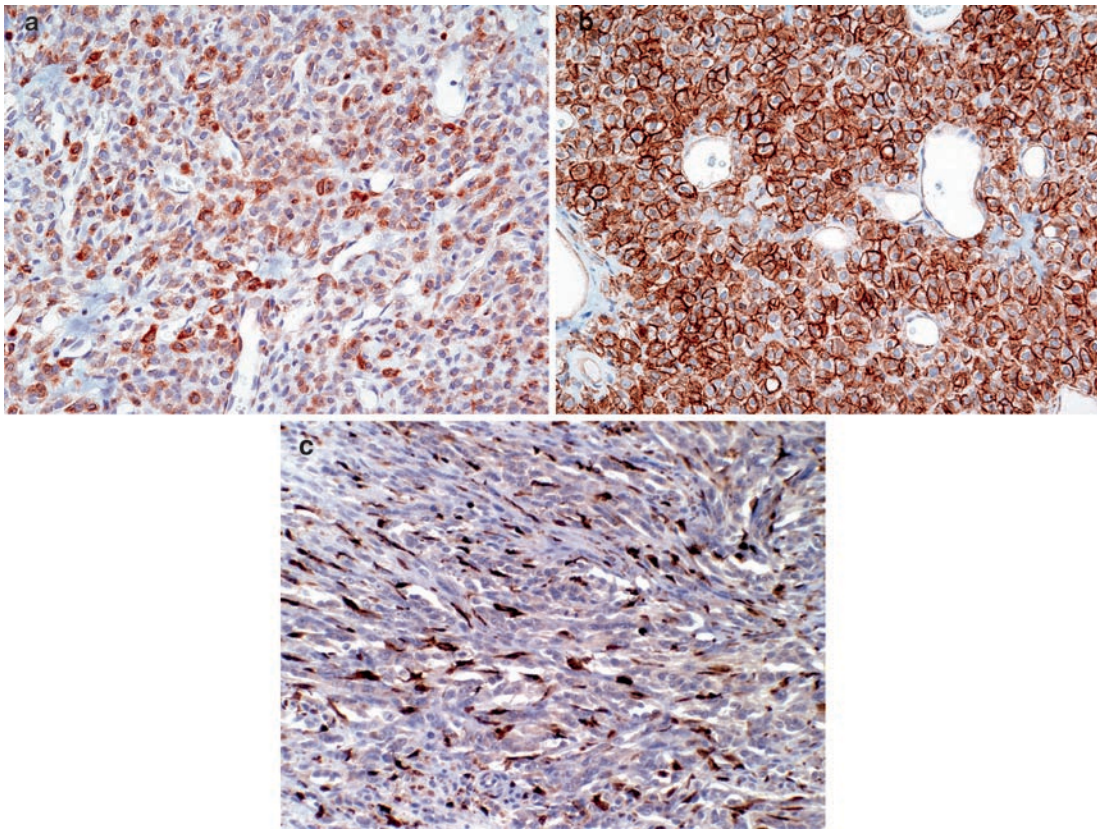
Fig. 10.5. Hemangiopericytoma is consistently positive for bcl-2 (**a**) and CD99 (**b**). Factor XIIIa stains scattered individual tumor cells (**c**), though this staining pattern may similarly be encountered in meningiomas (Pictures courtesy of Dr Arie Perry, Washington University, St Louis, MO, USA).

Melanocytic Lesions

Christine E. Fuller

11.1 OVERVIEW

- Dural-based lesions thought to derive from the leptomeningeal melanocytes. These include both circumscribed mass lesions *melanocytoma* and *malignant melanoma*, as well as diffuse *leptomeningeal melanocytosis* and its malignant counterpart *melanomatosis.*
- Diffuse melanocytosis is strongly linked to the rare congenital autosomal dominant phakomatosis neurocutaneous melanosis (Touraine syndrome), the affected patients in addition harbor large and/or multiple cutaneous congenital nevi.
- These patients are at significantly heightened risk for development of leptomeningeal melanoma or melanomatosis.

11.2 CLINICAL FEATURES

- Leptomeningeal melanocytosis and primary melanomas make up the bulk of pediatric melanocytic lesions; melanocytomas may occur in all age groups, though most arise in middle-age adults.
- Children with neurocutaneous melanosis and melanocytosis typically present before 2 years of age, and there is no gender or racial bias.
- Primary CNS melanomas are rarely reported below the 2nd decade of age, apart from when they arise in the context of neurocutaneous melanosis.
- The clinical presentation is variable and relates either to increased intracranial pressure secondary to hydrocephalus, or localized parenchymal compromise due to compression/mass effect or direct parenchymal infiltration (in the case of the malignant lesions).

11.3 NEUROIMAGING

- Leptomeningeal melanocytosis and melanomatosis may involve large expanses of the leptomeninges, with a predilection for the regions of the temporal lobes, cerebellum, and brainstem.
- Both may appear as diffuse thickening and contrast enhancement of the leptomeninges, sometime with foci of nodularity.
- Though they have been described throughout the neuroaxis, melanocytomas most frequently involve the cervical and thoracic spinal regions, presenting as dural-based lesions or in association with the nerve roots. Because of their high melanin content, they are characteristically iso-intense to hyperintense on *T1* weighted MR images, hypo-intense on *T2*, and show homogeneous contrast enhancement (Fig. 11.1a).
- Melanocytomas of Meckel's cave are associated with ipsilateral nevus of Ota.
- Melanomas often show similar neuroimaging characteristic to melanocytoma (depending upon their melanin content); in addition they often have associated *T2*-hyperintense vasogenic edema in the nearby parenchyma.

11.4 PATHOLOGY

- *Gross pathology:*
  - Diffuse lesions (melanocytosis/melanomatosis) present as dense discoloration of the leptomeninges, ranging from a dusky clouding to dense dark brown to black hyperpigmentation.
  - Melanocytoma and melanoma appear as solid extraaxial masses, their coloration dependent upon their overall melanin content; they may be black, brown, blue, or flesh-colored.
- *Cytology findings:*
  - Smear preparations of melanocytoma contain dispersed and perivascular aggregates of bland oval to spindle-shaped cells with small nucleoli and long cytoplasmic processes. Fine or course melanin pigment are easily detected, often more so than in frozen intraoperative specimens.
  - Malignant melanoma cells detected on smears or in CSF samples have a similar appearance to peripheral malignant melanomas, being epithelioid to spindled with significant nuclear pleomorphism; cytoplasmic melanin may or may not be present.
- *Histology:*
- All of these lesions are composed of cells with melanocytic differentiation, most showing melanin pigment within the tumor cells themselves, intermixed stromal cells and melanophages.
- Rare amelanotic examples of melanoma or melanocytoma occur, the diagnosis in these instances is reliant upon immunohistochemical and ultrastructural analysis.
- *Diffuse leptomeningeal melanocytosis* is a diffuse proliferation of cytologically bland leptomeningeal melanocytes of variable shape (spindled to epithelioid).
  - These cells often accumulate within Virchow-Robin spaces; overt invasion into CNS parenchyma constitutes evidence of malignant progression *(melanomatosis).*
- *Melanocytomas* are composed of variably-pigmented spindled to oval cells forming syncytial nests, sometimes with whorl formations resembling meningioma. Fascicular or sheeted architecture may be seen.

–   The cells have rounded to oval bland nuclei and small nucleoli.
–   Atypia and mitoses are not features.
–   CNS parenchymal invasion and elevated mitotic rate are features indicative of propensity for more aggressive biologic behavior (Fig. 11.1b–e).
*   *Malignant melanomas* are histologically akin to melanomas elsewhere in the body, composed of spindled to epithelioid cells with variable cytoplasmic pigment, arranged in cohesive nests, sheets, or sweeping fascicles.
–   They frequently show significant cytological atypia with enlarged pleomorphic nuclei, prominent nucleoli, and numerous mitoses, including atypical forms (Fig. 11.2a–c).
–   Overt CNS parenchymal invasion and/or necrosis are commonly present.

11.5 IMMUNOHISTOCHEMISTRY

*   All of these pigmented lesions share a similar immunohistochemical profile, being positive for *S-100* (Fig. 11.3a) and melanocytic markers *HMB-45* and *MART1* (Melan A) (Fig. 11.3b), with variable positivity for vimentin and NSE.
*   They are negative for EMA, GFAP, and cytokeratin.
*   *Ki67* labeling is elevated in melanomatosis and melanomas.

11.6 ELECTRON MICROSCOPY

*   Similarly, they all contain melanosomes, and all lack desmosomes and interdigitating cell processes typical of meningiomas and basement membrane material surrounding individual cells as seen in schwannomas.

11.7 MOLECULAR PATHOLOGY

*   Apart from the aforementioned link between diffuse leptomeningeal melanocytosis and neurocutaneous melanosis syndrome, thus far no specific genetic/molecular alterations have been identified in any of these pigmented lesions.

11.8 DIFFERENTIAL DIAGNOSIS

*   All of these primary CNS melanocytic lesions need to be differentiated from the following tumors:
–   Metastatic malignant melanoma, as this shares identical histologic, immunohistochemical, and ultrastructural features with primary CNS melanoma, identification of a primary lesion outside the CNS by radioimaging or other studies is critical.
–   Meningioma may mimic these melanocytic lesions, especially melanocytoma; as noted above, meningiomas are typically EMA positive, will lack melanocytic markers

and melanosomes, and will have interdigitating cell processes and desmosomes.
–   A number of other primary CNS tumors may show pigmentation, including schwannoma, neurofibroma, medulloblastoma, choroid plexus tumors, and some gliomas. Thankfully, most of these do not resemble these melanocytic tumors from a histologic standpoint; in diagnostically difficult instances, immunohistochemical and ultrastructural evidence of the corresponding cell of origin can be accurately ascertained. Schwannomas, for instance, have intervening basement membrane surrounding individual tumor cells. GFAP-positive intermediate filaments are a feature of gliomas, and choroid plexus tumors are positive for transthyretin and have surface microvilli and cilia.

11.9 PROGNOSIS

*   Diffuse leptomeningeal melanocytosis has a generally poor prognosis, independent of the increased risk of malignant progression to melanomatosis.
*   Melanocytomas are unpredictable; often there is cure with complete resection, however occasional lesions will show local recurrence or may undergo malignant transformation.
*   Frank CNS parenchymal infiltration correlates strongly with this tendency for aggressive biologic behavior.
*   Melanomas are highly aggressive tumors, radioresistant, and carry a very poor prognosis with frequent metastasis both within and outside the CNS to peripheral organs.

SUGGESTED READINGS

Ahluwalia S, Ashkan K, Casey AT (2003) Meningeal melanocytoma: clinical features and review of the literature. Br J Neurosurg 17(4):347–351

Alcutt D, Michowiz S, Weitzman S, Becker L, Blaser S, Hoffman H et al (1993) Primary leptomeningeal melanoma: an unusually aggressive tumor in childhood. Neurosurgery 32(5):721–729

Brat D, Giannini C, Scheithauer BW, Burger PC (1999) Primary melanocytic neoplasms of the central nervous system. Am J Surg Pathol 23(7):745–754

Chen KT (2003) Crush cytology of melanocytoma of the spinal cord. A case report. Acta Cytol 47(6):1091–1094

Kadonaga JN, Frieden IJ (1991) Neurocutaneous melanosis: definition and review of the literature. J Am Acad Dermatol 24(5):747–755

Lopez-Castilla J, Diaz-Fernandez F, Soult JA, Munoz M, Barriga R (2001) Primary leptomeningeal melanoma in a child. Pediatr Neurol 24(5):390–392

Makin GW, Eden OB, Lashford LS, Moppett J, Gerrard MP, Davies HA et al (1999) Leptomeningeal melanoma in childhood. Cancer 86(5):878–886

Nicolaides P, Newton RW, Kelsey A (1995) Primary malignant melanoma of meninges: atypical presentation of subacute meningitis. Pediatr Neurol 12(2):172–174

O'Brien DF, Crooks D, Mallucci C, Javadpour M, Williams D, du Plessis D et al (2006) Meningeal melanocytoma. Child's Nerv Syst 22(6):556–561

Reyes-Mugica M, Chou P, Byrd S, Ray V, Castelli M, Gattuso P et al (1993) Nevomelanocytic proliferations in the central nervous system of children. Cancer 72(7):2277–2285
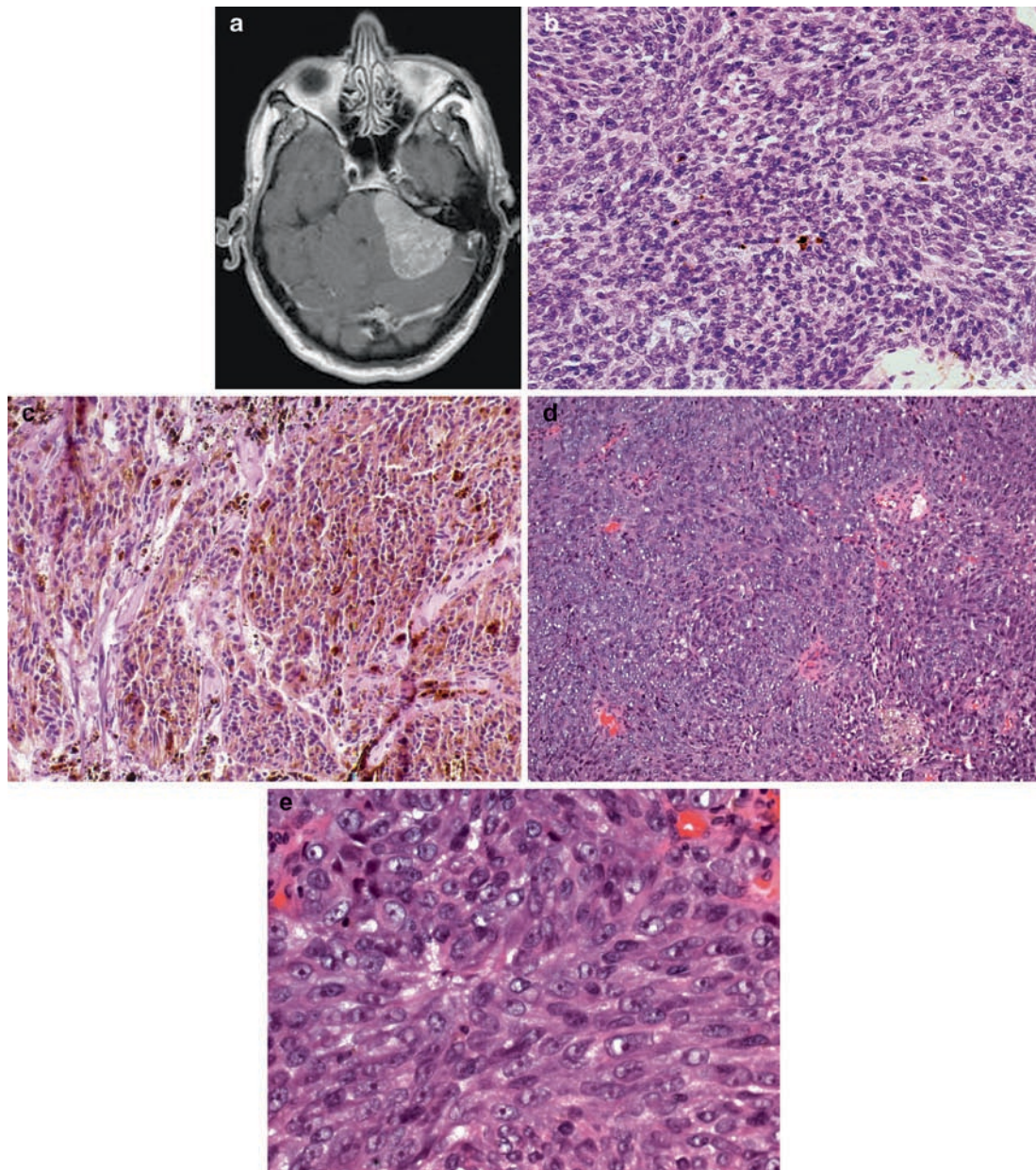
Fig. 11.1. (**a**) This axial *T1*-weighted post-gadolinium MR image shows a well-demarcated homogeneously-enhancing melanocytoma situated in the cerebellopontine angle, an uncommon location for this tumor. (**b**) At low power, this melanocytoma superficially resembles meningioma with bland spindle cells forming broad fascicles. Note occasional darkly pigmented cells. (**c**) Pigmentation is more obvious in this example. (**d**) This melanocytoma showed vague whorl formations, a small nest of lightly pigmented cells notable in the lower right corner. (**e**) At higher power, the same melanocytoma as in B contains bland oval nuclei with small nucleoli. Pleomorphism and mitotic figures are lacking. (Pictures courtesy of Drs Robert Schmidt and Arie Perry, Washington University, St Louis, MO and Dr Murat Gokden, University of Arkansas, Little Rock, AR).
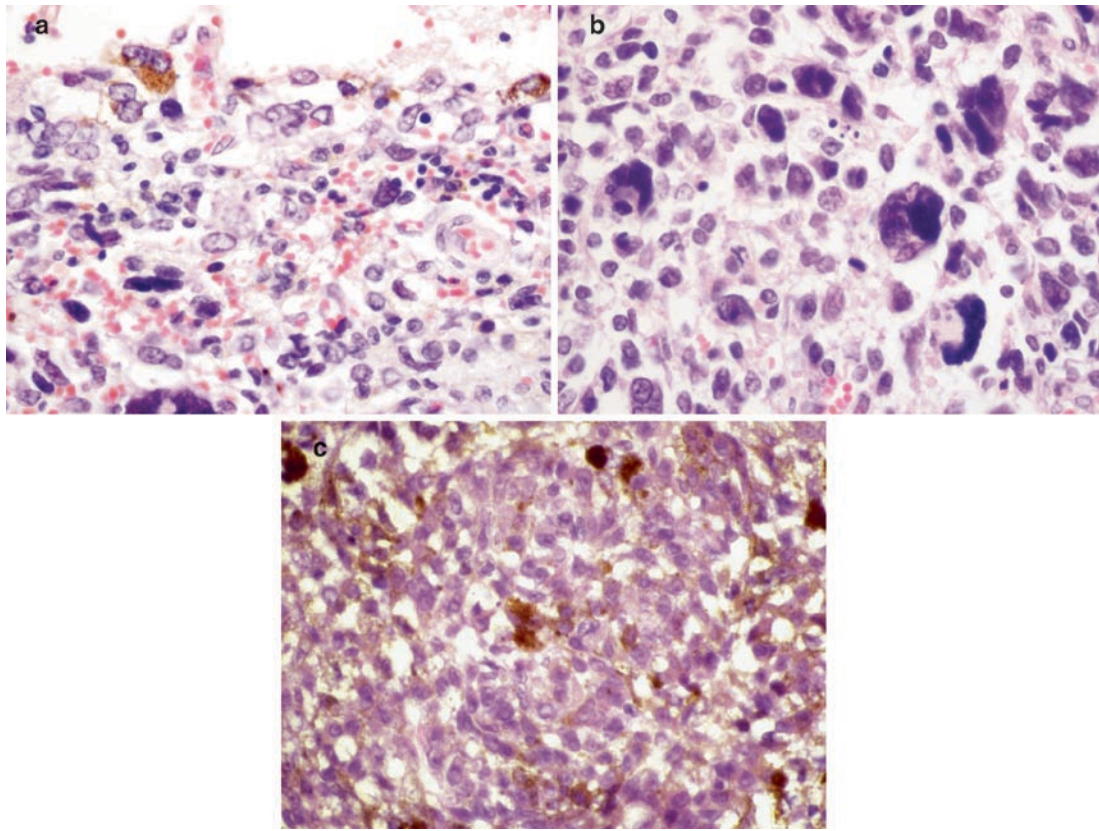
Fig. 11.2. (**a–c**) Primary pediatric leptomeningeal melanoma containing a generally patternless arrangement of variably pigmented cells, many with striking nuclear pleomorphism. Note atypical mitotic figure to the left of center in Fig. 11.2b.
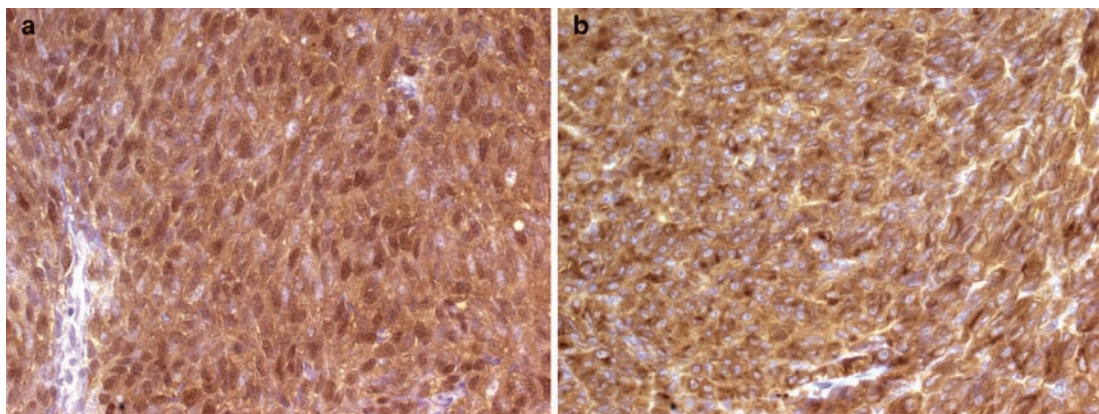
Fig. 11.3. Immunohistochemical staining of the melanocytoma in Fig. 11.1b demonstrating strong diffuse positivity for (**a**) *S-100* and (**b**) *MART1* (Melan A) (Pictures courtesy of Dr Murat Gokden).

Hemangioblastoma

Christine E. Fuller

12.1 OVERVIEW

- Hemangioblastomas are highly vascular tumors that are typically benign and slow-growing, corresponding to WHO grade I.
- They may occur sporadically or in the context of Von Hippel-Lindau (VHL) syndrome (see Sect. F); the former predominates.
- They have also been referred to as capillary hemangioblastomas. Though it is clearly the stromal cell that is the neoplastic component in these tumors, the underlying cell of origin has yet to be determined.

12.2 CLINICAL FEATURES

- They are uncommon CNS tumors in all age groups, most frequently arising in adults, though often presenting in children when associated with VHL. No gender predilection is apparent.
- Clinical signs and symptoms are most often encountered with large tumors and are related to mass effect either from the tumor itself, expansion of an accompanying cyst, or peritumoral edema. Intracranial examples may, therefore, cause ataxia, dysmetria, or hydrocephalus with signs/symptoms of increased intracranial pressure. Spinal tumors may cause radiculopathies and/or pain.
- Tumor production of erythropoietin may lead to polycythemia.
- Spontaneous hemorrhage has occasionally been documented.

12.3 NEUROIMAGING

- Sporadic hemangioblastomas most often arise within the cerebellar hemispheres, whereas those arising within the context of VHL may occur anywhere within the CNS, including the brain stem/cerebellopontine angle, spinal cord, and cranial nerves and nerve roots.
- Supratentorial localization is quite uncommon; unusual sites of occurrence include the pineal region, filum terminale, and extraneural locations. Tumor multiplicity may be encountered in VHL patients.
- Neuroimaging studies typically demonstrate a cystic lesion with heterogeneously contrast-enhancing mural nodule (Fig. 12.1a).
- Solid portions of tumor are typically isointense on T1 and hyperintense on T2-weighted MR images (Fig. 12.1b and 12.2a). They typically show high signal on apparent diffusion coefficient (ADC) map (Fig. 12.1c).

- Flow voids corresponding to large vessels may be encountered, angiography often showing an arteriovenous malformation-like tangle of vessels (Fig. 12.2b).

12.4 PATHOLOGY

- *Gross pathology*: Resection specimens are usually composed of firm, fleshy to overtly hemorrhagic tissue, often with grossly visible vascular spaces (Fig. 12.3a, b).
- *Intraoperative cytologic imprints/smears*: Intraoperative smears and samples of cystic fluid typically contain blood along with abundant stromal cells with hyperchromatic nuclei and lace-like vacuolated cytoplasm. (Fig. 12.4). Small vessels/stripped endothelial cells, macrophages, and calcified material may also be present.
- *Histology*: Hemangioblastomas are composed of a combination of stromal cells and a rich vascular network.
    - The stromal cells, representing the neoplastic component of this lesion, are quite variable in their morphologic appearance. Characteristically, they contain small bland nuclei and abundant vacuolated, lipid-rich cytoplasm (Fig. 12.5a, b). On occasion, they may take on a more spindled morphology with less obvious cytoplasmic vacuolization, and nuclear pleomorphism may be prominent (Fig. 12.5c, d).
    - The vascular component consists of numerous capillaries sprinkled throughout the tumor, together with scattered larger feeding (and draining) vessels.
    - Either of these two components may range from predominant to inconspicuous and sometimes abundant vasculature (Fig. 12.6a), intratumoral hemorrhage or extensive sclerosis may significantly mask the stromal cell component.
    - A reticulin-rich network is invariably present (Fig. 12.6b); it is especially prominent in the highly-vascular reticular variant, notable for small compact nests of stromal cells; in the cellular variant, broad sheets of stromal cells are uninterrupted by reticulin.
    - Whereas mitotic figures are quite uncommon, mast cells and extramedullary hematopoiesis are frequently present.
    - These lesions are sharply demarcated, the surrounding brain often showing a striking astrogliosis sometimes mimicking a pilocytic astrocytoma, replete with Rosenthal fibers and eosinophilic granular bodies.

12.5 IMMUNOHISTOCHEMISTRY

- The stromal cell and vascular components show significantly different immunoexpression patterns:

- Stromal cells are consistently positive for vimentin, alpha-inhibin, D2-40, and aquaporin, while variably positive for S-100, NCAM, NSE, erythropoietin, EGFR, VEGF, alpha-1-antitrypsin and antichymotrypsin. (Fig. 12.7a–c).
- Progesterone receptor and Factor XIIIa positivity have also been reported in a high percentage of cases. They may be focally positive for GFAP, keratin, EMA, or desmin, while specific neuronal markers (neurofilament, synaptophysin, and chromogranin) and endothelial cell markers CD31, CD34 and VWF are typically negative.
- Endothelial cells are consistently positive for CD31, CD34, and VWF (Fig. 12.7d).

12.6 ELECTRON MICROSCOPY

- At the ultrastructural level, hemangioblastomas contain three cell types: endothelial cells lining fenestrated vascular channels, pericytes ensheathed by basal lamina, and stromal cells. Stromal cells often contain lipid droplets, and may contain intracellular caveolae consistent with early capillary lumina, or small Weibel-Palade bodies.
- Transitional forms of these three cellular constituents may be present.

12.7 MOLECULAR PATHOLOGY

- Whereas germline mutations of the VHL gene are the norm in familial (VHL disease-associated) hemangioblastoma, loss or inactivation of this gene occurs in up to 50% of sporadic cases.
- Recent studies have indicated that inactivation of the ZAC1 gene (6q24-25) may also play a role in the development of hemangioblastoma, particularly non-VHL-associated cases.

12.8 DIFFERENTIAL DIAGNOSIS

- Clear cell renal cell carcinoma (RCC) is an important diagnostic consideration, particularly in VHL patients who may have both hemangioblastoma and RCC.
  - Both contain cells with clear, lipid-rich cytoplasm with variable vascular investments, though the cells of RCC tend to have more monotonous nuclear profiles and less reticulin positivity compared to hemangioblastoma.
  - Definitive diagnosis typically relies upon demonstration of immunopositivity for markers such as D2-40, inhibin, and aquaporin 1 in hemangioblastoma and for CD10, RCC, EMA, and cytokeratin AE1/AE3 in RCC.
- Several meningioma variants may mimic hemangioblastoma, especially the microcystic, clear cell, and angiomatous subtypes, as well as those with xanthomatous areas.
  - Unlike hemangioblastoma, all of these meningiomas are expected to show diffuse EMA positivity and should lack expression of the multiple markers of hemangioblastoma listed above.

- Hemangioblastoma may mimic intraparenchymal vascular lesions, especially capillary hemangioma; the latter will lack vacuolated stromal cells.
- Macrophages may closely resemble the bubbly stromal cells of hemangioblastoma; CD68 will confirm the identity of the former.

12.9 PROGNOSIS

- Surgical resection is the treatment of choice, and affords excellent recurrence-free and overall survival outcomes.
- Management of hemangioblastoma in VHL patients is more difficult, given the tendency of these patients to develop multiple lesions.
- Lifelong follow-up is required, with treatment indicated for symptomatic lesions and also for those asymptomatic tumors exhibiting radiographic progression.
- Fractionated external beam radiotherapy may be helpful in those patients with extensive intracranial and/or spinal disease, and in treating residual or recurrent lesions.
- Tumor embolization in select cases may facilitate complete resection with reduced blood loss.

SUGGESTED READING

Conway JE, Chou D, Clatterbuck RE, Brem H, Long DM, Rigamonti D (2001) Hemangioblastomas of the central nervous system in von Hippel-Lindau syndrome and sporadic disease. Neurosurgery 48(1):55–62

Lach B, Gregor A, Rippstein P, Omulecka A (1999) Angiogenic histogenesis of stromal cells in hemangioblastoma: Ultrastructural and immunohistochemical study. Ultrastruct Pathol 23(5):299–310

Chaudhry AP, Montes M, Cohn GA (1978) Ultrastructure of cerebellar hemangioblastoma. Cancer 42(4):1834–1850

Roy S, Chu A, Trojanowski JQ, Zhang PJ (2005) D2-40, a novel monoclonal antibody against the M2A antigen as a marker to distinguish hemangioblastomas from renal cell carcinomas. Acta Neuropathol (Berl) 109(5):497–502

Weinbreck N, Marie B, Bressenot A, Montagne K, Joud A, Baumann C et al (2008) Immunohistochemical markers to distinguish between hemangioblastoma and metastatic clear-cell renal cell carcinoma in the brain: Utility of aquaporin1 combined with cytokeratin AE1/AE3 immunostaining. Am J Surg Pathol 32(7):1051–1059

Lallu S, Naran S, Palmer D, Bethwaite P (2008) Cyst fluid cytology of cerebellar hemangioblastoma: A case report. Diagn Cytopathol 36(5):341–343

Jagannathan J, Lonser RR, Smith R, DeVroom HL, Oldfield EH (2008) Surgical management of cerebellar hemangioblastomas in patients with von Hippel-Lindau disease. J Neurosurg 108(2):210–222

Rodesch G, Gaillard S, Loiseau H, Brotchi J (2008) Embolization of intradural vascular spinal cord tumors: Report of five cases and review of the literature. Neuroradiology 50(2):145–151

Koh ES, Nichol A, Millar BA, Menard C, Pond G, Laperriere NJ (2007) Role of fractionated external beam radiotherapy in hemangioblastoma of the central nervous system. Int J Radiat Oncol Biol Phys 69(5):1521–1526

Lemeta S, Jarmalaite S, Pylkkanen L, Bohling T, Husgafvel-Pursiainen K (2007) Preferential loss of the nonimprinted allele of ZAC1 tumor suppressor gene in human capillary hemangioblastoma. J Neuropathol Exp Neurol 66(9):860–867

Glasker S (2005) Central nervous system manifestations in VHL: Genetics, pathology and clinical phenotypic features. Fam Cancer 4(1):37–42
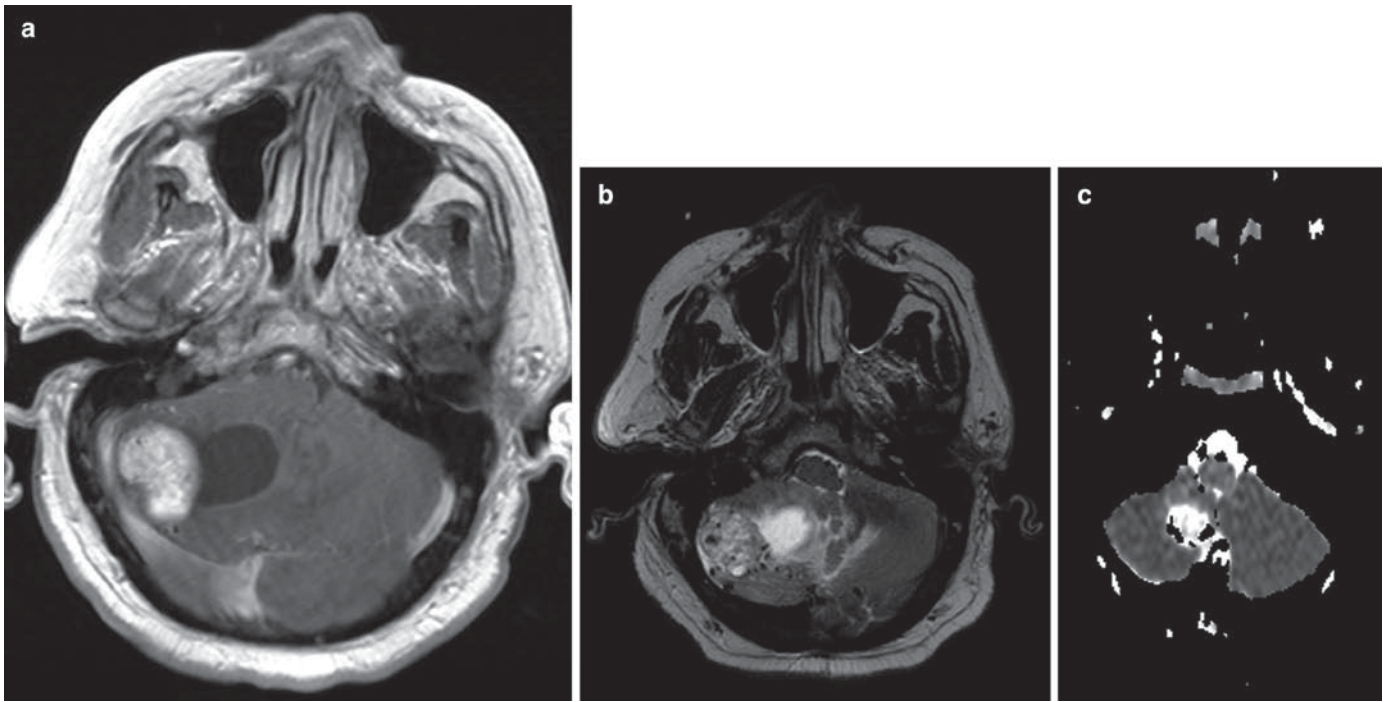
Fig. 12.1. Axial MR imaging (**a**) TI-w post-Gd showing classic posterior fossa localization with cyst bearing an enhancing mural nodule, and (**b**) T2-weighted image of same patient showing hyperintense cyst fluid and solid nodule of heterogeneous intensity with scattered flow voids. (**c**) Axial ADC map shows a high signal corresponding to this tumor.
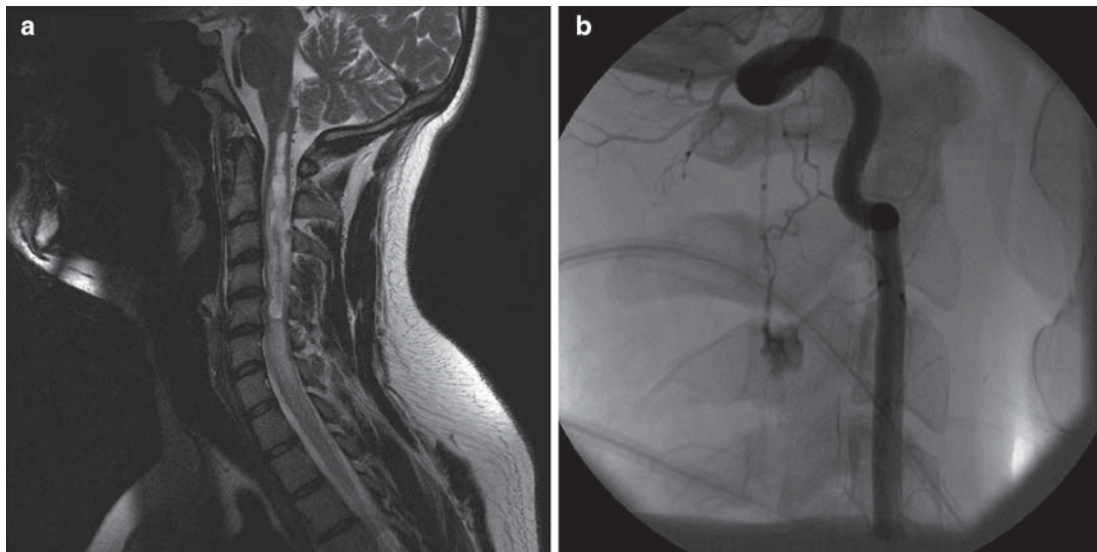
Fig. 12.2. Sagittal T2-w MR image (**a**) showing heterogeneously hyperintense hemangioblastoma arising in the cervical cord, while angiography (**b**) confirms an AVM-like tangle of vessels within the lesion.

Fig. 12.4. H & E cytologic smear preparation showing sheets of cells with abundant sometimes vacuolated cytoplasm with hyperchromatic nuclei of variable configuration.

Fig. 12.3. (**a**) Intraoperative view of a cervicomedullary fleshy red nodule with adjacent cyst and large feeder vessels. (**b**) Cut surface of hemangioblastoma surgical specimen from a different patient shows firm red-brown hemorrhagic tissue with variably sized vascular spaces.
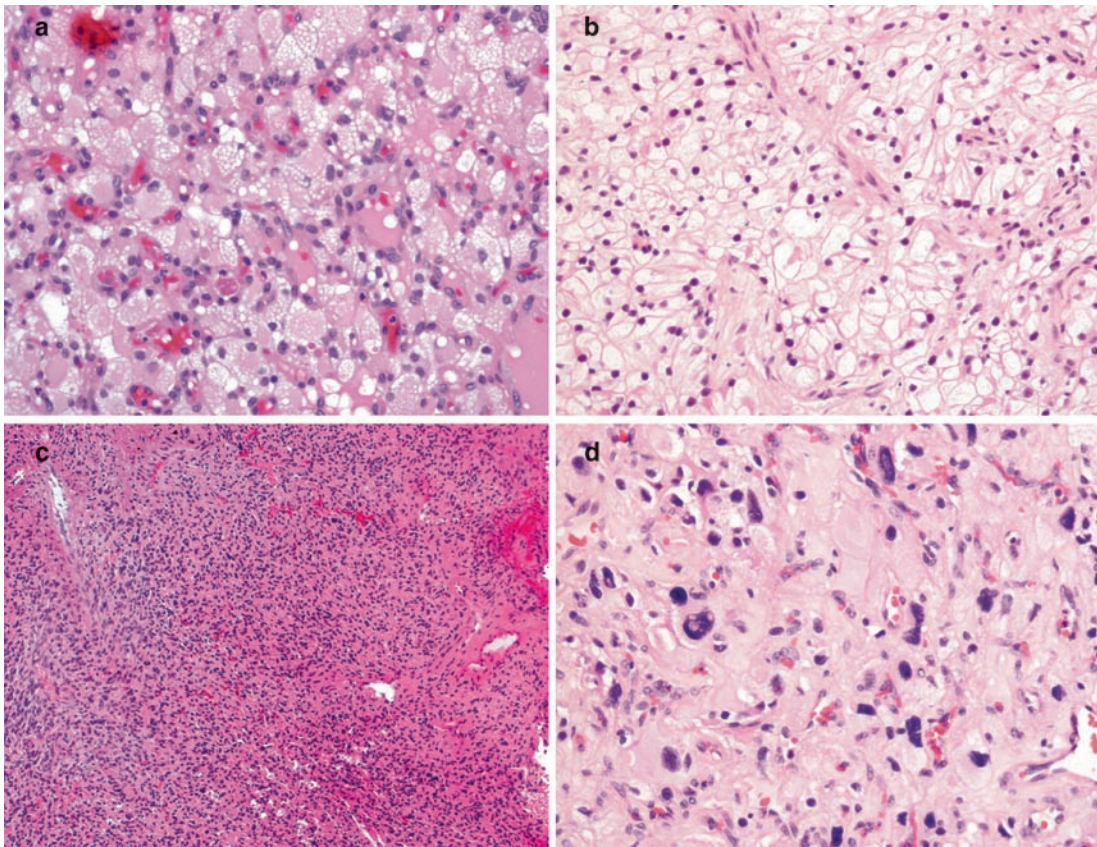
Fig. 12.5. Stromal cells of hemangioblastoma characteristically have small bland nuclei and abundant vacuolated cytoplasm (**a**), one may also encounter cells resembling clear cell renal cell carcinoma (**b**), spindle cell morphology (**c**), or cells with striking nuclear pleomorphism (**d**).
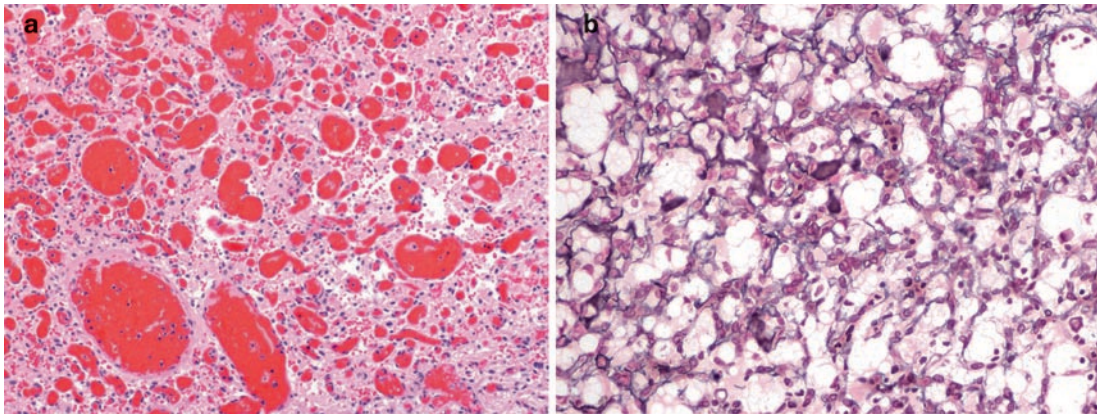
Fig. 12.6. (**a**) Abundant vasculature in this example effectively masks the diagnostic stromal cells. (**b**) Hemangioblastomas characteristically harbor a rich reticulin network.
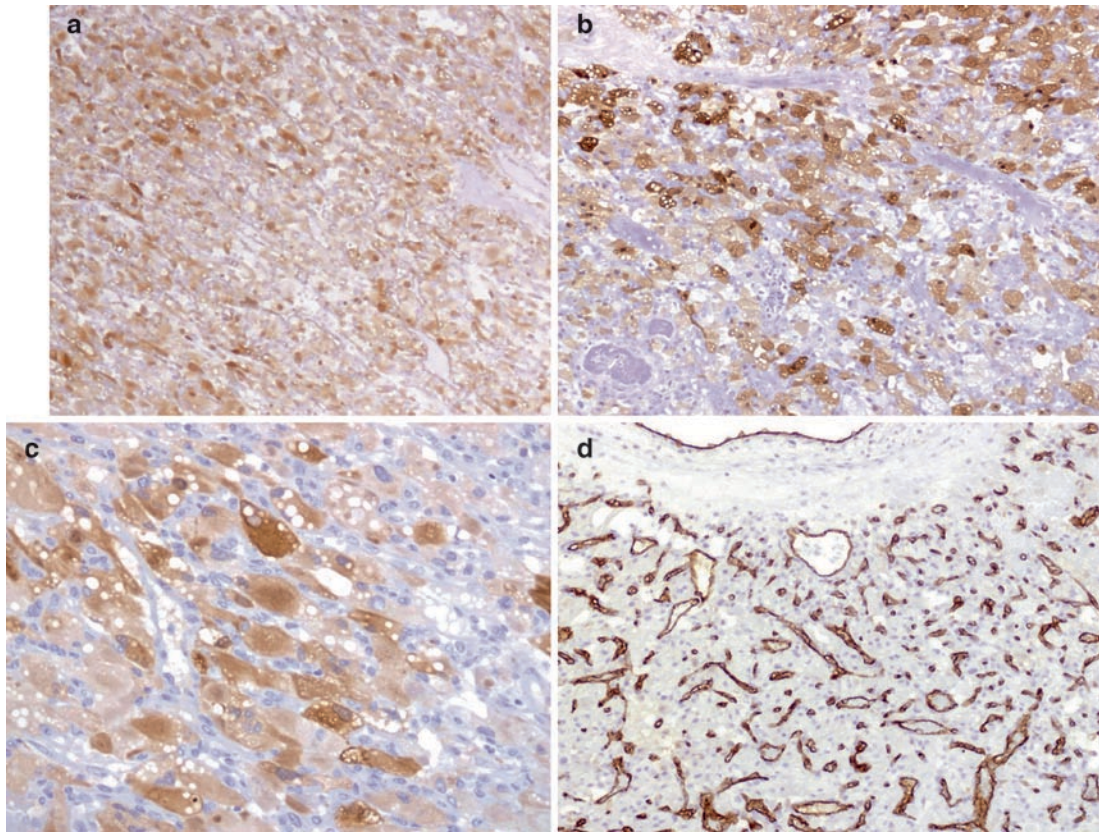
Fig. 12.7 Stromal cells of hemangioblastoma are diffusely positive for vimentin (**a**) and variably positive for S-100 (**b**) and neuron specific enolase (**c**); CD31-positive vessels (**d**) stand out from the background of non-staining stromal cells.

Section D: Tumors of Cranial and Spinal Nerves

Tarik Tihan

Abstract   This section presents (in three separate chapters) the major subgroups of tumors associated with cranial and spinal nerves including benign peripheral nerve sheath tumors (schwannoma and neurofibroma), followed by the chapter on malignant peripheral nerve sheath tumors.

Schwannoma

Tarik Tihan

13.1 OVERVIEW

- A well-defined, benign neoplasm believed to arise from schwann cells, also known as neurilemmocytes, thus the alternate name neurilemmoma.
- Schwannomas are typically seen in adults between the fourth and the sixth decades, and are extremely rare in children.
  - In a large referral center, only 0.7% of all schwannomas occurred in children during a 10-year period.
  - Pediatric schwannomas often occur in the setting of NF2.
- Both spinal and intracranial schwannomas show a predilection for sensory nerves, and the most common intracranial location is the 7–8th vestibulo-acoustic nerve complex.
- The incidence for schwannomas of the 8th nerve (vestibular schwannomas) has been reported as 0.6 per 100,000 person years.
- Schwannomas may be associated with irradiation during childhood, but such tumors are typically diagnosed later in life.
- Schwannomatosis, a disorder genetically distinct from NF2, includes multiple peripheral and intracranial schwannomas.

13.2 CLINICAL FEATURES

- Most children would suffer tinnitus or hearing loss, but schwannomas may go unnoticed for many months or years until cerebellar symptoms or signs of increased intracranial pressure emerge.
- The standard treatment for schwannomas is surgical resection.
  - Some reports also suggest using vascular embolization prior to surgery.
  - It is important to be aware of prior embolization when interpreting histological features of a schwannoma as there may be significant architectural distortion and degenerative changes.
- Outcomes of patients with NF2 are typically worse than those of patients with sporadic schwannomas.

13.3 NEUROIMAGING

- Schwannomas are often solid and occasionally solid and cystic extra-axial masses.
- On CT scans, tumors often distort or enlarge the acoustic canal and rarely can cause bony erosion.

- MRI reveals a well-defined mass that is isointense or hypointense on T1-weighted images, and hyperintense on T2-weighted images (Figs. 13.1 and 13.2).
- The majority of tumors show moderate to strong homogenous enhancement on post-contrast T1-weighted images.
  - Cystic tumors and tumors that have been embolized demonstrate variable contrast enhancement.
- Solid portions of schwannomas are isointense to normal parenchyma on DWI images (no restriction).
- Schwannomas are often seen as hypovascular masses on angiography.

13.4 PATHOLOGY

- Histopathological features of schwannomas in children are essentially similar to those in their adult counterparts.
  - However, due to the rarity of these neoplasms in children, a detailed comparison of histological patterns in both age groups is lacking.
- Intraoperative smears:
  - The cohesive nature of schwannomas does not allow easy smearing and disaggregation into individual cells, even in forcefully prepared samples. This alone is often a hint of the possibility of diagnosis in the right clinical setting (Fig. 13.3).
  - Smears often yield valuable information on the mesenchymal and collagenous background and highly convoluted, irregular nuclei that distinguish them from meningiomas.
  - In most smears, there is a mild nuclear pleomorphism, degenerative nuclear atypia, and rare pseudo-inclusions or calcifications.
    It is often difficult to exclude or confirm the presence of a low grade malignant peripheral nerve sheath tumor on the basis of cytological features alone.
- Frozen section:
  - Schwannomas often demonstrate marked nuclear freezing artifacts, and this may lead to an impression of a malignant neoplasm (Fig. 13.4).
  - Tumors in children tend to appear much more cellular and homogenous than those in adults. Therefore, it is advisable to be cautious in interpreting the cellularity of schwannomas in frozen sections.
- Routine microscopic features:
  - The classical biphasic appearance of schwannoma is not a common feature in pediatric schwannomas (Fig. 13.5).
  - Pediatric schwannomas are usually uniformly hypercellular, and often demonstrate the cellular patterns which include palisaded arrangement of cells termed Verocay bodies.
  - The thickened and hyalinized vasculature of adult schwannomas is not a typical finding in pediatric tumors.

- – Schwannomas in children can have pleomorphic or bizarre nuclei, but these are few in number and degenerative changes leading to such designations as "ancient" schwannoma are rare.
  - – While a typical schwannoma lacks mitotic figures, rare mitoses may be seen in a pediatric schwannoma (Fig. 13.6).
  - – Intracranial schwannomas in children are also likely to demonstrate hemosiderin deposits and reactive vascular changes.
  - – While most schwannomas in children appear somewhat hypercellular, true "cellular schwannoma", which is usually diffusely hypercellular, is extremely uncommon.
  - – Exceedingly rare are peritumoral chronic inflammatory infiltrates, melanin or lipofuscin pigment, or an epithelioid pattern.
  - – Plexiform schwannomas are also rare variants regardless of age group, although they have been reported in children.
- Cellular schwannoma is a variant showing a predominantly compact cellular growth, without appreciable cellular palisades or Verocay bodies, but with the typical ultrastructure of schwannomas.
  - – Architecturally, these tumors differ from conventional schwannomas by their lack of well-formed capsules and degenerative changes.
  - – The plexiform variant of cellular Schwannoma has also been reported in children.

13.5 IMMUNOHISTOCHEMISTRY

- Schwannomas show strong and diffuse cytoplasmic and nuclear immunoreactivity with antibodies against S-100 protein, as well as cytoplasmic positivity for vimentin.
  - – This immunopositivity is also readily observed in cellular schwannomas.
- Most schwannomas are reactive for Leu 7, a monoclonal antibody against human natural killer cells with the same antigenic determinant as myelin-associated glycoprotein.
  - – Calretinin is also suggested to be positive in most schwannomas.
- Staining for laminin and collagen type IV highlights the elaborate basement membrane material and can aid in differentiating schwannomas from meningiomas.
- Even though the majority of Schwannomas are negative for neurofilament protein thus allowing differentiation from neurofibromas, some neurofilament-positive axons may be present in the conventional and cellular variants of some schwannomas, confounding this issue (Fig. 13.8).
- Cellular schwannomas share the same immunohistochemical profile as conventional schwannomas.
- Schwannomas lack immunohistochemical staining for epithelial membrane antigen (EMA) and glial fibrillary acidic protein (GFAP).

13.6 ELECTRON MICROSCOPY

- Schwannomas feature spindle, bipolar cells with aligned and tangled processes.
- A single or duplicated layer of pericellular basement membrane separates the cells lacking highly specialized intercellular junctions with only rudimentary forms.
- Striated clusters of "long spacing collagen" also known as "Luse bodies" are present in many conventional schwannomas.

- There are scattered arrays of intracellular and extracellular intermediate filaments (Fig. 13.7).
- Schwann cells often contain elaborate perinuclear collections of lysosomes, and demonstrate a rich rough endoplasmic reticulum network.

The vessels often reflect the extent of hyalinization through thick and prominent basement membranes.

13.7 MOLECULAR PATHOLOGY

- Recent advances in molecular biology have led to a better understanding of the cause of schwannomas. Mutations in the NF2 gene have been well known both in sporadic and NF-associated tumors.
- A significant portion of schwannomas demonstrate allelic losses in chromosome 22 and NF-2 gene inactivation, which is considered an early event in tumor development.
  - – Interactions of merlin, the protein product of the NF2 gene, with other cellular proteins are beginning to give us a better idea of NF2 function and the pathogenesis of vestibular schwannomas.

13.8 DIFFERENTIAL DIAGNOSIS

- The differential diagnosis of a schwannoma is considered in terms of its location in the spinal cord, skull base, or cerebellopontine angle.
  - – At each of these locations, the differential diagnosis includes a host of lesions, but typically narrows down to a small group of extra-axial entities including meningiomas, mesenchymal non-meningothelial tumors, and other rare entities including non-neoplastic lesions.
- Schwannomas and meningiomas share common features such as spindled cells, foci rich in collagen, xanthoma cells, and rarely palisading of cells.
  - – Psammoma bodies and tight whorls are distinctive features of the meningiomas, but poorly-formed whorls may be seen in NF2-associated schwannomas, and some can even harbor psammoma bodies.
  - – Reticulin stains show a rich, elaborate, and distinctly pericellular network of basal membrane formation in schwannomas, and this feature is also highlighted by laminin or collagen IV immunostaining; this feature is not typically seen in meningiomas.
  - – Staining for S-100 protein, although typical of schwannomas, is not a reliable criterion. Approximately 20% of meningiomas show immunoreactivity for this protein, yet staining is typically more focal and less intense than in schwannomas.
  - – In addition, meningiomas are reactive for epithelial membrane antigen, whereas schwannomas do so only infrequently, and lack membranous staining.
- A second differential diagnosis is between neurofibroma and schwannoma, and more often problematic than with meningioma. While neurofibromas appear to blend with or infiltrate into peripheral nerves, schwannomas are often solid and have a well-defined capsule. Staining for neurofilament protein highlights far more of the background axonal elements in neurofibroma as compared to that in schwannoma.

SUGGESTED READING

Propp JM, McCarthy BJ, Davis FG, Preston-Martin S (2006) Descriptive epidemiology of vestibular schwannomas. Neuro-oncology 8(1):1–11

Sznajder L, Abrahams C, Parry DM, Gierlowski TC, Shore-Freedman E, Schneider AB (1996) Multiple schwannomas and meningiomas associated with irradiation in childhood. Arch Intern Med 156(16):1873–1878

Pothula VB, Lesser T, Mallucci C, May P, Foy P (2001) Vestibular schwannomas in children. Otol Neurotol 22(6):903–907

Allcutt DA, Hoffman HJ, Isla A, Becker LE, Humphreys RP (1991) Acoustic schwannomas in children. Neurosurgery 29(1):14–18

Pinto RG, Mandreker S, Nadkarni N, Amonkar SS, Lobo D, Noronha FP (1995) Plexiform (multinodular) schwannoma in a child – a rare variant of schwannoma. J Indian Med Assoc 93(8):317–318

Woodruff JM, Scheithauer BW, Kurtkaya-Yapicier O, Raffel C, Amr SS, LaQuaglia MP, Antonescu CR (2003) Congenital and childhood plexiform (multinodular) cellular schwannoma: A troublesome mimic of malignant peripheral nerve sheath tumor. Am J Surg Pathol 27(10):1321–1329

Woodruff JM, Godwin TA, Erlandson RA, Susin M, Martini N (1981) Cellular schwannoma: A variety of schwannoma sometimes mistaken for a malignant tumor. Am J Surg Pathol 5(8):733–744

Nascimento AF, Fletcher CD (2007) The controversial nosology of benign nerve sheath tumors: Neurofilament protein staining demonstrates intratumoral axons in many sporadic schwannomas. Am J Surg Pathol 31(9):1363–1370

Irving RM, Moffat DA, Hardy DG, Barton DE, Xuereb JH, Holland FJ, Maher ER (1997) A molecular, clinical, and immunohistochemical study of vestibular schwannoma. Otolaryngol Head Neck Surg 116(4):426–430

Neff BA, Welling DB, Akhmametyeva E, Chang LS (2006) The molecular biology of vestibular schwannomas: Dissecting the pathogenic process at the molecular level. Otol Neurotol 27(2):197–208
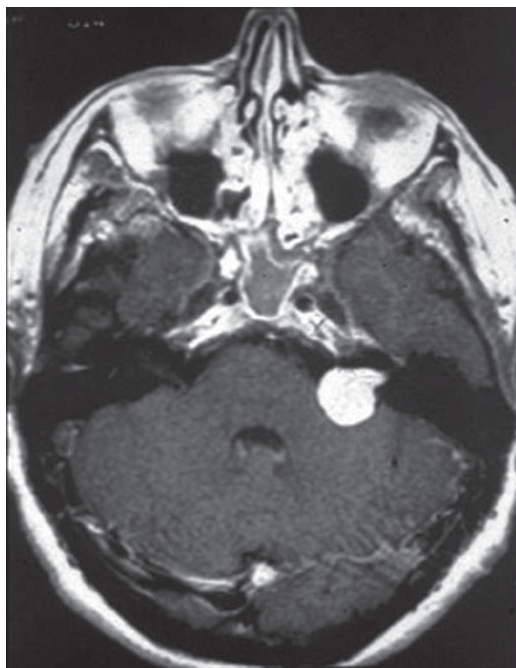
Fig. 13.1. Axial MR contrast enhanced T1-weighted image of a cerebellopontine angle schwannoma in a 16-year-old child with NF2.
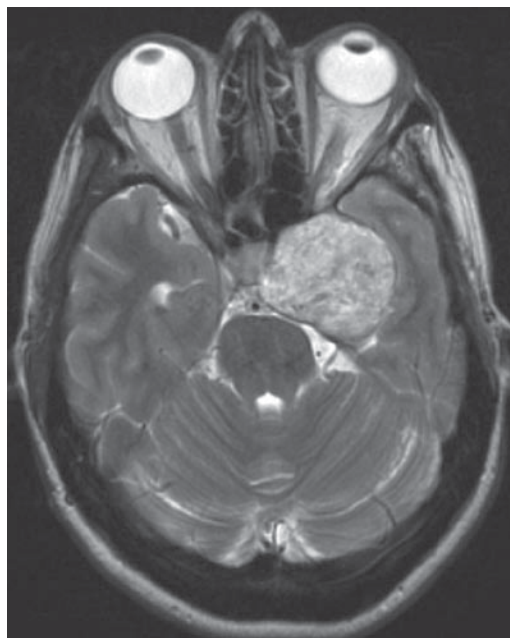
Fig. 13.2. Axial T2-weighted image of a schwannoma in the region of left Meckel's cave and cavernous sinus. Note the variable T2 hyperintensity.
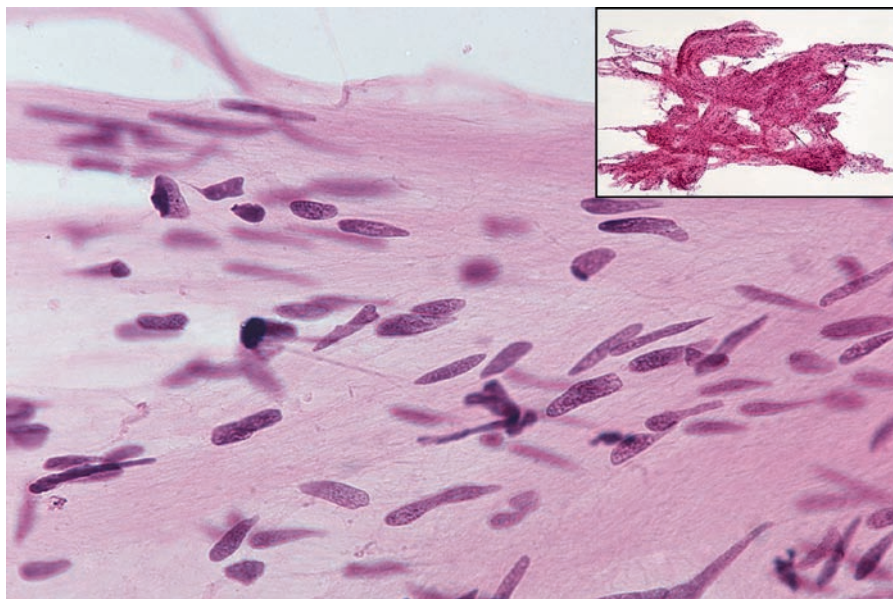
Fig. 13.3. Intraoperative smears typically reveal markedly irregular convoluted nuclear morphology. Note the inability to disaggregate the tissue on smears which can be a clue to the diagnosis (*inset*).
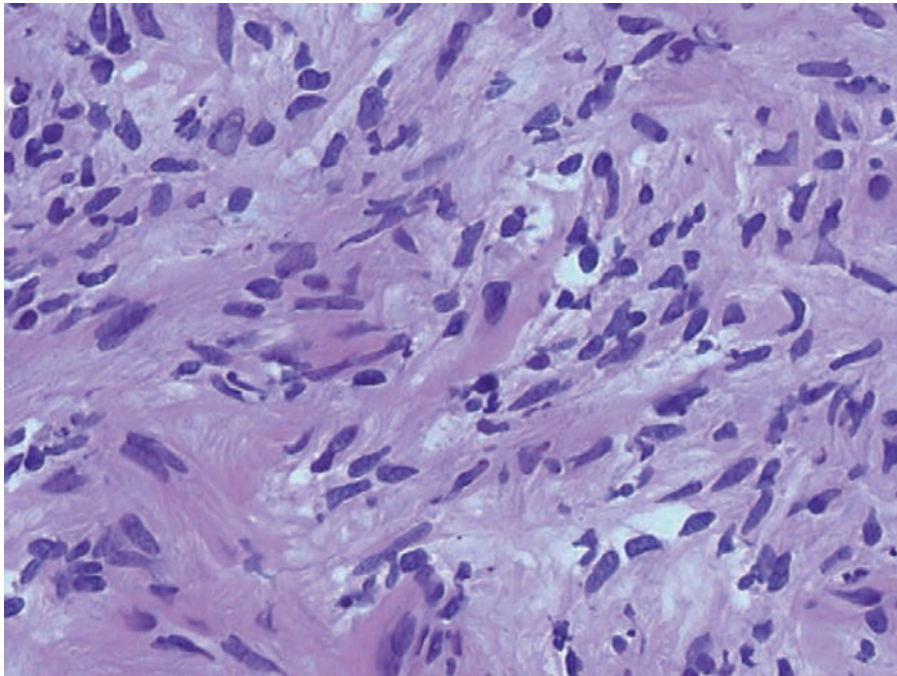
Fig. 13.4. Frozen section of a cerebellopontine angle schwannoma in a 6-year-old child showing a dense hyalin background and marked nuclear pleomorphism, caused partially by the freezing artifact.
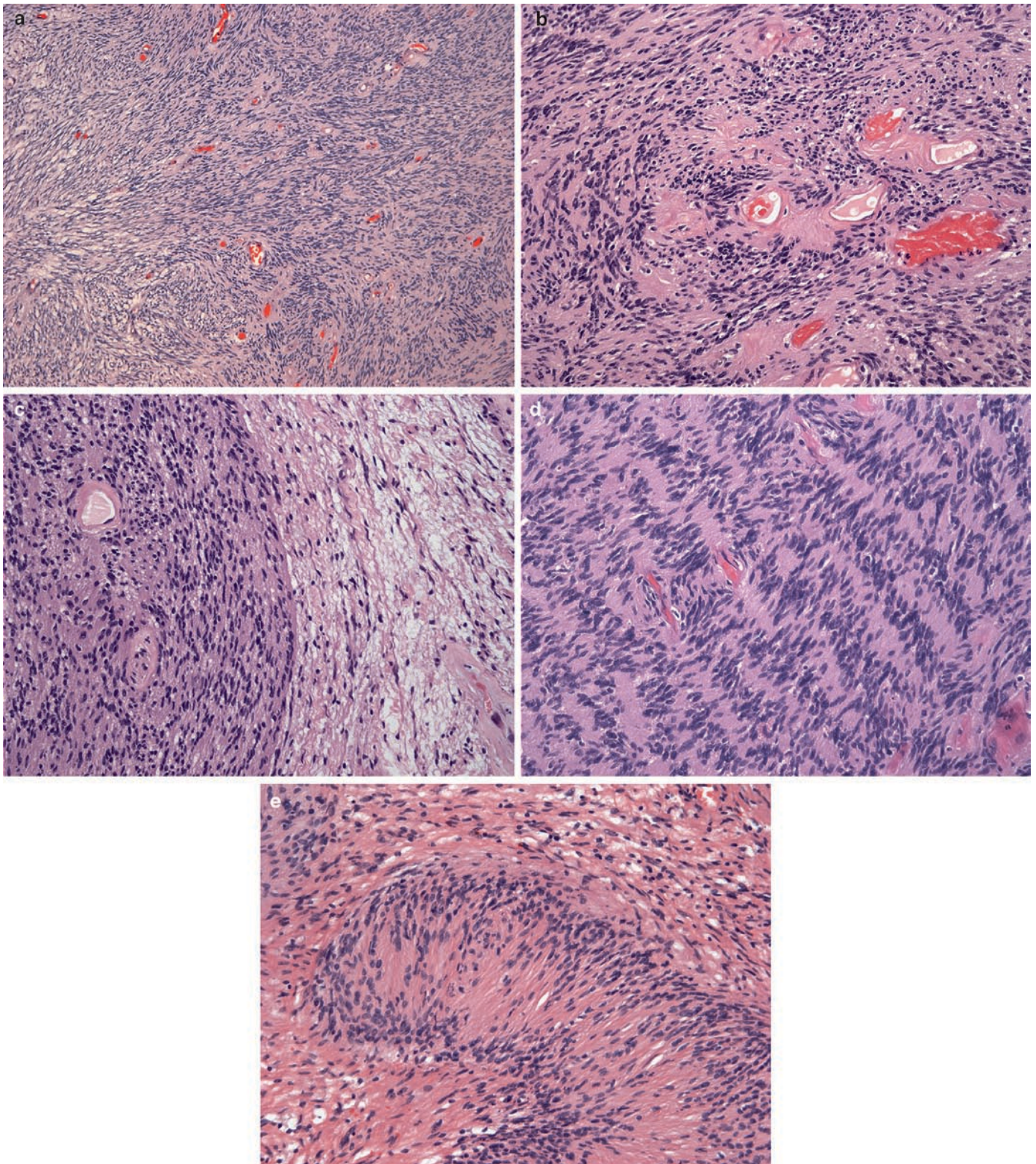
Fig. 13.5. Histological appearance of schwannomas in children. The classical biphasic appearance seen in adults in often not conspicuous in pediatric tumors: (**a**) spindled densely cellular tumor with collagenous stroma; (**b**) markedly hyalinized vasculature and abortive Verocay body formations; (**c**) hypercellular nodule with distinct boundary; (**d**) palisaded, polar-spongioblastoma-like pattern; (**e**) prominent Verocay body formation.
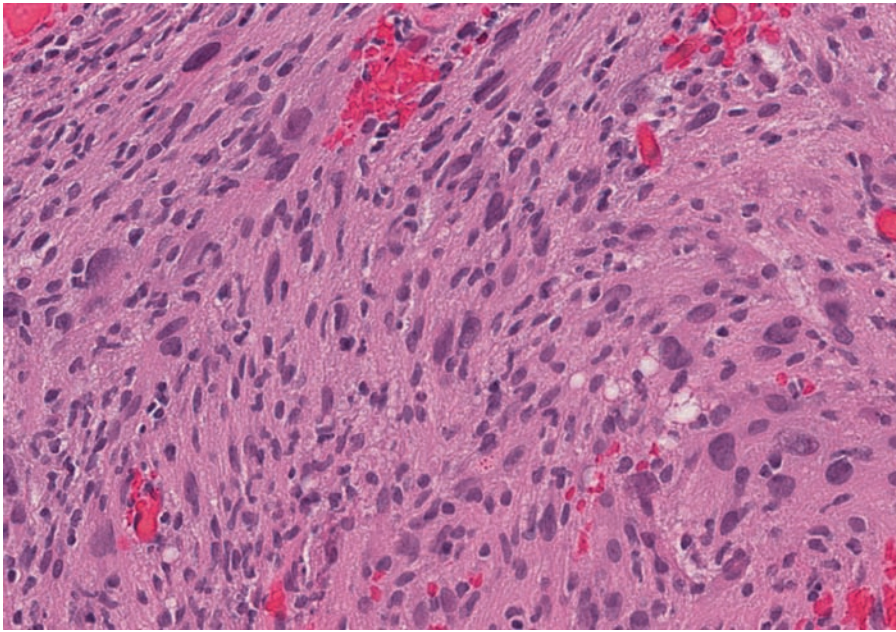
Fig. 13.6. Increased pleomorphism in a schwannoma from the cerebellopontine angle of a 9-year-old child.
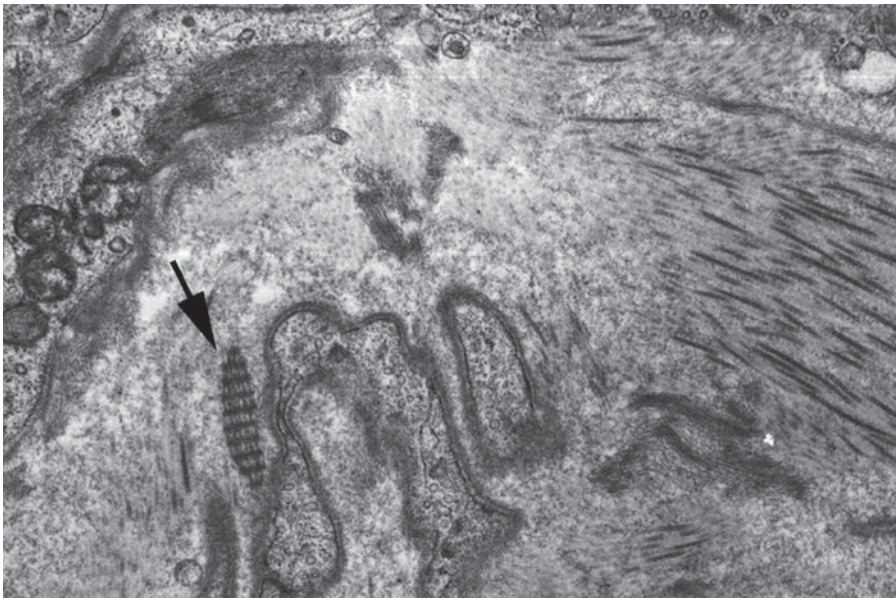
Fig. 13.7. Ultrastructural features of Schwannoma: The typical finding is the "long-spaced" collagen, also known as the Luse body (*arrow*) and the prominent basement membrane formation around tumor cells. Also note the abundant extracellular collagen.
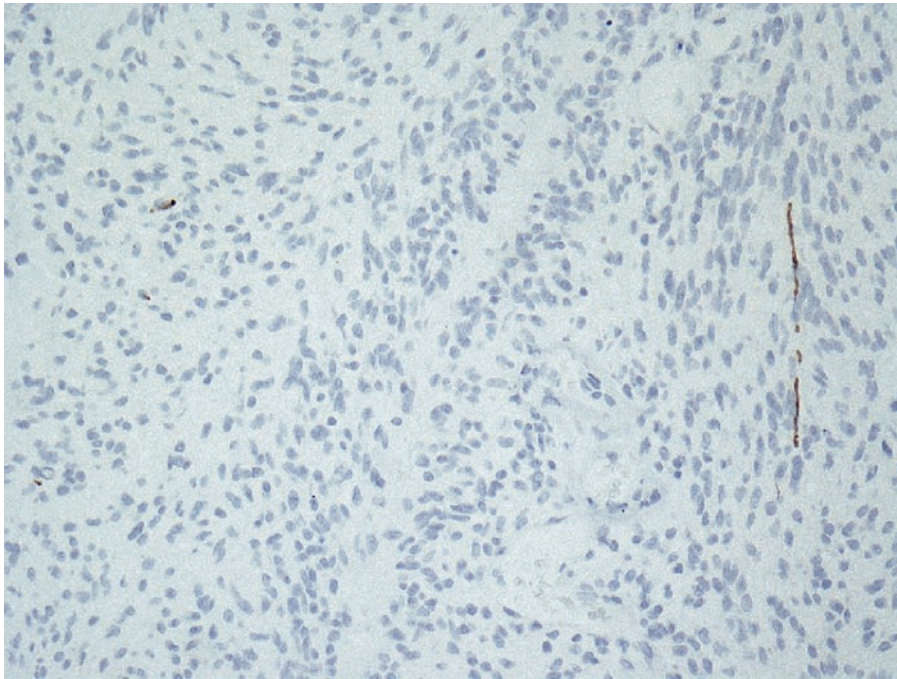
Fig. 13.8. Immunohistochemical staining for neurofilament protein (SM311) showing a rare neurofilament-positive fibril. Neurofilament positivity is far less prominent in schwannomas compared to that in neurofibromas and can be used in the differential diagnosis.

Neurofibroma

Tarik Tihan

Keywords Neurofibroma (localized, diffuse, intraneural, plexiform); Neurofibromin; NF1; Schwann cell

14.1 OVERVIEW

- Infiltrative and typically benign tumor of peripheral nerves that can occur as a solitary or diffuse mass in the subcutis, soft tissue, or along peripheral nerves.
- The tumor is believed to consist of a mixture of cell types including schwann cells, perineurial cells, and fibroblasts.
- Neurofibromas are considered WHO Grade I neoplasms.
- Some neurofibromas, especially plexiform neurofibromas, often occur in the setting of neurofibromatosis-1 (NF1).

14.2 CLINICAL FEATURES

- Most cutaneous neurofibromas present as slow-growing painless masses that are freely movable under the skin.
- Spinal cord examples can present with sensory loss and weakness, and are typically seen in the setting of NF1.
  - Spinal neurofibromas in NF1 are more likely to result in the sacrifice of the nerve root.
- Stigmata for NF1 should be sought in patients with neurofibromas, especially with multiple or plexiform lesions.

14.3 NEUROIMAGING

- Neurofibromas are moderately to strongly enhancing infiltrating masses that appear "worm-like" within the scalp or the orbit.
- Plexiform neurofibromas are highly tortuous enhancing masses along the larger peripheral nerves (Fig. 14.1).
- On MRI, neurofibroma is isointense on T1-weighted MR images and hyperintense on T2-weighted images, and often enhances strongly post contrast.
- Tumors can be seen in close association with nerve roots or peripheral nerves (Fig. 14.2). They may demonstrate the "target sign" on MR with central T2 dark (nerve fibers) and peripherally T2 bright (myxoid) appearance.

14.4 PATHOLOGY

- Intraoperative smears:
  - Like schwannomas, neurofibromas are difficult to smear and often do not yield single cells or small cell clusters.

The large fragments in smear preparations can suggest a spindled neoplasm with variably myxoid background (Fig. 14.3).
- Frozen section:
  - Neurofibromas may show marked pleomorphism on frozen sections, but the spindled and wavy nature of the tumor cells is characteristic (Fig. 14.4).
  - There is a variable amount of myxoid matrix and a variable degree of collagenous background.
  - Some cellular neurofibromas are difficult to distinguish from schwannomas on frozen section.
- Microscopic features:
  - Neurofibromas typically expand and distort the peripheral nerve and are composed of a haphazard proliferation of wavy spindle cells in a myxoid and collagenous background.
  - While most tumor cells have slender, moderately hyperchromatic nuclei, rare tumor cells exhibit large and occasionally bizarre nuclei (Fig. 14.5).
  - The tumors often blend imperceptively with the adjacent normal peripheral nerve, and in such areas, a clear separation is not possible.
  - Most neurofibromas contain occasional, but easily identifiable mast cells (Fig. 14.6).
  - Reactive changes, hemosiderin, or pigmentation is extremely rare.
  - The vascular network is often delicate, and hyalinized vessels (typical of schwannomas) are rare.
  - The myxoid matrix in neurofibromas is often positive with Alcian blue stain.
- Variants:
  - Localized cutaneous neurofibroma is typically a solitary subcutaneous nodule that is well-defined but not encapsulated. The lesion is usually not associated with a peripheral nerve, and located within the subcutis.
  - Diffuse neurofibroma is a larger and poorly delineated lesion, and often involves the adjacent soft tissue beyond the peripheral nerve. Growth of tumor cells around vessels and adnexal structures is often seen.
  - Plexiform neurofibroma is composed of large and small bundles of distended abnormal fascicles harboring a haphazard growth of cells in a myxoid background.
- The proportion of myxoid and collagenous elements, as well as cellularity, varies greatly.
- Foci of tumor may show patterns resembling specialized neural structures such as Pacinian corpuscles (Fig. 14.7).

- Typical plexiform neurofibromas do not harbor hypercellular regions, mitotic figures, or frank anaplastic change, any of which constitutes evidence for the emergence of a malignant peripheral nerve sheath tumor.

14.5 IMMUNOHISTOCHEMISTRY

- Neurofibromas show strong and diffuse cytoplasmic positivity for vimentin, as well as cytoplasmic and nuclear immunoreactivity with antibodies against S-100 protein.
- Neurofibromas harbor many neurofilament-positive axons than can aid in differentiating these lesions from schwannoma variants (Fig. 14.8).
- CD34 is focally and variably positive in most neurofibromas.
- Plexiform neurofibromas share the same immunohistochemical profile as conventional neurofibromas.
- It is pertinent to note that epithelial membrane antigen (EMA) and glial fibrillary acidic protein (GFAP) positivity are not demonstrable in neurofibromas.

14.6 ELECTRON MICROSCOPY

- Neurofibromas feature spindle, bipolar cells with aligned and tangled processes, in addition to perineurial-like cells with stumped processes and incomplete basal lamina, and fibroblasts without basal lamina and abundant rough endoplasmic reticulum.
- The typical long-spaced collagen or Luse body seen in schwannomas is not found in neurofibromas.

14.7 MOLECULAR PATHOLOGY

- Allelic loss of the NF1 gene region in chromosome 17 occurs in both NF-1 related, as well as sporadic neurofibromas.
- The NF1 gene and its product neurofibromin act as tumor suppressors and negative regulators of the ras proto-oncogene.
- For additional information see section on NF1.

14.8 DIFFERENTIAL DIAGNOSIS

- The differential diagnosis of neurofibroma is considered in terms of tumor location: spinal cord, peripheral nerve, soft tissue, or skin.
    - In each of these locations the differential potentially includes a host of lesions, but typically narrows down to schwannoma, meningioma, and other rare mesenchymal lesions.
- Some schwannomas appear indistinguishable from neurofibromas.
    - Neurofibromas often blend with or infiltrate into peripheral nerves, while schwannomas are often solid with a well-defined fibrous rim/capsule.
    - Staining for neurofilament protein highlights far more of the background axonal elements in neurofibroma as opposed to that in schwannoma.
    - It has been suggested that weak and rare calretinin positivity can distinguish neurofibromas from schwannomas that are diffusely and strongly positive for this antibody.
- Rarely, a solitary fibrous tumor or a myxofibrosarcoma can be considered in the differential diagnosis of soft tissue lesions, but can be easily distinguished on both morphological and immunohistochemical grounds.

SUGGESTED READINGS

Raffensperger J, Cohen R (1972) Plexiform neurofibromas in childhood. J Pediatr Surg 7:144–151

Smith TW, Bhawan J (1980) Tactile-like structures in neurofibromas. An ultrastructural study. Acta Neuropathol 50:233–236

Coffin CM, Dehner LP (1990) Cellular peripheral neural tumors (neurofibromas) in children and adolescents: A clinicopathological and immunohistochemical study. Pediatr Pathol 10:351–361

Feany MB, Anthony DC, Fletcher CD (1998) Nerve sheath tumours with hybrid features of neurofibroma and schwannoma: A conceptual challenge. Histopathology 32:405–410

Rosser T, Packer RJ (2002) Neurofibromas in children with neurofibromatosis 1. J Child Neurol 17:585–591 discussion 602–584, 646–551

Mentzel HJ, Seidel J, Fitzek C, Eichhorn A, Vogt S, Reichenbach JR, Zintl F, Kaiser WA (2005) Pediatric brain MRI in neurofibromatosis type I. Eur Radiol 15:814–822
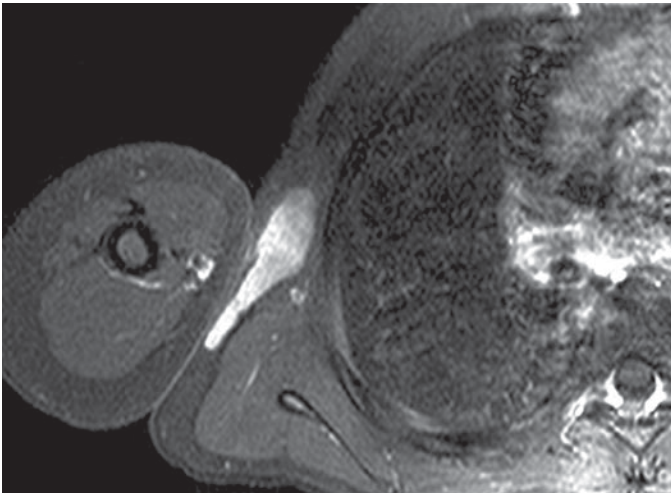
Fig. 14.1. Contrast-enhanced CT image of plexiform neurofibroma involving the brachial plexus in a 16 year-old child with NF-1.
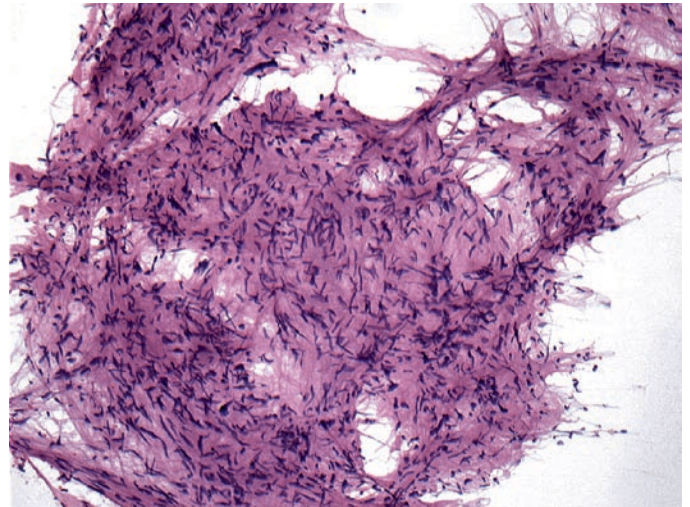
Fig. 14.3. Intraoperative smear of a neurofibroma showing dense clusters of cells with a variably myxoid background and irregular wavy nuclei.

Fig. 14.4. Frozen section from a brachial plexus neurofibroma, with wavy and some larger irregular-shaped nuclei, in a fibromyxoid background.

Fig. 14.2. Coronal contrast-enhanced T1-weighted MR image showing multiple neurofibromas involving nerve roots in a 12 year old child with NF-1.
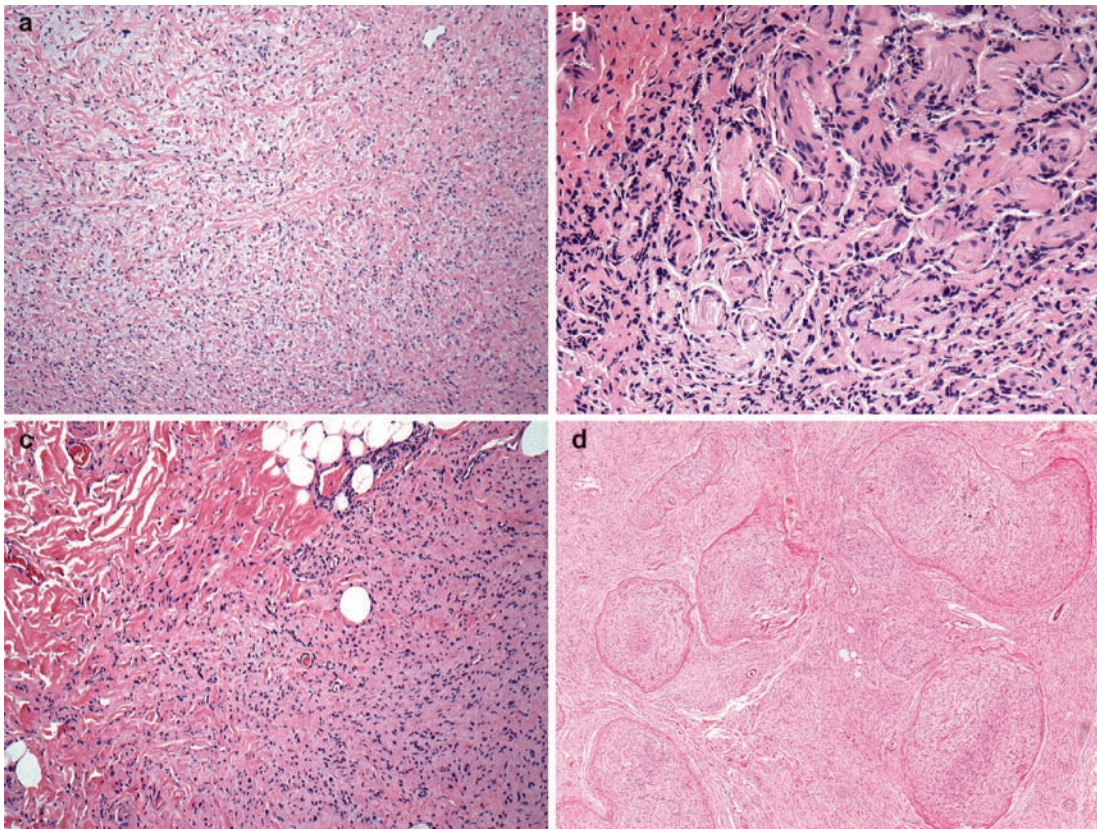
Fig. 14.5. Typical histological features of neurofibroma: (**a**) markedly myxoid background and monotonous, wavy nuclei; (**b**) nodular formations reminiscent of Verocay bodies; (**c**) infiltrative border; (**d**) plexiform neurofibroma. Note the multiple expanded fascicles and surrounding infiltrative tumor.
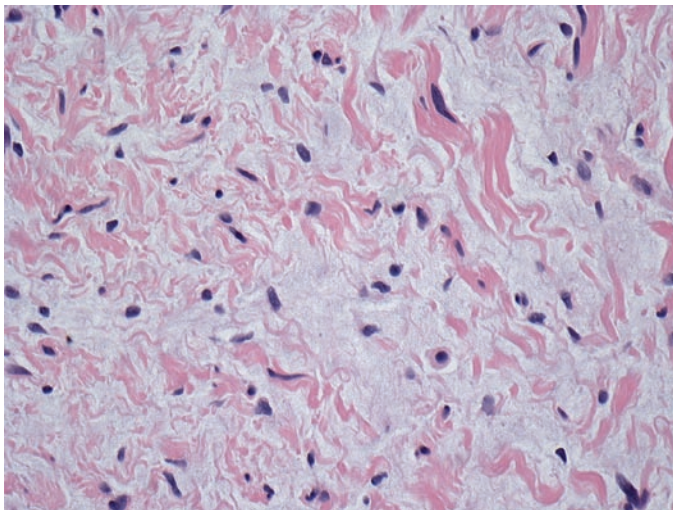
Fig. 14.6. High power magnification of a neurofibroma with mast cells.
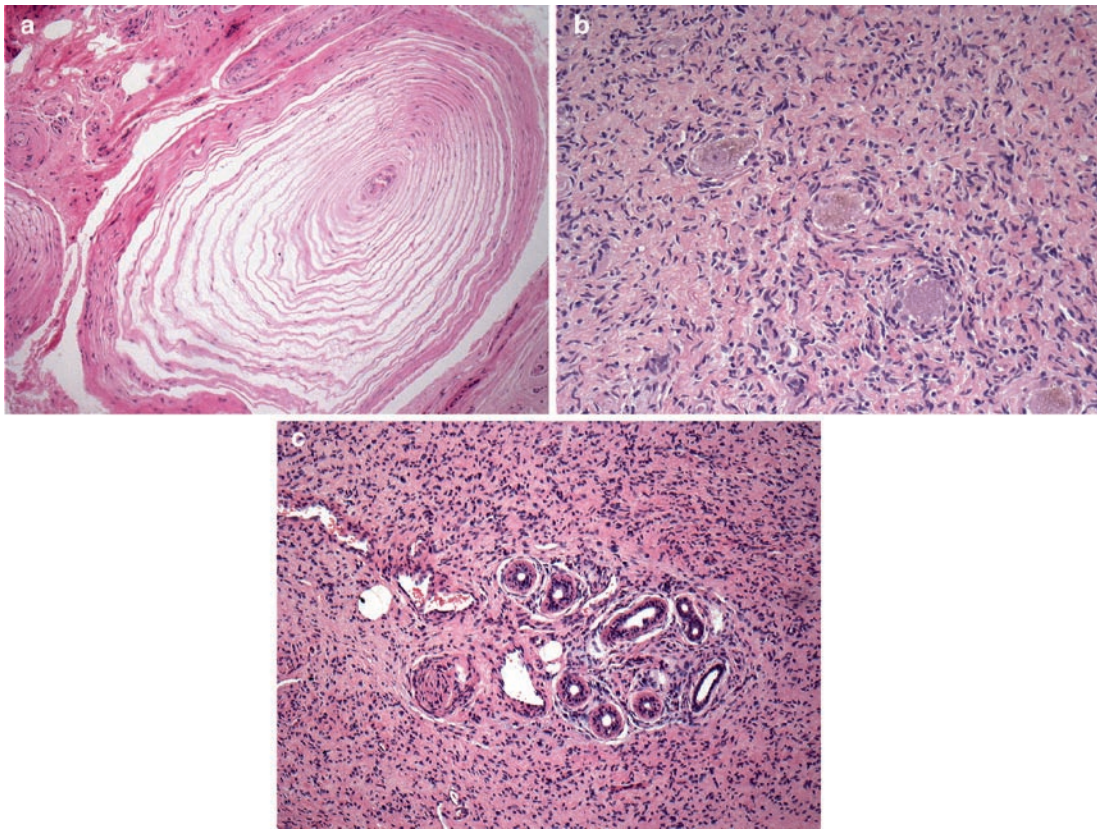
Fig. 14.7. (**a**) Pacinian corpuscle-like formations in a plexiform neurofibroma; (**b**) trapped ganglion cells in a spinal tumor; and (**c**) trapped adnexal structures in a dermal neurofibroma.
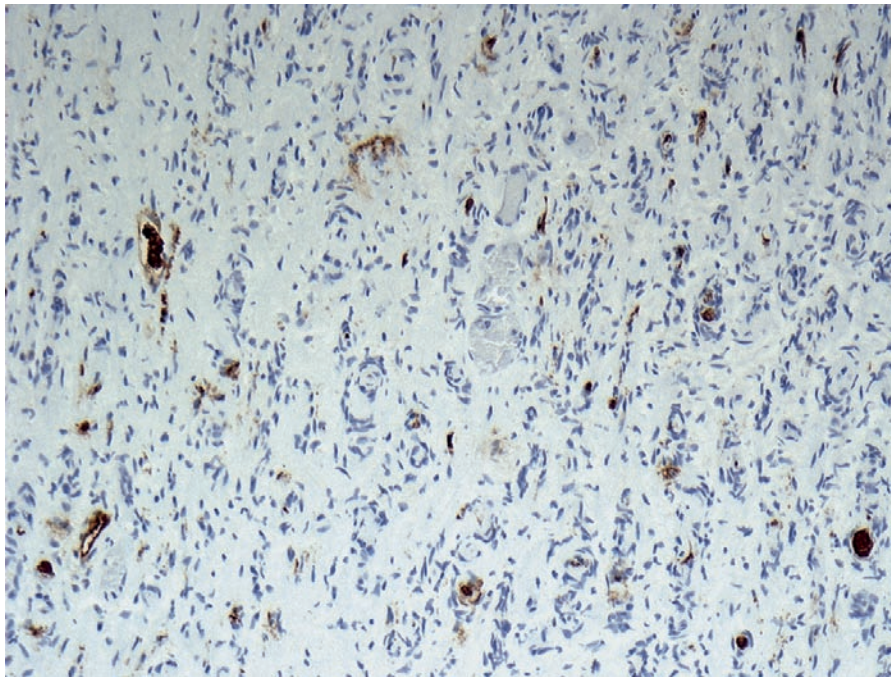
Fig. 14.8. Immunohistochemical staining for phosphorylated neurofilament protein in a typical neurofibroma demonstrating numerous neural processes. This feature is helpful in differentiating neurofibromas from schwannomas.

Malignant Peripheral Nerve Sheath Tumors

Tarik Tihan

15.1 OVERVIEW

- Malignant neoplasms arising in association with peripheral nerves and resembling elements of the peripheral nerve are considered in this category.
- These tumors may arise in the setting of neurofibromatosis or may be seen sporadically in children.
- The unequivocal recognition of a high grade sarcoma as malignant peripheral nerve sheath tumor (MPNST) requires that the tumor clearly arises from a peripheral nerve, emerge from a benign peripheral nerve sheath tumor such as neurofibroma or schwannoma, or demonstrate histological, immunohistochemical, and ultrastructural evidence of peripheral nerve tissue differentiation.

15.2 CLINICAL FEATURES

- MPNSTs can occur in children with NF-1 but are otherwise distinctly uncommon in children in comparison to that in adult population.
- The tumor often presents as an enlarging mass, and may be associated with pain or dysesthesia, but may not cause either in most cases.
- The patients or their parents observe a recent enlargement of a preexisting mass.
- Weakness, paresthesias, and pain can be observed in some examples, but are not consistently identified in all patients.
- Most MPNSTs present after the first decade, yet rare examples affect younger patients or occur as congenital tumors.
- A significant percentage of children with MPNST suffer from NF-1.
- Majority of tumors arise in the extremities, followed by trunk, and head and neck region.

15.3 NEUROIMAGING

- Most MPNSTs are not readily distinguishable, from other soft tissue neoplasms that can occur in the same anatomic regions.
  - The tumors are typically well-circumscribed and associated with a peripheral nerve.
- Typical MRI appearance is an isointense to hypointense mass on T1-weighted images, hyperintense on T2-weighted images with heterogenous contrast enhancement (Fig. 15.1).

15.4 PATHOLOGY

- Resection specimens are often large, fusiform, multi-lobular expansions of peripheral nerves.
- A variegated macroscopic appearance with hemorrhagic or necrotic foci is seen in most MPNSTs (Fig. 15.2).
- Intraoperative smears:
  - Similar to most mesenchymal tumors, smears from MPNST often yield cohesive clusters and rare individual cells (Fig. 15.3).
  - Mostly, they are reminiscent of a neurofibroma, but have more hyperchromatic and pleomorphic nuclei.
  - May also demonstrate mitotic figures or cellular debris suggestive of necrosis.
  - May be indistinguishable from other mesenchymal neoplasms.
- Frozen section:
  - Varied histologic patterns may be seen in frozen sections, but typically the overall impression is that of a sarcoma (Fig. 15.4).
  - Cellular pleomorphism is often exaggerated and the typical architectural features may not be readily identifiable.
  - One distinctive pattern is the palisaded or the polar spongioblastoma-like appearance (Fig. 15.5).
- Histology
  - Microscopically, most tumors are highly cellular and are composed of spindle cells with hyperchromatic nuclei and indistinct cytoplasm. Tumors can show a variety of architectural patterns including fascicular, whorled, palisaded, biphasic, nested, and focally myxoid designs (Fig. 15.6).
  - Tumor nuclei are typically hyperchromatic and spindled. Most tumors have foci with highly convoluted or wavy nuclei reminiscent of a neurofibroma (Fig. 15.3).
  - The tumor cells may form loose angiocentric arrangement around thin-walled, delicate blood vessels (Fig. 15.6).
  - Rare examples have foci of small cells reminiscent of PNET.
  - Extremely rare examples demonstrate epithelioid pattern with gland-like formations, goblet cells, or columnar epithelial arrangement.
  - Rhabdoid or hemangiopericytoma-like patterns can be observed in some pediatric tumors.
  - Divergent differentiation can be seen in about a quarter of the tumors and may include osteoid, chondromatous, angiosarcomatous, and liposarcomatous areas. Some tumors may arise in the setting of a neurofibroma (or less commonly schwannoma) and can show rhabdomyosarcomatous, primitive neuroectodermal tumor-like and epithelial/glandular differentiation.

- Variants
  - Triton Tumor or malignant triton tumor is a variant of MPNST with rhabdomyoblastomatous differentiation and carries a grim prognosis.
  - Triton tumors have been described in children, but are distinctly rare.
  - These tumors are often high grade sarcomas and have been reported mostly in young adults and occasionally in children.
- Electron microscopy
  - Rhabdoid or hemangiopericytoma-like patterns can be observed in some pediatric tumors.

15.5 IMMUNOHISTOCHEMISTRY

- The immunohistochemical identification of MPNST can be challenging, especially for poorly differentiated and highly anaplastic neoplasms.
- The typical S-100 protein positivity of benign and well-differentiated MPNSTs may not be readily observed in high grade examples, or S-100 protein positivity may be focal or weak. This vague pattern of staining may not always help in differential diagnosis.

15.6 MOLECULAR PATHOLOGY

- MPNST is presumed to arise from poorly defined stem cells.
- In NF1, these stem cells appear to originate from "de-differentiated" schwann cells and proliferate secondary to deregulated Ras/Raf/ERK signaling in NF1.

15.7 DIFFERENTIAL DIAGNOSIS

- The most critical differential diagnosis of a low grade MPNST in the setting of NF-1 includes a cellular benign peripheral nerve sheath tumor.
  - Although the boundary between a cellular schwannoma and a low grade MPNST may be subjective, a low grade MPNST should be favored in the presence of increased cellularity, atypia, and frequent mitosis.
- A second set of neoplasms considered in the differential diagnosis of high grade MPNSTs, includes primary soft tissue neoplasms such as fibrosarcoma, leiomyosarcoma, synovial sarcoma, mesenchymal chondrosarcoma and hemangiopericytoma/solitary fibrous tumor.
  - The combination of clinical, histopathological, and immunohistochemical features, as well as ultrastructural findings can identify a nerve sheath origin (or differentiation) and distinguish MPNST from other sarcomas.
- Differentiating a malignant melanoma from a high grade MPNST can also be challenging on rare occasions.
  - Both neoplasms can be composed of spindle cells and show variable S-100 positivity, and some melanomas do not contain appreciable amounts of melanin pigment.
  - Use of additional stains such as melan-A, HMB-45, tyrosinase, neurofilament, Leu-7, and myelin basic protein, and sometimes electron microscopy can aid in the recognition of a melanoma and its distinction from MPNST.

15.8 PROGNOSIS

- The following clinical characteristics have been suggested as significant prognostic variables:
  - Histologic grade and type (such as triton tumor).
  - Tumor location (superficial vs. deep) and size.
  - Younger age in some studies was suggested as a worse prognostic factor.
  - Presence of NF-1.

SUGGESTED READING

Meis JM, Enzinger FM, Martz KL, Neal JA (1992) Malignant peripheral nerve sheath tumors (malignant schwannomas) in children. Am J Surg Pathol 16(7):694–707

Casanova M, Ferrari A, Spreafico F et al (1999) Malignant peripheral nerve sheath tumors in children: A single-institution twenty-year experience. J Pediatr Hematol Oncol 21(6):509–513

Mautner VF, Friedrich RE, von Deimling A et al (2003) Malignant peripheral nerve sheath tumours in neurofibromatosis type 1: MRI supports the diagnosis of malignant plexiform neurofibroma. Neuroradiology 45(9):618–625

Carli M, Ferrari A, Mattke A et al (2005) Pediatric malignant peripheral nerve sheath tumor: The Italian and German soft tissue sarcoma cooperative group. J Clin Oncol 23(33):8422–8430

Friedrich RE, Hartmann M, Mautner VF (2007) Malignant peripheral nerve sheath tumors (MPNST) in NF1-affected children. Anticancer Res 27(4A):1957–1960

Harrisingh MC, Lloyd AC (2004) *Ras/Raf/ERK* signaling and NF1. Cell Cycle 3(10):1255–1258

Fig. 15.1. Coronal, contrast-enhanced T1-weighted MR image of a retroperitoneal MPNST in a 14-year-old child.
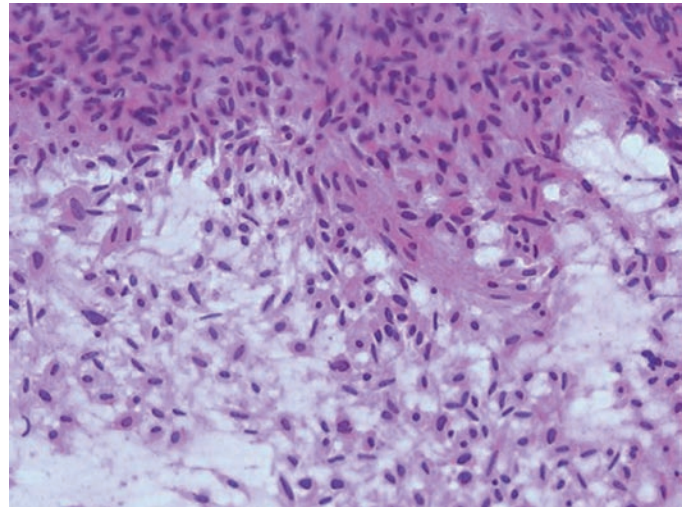
Fig. 15.3. Intraoperative smear of an MPNST showing cohesive clusters of cells with wavy hyperchromatic overlapping nuclei and scant cytoplasm.
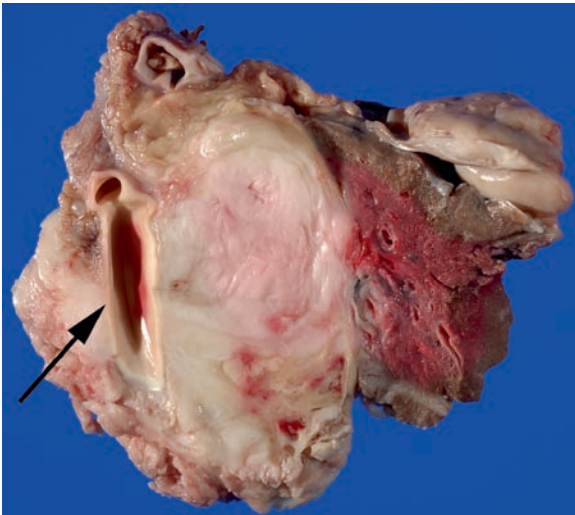
Fig. 15.2. Gross appearance of an MPNST in a 10-year-old child with NF1. Note the tumor wraps around a major vessel (*arrow*).
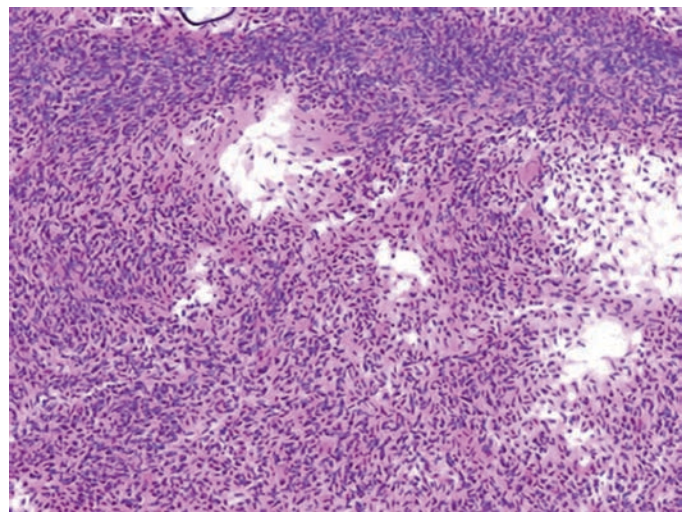
Fig. 15.4. Frozen section of MPSNT with marked cellularity and collagenous background. Note the histological features that are indistinguishable from those of a cellular schwannoma.

Fig. 15.5. Histological features of MPNST with a palisaded appearance, also referred to as polar spongioblastoma-like pattern. As such a pattern can also occur in benign peripheral nerve sheath tumors, it is not considered diagnostic of MPNST.
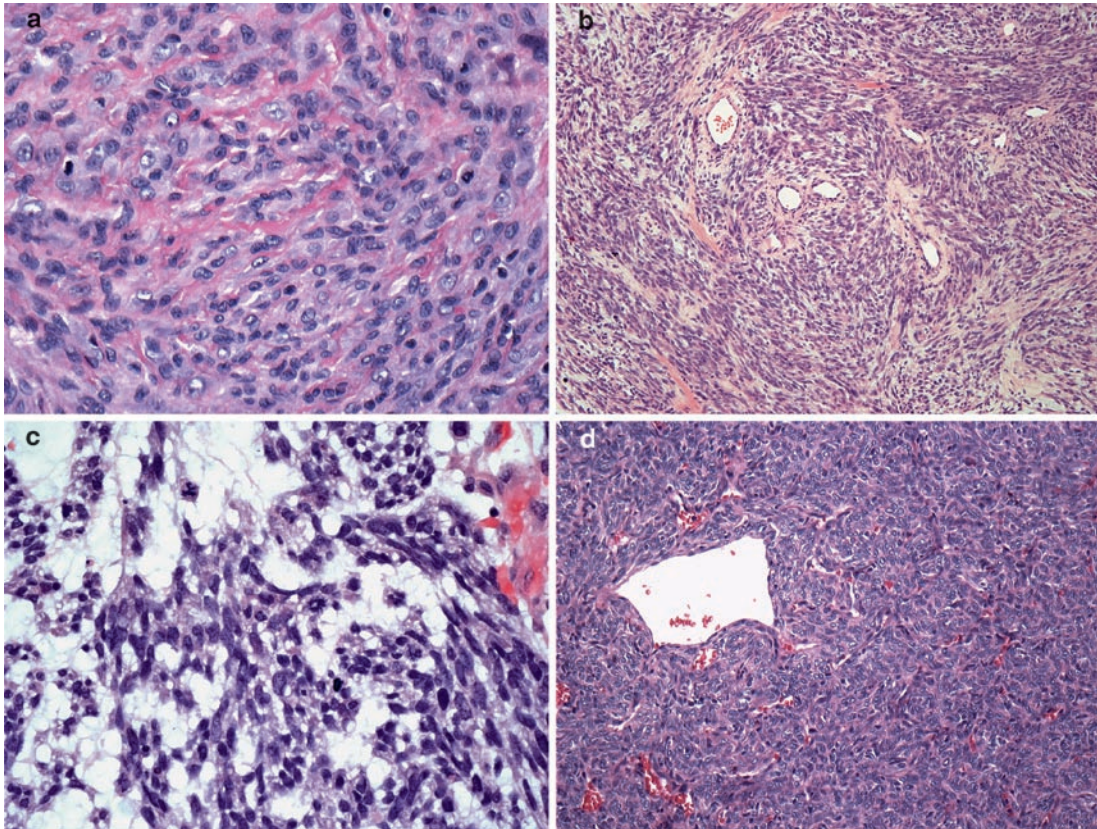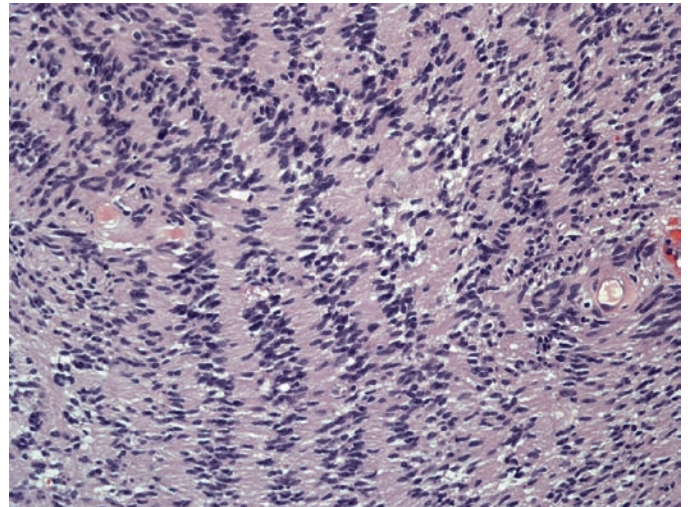
Fig. 15.6. Histological patterns in MPNST include (**a**) epithelioid, (**b**) fascicular, (**c**) myxoid, and (**d**) hemangiopericytoma-like with staghorn-like vasculature

Section E: Neuronal and Mixed Neuronal–Glial Tumors

Adekunle M. Adesina

Abstract Glioneuronal tumors represent an important group of tumors in children. They pose diagnostic difficulties because of their diversity and variable histologic features. However, a consensus on a number of new entities is beginning to emerge. In this section, we describe the well-established entities, such as ganglioglioma, desmoplastic infantile atsrocytoma/ganglioglioma, and dysembryoplastic neuroepithelial tumor. Predominantly neurocytic tumors such as central neurocytoma and paraganglioma are also presented. Rare and newly codified entities such as papillary glioneuronal tumor and rosetted (rosette forming) glioneuronal tumor of the fourth ventricle are presented in separate chapters, respectively. We also present the unique histologic features of an increasingly observed but yet to be codified new group of "malignant epithelioid glioneuronal tumors" in a separate chapter.

Desmoplastic Infantile Astrocytoma and Ganglioglioma

Adekunle M. Adesina

16.1 OVERVIEW

- Rare superficial cerebral cortical and leptomeningeal large cystic tumors with dural attachment primarily occurring in infants. Most patients are under 2 years of age.
- Account for 1.25% of all childhood brain tumors with a 1.5:1 male to female ratio.
- Characterized by neoplastic neuroepithelial cells in a desmoplastic stroma showing variable astrocytic differentiation [desmoplastic infantile astrocytoma, (DIA)] or combined astrocytic and neuronal differentiation [desmoplastic infantile ganglioglioma, (DIG)].
  - Immature neuroepithelial component is often present.
- Classified as a WHO grade I with favorable prognosis

16.2 CLINICAL FEATURES

- Patients often have massive tumors resulting in macrocephaly and associated features of raised intracranial pressure.
- Rapidly increasing head circumference, progressive lethargy, seizures, and localizing signs such as hemiplegia are consistent with a massive intracranial mass lesion.

16.3 NEUROIMAGING

- Presents as large multicystic mass, often mainly cystic mass, with a solid component. On MRI, the solid component is isointense to adjacent cortex on T1 weighted images and hyperintense on T2-w images and shows enhancement after contrast administration (Figs. 16.1 and 16.2).
- MR spectroscopy shows slight elevation of the choline peak and only a slight reduction of the NAA peak consistent with low cellularity.

16.4 PATHOLOGY

- These are large uni or multiloculated, firm, grey white fleshy tissue with attached dura.
- Tumor border is well demarcated.
- Characterized by three components including the following:
  - Fibroblastic spindled cells forming reticulin or collagenous matrix (Fig. 16.3a).
  - Neoplastic astrocytic cells, some with abundant (gemistocyte-like) eosinophilic cytoplasm (Fig. 16.3b).
- Spindled forms may be arranged in fascicles or storiform pattern (Fig. 16.3c).
  In DIG, a component of ganglionic or ganglioid cells with neuronal differentiation is present as well.
  - Variable population of immature small round hyperchromatic neuroepithelial cells are present (Fig. 16.3d).
- Calcification may be present.
- Mitosis is infrequent and necrosis is uncommon.
- No endothelial proliferation is seen.
- Rare examples of DIG with anaplastic features, frequent mitosis and elevated proliferation index as high as 40% have been reported.

16.5 IMMUNOHISTOCHEMISTRY

- Immunoreactivity for GFAP is widespread (Figs. 16.4a, b) and is seen in all of the components of DIA.
- Vimentin expression and pericellular reticulin demonstrable by reticulin silver stain or anti-collagen type IV antibody are present.
- Neuronal markers such as synaptophysin, neurofilament protein (NF-H), MAP2 (Fig. 16.5a), and NeuN (Fig. 16.5b) are often demonstrable in DIG.
- Smooth muscle actin and desmin may be demonstrable.
- A lack of expression of myogenin or MyoD excludes myoid differentiation.
- Ki67 shows a low proliferation index of less than 2%.
- Epithelial markers such as EMA, pancytokeratin (AE1/AE3), and CAM 5.2 are absent.

16.6 DIFFERENTIAL DIAGNOSIS

- Prominent spindle cell fibroblastic components raise the differential diagnosis of fibromatosis or solitary fibrous tumor.

16.7 PROGNOSIS

- This is a tumor with good prognosis, some reports showing good survival with a 15.1-year follow-up.
- The rare anaplastic variants are also reported with good survival.

SUGGESTED READING

Tamburrini G, Colosimo C Jr, Giangaspero F, Riccardi R, Di Rocco C (2003) Desmoplastic infantile ganglioglioma. Childs Nerv Syst 19(5–6):292–297

Trehan G, Bruge H, Vinchon M, Khalil C, Ruchoux MM, Dhellemmes P, Ares GS (2004) MR imaging in the diagnosis of desmoplastic infantile tumor: Retrospective study of six cases. Am J Neuroradiol 25(6): 1028–1033

Koeller KK, Henry JM (2001) From the archives of the AFIP: Superficial gliomas: Radiologic-pathologic correlation. Armed Forces Institute of Pathology. Radiographics 21(6):1533–1556 Review

Setty SN, Miller DC, Camras L, Charbel F, Schmidt ML (1997) Desmoplastic infantile astrocytoma with metastases at presentation. Mod Pathol 10(9):945–951 Review

Mallucci C, Lellouch-Tubiana A, Salazar C, Cinalli G, Renier D, Sainte-Rose C, Pierre-Kahn A, Zerah M (2000) The management of desmoplastic neuroepithelial tumours in childhood. Childs Nerv Syst 16(1):8–14

Kros JM, Delwel EJ, de Jong TH, Tanghe HL, van Run PR, Vissers K, Alers JC (2002) Desmoplastic infantile astrocytoma and ganglioglioma: a search for genomic characteristics. Acta Neuropathol 104(2):144–148

Sugiyama K, Arita K, Shima T, Nakaoka M, Matsuoka T, Taniguchi E, Okamura T, Yamasaki H, Kajiwara Y, Kurisu K (2002) Good clinical course in infants with desmoplastic cerebral neuroepithelial tumor treated by surgery alone. J Neurooncol 59(1):63–69

Louis DN, von Deimling A, Dickersin GR, Dooling EC, Seizinger BR (1992) Desmoplastic cerebral astrocytomas of infancy: a histopathologic, immunohistochemical, ultrastructural, and molecular genetic study. Hum Pathol 23(12):1402–1409

VandenBerg SR (1993) Desmoplastic infantile ganglioglioma and desmoplastic cerebral astrocytoma of infancy. Brain Pathol 3(3):275–281 Review

Duffner PK, Burger PC, Cohen ME, Sanford RA, Krischer JP, Elterman R, Aronin PA, Pullen J, Horowitz ME, Parent A et al (1994) Desmoplastic infantile gangliogliomas: an approach to therapy. Neurosurgery 34(4):583–589 discussion 589
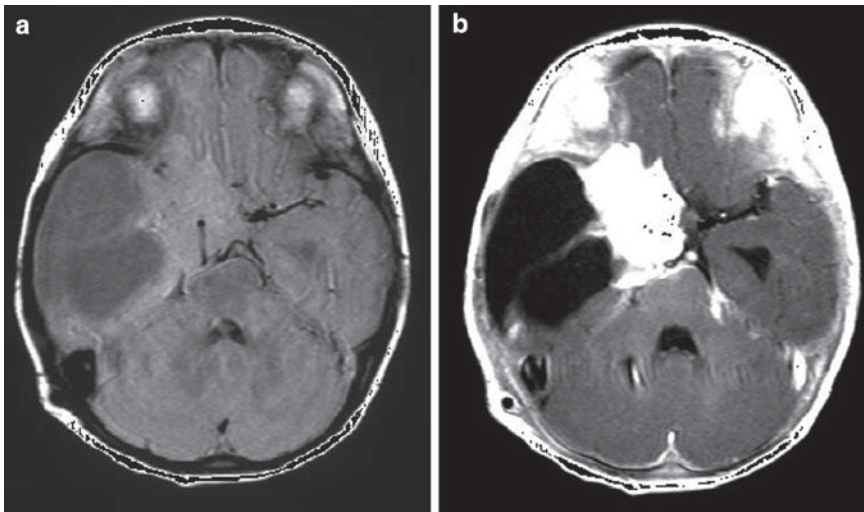
Fig. 16.1. (**a**) Multicystic hemispheric mass, isointense on axial T1-weighted images, and (**b**) same tumor showing contrast enhancement.
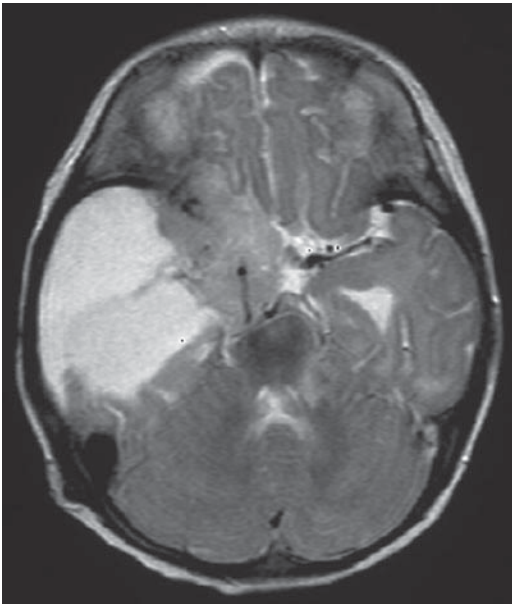
Fig. 16.2. Same patient as in Fig. 16.1 with axial T2 image post contrast demonstrating hyperintensity within the cysts and mild hypointensity in the solid component.
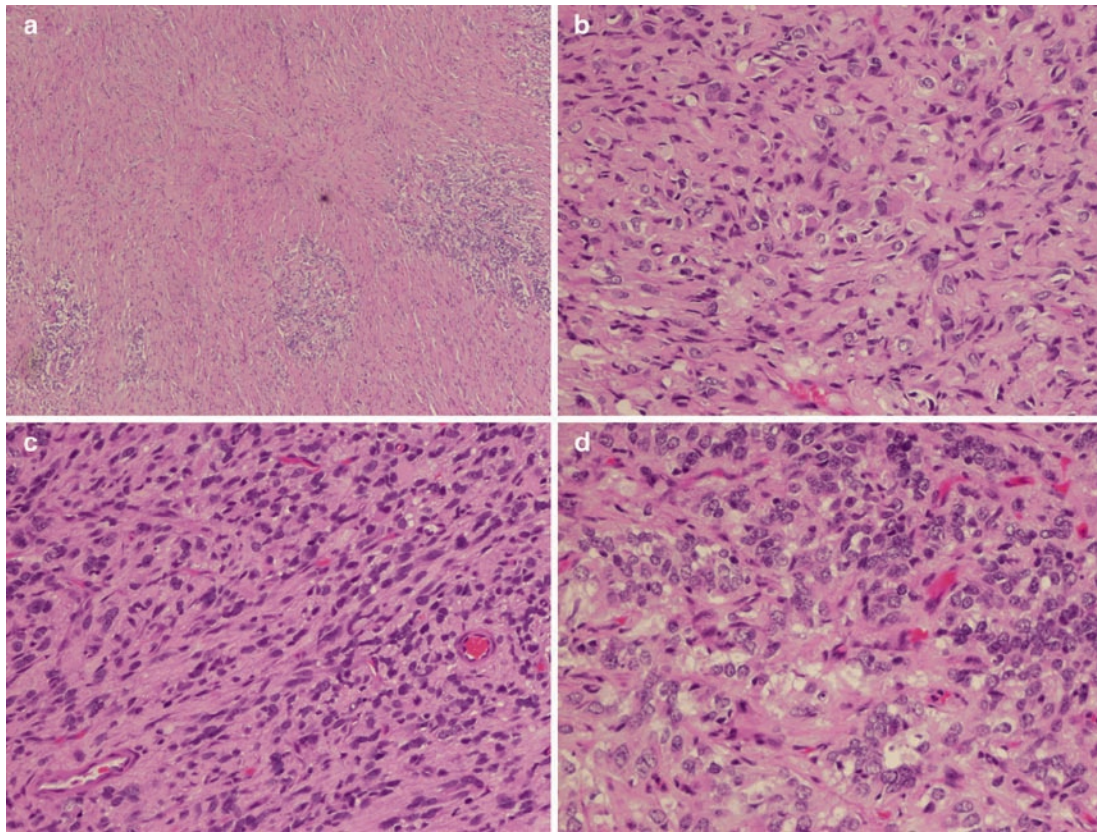
Fig. 16.3. Variable histologic features of DIG include (**a**) florid desmoplasia, (**b**) gemistocytic astrocytes in a desmoplastic matrix, (**c**) astrocytes in a spindled or fascicular pattern, and (**d**) interface between astrocytic component and a small cell, poorly differentiated neuroepithelial component.
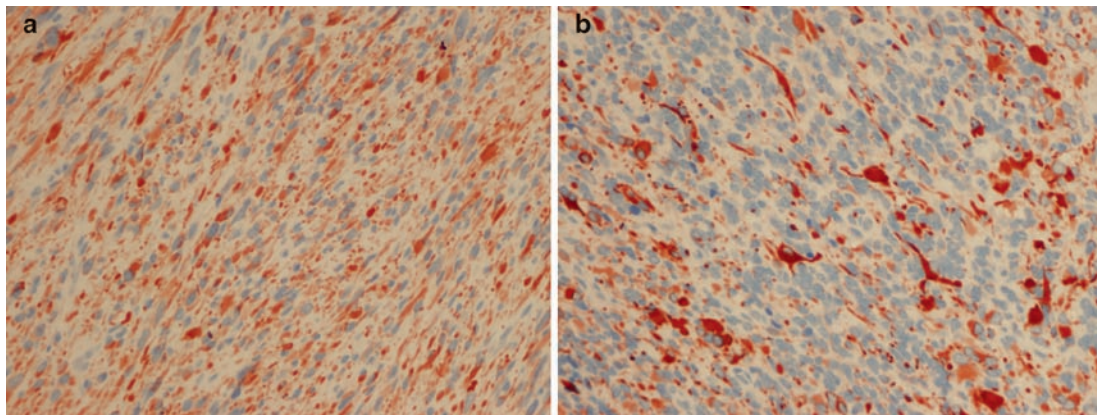
Fig. 16.4. Variable expression of GFAP is seen between the (**a**) astrocytic spindled cell region, and (**b**) small cell neuroepithelial component.
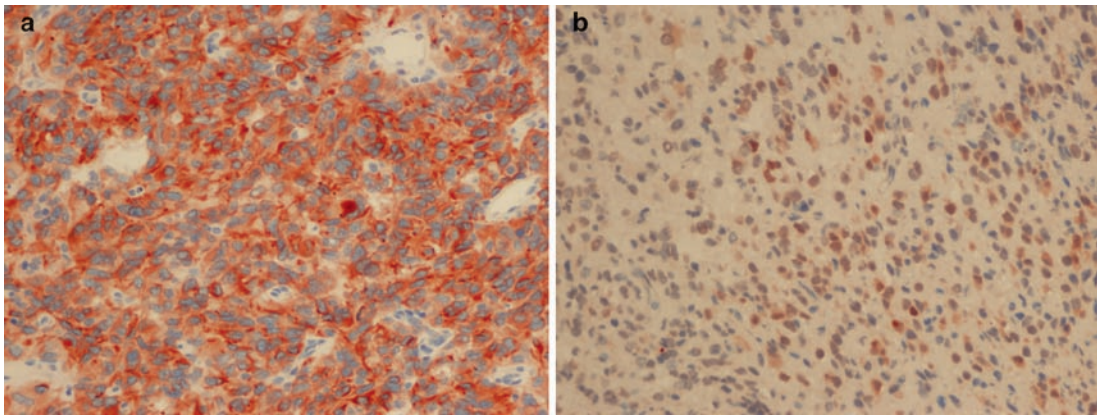
Fig. 16.5. Neuronal markers (**a**) MAP2, and (**b**) NeuN are expressed in the small neuroepithelial component of this DIG.

Dysembryoplastic Neuroepithelial Tumor

Adekunle M. Adesina and Ronald A. Rauch

Keywords Microcystic pattern, glioneuronal tumor, developmental tumor, cortical dysplasia, seizure related neoplasia

17.1 OVERVIEW

- Superficial cortical, benign glioneuronal neoplasms, WHO grade I, often associated with the long-standing history of refractory partial complex seizures.
- Characteristically uninodular or multinodular lesions accompanied by cortical dysplasia.
- Represents 12 and 13.5% of histologic findings in adults and children, respectively, receiving epileptic surgery.
- Although cases of DNT have been observed in young adults, most patients are less than 20 years of age at presentation and show a male predominance.

17.2 CLINICAL FEATURES

- Majority of patients present with long standing history of partial complex seizures that are poorly responsive or resistant to standard antiepileptic therapy.
- Presentation as mass lesions in noncortical sites such as basal ganglia, brainstem, and cerebellum have been reported.
- Occasional presentation in the context of neurofibromatosis 1 (NF1) and XYY syndrome has been reported.

17.3 NEUROIMAGING

- It shows a primary superficial cortical location often without mass effect or peritumoral edema (Fig. 17.1).
- The cortical lesions are best seen on MRI as well-defined hypointense lesions on T1-weighted images (Fig. 17.2a) and hyperintense on T2-weighted images (Fig. 17.1b).
  - The tumor may contain cystic regions.
- Enhancement after contrast administration is variable (Figs. 17.2b, 17.3, and 17.4) and may be nonenhancing.
  - In up to 33% of cases, enhancement may be solid or heterogeneous.
- Usually shows increased diffusion on diffusion images (Fig. 17.5).
- Appearance as malformed gyri with or without a pseudocystic component is common.
- Abnormalities of the overlying calvarium due to skull remodeling may be seen. This is probably more common in DNET than other tumors due to superficial location and slow growth of these tumors.
- Tumor is usually hypodense to white matter without associated edema on CT scan (Fig. 17.6a, b).

- Intratumoral calcification (approximately 20%) when present is demonstrable on CT scans (Fig. 17.6c, d) but may be suggested on MRI.
- MR spectroscopy may show normal spectra or an elevated choline peak (Fig. 17.7).

17.4 PATHOLOGY

- Grossly may appear as elevated and expanded "macrogyri" varying in size from a few millimeters to several centimeters.
- Histopathologic features are classified as:
  - **Complex form**
- Composed of a mixture of a multinodular component of glial nodules and intervening "specific glioneuronal" component (Fig. 17.8).
- Glial nodules are composed of oligodendroglia-like cells (Fig. 17.9) with perinuclear halo, mucinous matrix, and delicate vasculature (Fig. 17.10) and may show calcification (Fig. 17.11).
- Intraoperative smears often show a population of uniform or monomorphic small round cells representing oligodendroglia-like cells with interspersed cells having larger vesicular nuclei and prominent nucleoli representing the neuronal component (Fig. 17.12).
- Nodules may also have histologic features of pilocytic astrocytoma, (Fig. 17.13), diffuse astrocytoma or ganglioglioma.
- The specific glioneuronal component is composed of (1) vertical columns of neuritic processes perpendicular to the cortical surface, on which are arranged columns of oligodendroglia-like cells in a microcystic (Figs. 17.14 and 17.15), mucinous, alcian blue positive matrix, and (2) mature ganglion cells referred to as "floating neurons" seen in the pools of mucin present between the columns (Fig. 17.16).
  - **Simple form**
- Consists primarily of the specific glioneuronal component without the nodular pattern as a component.
  - **"Nonspecific" histologic variants**
- Histologically similar to classic low-grade gliomas and has neither the specific glioneuronal component nor the multinodular architecture.
  - Classification of nonspecific histologic variants as DNET is largely influenced by the clinical presentation.
- They present with similar clinical features of long-standing history of partial seizures and radiologic features as may be seen in the complex form of DNET.
- The need for clinical features to classify these otherwise-low-grade gliomas as DNET makes this category controversial.
  - **Cortical dysplasia**

- Cortical tissue adjoining the DNET mass-lesion often shows varying degrees of cortical dysplasia with features of cortical dyslamination or disorganization (microdysgenesis), including irregular neuronal clustering, irregular neuronal orientation, accentuation of vertical columnar architecture, and diffuse white matter neuronal heterotopia.
- The association of DNETs with cortical dysplasia suggests a developmental malformative origin.

17.5 IMMUNOHISTOCHEMISTRY

- Immunostaining for glial marker GFAP identifies an astrocytic component (Fig. 17.17 and 17.18).
- Oligodendroglia-like cells show diffuse immunoreactivity for S-100 and focal positivity for neuronal markers, including NeuN, neurofilament protein, and class III β-tubulin.
  - Dense core neurosecretory granules can be demonstarted within some of these neurocytic cells (Fig. 17.19).
- Synaptophysin is frequently diffusely positive in the neuropil (Fig. 17.20a) and the neuronal components of the "specific glioneuronal element," but weakly positive to negative in the oligodendroglia-like cells.
  - Neuronal component is also positive for chromogranin (Fig. 17.20b) and other neuronal markers.
- Reported demonstration of myelin-associated glycoprotein in some oligodendoglial-like cells suggests oligodendroglial differentiation in these cells.
- Proliferation index by MIB1 immunostaining is usually less than 1% (Fig. 17.21).
  - Proliferation index as high as 8% has been reported.

17.6 MOLECULAR PATHOLOGY

  - Molecular events associated with prognosis in oligodendroglioma, such as 1p36 and 19q13 deletions, or progression-related genetic events in fibrillary astrocytoma, such as 17p13 deletion or p53 gene mutation, are absent in DNET.

17.7 DIFFERENTIAL DIAGNOSIS

  - Identification of the specific glioneuronal element is key to recognition of the simple and complex forms of DNET.
  - Tumors with the presence of nonspecific histologic patterns, including pilocytic astrocytoma and oligodendroglioma-like or ganglioglioma-like patterns in addition to the specific glioneuronal component, should be classified as DNET.
  - In the absence of the specific glioneuronal element, diagnosis of nonspecific histologic patterns as DNET can be problematic and is currently controversial. Designation of such lesions as DNET is favored by the presence of a classic history of poorly controlled longstanding seizures and radiologic findings compatible with a diagnosis of DNET.

17.8 PROGNOSIS

- They are generally regarded as benign tumors. Long-term follow-up shows no evidence of recurrence following gross total resection or progression following subtotal resection.
- Rare case of malignant transformation has been reported following radiation and chemotherapy.

SUGGESTED READING

Sung CO, Suh YL (2009) Different pattern of expression of nestin in the non-specific form of dysembryoplastic neuroepithelial tumors compared to the simple and complex forms. J Neurooncol 92(1):7–13

Maher CO, White JB, Scheithauer BW, Raffel C (2008) Recurrence of dysembryoplastic neuroepithelial tumor following resection. Pediatr Neurosurg 44(4):333–336

O'Brien DF, Farrell M, Delanty N, Traunecker H, Perrin R, Smyth MD, Park TS (2007) The Children's Cancer and Leukaemia Group guidelines for the diagnosis and management of dysembryoplastic neuroepithelial tumours. Br J Neurosurg 21(6):539–549

Ishizawa K, Terao S, Kobayashi K, Yoshida K, Hirose T (2007) A neuroepithelial tumor showing combined histological features of dysembryoplastic neuroepithelial tumor and pleomorphic xanthoastrocytoma–a case report and review of the literature. Clin Neuropathol 26(4):169–175 Review

Sherburn EW, Bahn MM, Gokden M, Silbergeld DL, Rich KM (1998) Dysembryoplastic neuroepithelial tumor and oligodendroglioma: The diagnostic value of magnetic resonance spectroscopy. Case report and review of the literature. Neurosurg Focus 4(4):e6

Deb P, Sharma MC, Tripathi M, Sarat Chandra P, Gupta A, Sarkar C (2006) Expression of CD34 as a novel marker for glioneuronal lesions associated with chronic intractable epilepsy. Neuropathol Appl Neurobiol 32(5):461–468

Takahashi A, Hong SC, Seo DW, Hong SB, Lee M, Suh YL (2005) Frequent association of cortical dysplasia in dysembryoplastic neuroepithelial tumor treated by epilepsy surgery. Surg Neurol 64(5):419–427

Sakuta R, Otsubo H, Nolan MA, Weiss SK, Hawkins C, Rutka JT, Chuang NA, Chuang SH, Snead OC III (2005) Recurrent intractable seizures in children with cortical dysplasia adjacent to dysembryoplastic neuroepithelial tumor. J Child Neurol 20(4):377–384

Park JY, Suh YL, Han J (2003) Dysembryoplastic neuroepithelial tumor. Features distinguishing it from oligodendroglioma on cytologic squash preparations. Acta Cytol 47(4):624–629

Prayson RA, Castilla EA, Hartke M, Pettay J, Tubbs RR, Barnett GH (2002) Chromosome 1p allelic loss by fluorescence in situ hybridization is not observed in dysembryoplastic neuroepithelial tumors. Am J Clin Pathol 118(4):512–517

Stanescu Cosson R, Varlet P, Beuvon F, Daumas Duport C, Devaux B, Chassoux F, Frédy D, Meder JF (2001) Dysembryoplastic neuroepithelial tumors: CT, MR findings and imaging follow-up: A study of 53 cases. J Neuroradiol 28(4):230–240

Daumas-Duport C, Varlet P, Bacha S, Beuvon F, Cervera-Pierot P, Chodkiewicz JP (1999) Dysembryoplastic neuroepithelial tumors: Nonspecific histological forms – a study of 40 cases. J Neurooncol 41(3):267–280

Honavar M, Janota I, Polkey CE (1999) Histological heterogeneity of dysembryoplastic neuroepithelial tumour: Identification and differential diagnosis in a series of 74 cases. Histopathology 34(4):342–356

Prayson RA (1999) Composite ganglioglioma and dysembryoplastic neuroepithelial tumor. Arch Pathol Lab Med 123(3):247–250

Hirose T, Scheithauer BW (1998) Mixed dysembryoplastic neuroepithelial tumor and ganglioglioma. Acta Neuropathol 95(6):649–654 Review

Ostertun B, Wolf HK, Campos MG, Matus C, Solymosi L, Elger CE, Schramm J, Schild HH (1996) Dysembryoplastic neuroepithelial tumors: MR and CT evaluation. AJNR Am J Neuroradiol 17(3):419–430

Taratuto AL, Pomata H, Sevlever G, Gallo G, Monges J (1995) Dysembryoplastic neuroepithelial tumor: Morphological, immunocytochemical, and deoxyribonucleic acid analyses in a pediatric series. Neurosurgery 36(3):474–481

Hirose T, Scheithauer BW, Lopes MB, VandenBerg SR (1994) Dysembryoplastic neuroeptihelial tumor (DNT): An immunohistochemical and ultrastructural study. J Neuropathol Exp Neurol 53(2):184–195

Daumas-Duport C (1993) Dysembryoplastic neuroepithelial tumours. Brain Pathol 3(3):283–295 Review

Daumas-Duport C, Scheithauer BW, Chodkiewicz JP, Laws ER Jr, Vedrenne C (1988) Dysembryoplastic neuroepithelial tumor: A surgically curable tumor of young patients with intractable partial seizures. Report of thirty-nine cases. Neurosurgery 23(5):545–556
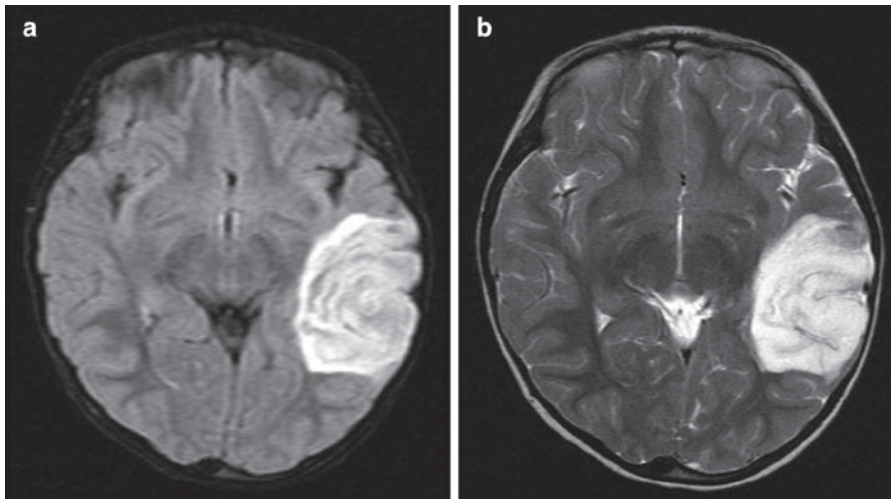
Fig. 17.1. (**a**) Axial FLAIR and (**b**) axial T-2w images showing bright (hyperintense) left temporal lobe lesion with no mass effect or midline shift.
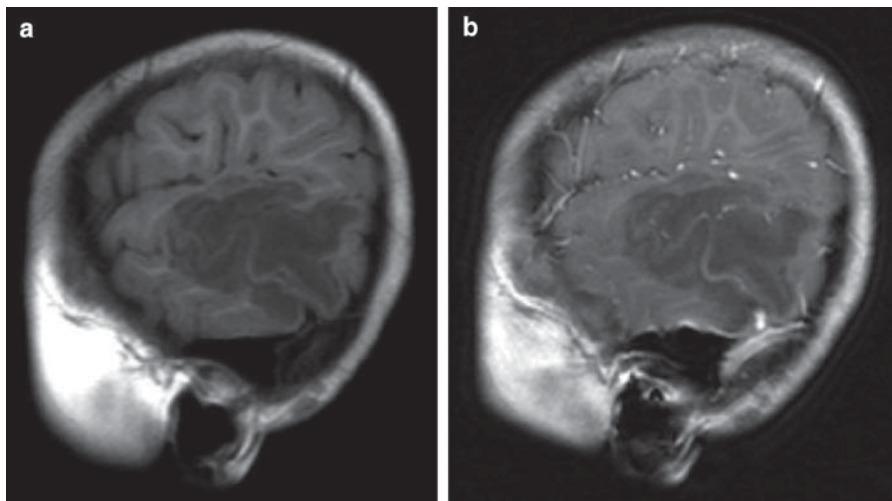
Fig. 17.2. (**a**) Dark (hypointense) cortical lesion on sagittal T1-w precontrast and (**b**) same lesion on sagittal T1-w postcontrast with no enhancement.
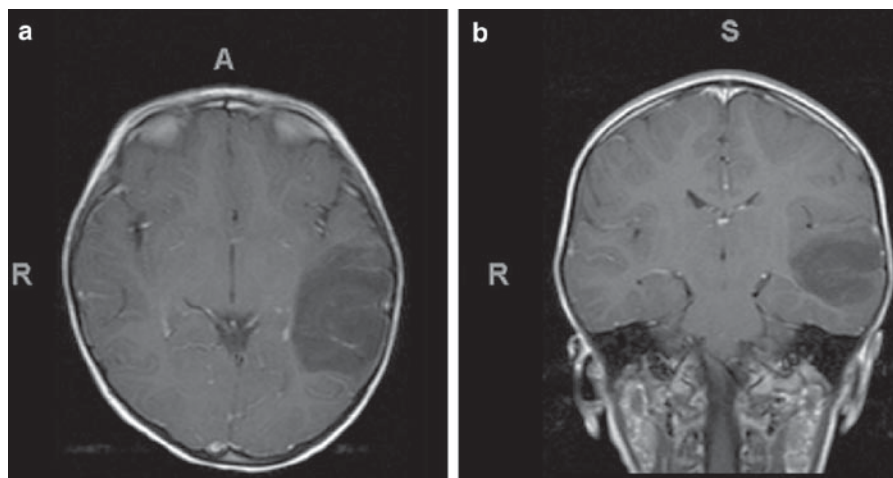
Fig 17.3. (**a**) Axial and (**b**) coronal T1-w postcontrast images showing lack of enhancement in the left temporal hyperintense mass lesions with confirmed histologic features of a complex DNET.
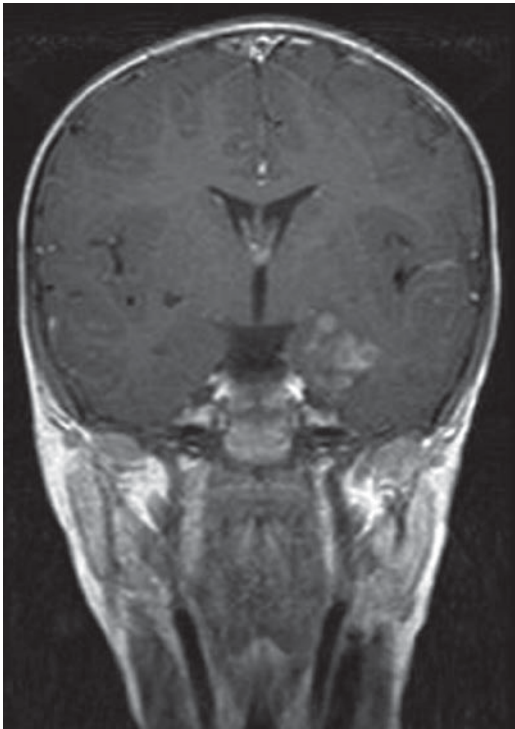
Fig 17.4. Coronal T1-w postcontrast image showing enhancement of a left mesiotemporal mass lesion.
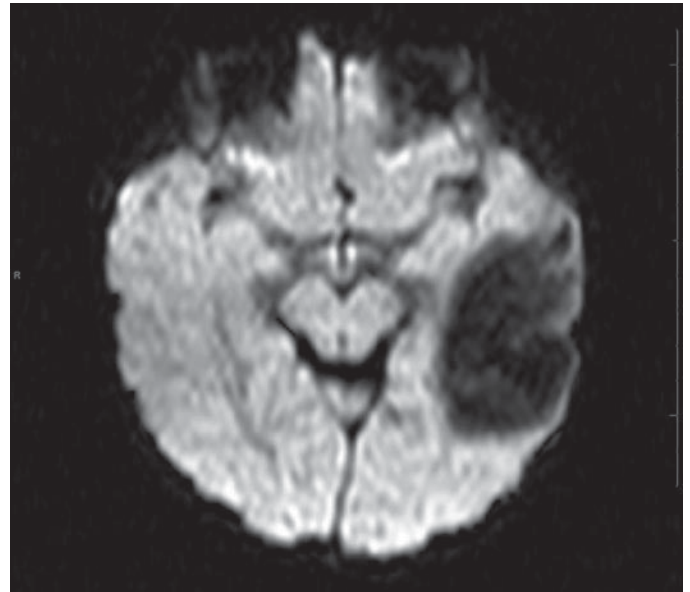
Fig 17.5. Axial diffusion weighted image showing unrestricted diffusion in the same lesion as in Fig. 17.1.
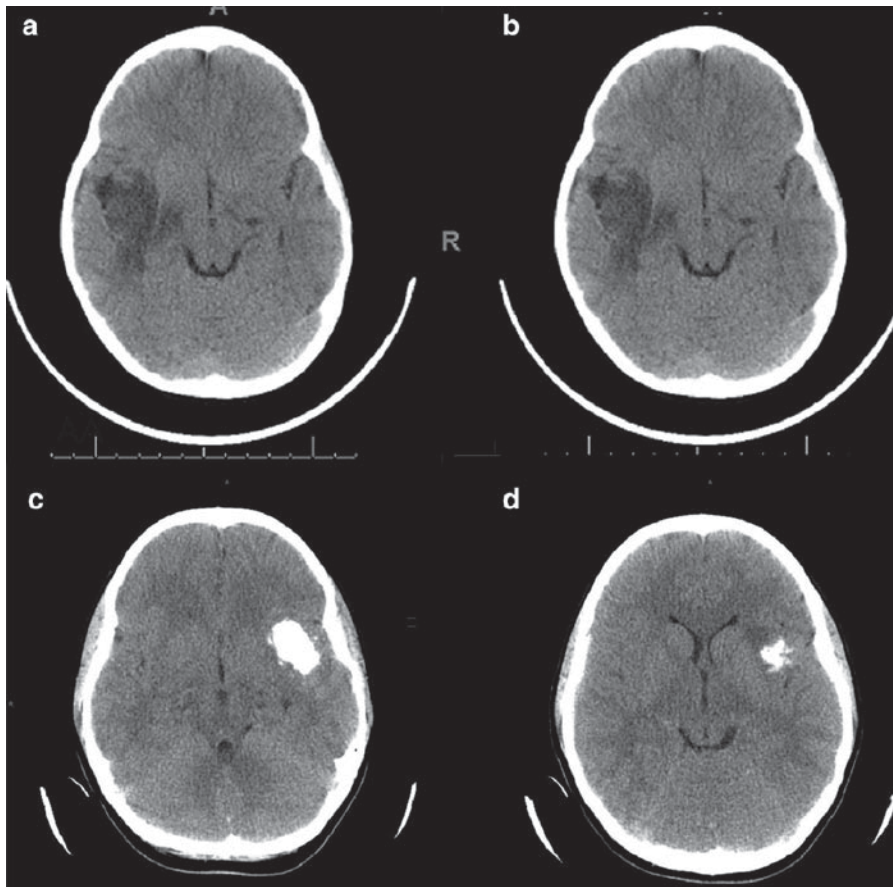
Fig. 17.6. (**a** and **b**) Axial CT scans of a right temporal lobe DNET showing no calcification. (**c** and **d**) Axial CT scans of a left temporal lobe DNET showing the presence of calcification.
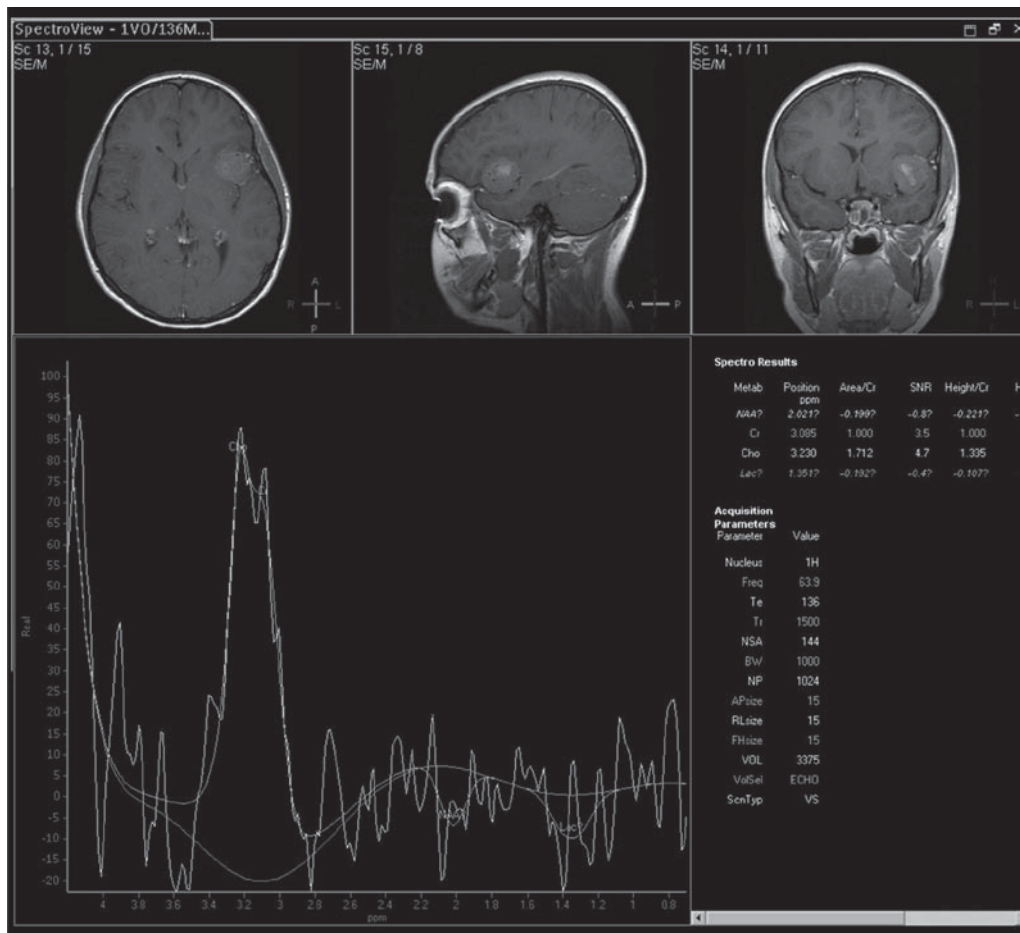
Fig. 17.7. MR spectroscopy at TE of 136 ms showing elevated choline and small NAA peak.
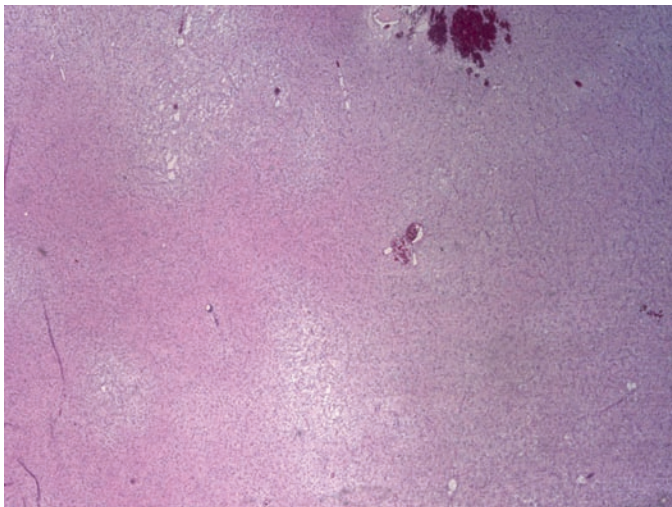
Fig. 17.8. Low-power view of a complex DNET with multiple nodules of the "glioneuronal" component.
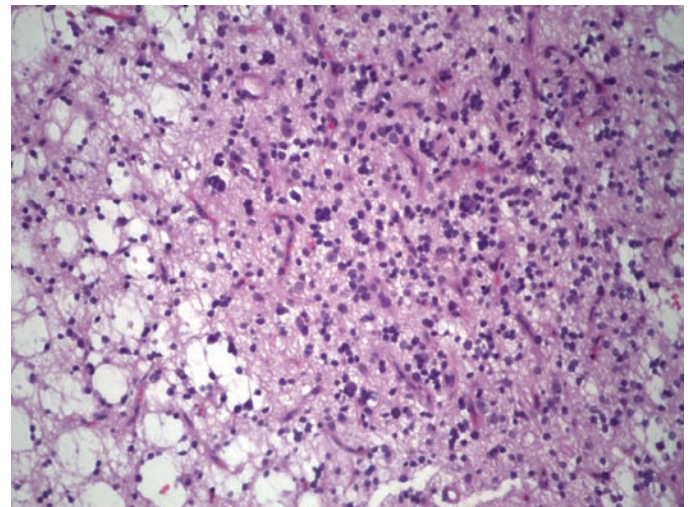
Fig. 17.9. Regional cluster of proliferating "oligo-like" cells in a microcystic background.
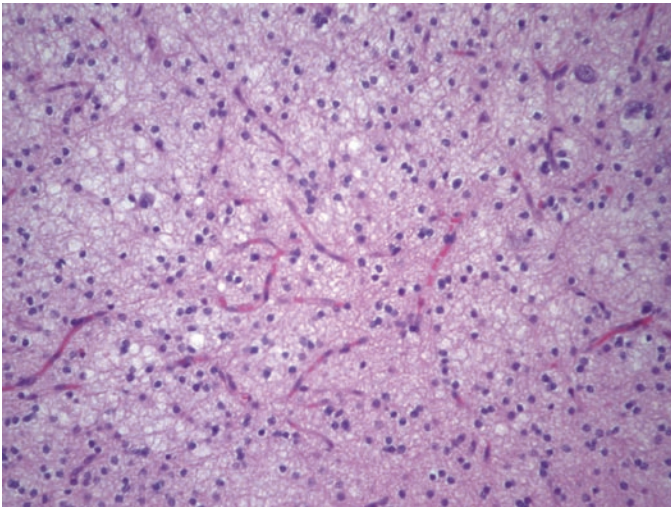
Fig. 17.10. Delicate vasculature arranged in a "chicken wire" configuration and intermixed with "oligo-like" cells.
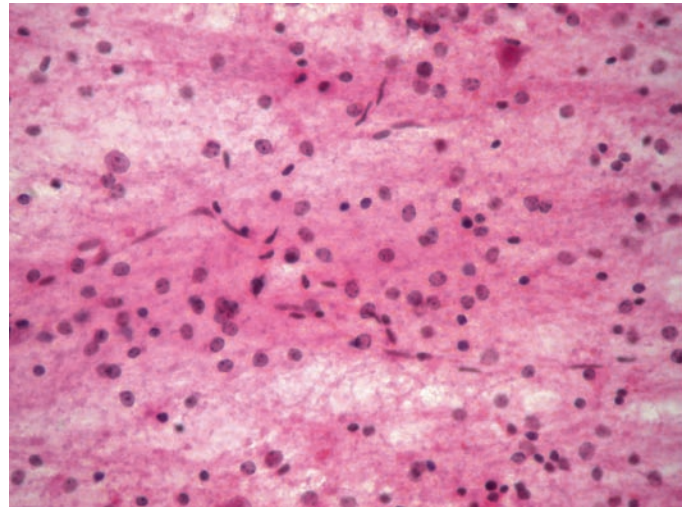
Fig. 17.12. Smear preparation showing a uniform population of oligo-like cells, few interspersed neuronal nuclei, and delicate capillaries in a fibrillary background.
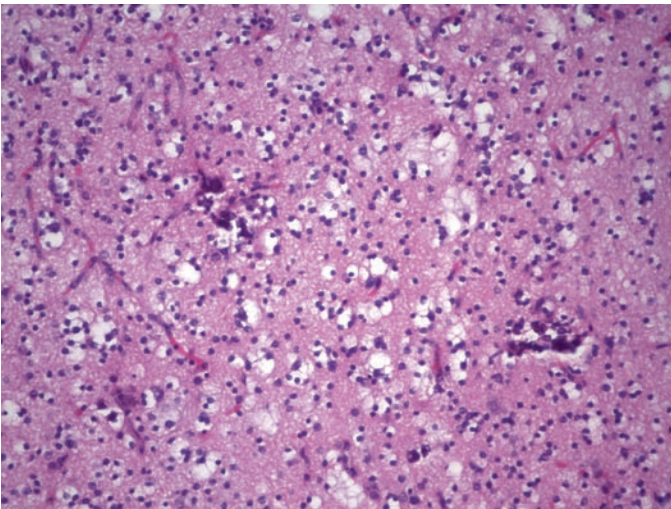
Fig. 17.11. Multifocal calcification randomly distributed within a DNET.
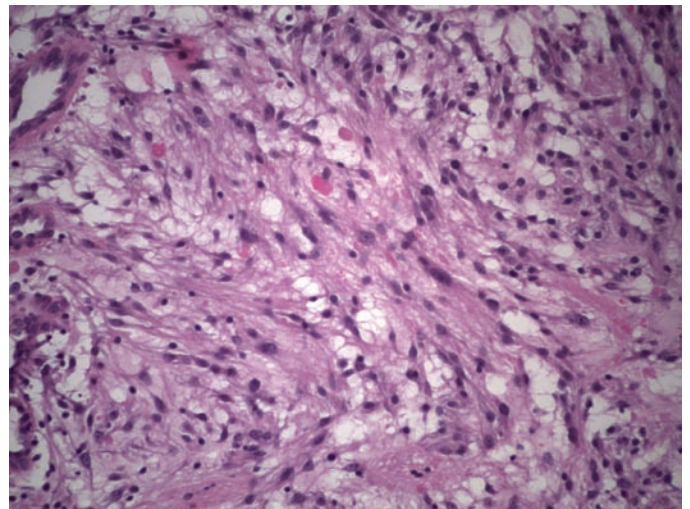
Fig. 17.13. Region of pilocytic astrocytoma within a DNET. Note the piloid astrocytic cells, Rosenthal fibers, and numerous microcysts.
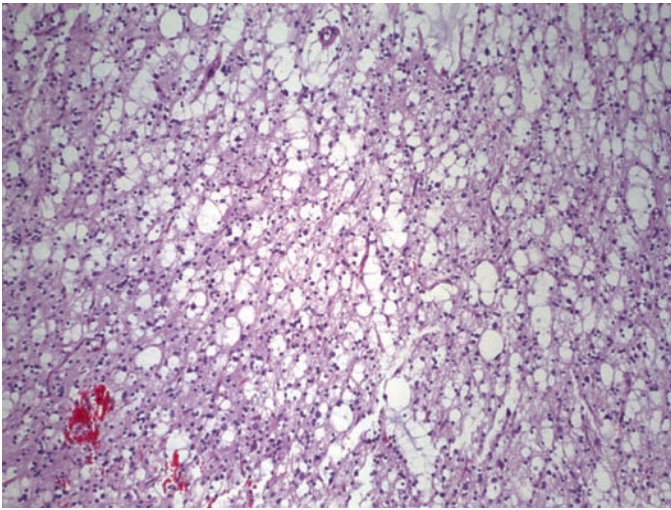
Fig. 17.14. Diffuse microcystic pattern.
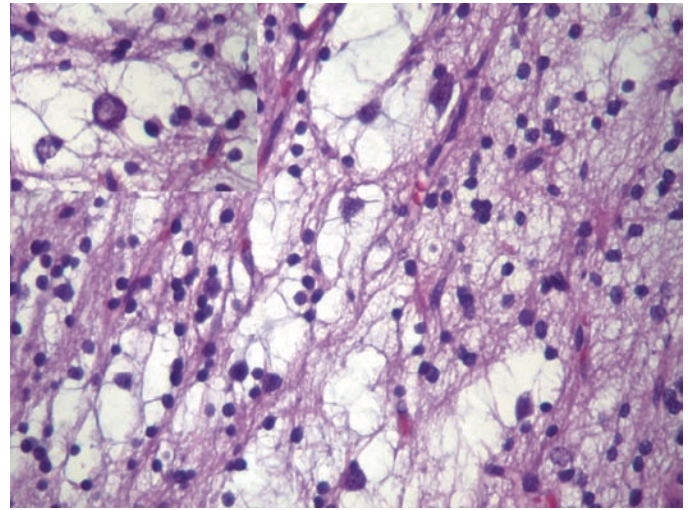
Fig. 17.16. Columns of oligodroglial-like cells, a diffuse microcystic pattern with a mucinous content and intracystic "floating" neurons (top left corner inset) represent the classic features of the specific glioneuronal component of a DNET.
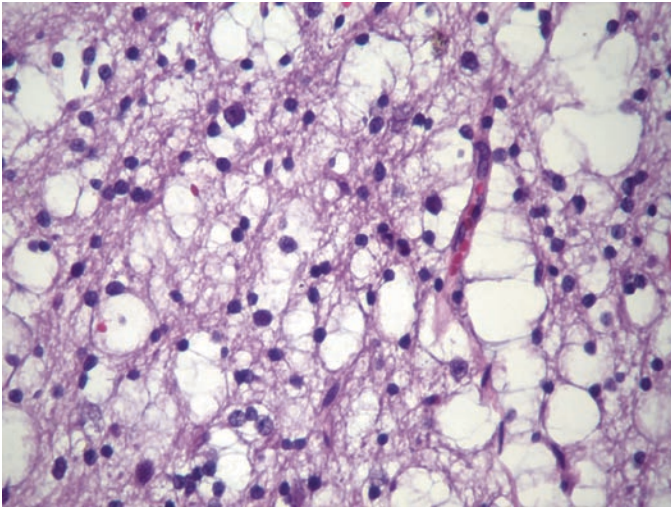
Fig. 17.15. Diffuse microcystic pattern at a higher magnification.
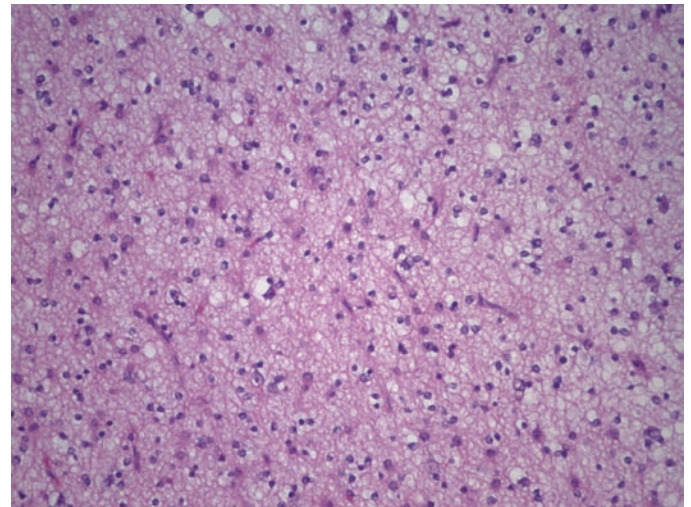
Fig. 17.17. Region of a more distinct astrocytic differentiation within a DNET.
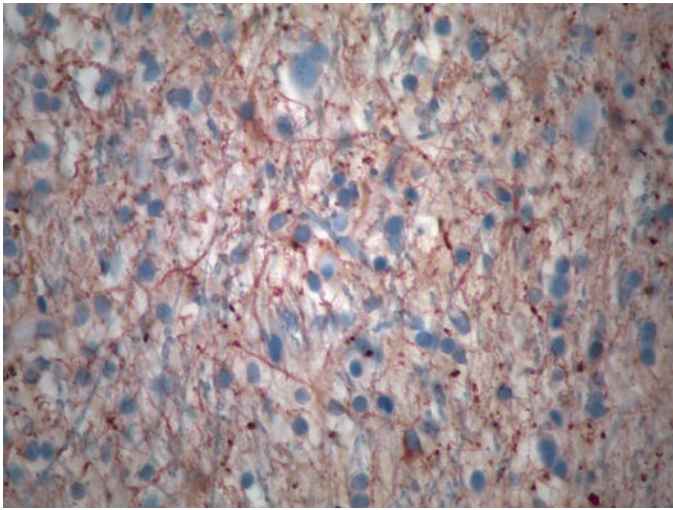
Fig. 17.18 GFAP immunostain showing a diffuse and fibrillary stromal positivity as well as cytoplasmic positivity in differentiating astrocytic cells.
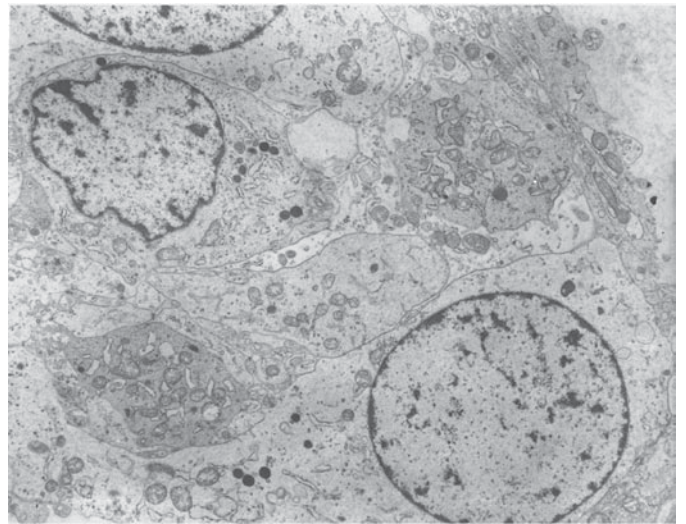
Fig. 17.19 Electron micrograph of the neurocytic cells within a DNET showing dense core neurosecretory granules consistent with neuronal differentiation.
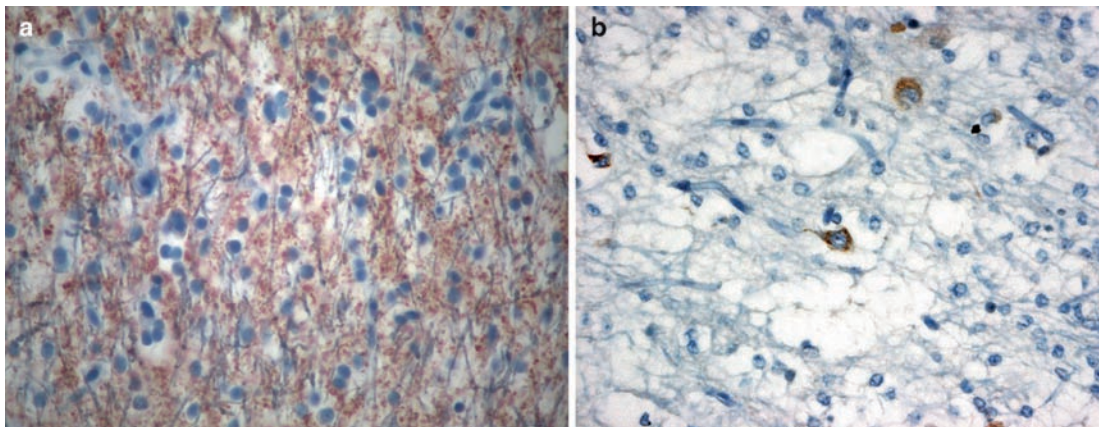
Fig. 17.20. (**a**) Diffuse stromal positivity for synaptophysin in a DNET (**b**) Floating neurons showing immunopositivity for chromogranin in a DNET.
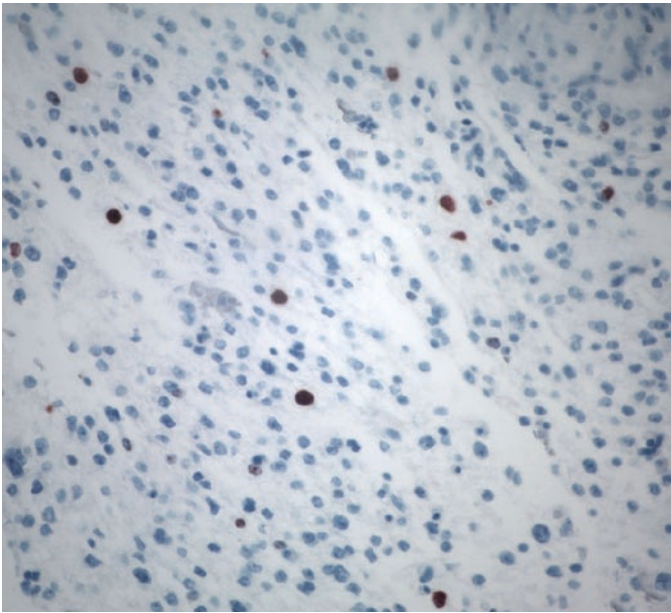
Fig. 17.21. Immunostain with the MIB1 antibody showing a paucity of Ki-67 positive cells consistent with a low proliferation index.

Ganglioglioma and Gangliocytoma

Adekunle M. Adesina and Ronald A. Rauch

18.1 OVERVIEW

- These are neuroepithelial tumors composed of mature neurons (gangliocytoma) or a mixed population of ganglion cells and glial cells (ganglioglioma).
- Well differentiated gangliocytomas are classified as WHO grade I while gangliogliomas may be classified as WHO grade I or II.
- Anaplastic ganglioglioma with a malignant glial component is classified as WHO grade III.
- Gangliogliomas and gangliocytomas may occur in all age groups but they are frequently seen in the young with a peak between the age of 10 and 30 years and representing about 0.4% of all tumors in the central nervous system.
- May occur in all regions of the CNS but occur with a higher frequency in the brain with an incidence of 1.3% of all brain tumors.
- Greater than 80% of gangliogliomas and gangliocytomas occur in the temporal lobe and represent the most frequent tumors associated with epilepsy.

18.2 CLINICAL FEATURES

- Clinical presentation reflects localized tumor effect and complications of raised intracranial pressure.
- Longstanding history of seizures ranging from a few months to decades is frequent in tumors involving the cerebral hemisphere.
- Represent the most frequent tumors in patients with temporal lobe epilepsy requiring surgical intervention for control of seizures.
- Tumors involving the brain stem and spinal cord often have a short duration of symptomatology related to pressure effect.

18.3 NEUROIMAGING

- Classically the tumors present as cysts with a mural nodule (Fig. 18.1) but may also present as circumscribed solid masses (Fig. 18.2) or masses with multiple cysts.
- On MRI, the tumors typically appear hypointense on T1-weighted images (Fig. 18.3) and hyperintense on T2-weighted images (Fig. 18.4). Enhancement with contrast is variable but often present (Figs. 18.5 and 18.6).
- CT scans may show calcification (Fig. 18.7). The solid portion of the tumor itself is often hypodense but may be isodense compared to brain.
- Calvarial bone remodeling changes due to prolonged tumor impingement on skull may be seen.

18.4 PATHOLOGY

- Macroscopically, often the tumors are seen as cystic lesions with a mural nodule. May also be seen as well circumscribed mass lesions.
- Intraoperative smear preparations show a mixed population of fibrillary astrocytic cells and variable number of ganglioid and ganglion cells with vesicular nuclei and prominent nucleoli (Figs. 18.8 and 18.9).

18.4.1 HISTOLOGY

- Histologic hallmark of a gangliocytoma is a tumor with disorganized, variably cellular, non-infiltrative (well circumscribed) aggregates of large and small neurons (Fig. 18.10) and no glial component.
- Neuronal differentiation is recognized by the presence of large cells with vesicular nuclei, prominent nucleoli, and variably abundant amphophilic cytoplasm (Fig. 18.11).
- Neurons show varying degrees of dysmorphism including irregular accumulation of Nissl substance, cytoplasmic vacuolation, neurofibrillary tangles, granulovacuolar degeneration and binucleated cells (Fig. 18.12).
- Less mature neurons with intermediate differentiation designated as "ganglioid cells" are often present (Fig. 18.13).
- Gangliogliomas show both populations of neoplastic neurons and glia (astrocytes) which may be arranged as separate and distinct clusters of cell populations or may be intimately mixed.
- Reticulin and collagen rich stroma may be seen in the lobular clusters of ganglion cells.
- The proportion of neuronal component is variable ranging from being predominant to being a minor component (Figs. 18.14–18.16).
- The glial component may represent a diffuse fibrillary or a pilocytic pattern (Fig. 18.17). Rare examples of composite pleomorphic xanthoastrocytoma and ganglioglioma have been reported.
- PAS positive eosinophilic granular bodies (EGBs) are a frequent feature of ganglion cell tumors.
- Lymphocytic infiltrate arranged in a perivascular pattern is also common. Microcalcification and a florid microcystic change may be seen.
- A delicate capillary network may be seen especially in gangliocytomas.
- Subarachnoid tumor growth is a frequent histologic observation which does not imply subarachnoid dissemination or poor prognosis.

- Cortical dysplasia may occur in adjoining cortical tissue especially in lesions removed for seizure control.
- High grade astrocytic features including increased cellularity, pleomorphism, and mitotic activity suggest anaplastic ganglioglioma which is usually due to malignant progression in the glial component (Figs. 18.18, 18.19a and 18.19b).

18.5 IMMUNOHISTOCHEMISTRY

- Use of a panel of neuronal markers including synaptophysin (Fig. 18.20), MAP 2 (Fig. 18.21), chromogranin, NFP, and NeuN to demonstrate neuronal differentiation is recommended.
  - Synaptophysin shows a granular surface membrane staining of perisomatic synapses with or without cytoplasmic staining.
  - MAP 2 frequently shows strong cytoplasmic staining, while chromogranin shows granular cytoplasmic staining but may be less diffusely positive.
  - NFP shows variable cytoplasmic staining while NeuN shows nuclear positivity.
  - Although MAP 2 positivity may be seen in diffuse gliomas, it is less frequently positive in the astrocytic component of gangliogliomas.
- CD34 has been reported as frequently positive in gangliogliomas with a frequency of about 70–80%.
- GFAP positivity is present in the astrocytic component of gangliogliomas (Fig. 18.22).

18.6 ELECTRON MICROSCOPY

- Neuronal differentiation in a ganglion cell tumor is readily demonstrable by the presence of dense core neurosecretory granules which are often abundant in the more differentiated cells.
- Abundant microtubules and demonstrable synaptic type junctions support neuronal differentiation.

18.7 DIFFERENTIAL DIAGNOSIS

- The major differential diagnostic issue is the need to differentiate between a ganglion cell tumor and an infiltrating glioma with entrapped neurons. Helpful clues in making the distinction include the following:
  - Neoplastic ganglion cells tend to form abnormal clusters and are variable in size with abnormal orientation of neuronal apical dendrites.
  - Binucleation is the ultimate proof of neoplasia.
  - Dysmorphic neurons are frequently seen in ganglion cell tumors.
- Dysembryoplastic neuroepithelial tumors may show a mixed glioneuronal phenotype.
  - Characteristic mucinous components with "floating" neurons are features of DNET, not seen in ganglion cell tumors.
  - Multinodular architecture with oligodendroglia-like cells and characteristic neuroimaging features including superficial location favor a DNET.
  - Transitional tumors with mixed features of DNET and ganglioglioma occur but are very rare (Figs. 18.23 and 18.24) and pose a significant diagnostic dilemma when attempts

are made to fit such tumors into either the DNET or ganglioglioma categories.

18.8 MOLECULAR PATHOLOGY

- Although examples of occurrence of ganglioglioma in patients with NF1, NF2 and Peutz-Jeghers' syndrome have been reported, no mutations in the NF1 or NF2 or LKB1 genes, respectively have been demonstrated in gangliogliomas.
- Gains of chromosome 7 have been reported.
- Genetic events described in typical fibrillary astrocytomas such as p53 and PTEN mutations, CDK4 and EGFR amplification are infrequent in ganglioglioma.
- Polymorphisms in intron 4 and exon 41 of TSC2 are over-represented in individuals with ganglioglioma.

18.9 PROGNOSIS

- Generally slow growing, low grade, classified as WHO grade 1 with a 7.5 year progression free survival rate of 94%.
- Malignant progression is uncommon but when it occurs it is usually related to malignant progression of the glial/astrocytic component showing increased cellularity, increased mitotic activity, endothelial proliferation and necrosis with poorer prognosis.

SUGGESTED READING

McLendon RE, Provenzale J (2002) Glioneuronal tumors of the central nervous system. Brain Tumor Pathol 19(2):51–58 Review

Shin JH, Lee HK, Khang SK, Kim DW, Jeong AK, Ahn KJ, Choi CG, Suh DC (2002a) Neuronal tumors of the central nervous system: Radiologic findings and pathologic correlation. Radiographics 22(5): 1177–1189

Hayashi Y, Iwato M, Hasegawa M, Tachibana O, von Deimling A, Yamashita J (2001) Malignant transformation of a gangliocytoma/ganglioglioma into a glioblastoma multiforme: A molecular genetic analysis Case report. J Neurosurg 95(1):138–142

Karremann M, Pietsch T, Janssen G, Kramm CM, Wolff JE (2009) Anaplastic ganglioglioma in children. J Neurooncol 92(2):152–163

Rogojan L, Olinici CD (2008) Ganglioglioma with glioblastoma component. Rom J Morphol Embryol 49(3):403–406

Brat DJ, Parisi JE, Kleinschmidt-DeMasters BK, Yachnis AT, Montine TJ, Boyer PJ, Powell SZ, Prayson RA, McLendon RE (2008) Surgical neuropathology update: A review of changes introduced by the WHO classification of tumours of the central nervous system, 4th edn. Arch Pathol Lab Med 132(6):993–1007, Review

Adachi Y, Yagishita A (2008) Gangliogliomas: Characteristic imaging findings and role in the temporal lobe epilepsy. Neuroradiology 50(10):829–834

Takei H, Dauser R, Su J, Chintagumpala M, Bhattacharjee MB, Jones J, Adesina AM (2007) Anaplastic ganglioglioma arising from a Lhermitte-Duclos-like lesion. J Neurosurg 107(2):137–142

Mittelbronn M, Schittenhelm J, Lemke D, Ritz R, Nägele T, Weller M, Meyermann R, Beschorner R (2007) Low grade ganglioglioma rapidly progressing to a WHO grade IV tumor showing malignant transformation in both astroglial and neuronal cell components. Neuropathology 27(5):463–467

Rosenblum MK (2007) The 2007 WHO Classification of Nervous System Tumors: Newly recognized members of the mixed glioneuronal group. Brain Pathol 17(3):308–313

Pandita A, Balasubramaniam A, Perrin R, Shannon P, Guha A (2007) Malignant and benign ganglioglioma: A pathological and molecular study. Neuro Oncol 9(2):124–134

Luyken C, Blümcke I, Fimmers R, Urbach H, Wiestler OD, Schramm J (2004) Supratentorial gangliogliomas: Histopathologic grading and tumor recurrence in 184 patients with a median follow-up of 8 years. Cancer 101(1): 146–155

Jallo GI, Freed D, Epstein FJ (2004) Spinal cord gangliogliomas: A review of 56 patients. J Neurooncol 68(1):71–77

Shin JH, Lee HK, Khang SK, Kim DW, Jeong AK, Ahn KJ, Choi CG, Suh DC (2002b) Neuronal tumors of the central nervous system: Radiologic findings and pathologic correlation. Radiographics 22(5):1177–1189

Whittle IR, Mitchener A, Atkinson HD, Wharton SB (2002) Anaplastic progression in low grade glioneural neoplasms. Acta Neuropathol 104(2):215

Blümcke I, Wiestler OD (2002) Gangliogliomas: An intriguing tumor entity associated with focal epilepsies. J Neuropathol Exp Neurol 61(7):575–584 Review

Bleggi-Torres LF, Netto MR, Gasparetto EL, Gonçalves E, Silva A, Moro M (2002) Dysembryoplastic neuroepithelial tumor: Cytological diagnosis by intraoperative smear preparation. Diagn Cytopathol 26(2):92–94

Lagares A, Gómez PA, Lobato RD, Ricoy JR, Ramos A, de la Lama A (2001) Ganglioglioma of the brainstem: Report of three cases and review of the literature. Surg Neurol 56(5):315–322 discussion 322–324, review

Nishio S, Morioka T, Mihara F, Gondo K, Fukui M (2001) Cerebral ganglioglioma with epilepsy: Neuroimaging features and treatment. Neurosurg Rev 24(1):14–19

Moreno A, de Felipe J, García Sola R, Navarro A, Ramón y Cajal S (2001) Neuronal and mixed neuronal glial tumors associated to epilepsy. A heterogeneous and related group of tumours. Histol Histopathol 16(2): 613–622 Review

Hayashi S, Kameyama S, Fukuda M, Takahashi H (2000) Ganglioglioma with a tanycytic ependymoma as the glial component. Acta Neuropathol 99(3):310–316

Prayson RA (1999) Composite ganglioglioma and dysembryoplastic neuroepithelial tumor. Arch Pathol Lab Med 123(3):247–250

Hirose T, Scheithauer BW (1998) Mixed dysembryoplastic neuroepithelial tumor and ganglioglioma. Acta Neuropathol 95(6):649–654 Review

Perry A, Giannini C, Scheithauer BW, Rojiani AM, Yachnis AT, Seo IS, Johnson PC, Kho J, Shapiro S (1997) Composite pleomorphic xanthoastrocytoma and ganglioglioma: Report of four cases and review of the literature. Am J Surg Pathol 21(7):763–771 Review

Hirose T, Scheithauer BW, Lopes MB, Gerber HA, Altermatt HJ, VandenBerg SR (1997) Ganglioglioma: An ultrastructural and immunohistochemical study. Cancer 79(5):989–1003
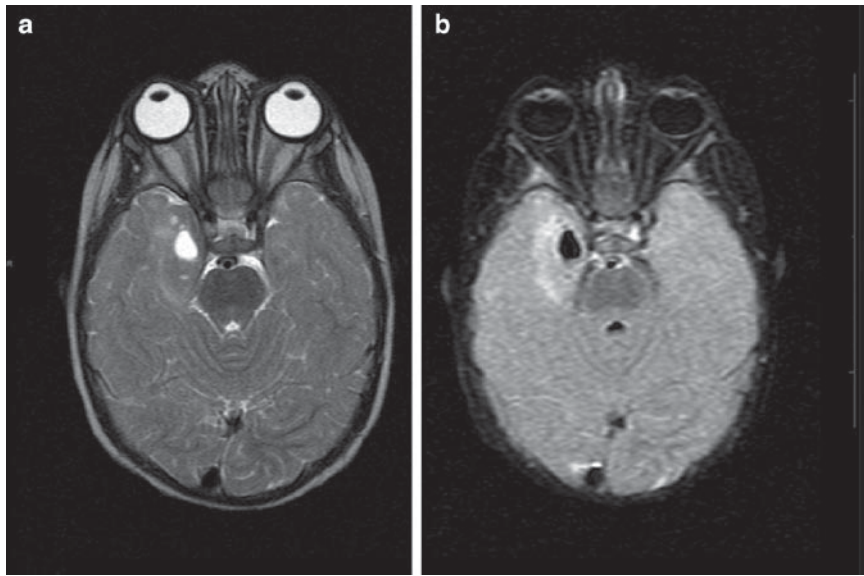
Fig. 18.1. (**a**) Axial T2-w, and (**b**) axial flair showing a cystic right temporal lobe mass with mural nodule and subtle T2-w hyperintensity.

Fig. 18.2. Non-contrast CT scan 15 months earlier from same patient as in Fig. 18.1 above showing calcified mass of right temporal lobe.
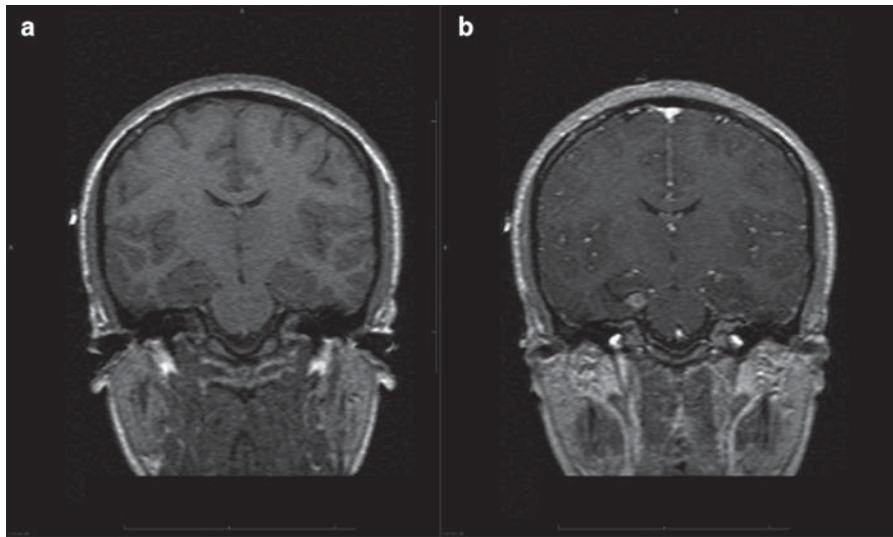
Fig. 18.3. (**a**) Coronal T1-w pre gadolinium (Gd) shows hypointense to isointense right temporal lobe lesion inferior to the hippocampus, and (**b**) Coronal T1-w post Gd shows enhancing nodule of right temporal lobe.
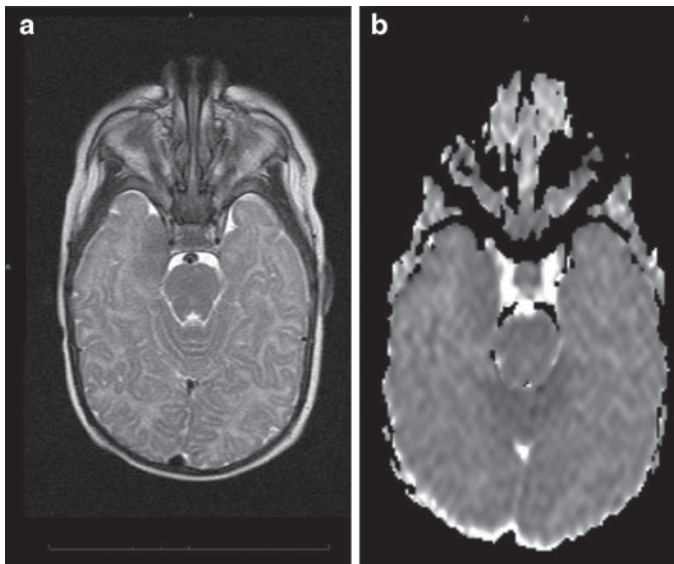
Fig. 18.4. (**a**) Axial T2-w image 15 months earlier from same patient as in Fig. 18.1 above showing lesion of right temporal lobe that is isointense to gray matter, and (**b**) ADC map showing no diffusion restriction.
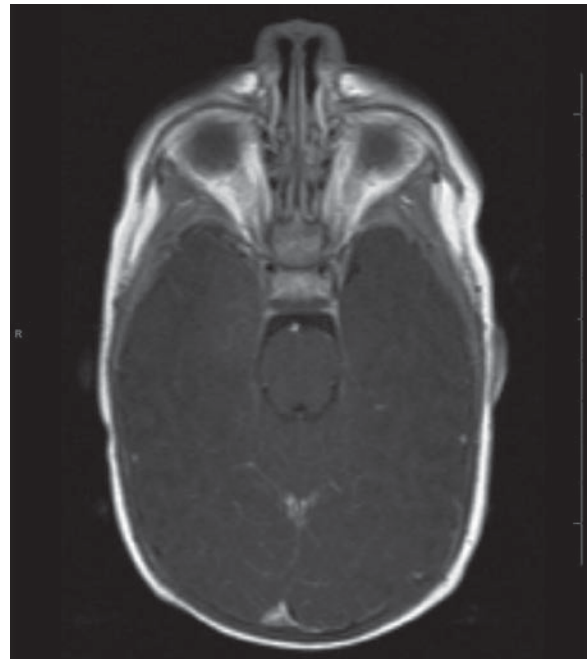
Fig. 18.5. Axial T1 post Gd 15 months earlier from same patient as in Fig. 18.1 above shows lesion of right temporal lobe with subtle/minimal enhancement.
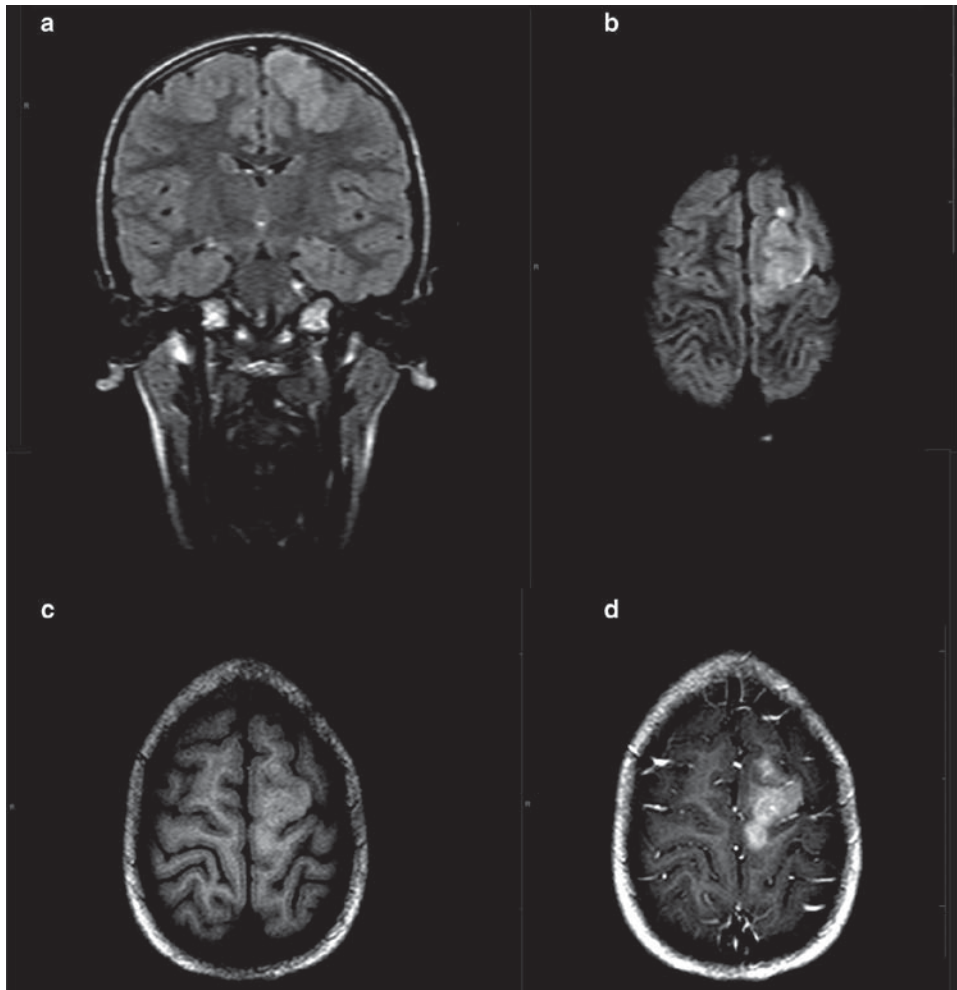
Fig. 18.6. (**a**) Coronal flair (**b**) axial flair (**c**) axial T1-w pre Gd, and (**d**) axial T1-w post Gd images showing T2-w hyperintense and contrast enhancing lesion of left frontal cortex with expansion of the involved cortex.
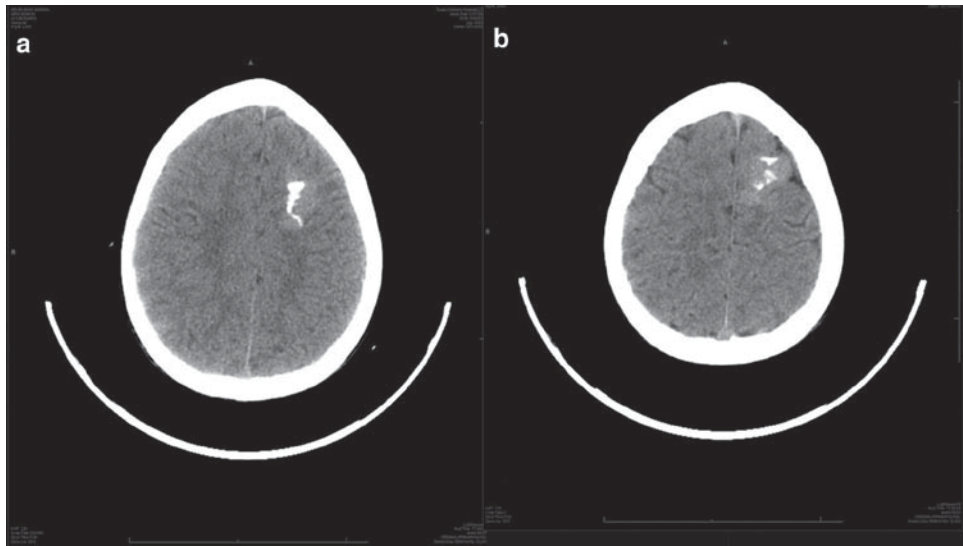
Fig. 18.7. Non contrast CT scan showing tumor calcification.
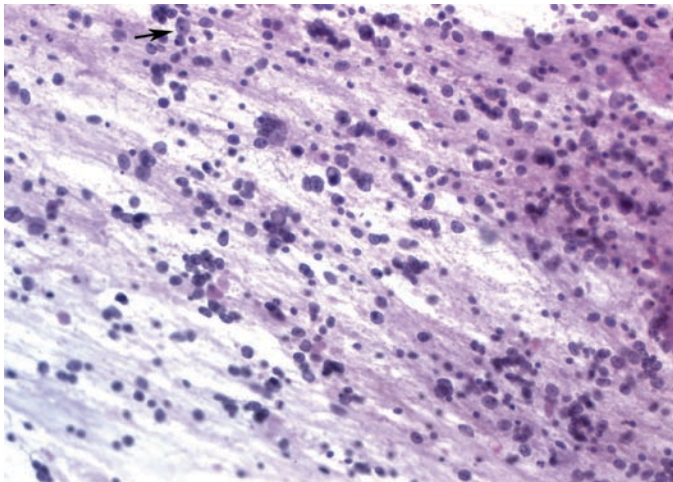
Fig. 18.8. Cellular smear preparation showing many "ganglioid" cells with vesicular nuclei and distinct nucleoli in a fibrillary astrocytic matrix.
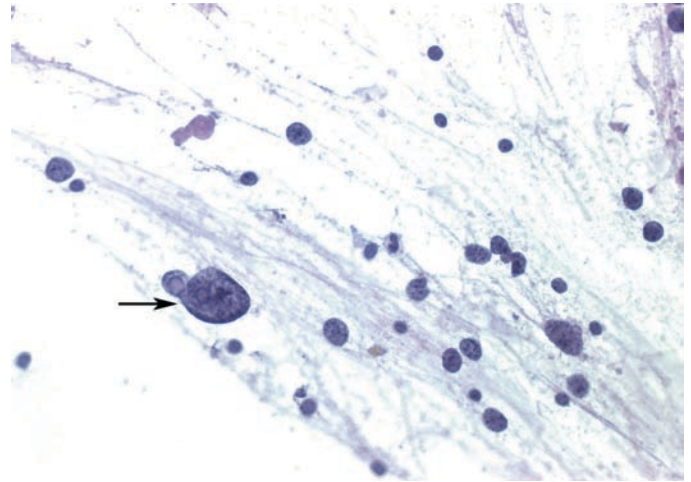
Fig 18.9. Higher magnification of same region as in Fig. 18.8.
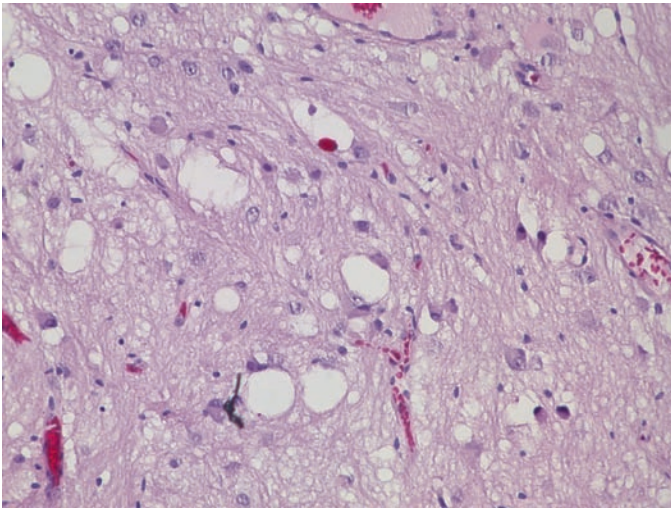
Fig. 18.10. Gangliocytoma with atypical ganglion cells in a microcystic and vacuolated stroma. Note the lack of a proliferating glial component.
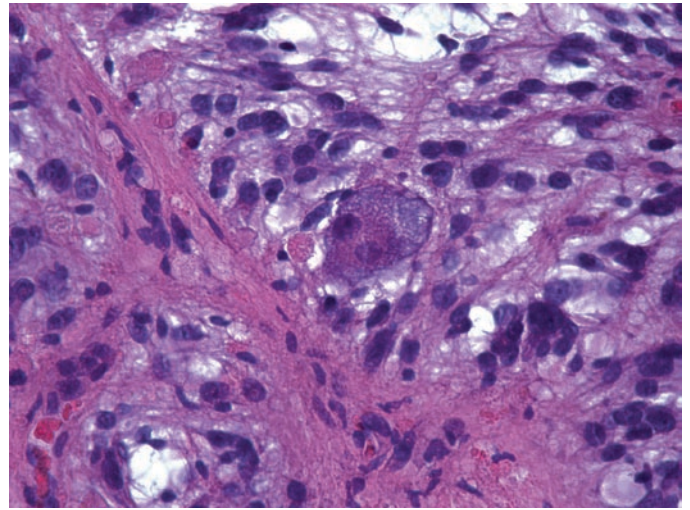
Fig. 18.12. Ganglioglioma showing a binucleated ganglion cell in a background of proliferating glial cells.
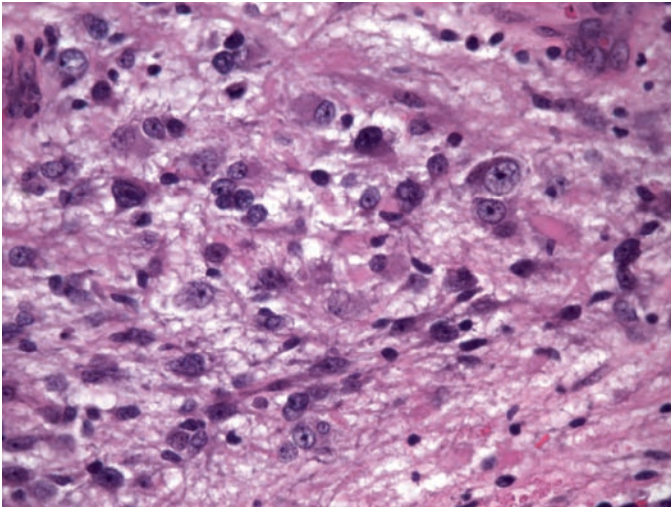
Fig. 18.11. Aggregates of tumor cells showing varying degrees of neuronal differentiation from "ganglioid" cells to well differentiated ganglion cells.
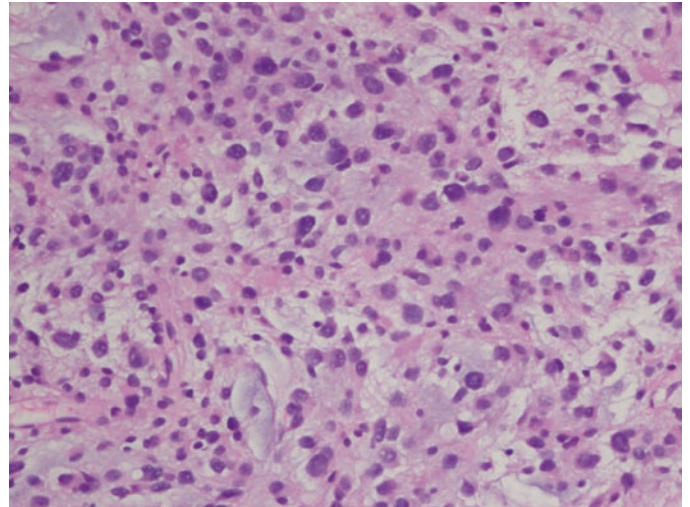
Fig. 18.13. Ganglioglioma with regional predominance of proliferating ganglioid and ganglion cells.
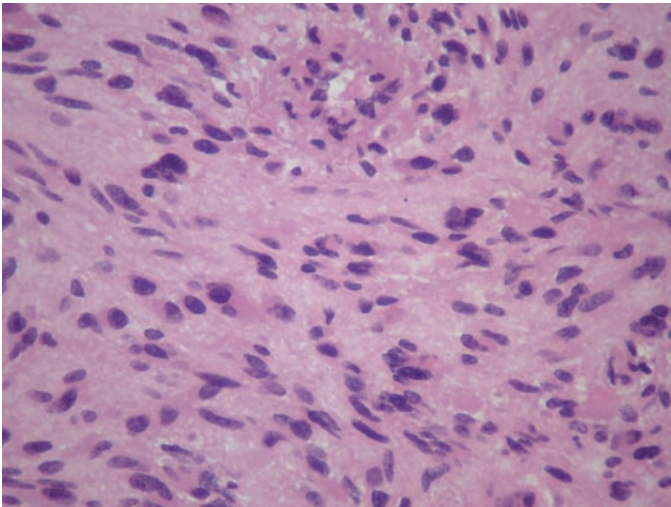
Fig. 18.14. Ganglioglioma with regional predominance of proliferating glial cells.
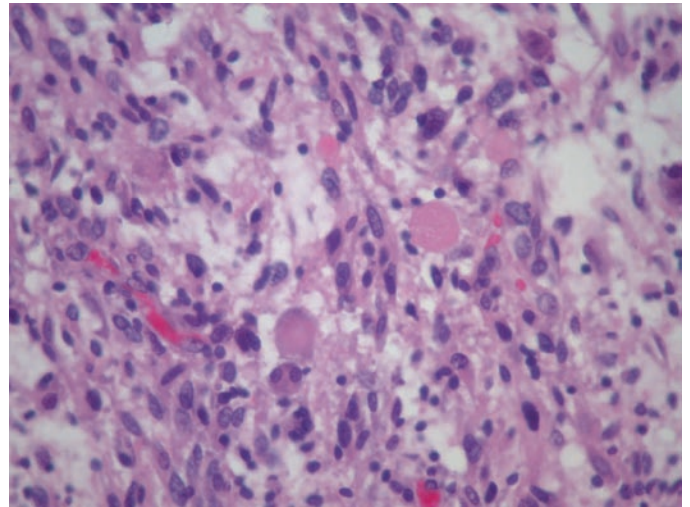
Fig. 18.16. Eosinophilic granular bodies (EGB) in a ganglioglioma with mixed population of proliferating ganglion and glial cells.
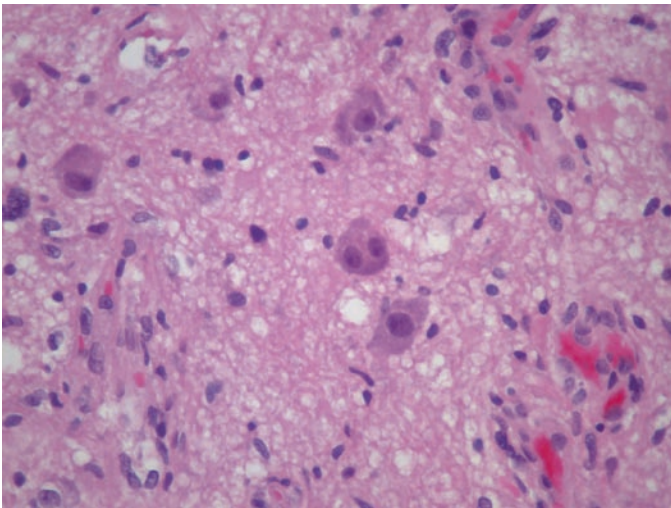
Fig. 18.15. Low cellularity glial component and proliferating ganglion cells in a ganglioglioma grade I.
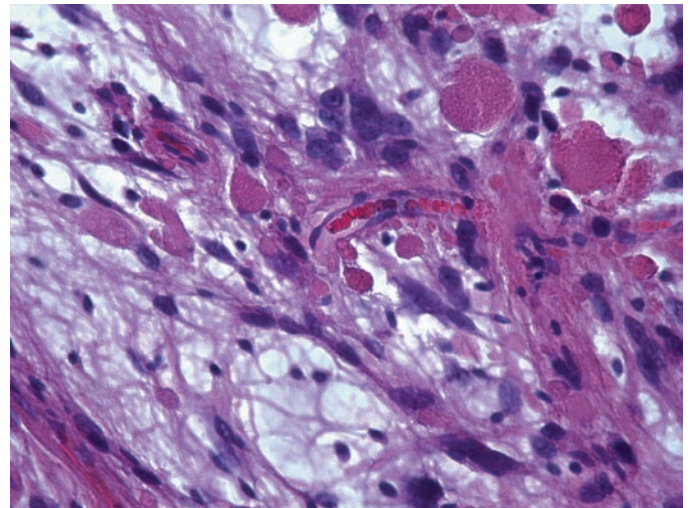
Fig. 18.17. Pilocytic glial component of a ganglioglioma showing abundant EGBs.
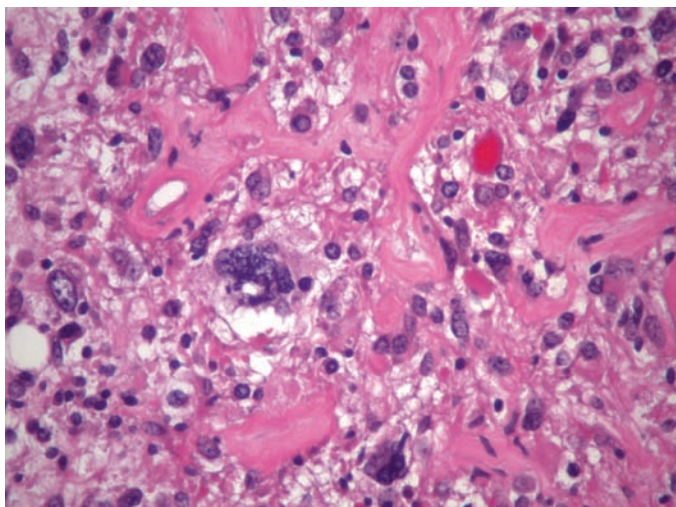
Fig. 18.18. Ganglioglioma showing increased cellularity and pleomorphism following progression to a WHO Grade III.
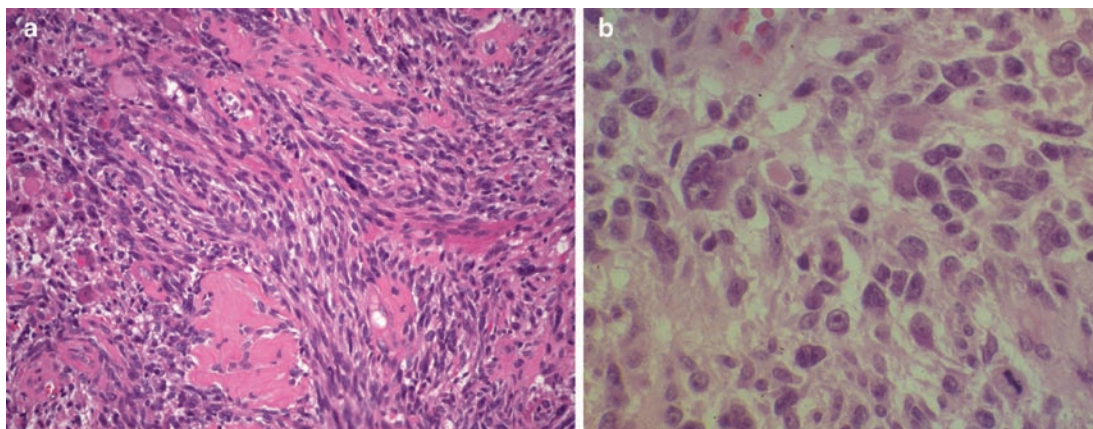
Fig. 18.19. Anaplastic ganglioglioma with (**a**) spindle cell appearance of the glial component, increased cellularity, and (**b**) increased mitotic activity.
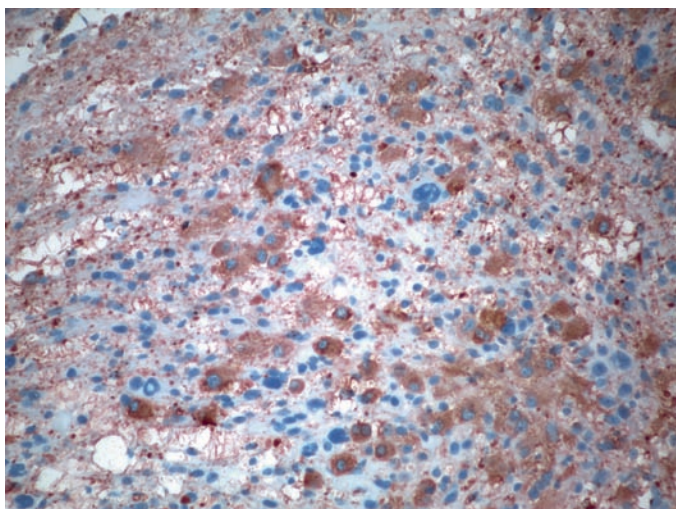
Fig. 18.20. Ganglion cell component of a ganglioglioma showing positivity for synaptophysin.
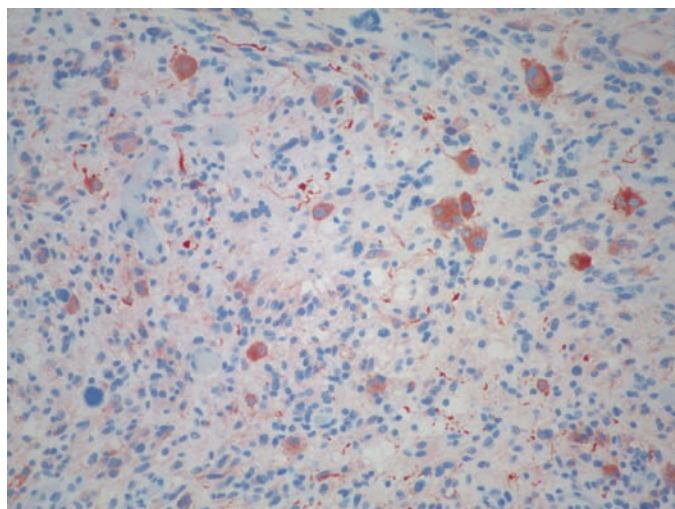
Fig. 18.21. MAP 2 positive ganglion cell component of a ganglioglioma.
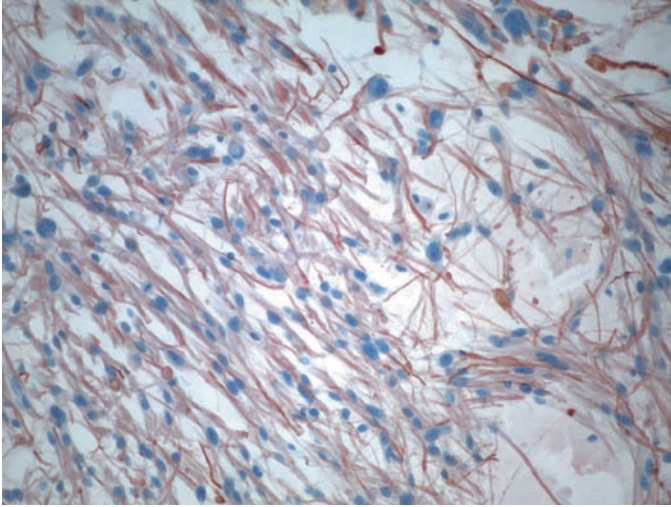
Fig. 18.22. GFAP positive astrocytic glial component of a ganglioglioma.
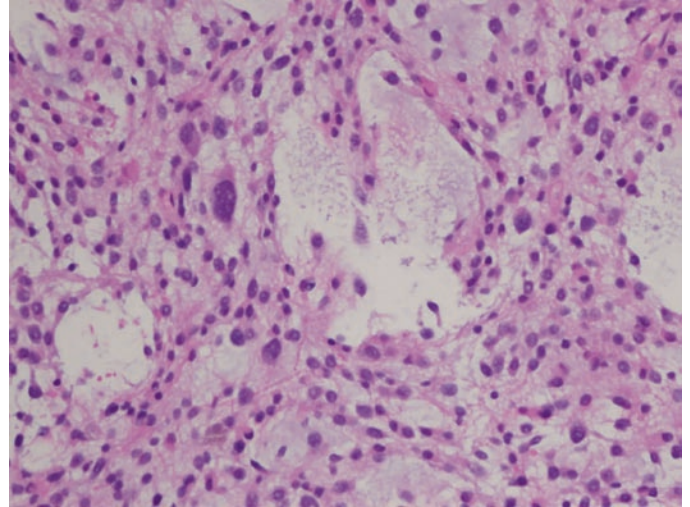
Fig. 18.23. Proliferating ganglioid cells in a background of microcysts and floating neurons in a transitional tumor with DNET-ganglioglioma phenotypic overlap.
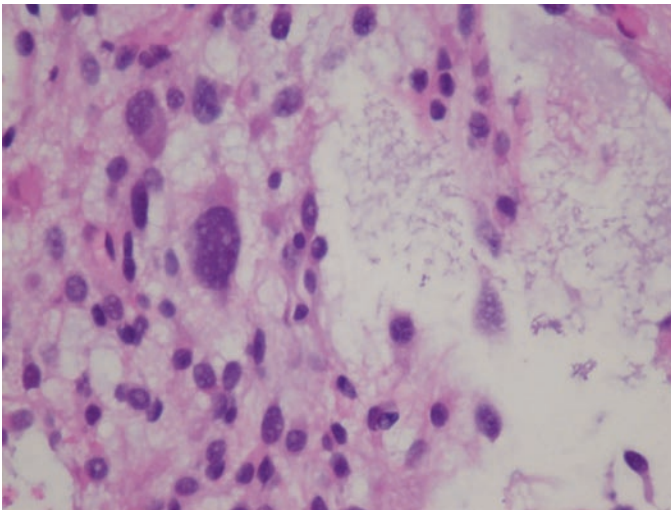
Fig. 18.24. High magnification from the same tumor as in Fig. 18.23 showing proliferating ganglioid cells in a background of microcysts and floating neurons in a transitional tumor with DNET-ganglioglioma phenotypic overlap.

Central Neurocytoma and Extraventricular Neurocytoma

Adekunle M. Adesina and Ronald A. Rauch

19.1 OVERVIEW

- A low-grade (WHO 2007, grade II) ventricular (central neurocytoma) or extraventricular tumor composed of a monomorphic population of uniform round neurocytic cells.
- More common in the lateral and third ventricles but may occur in the fourth ventricle and extraventricular sites including the cerebral hemispheric parenchyma and spinal cord.
- Occurs predominantly in young adults with a peak incidence in the third and fourth decades, and with a low incidence in the first and second decades.

19.2 CLINICAL FEATURES

- Localization in the region of the foramen of Monroe and third ventricle leads to raised intracranial pressure.
- Pressure effect on the hypothalamus may be associated with hormonal disturbance.

19.3 NEUROIMAGING

- Tumors are well-circumscribed and usually attached to the intraventricular septum.
- On CT, tumors are isodense or slightly hypodense and associated with contrast enhancement.
- Calcification and cystic degeneration may occur.
- MRI shows a well-circumscribed mass lesion isointense to gray matter on T1-w (Figs. 19.1b and 19.2a), and variably hyperintense on T2-w (Fig. 19.1a) and FLAIR imaging with variable mild to marked gadolinium enhancement (Figs. 19.2b and 19.3).

19.4 PATHOLOGY

- Macroscopically, these tumors are grey and friable; they may be calcified.
- The classic histologic features are those of a monomorphic population of round cells arranged in variable clusters with intervening fibrillary neuropil-like regions (Fig. 19.4a).
- Oligodendroglioma-like features with perinuclear halo and delicate arborizing capillary vasculature may be present (Fig. 19.4b).
- Areas showing perivascular pseudo-rosetting may cause confusion with an ependymoma.
- Homer Wright rosettes and ganglioid/ganglionic differentiation (Figs. 19.5 and 19.6) are rare and may be more common with the extraventricular variant.

- Mitoses are rare and tumors generally show a low proliferation index.
- Anaplastic transformation is rare, and when present, it is characterized by brisk mitosis and microvascular proliferation.

19.5 IMMUNOHISTOCHEMISTRY

- The hallmark of central neurocytoma is a diffuse neuropil and perivascular immunoreactivity for synaptophysin (Fig. 19.7). Diffuse nuclear positivity for Neu N and cytoplasmic positivity for MAP2 (Fig. 19.8) are common.
- Ganglioid cells when present are immunopositive for neurofilament protein and chromogrannin A, while the neurocytes are generally negative for these markers.
- Proliferation index (MIB-1 staining) is usually low and often less than 2%.
- "Atypical" neurocytoma with proliferation index greater than 2% is associated with shorter recurrence/progression-free survival.

19.6 ELECTRON MICROSCOPY

- Neurocytic differentiation is present and is characterized by the formation of intermingled cell processes containing microtubules, dense core neurosecretory granules, and clear vesicles.
- Synaptic junctions may be seen.
- Other organelles including the presence of mitochondria, rough endoplasmic reticulum, and prominent Golgi are nonspecific.

19.7 DIFFERENTIAL DIAGNOSIS

- Central neurocytoma shares the characteristic perinuclear halo and delicate vasculature with oligodendroglioma. Unlike central neurocytoma, oligodendrogliomas do not have the acellular, synaptophysin positive intervening neuropil.
- In addition, the uncommon tendency to form vague perivascular pseudorosettes and the presence of perinuclear halos raise a differential diagnosis of clear cell ependymoma. Ependymomas show dot-like EMA positivity, a feature not seen with neurocytomas and it allows a distinction between these two entities.

19.8 MOLECULAR GENETICS AND HISTOGENESIS

- No consistent genetic signature has been described. 1p36 and 19q13 deletions are uncommon in central neurocytomas.
- Rare examples of chromosomal gains involving chromosomes 7, 2p, 10q, 18q, and 13q have been reported.

- TP53 mutation is uncommon in central neurocytoma.
- Rare occurrence in association with von Hippel Lindau disease has been described.
- Cell of origin is unknown but a putative origin from a neuroglial precursor cell from the subependymal region or from the circumventricular organ has been suggested.

19.9 PROGNOSIS

- Generally runs a benign course following gross total resection whereas incomplete resection is often associated with local recurrence.
- Anaplastic features including proliferation index greater than 2% are associated with poorer prognosis and shorter recurrence free intervals.
- Infiltration of periventricular tissue is likewise a poor prognostic feature.

SUGGESTED READING

Yang GF, Wu SY, Zhang LJ, Lu GM, Tian W, Shah K (2009) Imaging findings of extraventricular neurocytoma: Report of 3 cases and review of the literature. AJNR Am J Neuroradiol 30(3):581–585

Kocaoglu M, Ors F, Bulakbasi N, Onguru O, Ulutin C, Secer HI (2008) Central neurocytoma: Proton MR spectroscopy and diffusion weighted MR imaging findings. Magn Reson Imaging 27(3):434–440

Kerkovský M, Zitterbart K, Svoboda K, Hrivnacká J, Skotáková J, Sprláková-Puková A, Mechl M (2008) Central neurocytoma: The neuroradiological perspective. Childs Nerv Syst 24(11):1361–1369

Kurose A, Arai H, Beppu T, Wada T, Sato Y, Kubo Y, Jin R, Ogawa A, Sawai T (2007) Ganglioneurocytoma: Distinctive variant of central neurocytoma. Pathol Int 57(12):799–803

Leenstra JL, Rodriguez FJ, Frechette CM, Giannini C, Stafford SL, Pollock BE, Schild SE, Scheithauer BW, Jenkins RB, Buckner JC, Brown PD (2007) Central neurocytoma: Management recommendations based on a 35-year experience. Int J Radiat Oncol Biol Phys 67(4):1145–1154

Zhang D, Wen L, Henning TD, Feng XY, Zhang YL, Zou LG, Zhang ZG (2006) Central neurocytoma: Clinical, pathological and neuroradiological findings. Clin Radiol 61(4):348–357

Favereaux A, Vital A, Loiseau H, Dousset V, Caille J, Petry K (2000) Histopathological variants of central neurocytoma: Report of 10 cases. Ann Pathol 20(6):558–563

Tong CY, Ng HK, Pang JC, Hu J, Hui AB, Poon WS (2000) Central neurocytomas are genetically distinct from oligodendrogliomas and neuroblastomas. Histopathology 37(2):160–165

Ishiuchi S, Tamura M (1997) Central neurocytoma: An immunohistochemical, ultrastructural and cell culture study. Acta Neuropathol 94(5):425–435

Söylemezoglu F, Scheithauer BW, Esteve J, Kleihues P (1997) Atypical central neurocytoma. J Neuropathol Exp Neurol 56(5):551–556

Schild SE, Scheithauer BW, Haddock MG, Schiff D, Burger PC, Wong WW, Lyons MK (1997) Central neurocytomas. Cancer 79(4):790–795

Giangaspero F, Cenacchi G, Losi L, Cerasoli S, Bisceglia M, Burger PC (1997) Extraventricular neoplasms with neurocytoma features. A clinicopathological study of 11 cases. Am J Surg Pathol 21(2):206–212

Hassoun J, Söylemezoglu F, Gambarelli D, Figarella-Branger D, von Ammon K, Kleihues P (1993) Central neurocytoma: A synopsis of clinical and histological features. Brain Pathol 3(3):297–306 Review

Townsend JJ, Seaman JP (1986) Central neurocytoma-a rare benign intraventricular tumor. Acta Neuropathol 71(1–2):167–170
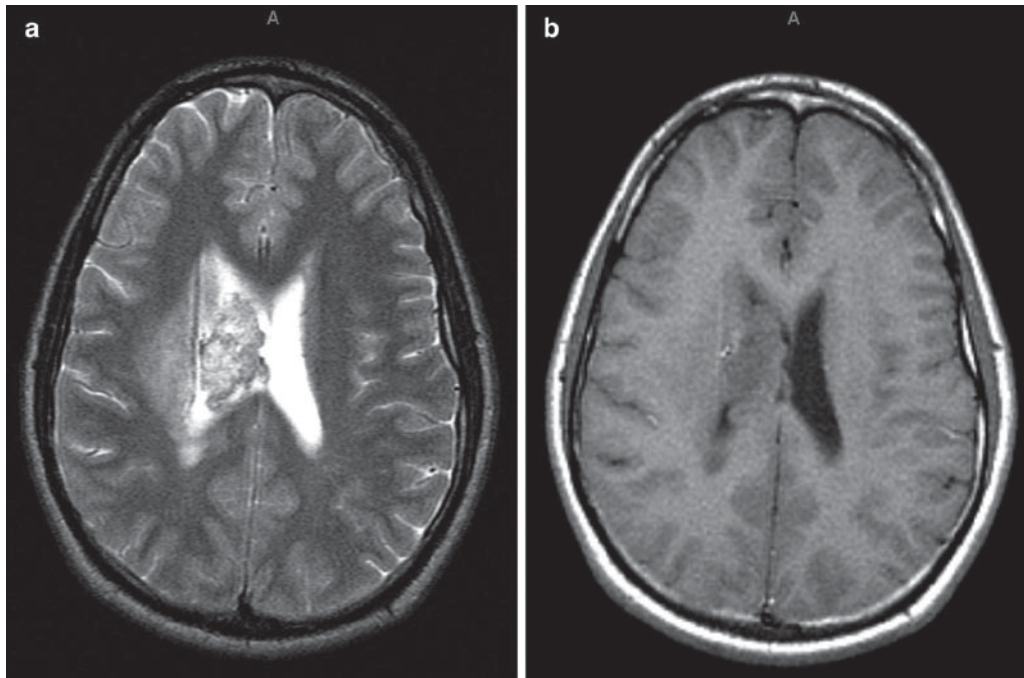
Fig. 19.1. Intraventricular central neurocytoma illustrated in axial (**a**) T2-w and (**b**) T1-w pre-contrast images showing hyperintensity on T2 images and isointensity on T1 images, respectively.
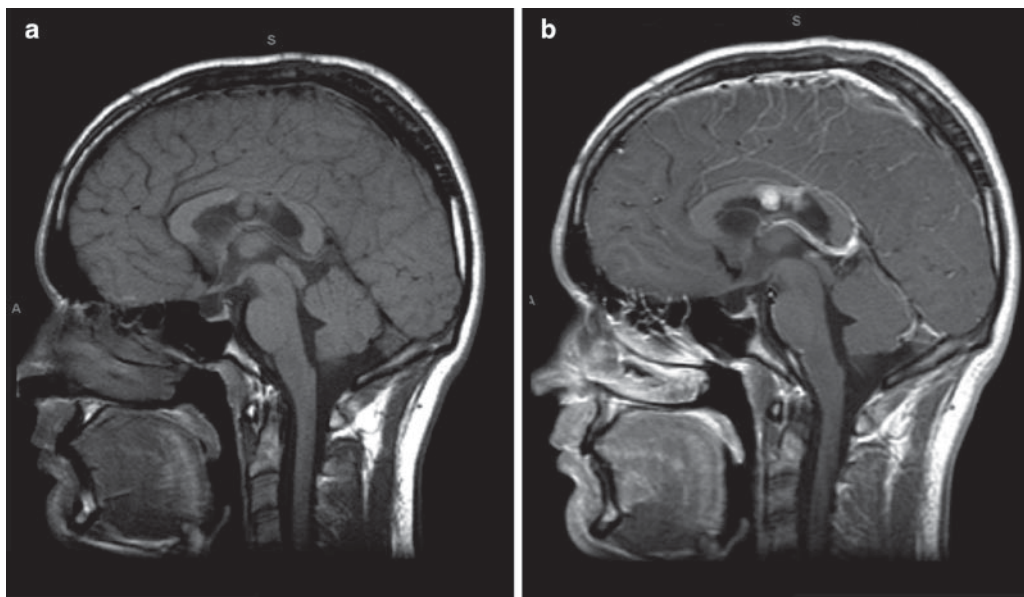
Fig. 19.2. Another example (sagittal view) of central neurocytoma showing isointensity on (**a**) precontrast T1-w imaging and homogenous enhancement (**b**) on T1-w post-contrast imaging.
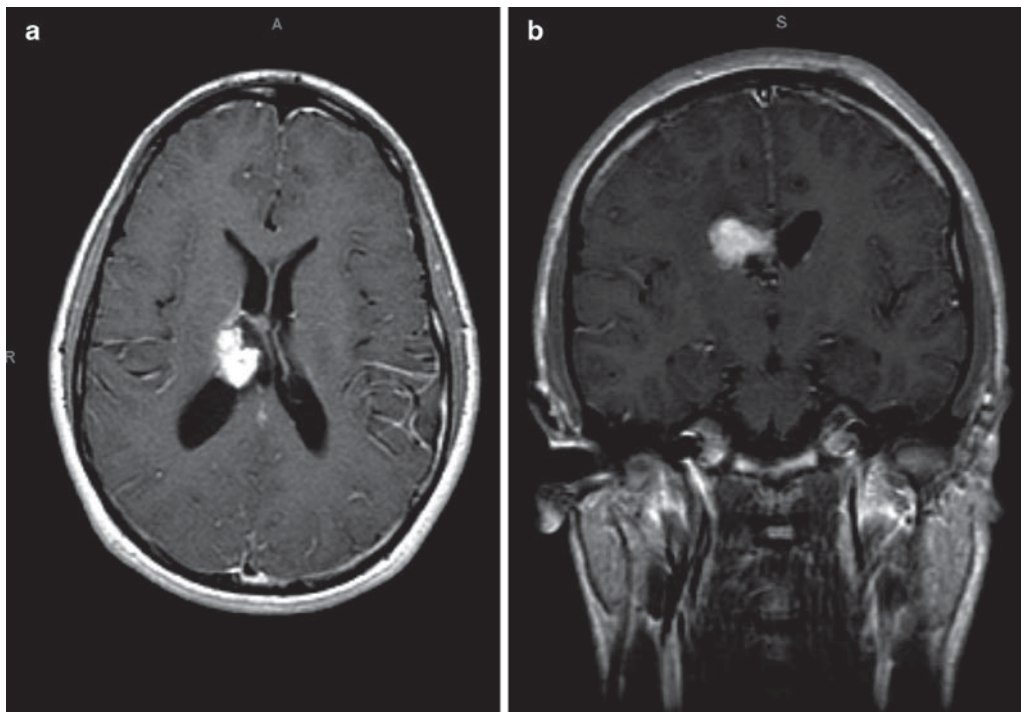
Fig. 19.3. (**a**) Axial T1-w and (**b**) coronal T1-w post-contrast images on the same patient in Fig. 19.2 confirming homogenous tumor enhancement.
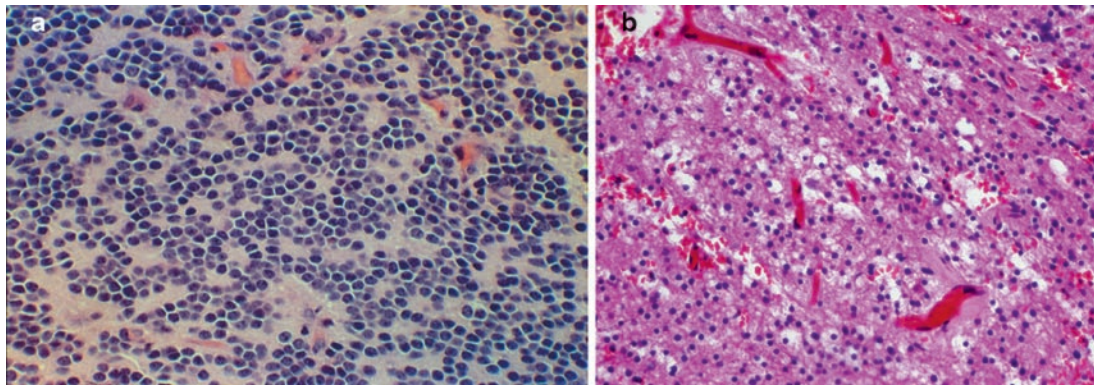
Fig. 19.4. (**a**) Histology of central neurocytoma showing a monomorphic population of round cells arranged in irregular clusters with intervening acellular neuropil islands; (**b**) oligo-like histologic features with perinuclear halo and delicate vasculature may be seen.
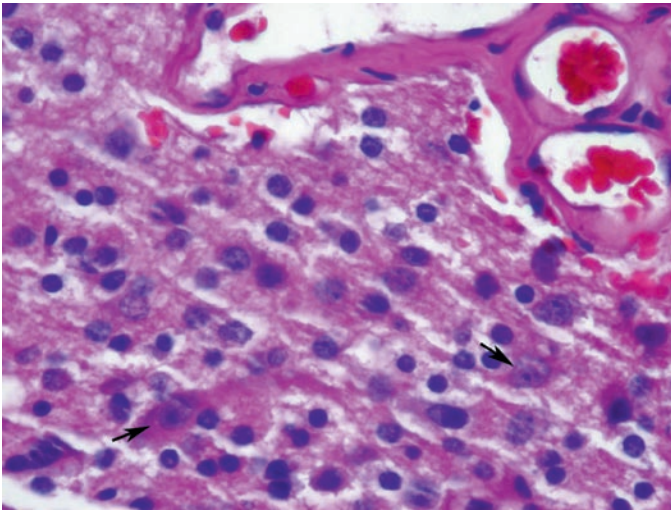
Fig. 19.5. Regions of ganglioid cells with vesicular nuclei and distinct nucleoli are illustrated (*arrows*).
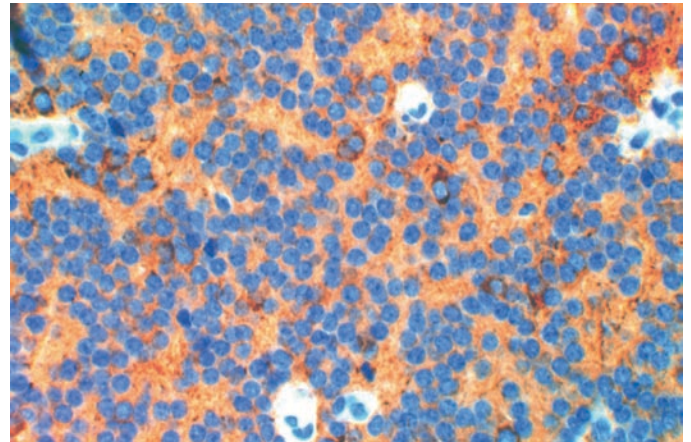
Fig. 19.7. Diffuse perikaryal immunopositivity for synaptophysin in central neurocytoma. Note the presence of and positivity in acellular islands which is a major distinguishing feature from an oligodendroglioma.
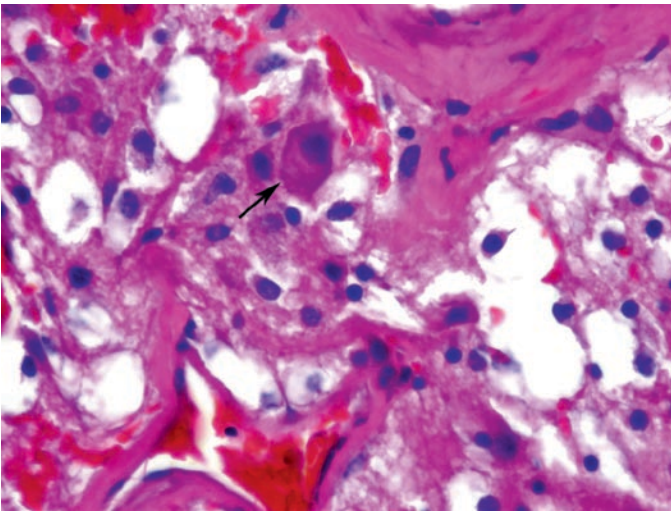
Fig. 19.6. Mature ganglionic differentiation (*arrow*) is seen focally in this example of central neurocytoma.
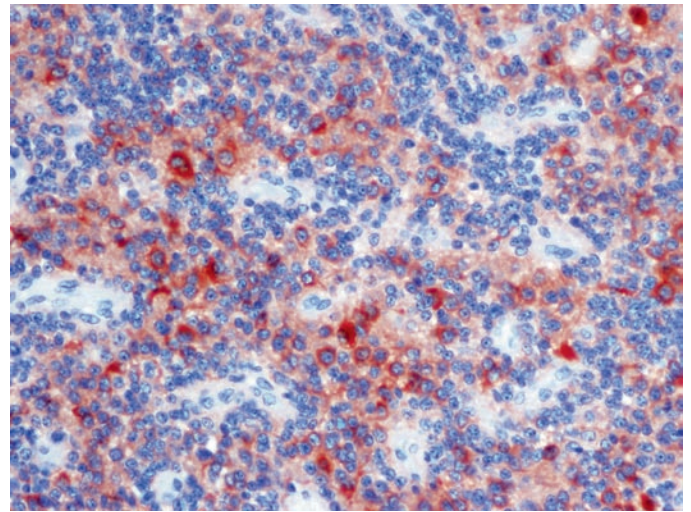
Fig. 19.8. Immunostaining for MAP2 with regional positivity in central neurocytoma.

Papillary Glioneuronal Tumor

M. Rivera-Zengotita, A. Illner and Adekunle M. Adesina

Keywords Mixed glioneuronal tumors; Papillary glioneuronal tumor; Pseudopapillary ganglioglioneurocytoma; Pseudopapillary neurocytoma with glial differentiation

20.1 OVERVIEW

- A benign (WHO grade I), relatively circumscribed, biphasic cerebral neoplasm occurring predominantly in the temporal lobe and most commonly affecting young adults.
- No population-based epidemiologic data are available to date.
- Papillary glioneuronal tumor (PGNT) was initially described as "pseudopapillary ganglioglioneurocytoma" or "pseudoapillary neurocytoma with glial differentiation."
  - Established as a distinct clinicopathologic entity in 1998 by Komori et al.
  - Regarded as a variant of ganglioglioma in the 2000 WHO classification of central nervous system tumors.
  - Recently added as a new entity in the 2007 WHO classification.

20.2 CLINICAL FEATURES

- PGNT occurs over a wide age range (4–75 years) with a mean age at presentation of 27 years. It is more prevalent in the second and third decades of life.
- No gender predilection has been reported.
- The most common clinical manifestations include headache and seizures.
- Patients may also present with nausea, vertigo, visual and gait disturbances, focal sensorimotor deficits, syncope, memory loss, and mood changes.

20.3 NEUROIMAGING

- Presents as a well-defined, circumscribed lesion centered in subcortical or periventricular cerebral white matter. Small lesions lack peritumoral edema. Mass effect and mild peritumoral edema are present in large lesions.
  - Occurs in all lobes with the temporal being the most common lobe involved.
  - MRI: Typically heterogeneous on T2-w imaging although small lesions may be homogeneous and marked hyperintensity may be present in cyst-like regions (Figs. 20.1 and 20.2).
  - Usually hypointense on T1-w imaging (Fig. 20.3) unless intratumoral hemorrhage is present.
  - May show post-contrast enhancement (Fig. 20.4) with the enhancing component iso- or hyperintense to cortex on T2-w imaging.

- Enhancement may be peripheral, solid, or peripheral with mural nodule.
- Diffusion weighted imaging usually shows no restriction of diffusion (Fig. 20.5).
- CT: Calcification and intratumoral hemorrhage are uncommon.

20.4 PATHOLOGY

- Smear preparations reveal a mixture of cells (Figs 20.6–20.8) including ganglion cells with large eccentric nuclei, prominent nucleoli, delicate nuclear membranes and Nissl substance in the cytoplasm. Also intermediate cells with less prominent nucleoli and relatively scant cytoplasm are seen. Cells with dense nuclei, scant cytoplasm, and occasional processes represent perivascular astrocytes.
- Two distinct histologic components are identified, one glial and the other neuronal.
  - The glial component consists of pseudopapillary structures with hyalinized blood vessels surrounded by a single or pseudostratified layer of cuboidal glial cells (Figs. 20.9 and 20.10). These cells have rounded nuclei, moderately dense chromatin, and scant eosinophilic cytoplasm and do not elaborate perivascular cytoplasmic processes. Mitotic activity and cellular atypia are absent in this component.
  - The neuronal component consists of interpapillary sheets or focal collections of neurocytes, ganglion cells, and intermediate "ganglioid cells" in a fibrillary, neuropil-like matrix.
- Neurocytic cells have dark, round, uniform nuclei and scant cytoplasm, and sometimes oligo-like halo (Fig. 20.11) while the ganglion cells feature large, vesicular nuclei, prominent nucleoli, and abundant cytoplasm with well developed Nissl substance.
  - The intermediate-sized "ganglioid cells" feature less abundant cytoplasm and smaller nucleoli.
  - Occasional pleomorphic and binucleated ganglion cells are identified.
- Minigemistocytes with eccentrically placed nuclei and eosinophilic hyaline cytoplasm may be found in the interpapillary regions or nestled among neuronal cell types (Figs. 20.6 and 20.10).
- A narrow zone of tumor infiltration or a discrete pushing border may be seen with the adjacent neural parenchyma. In this region, prominent gliosis, Rosenthal fibers, eosinophilic granular bodies, hemosiderin deposition, foamy cell infiltration, and dystrophic calcifications may be identified.
- Mitotic activity is usually inconspicuous.
- Necrosis and microvascular proliferation are exceptional when present.

20.5 IMMUNOHISTOCHEMISTRY

- The small cuboidal glial cells surrounding the hyalinized vascular pseudopapillae are positive for GFAP (Fig. 20.12) and S-100.
- Neuronal cells of all sizes are immunopositive for synaptophysin (Fig. 20.13), NSE, and class III β-tubulin (MAP-2) (Fig. 20.14).
- Most of the neuronal cells are also positive for NeuN while neurofilament protein (NFP) immunopositivity is confined to ganglion cells and intermediate "ganglioid cells."
- Chromogranin A expression has not been observed.
- Minigemistocytes show intense GFAP immunoreactivity.
- Tanaka et al described a subpopulation of cells that fail to label with GFAP and neuronal markers but express the Olig2 transcription factor. These cells are mainly found in the interpapillary areas surrounding GFAP positive perivascular elements. They also found that minigemistocytes are in close association with these Olig2 positive cells and may be derived from them.
- MIB-1 labeling indices are low and in the range of 1–2%.

20.6 ELECTRON MICROSCOPY

- The perivascular glial cells show cytoplasmic bundles of intermediate filaments and form juxtavascular basal lamina.
- The neuronal cells exhibit cytoplasmic extensions filled with aligned microtubules, dense-core granules, clear vesicles, and synaptic contacts of varying organization.
- A third cell component of poorly differentiated cells has been described at the ultrastructural level. These cells contain mitochondria, ribosomes, occasional dense bodies, intermediate filaments, and microtubules but no definitive dense core granules. They are thought to represent glioneuronal progenitor cells.
- Hybrid glioneuronal cells have not been described.

20.7 MOLECULAR PATHOLOGY

- PGNT has been reported in patients with cleft lip and orbital schwannoma but association with familial syndromes has not been established.
- Several cases have been studied for 1p status by FISH and have been found to be intact.
- Faria et al reported a case of PGNT with gains and alterations involving chromosome 7p22. Using comparative genomic hybridization, they also observed high-level amplification at 7p14~q12.

20.8 DIFFERENTIAL DIAGNOSIS

- The pseudopapillae with surrounding astrocytic cells may resemble the perivascular pseudorosettes of ependymoma. However, cellular processes radiating to the vessel wall are not seen in PGNT. In addition, PGNT does not show ultrastructural evidence of ependymal differentiation.
- The presence of neurocytic, ganglionic, and glial components may raise the possibility of ganglioglioneurocytoma as a differential diagnosis.
  - The presence of pseudopapillary glio-vascular structures and the broad spectrum of neuronal differentiation in PGNT help distinguish between the two entities.
- PGNT should be distinguished from dysembryoplastic neuroepithelial tumor (DNET) which also presents at a young age with seizures.
  - Histologically, DNET is characterized by the specific glioneuronal element, microcysts with floating neurons and cortical dysplasia in the adjacent cortex. None of these features are seen in PGNT.

20.9 PROGNOSIS

- In general, PGNT shows a favorable clinical outcome.
- Gross total resection without adjuvant therapy results in recurrence-free, long term survival in the majority of cases.
- One case of atypical papillary glioneuronal tumor has been reported as showing mitotic activity and MIB-1 labeling index of 15%. The patient remained symptom-free without tumor recurrence 5 years after radical resection and radiotherapy.
- Very rare examples of tumor recurrence or progression have also been reported.

SUGGESTED READING

Faria C, Miguéns J, Antunes JL, Barroso C, Pimentel J, Martins Mdo C, Moura-Nunes V, Roque L (2008) Genetic alterations in a papillary glioneuronal tumor. J Neurosurg Pediatr 1(1):99–102

Hainfellner JA, Scheithauer BW, Giangaspero F, Rosenblum MK (2007) Rosette-forming glioneuronal tumour of the fourth ventricle. In: Louis DN, Ohgaki H, Wiestler OD, Cavenee WK (eds) WHO Classification of tumours of the central nervous system, 4th edn. International Agency for Research on Cancer, Lyon, pp 113–114

Louis DN, Ohgaki H, Wiestler OD, Cavenee WK, Burger PC, Jouvet A, Scheithauer BW, Kleihues P (2007) The 2007 WHO classification of tumours of the central nervous system. Acta Neuropathol 114:97–109

Komori T, Scheithauer BW, Anthony DC, Rosenblum MK, McLendon RE, Scott RM, Okazaki H, Kobayashi M (1998) Papillary glioneuronal tumor: a new variant of mixed neuronal-glial neoplasm. Am J Surg Pathol 22(10):1171–1183

Rosenblum MK (2007) The 2007 WHO classification of nervous system tumors: newly recognized members of the mixed glioneuronal group. Brain Pathol 17(3):308–313

Tanaka Y, Yokoo H, Komori T, Makita Y, Ishizawa T, Hirose T, Ebato M, Shibahara J, Tsuksyama C, Shibuya M, Nakazato Y (2005) A distinct pattern of Olig2-positive cellular distribution in papillary glioneuronal tumors: a manifestation of the oligodendroglial phenotype? Acta Neuropathol 110:39–47

Vaquero J, Coca S (2007) Atypical papillary glioneuronal tumor. J Neurooncol 83(3):319–323
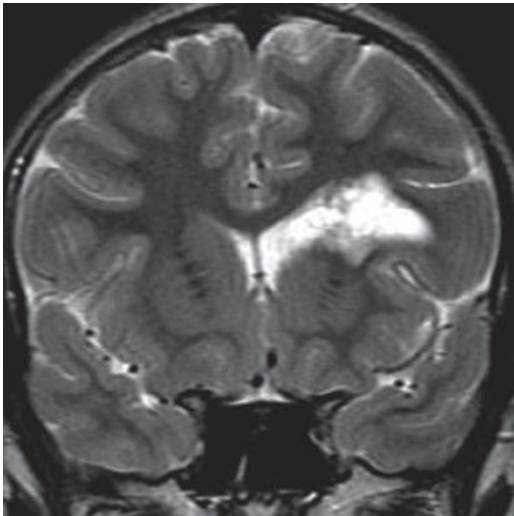
Fig. 20.1. Coronal T2-w MRI showing a heterogeneous tumor in the left periventricular white matter with markedly hyperintense central cyst-like component and less intense peripheral, nodular component.
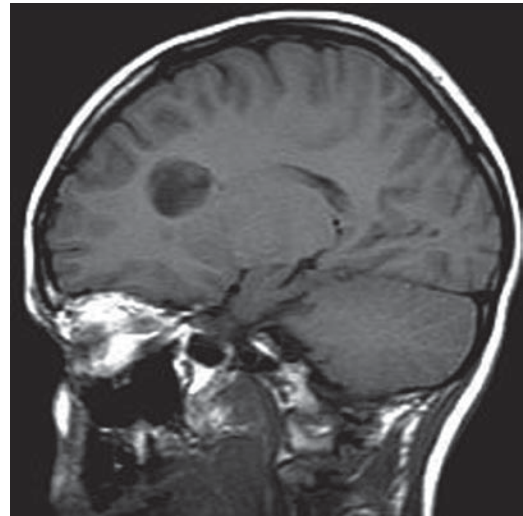
Fig. 20.3. Sagittal T1-w MRI showing a well-circumscribed tumor with marked hypointensity in the central, cyst-like component.
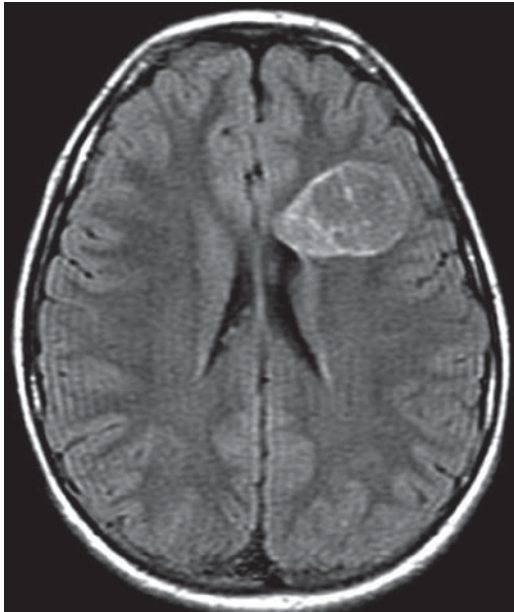
Fig. 20.2. Axial FLAIR MRI showing attenuation of signal in the central, cyst-like component. Note lack of peritumoral edema.
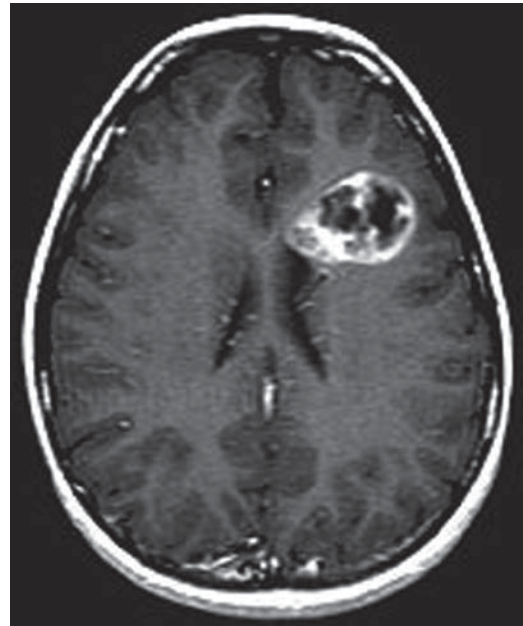
Fig. 20.4. Axial T1-w post contrast images showing tumor demonstrating irregular, peripheral nodular enhancement. The central, cyst-like component does not enhance.
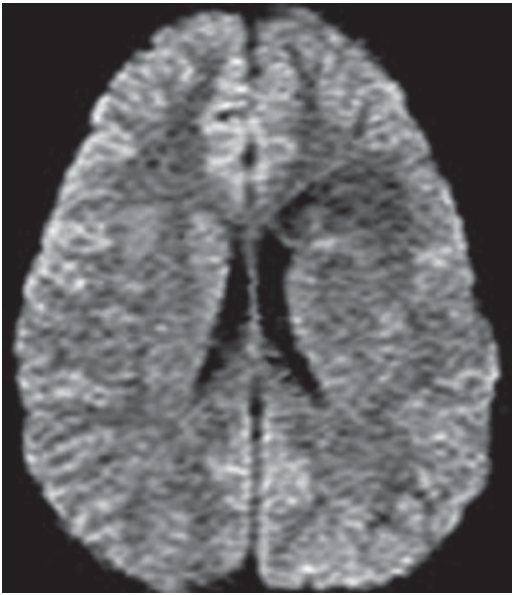
Fig. 20.5. Axial DWI images showing no diffusion restriction within the tumor.
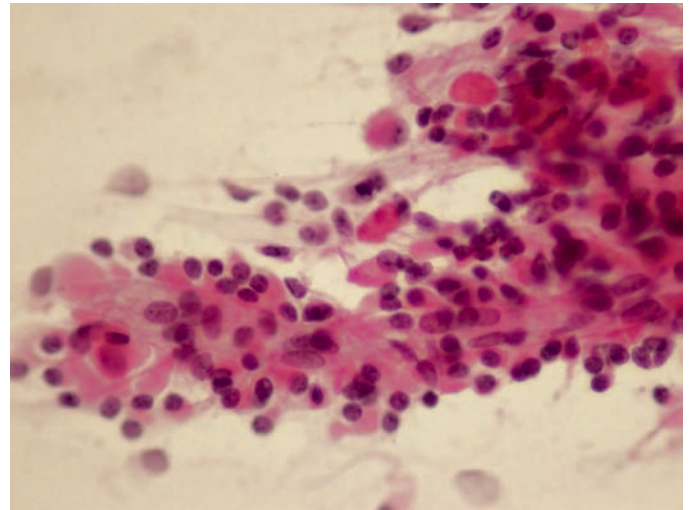
Fig. 20.6. Intraoperative cytologic preparation showing pseudopapillary architecture and fibrillary background. There is a mixed cell population with some of the cells having eosinophilic cytoplasm and eccentric nuclei.
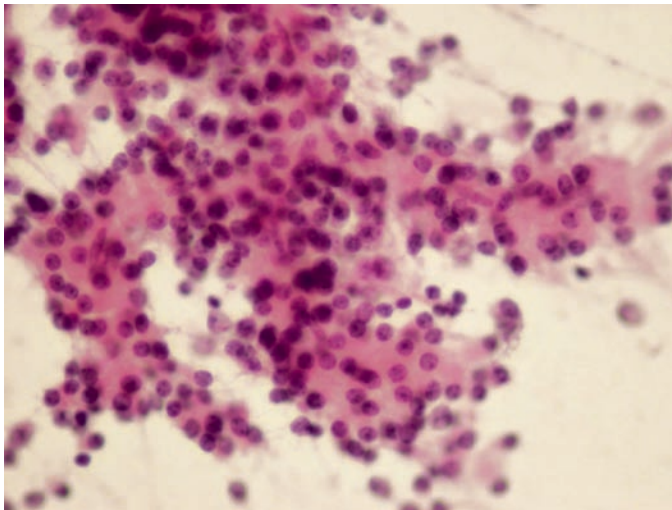
Fig. 20.7. Intraoperative cytologic preparation showing pseudopapillary architecture and fibrillary background. There is a mixed cell population with some of the cells having eosinophilic cytoplasm and eccentric nuclei.
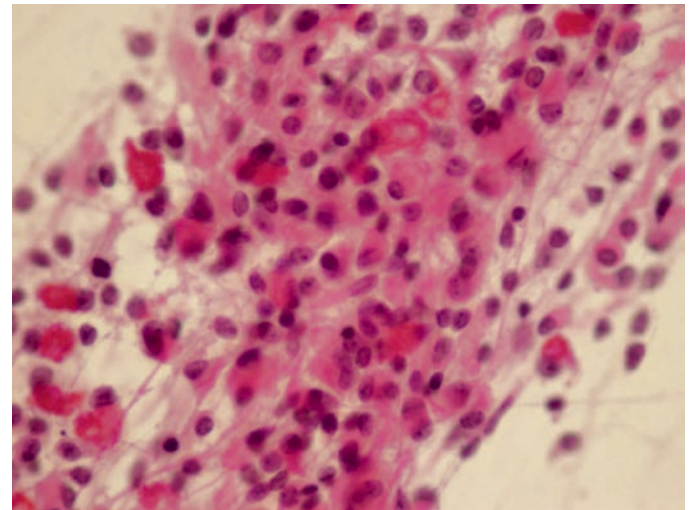
Fig. 20.8. Intraoperative cytologic preparation showing pseudopapillary architecture and fibrillary background. There is a mixed cell population with some of the cells having eosinophilic cytoplasm and eccentric nuclei.
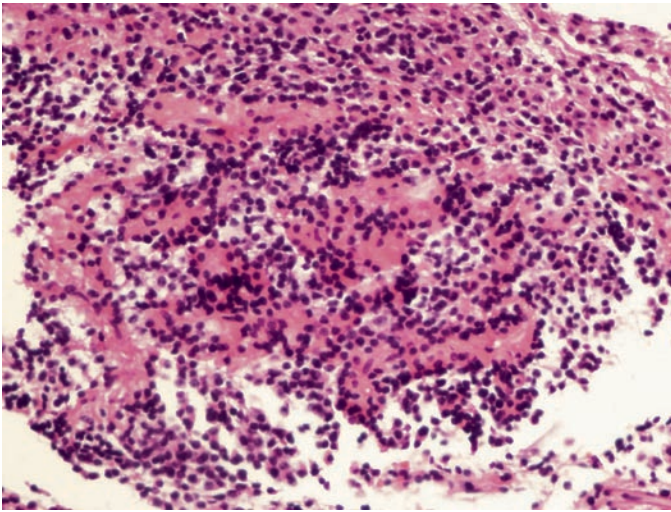
Fig. 20.9. Characteristic pseudopapillary pattern in PGNT.
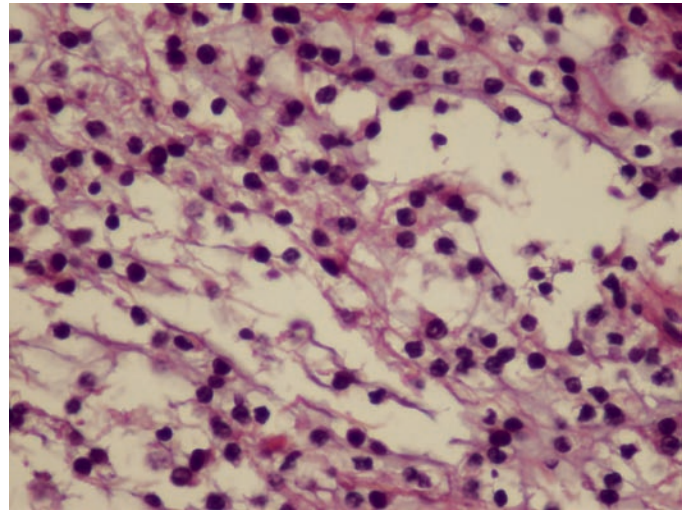
Fig. 20.11. Mixed glioneuronal populations of cells with clear cytoplasm and halo-like appearance may be seen.
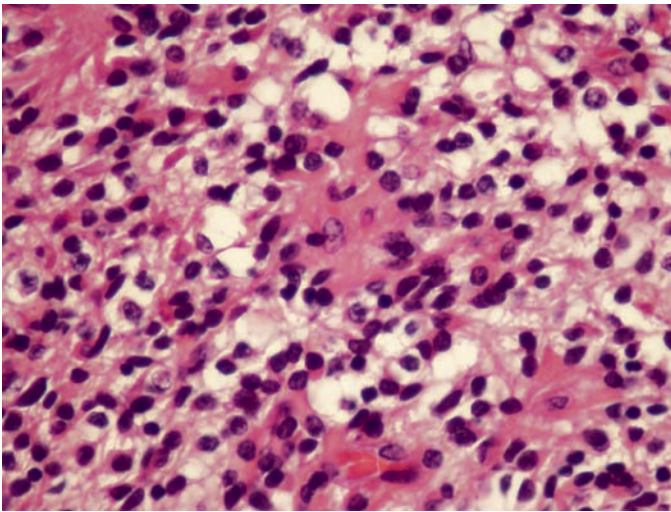
Fig. 20.10. Mixed glioneuronal populations of cells with sometimes variable histology as seen here characterize this tumor.
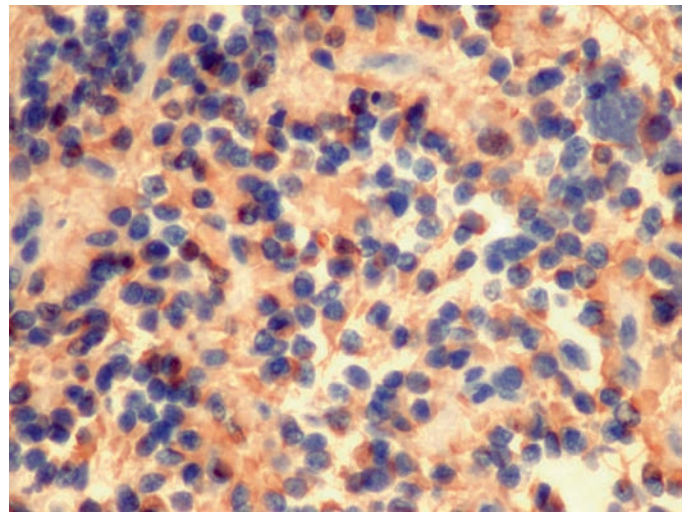
Fig. 20.12. A large subpopulation of tumor cells are GFAP positive.
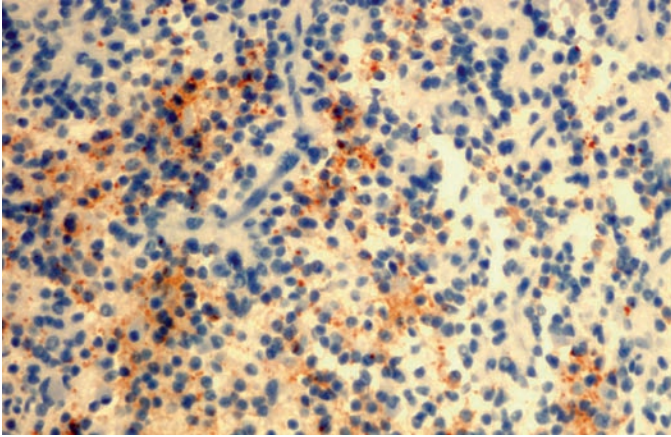
Fig. 20.13. Synaptophysin positivity is granular but patchy.
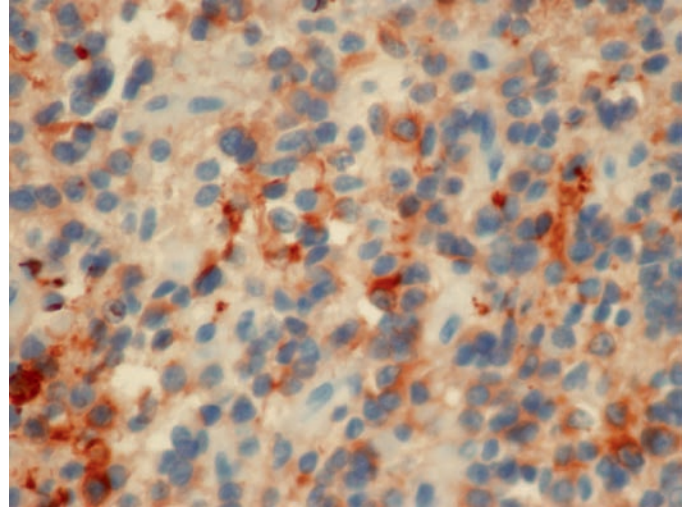
Fig. 20.14. A diffuse positivity for MAP2 is observed in this tumor.

Rosette-Forming Glioneuronal Tumor of the Fourth Ventricle

M. Rivera-Zengotita and Adekunle M. Adesina

Keywords Mixed glioneuronal tumors; Cerebellar dysembryoplastic neuroepithelial tumor; Cerebellar neurocytoma; Rosette-forming tumor of fourth ventricle

21.1 OVERVIEW

- A rare, slow growing biphenotypic tumor arising in the region of the fourth ventricle.
- It shows a benign histology and favorable postoperative course corresponding to WHO 2007 grade I.
- Rosette-forming glioneuronal tumor (RGNT) of the fourth ventricle affects young adults most commonly. Population-based incidence rates are not yet available.
- RGNT was first recognized and characterized as a distinct disease in a report of 11 cases by Komori et al. in 2002 and recently added as a new entity in the 2007 WHO classification of tumors of the central nervous system.
  - Previous reports of cerebellar dysembryoplastic neuroepithelial tumors (DNET) may represent the same entity.

21.2 CLINICAL FEATURES

- RGNT affects predominantly young adults (mean age 33 years).
- The age range of reported cases is between 12 and 59 years with a slight female predominance.
- The most common signs and symptoms include ataxia and headache secondary to obstructive hydrocephalus.
- Patients have also presented with visual disturbances, vertigo, neck pain, and rigidity.

21.3 NEUROIMAGING

- RGNTs arise in the posterior fossa, often in the midline and are centered in the fourth ventricle.
  - It may extend to the cerebellar vermis, brainstem, pineal gland, thalamus, and cerebral aqueduct.
- MRI reveals a relatively circumscribed solid or multicystic tumor that is hyperintense on T2-weighted images and hypointense on T1.
- They show focal or multifocal contrast enhancement with a nodular, linear, ring, or spot-like pattern.
- Peritumoral edema is minimal.
- Multicentric cases have been described.

21.4 PATHOLOGY

- *Intraoperative smear preparations* usually demonstrate the biphenotypic nature of the tumor, including neurocytic cells with round uniform nuclei, granular chromatin, inconspicuous nucleoli and scant cytoplasm, and a glial piloid component.
  - Rosettes and ganglion cells are not usually identified on smear preparations.
- Two main distinct histological components are seen; neurocytic and glial.
- The neurocytic component consists of a uniform population of small cells with round nuclei, finely granular chromatin, inconspicuous nucleoli, and scant cytoplasm with delicate cytoplasmic processes (Figs. 21.1 and 21.2).
  - These cells form neurocytic and/or perivascular pseudorosettes.
  - When viewed along the longitudinal plane, the rosettes assume a columnar arrangement resembling the specific glioneuronal element of DNET.
  - Microcysts with myxoid material may also be seen.
- The glial component usually predominates and consists of spindled astrocytic tumor cells with oval nuclei, dense chromatin and cytoplasmic processes that form a compact fibrillary background (Figs. 21.1 and 21.2).
  - Microcysts, oligodendroglial-like cells, Rosenthal fibers, eosinophilic granular bodies, microcalcifications, and hemosiderin deposits may be encountered.
  - The glial component resembles pilocytic astrocytoma.
- Occasionally, dysmorphic ganglion-like cells may be embedded in the astrocytic component.
- Mitoses are inconspicuous and necrosis is usually absent.
- Dilated, hyalinized, thrombosed, and glomeruloid vessels may be present.
- Cortical dysplasia or neuronal ectopias are not found in the adjacent cerebellar cortex.
- RGNT usually shows a relatively sharp margin with the adjacent cerebellar parenchyma and lacks diffuse infiltration.

21.5 IMMUNOHISTOCHEMISTRY

- The center of the neurocytic rosettes and the neuropil of the perivascular pseudorosettes are positive for synaptophysin with a granular pattern of staining (Fig. 21.3).
- The cytoplasm and cytoplasmic processes of neurocytic cells are positive for MAP-2 and neuron-specific enolase (NSE).
- Ganglion cells are immunopositive for synaptophysin and neurofilament protein (NFP) and often negative for chromogranin A.
- The glial component is positive for GFAP and S-100.
- Oligodendroglial-like cells are negative for GFAP and synaptophysin and immunopositive for S-100.
- MIB-1 labeling indices are low (range 0.35–3.07%; mean 1.58%).

21.6 ELECTRON MICROSCOPY

- The neurocytic cells show cytoplasmic processes containing parallel microtubules, and dense-core granules and forming well-developed synaptic contacts.
- When forming rosettes, these neurocytic cells are closely apposed with the cytoplasmic processes seen toward the center of the rosette.
- The glial component shows numerous bundles of intermediate filaments within the cytoplasm.
- Cilia or microvilli are not present.

21.7 MOLECULAR PATHOLOGY

- No association with familial tumor syndromes has been reported.
- Only one reported patient had a Chiari type I malformation.

21.8 DIFFERENTIAL DIAGNOSIS

- The main differential diagnosis is DNET. DNET is a supratentorial, benign, intracortical tumor occurring in children and young adults (usually less than 20 years of age) and highly associated with seizures.
- Key histological feature of DNET is the specific glioneuronal element composed of a columnar arrangement of oligodendroglial-like cells and microcysts with "floating neurons."
  - In addition, cortical dysplasia is commonly found in the adjacent cortex in DNET.
  - On the contrary, all reported cases of RGNT have been described in the posterior fossa. Patients usually present at an older age and with progressive neurologic deficits; these features are atypical for a DNET.
  - Seizures are not a characteristic finding in RGNT.
  - Histologically, a distinguishing feature of RGNT is the formation of neurocytic and perivascular pseudorosettes, which are not seen in DNETs.

- Another diagnostic consideration is central neurocytoma. A prominent glial component as seen in RGNT is not a feature of neurocytoma.

21.9 PROGNOSIS

- RGNT shows an indolent clinical behavior and, as such, it is classified as a WHO 2007 grade I tumor.
- Gross total resection without adjuvant therapy results in recurrence-free, long-term survival.
  - Only one example of tumor recurrence occurring 10 years after initial resection, has been reported.
  - Only one example of tumor-associated fatality is on record. In this example, the patient was a 52-year-old woman who was treated with partial resection and irradiation. She subsequently developed progressive bulbar dysfunction and a new ring-enhancing lesion near the operative bed. Autopsy was not performed and the cause of death remains unclear.

SUGGESTED READING

Hainfellner JA, Scheithauer BW, Giangaspero F, Rosenblum MK (2007) Rosette-forming glioneuronal tumour of the fourth ventricle. In: Louis DN, Ohgaki H, Wiestler OD, Cavenee WK (eds) WHO Classification of tumours of the central nervous system, 4th edn. International Agency for Research on Cancer, Lyon, pp 115–116

Louis DN, Ohgaki H, Wiestler OD, Cavence WK, Burger PC, Jouvet A, Scheithauer BW, Kleihues P (2007) The 2007 WHO classification of tumours of the central nervous system. Acta Neuropathol 114: 97–109

Komori T, Scheithauer BW, Hirose T (2002) A rosette-forming glioneuronal tumor of the fourth ventricle: infratentorial form of dysembryoplastic neuroepithelial tumor? Am J Surg Pathol 26(5):582–591

Rosenblum MK (2007) The 2007 WHO classification of nervous system tumors: newly recognized members of the mixed glioneuronal group. Brain Pathol 17(3):308–313
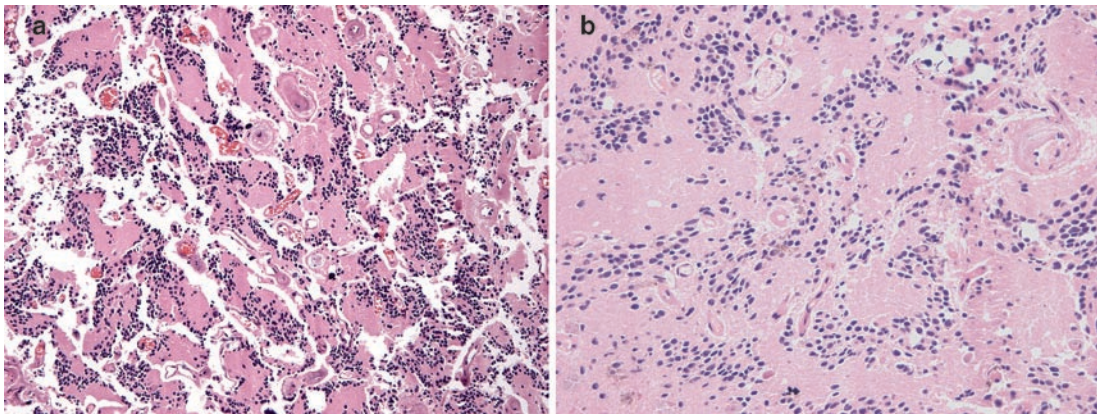
Fig. 21.1. (**a**) Low and (**b**) intermediate magnifications showing a diffuse resetting pattern in an example of RGNT of the fourth ventricle.
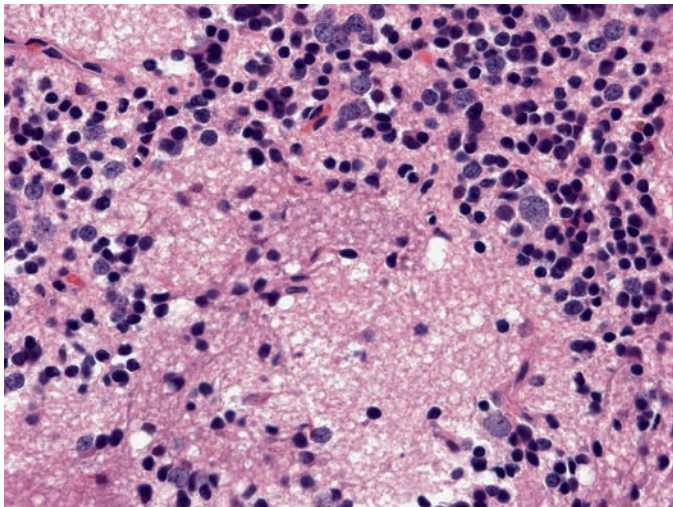
Fig. 21.2. Higher magnification showing the biphenotypic cellular population often seen in RGNT.
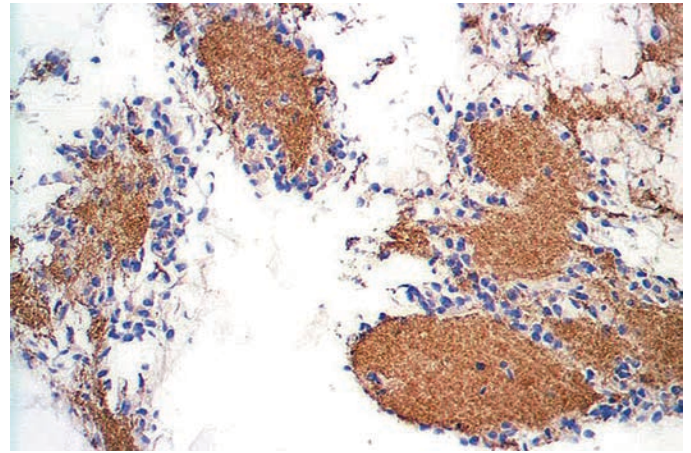
Fig. 21.3. Synaptophysin immunopositivity is present in the acellular core of the rosettes in RGNT.

Malignant Epithelioid Glioneuronal Tumor

M. Rivera-Zengotita, R. Rauch and Adekunle M. Adesina

Keywords Glioneuronal tumors; Malignant glioneuronal tumors; Epithelioid tumors

22.1 OVERVIEW

- Malignant epithelioid glioneuronal tumor (MEGNT) is the name proposed for a high-grade tumor showing both glial and neuronal differentiation. This tumor is not included in the current 2007 WHO classification of tumors of the central nervous system, but examples described so far have shown an aggressive behavior.

22.2 CLINICAL FEATURES

- Three pediatric and three adult cases have been described so far with an age range between 5 and 84 years.
- The three pediatric cases occurred in males, while the adult cases occurred in one female and two males.
- Patients usually present with signs and symptoms of increased intracranial pressure or symptoms related to the location of the lesion.

22.3 NEUROIMAGING

- All reported cases are supratentorial with a predilection for the frontoparietal region.
- MRI scans show large heterogeneous lesions with associated edema and mass effect (Figs. 22.1–22.3).
- The lesions enhance after contrast administration either with a ring-enhancing pattern (Fig. 22.1b), a solid enhancing component (Fig. 22.2b), or heterogeneous contrast enhancement (Fig. 22.3b).
- A cystic, necrotic appearing component may be seen.
- Multicentric lesions were described in two adult patients.
- CT scans are characterized by hyperdense lesions.

22.4 PATHOLOGY

- At surgery, the tumors are relatively well circumscribed and highly vascular.
- Dural attachment has been described in two cases.
- Grossly, the tumors are circumscribed and show a variegated appearance with solid, cystic, and necrotic regions (Figs. 22.4 and 22.5).
- Intraoperative cytologic imprints or smears are characterized by hypercellularity with a mixed population of tumor cells (Fig. 22.6), including large epithelioid cells, small undifferentiated cells, spindle cells, and sometimes infiltrating lymphocytes (Fig. 22.7).
- Cell-wrapping may be prominent (Fig. 22.6).

- The most striking histologic feature of these tumors is an epithelioid cell component consisting of large cells with open chromatin and prominent nucleoli (Figs. 22.8 and 22.9).
- Epithelioid cells have abundant eosinophilic, often vacuolated (Fig. 22.10) or clear cell (Fig. 22.10) or xanthomatous (Fig. 22.11) cytoplasm and well-defined cell borders.
- Multinucleated forms may be present.
- Cells may have a ganglioid and/or rhabdoid appearance (Fig. 22.12).
- Other cellular components include small undifferentiated, PNET-like cells (Figs. 22.13 and 22.14), an undifferentiated cell-epithelioid cell transition (Fig. 22.15) and spindle cells arranged in short fascicles (Fig. 22.16).
- The tumors may have an ill-defined nodular architecture. In some areas, a sharp circumscription with adjacent brain is identified, while in other regions tumor cells are seen infiltrating brain parenchyma.
- Vascular proliferation has been identified in all pediatric cases.
- Necrosis, including pseudopalisading necrosis (Fig. 22.17), is usually present.
- Mitotic activity is conspicuous.

22.5 IMMUNOHISTOCHEMISTRY

- The tumors are positive for GFAP (Fig. 22.18), vimentin (Fig. 22.19), S-100, and one or a combination of the following neuronal markers: synaptophysin (Fig. 22.20a), chromogranin A (Fig. 22.20b), neurofilament protein (Fig. 22.20c), Neu-N (Fig. 22.20d), and MAP-2 (Fig. 22.20e).
- P53 immunoreactivity has also been described.
- Co-expression of GFAP, synaptophysin, and chromogranin A has been observed.
- EMA (Fig. 22.21) and aberrant desmin (Fig. 22.22) positivity have been described in the pediatric tumors.
- All pediatric tumors were positive for INI-1 protein expression (Fig. 22.23).
- Tumor cells are consistently negative for cytokeratins, smooth muscle actin, myogenin, and Myo-D1.
- MIB-1 shows variable but generally high labeling indices with up to 60% proliferation index (Fig. 22.24).

22.6 ELECTRON MICROSCOPY

- A mixed population of tumor cells is identified including large and small undifferentiated cells.
- Evidence of neuronal differentiation includes synaptic junctions (Fig. 22.25), dense core neurosecretory granules, and cytoplasmic processes with microtubules (Fig. 22.26).
- Intermediate filaments are also identified (Fig. 22.27).

22.7 MOLECULAR PATHOLOGY

- Cytogenetic studies performed in two of the pediatric cases failed to show any consistent abnormality.
- FISH for HSNF5/INI1 locus deletion and chromosome 22 monosomy performed in one pediatric case showed no abnormalities.

22.8 DIFFERENTIAL DIAGNOSIS

- The mixed population of large epithelioid cells and small undifferentiated cells may raise atypical teratoid rhabdoid tumor (ATRT) as a major differential diagnosis, especially in the pediatric population.
- However, ATRT is more common in the posterior fossa.
- FISH with INI-1 locus-specific probe shows allelic deletion in ATRT giving rise to negative INI-1 immunohistochemistry. This deletion is not seen in MEGNT.
- The biphenotypic population of cells also raises anaplastic ganglioglioma as part of the differential diagnosis.
- Evidence of a preceding low-grade ganglioglioma is not found in MEGNT cases.
- The rhabdoid appearance of the epithelioid cells may raise the possibility of pleomorphic rhabdomyosarcoma. However, MEGNT is negative for Myo-D1 and myogenin, which are positive in pleomorphic rhabdomyosarcoma.
- In addition, there is no ultrastructural evidence of myogenic differentiation in MEGNT.
- Epithelioid glioblastoma is another important differential diagnosis especially in adults. The epithelioid cells in glioblastoma should not show immunopositivity for neuronal markers as is seen in MEGNT.

22.9 PROGNOSIS

- The described cases have shown an aggressive behavior with rapid progression and death in less than a year after diagnosis, despite aggressive surgery, radiation, and chemotherapy.
- Varlet et al. described 40 cases of malignant glioneuronal tumors of which 22 (55%) had epithelioid features. They reported that their subset of malignant glioneuronal tumors may have a better prognosis than typical malignant gliomas with gross total surgical resection being curative in some cases.
  - These tumors reported by Varlet et al. may represent a different subset of glioneuronal tumors distinct from the ones described above as MEGNT.
- Further characterization of subgroups of glioneuronal tumors should allow more appropriate classification and reliable definition of prognosis.

SUGGESTED READING

Rodriguez FJ, Scheithauer BW, Port JD (2006) Unusual malignant glioneuronal tumors of the cerebrum of adults: a clinicopathologic study of three cases. Acta Neuropathol 112:727–737

Varlet P, Deepa S, Miguel C, Roux FX, Meder JF, Chneiweiss H, Daumas–Duport C (2004) New variants of malignant glioneuronal tumors: a clinicopathologic study of 40 cases. Neurosurgery 55(6):1377–1392

Rivera-Zengotita M, Whitehead W, Jea A, Chintagumpala M, Fuller GN, Jones J, Adesina AM (2008) Malignant epithelioid glioneuronal tumor: unusual phenotype or new entity? Mod Pathol 21(Suppl 1):324A
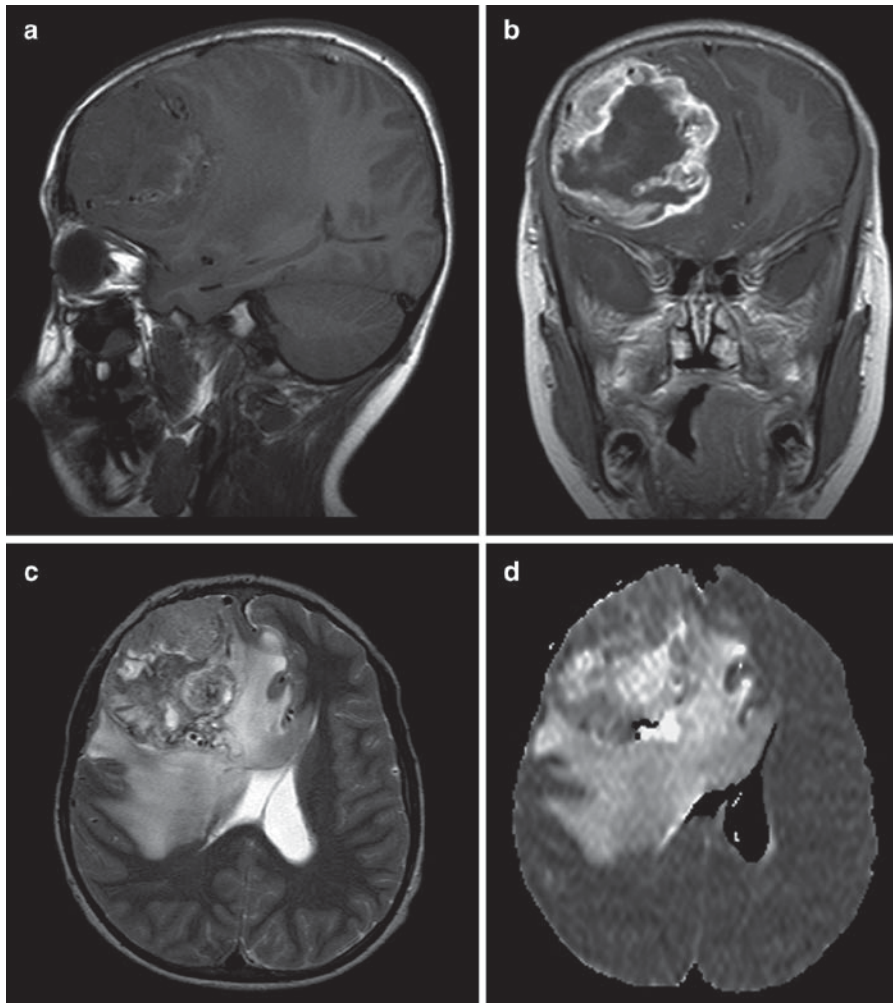
Fig. 22.1. (**a**) Sagittal T1-w image showing a frontal lobe mass lesion, (**b**) Coronal T1-w postcontrast image with heterogeneity, and ring-type contrast enhancement, and (**c**) axial T2-w image with massive peritumoral edema. (**d**) Diffusion weighted image showing regions of increased and mild restricted diffusion.
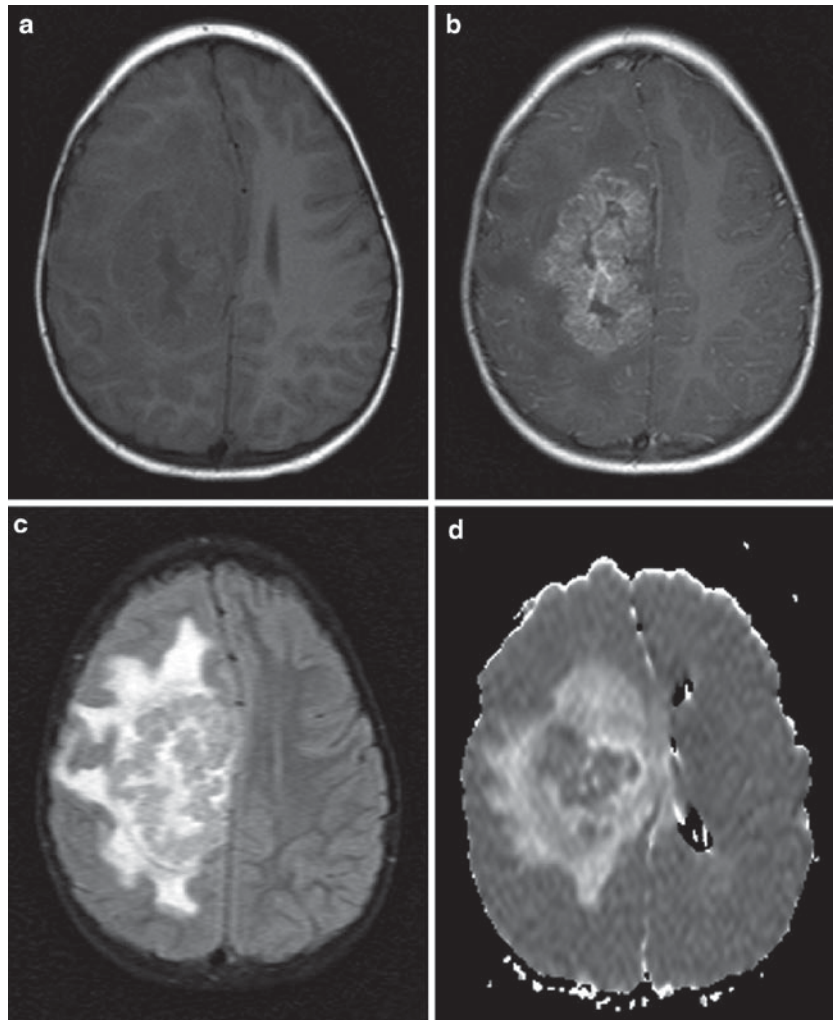
Fig. 22.2. (**a**) Axial T1-w image showing a partially cystic fronto-parietal mass, (**b**) axial T1-w postcontrast image showing heterogenous enhancement, and (**c**) axial T2-w image showing heterogeneous signal intensity in mass with surrounding edema. (**d**) ADC map showing increased diffusion around the mass and restricted diffusion in the central parts of the mass.
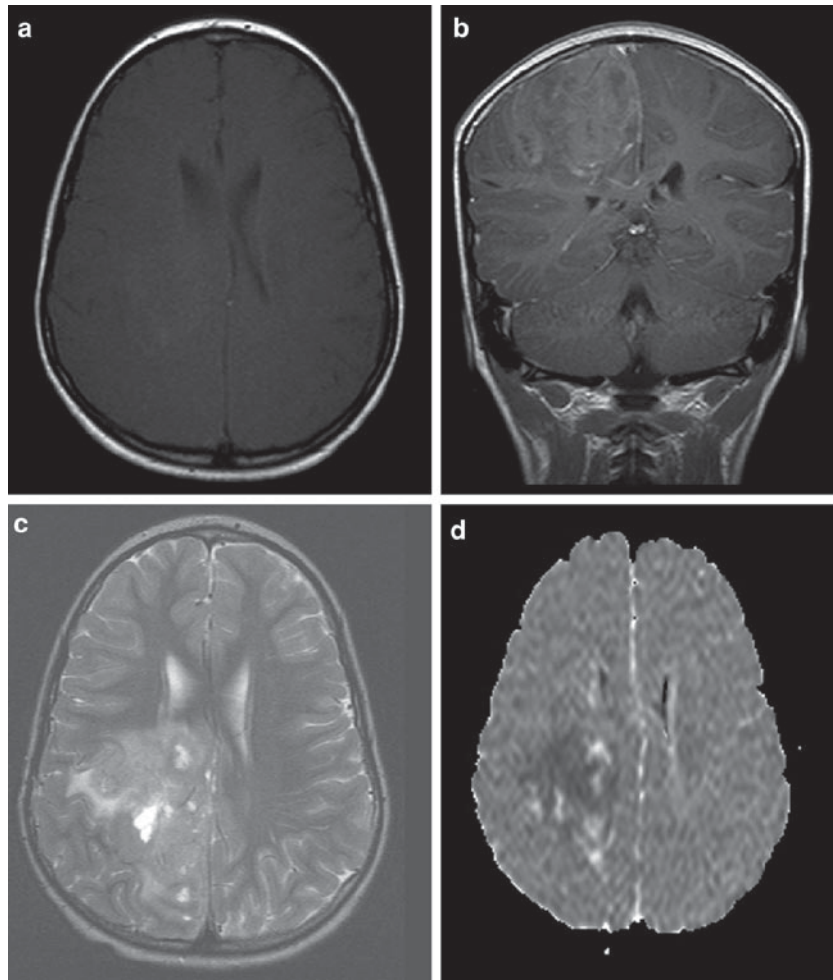
Fig. 22.3. (**a**) Axial T1-w image showing a parietal lobe mass lesion, (**b**) coronal T1-w postcontrast image with heterogenous, contrast enhancement, and (**c**) axial T2-w image with a cystic component and minimal peritumoral edema. (**d**) Diffusion-weighted image showing mild restricted diffusion in mass.

Fig. 22.4. Well-circumscribed tumor excised from the same patient as in Fig. 22.1.
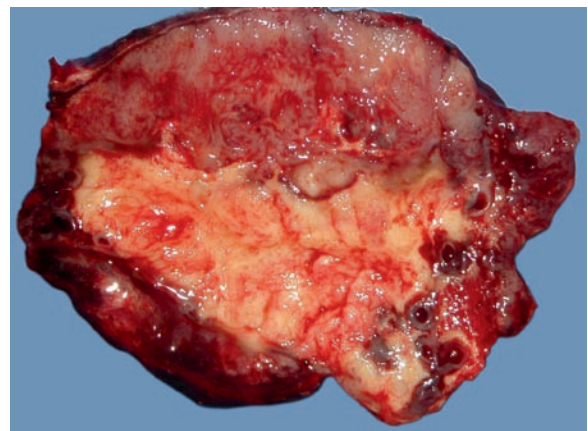
Fig. 22.5. Cut surface shows a tan fish flesh solid component and a yellow necrotic component.
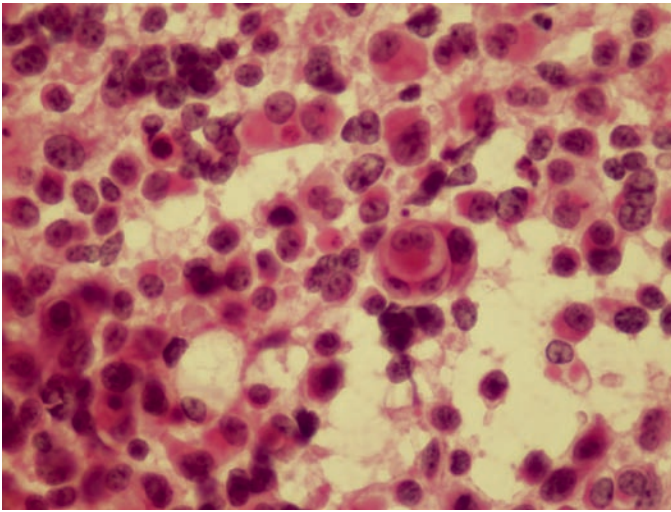
Fig. 22.6. Intraoperative smear preparation showing discohesive cells with large vesicular nuclei and nucleoli. Some of the cells have a rhabdoid appearance with abundant eosinophilic cytoplasm and eccentric nucleus. Cell wrapping is readily appreciated. There is a background tumor diathesis in this touch preparation.
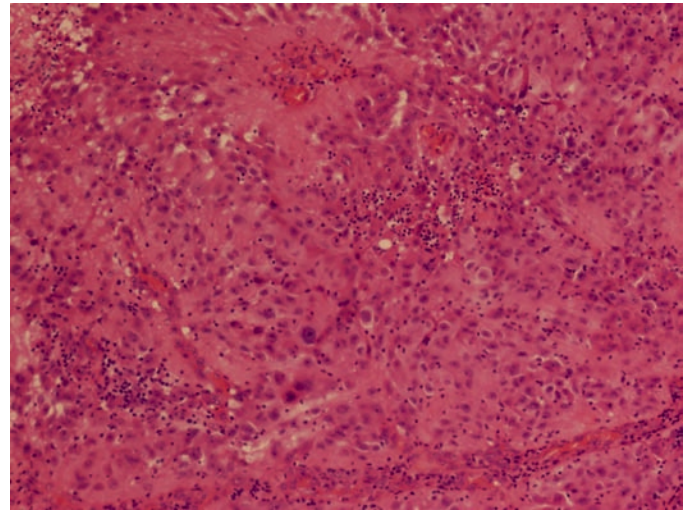
Fig. 22.8. Low-power overview showing a mixed population of epithelioid tumor cells and lymphocytes.
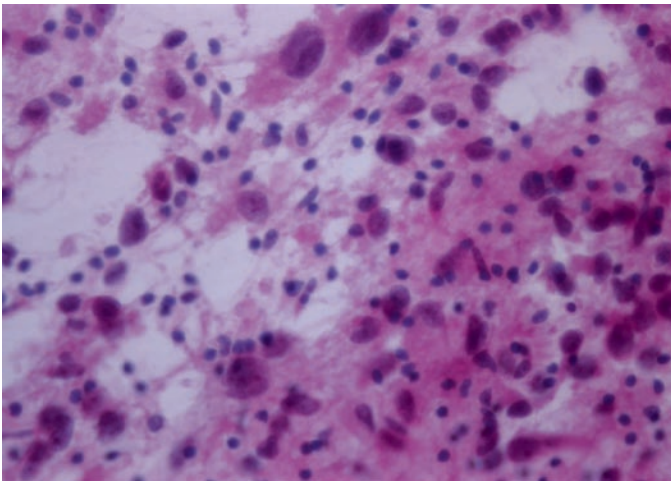
Fig. 22.7. Intraoperative smear preparation from another example with a component of infiltrating lymphoid cells.
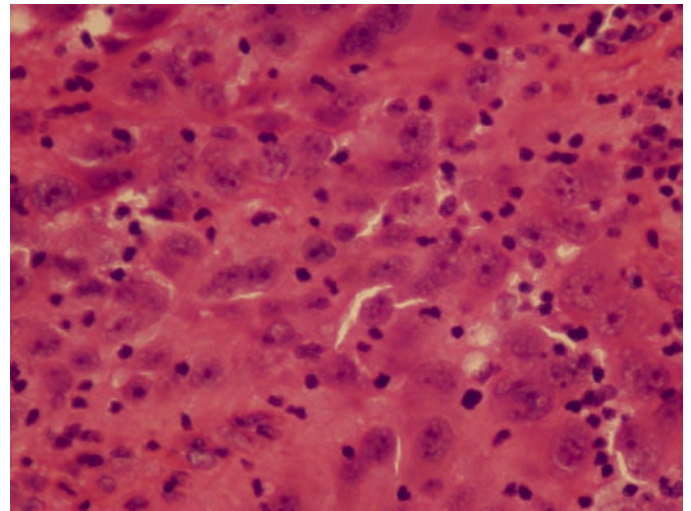
Fig. 22.9. Higher magnification showing sheets of epithelioid cells with large vesicular nuclei and prominent nucleoli.
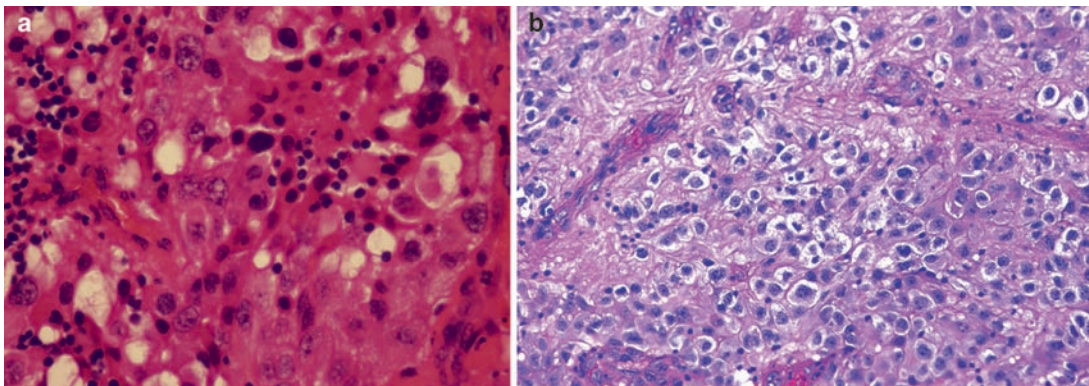
Fig. 22.10. (**a**) Epithelioid cells with variable number of infiltrating lymphocytes and few cells with cytoplasmic vacuolation and (**b**) epithelioid cells with clear cell features.
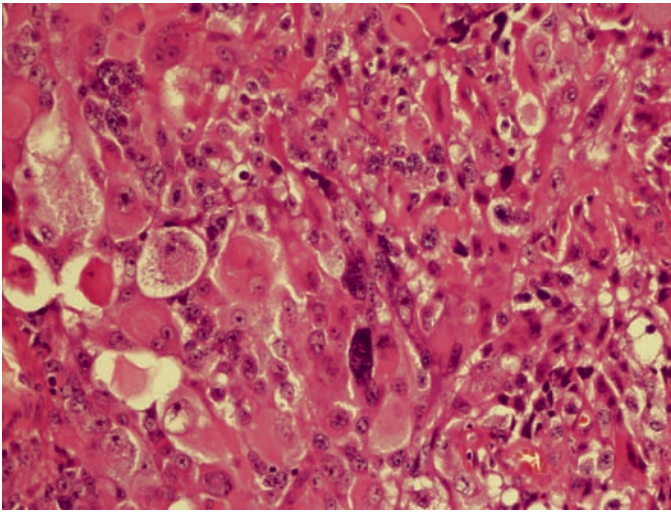
Fig. 22.11. Region of epithelioid cells with some of the cells showing xanthomatous change.
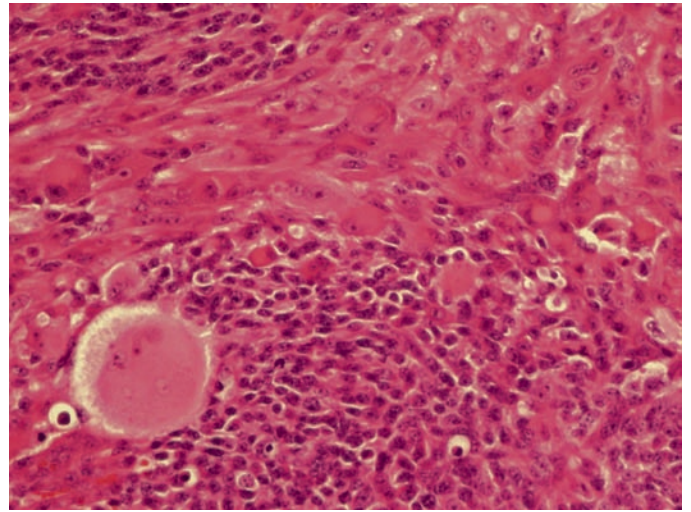
Fig. 22.12. Region of tumor showing epithelioid cells with a rhabdoid or ganglioid appearance (*upper field*) and sheet of undifferentiated small cells (*lower field*) with little indistinct cytoplasm.
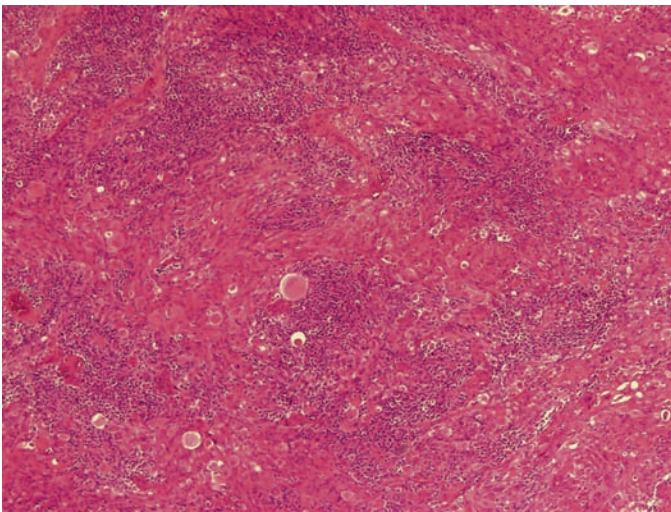
Fig. 22.13. An overview of the intimate intermixture of epithelioid cell clusters and undifferentiated small cells.
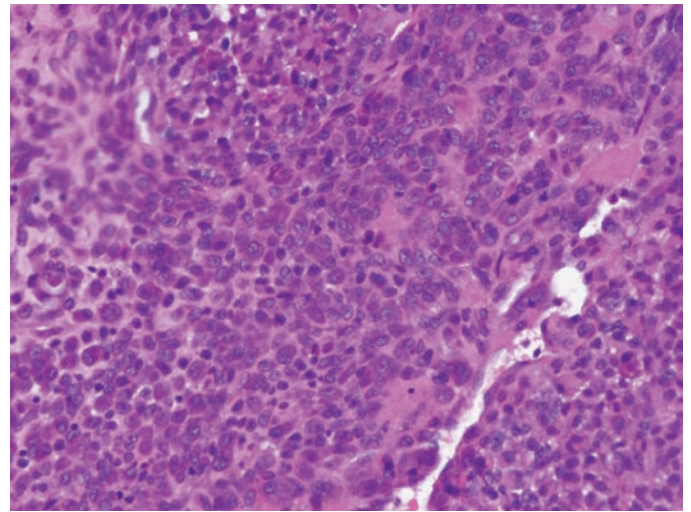
Fig. 22.14. A close-up showing the poorly differentiated small cell component in another tumor.
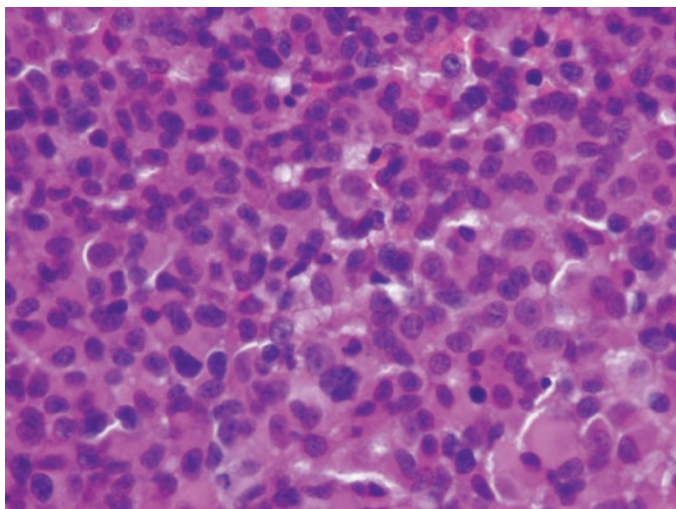
Fig. 22.15. A transition or progressive differentiation from small undifferentiated cells (*left upper field*) to epithelioid cells (*right lower field*) is present in this tumor.
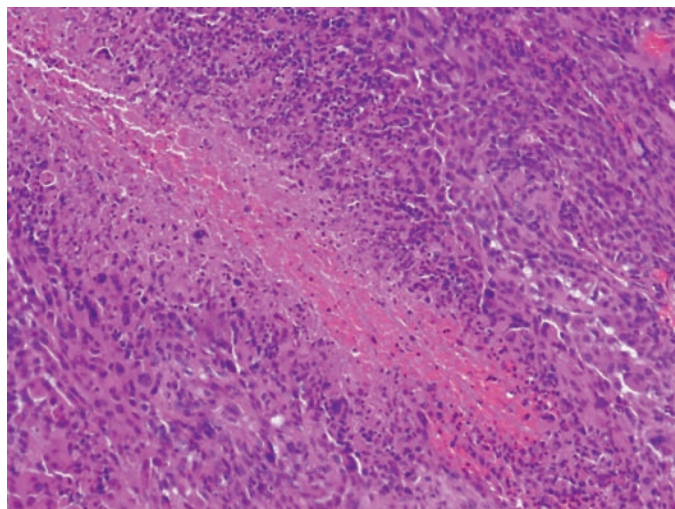
Fig. 22.17. Pseudopallisaded necrosis may be present and is a feature shared with high-grade glioma, glioblastoma.
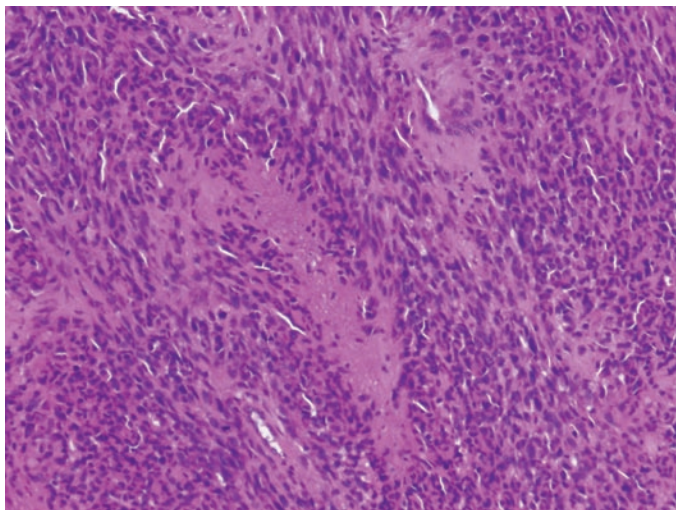
Fig. 22.16. Region with tumor cells showing an oval to spindle cell configuration.
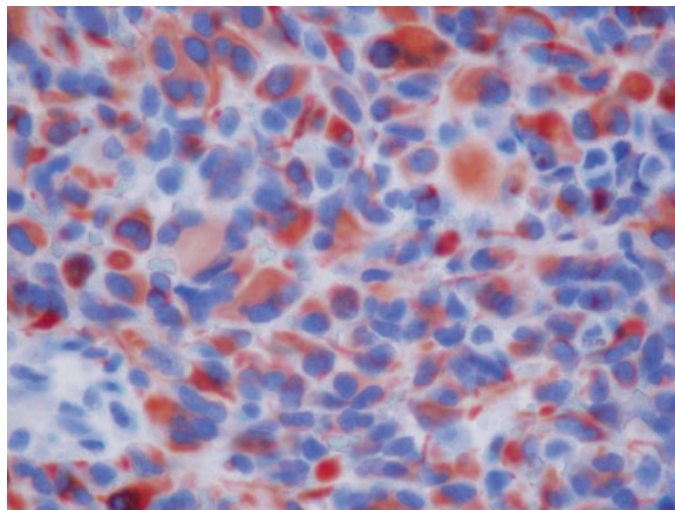
Fig. 22.18. Strong GFAP positivity is seen in the tumor cells.
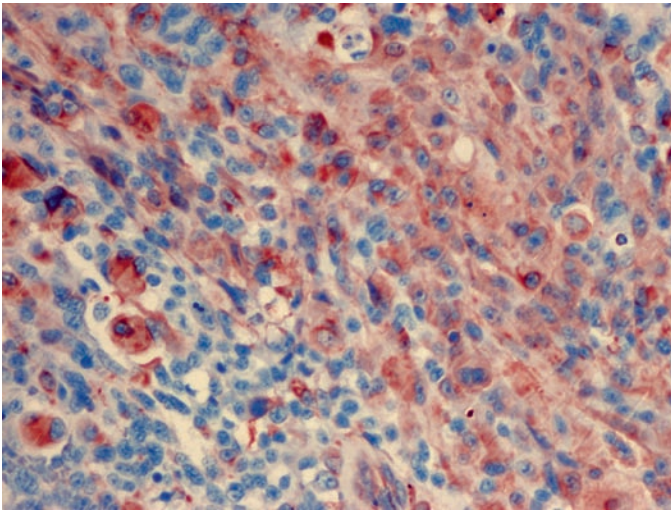
Fig. 22.19. Variable expression of vimentin is often present.
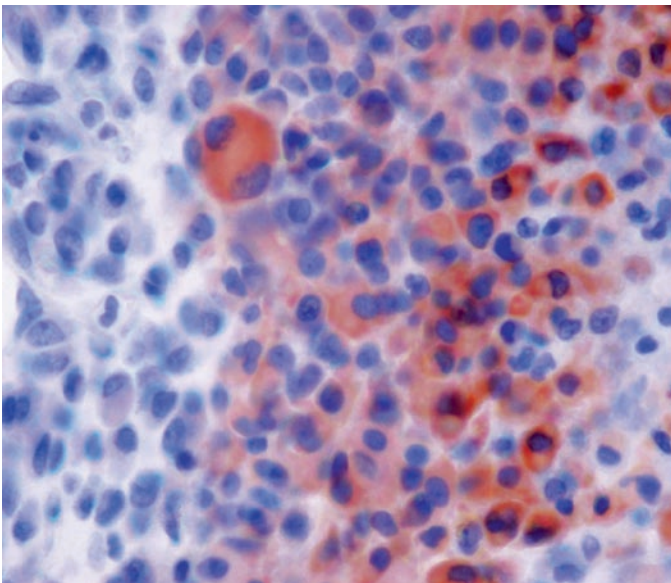
Fig. 22.21. Expression of EMA is seen in a subset of tumor cells.
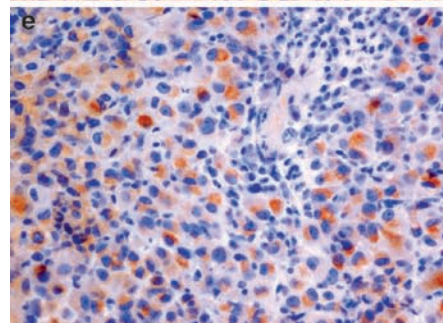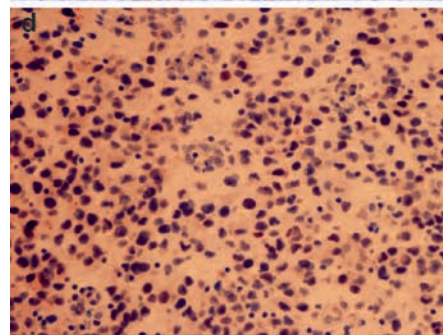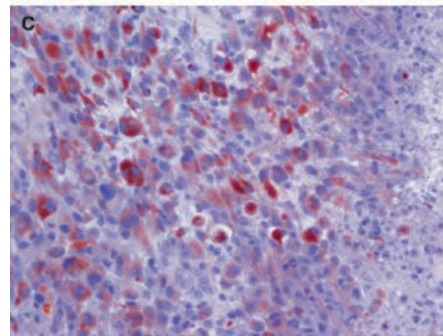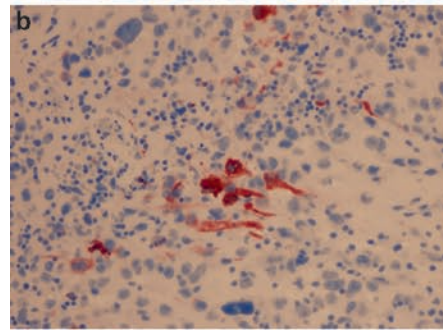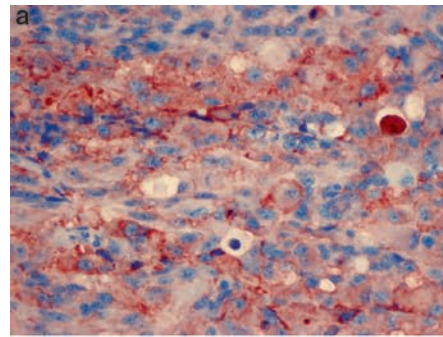
Fig. 22.20. Expression of neuromarkers may include (**a**) diffuse expression of synaptophysin, (**b**) focal expression of chromogranin, (**c**) a diffuse expression of neurofilament protein, (**d**) nuclear expression of Neu-N, and (**e**) diffuse expression of MAP2.
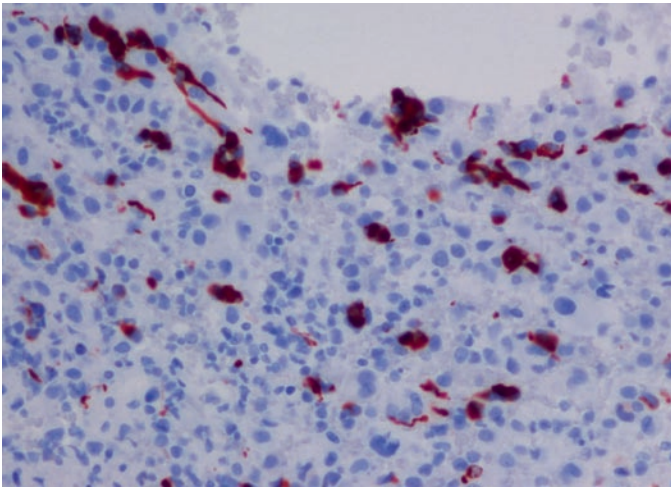
Fig. 22.22. Aberrant expression of desmin in the absence of myogenin or myoD1 may be seen.
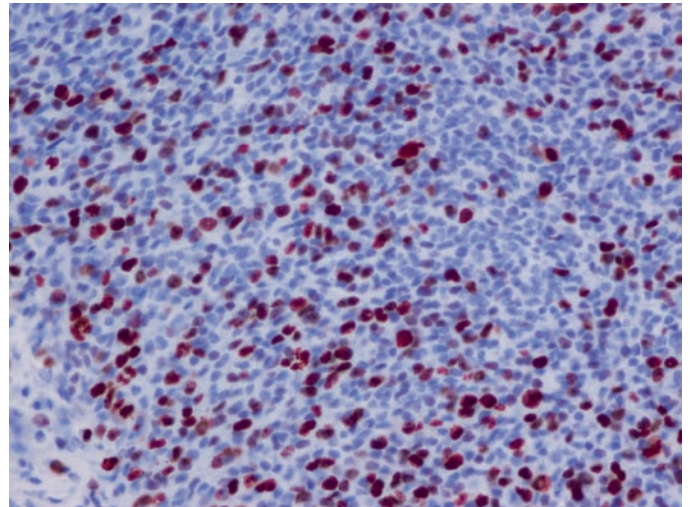
Fig. 22.24. Immunostain for Ki67 in a tumor showing high proliferation index.
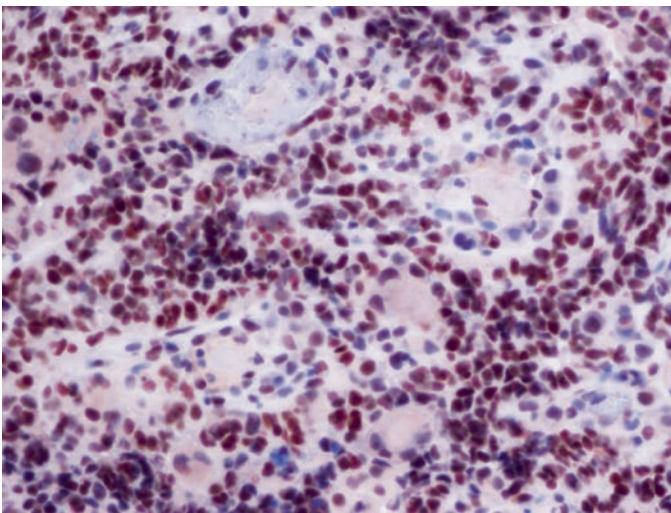
Fig. 22.23. Tumor cells showing INI1 protein expression, a feature excluding this entity from the group of atypical teratoid rhabdoid tumors.
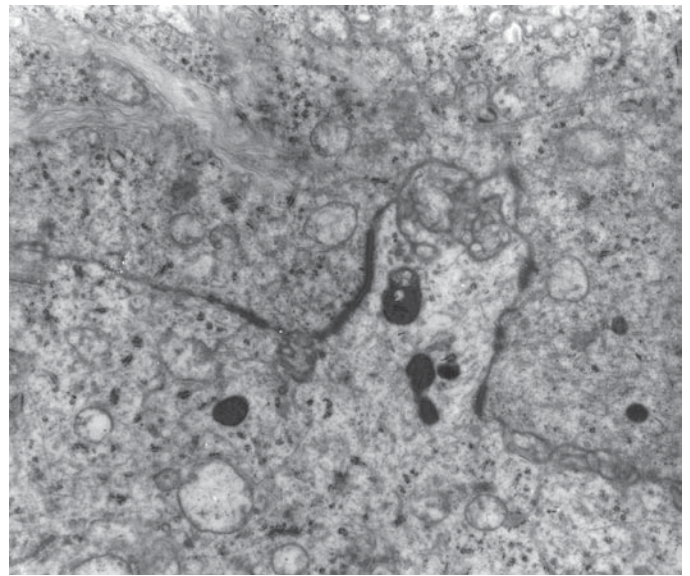
Fig. 22.25. Electron microscopy showing cellular formation of synaptic junction.
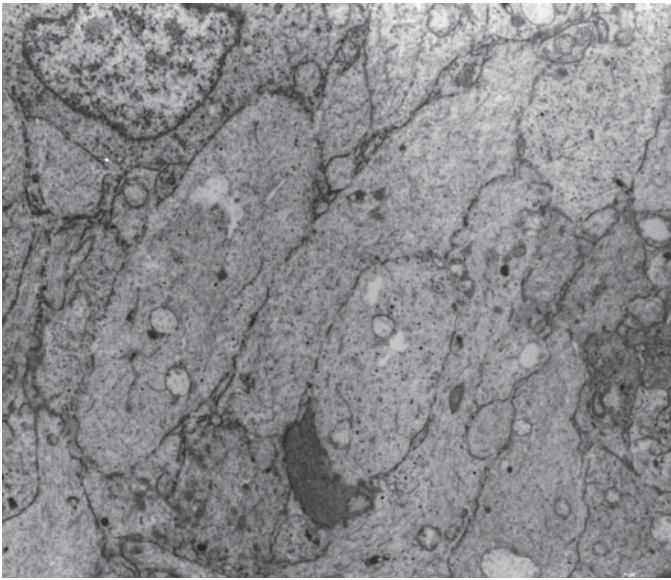
Fig. 22.26. Tumor cells form cytoplasmic processes containing micro-tubules and dense core neurosecretory ganules.
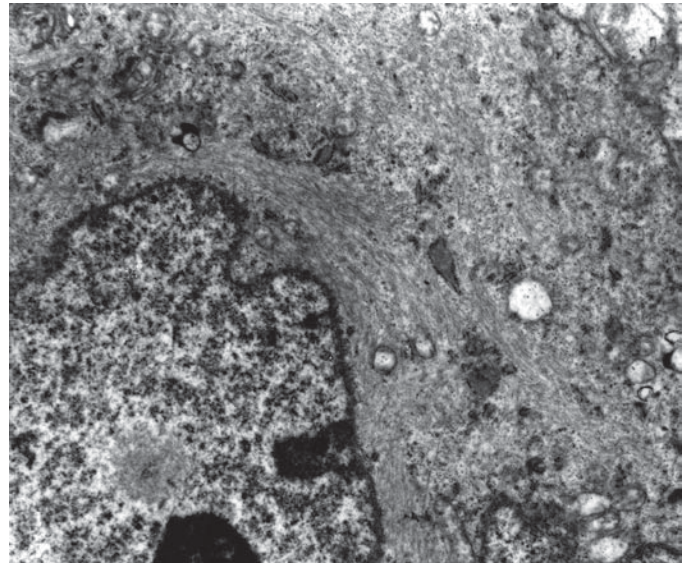
Fig. 22.27. Intermediate filaments consistent with glial differentiation are present in tumor cells.

Paraganglioma

A. Rivera and Adekunle M. Adesina

Keywords Paraganglioma; Extra-adrenal; Filum terminale; Melanotic paraganglioma

23.1 OVERVIEW

- Encapsulated, benign neoplasm composed of neuroendocrine cells arranged in a lobular fashion arising from the autonomic ganglia (paraganglia) of the sympathetic and parasympathetic chains.
- The parasympathetic variety tends to arise predominantly in the head and neck region often along the jugular veins and carotid arteries, with direct extension into the cranial vault.
- Sympathetic paragangliomas are typically retroperitoneal.
- Best characterized paragangliomas of the central nervous system (CNS) are those of the filum terminale (WHO grade I).

23.2 CLINICAL FEATURES

- Paragangliomas of the CNS are relatively uncommon with the majority located in the lumbar cistern (particularly associated with the cauda equina).
- Of cauda equina lesions, paragangliomas only make up approximately 3–4%. Other spinal levels are far less commonly involved.
- Intracranial paragangliomas are usually seen as a result of direct extension of jugular (glomus jugulare) or carotid body lesions. Rare, purely intracranial paragangliomas have been reported in the sellar region, cerebellum and in the cerebral hemispheres.
- Age distribution is wide ranging from children to older adults with peak age in the fifth decade. There is a slight male predominance.
- Presenting symptoms are typically related to location of the lesion.
- Intracranial lesions, particularly glomus jugulare, present with pulsatile tinnitus or cranial nerve dysfunction.
- Paragangliomas of the cauda equina often present with low back pain and rarely, paralysis or sensory deficits can occur.
- The vast majority of paragangliomas of the CNS are non-functional, though rare functional intracranial and cauda equina lesions have been reported.

23.3 NEUROIMAGING

- There are no specific imaging findings purely associated with paragangliomas.
- On MRI, the lesions often have a well-circumscribed, cystic appearance that is hypointense or isointense to the spinal cord on T1-weighted images (Fig. 23.1).
- In the cauda equina, the presence of congested, ectatic vessels and a rim of low signal intensity or "cap sign" on T2-weighted images may be helpful in distinguishing this lesion from myxopapillary ependymoma radiographically, given the vascularity of paragangliomas compared to that of ependymomas.
- A rare intracranial and hemispheric paraganglioma is isointense on T1 and hyperintense on T2 weighted imaging with diffuse contrast enhancement post-gadolinium (Figs. 23.2 and 23.3).
- Computed tomography shows the lesion as an isodense, homogenously enhancing mass lesion post-contrast; however, noncontrast scans may not detect the lesion.

23.4 PATHOLOGY

- Gross appearance:
  - Soft, tan-pink to red-brown, encapsulated tissue. Lesions of the cauda equina have a classic ovoid or "sausage" shaped appearance, are well encapsulated, and are often attached to the filum or nerve root.
- Histology:
  - Despite location, paragangliomas have a microscopic appearance that closely resembles normal paraganglia.
  - They are composed of bland neuroendocrine cells (chief cells) arranged in nests or "Zellballen" structures separated by fine fibrovascular septa (Figs. 23.4–23.7).
  - Interspersed among the nests of chief cells are spindled cells with long inconspicuous processes termed sustentacular cells; these are better visualized with S-100 protein immunostain (Fig. 23.8).
  - Some paragangliomas can have ganglion cell differentiation with presence of ganglion cells in varying proportions.
  - Melanotic paragangliomas have also been reported (Figs. 23.9–23.13).
  - Focal necrosis and rare mitoses can be seen and do not impact prognosis.

23.5 IMMUNOHISTOCHEMISTRY

- The chief cells are positive for neuronal markers such as synaptophysin and chromogranin.
  - Neurofilament and neuron specific enolase can also be used, but are less sensitive.
- The sustentacular cells are positive for S-100 protein, and may show focal positivity with GFAP (Figs. 23.8–23.11).

23.6 ELECTRON MICROSCOPY

- The classic feature is the presence of neurosecretory granules in the chief cells which also have interdigitating processes.

- Basal lamina is seen at the interface between the "Zellballen" structures and intervening septa.

23.7 MOLECULAR PATHOLOGY

- While there is no genetic alteration specific for CNS paragangliomas, some genes have been associated with predisposition to formation of paragangliomas and pheochromocytomas.
- Familial or inherited syndromes associated with paragangliomas include von Hippel Lindau disease (*VHL* gene 3p25-26), neurofibromatosis type 1 (*NF1* gene 17q11.2), and multiple endocrine neoplasia type 2 (*RET* gene 10q11.2).
- Mutations in the succinate dehydrogenase genes subunits B, C, and D (SDHB, SDHC, SDHD) have been shown to be associated with systemic paragangliomas, SDHD with multiple paragangliomas of the head and neck and SDHB with pheochromocytomas.

23.8 DIFFERENTIAL DIAGNOSIS

- The main differential diagnosis for cauda equina paragangliomas is myxopapillary ependymoma with nearly identical clinical presentation, location, and gross appearance.
- However, these lesions can be easily differentiated microscopically.
- Primary cerebral melanotic paraganglioma must be distinguished from primary CNS malignant melanoma or pigmented choroid plexus carcinoma, both of which are relatively easily distinguished by their high grade anaplastic features and from meningeal melanocytoma which shows a diffuse nuclear immunopositivity for S-100 protein.

23.9 PROGNOSIS

- Prognosis of CNS paragangliomas is favorable with outcome correlating more closely with location and extent of tumor growth at time of presentation than with histologic appearance.
- Metastasis of CNS paragangliomas is rare.
  - Metastasis occurs in approximately 5% of carotid body and glomus jugulare tumors.
  - Recurrence is commonly seen in these locations.
- In the cauda equina, paragangliomas are curable with complete resection.

- Recurrence occurs in 4% of cases.
- Cerebrospinal fluid seeding has been reported.
- Metastasis of a spinal paraganglioma is exceedingly rare with few cases reported.

SUGGESTED READING

Scheithauer BW, Brandner S, Soffer D (2007) Spinal paraganglioma. In: Louis DN, Ohgaki H, Wiestler OD, WK C (eds) WHO Classification of tumours of the central nervous system. 4th edn. WHO Press (IARC), Lyon, France pp 117–119

Naggara O, Varlet P, Page P, Oppenheim C, Meder JF (2005) Suprasellar paraganglioma: A case report and review of the literature. Neuroradiology 47:753–757

Prayson RA, Chahlavi A, Luciano M (2004) Cerebellar paraganglioma. Ann Diagn Pathol 8:219–223

Reithmeier T, Gumprecht H, Stolzle A, Lumenta CB (2000) Intracerebral paraganglioma. Acta Neurochir (Wien) 142:1063–1066

Yoo JH, Rivera A, Naeini RM, Yedururi S, Bayindir P, Megahead H, Fuller GN, Suh JS, Adesina AM, Hunter JV (2008) Melanotic paraganglioma arising in the temporal horn following Langerhans cell histiocytosis. Pediatr Radiol 38:571–574

Levy RA (1993) Paraganglioma of the filum terminale: MR findings. AJR Am J Roentgenol 160:851–852

Yang SY, Jin YJ, Park SH, Jahng TA, Kim HJ, Chung CK (2005) Paragangliomas in the cauda equina region: Clinicopathoradiologic findings in four cases. J Neurooncol 72:49–55

Moran CA, Rush W, Mena H (1997) Primary spinal paragangliomas: A clinicopathological and immunohistochemical study of 30 cases. Histopathology 31:167–173

Sonneland PR, Scheithauer BW, LeChago J, Crawford BG, Onofrio BM (1986) Paraganglioma of the cauda equina region. Clinicopathologic study of 31 cases with special reference to immunocytology and ultrastructure. Cancer 58:1720–1735

Masuoka J, Brandner S, Paulus W et al (2001) Germline SDHD mutation in paraganglioma of the spinal cord. Oncogene 20:5084–5086

Kliewer KE, Wen DR, Cancilla PA, Cochran AJ (1989) Paragangliomas: Assessment of prognosis by histologic, immunohistochemical, and ultrastructural techniques. Hum Pathol 20:29–39

Lack EE, Cubilla AL, Woodruff JM (1979) Paragangliomas of the head and neck region. A pathologic study of tumors from 71 patients. Hum Pathol 10:191–218

Strommer KN, Brandner S, Sarioglu AC, Sure U, Yonekawa Y (1995) Symptomatic cerebellar metastasis and late local recurrence of a cauda equina paraganglioma. Case report. J Neurosurg 83:166–169
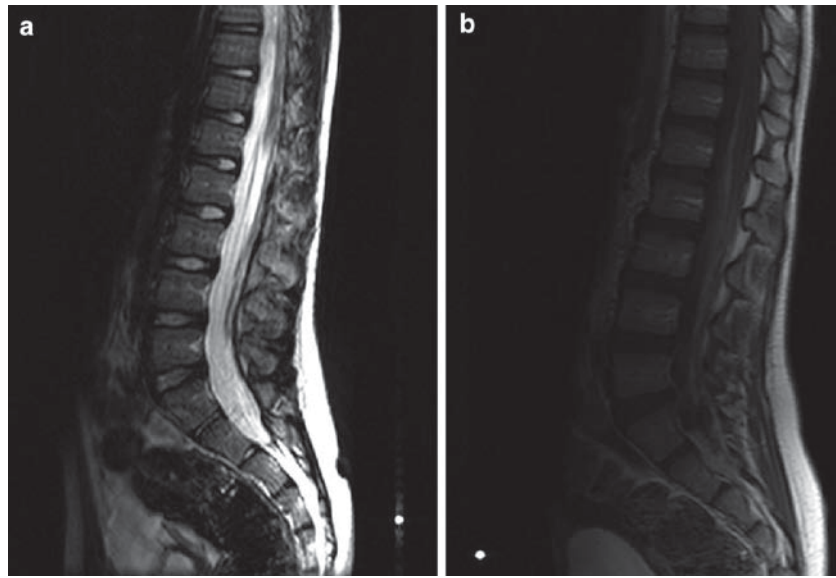
Fig. 23.1. Abnormal expansion of cauda equina by a mass lesion (**a**) hyperintense on T2-w imaging, and (**b**) isointense on T-1 w imaging. Radiologic differential diagnosis includes paraganglioma and myxopapillary ependymoma.
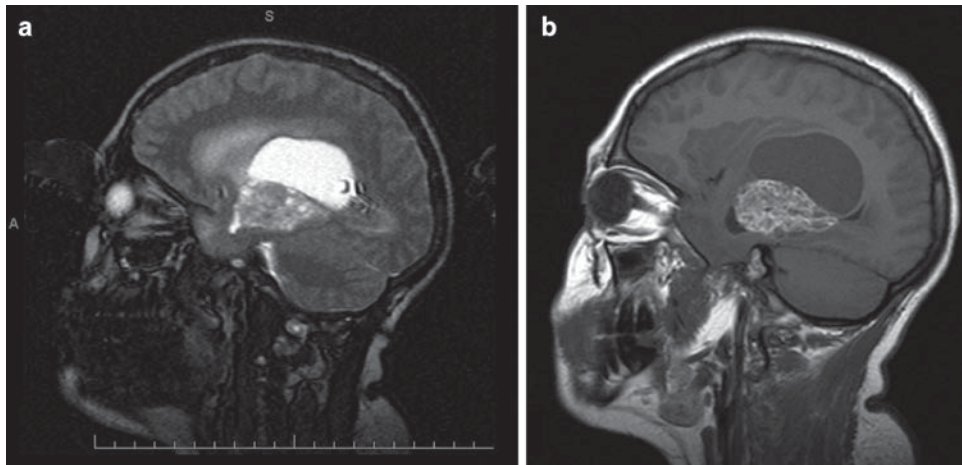
Fig. 23.2. Melanotic paraganglioma arising in the temporal horn of the lateral ventricle post radiation therapy for Langerhan's histiocytosis and showing (**a**) sagittal T-2-w image and (**b**) sagittal T1-w image with intraventricular cyst and diffuse enhancement of solid component post gadolinium.
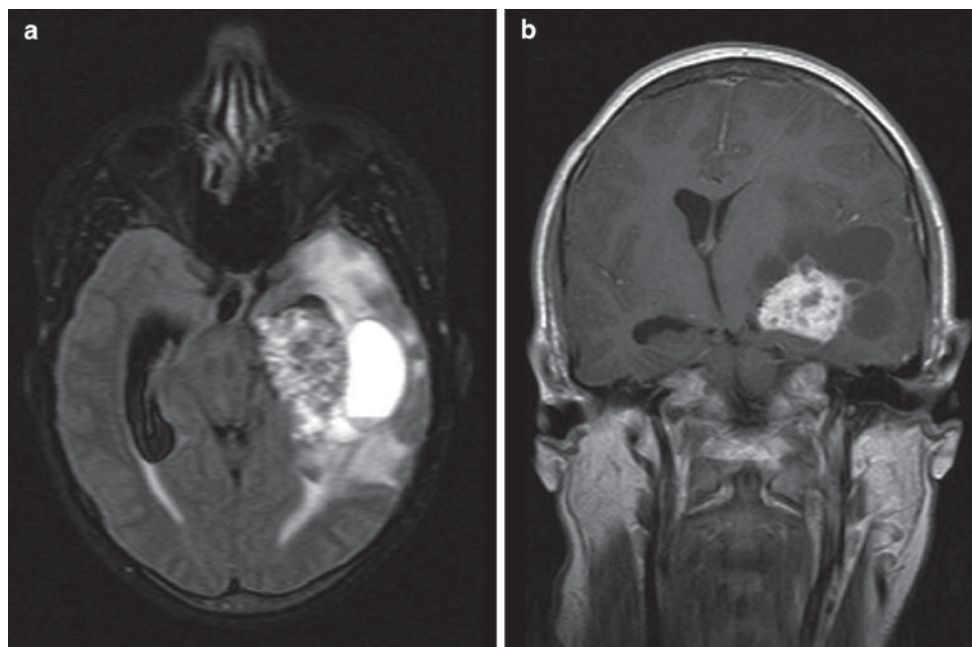
Fig. 23.3. (**a**) Axial FLAIR and (**b**) coronal T1-w images post gadolinium showing a cystic component, solid component, and peritumoral edema.
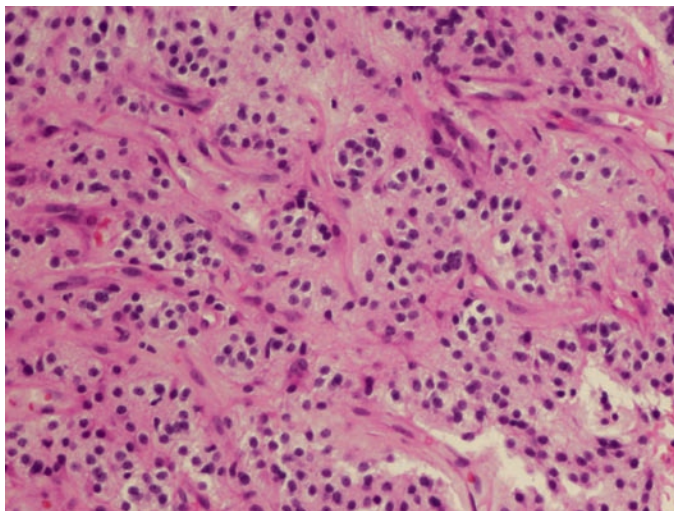
Fig. 23.4. A lobulated or organoid/nesting pattern with intervening fibrovascular septa.
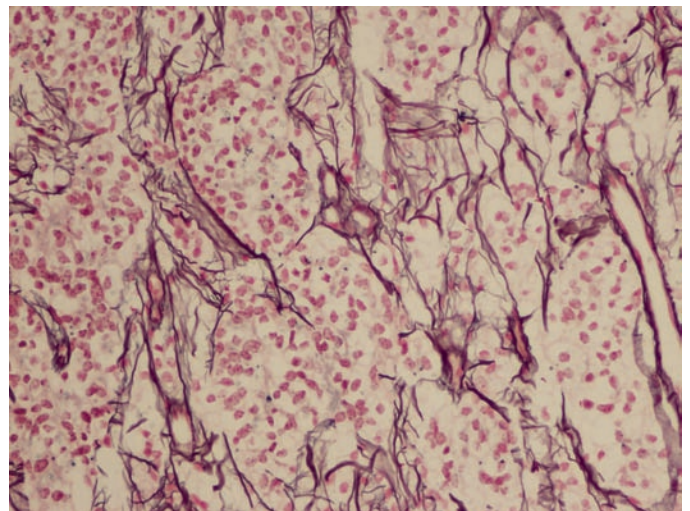
Fig. 23.5. Reticulin stains demonstrating the reticulin framework underlying the nesting pattern.
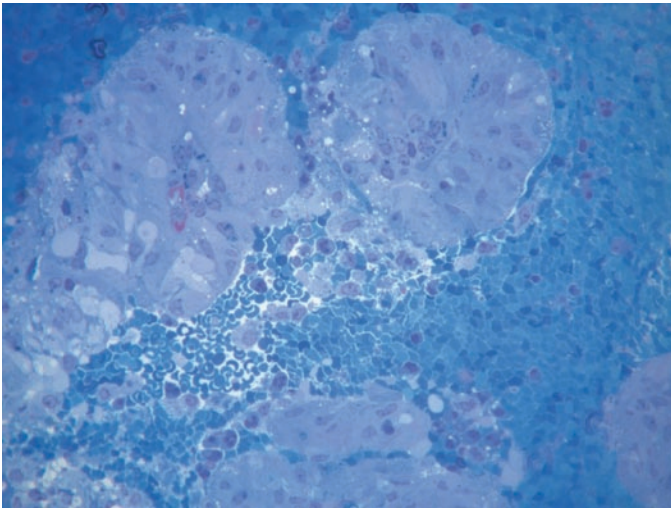
Fig. 23.6. Plastic section showing the classic "Zellballen" pattern characteristic of paraganglioma.
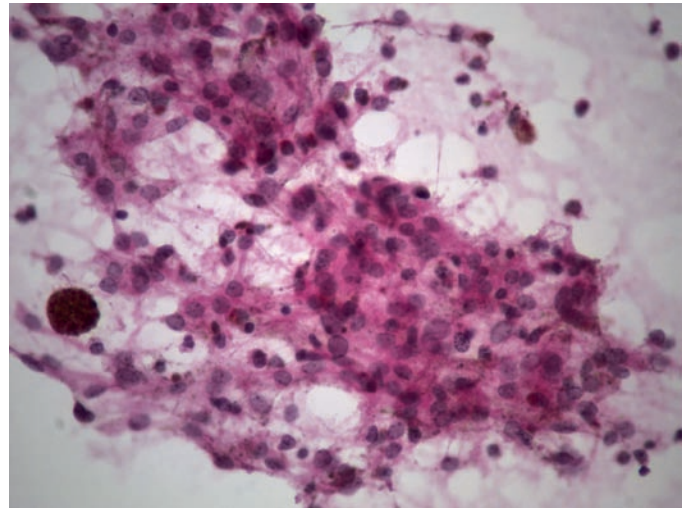
Fig. 23.9. Intraoperative touch preparation showing the monomorphic population of benign tumor cells and pigmentation in a melanotic paraganglioma. Note the lack of anaplasia that is typically seen in malignant melanoma.
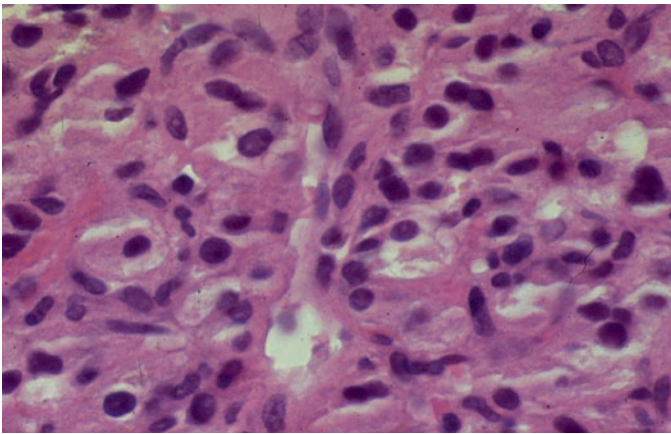
Fig. 23.7. Close up view of the "Chief" cells representing the neoplastic cells of paraganglioma.
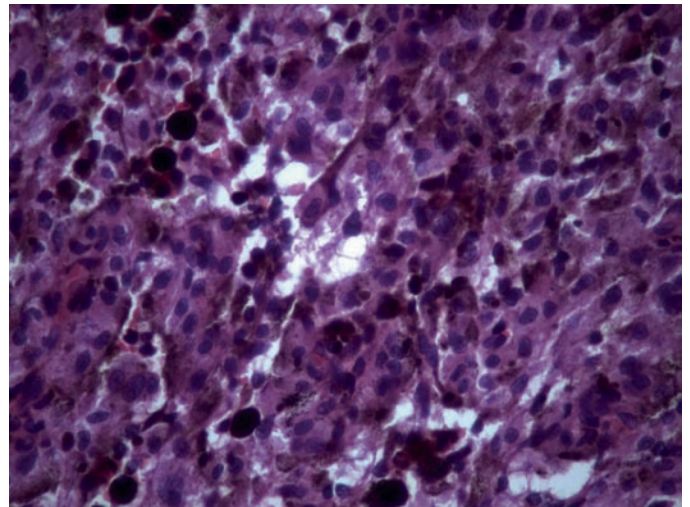
Fig. 23.10. Diffuse pigmentation resulting from melanocytic differentiation as seen here is uncommon in paraganglioma.
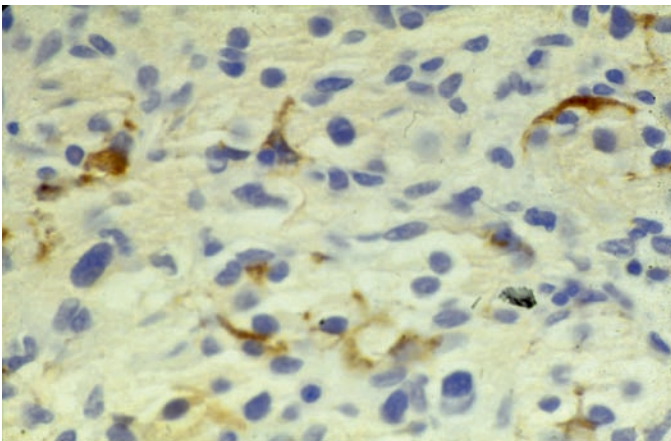
Fig. 23.8. Immunostain for S-100 protein highlights the sustentacular cells.
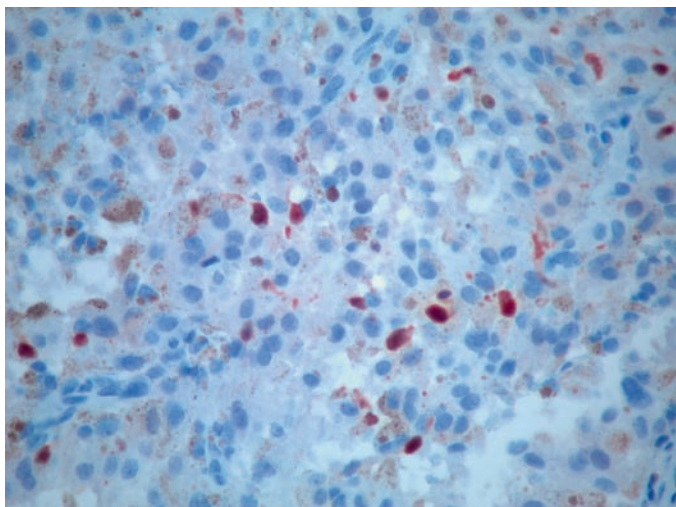
Fig. 23.11. Immunopositivity for S-100 protein in the sustentacular cells allows a differentiation of melanotic paraganglioma from meningeal melanocytoma and malignant melanoma.
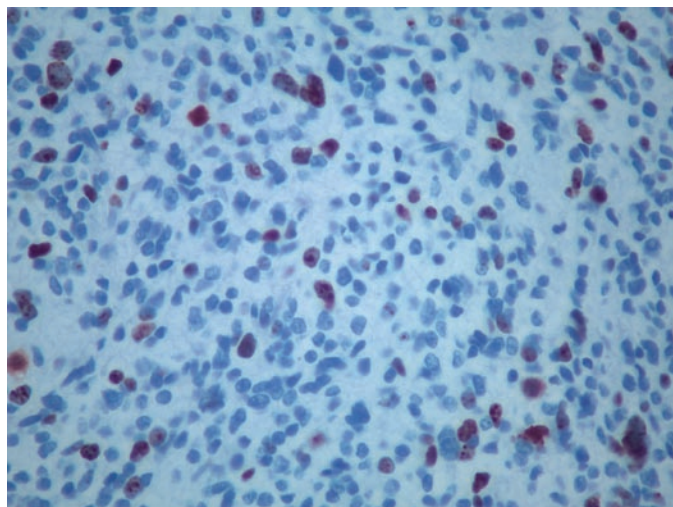
Fig. 23.13. Paragangliomas show variable but generally low proliferation index by immunostaining for Ki-67.
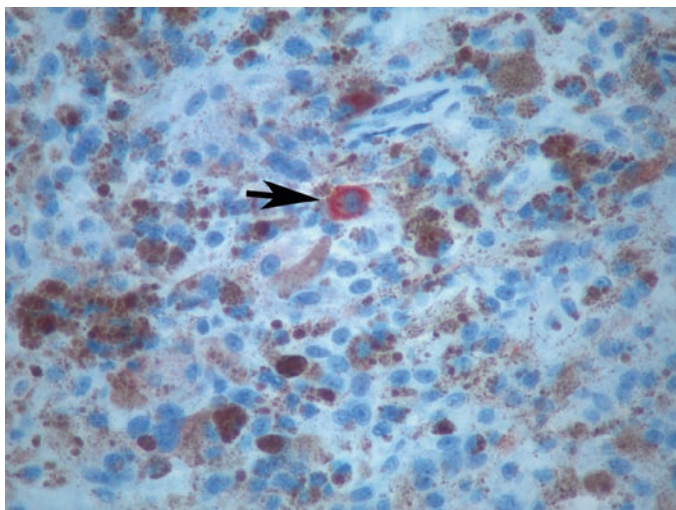
Fig. 23.12. Melanotic paraganglioma demonstrating only a rare cell positivity for HMB-45.

Section F: Neurocutaneous Syndromes

Tarik Tihan

Abstract This section includes a unique set of tumor predisposing syndromes characterized by the presence of cutaneous lesions or tumors, as well as tumors involving the CNS and other organ systems. Notable are the neurofibromatosis 1 and 2, tuberous sclerosis, Von Hippel–Lindau disease, Cowden disease and L'hermitte Duclos disease. Rhabdoid predisposition syndrome represents another member of the group of tumor predisposition syndromes, but it is discussed in a different section along with ATRT.

Neurofibromatosis 1

Tarik Tihan

24.1 OVERVIEW

- Neurofibromatosis 1 (NF1) is an inherited, multisystem disorder that is characterized by the formation of numerous tumors, among which neurofibromas constitute the majority.
- The incidence of NF1 is approximately one in every 2,500–3,000 births.
- A set of diagnostic criteria has been established by the NIH for NF1 as listed below.

24.2 CLINICAL FEATURES

- The diagnosis of NF1 requires two or more of the following:
  - Six or more "cafe-au-lait" macules that are greater than 0.5 cm in children.
  - Two or more cutaneous/subcutaneous neurofibromas or one plexiform neurofibroma.
  - Axillary or groin freckling.
  - Optic glioma; i.e., pilocytic astrocytoma of the optic tract.
  - Two or more Lisch nodules.
  - Bone dysplasia with or without pseudoarthrosis.
  - First degree relative with documented NF1.

24.3 NEUROIMAGING

- Typically the neuroimaging features of lesions in NF1 are those of neurofibromas (Chapter 14) and astrocytic neoplasms. Plexiform neurofibromas are detected radiologically in up to half of all patients with NF1.
- Plexiform neurofibromas appear as heterogeneous masses which extend along nerve fascicles with low T1 signal intensity as compared to brain tissue and can be hyperintense on T2 images with central hypointensity called the "target sign."
  - They may show variable gadolinium enhancement.
  - Plexiform neurofibromas rarely occur intracranially, in which case they can extend into the orbit, cavernous sinus, and paranasal sinuses.
  - Intra or paraspinal plexiform neurofibromas have a slightly higher signal intensity compared to skeletal muscle on T1-weighted images and have variable intensity on T2-weighted images.
  - Pilocytic astrocytomas often involve the optic nerve in a fusiform fashion and are hyperintense on T2-weighted images.
  - Contrast enhanced images demonstrate tumor filling the optic nerve sheath without a cystic component.
  - Pilocytic astrocytomas can also occur outside the optic nerve and are similar to sporadic examples.
- T2-weighted and FLAIR images often demonstrate small, multiple hyperintense lesions within the brainstem, basal ganglia, splenium of the corpus callosum, and cerebellar white matter in patients with NF1.
  - These abnormalities are nonenhancing after contrast, and signal on T1 images is often normal.
  - They appear around the age of 3 years, increase in size and number until age 12, and then decrease subsequently (Figs. 24.1–24.3).

24.4 PATHOLOGY

- Neurofibromas
  - Plexiform neurofibromas are typical of NF1, cause diffuse enlargement of large nerves, and involve multiple roots or fascicles, resulting in a typical "rope-like" or bosselated appearance (Fig. 24.4).
  - Plexiform neurofibromas are microscopically ill defined with a nodular architecture and infiltrative pattern (Fig. 24.5).
  - Some neurofibromas in the setting of NF1 may have cellular and atypical histological features (Fig. 24.6).
- Malignant peripheral nerve sheath tumors (MPNSTs)
  - The majority of MPNSTs that occur in the setting of NF1 are high grade sarcomas.
  - The tumors often have regions resembling benign peripheral nerve sheath tumors, but also harbor pleomorphic, epithelioid, and myxoid patterns (Fig. 24.6).
  - The definition of a high grade MPNST is difficult, but markedly increased mitotic rate, necrosis, and cellular anaplasia are most commonly accepted criteria (see section on MPNST).
- Astrocytomas
  - While most astrocytic neoplasms seen in the setting of NF1 are pilocytic astrocytomas, infiltrating astrocytomas including glioblastomas can also be seen.
  - Macroscopic and histological features of infiltrating astrocytomas in NF1 are essentially identical to those of the sporadic examples.

- Other non-CNS tumors
  - NF1 is associated with an increased incidence of a number of non-CNS neoplasms including the following:
- Soft tissue neoplasms such as rhabdomyosarcoma, juvenile xanthogranuloma, gastrointestinal stromal tumor, and paraganglioma.
- Neuroendocrine neoplasms such as pheochromocytoma, ganglioneuroma, carcinoid tumors, and medullary thyroid carcinoma.

24.5 MOLECULAR PATHOLOGY

- The gene for NF1 was cloned on chromosome 17q11.2 and is composed of 60 exons. The cytoplasmic protein product of the gene is neurofibromin, which acts as a tumor suppressor and is widely expressed in the CNS. Neurofibromin is considered within the GTP-ase activating protein (GAP) family.
- Almost half of the cases represent new mutations, while the rest are familial.
- One of the major functions of neurofibromin is to inactivate p21ras, thereby inhibiting cell proliferation.

24.6 PROGNOSIS

- Prognosis of NF1 is highly dependent on the extent and location, as well as types of tumors in a patient, and is therefore difficult to predict. Features associated with a poor prognosis include the following:
  - Emergence of MPNST.
  - High grade infiltrating astrocytomas.
  - Late-onset long bone fractures with non-union.

SUGGESTED READING

Ferner RE, Golding JF, Smith M, Calonje E, Jan W, Sanjayanathan V, O'Doherty M (2008) [18F]2-fluoro-2-deoxy-D-glucose positron emission tomography (FDG PET) as a diagnostic tool for neurofibromatosis 1 (NF1) associated malignant peripheral nerve sheath tumours (MPNSTs): A long-term clinical study. Ann Oncol 19:390–394

Friedrich RE, Hartmann M, Mautner VF (2007) Malignant peripheral nerve sheath tumors (MPNST) in NF1-affected children. Anticancer Res 27:1957–1960

Ferner RE, Huson SM, Thomas N, Moss C, Willshaw H, Evans DG, Upadhyaya M, Towers R, Gleeson M, Steiger C, Kirby A (2007) Guidelines for the diagnosis and management of individuals with neurofibromatosis 1. J Med Genet 44:81–88

Ferner RE (2007) Neurofibromatosis 1. Eur J Hum Genet 15:131–138

Kluwe L, Tatagiba M, Funsterer C, Mautner VF (2003) NF1 mutations and clinical spectrum in patients with spinal neurofibromas. J Med Genet 40:368–371

Rosser T, Packer RJ (2002) Neurofibromas in children with neurofibromatosis 1. J Child Neurol 17:585–591

Ferner RE, Gutmann DH (2002) International consensus statement on malignant peripheral nerve sheath tumors in neurofibromatosis. Cancer Res 62:1573–1577

Packer RJ, Rosser T (2002) Therapy for plexiform neurofibromas in children with neurofibromatosis 1: An overview. J Child Neurol 17:638–641

Caldemeyer KS, Mirowski GW (2001) Neurofibromatosis type 1. Part I. Clinical and central nervous system manifestations. J Am Acad Dermatol 44:1025–1026

Chung CJ, Armfield KB, Mukherji SK, Fordham LA, Krause WL (1999) Cervical neurofibromas in children with NF-1. Pediatr Radiol 29:353–356

Mukonoweshuro W, Griffiths PD, Blaser S (1999) Neurofibromatosis type 1: The role of neuroradiology. Neuropediatrics 30:111–119

Goldberg Y, Dibbern K, Klein J, Riccardi VM, Graham JM Jr (1996) Neurofibromatosis type 1 – an update and review for the primary pediatrician. Clin Pediatr (Phila) 35:545–561

Riccardi VM (1992) Type 1 neurofibromatosis and the pediatric patient. Curr Probl Pediatr 22:66–106

DiPaolo DP, Zimmerman RA, Rorke LB, Zackai EH, Bilaniuk LT, Yachnis AT (1995) Neurofibromatosis type 1: Pathologic substrate of high-signal-intensity foci in the brain. Radiology 195:721–724

Fig. 24.3. Macroscopic appearance of a plexiform neurofibroma from a 14-year-old boy with NF-1.

Fig. 24.1. Axial T1 MR image showing enlargement and hyperintensity of the right optic nerve in a case of optic nerve glioma.
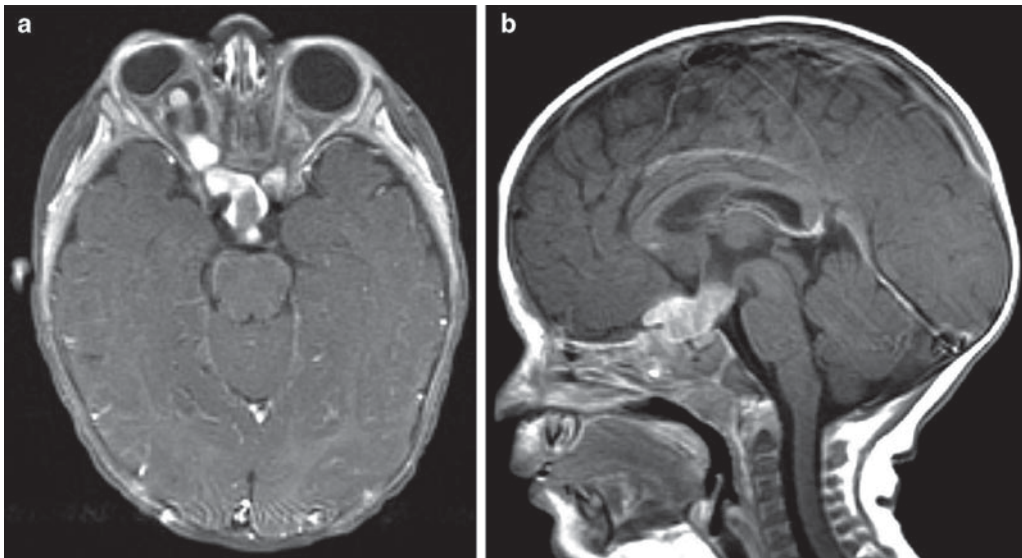
Fig. 24.2. (**a**) Axial T1 weighted MR image and (**b**) coronal T1 weighted MR image, post gadolinium in the same patient as in Fig. 24.1 showing posterior extension of tumor into the optic chiasm and suprasellar region.
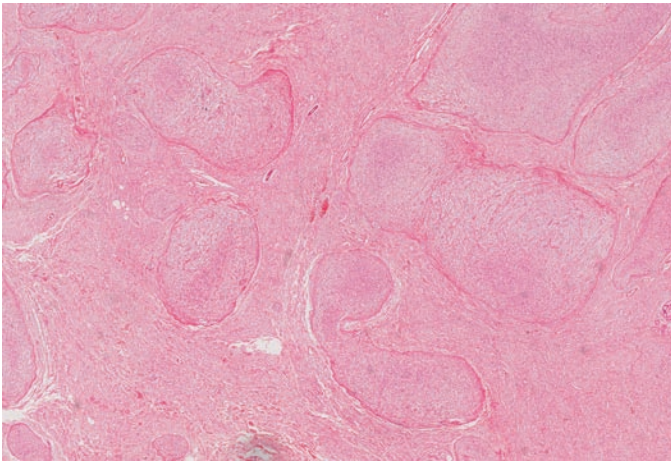
Fig. 24.4. Low power magnification of the plexiform neurofibroma from the 14-year-old boy with NF-1. Note the lobulated appearance and infiltrative pattern.
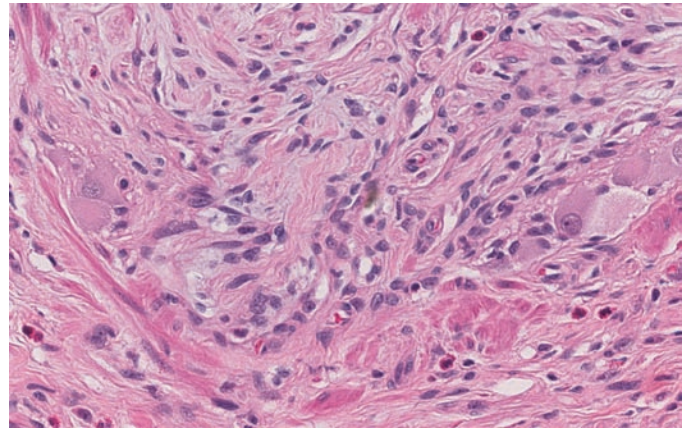
Fig. 24.5. High power magnification of plexiform neurofibroma with scattered atypical nuclei and increased cellularity.
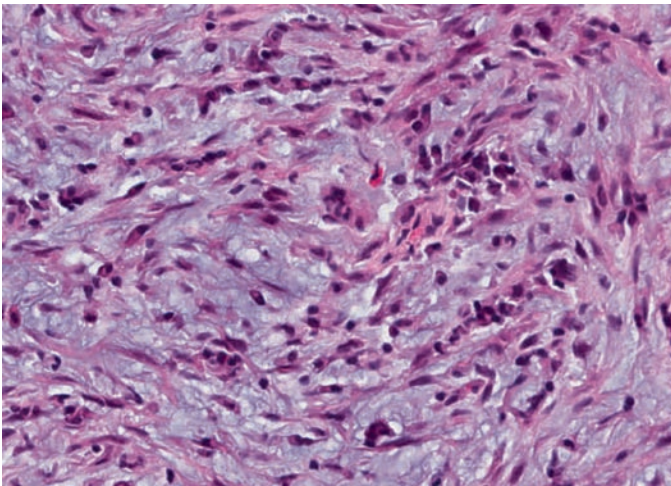
Fig. 24.6. Malignant peripheral nerve sheath tumor arising in the setting of NF-1 with a myxoid stroma.

Neurofibromatosis 2

Tarik Tihan

25.1 OVERVIEW

- Neurofibromatosis 2 (NF2) is an inherited autosomal dominant syndrome that is characterized by formation of numerous circumscribed neoplasms including schwannomas, meningiomas and ependymomas.

25.2 CLINICAL FEATURES

- NF2 has an incidence of approximately one in every 20,000 to 30,000 births.
- The most common tumor associated with the syndrome for all ages is vestibular schwannoma, but meningiomas are just as common in the pediatric population.
- The recently revised diagnostic criteria for NF2 include the following:
  - Bilateral vestibular schwannomas (Fig. 25.1) or
  - Early onset unilateral vestibular schwannoma (<30-years old) *and* two other lesions (schwannoma, meningioma, neurofibroma, glioma, or juvenile cortical cataract).
  - First-degree relative with NF2 *and* two other lesions (schwannoma, meningioma, neurofibroma, glioma, juvenile cortical cataract).
  - Multiple meningiomas *and* unilateral vestibular schwannoma *and* one other lesion (schwannoma, glioma, juvenile cortical cataract).
- Male and females are equally affected, and clinical presentation in children is more diverse than in adults.
- Typically, numerous tumors are present at diagnosis, and a careful search for all components of NF2 is critical.

25.3 NEUROIMAGING

- Neuroimaging features of neoplasms seen in the setting of NF2 are similar to those of sporadic examples and are discussed in their respective sections.
- The modality of choice for imaging NF2 is contrast-enhanced MRI, since small schwannomas and meningiomas are better visualized, as compared to CT.
- Both intracranial and intraspinal schwannomas are present in almost all patients.
  - Schwannomas can be intra or extradural in the spinal cord.
  - They are isointense to spinal cord on T1-weighted images and hyperintense on T2-weighted images.
  - They also show uniform (rarely variable) enhancement on gadolinium.
- Aneurysms and arteriovenous malformations may also be detected on MR imaging.

25.4 PATHOLOGY

- The histologic features of neoplasms seen in the setting of NF2 are similar to their sporadic counterparts and are discussed in their respective sections.
- In addition to the neoplasms mentioned above, the following lesions can be seen:
  - Meningioangiomatosis (Fig. 25.2a)
  - Intraneural schwann cell nodules
  - Heterotopic ependymal clusters, particularly in the spinal cord
  - Cortical hamartomas (Fig. 25.2b)
- Rare examples of other glial neoplasms such as pleomorphic xanthoastrocytoma have been reported in association with NF2.

25.5 MOLECULAR PATHOLOGY

- The gene for NF2 is located on chromosome 22q12 and contains 17 exons, encoding a 595 amino acid protein, Schwannomin (merlin).
- Schwannomin is widely expressed in schwann cells, arachnoid cells, and the lens. The protein functions in linking the actin cytoskeleton to cell membrane glycoproteins.
- The gene product is considered to be a tumor suppressor and regulator of schwann cell and arachnoidal cell proliferation.
- The most common genetic mutations in NF2-related schwannomas and meningiomas span exons 1–15 and involve C>T transitions that change arginine codons to stop codons.

25.6 PROGNOSIS

- Early onset of symptoms is associated with reduced survival in children with NF2.
- In general, children have a slightly less favorable prognosis compared to adults.
- Patients with small vestibular schwannomas at diagnosis (<2 cm in diameter) were shown to have a better survival probability.
- Other variables such as gender, additional tumors in the CNS, or dermal abnormalities do not appear to influence prognosis.

SUGGESTED READING

Ferner RE (2007) Neurofibromatosis 1 and neurofibromatosis 2: a twenty first century perspective. Lancet Neurol 6:340–351

Baser ME (2006) The distribution of constitutional and somatic mutations in the neurofibromatosis 2 gene. Hum Mutat 27:297–306

Otsuka G, Saito K, Nagatani T, Yoshida J (2003) Age at symptom onset and long-term survival in patients with neurofibromatosis Type 2. J Neurosurg 99:480–483

Baser ME, Friedman JM, Aeschliman D, Joe H, Wallace AJ, Ramsden RT, Evans DG (2002) Predictors of the risk of mortality in neurofibromatosis 2. Am J Hum Genet 71:715–723

Mohyuddin A, Neary WJ, Wallace A, Wu CL, Purcell S, Reid H, Ramsden RT, Read A, Black G, Evans DG (2002) Molecular genetic analysis of the NF2 gene in young patients with unilateral vestibular schwannomas. J Med Genet 39:315–322

Antinheimo J, Sallinen SL, Sallinen P, Haapasalo H, Helin H, Horelli-Kuitunen N, Wessman M, Sainio M, Jaaskelainen J, Carpen O (2000) Genetic aberrations in sporadic and neurofibromatosis 2 (NF2)-associated schwannomas studied by comparative genomic hybridization (CGH). Acta Neurochir (Wien) 142:1099–1104

Parry DM, Eldridge R, Kaiser-Kupfer MI, Bouzas EA, Pikus A, Patronas N (1994) Neurofibromatosis 2 (NF2): clinical characteristics of 63 affected individuals and clinical evidence for heterogeneity. Am J Med Genet 52:450–461
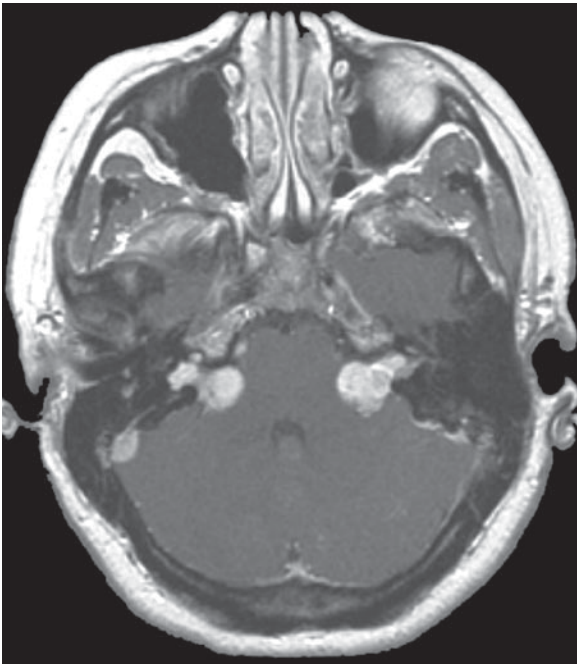
Fig. 25.1. Axial, contrast-enhanced T1-weighted MR image showing bilateral cerebellopontine angle vestibular schwannomas in a 12-year-old child with NF2.
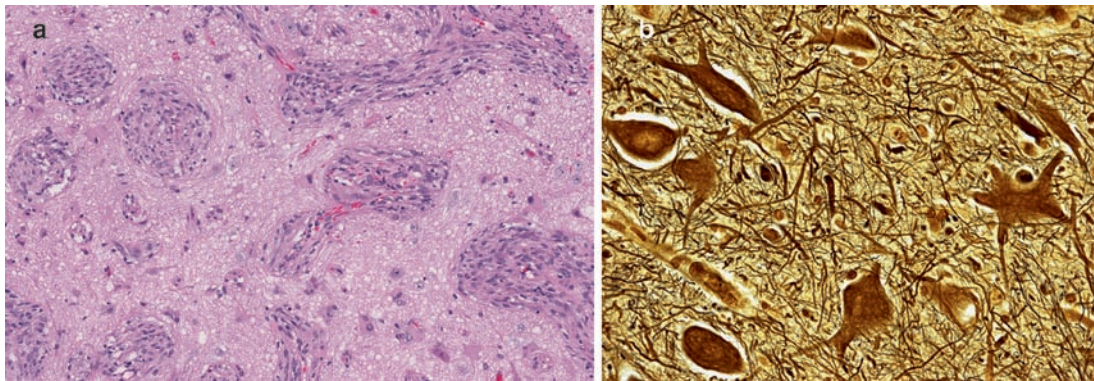
Fig. 25.2. Characteristic histologic features of lesions seen in the setting of NF2 (**a**) meningioangiomatosis and (**b**) dysplastic neurons in cortical hamartia (Bielschowsky stain).

Von Hippel–Lindau Disease

Tarik Tihan and Adekunle M. Adesina

Keywords Von Hippel–Lindau; Hemangioblastoma; Retinal angioma; Pheochromocytoma; Endolymphatic sac tumor

26.1 OVERVIEW

- Von Hippel–Lindau (vHL) disease has been attributed to Eugen von Hippel's descriptions of the retinal angiomatosis in 1904 and Arvid Lindau's descriptions of angiomatous tumors in the cerebellum and spinal cord in 1927. These tumors have subsequently been categorized as hemangioblastomas.
- vHL disease is an autosomal dominant disorder characterized by hemangioblastomas in the cerebellum, spine, and cerebum, retinal angiomas, clear cell renal carcinoma, pheochromocytoma, neuroendocrine tumors or cysts of the pancreas, epididymal cystadenomas, and endolymphatic sac tumors.
- The disease is caused by mutations of the vHL gene located on chromosome 3p25–26.
- The germline mutation is present in the majority of patients with vHL disease. The disease has high penetration, and almost all individuals with germline mutations develop vHL disease during their lifetime.

26.2 CLINICAL FEATURES

- Type 1 vHL syndrome refers to angiomas without pheochromocytoma, and Type 2 refers to angiomas with pheochromocytoma.
- Loss or limited vision is one of the more common presentations of patients with vHL due to retinal hemangioblastomas (angiomas).
- Retinal hemangioblastomas occur in one out of every three patients with vHL disease. They can be multiple, often located in the peripheral retina.
- Patients with cerebellar hemangioblastomas may present with ataxia, dysmetria and coordination difficulties.
- Patients with spinal hemangioblastomas present with various motor or sensory problems based on the tumor location.
- Patients with pheochromocytomas can present with paroxysmal or sustained hypertension.
- Hearing loss is often associated with endolymphatic sac tumors.
- Paraneoplastic polycythemia is seen in some patients with vHL because of decreased inactivation of erythropoietin.

26.3 NEUROIMAGING

- Tumors at various anatomic sites require different modalities, and MRI is the modality of choice for diagnosis, as well as for screening the CNS in patients with vHL syndrome.

- Hemangioblastomas are typically well-defined, solid or solid-cystic masses with a homogenous enhancement of the solid component (Fig. 26.1a–c).
- The solid component shows increased diffusion on ADC maps (Fig. 26.2a, b).
- Endolymphatic sac tumors can be detected both on CT and MRI, and they appear as irregular, bone-destructive masses with "moth-eaten" borders. Most endolymphatic sac tumors have multiple calcified foci, and they variably enhance on contrast administration.
- While CT can be helpful in detecting renal cell carcinomas, some cortical or multifocal tumors cannot be readily detected on CT and may require additional imaging modalities.

26.4 PATHOLOGY

- Hemangioblastomas in vHL syndrome are essentially identical to sporadic hemangioblastomas on histologic grounds (Fig. 26.3a–c) and are discussed in greater detail in the hemangioblastoma section.
- Retinal angiomas are also considered capillary hemangioblastomas and are histologically indistinguishable from cerebellar or spinal examples.
- Endolymphatic sac tumors arise from the petrous aspect of the temporal bone and are characterized by papillary architecture with gland formation in a colloid-like matrix. The papillae are often lined by a single layer of columnar epithelium with variable cytologic atypia. The tumor often shows erosion into the bone and may be associated with an inflammatory infiltrate. Occasionally, cuboidal epithelial cells may have cilia.
- Endolymphatic sac tumors are often positive for cytokeratins, EMA, and Vimentin, and negative for S-100 protein, GFAP, synaptophysin or chromogranin.
- Pheochromocytomas are more common in children with vHL and have histological features identical to sporadic pheochromocytomas.
- Renal cell carcinomas can complicate vHL, but they are distinctly more common in adults.

26.5 MOLECULAR PATHOLOGY

- The vHL gene is located on the short arm of chromosome 3 and encodes a 4.7 kb mRNA with three alternately spliced exons, resulting in two different vHL proteins.
- The vHL protein complexes with a number of other proteins and functions to ubiquitinate various substrates for degradation. Two of the key targets of the vHL protein are hypoxia inducible factors (HIFs), HIF-1alpha and HIF-2alpha.

- Loss of vHL protein results in the accumulation of HIFs that leads to the transcription of numerous hypoxia response genes, such as genes encoding vascular endothelial growth factor (VEGF), and platelet derived growth factor (PDGF).
- The fate of cells lacking vHL gene is increased proliferation, and limited or disrupted differentiation.
- Genetic counseling and screening are critical components of care for vHL patients and their relatives, and should be implemented.

26.6 PROGNOSIS

- The outcome of patients with vHL disease is varied and partly depends on the type of tumors in a given patient.
- The most serious cause of mortality is the presence of renal cell carcinoma, which accounts for about half of all deaths in vHL disease. This is followed by intracranial hemangioblastomas. However, the occurrence of renal cell carcinoma in children with vHL disease is distinctly rare.
- Retinal capillary hemangioblastomas can cause retinal detachment or serious visual loss unless they are detected and treated early.

SUGGESTED READING

Keeler LL III, Klauber GT (1992) Von Hippel-Lindau disease and renal cell carcinoma in a 16-year-old boy. J Urol 147(6):1588–1591

Friedrich CA (2001) Genotype-phenotype correlation in von Hippel-Lindau syndrome. Hum Mol Genet 10(7):763–767

Smirniotopoulos JG (2004) Neuroimaging of phakomatoses: Sturge-Weber syndrome, tuberous sclerosis, von Hippel-Lindau syndrome. Neuroimaging clin N Am 14(2):171–183, vii

Bornfeld N, Kreusel KM (2007) [Capillary hemangioma of the retina in cases of von Hippel-Lindau syndrome. New therapeutic directions]. Ophthalmologe 104(2):114–118
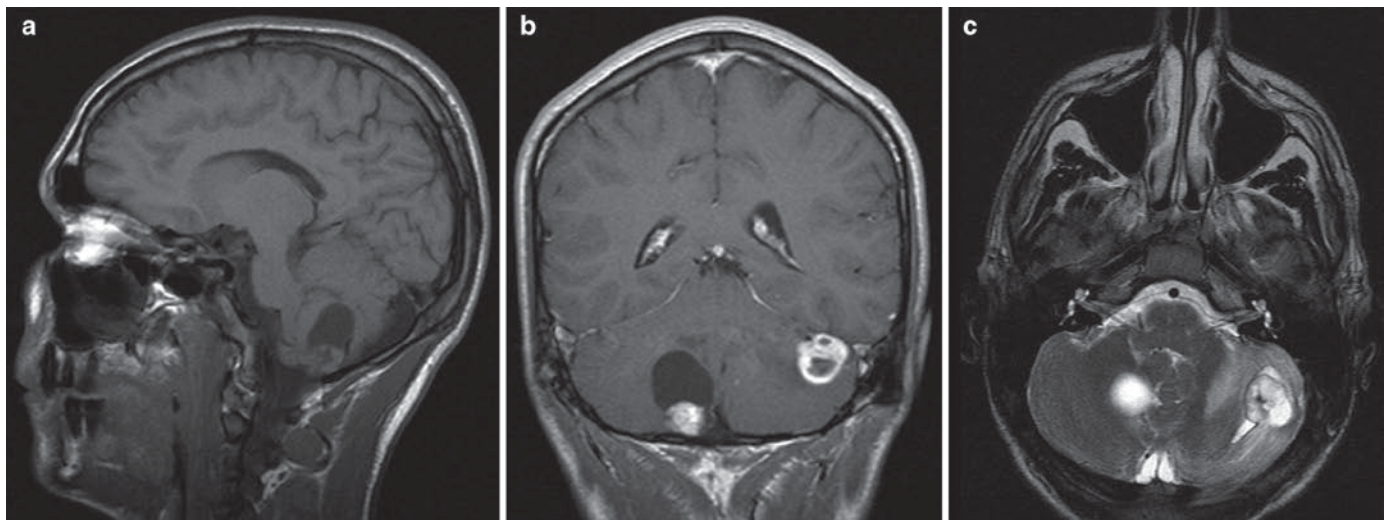
Fig. 26.1. An example of vHL disease with multiple cerebellar lesions, one of which on (**a**) sagittal T1 MRI shows a partially cystic cerebellar mass with isointense mural nodule/solid component. On (**b**) and (**c**) coronal T1 and T2 MRI respectively, it shows a second purely solid lesion with contrast enhancement post gadolinium administration. A third lesion (not shown) was present in the brainstem in this patient.
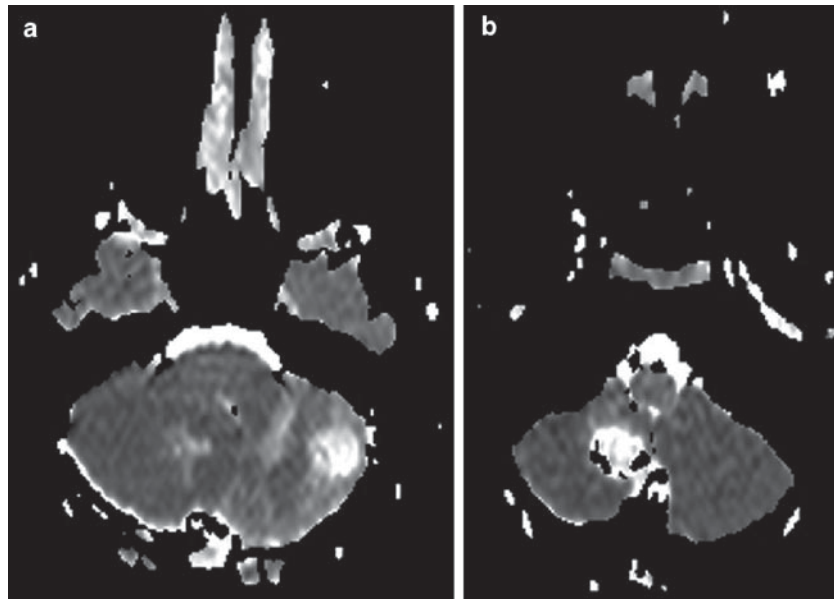
Fig. 26.2. Diffusion weighted images (**a**) and (**b**) showing increased diffusion.
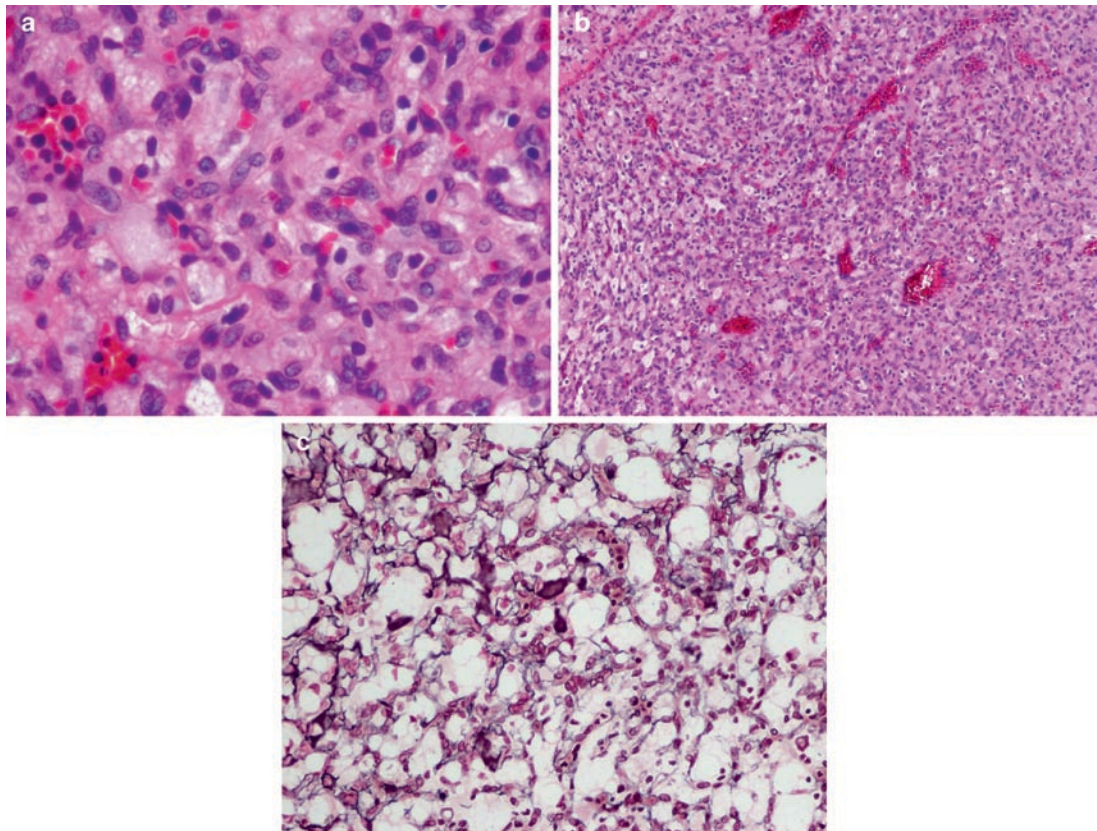
Fig. 26.3. (**a**) Low magnification, and (**b**) high magnification microscopy showing diffuse capillary proliferation with interspersed pale, foamy stromal cells characteristic of hemangioblastoma. (**c**) Reticulin stain outlining the proliferating capillaries.

Tuberous Sclerosis Complex

Tarik Tihan and Adekunle M. Adesina

27.1 OVERVIEW

- Tuberous Sclerosis Complex is an autosomal dominant dysgenetic disorder characterized by hamartomas and neoplasms involving the CNS, as well as various other tissues.
- The causative mutations involve TSC 1 and TSC 2 genes located on 9q and 16p, respectively.
- The definitive diagnosis of TSC is established if at least one major and two minor criteria are present (see below).

27.2 CLINICAL FEATURES

- There are 1–2 million individuals affected by TSC worldwide. TSC has an estimated prevalence of one out of every 5,000–6,000 births.
- About half of TSC patients have a positive family history.
- The MAJOR diagnostic criteria include:
  - Cortical hamartomas (tubers).
  - Subependymal nodules.
  - Subependymal giant cell astrocytoma (SEGA).
  - Retinal nodular hamartomas.
  - Cutaneous angiofibromas or adenoma sebaceum.
  - Angiomyolipomas.
  - Subungual fibromas.
  - Cardiac rhabdomyomas.
  - Pulmonary lymphangioleiomyomatosis.
  - Shagreen patch.
  - Multiple (>3) hypomelanotic macules.
- The MINOR diagnostic criteria include:
  - Hamartomatous rectal polyps.
  - Gingival fibromas.
  - Bone cysts.
  - Hamartomas other than CNS/retina.
  - Multiple renal cysts.
  - Skin lesions (various).

27.3 NEUROIMAGING

- Several characteristic CNS lesions can be seen in patients with TSC:
  - Cortical tubers are often multiple cerebral lesions with variable calcifications, sometimes in a gyriform fashion.
- The MR appearance of cortical tubers varies with the age of the patient; in babies, it is T1 hyperintense and T2 hypointense to white matter, becoming isointense to white matter as the CNS is myelinated, and then changes to T1-hypointense (Fig. 27.1) and T2 hyperintense (Fig. 27.2).
- Cortical tubers typically do not enhance.
  - Subependymal nodules occur along the ventricular surface, and the imaging appearance varies with the age of the patient.
- In infants, the nodules are T1 hyperintense and T2 hypointense.
- With myelination, they are often isointense to white matter on T1-weighted images (Fig. 27.1) and T2-weighted images (Fig. 27.2).
- They show limited and variable enhancement after contrast administration.
  - SEGA is almost entirely an intraventricular tumor and rarely demonstrates a parenchymal component.
- Tumors are isointense to hypointense on T1-weighted images and isointense to hyperintense on T2-weighted images (Fig. 27.3a), and show strong diffuse enhancement on gadolinium administration (Fig. 27.3b).
- They often show increased diffusion on ADC maps (Fig. 27.4).

27.4 PATHOLOGY

- Cortical tubers are firm, wart-like protrusions (Fig. 27.5).
  - They are composed of jumbled-up elements of neuropil with bizarre, ganglion-like cells having short processes. These bizarre cells are often found in clusters in a marked gliotic background with large collections of glial processes (Fig. 27.6).
  - Microcalcifications are often present.
- Subependymal nodules are often calcified and partially covered by a layer of ependymal cells.
  - They are mostly composed of large cells with glial phenotypes and multinucleated cells with extensive glial processes.
  - There is little or no cytological difference between the predominant cell in a subependymal nodule and the cells of SEGA.
  - Most cells in subependymal nodules have an ambiguous expression of glial and neuronal markers as in SEGA.
- SEGA is a well-circumscribed neoplasm and is considered WHO grade I.
  - The tumor is characterized by gemistocyte-like cells with ample glassy, eosinophilic cytoplasm (Fig. 27.7a) and eccentric nuclei with prominent nucleoli in a "streaming" pattern (Fig. 27.7b, c).
  - This pattern portends a more spindled morphology to some of the tumor cells, and some tumors may display a striking pleomorphism.
  - There is a striking glial background with rich fibrillarity.

- There are often binucleated or occasionally multinucleated cells, as well as rare mast cells within the neoplasm.
- Some tumors demonstrate perivascular lymphocytic infiltrates.
- Rare mitotic figures can be encountered in SEGA.
- Exceptional cases demonstrate necrosis, but this is often in the form of geographic necrosis.
- Microcalcification may be present (Fig. 27.7d).

27.5 IMMUNOHISTOCHEMISTRY

- Ganglion-like cells in cortical tubers often show a strong positivity for vimentin (Fig. 27.8a) and weak to no staining for NFP (Fig. 27.8b) and GFAP (Fig. 27.8c).
  - In contrast, dysmorphic neurons, which are also often seen in tubers, demonstrate positivity for NFP (Fig. 27.8b).
- SEGA is variably positive for GFAP and S-100 protein antibodies.
  - Although the tumor cells are typically GFAP positive, many cells in SEGA demonstrate an ambiguous glial/neuronal immunohistochemical pattern, as in subependymal nodules.
  - The proliferation indices are often very low.
  - Neuronal antibodies, such as neurofilament proteins, class III beta-tubulin, synaptophysin and Neu-N are only focally positive in a small percentage of the cells, but the staining is variable among tumors.

27.6 ELECTRON MICROSCOPY

- SEGA shows evidence of glial as well as neuronal differentiation, including microtubules, occasional dense-core granules, and, rarely, synapses can be observed.

27.7 MOLECULAR PATHOLOGY

- Linkage studies have provided evidence for two distinct TSC loci on chromosome 9q34 (TSC1), and on chromosome 16p13.3 (TSC2).
- TSC1 and TSC2 gene products are components of a heterodimer that is critical in the regulation of a number of cellular functions, including proliferation, and are considered to be tumor suppressor genes.

- Gene products, tuberin and hamartin, form a complex and integrate and transmit cellular growth factor and stress signals to the PI3K/PKB signaling pathway, and negatively regulate mTOR activity.
- Loss of both TSC1 and TSC2 seems to result in a similar clinical picture, supporting the suggestion that both the genes are involved in the same regulatory pathway.
- Mutations of the TSC2 gene are more common than those of the TSC1 gene.
- Virtually all mutations of TSC1 seem to result in a truncated gene product.
- Mutations in the TSC2 gene are more varied and include deletions, missense, nonsense, frameshift deletions/insertions and splice junction mutations.

27.8 PROGNOSIS

- SEGA is essentially a benign neoplasm and can often be cured by resection.
- In recent years, rapamycin therapy has been suggested for cases where a gross total resection cannot be achieved.
- Even though prognosis of SEGA is quite favorable, the overall prognosis of TSC patients is dependent on the extent of CNS, as well as extra-CNS lesions.

SUGGESTED READING

Short MP, Richardson EP Jr, Haines JL, Kwiatkowski DJ (1995) Clinical, neuropathological and genetic aspects of the tuberous sclerosis complex. Brain Pathol 5(2):173–179

Roach ES, Gomez MR, Northrup H (1998) Tuberous sclerosis complex consensus conference: revised clinical diagnostic criteria. J Child Neurol 13(12): 624–628

Christophe C, Sekhara T, Rypens F et al (2000) MRI spectrum of cortical malformations in tuberous sclerosis complex. Brain Dev 22(8):487–493

Hyman MH, Whittemore VH (2000) National Institutes of Health consensus conference: tuberous sclerosis complex. Arch Neurol 57(5):662–665

Marcotte L, Crino PB (2006) The neurobiology of the tuberous sclerosis complex. Neuromolecular Med 8(4):531–546

Schwartz RA, Fernandez G, Kotulska K, Jozwiak S (2007) Tuberous sclerosis complex: advances in diagnosis, genetics, and management. J Am Acad Dermatol 57(2):189–202

Datta AN, Hahn CD, Sahin M (2008) Clinical presentation and diagnosis of tuberous sclerosis complex in infancy. J Child Neurol 23(3):268–273
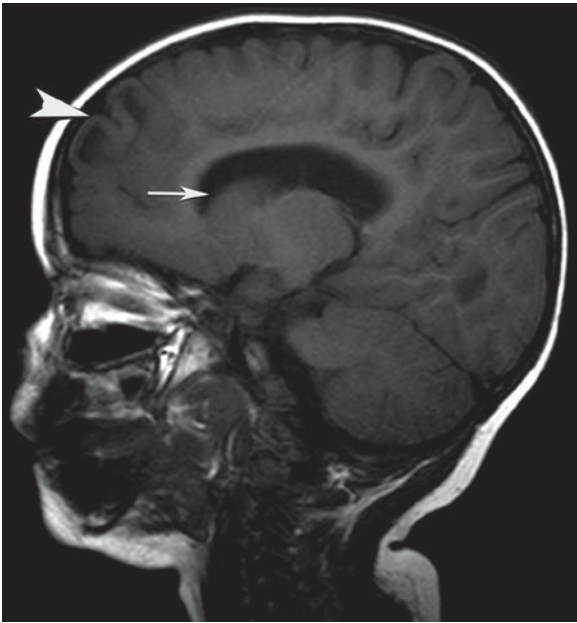
Fig. 27.1. Sagittal T1 MR image showing hypointense lesions in the frontal lobe consistent with tubers.
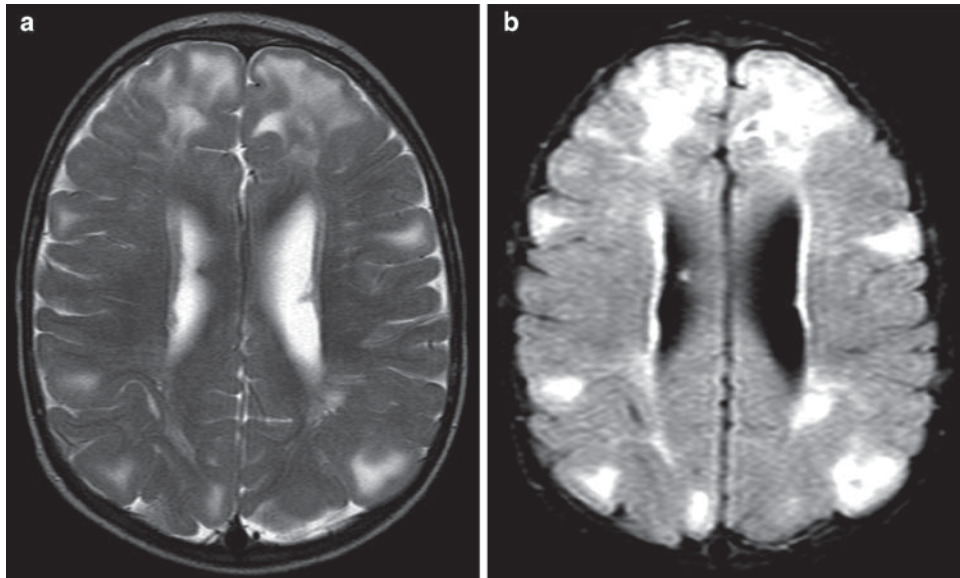
Fig. 27.2. (**a**) Axial T2 MR image with multiple subcortical white matter hyperintensities, and (**b**) axial FLAIR with multiple subcortical hyperintensities, consistent with tubers.
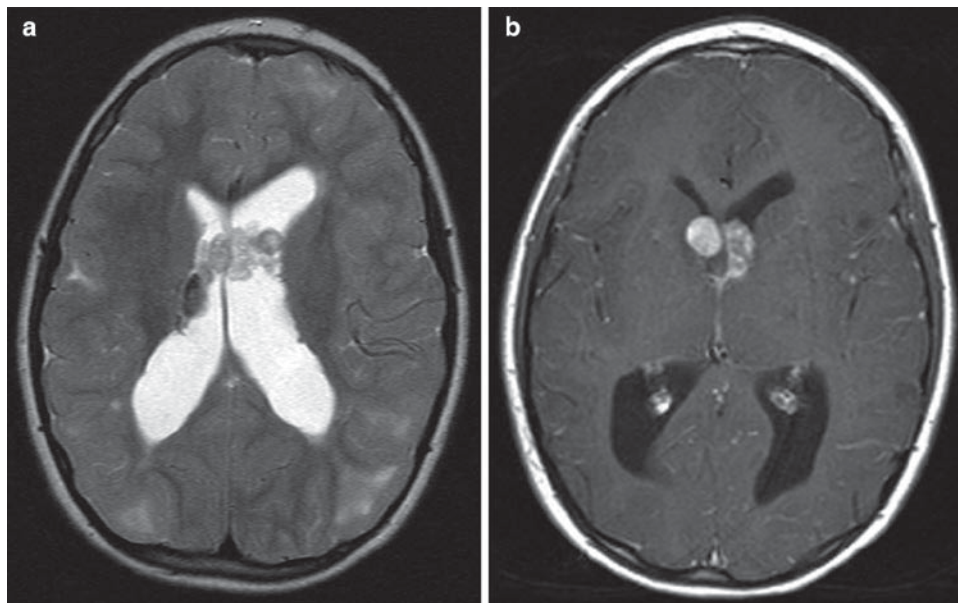
Fig. 27.3. SEGA seen as intraventricular hyperintense mass on (**a**) Axial T2 MR image, and (**b**) showing moderate enhancement on axial T1 MR image, post-contrast.
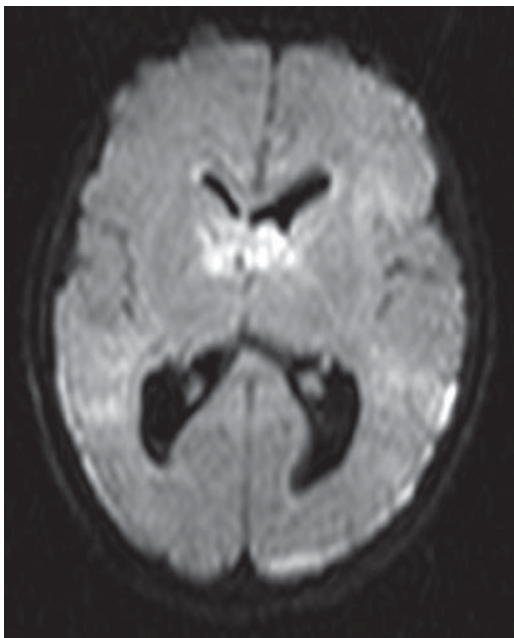
Fig. 27.4. SEGA showing increased diffusion on diffusion weighted images.
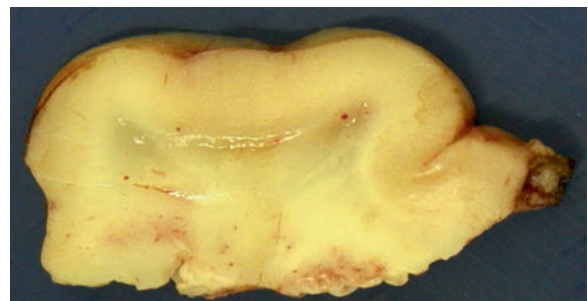
Fig. 27.5. Cortical pallor with poor gray white matter distinction is seen in this coronal section of a cortical tuber.
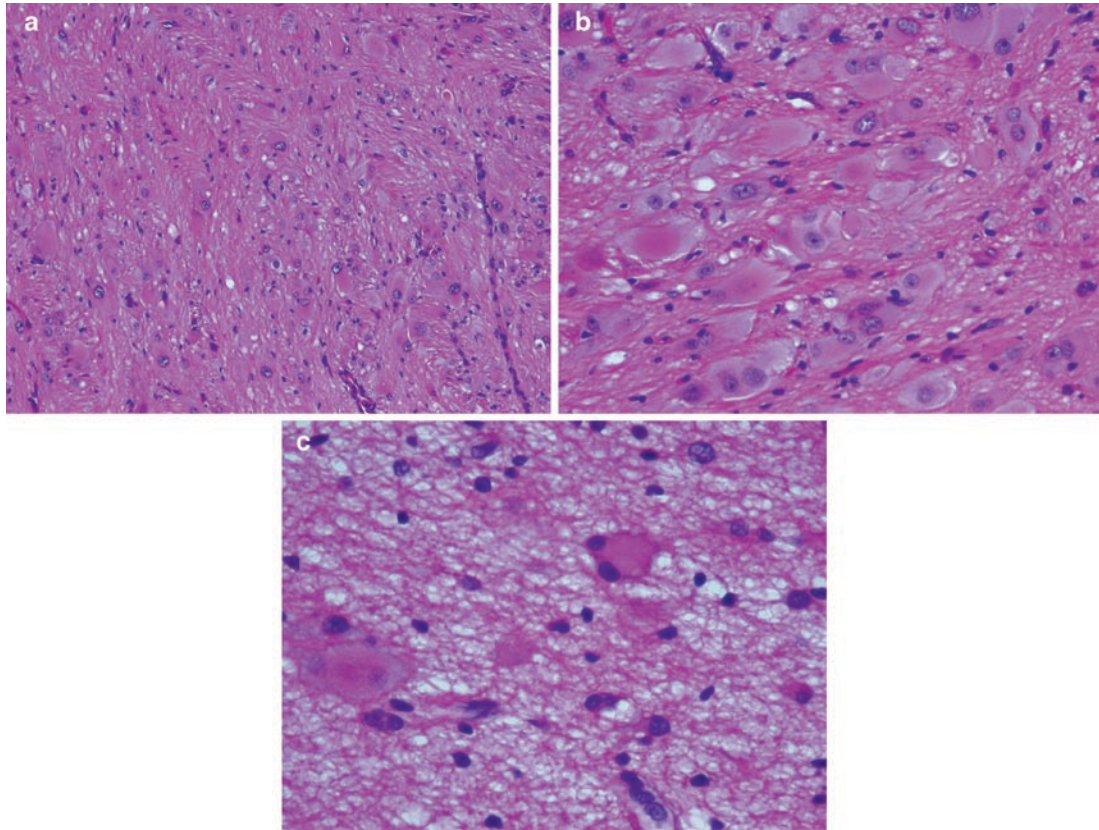
Fig. 27.6. (**a**) Low magnification, (**b**) high magnification microscopy of the cortex, and (**c**) white matter of a cortical tuber showing the characteristic "disorderly" arrangement of ballooned neurons in a densely fibrillary and "gliotic" neuropil.
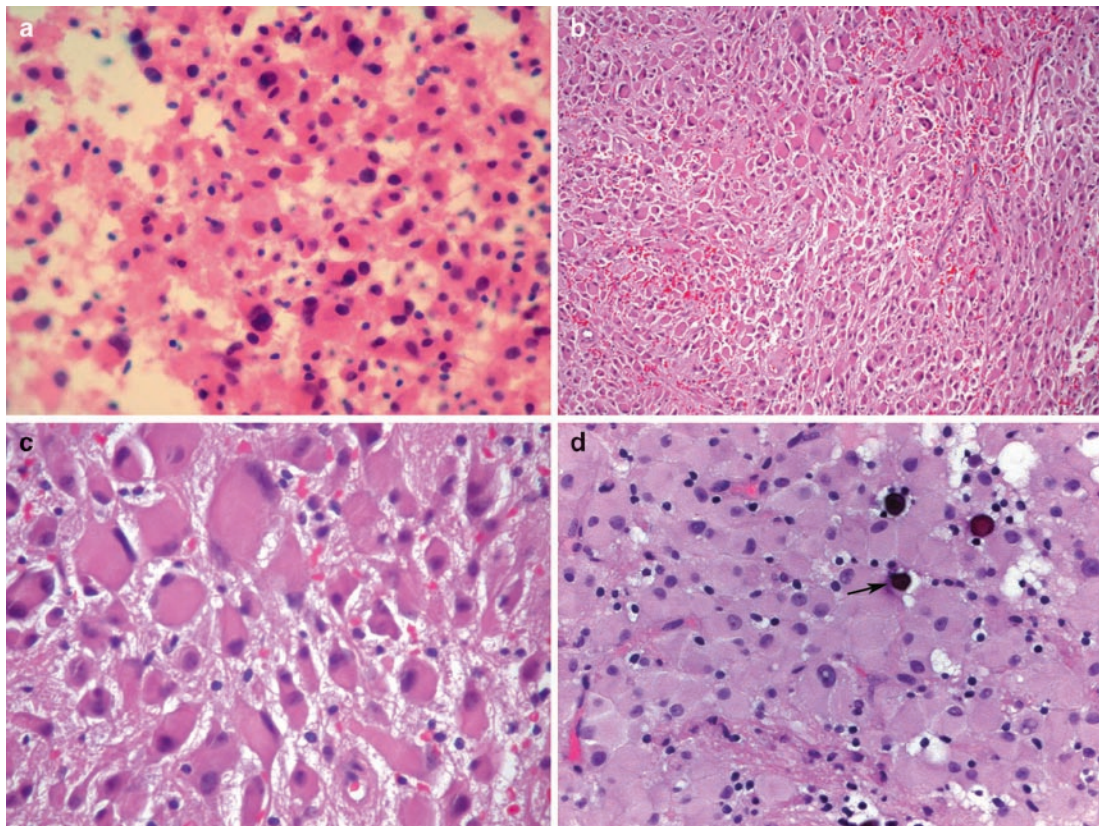
Fig. 27.7. (**a**) Intraoperative cytologic preparation of a SEGA showing the characteristic plump gemistocytic astrocyte-like cells. The same cells are seen in tissue sections from the same tumor in (**b**) and (**c**). (**d**) Another example of a SEGA with microcalcifications (*arrow*).
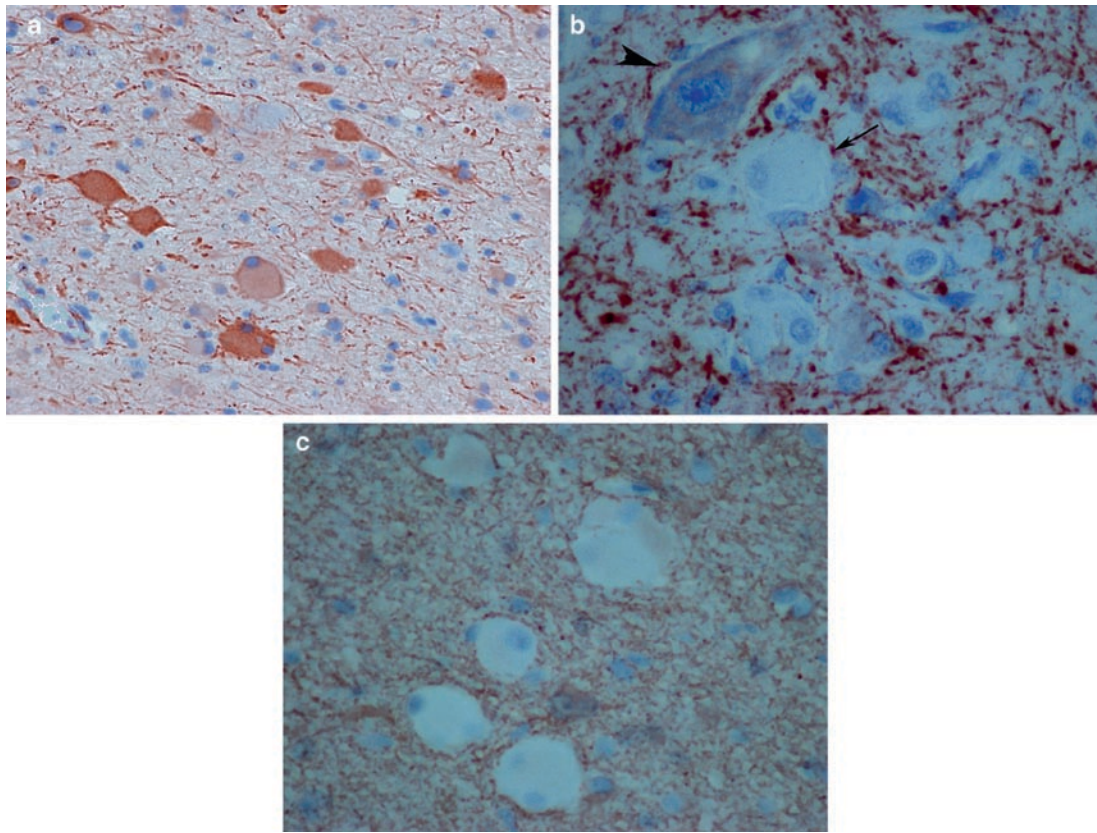
Fig. 27.8. Immunostains of cortical tubers showing (**a**) diffuse positivity for vimentin, (**b**) a ballooned cell (arrow) and a dysmorphic neuron (*arrow head*) with negative and a weak positivity for NFP, respectively. (**c**) Variable weak to no positivity for GFAP in the ballooned cells of a cortical tuber.

L'hermitte–Duclos Disease and Cowden Disease

T. Hidehiro, S. Hiroyoshi, and Adekunle M. Adesina

Keywords L'hermitte–Duclos disease; Dysplastic gangliocytoma of the cerebellum; Cowden disease

28.1 OVERVIEW

28.1.1 L'hermitte–Duclos Disease

- L'hermitte–Duclos disease (LDD) also known as dysplastic cerebellar gangliocytoma is a rare slowly enlarging cerebellar mass lesion composed of dysplastic ganglion cells.
- It has features of both hamartoma and benign neoplasm (WHO grade I).
- The exact incidence is unknown although most reports indicate that this is a rare condition.
- In the cerebellum, no cases of gangliocytoma have been reported except in the context of LDD.

28.1.1 Cowden Disease

- Cowden disease (CD) is an autosomal dominant disorder with age-related penetrance.
- The incidence of CD is estimated at 1/200,000–250,000, which is probably underestimated due to underrecognition of this disease.
- It is characterized by multiple hamartomas in a variety of tissues (i.e., multiple hamartoma syndrome) and a high risk of breast, thyroid, and endometrial cancers.
- It is caused by germline mutations in the *PTEN* gene, a tumor suppressor gene located at chromosome10q23.3, and is allelic to the Bannayan–Riley–Ruvalcaba syndrome with overlapping clinical phenotypes.
- When the diagnosis of CD is made, a long-term follow-up of the patient, as well as a thorough familial screening (and genetic consultation) is necessary.

28.1.3 Association Between LDD and CD

- LDD may occur as a sporadic, isolated disease or in association with CD.
- LDD is listed as one of the major diagnostic criteria of CD established by the International Cowden Consortium.
- The frequency of LDD in patients with CS is unknown.
- In most cases, the diagnosis of LDD precedes the final diagnosis of CD.
- All patients with LDD must be thoroughly investigated for concomitant neoplasms associated with CD.

28.2 CLINICAL FEATURES

28.2.1 L'hermitte–Duclos Disease

- LDD presents with a longstanding history of vague neurological symptoms or cerebellar signs related to a progressive posterior fossa mass. Additional signs and symptoms attributable to increased intracranial pressure may be seen.
- Occasionally manifests as sudden neurological deterioration due to acute or decompensated chronic hydrocephalus.
- Most cases have been identified in young adults, although there is reportedly a broad range of age at diagnosis from neonatal period to the eighth decade of life.
- The treatment is surgical resection for decompression of the posterior fossa. Recurrence is not rare, probably due to the ill-defined margins of the lesion that preclude complete excision, however, no malignant transformation has so far been reported.

28.2.2 Cowden's Disease

- Cowden's disease presents with pathognomonic mucocutaneous lesions, characterized by facial trichilemmomas, acral keratosis, and papillomatous papules, which occur in over 90% of patients.
- Other tumors which are part of the major diagnostic criteria include breast carcinoma, thyroid (non-medullary) carcinoma, macrocephaly (megalencephaly), LDD, and endometrial carcinoma.
- CNS manifestations reported include LDD, mental retardation (minor diagnostic criterion), and vascular malformations (e.g., venous and cavernous angiomas)/developmental venous anomalies.

28.3 NEUROIMAGING OF LDD

- MRI demonstrates the characteristic "tiger-striped" appearance of the cerebellum and this feature is often sufficient for diagnosis, although the histopathological findings definitively confirm the diagnosis.
- On T2-weighted MR images, the lesion has a unique striated pattern consisting of alternating bands of high signal intensity and normal signal intensity relative to cerebellar gray matter (Fig. 28.1).
- On T1-weighted MR images, the striations are hypointense and isointense, respectively, to cerebellar gray matter, with

- slight or no enhancement following gadolinium-DTPA administration.
- Evidence of mass effect and hydrocephalus is common with the compression of the fourth ventricle and occasional tonsillar herniation.

28.4. PATHOLOGY

28.4.1. Histopathology of LDD

- Macroscopically, thickened and distorted folia are observed.
- Microscopically, overgrowth of dysplastic/hypertrophic ganglion cells with massive replacement of the internal granule cell layer of cerebellum is seen (Fig. 28.2a, b).
- The overlying molecular layer contains abnormally myelinated fibers, in parallel arrays primarily in its outer portion (Fig. 28.2c), which are highlighted with myelin stain (Luxol Fast Blue) (Fig. 28.2d). Increased cellularity composed of neuronal elements may be seen in the molecular layer or subpial region.
- The Purkinje cell layer is attenuated or absent.
- Microscopic calcification and hypervascular parenchyma is common.
- Vacuolization of the cerebellar white matter and molecular layer is often seen.
- Mitotic figures are absent.

28.5. IMMUNOHISTOCHEMISTRY OF LDD

- Dysplastic ganglion cells express neuronal markers including synaptophysin (ring-like pattern of membranous labeling (Fig. 28.3a), neurofilament protein (Fig. 28.3b) and neuronal nuclear antigen (NeuN) (Fig. 28.3c)). NeuN immunoreactivity is characteristically seen in native granule cell neurons, but is not usually expressed by Purkinje cells and dentate nuclei neurons in the cerebellum.
- The MIB-1 (Ki-67) labeling index of dysplastic ganglion cells is usually zero.
- Loss of *PTEN* protein (Fig. 28.4a) and expression of phospho-*AKT* and phospho-*S6* (Fig. 28.4b) is reportedly observed in the dysplastic ganglion cells, indicating activation of the *PTEN/AKT/mTOR* pathway.
  - Demonstrable mTOR positivity supports this hypothesis (Fig. 28.4c).

28.6. MOLECULAR PATHOLOGY

- Germline intragenic mutations in *PTEN* are detectable in approximately 80% of patients with CD. Most germline *PTEN* mutations are found in exon 5 (31.5%), which encodes for the phosphatase core motif.
  - *PT*EN is a tumor suppressor gene, which codes for a phosphatase that negatively regulates the phosphatidylinositol 3-kinase (*PI3K*)/*Akt/mTOR* pathway. *mTOR* phosphorylates *ribosomal S6 kinase (S6K)* which, in turn, leads to increased levels of *phospho-S6*.
  - Proper *PTEN* signaling leads to G1 cell-cycle arrest and/or apoptosis.
- Mutations in the *PTEN* promoter are reported to account for a subset of apparently mutation-negative patients with CD.

- Mouse studies reveal that selective inactivation of *Pten* in cerebellar neurons results in a progressive increase in neuronal soma size with no change in cell number, producing a phenotype with striking similarities to human LDD, and elevated phosphorylation of *Akt*.
- It is reported that a *PTEN* mutation was detected in all tissue samples from patients with adult-onset LDD, in contrast to samples from patients with childhood-onset LDD, which were all found to be without mutations.
- Immunohistochemical pattern of *PTEN*(−)/phospho-*AKT*(+)/*mTOR*(+)/phospho-*S6*(+), seen in dysplastic ganglion cells in LDD, indicates dysregulation of the *PTEN/AKT/mTOR* pathway, which supports the hypothesis that this signaling pathway plays a major role in histogenesis of LDD.

27.7. DIFFERENTIAL DIAGNOSIS OF LDD – CEREBELLAR GANGLIOGLIOMA

- The main differential diagnosis of LDD is cerebellar ganglioglioma (GG) which is an uncommon tumor in the posterior fossa.
- LDD may have areas of reactive glial cells in addition to typical dysplastic ganglion cells, thus raising GG as a major histologic differential diagnosis, especially in a small biopsy.
- The histological distinction between "reactive" glial cells in LDD and "neoplastic" glial cells in GG is virtually impossible.
- The most common presenting symptoms of cerebellar GG are similar to those of LDD, in contrast to supratentorial GGs, which commonly present with a long history of seizures.
- Radiologically, nearly half of cerebellar GG are cystic and the majority also show contrast enhancement. Without clinicoradiological correlation, the histologic distinction from LDD may be very difficult.

SUGGESTED READING

Eberhart CG, Wiestler OD, Eng C (2007) Cowden disease and dysplastic gangliocytoma of the cerebellum/ Lhermitte-Duclos disease. In: Louis DN, Ohgaki H, Wiestler OD, Cavenee WK (eds) World Health Organization classification of tumours of the central nervous system. IARC Press, Lyon, pp 226–228

Eng C (2000) Will the real Cowden syndrome please stand up: revised diagnostic criteria. J Med Genet 37:828–830

Lok C, Viseux V, Avril MF et al (2005) Brain magnetic resonance imaging in patients with Cowden syndrome. Medicine 84:129–136

Tan WH, Baris HN, Burrows PE et al (2007) The spectrum of vascular anomalies in patients with PTEN mutations: implications for diagnosis and management. J Med Genet 44:594–602

Meltzer CC, Smirniotopoulos JG, Jones RV (1995) The striated cerebellum: an MR imaging sign in Lhermitte-Duclos disease (dysplastic gangliocytoma). Radiology 194:699–703

Abel TY, Baker SJ, Fraser MM et al (2005) Lhermitte-Duclos disease: a report of 31 cases with immunohistochemical analysis of the PTEN/AKT/mTOR pathway. J Neuropathol Exp Neurol 64:341–349

Rosenblum MK, Yachnis AT (2006) Dysplastic gangliocytoma of the cerebellum (Lhermitte-Duclos disease). In: McLendon RE, Rosenblum MK, Bigner DD (eds) Russell & Rubinstein's pathology of tumors of the nervous system, 7th edn. Hodder Arnold, London, pp 379–389

Wolf HK, Buslei R, Schmidt-Kastner R et al (1996) NeuN: a useful neuronal marker for diagnostic histopathology. J Histochem Cytochem 44: 1167–1171

Waite KA, Eng C (2002) Protean PTEN: form and function. Am J Hum Genet 70:829–844

Liaw D, Marsh DJ, Li J et al (1997) Germline mutations of the *PTEN* gene in Cowden disease, an inherited breast and thyroid cancer syndrome. Nat Genet 16:64–67

Marsh DJ, Coulon V, Lunetta KL et al (1998) Mutation spectrum and genotype-phenotype analysis in Cowden disease and Bannayan-Zonana syndrome, two hamartoma syndromes with germline *PTEN* mutation. Hum Mol Genet 7:507–515

Bonneau D, Longy M (2000) Mutation of the human *PTEN* gene. Hum Mutat 16:109–122

Zhou XP, Waite KA, Pilarski R et al (2003a) Germline *PTEN* promoter mutations and deletions in Cowden/Bannayan-Riley-Ruvalcaba syndrome result in aberrant *PTEN* protein and dysregulation of the phosphoinostol-3-kinase/ Akt pathway. Am J Hum Genet 73:404–411

Backman SA, Stambolic V, Suzuki A et al (2001) Deletion of Pten in mouse brain causes seizures, ataxia and defects in soma size resembling Lhermitte-Duclos disease. Nat Genet 29:396–403

Zhou XP, Marsh DJ, Morrison CD et al (2003b) Germline inactivation of *PTEN* and dysregulation of the phosphoinositol-3-kinase/Akt pathway cause human L'hermitte-Duclos disease in adults. Am J Hum Genet 73:1191–1198
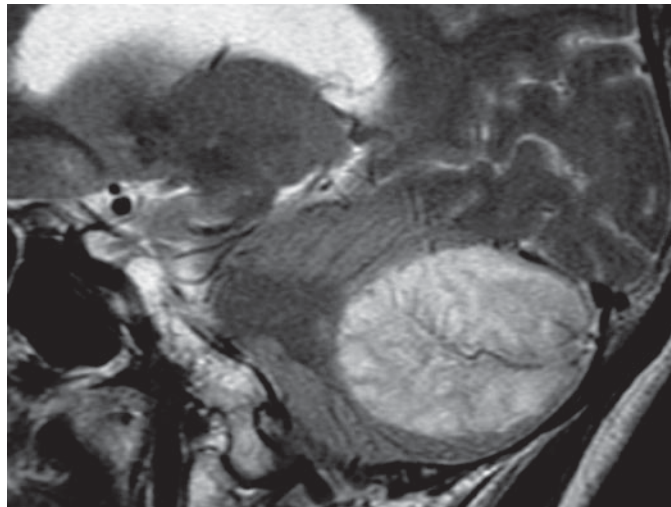
Fig. 28.1. T2-weighted MR images, showing a striated tigroid pattern consisting of alternating bands of high signal intensity and normal signal intensity in the cerebellum.
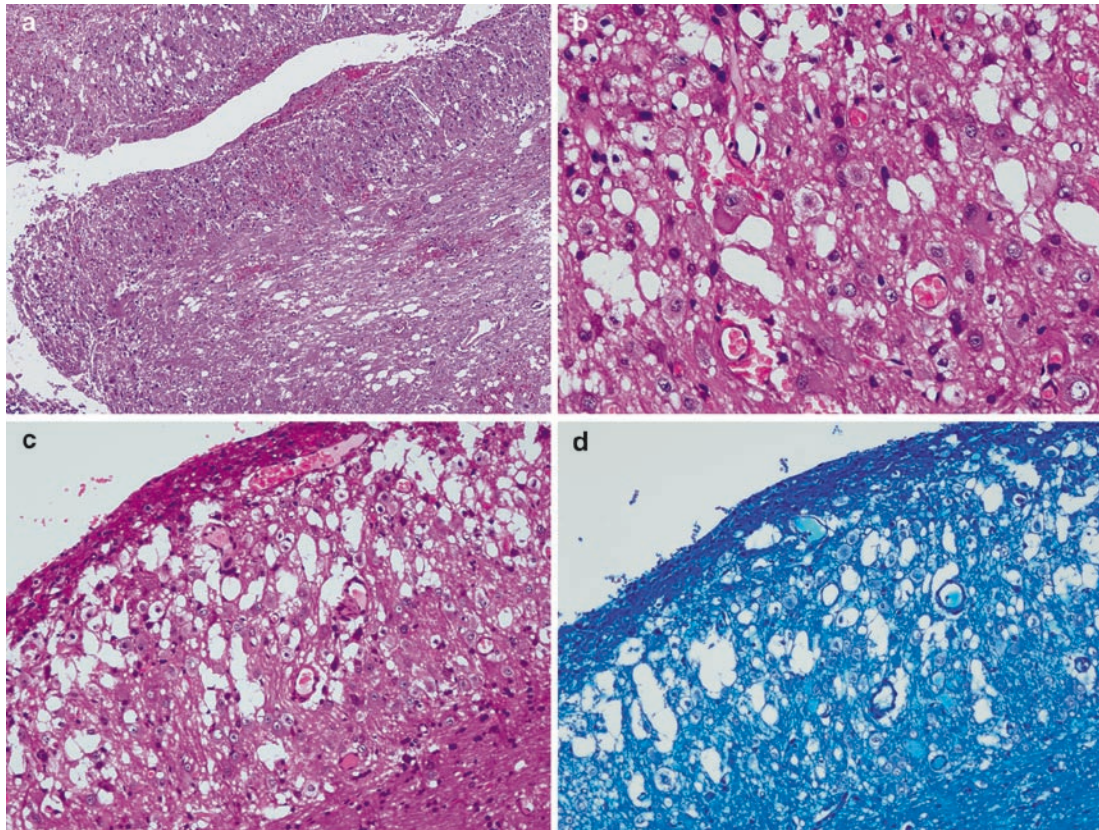
Fig. 28.2. (**a**, **b**) Cerebellum showing distortion of normal cerebellar architecture by overgrowth of dysplastic/hypertrophic ganglion cells with massive replacement of the internal granule cell layer of the cerebellum. (**c**) Abnormally myelinated fibers in parallel arrays are seen in the peripheral region of the molecular layer and are highlighted with the (**d**) LFB (myelin) stain.
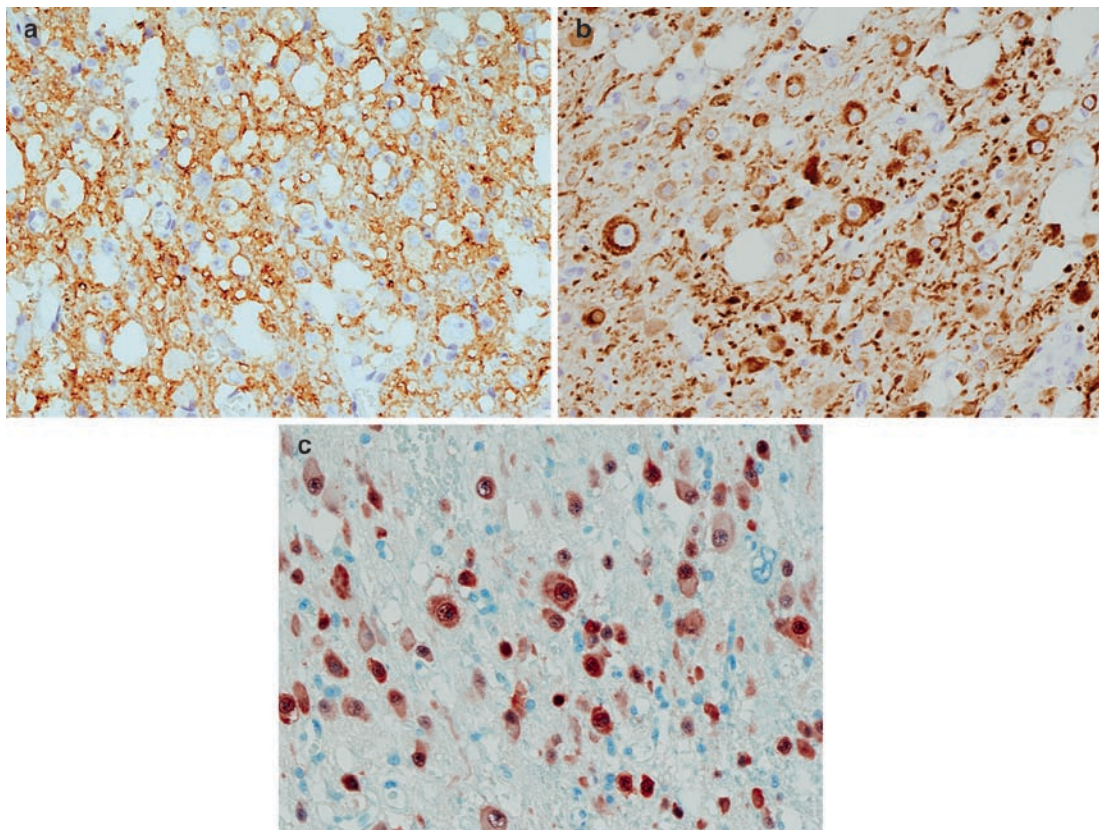
Fig. 28.3. Dysplastic ganglion cells are identified by neuronal markers including (**a**) synaptophysin with cells displaying a ring-like pattern of membranous labeling, (**b**) neurofilament protein and (**c**) NeuN.
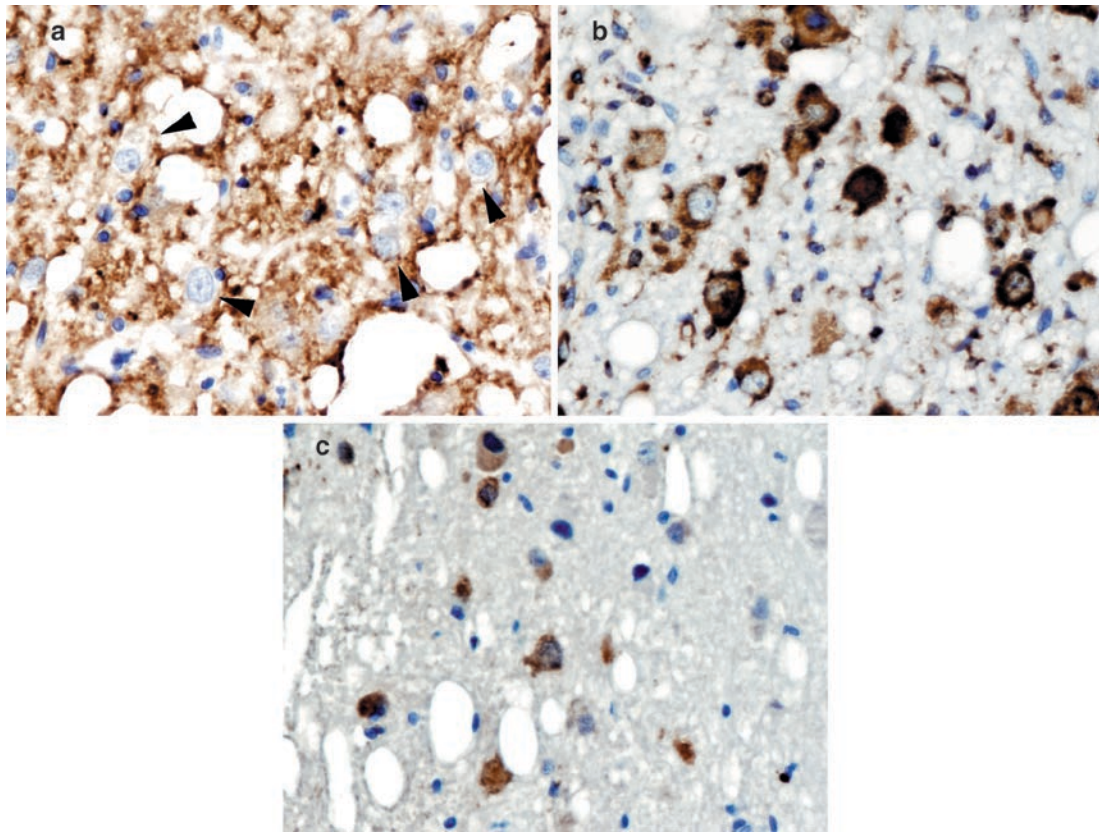
Fig. 28.4. Dysplastic ganglion cells showing (**a**) loss of *PTEN* protein expression (*arrow*). The loss of PTEN expression is associated with downstream expression and immunopositivity for (**b**) phospho-S6, and (**c**) mTOR and is consistent with constitutive activation of the *PTEN/AKT/mTOR* pathway.

Section G: Tumors in the Region of the Pituitary Fossa

Tarik Tihan

Abstract This section presents the diverse tumors that occur in the region of the pituitary fossa including pituitary adenoma, pituicytoma and rare entities like granular cell tumor and spindle cell oncocytoma followed by craniopharyngioma.

Pituitary Tumors

Tarik Tihan and Christine E. Fuller

29.1 OVERVIEW

- *Pituitary adenomas*:
  - Benign neoplasms arising from adenohypophysis and are reviewed within the context of tumors of endocrine organs in WHO classification schemes.
  - Represent the most common lesion of the pituitary fossa/sella region. Most are sporadic, although a small percentage arise in the context of Multiple Endocrine Neoplasia (MEN) type 1, in association with hyperplasia/neoplasia of the pancreas and parathyroid adenomas.
  - They are distinctly less common in children than in adults; less than 10% of all pituitary adenomas present in the pediatric age group.
- They are approximately twice as common in females than in males.
  - By convention, macroadenomas are >10 mm while microadenomas are <10 mm in dimension. The former are more frequently nonfunctioning from a hormonal standpoint, while most microadenomas come to clinical attention due to endocrinopathy. Microadenomas are not infrequently encountered within the pituitaries of elderly adults as incidental autopsy findings.
- Rare tumors that occur within the sellar region include the *granular cell tumor of the neurohypophysis, pituicytoma (infundibuloma)*, and *spindle cell oncocytoma of the adenohypophysis*.
  - Our experience thus far with these rare lesions is virtually limited to adults, and the incidence of any of these in children is unknown.
  - Granular cell tumor and pituicytoma are thought to be of glial derivation, while folliculostellate cells represent the possible origin of spindle cell oncocytoma.
  - Given their rarity, detailed information on the nature and behavior of these neoplasms is limited.

29.2 CLINICAL FEATURES

- Typical signs and symptoms of pituitary neoplasia in adults are also commonly seen in children. Visual deterioration, headaches, and endocrinopathies constitute the most common presenting problems. Seizures are an uncommon form of presentation.
- The majority of pituitary adenomas in children are hormonally active.

- Pituitary apoplexy can occur in children with pituitary adenomas.
  - Sudden development of headaches, vomiting, fever and meningeal syndrome along with deficiencies of one or more serum pituitary hormones are indicative of pituitary apoplexy.
- None of the rarer tumors of this region (granular cell tumor, pituicytoma, or spindle cell oncocytoma) present with distinguishing signs/symptoms to differentiate them from pituitary adenomas.

29.3 NEUROIMAGING

- Radioimaging characteristics of *pituitary adenomas* in children are likewise similar to those in adults. There is often distortion of the sella turcica and the tumor may extend into the suprasellar space.
- MRI typically reveals a T1-hypointense and a T2-hyperintense or isointense mass.
- Occasionally in children with macroadenomas, there may be areas of associated hemorrhage that are T1-hyperintense.
- Pituitary microadenomas are typically nonenhancing on enhanced MRI contrast.
- Most pituitary macroadenomas show diffuse enhancement after gadolinium administration, but tumors with hemorrhage may show heterogeneous enhancement (Fig. 29.1).
- *Granular cell tumor*:
  - Some examples can be rather large, and most typically appear as solid T2-hyperintense masses that show prominent contrast enhancement.
- *Pituicytoma*:
  - They are located in proximity to the infundibulum and can be large, extending into suprasellar space.
  - These tumors clinically present like nonfunctioning adenomas and are radiologically solid and uniformly contrast enhancing.
- *Spindle cell oncocytoma*:
  - Distinguishing radioimaging characteristics for spindle cell oncocytoma have not been delineated.

29.4 PATHOLOGY

- *Gross*: adenomas are generally soft and tan, though may have areas of hemorrhage. The other tumors depicted above may have similar macroscopic characteristics, but our experience is limited.
- *Intraoperative smears/frozen section*:
  - Adenomas are often composed of a discohesive pattern of a monotonous population of cells with abundant, well-defined cytoplasm, and bland nuclei with fine "salt and pepper" chromatin pattern.

- Variability in nuclear size may be encountered.
- Nuclei are frequently eccentric, giving the cells a plasmacytoid appearance (Fig. 29.2).
  - Rarely, papillary structures can be observed.
  - When admixed with significant amount of normal pituitary, the homogenous characteristic of the smear may be lost.
  - Normal pituitary tissue is substantially more difficult to smear in comparison to adenomas.
- *Frozen Section*:
  - Typically, routine cases of pituitary adenomas do not necessitate a frozen section evaluation. Almost all cases that require frozen section are unusual examples and should be approached with caution.
  - The key to diagnosis of an adenoma is the architectural patterns i.e., loss of normal pituitary lobular architecture and loss of the normal heterogeneity of the epithelial cells (Fig. 29.3).
- Cytological features other than uniformity can be misleading.
  - In some cases, the nested appearance of the tumor may simulate normal pituitary, and rare tumors also show some cytological heterogeneity, confounding an accurate diagnosis (Fig. 29.4).
  - A tissue sample should always be saved for routine analysis.
- *Histology*
- *Pituitary adenoma*:
  - The tumor is composed of loosely cohesive epithelial cells forming nests, ribbons, festoon-like structures, diffuse sheets, and occasionally, papillary formations (Fig. 29.5).
  - Adenomas do not harbor any peritumoral fibrotic tissue or a true capsule.
  - Scattered mitotic figures can be seen in some adenomas, along with isolated cells with bizarre nuclear profiles. Mitoses can be more easily identified in adenomas from children compared to adults.
  - Most resection specimens also include a fragment of compressed and distorted normal pituitary at the periphery, which can aid in the diagnosis.
  - Microadenomas need to be sampled adequately for accurate diagnosis, and may necessitate special studies (see below).
  - Rare adenomas present with sudden hemorrhage, which may ultimately hamper accurate identification of the neoplasm on microscopic examination, necessitating special studies.
  - ACTH producing adenomas can exhibit Crooke's hyalin change, which can also be seen in non-neoplastic pituitary (Fig. 29.6).
  - One of the most useful special stains is Reticulin, which highlights the lobular architecture of the normal pituitary and the destruction of this network in adenomas. Use of this stain can be particularly helpful in microadenomas (Fig. 29.7).
- *Atypical pituitary adenoma*:
  - Some pituitary adenomas demonstrate "Atypical" histological features that have been associated with a slightly more aggressive behavior.
  - These features include: invasive growth, Ki-67 (MIB-1) labeling index greater than 3%, and positivity of p53 protein immunohistochemistry.
- *Granular cell tumor*: They are morphologically similar to granular cell tumors elsewhere in the body.

- Histologically, they are composed of large abundantly granular, eosinophilic cells forming clusters, nests, and large lobules.
  - They may show marked nuclear pleomorphism, scattered mitotic figures, and rare multi-nucleated cells.
  - Small asymptomatic clusters of granular cells, also termed "choristomas", are more common than true granular cell tumors.
- *Pituicytoma*:
  - These tumors are composed of spindled glial cells in fascicles and bundles intermixed with scattered lympho-plasmacytic cells.
- *Spindle cell oncocytoma*:
  - These tumors are composed of spindle cells with bright eosinophilic cytoplasm, the latter feature due to abundant mitochondria.

29.5 IMMUNOHISTOCHEMISTRY

- *Pituitary adenoma*:
  - The most common set of stains used for pituitary adenomas are the antibodies against pituitary hormones, and the majority of pediatric pituitary adenomas demonstrate positive staining with either prolactin (PRL), growth hormone (GH), Gonadotrophins, ACTH, or TSH.
    Bi- or plurihormonal positivity may rarely be seen.
    (a) Observed combinations include GH and PRL or GH–TSH or ACTH–LH.
    (b) Rare examples of other combinations have been reported.
    A minority show no hormonal staining compatible with a null-cell adenoma.
  - Tumors are diffusely positive for chromogranin (Fig. 29.8a) and synaptophysin, and can also demonstrate focal cytoplasmic keratin positivity, especially with low molecular weight cytokeratin antibodies.
- Absence of chromogranin stain should raise the suspicion of a technical error or a different neoplasm.
  - Staining for Collagen type IV is a more sensitive and expensive substitute for reticulin stain.
  - MIB-1 or Ki-67 labeling index has been used to determine biological aggressiveness.
- Atypical pituitary adenomas will have labeling index greater than 3%.
- Staining for p53 has similarly been associated with more aggressive biological behavior, as in atypical pituitary adenoma (Fig. 29.8b, c).
  - In rare instances, use of novel transcription factors specific for the pituitary, such as pit-1 and neuro-D1 may be helpful in identifying a tumor as a pituitary adenoma. These markers are often unavailable in standard clinical immunohistochemical laboratories.
- *Granular cell tumor*:
  - The tumors often stain strongly with S-100 protein, and more variably for CD68, and α-1 antitrypsin. They are negative for hormonal markers, GFAP, neurofilament, cytokeratin, chromogranin, and synaptophysin.
- *Pituicytoma*:
  - Pituicytomas are positive for Vimentin, S-100 protein, and variably for GFAP.

– They are negative for hormonal markers, chromogranin, synaptophysin and cytokeratins.
– A recent study has identified TTF-1 as another marker for pituicytomas.
• *Spindle cell oncocytoma*:
– These tumors are negative for hormonal stains, chromogranin or synaptophysin, as well as cytokeratins.
– They express Vimentin, S-100 protein, epithelial membrane antigen (EMA), as well as mitochondrial antigens that can be detected with mitochondria specific antibodies.

29.6 ELECTRON MICROSCOPY

• *Pituitary adenoma*:
– Ultrastructural analysis is often helpful in recognizing the neuroendocrine nature of pituitary adenomas, which have abundant neurosecretory granules within the cytoplasm of tumor cells (Fig. 29.9).
Most prolactinomas, however, show a limited number of neurosecretory granules.
– Cells also display cell junctions and a well-developed endoplasmic reticular network.
– Typically, intermediate filaments are sparse.
– Cells with Crooke's hyalin or Crooke cell adenomas demonstrate a marked perinuclear accumulation of intermediate filaments (cytokeratin), which may trap numerous neurosecretory granules.
• *Granular cell tumors* contain abundant intracytoplasmic lysosomes while *spindle cell oncocytoma* contain abundant mitochondria.

29.7 MOLECULAR PATHOLOGY

• Oncogenes such as Gsp, Ras, CyclinD1, and a group of other pituitary derived kinases, and tumor suppressor genes such as MEN1, p53, p16/CDKN2A, and p27/KIP1 have been associated with tumorigenesis in specific types of pituitary adenomas.

29.8 DIFFERENTIAL DIAGNOSIS

• The first important diagnostic consideration is ruling out that the tissue at hand represents something other than non-neoplastic pituitary gland
– Especially during intraoperative consultations, a normal or edematous pituitary gland may be mistaken for adenoma.
– A monomorphic population of pituitary cells that is discohesive on cytology preparations, with abnormal architectural patterns on tissue sections should be sought before a diagnosis of pituitary adenoma is rendered.
– Hyperplasia and lymphocytic or granulomatous hypophysitis should be considered in the differential diagnoses of a pituitary mass.

• Pituitary adenomas may be difficult to distinguish from olfactory neuroblastomas on pathological examination, especially if a clear understanding of tumor location and radioimaging features are not available to the pathologist.
– Both tumors will be synaptophysin and chromogranin positive and may have similar histological patterns.
– If staining for cytokeratin shows focal dot-like positivity, this can be considered supportive evidence for pituitary adenoma.
– Likewise staining for any of the pituitary hormones effectively rules out olfactory neuroblastoma, as well as any of the other rare lesions of the pituitary listed above.

29.9 PROGNOSIS

• Extent of resection remains the most critical prognostic factor in pituitary adenomas.
– Incompletely excised tumors may be treated with radiation therapy, which has been associated with a low rate of radiation-associated damage or tumorigenesis.
– Radiation treatment presents additional challenges in young children, due mainly to the increased possibility of significant neurocognitive deficits.
• The diagnosis of pituitary carcinoma requires documentation of discontinuous spread to other areas of the CNS or distant metastasis, and is not based solely on histopathologic findings.
• Granular cell tumors are benign lesions and total surgical removal is considered curative.
• Pituicytomas are considered to be indolent, although data on the outcome is very limited.
• The natural course and prognosis of spindle cell oncocytomas has not been fully characterized.

SUGGESTED READING

Pandey P, Ojha BK, Mahapatra AK (2005) Pediatric pituitary adenoma: a series of 42 patients. J Clin Neurosci 12:124–127
Lee AG, Sforza PD, Fard AK, Repka MX, Baskin DS, Dauser RC (1998) Pituitary adenoma in children. J Neuroophthalmol 18:102–105
Pinto G, Zerah M, Trivin C, Brauner R (1998) Pituitary apoplexy in an adolescent with prolactin-secreting adenoma. Horm Res 50:38–41
De Divitiis E, De Chiara A, Benvenuti D, Corriero G, Maiuri F, Spaziante R (1980) [Pituitary invasive adenoma in a child. Case report of unusual extensive invasion of the orbit (author's transl)]. Neurochirurgie 26:405–408
Cohen-Gadol AA, Pichelmann MA, Link MJ et al (2003) Granular cell tumor of the sellar and suprasellar region: clinicopathologic study of 11 cases and literature review. Mayo Clin proc 78(5):567–573
Rossi ML, Bevan JS, Esiri MM, Hughes JT, Adams CB (1987) Pituicytoma (pilocytic astrocytoma). Case report. J Neurosurg 67(5):768–772
Brat DJ, Scheithauer BW, Staugaitis SM et al (2000) Pituicytoma: a distinctive low-grade glioma of the neurohypophysis. Am J Surg Pathol 24(3):362–368
Kloub O, Perry A, Tu PH, Lipper M, Lopes MB (2005) Spindle cell oncocytoma of the adenohypophysis: report of two recurrent cases. Am J Surg Pathol 29(2):247–253
Roncaroli F, Scheithauer BW, Cenacchi G et al (2002) 'Spindle cell oncocytoma' of the adenohypophysis: a tumor of folliculostellate cells? Am J Surg Pathol 26(8):1048–1055
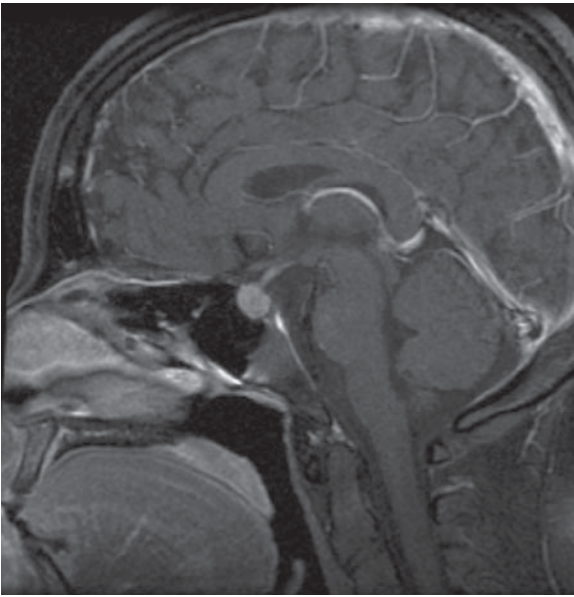
Fig. 29.1. Sagittal contrast-enhanced T1-weighted image of a pituitary adenoma in a 16 year old.
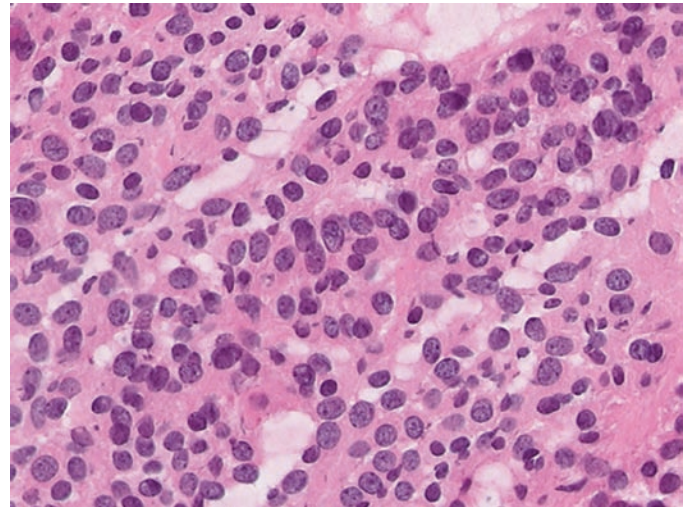
Fig. 29.3. Frozen section of a pituitary adenoma in a 14-year old child. Note the faded appearance of monotonous cells and vague nested pattern.
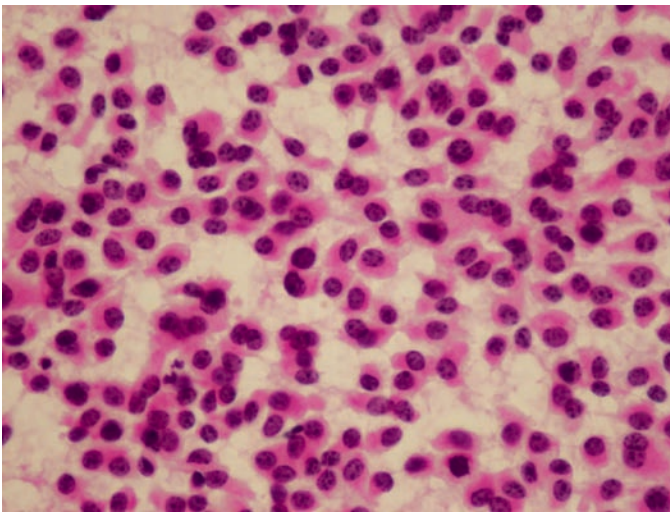
Fig. 29.2. Intraoperative smear preparation of a pituitary adenoma showing discohesive and monotonous epithelial cells.
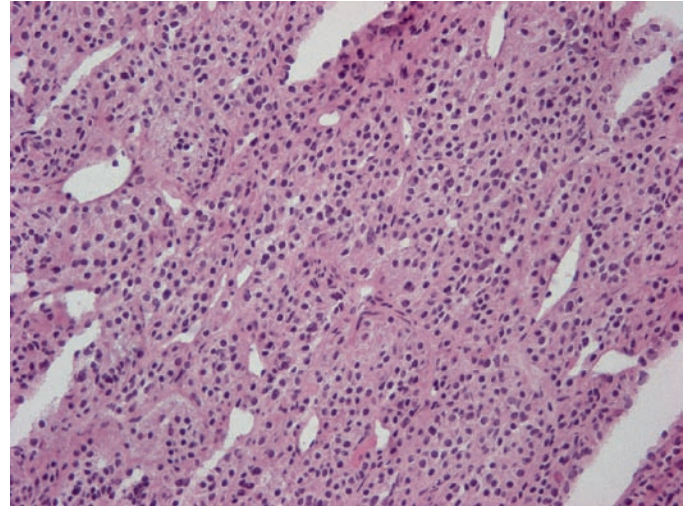
Fig. 29.4. Frozen section of a pituitary adenoma simulating normal pituitary with nested appearance and a heterogeneous population of cells.
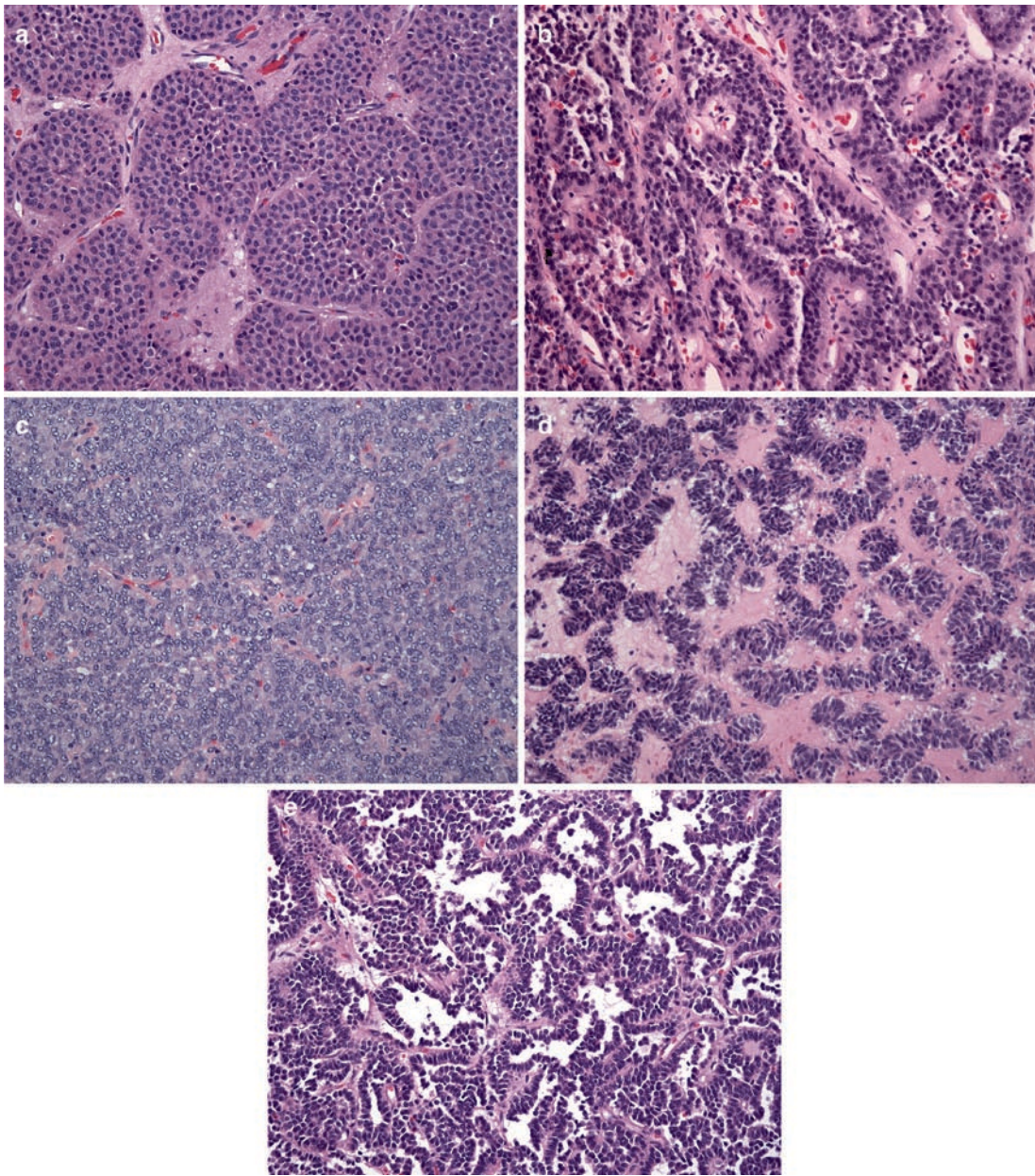
Fig. 29.5. Histological patterns of typical pituitary adenoma in children: (**a**) nested, (**b**) papillary, (**c**) diffuse, (**d**) ribbon-like, and (**e**) pseudoglandular architectures.
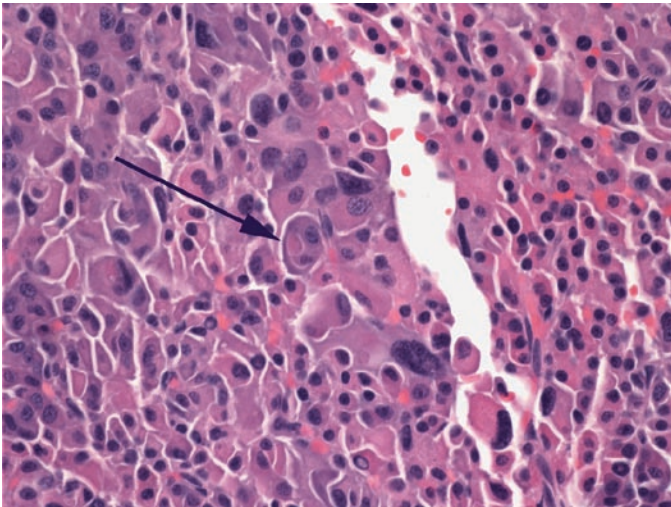
Fig. 29.6. Crooke's hyalin change (*arrow*) in an ACTH-producing adenoma.
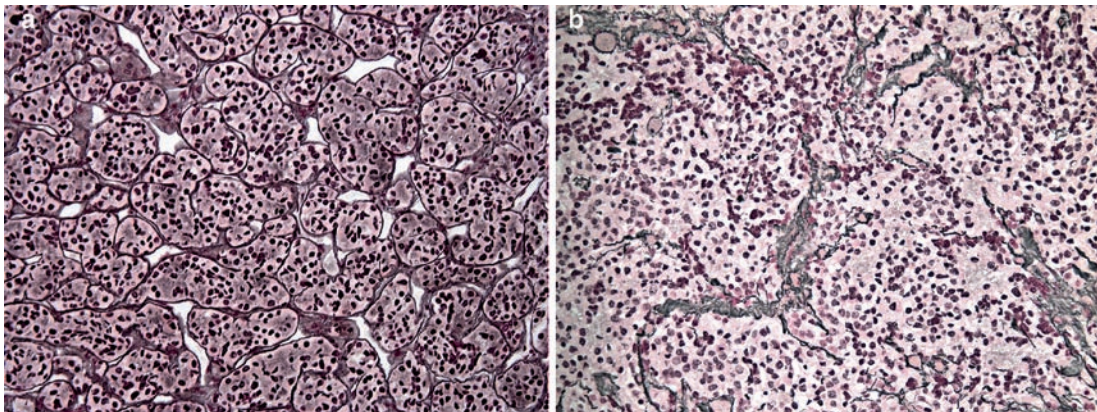
Fig. 29.7. Reticulin staining in (**a**) normal pituitary, (**b**) pituitary adenoma. Note the disruption of the nested reticulin pattern in the adenoma.
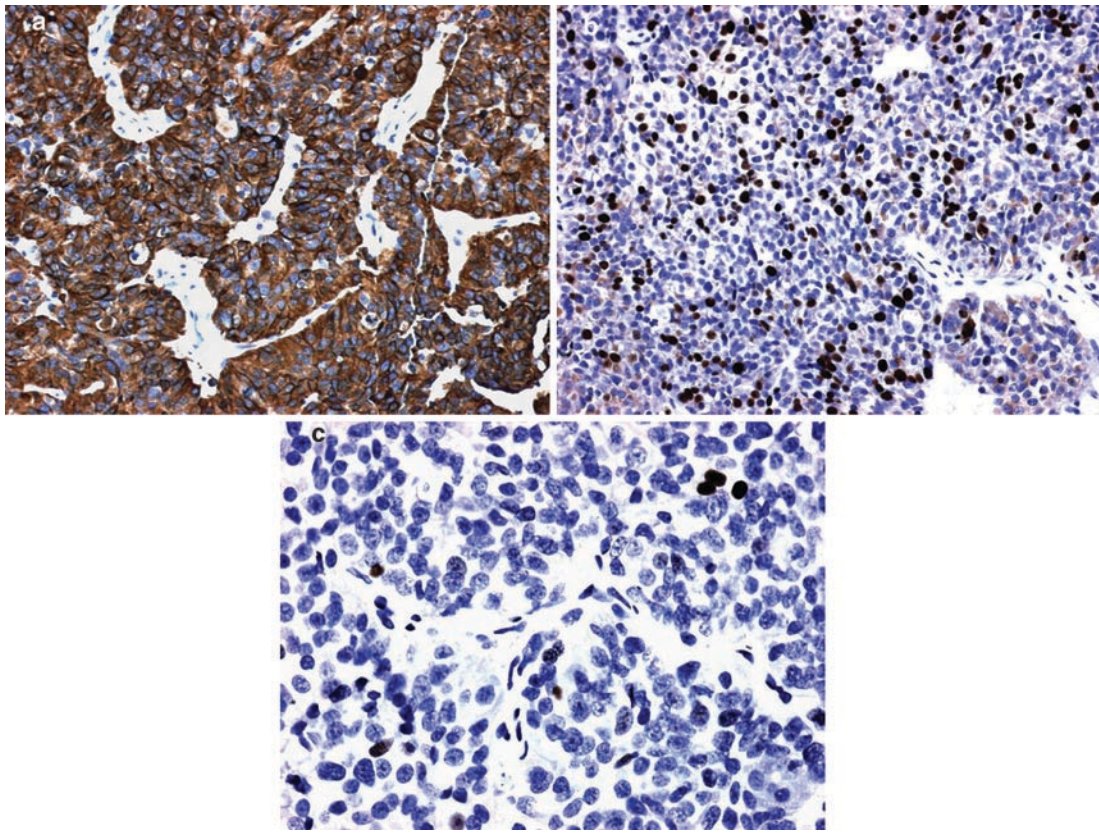
Fig. 29.8. (**a**) Chromogranin positivity is a consistent finding in pituitary adenoma, although it may vary from focal to diffuse. Immunohistochemical staining for (**b**) Ki-67 [MIB-1], and (**c**) p53 protein in an atypical pituitary adenoma; Ki-67 labeling index was approximately 5% and a significant number of adenoma cells show nuclear positivity with the p53 antibody.

Fig. 29.9. Ultrastructural features in a typical pituitary adenoma showing multiple neurosecretory granules.

Craniopharyngioma

Tarik Tihan

30.1 OVERVIEW

- Craniopharyngiomas are typically midline tumors and have two distinct variants; the adamantinomatous and papillary.
- Adamantinomatous variant is identical to adamantinoma of jaw bones. Papillary variant is similar to a squamous papilloma.
- Craniopharyngiomas are currently considered WHO grade I neoplasms.

30.2 CLINICAL FEATURES

- The adamantinomatous variant occurs mostly in children and young adults while the papillary variant is typical for older adults and exceedingly rare in children.
- The most common location is the third ventricle, followed by the pineal region and the posterior fossa.
- Endocrine, visual and behavioral symptoms can be encountered.
- Even though they were reported to be more common in males, the incidence is near equal between genders.

30.3 NEUROIMAGING

- CT is helpful to define the cystic component and calcifications in adamantinomatous craniopharyngioma.
- MRI offers a more detailed assessment of the tumor extent. The tumors often appear as lobulated masses and may encase larger vessels around the third ventricle.
- The cystic component of adamantinomatous craniopharyngioma is often uniformly bright on T2-weighted MR sequences (Fig. 30.1).
- On T1-weighted sequences, the cysts can be hypointense to hyperintense. Calcifications appear as T2-hypointense areas.
- The solid component of the tumor enhances post-contrast and there can also be peripheral enhancement around the cysts (Fig. 30.2).
- Papillary craniopharyngiomas are solid masses with homogenous enhancement and without obvious cystic elements.

30.4 PATHOLOGY

30.4.1 Histology

- Intraoperative smears
  - Often contain a mixture of necrotic-appearing acellular material with calcifications and cholesterol clefts and wet-keratin (Fig. 30.3).
  - In some smears, sheets of epithelial cells and stellate reticulum can be seen.

- Frozen section:
  - The typical frozen section features are cholesterol clefts and the amorphous "wet-keratin."
  - The epithelial component, as well as cells arranged in peripheral palisades may not be easily recognizable on frozen sections, and may appear simply as sheets of cohesive cells (Fig. 30.4).
  - The surrounding tissue may demonstrate multiple Rosenthal fibers, which could lead to an erroneous diagnosis of pilocytic astrocytoma.
- The contents of the cysts in craniopharyngiomas are often described as "machine oil."
- The adamantinomatous craniopharyngioma is composed of nodules of epithelial cells that are arranged in palisades around a loose stromal element with more spindled cells also known as "stellate reticulum" (Fig. 30.5).
- Wet keratin, cluster of eosinophilic and necrotic keratinized cells, is a classic histological finding and is often diagnostic (Fig. 30.6).
- Calcifications (dystrophic and psammomatous), necrotic tissue and cholesterol clefts are typical features (Fig. 30.7).
- Compact, sheet-like arrangement of epithelial cells can be seen in adamantinomatous craniopharyngiomas, which can be confused with the papillary variant.
- Some tumors also contain marked piloid gliosis surrounding the tumor.
- Other microscopic features include:
  - Degenerative and reactive changes including cholesterol clefts and multinucleated giant cells
  - Fibrotic and gliotic surrounding tissue with Rosenthal fibers.
- Variants
  - Papillary craniopharyngioma is a rare variant mostly seen in adults, and extremely uncommon in children.
    This lesion resembles a squamous papilloma.
    The papillary variants appear to be more common in the suprasellar region.

30.5 ELECTRON MICROSCOPY

- Electron microscopy is of little use in clinical practice for diagnosis of craniopharygioma.
- The typical characteristics of palisading epithelial cells are abundant cell junctions, well-formed desmosomes and basal lamina formation.

30.6 IMMUNOHISTOCHEMISTRY

- The epithelial component is strongly positive for cytokeratins, especially CK7, CK19 and other high molecular cytokeratin antibodies.

- The tumors are typically negative for germ cell markers (PLAP, AFP, HCG), GFAP and S-100 protein.
- High Ki-67 (MIB-1) labeling of tumors has been associated with a higher rate of recurrence, but Ki-67 does not have any role in the diagnosis of craniopharyngioma.

30.7 MOLECULAR PATHOLOGY

- Little is known about specific genetic alterations in craniopharyngiomas. Recent studies failed to determine chromosomal imbalances or specific genomic alterations.

30.8 DIFFERENTIAL DIAGNOSIS

- It is important to distinguish the two variants of craniopharyngioma, since the papillary variant is considered a more indolent neoplasm.
- Epidermoid cysts may be considered in the differential, but the presence of wet keratin alone excludes this possibility.
- The surrounding piloid gliosis with Rosenthal fibers should be distinguished from a pilocytic astrocytoma or less likely a subependymoma.

30.9 PROGNOSIS

- Prognosis in craniopharyngiomas is mostly influenced by
  – The extent of resection

  – Tumor size greater than 4 cm
  – Cystic tumors possibly suggesting adamantinomatous variant

SUGGESTED READING

Ohmori K, Collins J, Fukushima T (2007) Craniopharyngiomas in children. Pediatr Neurosurg 43:265–278

Puget S, Garnett M, Wray A, Grill J, Habrand JL, Bodaert N, Zerah M, Bezerra M, Renier D, Pierre-Kahn A, Sainte-Rose C (2007) Pediatric craniopharyngiomas: classification and treatment according to the degree of hypothalamic involvement. J Neurosurg 106:3–12

Di Rocco C, Caldarelli M, Tamburrini G, Massimi L (2006) Surgical management of craniopharyngiomas – experience with a pediatric series. J Pediatr Endocrinol Metab 19(Suppl 1):355–366

Rossi A, Cama A, Consales A, Gandolfo C, Garre ML, Milanaccio C, Pavanello M, Piatelli G, Ravegnani M, Tortori-Donati P (2006) Neuroimaging of pediatric craniopharyngiomas: a pictorial essay. J Pediatr Endocrinol Metab 19(Suppl 1):299–319

Kalapurakal JA (2005) Radiation therapy in the management of pediatric craniopharyngiomas – a review. Childs Nerv Syst 21:808–816

Fisher PG, Jenab J, Gopldthwaite PT, Tihan T, Wharam MD, Foer DR, Burger PC (1998) Outcomes and failure patterns in childhood craniopharyngiomas. Childs Nerv Syst 14:558–563

Miller DC (1994) Pathology of craniopharyngiomas: clinical import of pathological findings. Pediatr Neurosurg 21(Suppl 1):11–17

Yasargil MG, Curcic M, Kis M, Siegenthaler G, Teddy PJ, Roth P (1990) Total removal of craniopharyngiomas. Approaches and long-term results in 144 patients. J Neurosurg 73:3–11
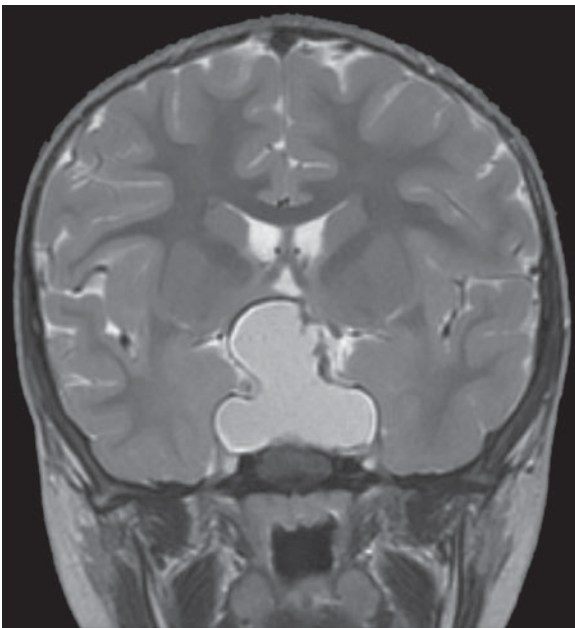
Fig. 30.1. T2-weighted coronal MR image of a suprasellar/hypothalamic midline mass consistent with a craniophayngioma in a 14-year-old child
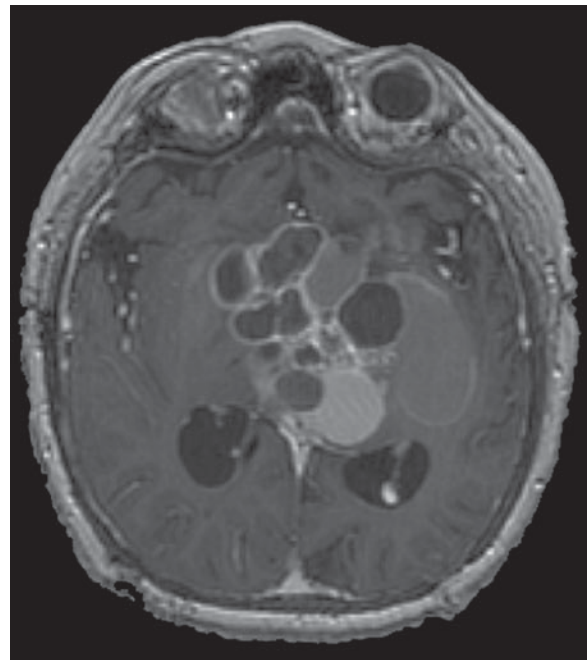
Fig. 30.2. T1-weighted axial MR image of a large multicystic midline mass compressing the third ventricle and showing an enhancing solid component post gadolinium in a 7-year-old male.
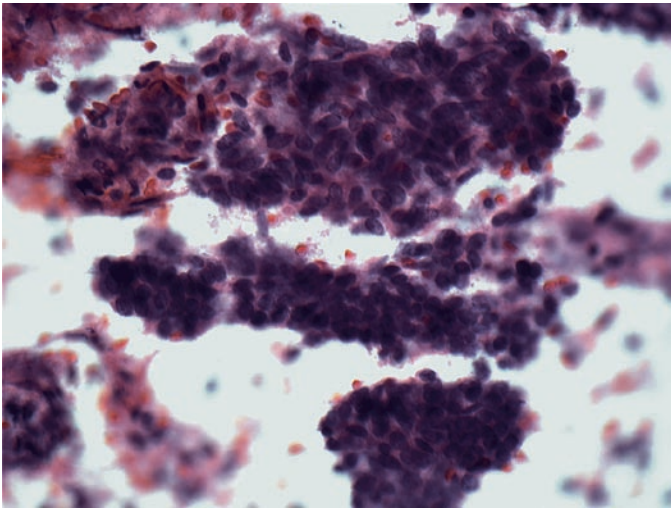
Fig. 30.3. Intraoperative smear of a craniopharyngioma; note the clustered and vaguely nested epithelial cells
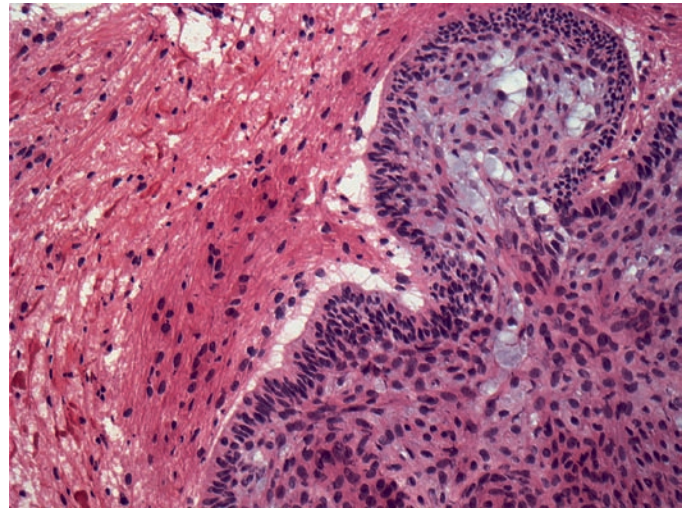
Fig. 30.4. Frozen section of a craniopharyngioma showing the surrounding piloid gliosis with Rosenthal fibers
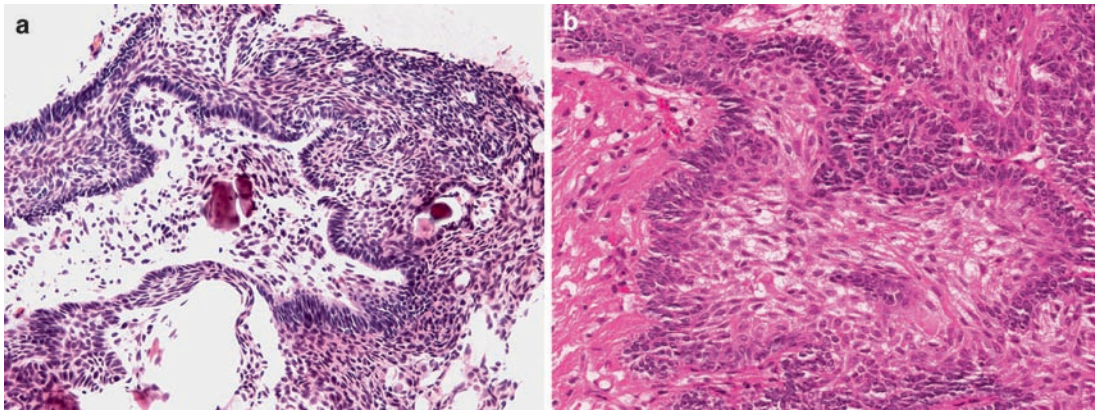
Fig. 30.5. Typical histological components of adamantinomatous craniopharyngioma: (**a**) epithelial component, (**b**) stellate reticulum
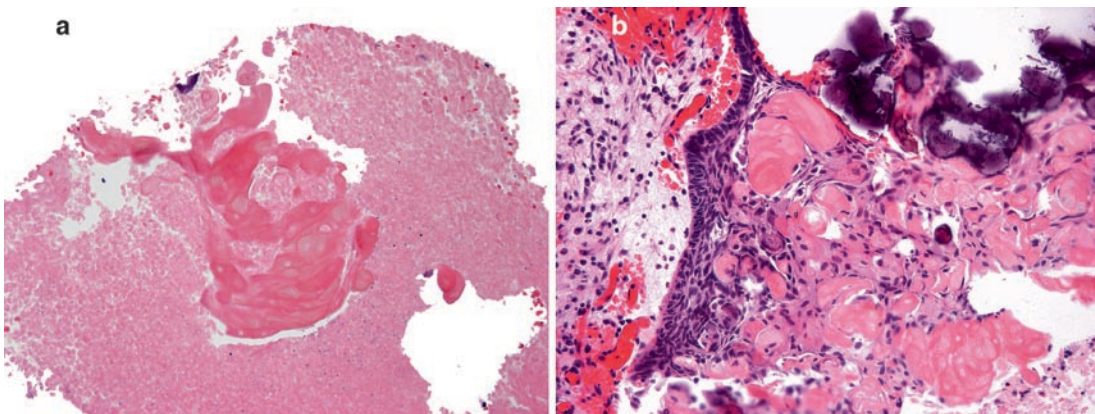
Fig. 30.6. Classical histological finding of "wet keratin" that can be observed both in (**a**) frozen sections and (**b**) paraffin embedded tissue
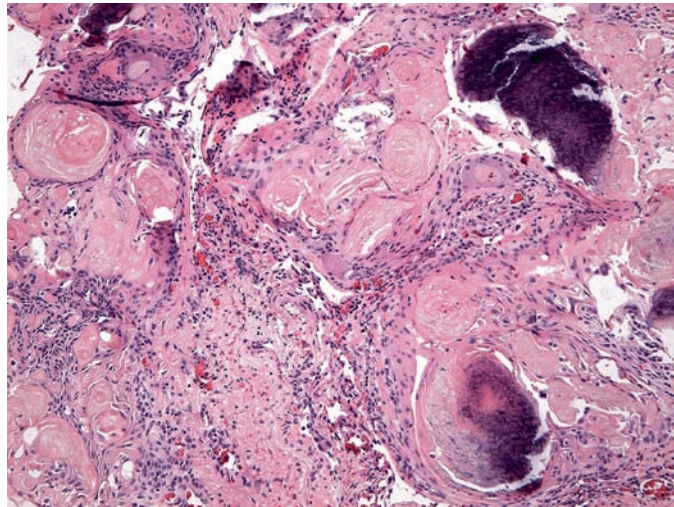
Fig. 30.7. Calcifications, cholesterol clefts and necrotic appearing tissue can suggest the diagnosis of craniopharyngioma in the absence of epithelial components or wet keratin

Section H: Choroid Plexus Neoplasms

Christine E. Fuller, Sonia Narendra and Ioana Tolocica

Abstract Choroid plexus tumors are presented in Sect. H. Included are numerous examples of classic (and not-so-classic) choroid plexus papillomas and choroid plexus carcinomas, as well as tumors of "intermediate" differentiation/so-called "atypical choroid plexus papilloma." Specific emphasis will be placed on the classic neuroimaging and pathologic characteristics of each of these entities, with careful consideration of differential diagnosis in each instance.

Choroid Plexus Neoplasms

Christine E. Fuller, Sonia Narendra and Ioana Tolocica

Keywords Choroid plexus papilloma; Choroid plexus carcinoma; Atypical choroid plexus papilloma; Rhabdoid predisposition syndrome

31.1 OVERVIEW

- Intraventricular neoplasms derived from choroid plexus epithelium including choroid plexus papilloma (WHO grade I), atypical choroid plexus papilloma (WHO grade II), and choroid plexus carcinoma (WHO grade III).
- The vast majority are sporadic, though rarely arise in association with hereditary cancer predisposition syndromes, including the Li Fraumeni and Rhabdoid Predisposition Syndromes, with germline mutations of TP53 and hSNF5/INI1/SMARCB1 respectively. Choroid plexus papillomas (CPP) are also a component of Aicardi syndrome, the affected patients showing agenesis of the corpus callosum, chorioretinal lacuna, and infantile spasms. Rarely CPP arise in the context of von Hippel-Lindau disease.
- Choroid plexus papillomas are at least five times more common than carcinomas (CPC).

31.2 CLINICAL FEATURES

- May occur at any age, however, the peak incidence is within the first decade. Rare congenital and fetal examples have been described.
- Though they are rare brain tumors overall, choroid plexus tumors are more frequent in the pediatric population, representing approximately 4% of all brain tumors in children under 15 years, and up to 20% of those arising within the first year of life.
- The majority of CPC occur in children, where they account for 1/3 of all choroid plexus tumors.
- Patients present with signs and symptoms related to blockage of CSF pathways and hydrocephalus, including macrocephaly and bulging fontanelles, papilledema, ataxia, headache, strabismus, irritability, and altered consciousness.

31.3 NEUROIMAGING

- Typically arise within the lateral (50%), fourth (40%), or third (5%) ventricles; rarely at the cerebellopontine angle or other locations (intraparenchymal, suprasellar, spinal epidural region). Rarely multiple ventricles are involved by tumor.
- Most lateral ventricular tumors present within the first two decades of life, whereas fourth ventricle tumors have a more diverse age distribution.
- CPP are characteristically solid, well-demarcated intraventricular masses that on MRI are isointense to grey matter on T1, hyperintense on T2, and show marked contrast enhancement (Fig. 31.1). They are isodense to hyperdense on CT images.
- CPCs are generally larger with MRI showing more heterogeneous intensities on both T1 and T2, with irregular enhancement, and edema (often indicative of invasion of adjacent brain); flow voids, cysts, and areas of intratumoral hemorrhage or necrosis are not uncommon (Fig. 31.2a and b). On CT they are heterogenous and isodense with calcifications and necrosis.
- Atypical CPP may show imaging features intermediate between typical CPP and CPCs, often with surrounding edema evident on T2 and FLAIR images (Fig. 31.3a and b).
- Hydrocephalus, sometimes massive, typically accompanies choroid plexus lesions (Fig. 31.1).
- Leptomeningeal enhancement correlates with CSF dissemination of tumor, which may be encountered with CPC (frequent) and CPP (rare).
- On MR spectroscopy, choroid plexus papillomas have higher levels of myoinositol and lower levels of choline than choroid plexus carcinomas.

31.4 PATHOLOGY FINDINGS

- *Gross pathology*:
  - Surgical specimens of CPP are typically globular, soft, red-brown or pink, with stippled surfaces (correlating with papillary microarchitecture); they sometimes have intratumoral hemorrhages, cysts, or calcification.
  - CPCs are often punctuated by areas of hemorrhage and necrosis.
  - In autopsy brains, CPPs are found as cauliflower-like masses, often adherent to the ventricular walls but otherwise well demarcated from the surrounding brain tissue. CPCs in contradistinction are frequently invasive into the periventricular brain parenchyma.
- *Intraoperative cytologic imprints/smears*:
  - Cytologic preparations of CPPs are typified by multiple well-formed papillary clusters, sheets/monolayers (often with honeycomb-type architecture), and isolated single tumor cells that are cuboidal to columnar with bland round or oval nuclei, dispersed chromatin, and moderate amount of cytoplasm. Microcalcifications may occasionally be present (Fig. 31.4a, b).
  - CPCs demonstrate tight three-dimensional clusters and isolated anaplastic-appearing cells with prominent nuclear irregularities (indentations or lobulations), high nuclear to cytoplasmic ratio, and frequent nucleoli.
  - Papillary architecture may be retained in some areas.
  - Mitotic figures may be seen (Fig. 31.5a, b).
- *Histology*: most choroid plexus papillomas show similar microscopic features, whereas higher-grade choroid plexus

lesions are quite variable in their appearance, particularly the CPCs.

- *Choroid plexus papilloma (WHO grade I)* contains numerous fibrovascular papillary projections covered by a single layer of cuboidal to columnar epithelium with monotonous bland nuclei (Fig. 31.6a).
  - Though they may superficially resemble non-neoplastic choroid plexus (Fig. 31.6b), CPP show more cellular crowding/stratification, mildly elevated nuclear to cytoplasmic ratio, nuclear hyperchromasia and/or mild nuclear pleomorphism, and rare mitoses.
  - The epithelial cytoplasm is quite variable and may be abundant and eosinophilic, vacuolated, or clear (Fig. 31.6c–e).
  - Notable but uncommon histologic features include: oncocytic change (Fig. 31.6f), glandular metaplasia, mucinous degeneration, melanin pigment, focal ependymal differentiation, neuropil-like islands, and osseous or cartilaginous metaplasia.
  - Degenerative changes may include xanthomatous change, angioma-like increase of blood vessels, hyalinization or calcification (Fig. 31.6g).
  - Foci of necrosis, increased cellularity, or loss of papillary architecture are rarely encountered in grade I CPP.
- *Atypical choroid plexus papillomas (WHO grade II)* represent those CPPs with elevated mitotic activity (>2 mitoses per 10 high power fields) (Fig. 31.7a).
  - Additional histologic features often present in atypical CPPs include hypercellularity, nuclear pleomorphism, focal loss of papillary architecture/solid growth pattern, and necrosis (Fig. 31.7b,c).
  - Complex architectural arrangements with cribriforming and anastomosing papillary formations may be seen.
- *Choroid plexus carcinoma (WHO grade III)* shows frank features of malignancy, with solid sheets of variably pleomorphic epithelioid cells with frequent mitoses (Fig. 31.8a,b).
  - Foci of papillary architecture may be retained in some CPCs (Fig. 31.8c).
  - Brain invasion and necrosis are common findings (Fig. 31.8d).
  - Malignant choroid plexus epithelium may have eosinophilic, amphophilic, or clear cytoplasm (Fig. 31.8a–c, e, and f, respectively)
  - Cells exhibiting a distinctly rhabdoid morphology may be the overwhelming feature of some CPCs, resulting in significant overlapping histology with atypical teratoid/rhabdoid tumors (Figs. 31.9a,b).
  - Likewise, some CPCs harbor smaller cells with a high nuclear to cytoplasmic ratio, reminiscent of PNET/medulloblastoma (Figs. 31.10a,b).
  - Other uncommon histologic features similar to those listed above for CPPs (particularly melanin pigment) may be rarely encountered.

31.5 IMMUNOHISTOCHEMISTRY

- *Choroid plexus papillomas* are almost uniformly positive for cytokeratins, vimentin, and podoplanin. Though variable patterns of positivity for CK7 and CK20 may be encountered, the most frequent is CK7+/CK20–.

  - EMA is usually negative, whereas up to 90% will show some positivity for S-100 protein.
  - Though it is not found in normal choroid plexus, GFAP staining may be detected at least focally in up to 50% of CPP.
  - Transthyretin is positive in the majority of CPPs, though this stain is not entirely specific to choroid plexus tumors.
  - Synaptophysin may be paradoxically positive in some cases.
- *Choroid plexus carcinomas* similarly show immunopositivity for cytokeratin, however, S-100 and transthyretin are less reliably positive compared to CPPs (Fig. 31.11a).
  - Synaptophysin, GFAP, EMA, CD44, CA19-9 may all be at least focally positive (Fig. 31.11b).
  - Retained nuclear staining for INI1 is helpful in differentiating these tumors from atypical teratoid/rhabdoid tumor (Fig. 31.11c).
  - Lack of staining for CEA, HEA 125, Ber EP4, or positive staining for EAAT1 (excitatory amino acid transporter-1) help to differentiate CPC from metastatic carcinomas from other body sites.
  - Proliferation index as detected by MIB-1 (Ki67) is variable, though typically brisk (Fig. 31.11d).
  - The majority of CPCs show nuclear positivity for p53.

31.6 ELECTRON MICROSCOPY

Electron microscopy for CPP or CPC may show tight junctions and membrane interdigitations, cell surface specializations including microvilli and cilia, and basement membrane (Fig. 31.11e).

31.7 MOLECULAR PATHOLOGY

- *Choroid plexus papillomas* are often hyperdiploid with multiple chromosomal gains including chromosomes 7,9,12,15, 17, and 18. Comparative genomic hybridization studies have likewise defined regions of gain on chromosome 5, 7, and 9p, as well as region of loss of 10q.
  - Chromosome 3 VHL allele loss may be encountered in those CPPs arising in association with von Hippel-Lindau disease.
  - *Notch* signaling pathway activation has been implicated in a subset of CPPs
- *Choroid plexus carcinoma* have been found to harbor regions of loss of heterozygosity on chromosomes 5, 18q, 22q; gains were observed on chromosomes 1, 4, 8q, 9p,12, 14q, 20q, and 21.
  - Immunohistochemical nuclear positivity for p53 is observed in most CPCs and few CPPs, though corresponding TP53 mutations are quite rare.
  - Accounts of INI1 gene mutations in CPCs appear in the literature, though more recent immunohistochemical studies indicate that INI1 protein expression is retained in CPCs and nuclear staining pattern with BAF-47 (anti-INI1) is a reliable method to differentiate CPCs with a rhabdoid phenotype from true AT/RTs (which lack nuclear INI1 staining) (Fig. 31.11c).
  - Expression and amplification of PDGF receptors is frequent in CPC.

31.8 DIFFERENTIAL DIAGNOSIS

- Choroid plexus papillomas need to be distinguished from non-neoplastic choroid plexus and villous hypertrophy, the latter a diffuse enlargement of the choroid plexus. Demonstrable mitoses and/or MIB-1/Ki67 (proliferation marker) labeling, together with cytomorphologic and architectural features as noted above, should reliably accomplish this differentiation in favor of CPP.

- Papillary ependymoma exhibits distinctive papillary architecture similar to CPP; however, the latter has basement membrane beneath epithelium, shows strong positivity for cytokeratin, and lacks the perivascular pseudorosettes and strong positivity for GFAP of the former. Similarly, choroid plexus carcinoma may resemble anaplastic ependymoma, and likewise can be differentiated from that tumor by virtue of strong cytokeratin positivity, lack of significant GFAP staining, and lack of true and perivascular pseudorosettes.

- Medulloepithelioma and the germ cell tumor embryonal carcinoma, both enter the differential of CPC. However, medulloepithelioma with its multilayered ribbons of primitive epithelioid-appearing cells is typically not immunoreactive for cytokeratin, and embryonal carcinomas are characteristically positive for placental alkaline phosphatase (PLAP).

- As discussed elsewhere, CPCs may contain variable populations of cells with rhabdoid morphology, thus raising AT/RT as a diagnostic consideration. Recent studies indicate that nuclear staining with anti-INI1 (BAF-47) in this context reliably differentiates the former from AT/RT, which characteristically has absence of staining with BAF-47.

- Transthyretin and/or S-100 protein expression may be helpful features in differentiating choroid plexus tumors from metastatic carcinomas (papillary or otherwise) from other sites, though are by no means 100% reliable. GFAP and synaptophysin positivity, often encountered in choroid plexus tumors, is likewise typically not a signature of metastatic carcinomas. Other immunostains (CEA, HEA 125, Ber EP4, EAAT1) may provide ancillary assistance in this differential diagnosis, as noted elsewhere.

31.9 PROGNOSIS

- Prolonged recurrence-free and overall survival is typical for CPP, with 5-year survival rates approaching 100% following complete surgical excision. CPCs are significantly more aggressive, with survival rates approximately half those encountered in CPPs. Survival rates for atypical CPPs fall somewhere between these two extremes.

- Resection of all choroid plexus tumors is technically difficult due to their extensive vascularity and propensity to bleed.

- Histologic features portending poor prognosis include:
  - Decreased S-100 protein expression
  - Mitoses
  - Lack of immunopositivity for transthyretin
  - Brain invasion
  - Necrosis

- Surgical excision is the standard first line therapy for all choroid plexus tumors, with gross total resection curative for most CPPs. Localized CPCs with complete resection have a favorable outcome realized with the addition of adjuvant chemo- or radiotherapy. Craniospinal irradiation may be necessary in those cases of CPC with subtotal resection and/or disseminated leptomeningeal disease.

SUGGESTED READING

Beschorner R, Schittenhelm J, Schimmel H, Iglesias-Rozas JR, Herberts T, Schlaszus H et al (2006) Choroid plexus tumors differ from metastatic carcinomas by expression of the excitatory amino acid transporter-1. Hum Pathol 37:854–860

Chow E, Reardon DA, Shah AB, Jenkins JJ, Langston J, Heideman R et al (1999) Pediatric choroid plexus neoplasms. Int J Radiat Oncol Biol Phys 44(2):249–254

Corcoran GM, Frazier SR, Prayson RA (2001) Choroid plexus papilloma with osseous and adipose metaplasia. Ann Diagn Pathol 5(1):43–47

Geerts Y, Gabreels F, Lippens R, Merx H, Wesseling P (1996) Choroid plexus carcinoma: a report of two cases and review of the literature. Neuropediatrics 27(3):143–148

Guermazi A, De Kerviler E, Zagdanski A-M, Frija J (2000) Diagnostic imaging of choroid plexus disease. Clin Radiol 55:503–516

Hasselblatt M, Bohm C, Tatenhorst L, Dinh V, Newrzella D, Keyvani K et al (2006) Identification of novel diagnostic markers for choroid plexus tumors. A microarray-based approach. Am J Surg Pathol 30(1)):66–74

Jeibmann A, Hasselblatt M, Gerss J, Wrede B, Egensperger R, Beschorner R et al (2006) Prognostic implications of atypical histologic features in choroid plexus papilloma. J Neuropathol Exp Neurol 65(11): 1069–1073

Jeibmann A, Wrede B, Peters O, Wolff JE, Paulus W, Hasselblatt M (2007) Malignant progression in choroid plexus papillomas. J Neurosurg 107:199–202

Judkins AR, Burger PC, Hamilton RL, Kleinschmidt-Demasters BK, Perry A, Pomeroy SL et al (2005) INI1 protein expression distinguishes atypical teratoid/rhabdoid tumor from choroid plexus carcinoma. J Neuropathol Exp Neurol 64(5):391–397

Louis DN, Ohgaki H, Wiestler OD, Cavenee WK (2007) WHO classification of tumours of the central nervous system, 4th edn. IARC, Lyon

Matsushima T, Inoue T, Takeshita I, Fukui M, Iwaki T, Kitamoto T (1988) Choroid plexus papillomas: an immunohistochemical study with particular reference to the coexpression of prealbumin. Neurosurgery 23(3):384–389

Paulus W, Janisch W (1990) Clinicopathologic correlations in epithelial choroid plexus neoplasms: a study of 52 cases. Acta Neuropathol (Berl) 80(6):635–641

Pencalet P, Sainte-Rose C, Lellouch-Tubiana A, Kalifa C, Brunelle F, Sgouros S et al (1998) Papillomas and carcinomas of the choroid plexus in children. J Neurosurg 88(3):521–528

Rickert CH, Wiestler OD, Paulus W (2002) Chromosomal imbalances in choroid plexus tumors. Am J Pathol 160:1105–1113

Stefanko SZ, Vuzevski VD (1985) Oncocytic variant of choroid plexus papilloma. Acta Neuropathol (Berl) 66(2):160–162

Tena-Suck ML, Gomez-Amador JL, Ortiz-Plata A, Salina-Lara C, Rembao-Bojorquez D, Vega-Orozco R (2007) Rhabdoid choroid plexus carcinoma: a rare histological type. Arq Neuropsiquiatr 65(3A):705–709

Wrede B, Liu P, Wolff JE (2007) Chemotherapy improves the survival of patients with choroid plexus carcinoma: a meta-analysis of individual cases with choroid plexus tumors. J Neurooncol 85(3):345–351

Fig. 31.1. Coronal T1-weighted postgadolinium MR image of a CPP showing an intraventricular densely-enhancing well-circumscribed lesion involving the left lateral and third ventricles with accompanying hydrocephalus.
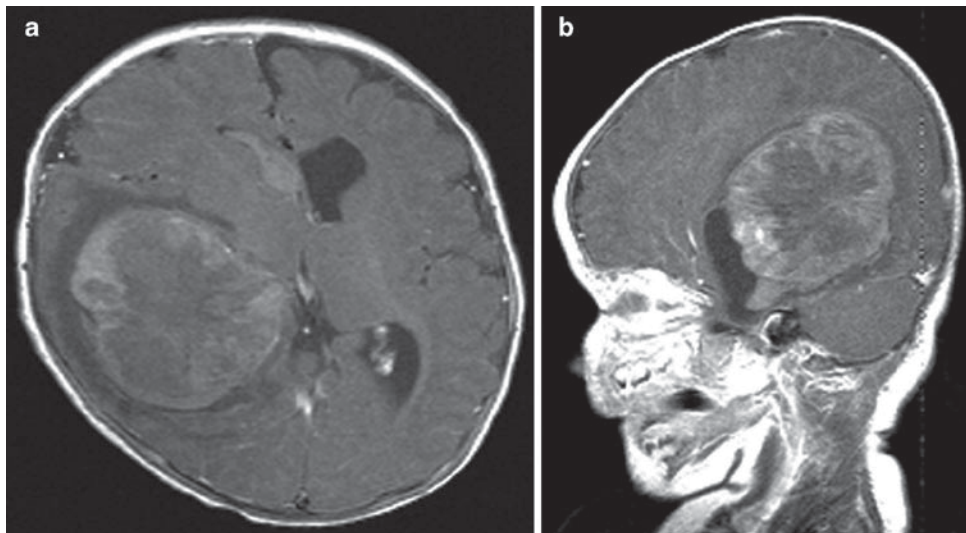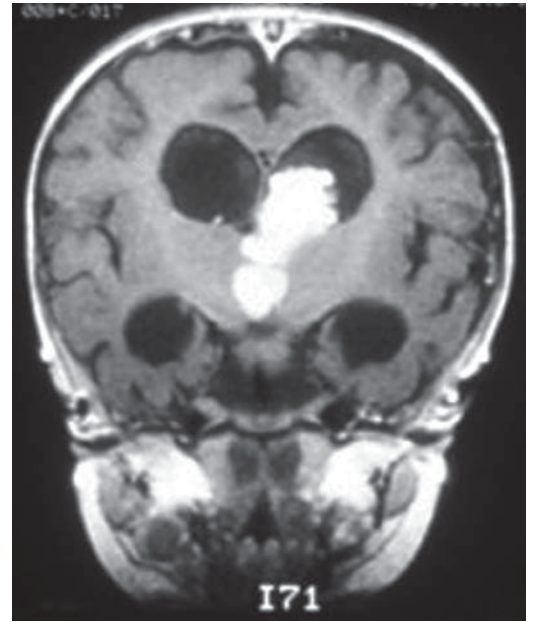
Fig. 31.2. Axial (**a**) and sagittal (**b**) T1-weighted postgadolinium MR images of a CPC showing a large mass arising within the right lateral ventricle with heterogeneous signal intensity and enhancement, central necrosis, hydrocephalus, and significant mass effect with midline shift.
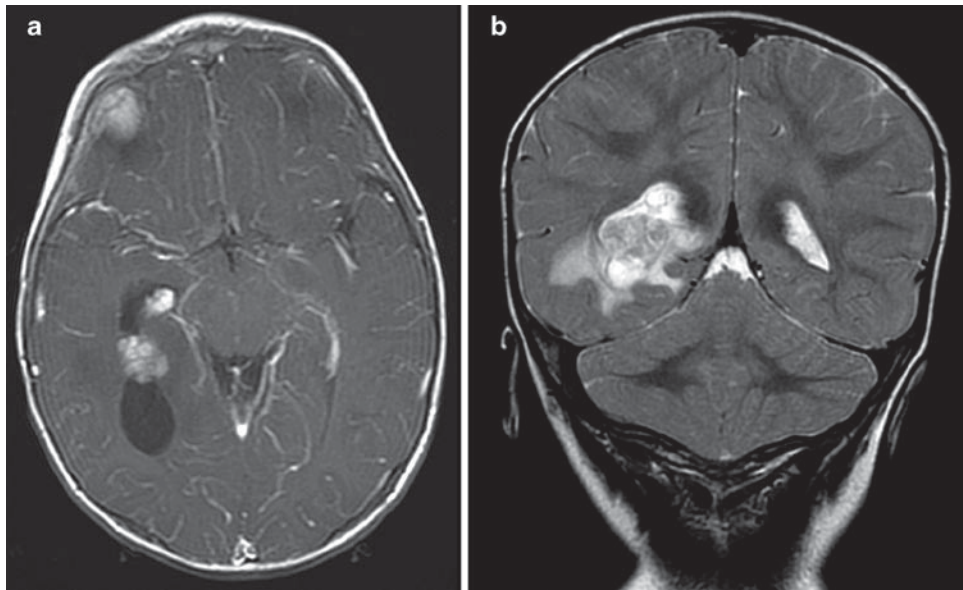
Fig. 31.3. These MR images depict a right intraventricular tumor which microscopically proved to be an atypical CPP (WHO grade II). Axial T1-weighted postgadolinium MR image (**a**) shows solid homogeneously enhancing tumor, whereas T2-weighted coronal MR image (**b**) indicates more heterogeneous signal intensity ranging from isointense to hyperintense, with associated periventricular edema. Hydrocephalus was not prominent in this case.
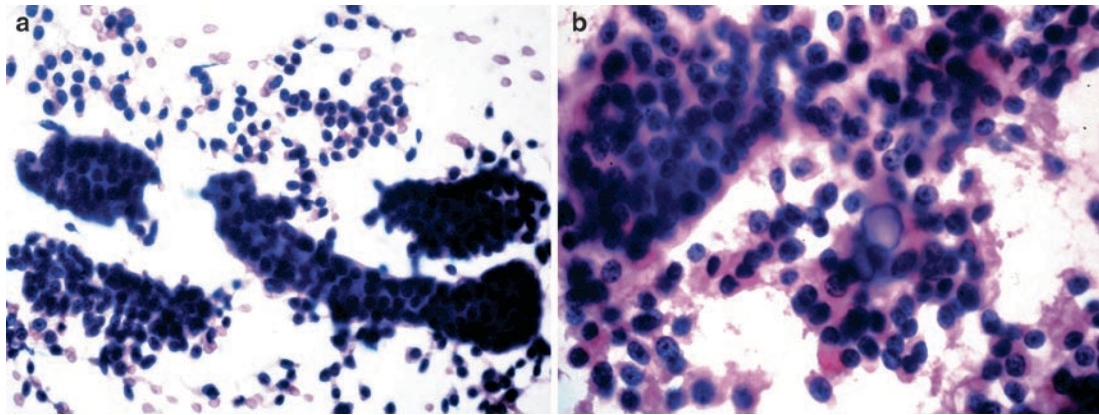
Fig. 31.4. (**a**) Cytologic squash preparation of CPP showing well-formed papillary structures along with scattered bland-appearing individual tumor cells. (**b**) Higher magnification of this CPP sample reveals cells with bland round to oval nuclei, micro-nucleoli, and a single microcalcification. Honeycomb architecture is noted in these cellular sheets.
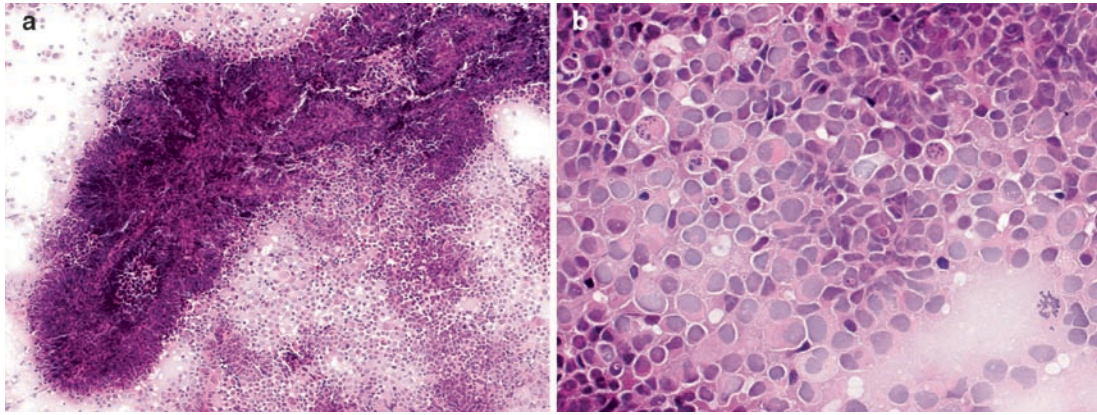
Fig. 31.5. (**a**) Squash preparation of a CPC showing three-dimensional clusters, some showing a papillary architecture with complex multilayer covering of neoplastic epithelium. (**b**) Numerous isolated anaplastic-appearing cells with prominent nuclear irregularities, many with a high nucleocytoplasmic ratio, are present as are scattered apoptotic cells and mitotic figures.
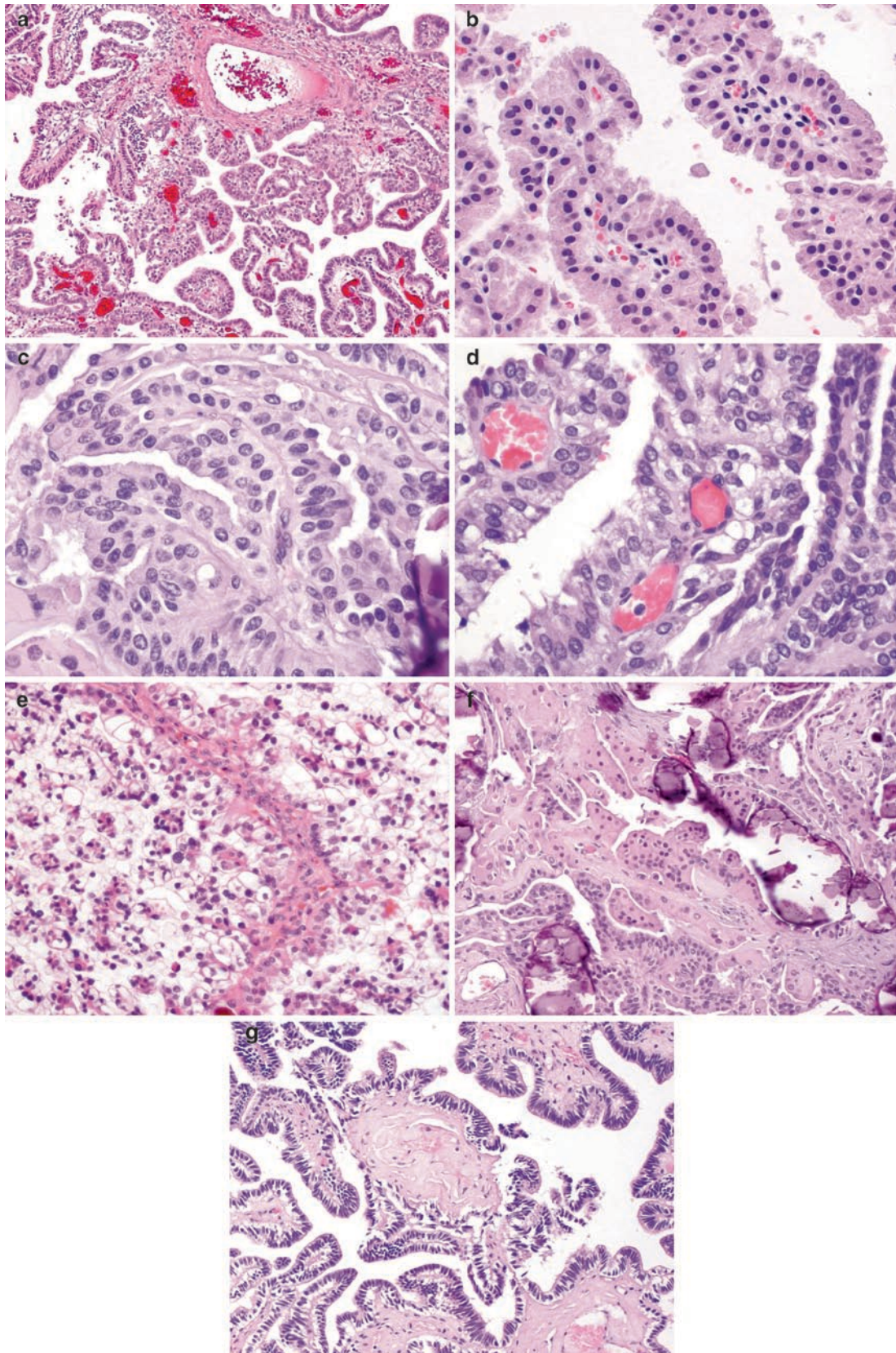
Fig. 31.6. (**a**) CPPs are characterized by fibrovascular papillary projections covered by a single layer of cuboidal to columnar epithelium. (**b**) Normal choroid plexus with small intercellular spaces, imparting a cobblestone appearance. In contradistinction, the epithelium of CPP lacks these spaces and may display abundant eosinophilic cytoplasm (**c**), cytoplasmic vacuoles (**d**), or optically clear cytoplasm (**e**). Though tumoral calcifications are not uncommon (**f**), oncocytic change as seen in the middle of this photomicrograph is infrequent. (**g**) Papilla may show dense hyalinization of stromal cores.
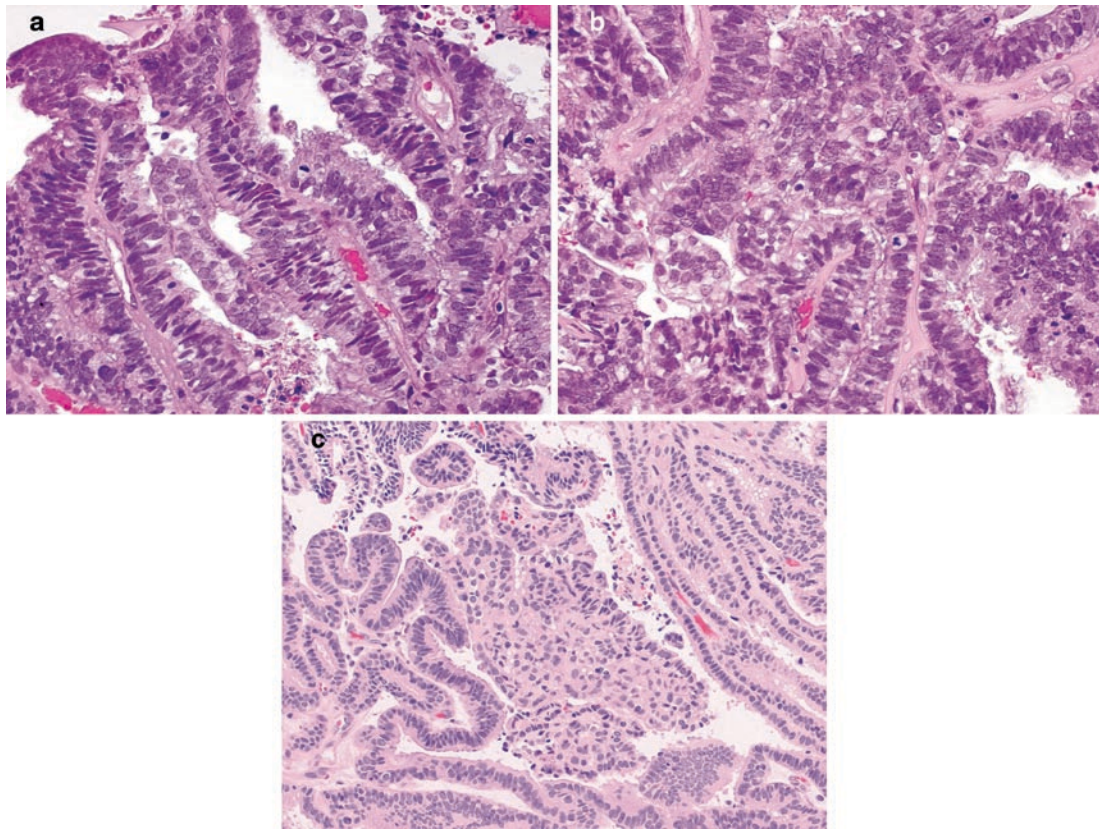
Fig. 31.7. (**a**) Atypical CPPs are defined by their elevated mitotic rate; in addition to multiple mitotic figures, cell crowding, pseudostratification, and focal nuclear pleomorphism are seen in this example. Complex architecture (**b**) and solid areas (**c**) are additional features.
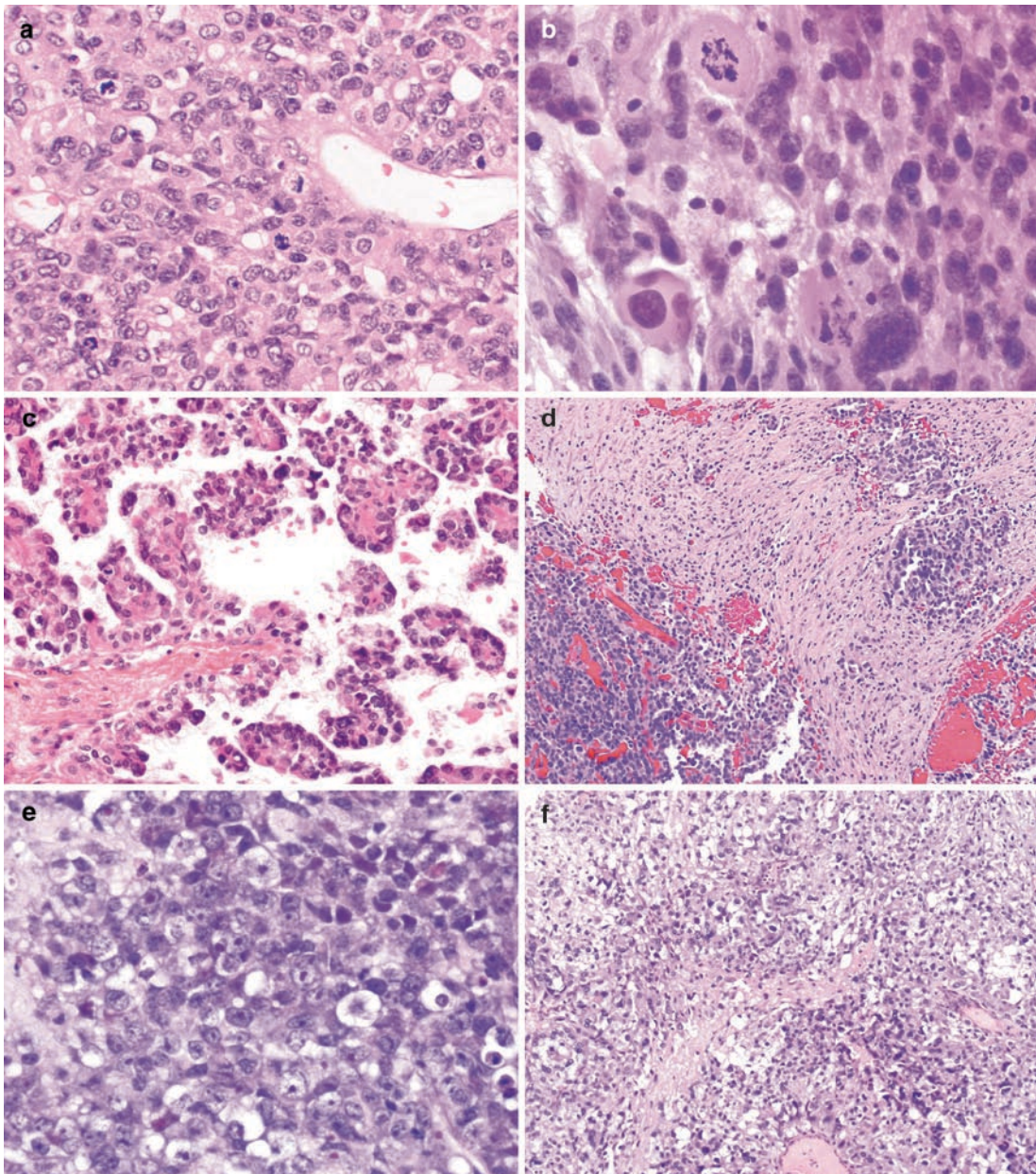
Fig. 31.8. (**a** and **b**) CPCs contain solid sheets of variably pleomorphic epithelioid cells with frequent mitoses, sometimes with focally retained papillary architecture (**c**). Invasion into the surrounding brain parenchyma is common (**d**). Though their cytoplasm is often eosinophilic, the malignant epithelioid cells of CPC may also have amphophilic (**e**) or clear cytoplasm (**f**).
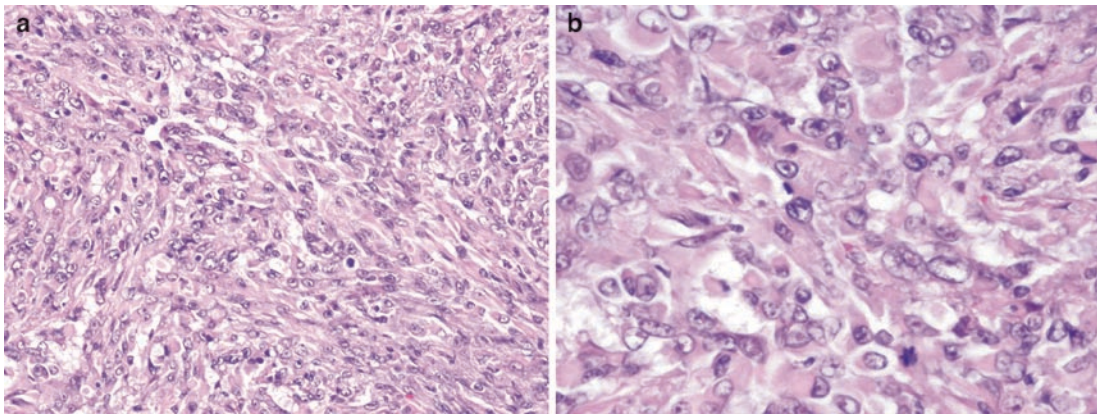
Fig. 31.9. CPCs may display a distinctly rhabdoid morphology; though often showing a rather spindled low power appearance (**a**), these lesions harbor cells with large eccentric vesicular nuclei and prominent nucleoli (**b**), virtually identical to the rhabdoid cells of AT/RT.
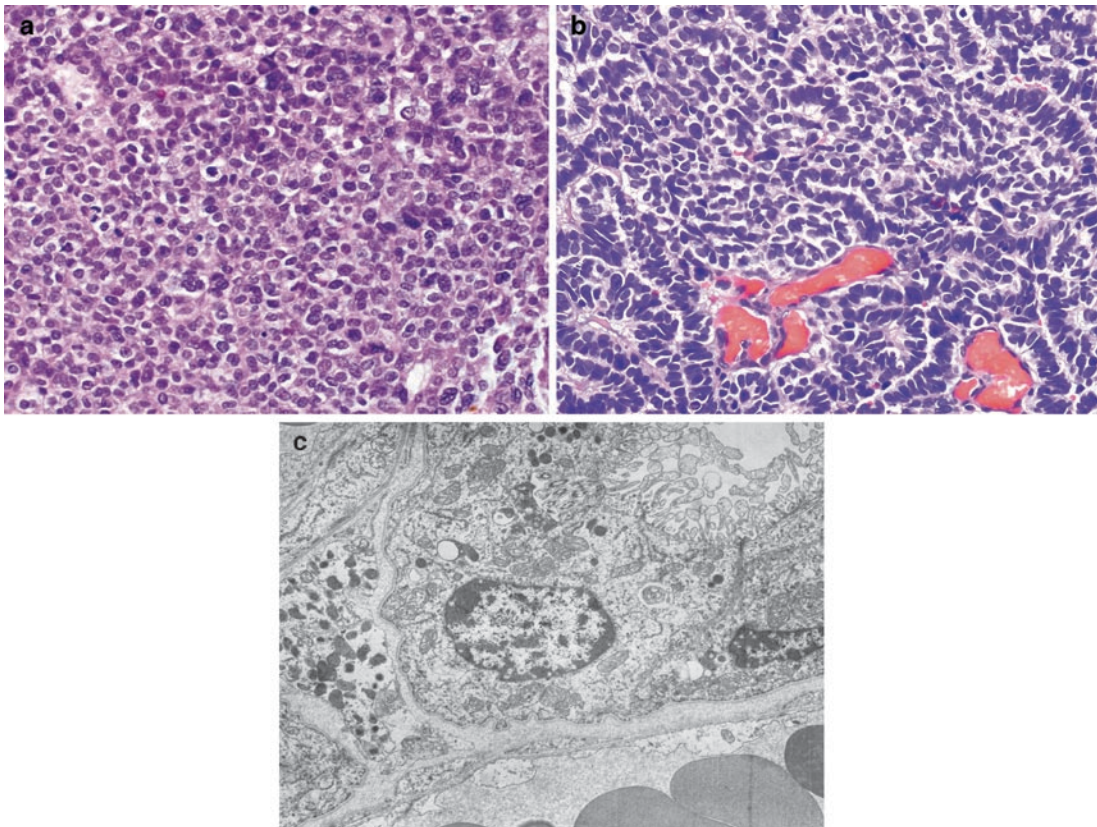
Fig. 31.10. Occasionally, CPCs may show a small cell morphology mimicking PNET and other small round blue cell tumors of infancy. The neoplastic cells, with their high nucleocytoplasmic ratio and minimal surrounding cytoplasm, may arrange in patternless sheets (**a**) or ribbon-like patterns (**b**). At the ultrastructural level (**c**), choroid plexus tumors contain epithelioid cells with surface microvilli and cilia, tight junctions (upper right), and they rest upon basement membrane.
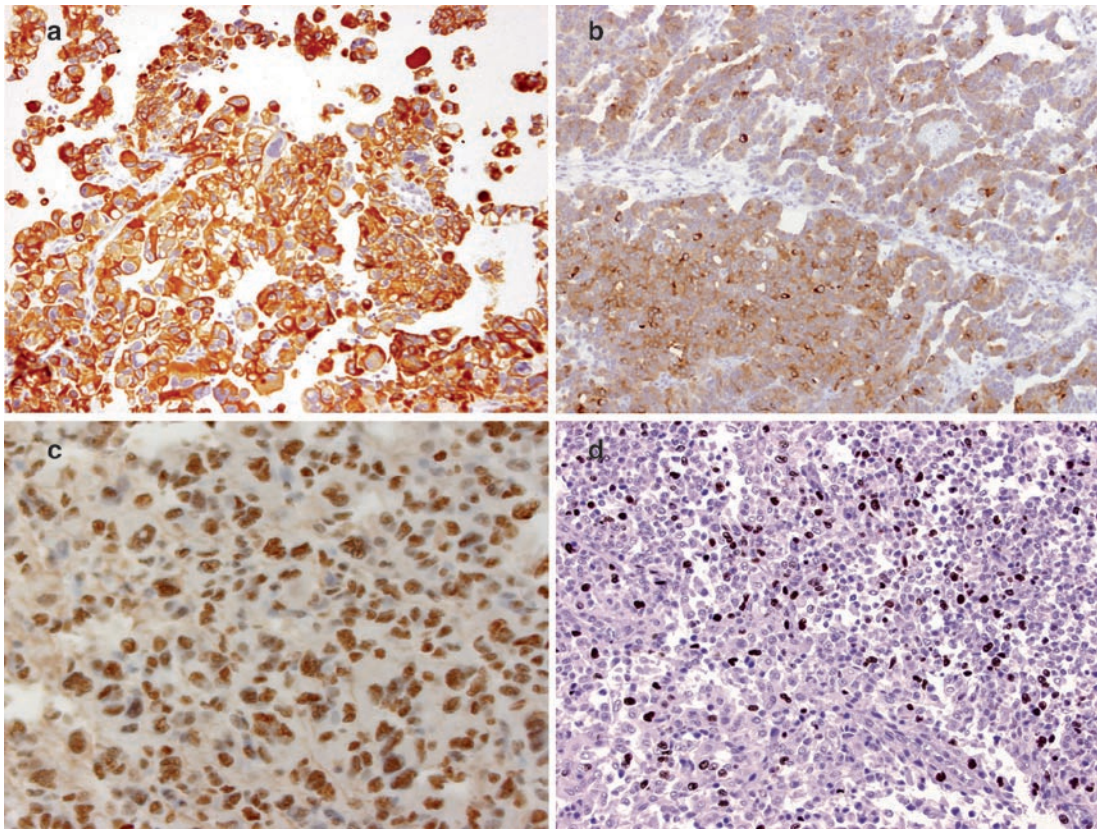
Fig. 31.11. CPCs are typically positive for cytokeratin (**a**) as well as synaptophysin (**b**). (**c**) Nuclear positivity for immunohistochemical stain for INI1 (BAF47) is a helpful discriminator of CPC from AT/RT. (**d**) Ki67 (Mib-1) labeling index of proliferation is often brisk.

Section I: Pineal-Based Tumors

Tarik Tihan

Abstract This section is focused on pineal-based tumors. It covers pineocytoma, pineal parenchymal tumor of intermediate differentiation (PPT-INT) and pineoblastoma. The salient features that allow the diagnosis of these entities are presented.

Pineal Parenchymal Tumors

Tarik Tihan

Keywords Pineocytic; Pineocytoma; Pineal Parenchymal Tumor; Pineoblastoma; RB gene

32.1 OVERVIEW

- A recently described rare neoplasm, papillary tumor of the pineal region, is typically a tumor in adults and will not be discussed in this chapter.

32.2 CLINICAL FEATURES

- All primary pineal parenchymal neoplasms, as well as other pineal region masses, may be associated with Parinaud's syndrome in children, a dorsal midbrain syndrome that includes upward gaze paralysis, accommodative paresis, nystagmus, and eyelid retraction.
- Pineal region masses can also cause significant CSF obstruction leading to headache, nausea and vomiting and other signs related to increased intracranial pressure. However, these symptoms are not specific to pineal parenchymal neoplasms.
- *PINEOCYTOMA (PC)* is less common in the pediatric age group, and the rare PC typically presents with signs of increased intracranial pressure and occasional visual disturbances.
  - The few available reports on PC in children document a clinical course that is more aggressive compared to PC in adults in terms of local recurrence.
- *PPT-INT* is even less frequent in children; its clinical presentation is less well defined, yet is considered similar to PC.
  - These tumors have a greater tendency for local recurrence, but an objective comparison between PPT-INT and PC with regard to recurrence risk is not possible.
- *PINEOBLASTOMA (PB)* is the most common pediatric pineal parenchymal tumor, and the majority of the tumors occur within the first two decades of life.
  - The interval between the initial symptoms and the presentation of the need for surgical intervention is much shorter than in other pineal parenchymal tumors.
  - Signs and symptoms of intracranial pressure are often present and may rapidly worsen with cerebrospinal dissemination.

32.3 NEUROIMAGING

- *PC* is often a well-defined mass, typically less than 3–4 cm, and is hypointense or isointense on T1, and hyperintense on T2-weighted images.
  - The tumors enhance avidly upon gadolinium administration.
  - Some PCs demonstrate calcifications on CT or MRI (Fig. 32.1).
- *PPT-INT* is often indistinguishable from PC and may also demonstrate calcifications or hemorrhage on imaging studies.
- *PB* is often a large tumor, rarely seen in association with unilateral or bilateral retinoblastoma (trilateral retinoblastoma).
  - The tumors are often larger, with hyperintense T2-weighted signals, and hypointense in T1-weighted images.
  - While there is a marked enhancement on gadolinium administration, the tumors are much more heterogenous in their appearance, with calcifications, necrosis or hemorrhage.
  - The boundaries of PB may not always be well-defined (Fig. 32.2).

32.4 PATHOLOGY

- Macroscopically, *PCs* are gray, granular and discrete masses, and often fill the pineal recess and the subjacent aqueduct.
  - The tumors are composed of cells with large nuclei and open chromatin density, and ample surrounding cytoplasm.
  - The tumor cells are typically monomorphous with only occasional cells with nuclear pleomorphism or hyperchromasia.
  - Necrosis and mitotic figures are exceptionally rare.
  - In some foci, cytological atypia can be interpreted as "degenerative change".
  - PC often harbors pineocytomatous rosettes formed by a conglomeration of tumor cell processes in a circular or stellate form; they are slightly more eosinophilic than the neuropil.
  - The structure of a pineocytomatous rosette is similar to that of a pineoblastic or Homer–Wright rosette, but it is conspicuously less cellular, larger, and the majority of the cells have ample cytoplasm.
  - PC can show large isolated or clustered ganglion-like cells, and focal islands of neuropil, but these findings are rare (Figs. 32.3 and 32.4).
- *PPT-INT*
  - The tumors show variable diffuse or lobular architecture, and are often composed of dense monomorphous, back-to-back, neuronal cells.
  - The tumors have high or moderate cellularity with focally overlapping nuclei, cells with scant cytoplasm, mild to moderate nuclear atypia, and scattered mitotic figures.
  - The tumors may harbor focal PC-like areas admixed with sheets of tumor cells or lobules with increased cellularity.
  - These tumors rarely contain giant cells, Homer Wright type rosettes or large ganglion-like cells (Fig. 32.5).

- *PB*
  - Macroscopically, these tumors are soft, gelatinous, focally hemorrhagic and necrotic.
  - These irregular neoplasms can be quite large.
  - They have been described as similar to medulloblastomas or to supratentorial PNETs.
  - The tumors are composed of small round blue cells with scant cytoplasm and hyperchromatic nuclei (Fig. 32.6).
  - The cells are often arranged in sheets or discohesive clusters.
  - As in retinoblastoma, the tumor cells may form Flexner–Wintersteiner rosettes (Fig. 32.7) in which the cells are radially arranged around a small luminal structure.
  - Neuroblastic-type Homer–Wright rosettes (Fig. 32.8) identical to those seen in medulloblastomas can be observed.
  - The tumor shows conspicuous mitotic figures, and in some areas these can be numerous.
  - Occasional giant cells, hemorrhage and calcification are also commonly present.
  - Rare tumor cells may harbor melanin pigment, but more often, the pigment is hemosiderin.

32.5 IMMUNOHISTOCHEMISTRY

- *PC*
  - It typically demonstrates a strong positivity for S-100 protein, synaptophysin and chromogranin, as well as a variable immunoreactivity to antibodies directed at neurofilament proteins.
  - The tumors are also focally positive for glial fibrillary acidic protein, retinal-S antigen, and rhodopsin (Fig. 32.9).
- *PPT-INT*
  - It is similar to PC with a strong positivity for synaptophysin, as well as S-100 protein.
  - Antibodies for neurofilament proteins stain the tumors focally, and in some cases isolated cells within the tumor show intense staining.
  - The staining for GFAP and retinal-S antigen is also variable, and some tumors may be negative for these two markers.
- *PB*
  - It exhibits a less pronounced retinoblastomatous differentiation but is often as positive with synaptophysin as other pineal parenchymal tumors.
  - Chromogranin is positive only in a small percentage of tumors and in a limited number of tumor cells.
  - S-100 protein and retinal-S antigen are typically negative, and only an occasional tumor may show a rare weak positivity.

32.6 MOLECULAR PATHOLOGY

- Trilateral retinoblastoma is a heritable form of bilateral retinoblastoma in association with PB, and has a rather dismal prognosis.
  - The disease is associated with germline deletion of the RB1 gene from chromosome 13.
    RB1 gene encodes a protein that acts as a cell cycle checkpoint control protein at the G1/S interphase.

32.7 DIFFERENTIAL DIAGNOSIS

- The differential diagnosis of the tumors in the pineal region of children primarily includes germ cell neoplasms.
- Both the pineal parenchymal tumors and germ cell neoplasms of the pineal region may have similar clinical and radiological characteristics.
- Typically, routine microscopy is all that is necessary to differentiate the various germ cell tumors from pineal parenchymal tumors, though immunohistochemistry for germ cell markers (PLAP, AFP, HCG) and neural markers may be employed in difficult cases.

32.8 PROGNOSIS

- The following clinical characteristics influence the outcome in pineal neoplasms:
  - Tumors with a pineoblastomatous component have a much worse overall survival compared to other histologic types.
  - Gross total resection seems to portend a better prognosis even in patients with PB.
  - Aggressive chemotherapy and radiotherapy have been suggested to improve survival for patients with PB.

SUGGESTED READING

Schild SE, Scheithauer BW, Schomberg PJ et al (1993) Pineal parenchymal tumors. Clinical, pathologic, and therapeutic aspects. Cancer 72:870–880

Min KW, Scheithauer BW, Bauserman SC (1994) Pineal parenchymal tumors: an ultrastructural study with prognostic implications. Ultrastruct Pathol 18:69–85

Chiechi MV, Smirniotopoulos JG, Mena H (1995) Pineal parenchymal tumors: CT and MR features. J Comput Assist Tomogr 19:509–517

Scheithauer BW (1999) Pathobiology of the pineal gland with emphasis on parenchymal tumors. Brain tumor pathology 16:1–9

Fauchon F, Jouvet A, Paquis P et al (2000) Parenchymal pineal tumors: a clinico-pathological study of 76 cases. Int J Radiat Oncol Biol Phys 46:959–968

Fevre-Montange M, Champier J, Szathmari A et al (2006) Microarray analysis reveals differential gene expression patterns in tumors of the pineal region. J Neuropathol Exp Neurol 65:675–684
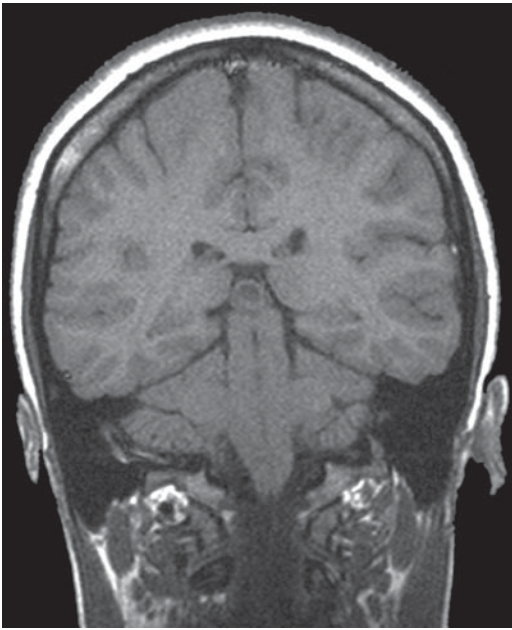
Fig. 32.1. Coronal non-contrast T1-weighted MR image of a pineal mass in a 17-year old male showing a small and cystic pineal gland. The lesion was histologically confirmed as a pineocytoma.

Fig. 32.2. Sagittal, contrast-enhanced T1-weighted MR image of a pineoblastoma, with mass effect and hydrocephalus, in a 4-year old child.
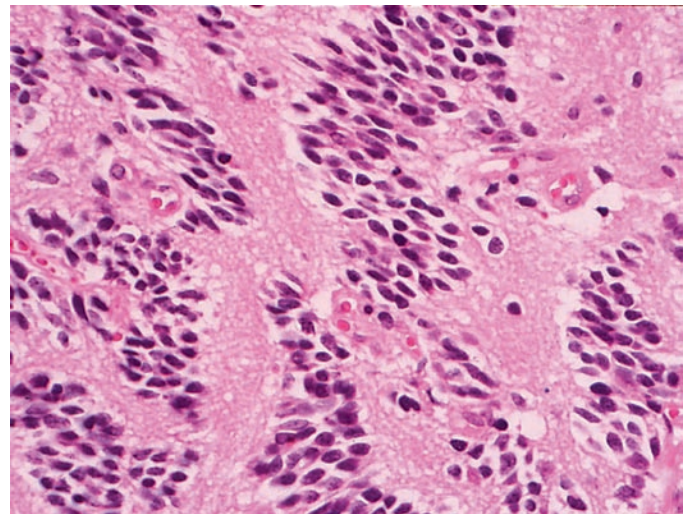
Fig. 32.3. Characteristic histological appearance of pineocytoma. The tumor is sparsely cellular and is composed of monomorphous, small mature neuronal cells and a neuropil-like background.
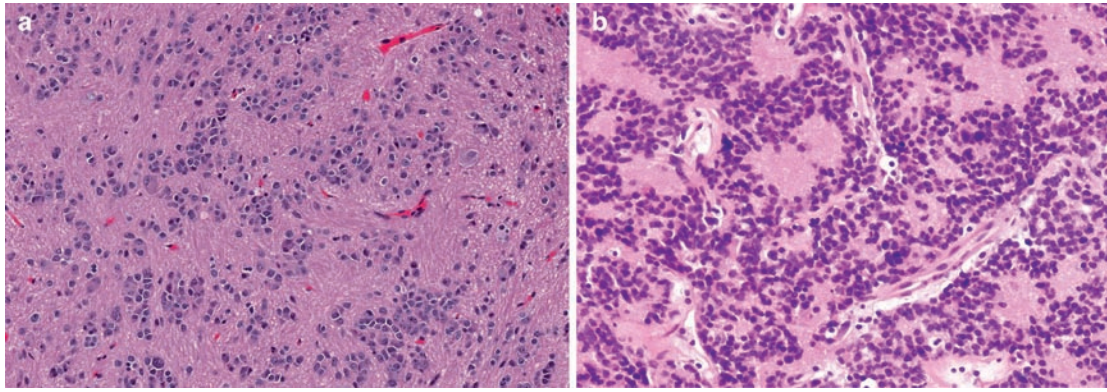
Fig. 32.4. Histological features of pineocytoma showing (**a**) the less common histologic feature of a rich neuropil-like matrix and rare ganglion-like cells, and (**b**) pineocytomatous rosettes.

Fig. 32.5. Pineal parenchymal tumor of intermediate differentiation (PPT-INT) composed of a mixture of small and mature cells presenting a mixed appearance between pineocytoma and pineoblastoma.
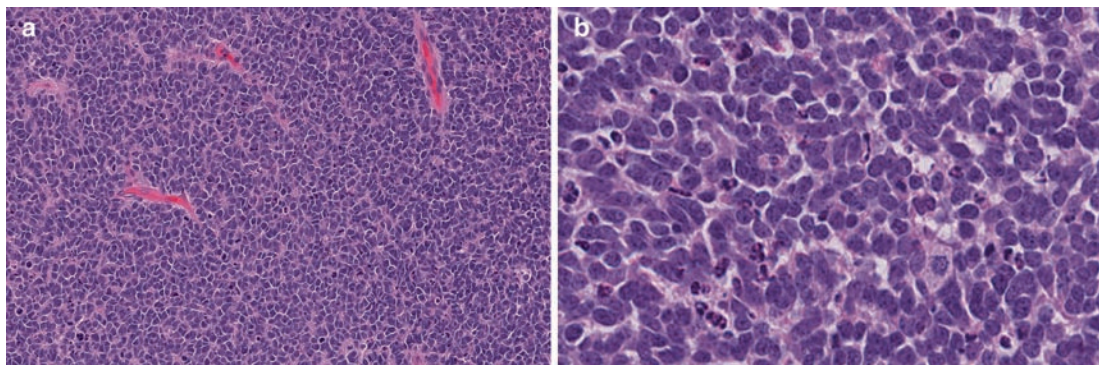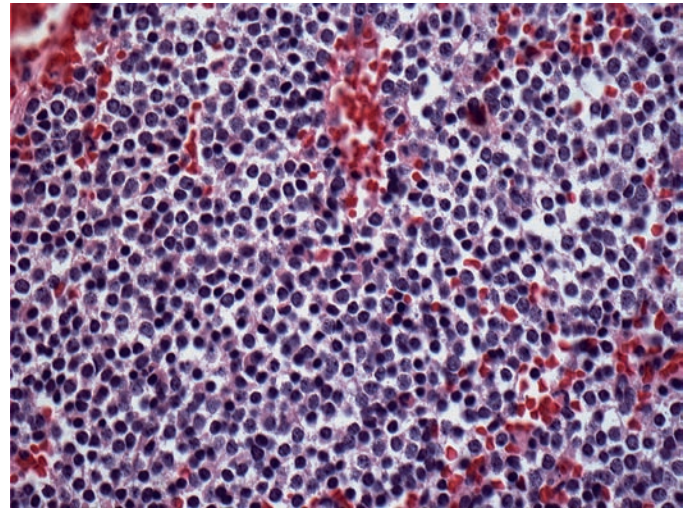
Fig. 32.6. (**a**) Low magnification, and (**b**) high magnification microscopy of pineoblastoma composed of highly cellular, small round blue cells with numerous mitotic figures.
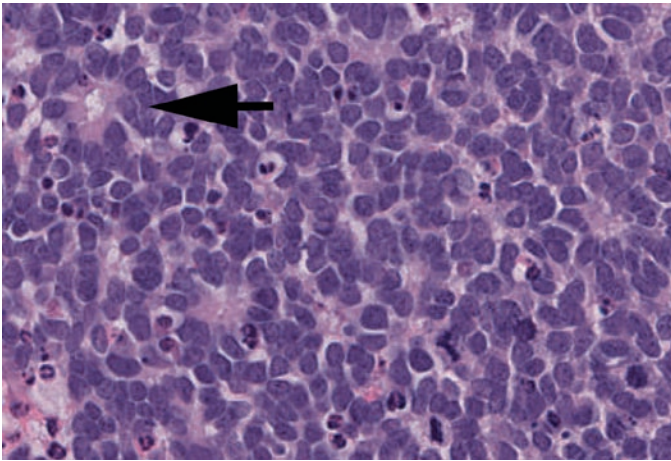
Fig. 32.7. Retinoblastic (Flexner–Wintersteiner) rosette in pineoblastoma (*arrow*).
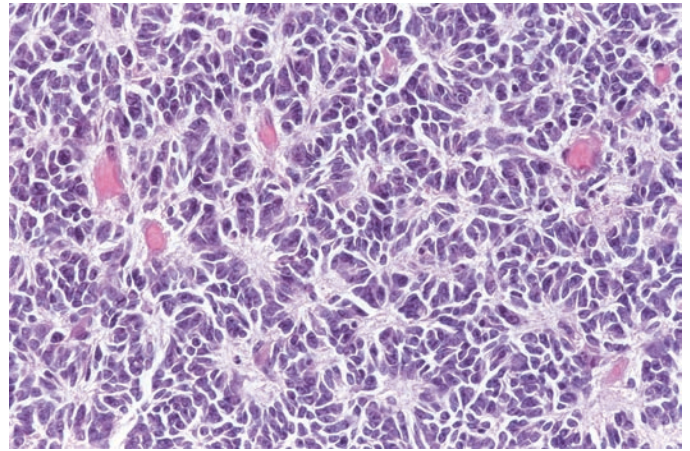
Fig. 32.8. Neuroblastic (Homer–Wright) rosettes in pineoblastoma.
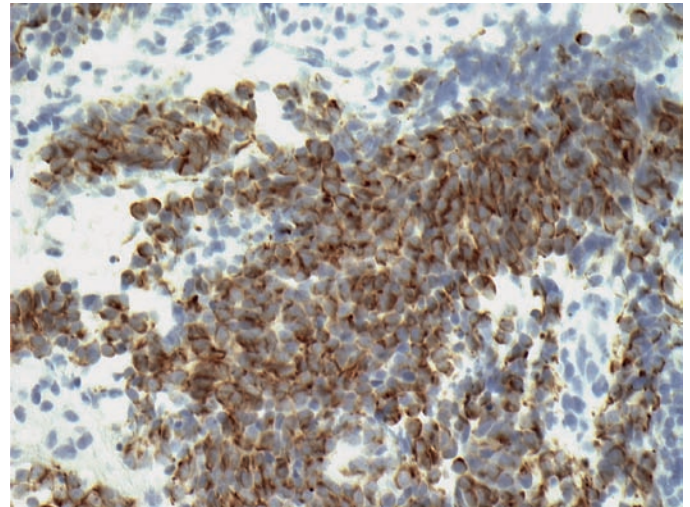
Fig. 32.9. Immunohistochemical staining for chromogranin in pineoblastoma. Note the patchy staining of the cytoplasm.

Section J: Germ Cell Tumors

Tarik Tihan

Abstract This section presents the pathology and the neuroimaging features of germ cell tumors including germinoma, yolk sac tumor, embryonal carcinoma, choriocarcinoma, and teratoma. The salient distinguishing features of these often overlapping entities are presented.

Germ Cell Tumors

Tarik Tihan

33.1 OVERVIEW

- Germ cell tumors of the CNS are typically midline lesions, commonly affecting the pineal and suprasellar regions, and are similar to their counterparts arising in the gonads.
- Types, histological and immunohistochemical features of CNS germ cell tumors are essentially the same as gonadal or extra-gonadal extracranial germ cell tumors.

33.2 CLINICAL FEATURES

- Germ cell tumors are more common in children and young adults, and the overwhelming majority occur within the first two decades. A unique exception to this is the congenital teratoma that is often discovered during the neonatal period or in utero.
- Males are slightly more commonly affected than females, particularly regarding germ cell tumors arising within the pineal region among which males outnumber females 2:1.
- The pineal region tumors often present with signs and symptoms of hydrocephalus as well as upward gaze palsy due to compression of midbrain, known as Parinaud's syndrome.
- One of the most common presentations of germ cell tumors in the suprasellar/infundibular region is diabetes inspidus.
- Suprasellar tumors can present with visual disturbance, pituitary failure or abnormal sexual maturation.
- Serum (or CSF) levels of alpha-fetoprotein (AFP), human chorionic gonadotrophin (b-HCG) and carcinoembryonic antigen (CEA) levels can be elevated and should be analyzed in a patient with a suspected germ cell tumor.

33.3 NEUROIMAGING

- Most germinomas involving the pineal are well-delineated and are hypo-intense on T1-weighted images, iso or hyper-intense on T2-weighted images, and demonstrate often strong and uniform contrast enhancement (Fig. 33.1).
- Suprasellar or infundibular examples can be less well defined and may appear more infiltrative.
- Mixed germ cell tumors and teratomas demonstrate more mixed elements, may have both hyper and hypo-intense regions on T2-weighted images, and may show heterogeneous enhancement.
- Subependymal linear enhancements often represent local tumor spread.
- Occasionally, there may be synchronous pineal and suprasellar masses with periventricular or infundibular involvement.
- In patients with diabetes insipidus, there can be absence of the posterior pituitary bright spot on the sagittal T1-weighted images.

33.4 HISTOPATHOLOGY

- The most common types of germ cell tumors in the CNS are germinomas (~50%) and teratomas (~20%), but all types of germ cell tumors can be observed.
- *GERMINOMA*
  - Most common histological form of germ cell tumor in the CNS.
  - Most biopsy specimens from germinomas are small, and suffer from crush artifact. Thus a thorough evaluation of the smear and frozen section slide is necessary.
  - Typical components are mitotically active large cells with vacuolated cytoplasm, round vesicular nuclei and central macronucleoli, and mature lymphocytes (Fig. 33.2).
  - The large neoplastic cells often appear discohesive, reminiscent of a malignant lymphoma.
  - Occasional examples can also show granuloma formation.
  - Syncytiotrophoblastic giant cells can be seen.
  - Recognition of the biphasic nature of the tumor is very helpful in smears and intraoperative consultations (Fig. 33.3).
  - Germinomas show focal positive cytoplasmic PAS staining that is digested by diastase treatment because of their glycogen-rich cytoplasm.
  - Germinomas may rarely involve the brain parenchyma, and give the false impression of an infiltrating malignant glioma.
- *TERATOMA*
  - Both mature and immature teratomas in the CNS are aggressive neoplasms. They are the second most common germ cell tumors after germinoma.
  - Typical mature teratoma consists of histologically mature tissue that differentiates along all three germ layers of ectoderm, mesoderm, and endoderm (Fig. 33.4).
  - Immature teratomas contain variable amounts of tissue resembling fetal tissue that may often include immature neural elements with rosettes. Even a minor component of fetal tissue is considered sufficient to classify a neoplasm in this category (Fig. 33.5).
  - Most common immature tissue type is the stroma reminiscent of fetal mesenchymal tissue, but immature epithelium, bone or cartilage can also be encountered.
  - In addition to mature and immature tissues, some teratomas contain foci that are reminiscent of malignant neoplasms such as a carcinoma or a sarcoma. These neoplasms are believed to act more aggressively, however, a detailed study of this phenomenon in the CNS is lacking.
  - Sampling is critical for teratomas since some elements may be present only focally.
- *YOLK SAC TUMOR (ENDODERMAL SINUS TUMOR)*
  - More likely to be seen in the pineal region.

- Primary intracranial yolk sac tumor is extremely rare, and constitutes a rare component of a mixed non-germinomatous germ cell tumor.
- Histological appearance is identical to yolk sac tumors of the gonads.
- Often, the tumor cells are arranged in a loose lacy network interrupted by characteristic Schiller–Duval bodies and other more obvious epithelial-appearing elements (Fig. 33.6).
- The tumors are often highly aggressive and are associated with poor prognosis.
- Pure or predominantly yolk sac tumors are exceedingly rare.

- *EMBYONAL CARCINOMA*
  - Histologically are composed of pleomorphic and anaplastic epithelial cells arranged in a variety of patterns, from patternless solid sheets to glandular sometimes cribriform arrangements to papillary structures.
  - This component tends to be more pleomorphic than the epithelium of yolk sac tumor and may resemble a poorly differentiated metastatic carcinoma (Fig. 33.7).
  - Mitotic figures are abundant, and giant cells can be seen.

- *CHORIOCARCINOMA*
  - Presence of multinucleated syncytiotrophoblasts and cytotrophoblasts define choricarcinoma (Fig. 33.8).
  - Choriocarcinomas are typically seen as hemorrhagic foci.
  - Choriocarcinoma portends a worse prognosis in a germ cell tumor.

33.5 IMMUNOHISTOCHEMISTRY

- *GERMINOMA*
  - The typical immunohistochemical profile of germinoma includes positive C-kit (CD117), OCT-4, D2-40, PLAP (Fig. 33.9), as well as the homeodomain transcription factor NANOG.
  - OCT-4 has been reported as a sensitive and specific marker for intracranial germinomas.
  - Rare cells may show CD30 or cytokeratin immunopositivity; beta-HCG positivity is detected in scattered syncytiotrophoblastic cells.

- *TERATOMA*
  - While immunohistochemistry is not essential, Ki-67 (MIB-1) staining may be helpful in confirming immature elements within teratomas.
  - Teratomas are often positive for EMA, and rarely positive for CD30.

- *YOLK SAC TUMOR (ENDODERMAL SINUS TUMOR)*
  - Most yolk sac tumors are AFP- and cytokeratin-positive.
  - PLAP and alpha-1 antitrypsin are occasionally positive in some tumors.
  - beta-HCG is often negative in yolk-sac tumors.

- *EMBYONAL CARCINOMA*
  - Embryonal carcinoma is often CD30, OCT-4 and cytokeratin-positive.
  - The tumors are negative or weakly positive for CEA, hCG, CD117, and D2-40.

- *CHORIOCARCINOMA*
  - Choriocarcinomas are positive for beta-HCG (syncytiotrophoblasts) and cytokeratin.
  - PLAP may be positive in one half of choriocarcinomas.

33.6 MOLECULAR PATHOLOGY

- Typically all types of CNS germ cell tumors demonstrate multiple genetic aberrations
- Gain of chromosome 12p appears to be the most common gain in CNS germ cell tumors, similar to testicular germ cell tumors in adults.
- Other gains include chromosomes 1q, 8q, and 20q.
- Chromosomal losses can be seen in 1p, 4q, 6q, 11, 13, 18.

33.7 PROGNOSIS

- The most common cited prognostic factors include age, tumor location, histological type and grade, tumor stage, extent of resection, and the tumor markers AFP and beta-HCG.
- Prognosis has been strongly related to pathological classification as either pure germinoma or mixed germ cell or non-germinomatous germ cell tumor.
- The presence of serum or cerebrospinal fluid tumor marker elevation has been helpful in determining response to treatment.
- Age of onset also influences the modality and success of treatment.

SUGGESTED READING

Santagata S, Hornick JL, Ligon KL (2006) Comparative analysis of germ cell transcription factors in CNS germinoma reveals diagnostic utility of NANOG. Am J Surg Pathol 30(12):1613–1618

Felix I, Becker LE (1990) Intracranial germ cell tumors in children: an immunohistochemical and electron microscopic study. Pediatr Neurosurg 16(3):156–162

Iczkowski KA et al (2008) Trials of new germ cell immunohistochemical stains in 93 extragonadal and metastatic germ cell tumors. Hum Pathol 39(2):275–281

Gobel U et al (2002) Management of germ cell tumors in children: approaches to cure. Onkologie 25(1):14–22

Schneider DT et al (2001) Genetic analysis of childhood germ cell tumors with comparative genomic hybridization. Klin Padiatr 213(4):204–211

Jaing TH et al (2002) Intracranial germ cell tumors: a retrospective study of 44 children. Pediatr Neurol 26(5):369–373
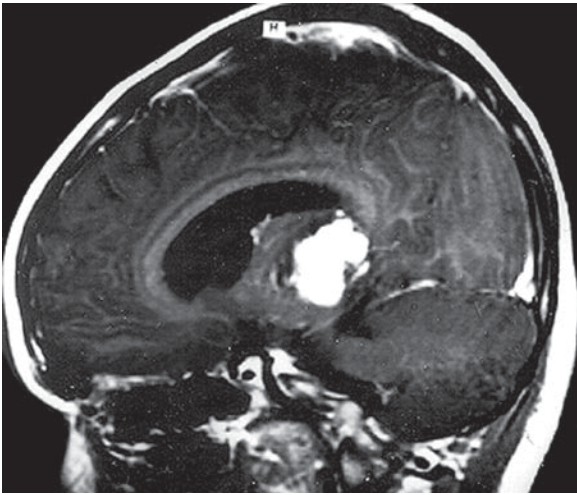
Fig. 33.1. Sagittal T1-weighted image of germinoma involving the pineal region with enhancement post contrast in a 12-year-old male.
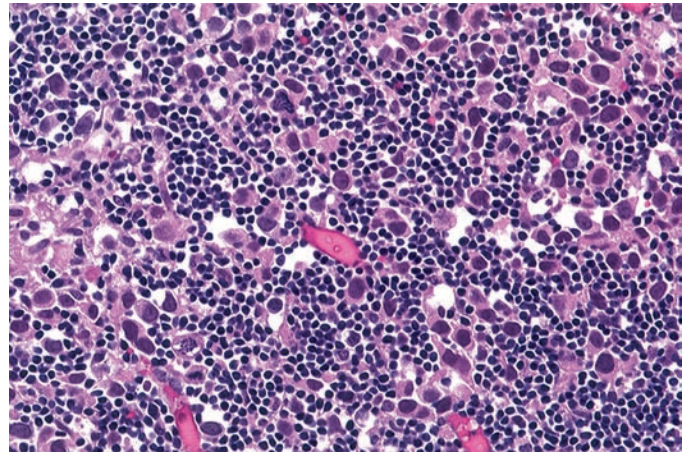
Fig. 33.2. Typical histological appearance of germinoma with two components of large malignant cells and mature appearing lymphocytes.

Fig. 33.3. Intraoperative smear of germinoma is often confounded by marked crush artifact, but the biphasic composition of large malignant cells with prominent central nuclei and mature lymphocytes is pathognomonic.
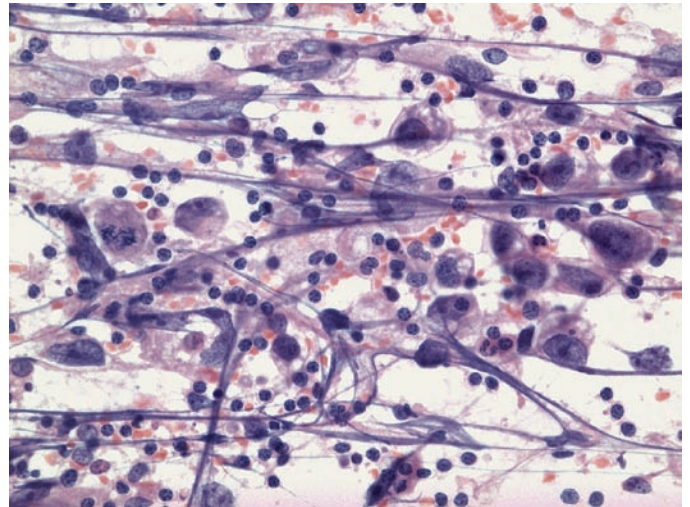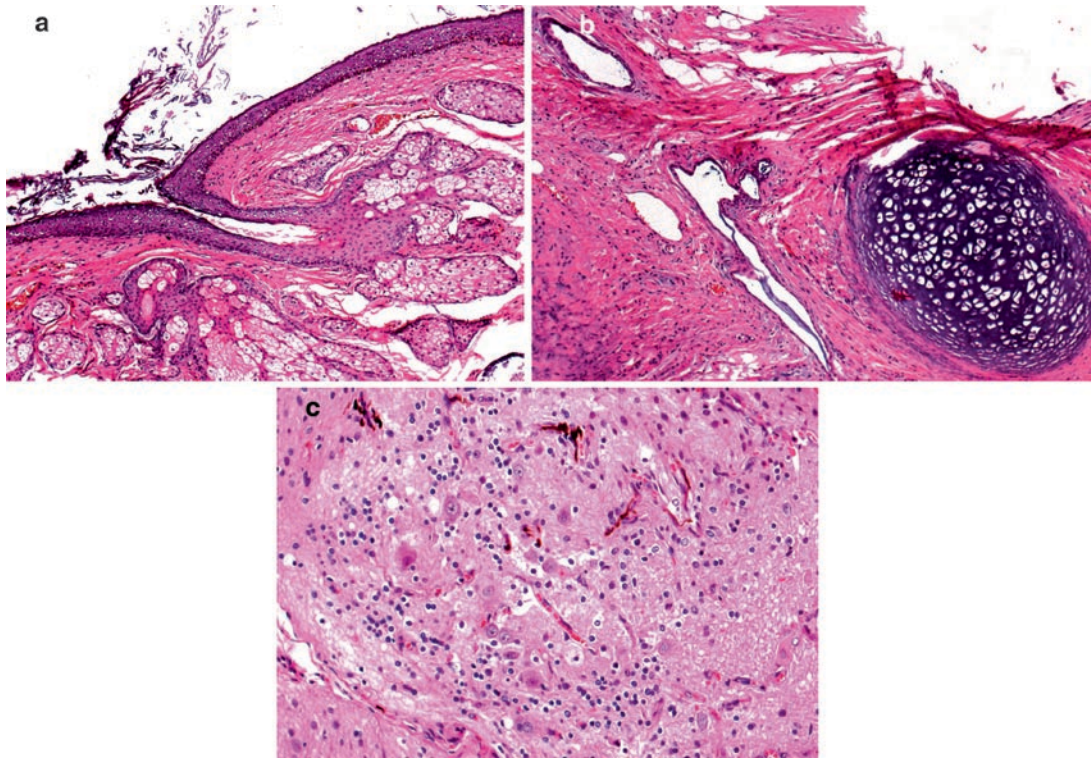
Fig. 33.4. Histological appearance and various components of mature teratoma: (**a**) dermal/epidermal, (**b**) cartilage, and (**c**) neural tissue.
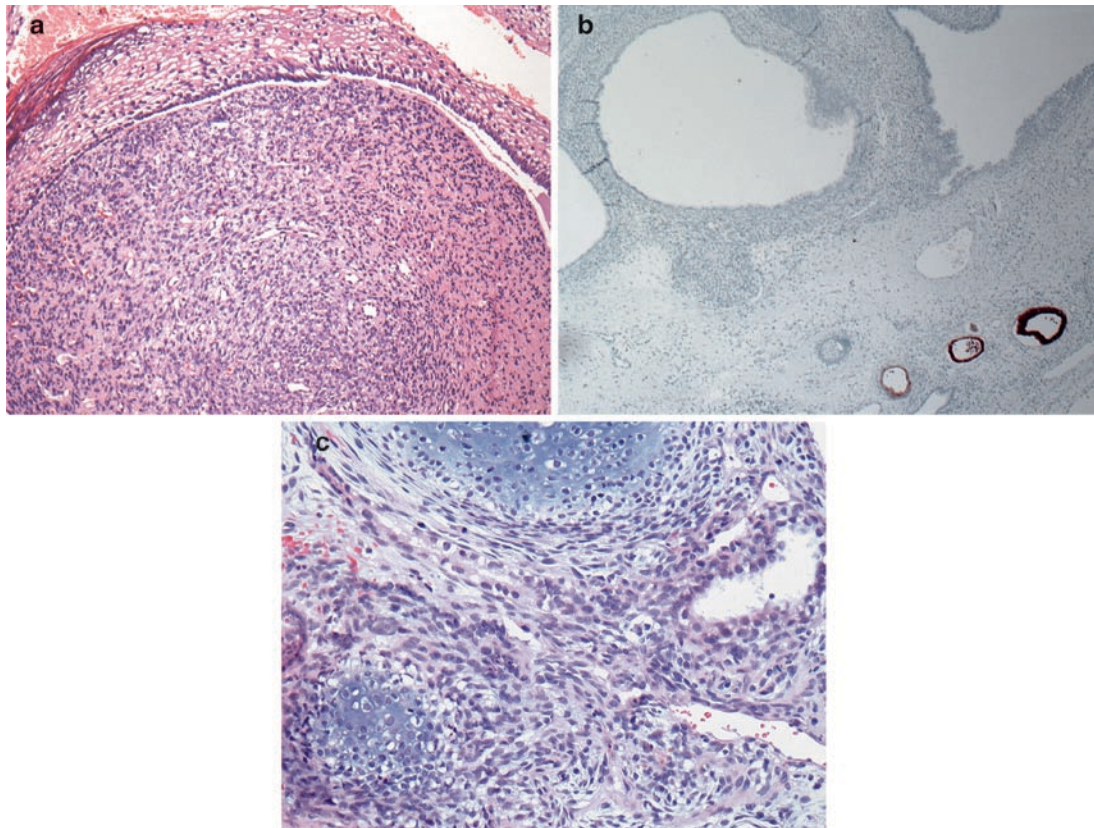
Fig. 33.5. Immature elements in teratoma: (**a**) fetal mesenchymal tissue, (**b**) immature epithelium as highlighted by positive AFP staining, and (**c**) immature cartilage.
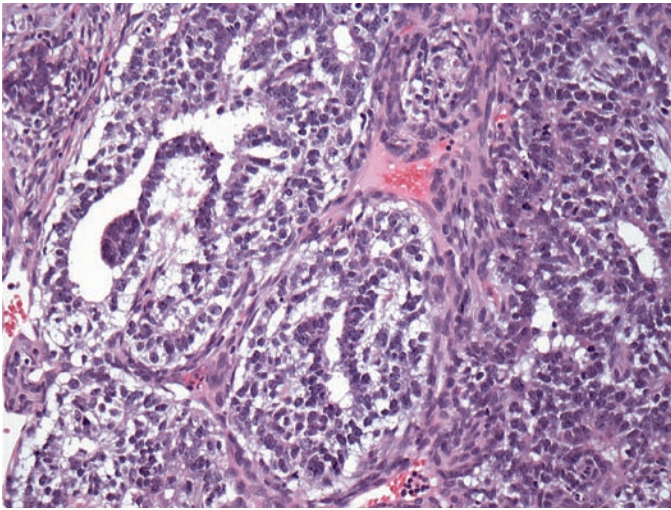
Fig. 33.6. Typical histological features of yolk sac (endodermal sinus) tumor with classical papillary-alveolar gland-like structures.
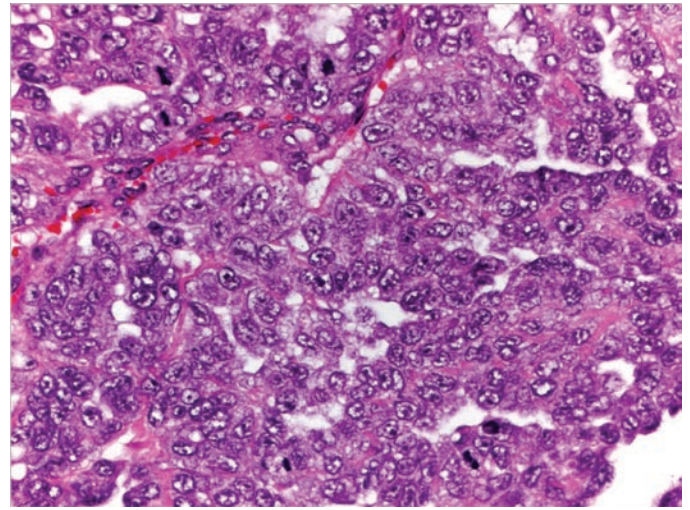
Fig. 33.7. Embryonal carcinoma showing high grade anaplastic epithelial features and no discernable glandular differentiation. Note the vesicular nuclei with distinct nucleoli and frequent mitotic figures.
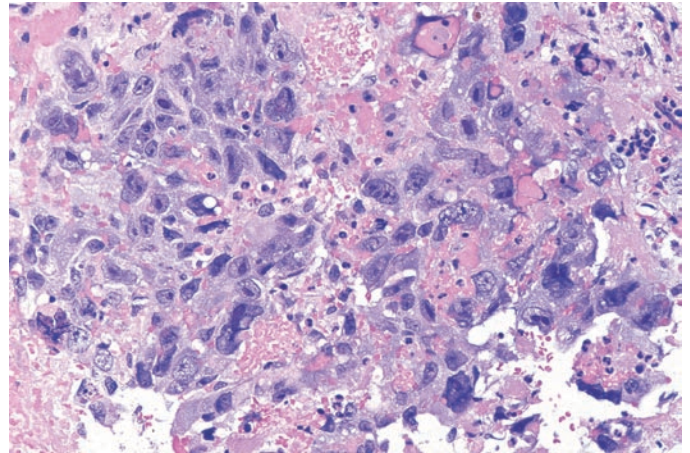
Fig. 33.8. Choricarcinoma with multinucleated syncytiotrophoblasts and cytotrophoblasts in a hemorrhagic background.
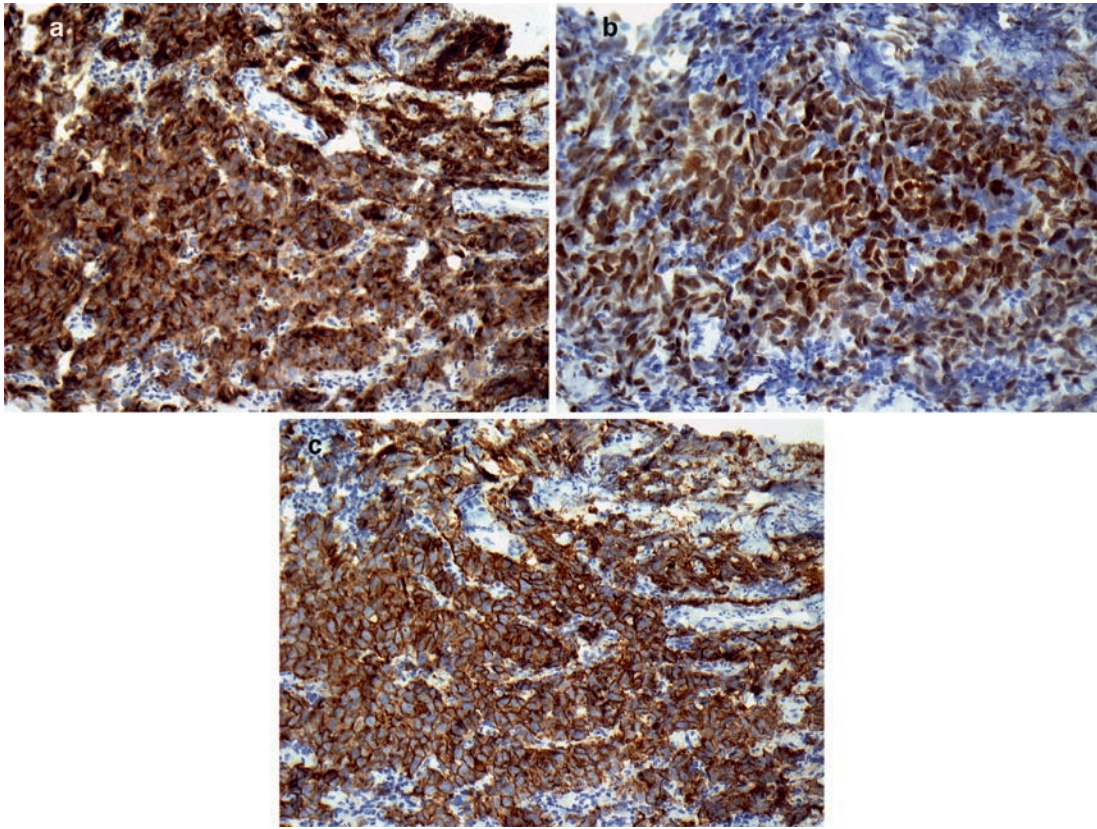
Fig. 33.9. Illustrations of immunohistochemical positivity for (**a**) PLAP, (**b**) oct-4, and (**c**) c-kit in germinoma.

Section K: Paraneoplastic Disorders

Christine E. Fuller and Sonia Narendra

Abstract Section K addresses paraneoplastic disorders involving the central nervous system. Paraneoplastic encephalomyelitis, cerebellar degeneration, and opsoclonus–myoclonus–ataxia are all presented, though the focus will be particularly on paraneoplastic CNS processes affecting children. Classic histologic findings are demonstrated.

Paraneoplastic Disorders of the Central Nervous System

Christine E. Fuller and Sonia Narendra

34.1 OVERVIEW

- Paraneoplastic disorders of the central nervous system are inflammatory disorders affecting various parts of the brain and spinal cord in the setting of a peripheral cancer.
- Ganglia, the peripheral nervous system, retina, and neuromuscular junction may also be involved.
- These syndromes appear to represent a group of autoimmune disorders in which antibodies mounted against peripheral cancers target antigens normally expressed within cells (particularly neurons) of the nervous system (i.e., onconeural antibodies).
- Main categories of disease include:
  - Paraneoplastic encephalomyelitis (PEM) – subcategories based on localization (limbic encephalitis, brainstem encephalitis, cerebellar encephalitis, and myelitis)
  - Paraneoplastic cerebellar degeneration (PCD)
  - Opsoclonus-myoclonus-ataxia syndrome (OMA)
- These syndromes occur in the absence of infiltration of the nervous system by tumor cells, side effects of cancer therapy, or other infections or metabolic/nutritional disturbances that may occur during the course of the disease. In addition, they may occasionally arise in the absence of demonstrable neoplasm.

34.2 CLINICAL FEATURES

- Though more frequently encountered in adults in association with lung, breast, or gynecologic malignancies, all of these disorders may present in children.
- In the pediatric age group, PEM most frequently accompanies neuroblastoma or rhabdomyosarcoma.
- PCD may be seen with Hodgkin's lymphoma, and OMA may occur with neuroblastoma.
- Often these syndromes will precede a diagnosis of cancer by weeks to months.
- Symptoms/signs reflect different patterns of CNS involvement:
  - Limbic encephalitis – short-term memory loss, seizures, confusion, psychosis.
  - Myelitis – pain, numbness, loss of proprioception.
  - OMA – eye movement disturbance, myoclonus ("dancing eyes and dancing feet"), ataxia, and sometimes developmental retardation. Unlike the other paraneoplastic disorders, OMA may have a relapsing-remitting course.
  - Cerebellar degeneration – ataxia, truncal and hemispheric cerebellar dysfunction.

34.3 NEUROIMAGING

- MR imaging in limbic encephalitis typically demonstrates hyperintense areas within limbic structures on T2-weighted and FLAIR sequences. Contrast enhancement is not a feature.
- MR may be normal in PCD, though edema or atrophy may be seen in some cases.
- MR is also frequently normal on OMA, though pontine tegmental abnormalities and cerebellar atrophy have been reported.
- Fluorodeoxyglucose-PET (FDG-PET) may be useful in confirming the presence of an occult neoplasm when conventional CT and MR imaging fail to detect a lesion. FDG-PET may sometimes reveal areas of increased uptake within the CNS itself correlating with the inflammatory process.

34.4 PATHOLOGIC FEATURES

- *Gross pathology*: With the exception of mild cerebellar cortical atrophy detectable in some cases of PCD, gross examination is typically unremarkable.
- *Cytology findings*: CSF samples often show a cellular pleocytosis; additional findings may include elevated protein level and/or oligoclonal bands.
- *Histology*:
  - The unifying theme for all of these disorders is the findings of:
    Neuronal loss
    Astrocytosis (gliosis)
    Microglial proliferation, often with microglial nodule formation or active neuronophagia
    Perivascular chronic inflammatory infiltrate of lymphocytes (mainly T cells) and occasional plasma cells (Fig. 34.1a–e)
  - Gray matter is predominantly involved, though there may be secondary white matter loss and leptomeningitis is frequently present.
  - Limbic encephalitis – neuronal loss/inflammation localized in the medial temporal and inferior frontal lobes, insular cortex, and cingulate gyrus.
  - Brainstem encephalitis – mainly involves the medulla.
  - Cerebellar encephalitis of PEM – neuronal loss in deep structures/nuclei of cerebellum with sparing of cortex.
  - PCD – severe loss of Purkinje cells with accompanying Bergman gliosis (cortex involved).

- Myelitis – neuronal loss/inflammation may diffusely involve most of the spinal cord or may be more localized to a few segments.
- OMA – there is no specific pathologic feature for this disorder. Approximately ½ will show loss of Purkinje cells. Often there is neuronal loss and inflammation within the brainstem, though localization is variable.
- Ganglioneuronopathy with loss of dorsal root ganglion cell loss/inflammation and dorsal column degeneration may accompany PEM (Fig. 34.1f).

34.5 IMMUNOHISTOCHEMISTRY

- CD68 will highlight microglia (Fig. 34.2a), whereas T and B cell markers (CD3 and CD20 respectively) decorate the perivascular lymphoid infiltrates.
- GFAP highlights numerous reactive astrocytes (Fig. 34.2b).
- Immunohistochemical assessment for various viral agents as well as routine stains for spirochetes (Warthin-Starry stain) or fungal organisms (GMS) may be helpful in ruling out various infectious encephalitides.

34.6 ELECTRON MICROSCOPY

- Electron microscopy serves no significant role in the direct diagnosis of paraneoplastic CNS disorders.
- It may, however, be useful in identifying some microorganisms that cause infectious encephalitis that may otherwise closely mimic the histologic features of paraneoplastic disorders, such as microgliosis and perivascular chronic inflammation.

34.6.1 Ancillary Testing

- The detection of specific antineuronal antibodies in the serum and CSF may serve as a diagnostic tool that directs the search of the tumor to specific organ system.
- Many different antibodies can be associated with the same neurologic syndrome or one antibody may be associated with different syndromes.
- Approximately 40% of patients with paraneoplastic CNS disorders do not have detectable antibodies and some antibodies can be found in low titers in patients who have cancer without paraneoplasia.
- Anti-Tr can be detected in the CSF of some children with PCD arising in the setting of Hodgkin's lymphoma.
- Autoantibodies of IgG3 subclass have been found in pediatric patients with OMA in the setting of neuroblastoma. Anti-Ri has been identified in some.

- Anti-Hu, Ma, and Ta antibodies have been found in cases of PEM.

34.7 DIFFERENTIAL DIAGNOSIS

- The histologic features of these paraneoplastic CNS disorders may closely mimic infectious (particularly viral) encephalomyelitis. Careful histologic inspection for viral cytopathic effect, use of immunohistochemical stains, and tissue culture are helpful adjuncts to diagnosis in ruling out infectious etiologies.

34.8 PROGNOSIS

- In most instances, the most effective treatment for the paraneoplastic CNS disorders is to remove/treat the primary peripheral neoplasm together with immunomodulatory therapies.
- With some cases of pediatric OMA, despite tumor resection and immunosuppressive therapy, poor outcomes may include developmental and behavioral problems. Rituximab therapy has shown some promising results in some instances.

SUGGESTED READING

Mitchell WG, Davalos-Gonzalez Y, Brumm VL, Aller SK, Burger E, Turkel SB et al (2002) Opsoclonus-ataxia caused by childhood neuroblastoma: developmental and neurologic sequelae. Pediatrics 109(1):86–98

Corapcioglu F, Mutlu H, Kara B, Inan N, Akansel G, Gurbuz Y et al (2008) Response of rituximab and prednisolone for opsoclonus-myoclonus-ataxia syndrome in a child with ganglioneuroblastoma. Pediatr Hematol Oncol 25(8):756–761

Rutherford GC, Dineen RA, O'Connor A (2007) Imaging in the investigation of paraneoplastic syndromes. Clin Radiol 62:1021–1035

Gultekin SH, Rosenfeld MR, Voltz R, Eichen J, Posner JB, Dalmau J (2000) Paraneoplastic limbic encephalitis: neurological symptoms, immunological findings and tumour association in 50 patients. Brain 123:1481–1494

Bernal F, Shams'ili S, Rojas I, Sanchez-Valle R, Saiz A, Dalmay J et al (2003) Anti-Tr antibodies as markers of paraneoplastic cerebellar degeneration and Hodgkin's disease. Neurology 60(2):230–234

Beck S, Fuhlhuber V, Krasenbrink I, Tschernatsch M, Kneifel N, Kirsten A et al (2007) IgG subclass distribution of autoantibodies in pediatric opsoclonus-myoclonus syndrome. J Neuroimmunol 185(1–2):145–149

Linke R, Voltz R (2008) FDG-pet in paraneoplastic syndromes. Recent Results Cancer Res 170:203–211

Graus F, Delattre JY, Antoine JC, Dalmau J, Giometto B, Griswold W et al (2004) Recommended diagnostic criteria for paraneoplastic neurological syndromes. J Neurol Neurosurg Psychiatry 75:1135–1140
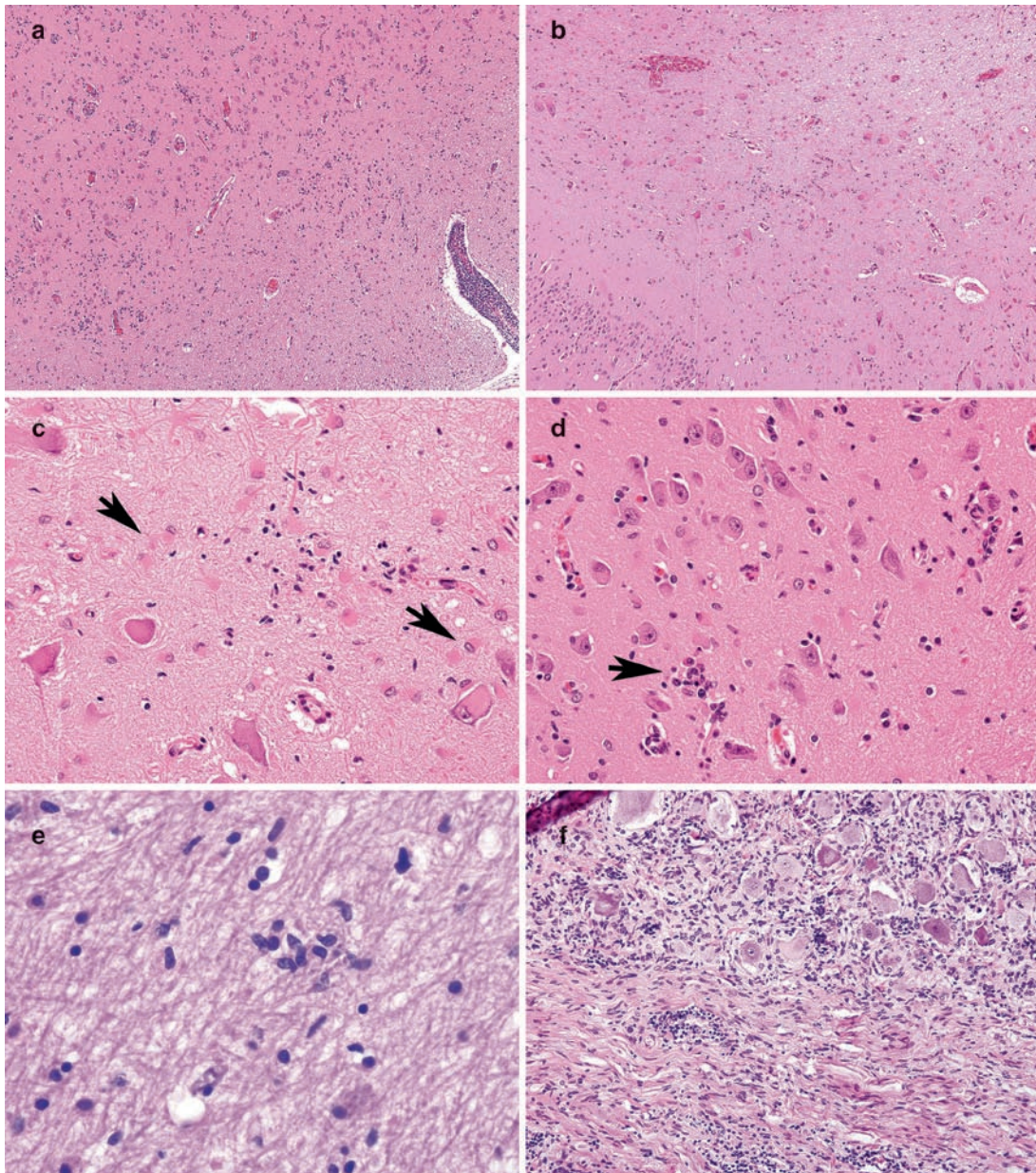
Fig. 34.1. (**a**) Low power view of a case of limbic encephalitis showing perivascular inflammatory infiltrate and increased cellularity within the gray matter with some cell clustering. (**b**) This area shows extensive reactive astrocytosis with accompanying neuronal loss in the hippocampal neurons. (**c**) Examination at higher magnification confirms the presence of numerous reactive astrocytes with brightly eosinophilic cytoplasmic "bellies" and elongated processes (*arrows*), together with a microglial proliferation (note hyperchromatic rod-shaped nuclei towards center of field). (**d**) Active neuronophagia is apparent (*arrow*). (**e**) Microglial nodules may also be seen. (**f**) This example of paraneoplastic ganglionitis shows the typical lymphocytic inflammatory infiltrate, in some areas surrounding individual ganglion cells (Courtesy of Dr Robert Schmidt, Washington University, St Louis, MO).
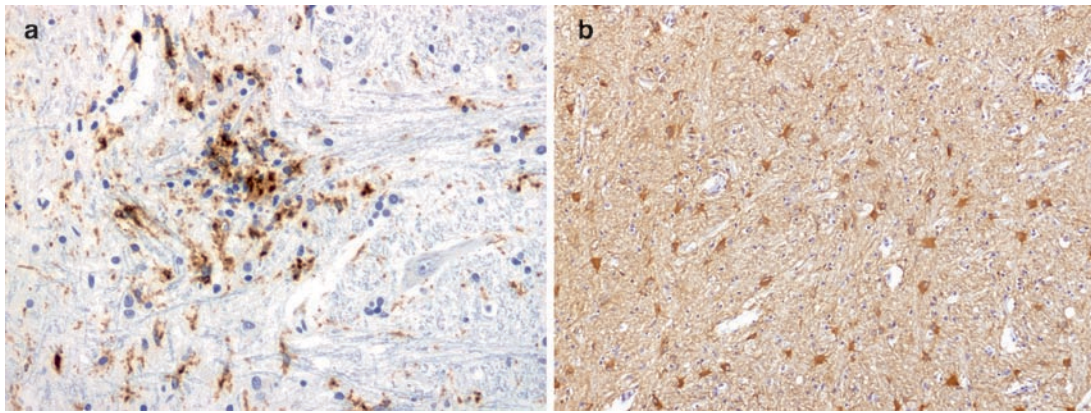
Fig. 34.2. (**a**) CD68 stain highlights the numerous microglia of these paraneoplastic processes, whereas GFAP (**b**) decorates the cytoplasm of reactive astrocytes.

Section L: Tumors of the Hematopoietic System

Adekunle M. Adesina

Abstract   Only two groups of hematopoietic neoplasms are discussed in this section. It is primarily focused on the heterogeneous groups of malignant lymphoma and histiocytic tumors.

Malignant Lymphoma

Adekunle M. Adesina

35.1 OVERVIEW

- Represent primary CNS extranodal lymphomas and should be distinguished from clinical scenarios in which the CNS is involved secondarily by a primary nodal or extranodal systemic lymphoma.
- Primary central nervous system lymphoma (PCNSL) represents 5% of all primary brain tumors in adults.
- Occurs primarily in older individuals or in immunocompromised states.
- Significant rise in incidence was noted in the 1980s and 1990s which was partly due to AIDS.
- An increased incidence was also noted in the immunocompetent and particularly young adults but current data suggest that incidence has stabilized.
- Secondary leptomeningeal involvement of the CNS is the more common form of involvement of the CNS by hematologic malignancies and is the rationale for CNS prophylaxis in childhood leukemias.
- PCNSL is frequently seen in the context of immunosuppression and may be associated with:
  - Acquired immunodeficiency syndrome (AIDS).
  - Post-transplant immunosuppression.
  - Inherited immunodeficiency states such as Wiskott-Aldrich syndrome and
  - Immunosuppression associated with treatment for immune-mediated disorders such as rheumatoid arthritis, Sjogren syndrome or treatment for malignancies such as Hodgkin's lymphoma or acute lymphoblastic leukemia.
- The demonstration of the presence of Epstein-Barr Virus genome (including EBNA 1-6, EBER1 and EBER2) in greater than 95% of tumors developing in patients who are immunocompromised implicates the loss of immune surveillance and EBV-induced cell proliferation in the pathogenesis of these tumors.
- Primary CNS lymphoma is uncommon in children and the young who are immunocompetent with children (18 years old and younger) representing only 1% of all PCNSL patients.
- In contrast to the adult population, when PCNSL occurs in children, it is more often seen in the immunocompetent.
- In the first two decades, there is also frequent association with inherited immunodeficiency syndromes and post-transplant immunosuppression.
- B cell lymphoma is the most common, accounting for about 80% of cases while T cell lymphoma accounts for approximately 20% of cases in children, with anaplastic large cell lymphoma representing a common histologic subtype.

35.2 CLINICAL FEATURES

- The typical PCNSL seen in immunocompetent adult individuals presents as a supratentorial, deep-seated, generally solitary mass. The most common locations are the frontal lobe, basal ganglia, corpus callosum, periventricular region and deep white matter.
- In children, the most frequent tumor locations are the parietal lobe, frontal lobe, cerebellum, pituitary stalk and hypothalamus.
- Often present as symptomatic mass lesions that may be associated with focal neurologic deficits, signs of raised intracranial pressure, seizures or a combination of these features.
- Post-transplantation CNS lymphoma may develop as early as within the first year in about 50% of patients post transplant.

35.3 NEUROIMAGING

- MRI shows tumors as isointense to hypointense on T2 or FLAIR images, isointense or hypointense on T1-weighted images relative to gray matter and homogeneous enhancement post contrast (Figs. 35.1–35.3).
- Lesions may be located in the central gray matter or may be cortical or involve the optic nerve or parasellar regions; rarely do they involve the spinal cord.
- Tumors are often accompanied by significant peritumoral edema.
- Location as bilateral symmetrical mass lesions in the deep gray matter is very characteristic of primary CNS lymphoma, but must be distinguished from toxoplasmosis by biopsy.
- In children, contrast-enhanced CT usually shows a characteristic heterogeneous pattern, marked edema, and a prominent mass effect with a ring-like peripheral pattern of enhancement (Figs. 35.1a and 35.2a).
- Occasionally may present with a predominant leptomeningeal involvement and no evidence of an intracranial mass.
- Diffusion imaging usually demonstrates restricted diffusion within the solid component of the mass.

35.4 PATHOLOGY

- They tend to be large (>2 cm) and vary in circumscription.
- Some are well-circumscribed masses that are pale in color with a relatively homogeneous appearance on the cut surface, while others are diffusely infiltrative and indistinguishable from surrounding brain.

35.4.1 Intraoperative Cytologic Smears

- Characterized by monomorphic population of discohesive cells often showing vesicular nuclei and variably-sized nucleoli in a necrotic background with frequent apoptosis.
- Lack of a fibrillary background allows the exclusion of a high-grade glioma.

35.4.2 Histopathology

- Histologic subtypes are similar to those seen in systemic lymphoma including high-grade diffuse large cell lymphoma, Burkitt's-type lymphoma, T cell lymphoma, anaplastic large cell lymphoma (ALCL), as well as, low-grade diffuse lymphocytic, lymphoplasmacytic, mucosa associated lymphoid tissue type (MALT) or marginal zone B cell lymphoma (MZBCL). Follicular lymphoma and primary intracranial Hodgkin's lymphoma are extremely rare.
  - In adults, the large B-cell lymphoma accounts for greater than 90% of PCNSL.
  - The diffuse large B cell lymphoma (Fig. 35.4) is also the most common subtype in children accounting for 30% of PCNSL in this age group.
  - Composed of large cells with distinct nucleoli representing cytologic equivalents of centroblasts or immunoblasts.
  - Distinct perivascular distribution (Fig. 35.5) and localization of viable tumor cells is often associated with perivascular reticulin formation and accounts for the now antiquated designation as reticulum cell sarcoma.
  - Necrosis is usually prominent.
  - Brain tumor interface may be well-delineated or may show an infiltrative pattern.
  - Prior steroid therapy may be associated with extensive tumor lysis, marked apoptosis, and an often non-diagnostic biopsy.
  - Morphologic subtypes similar to the T cell rich or anaplastic variants of large cell lymphoma have been reported.
  - Rare examples of precursor B-cell or T-cell lymphoma have also been reported.
  - ALCL including T-cell and null-cell tumors account for 21% of PCNSL in children while precursor B and T cell lymphoblastic lymphomas (Figs. 35.6–35.9) represent 16%; Burkitt's lymphoma and histiocytic lymphoma represent 12 and 5%, respectively; other less common variants represent 6%.
- Lymphomatoid granulomatosis represents a polymorphous angiocentric and invasive infiltrate including atypical T lymphocytes, plasmacytoid lymphocytes and macrophages.
  - May be associated with demonstrable EBV genome.
  - May occur as CNS disease alone or in combination with pulmonary manifestations.
  - May occur in the setting of AIDS.
- Intravascular lymphomatosis represents CNS involvement by a primarily systemic, intravascular, often large B cell lymphoma. Rarely, can be a T cell lymphoma.
  - Multifocal infarcts associated with vascular occlusion are common.

35.5 IMMUNOHISTOCHEMISTRY

- When a lymphoma is suspected and sufficient tissue is available, tissue should be submitted for flow cytometry.
- Diffuse large B cell lymphomas show positivity for pan-B cell markers such as CD19 and CD20 (Fig. 35.10a), although an often variable infiltrating T cell component is always present (Fig. 35.10b).
- The presence of EBV genome by in situ hybridization is often demonstrable (Fig. 35.10c).
- Most tumors express *BCL-2* and *BCL-6*.
- MZBCL express CD19, CD20, CD79a and occasionally CD5. CD3 and CD10 are usually negative.

35.6 MOLECULAR PATHOLOGY

- Loss of chromosome 6q is associated with poorer outcome.
- Copy gain of 18q21 which includes loci for MALT1 and BCL2 are common.
- Clonal abnormalities including t(1;14), t(6;14) and t(13;18) translocations have been reported.
- Global gene expression profiling of diffuse large B-cell lymphomas has allowed the identification of three distinct subsets with differing profiles and prognostic differences.
  - The germinal center B-cell-like diffuse large B-cell lymphomas characterized by the expression of genes of the normal germinal center B cells including *BCL-6, CD10* and *CD38* with a more favorable clinical outcome.
  - The activated B-cell-like diffuse large B-cell lymphomas characterized by the high levels of expression of genes that are normally induced during in vitro activation of peripheral blood B cells including a gene that is translocated in lymphoid malignancies, *IRF4 (MUM1/LSIRF),* anti-apoptoticgenes such as *FLIP* and *bcl2* and a subset of the genes that are characteristic of plasma cells.
  - The type 3 diffuse large B-cell lymphomas which express neither of these set of genes at a high level.

35.7 PROGNOSIS

- Most primary CNS lymphomas do not show systemic dissemination and yet show poor survival of only about $1\frac{1}{2}$ years.

SUGGESTED READING

Abla O, Weitzman S (2006) Primary central nervous system lymphoma in children. Neurosurg Focus 21(5):E8

Karikari IO, Thomas KK, Lagoo A, Cummings TJ, George TM (2007) Primary cerebral ALK-1-positive anaplastic large cell lymphoma in a child. Case report and literature review. Pediatr Neurosurg 43(6):516–521

Makino K, Nakamura H, Yano S, Kuratsu JI (2007) Pediatric primary CNS lymphoma: Long term survival after treatment with radiation monotherapy. Acta Neurochir (Wien) 149(3):295–297 discussion 297–298

Wilmshurst JM, Burgess J, Hartley P, Eley B (2006) Specific neurologic complications of human immunodeficiency virus type 1 (HIV-1) infection in children. J Child Neurol 21(9):788–794

Büyükpamukçu M, Varan A, Yazici N, Akalan N, Söylemezoğlu F, Zorlu F, Akyüz C, Kutluk MT (2006) Second malignant neoplasms following the treatment of brain tumors in children. J Child Neurol 21(5):433–436

Traum AZ, Rodig NM, Pilichowska ME, Somers MJ (2006) Central nervous system lymphoproliferative disorder in pediatric kidney transplant recipients. Pediatr Transplant 10(4):505–512

Brennan KC, Lowe LH, Yeaney GA (2005) Pediatric central nervous system posttransplant lymphoproliferative disorder. AJNR Am J Neuroradiol 26(7):1695–1697

Fallo A, De Matteo E, Preciado MV, Cerqueiro MC, Escoms S, Chabay P, López E (2005) Epstein-Barr virus associated with primary CNS lymphoma and disseminated BCG infection in a child with AIDS. Int J Infect Dis 9(2):96–103

Varan A, Büyükpamukçu M, Ersoy F, Sanal O, Akyüz C, Kutluk T, Yalçin B (2004) Malignant solid tumors associated with congenital immunodeficiency disorders. Pediatr Hematol Oncol 21(5):441–451

Hareema A (2003) Lymphomatoid granulomatosis: unusual presentation in a pediatric patient. Pediatr Dev Pathol 6(2):106–107

al-Ghamdi H, Sabbah R, Martin J, Patay Z (2000) Primary T-cell lymphoma of the brain in children: a case report and literature review. Pediatr Hematol Oncol 17(4):341–343

Douek P, Bertrand Y, Tran-Minh VA, Patet JD, Souillet G, Philippe N (1991) Primary lymphoma of the CNS in an infant with AIDS: imaging findings. AJR Am J Roentgenol 156(5):1037–1038

Egelhoff JC, Beatty EC Jr (1989) Primary B-cell lymphoma of the CNS in an infant. Pediatr Radiol 19(3):204–205

Dickson DW, Belman AL, Park YD, Wiley C, Horoupian DS, Llena J, Kure K, Lyman WD, Morecki R, Mitsudo S et al (1989) Central nervous system pathology in pediatric AIDS: an autopsy study. APMIS 8(Suppl):40–57

Nakamura M, Kishi M, Sakaki T, Hashimoto H, Nakase H, Shimada K, Ishida E, Konishi N (2003) Novel tumor suppressor loci on 6q22-23 in primary central nervous system lymphoma. Cancer Res 63:737–741

Itoyama T, Sadamori N, Tsutsumi K, Tokunaga Y, Soda H, Tomonaga M, Yamamori S, Masuda Y, Oshima K, Kikuchi M (1994) Primary central nervous system lymphomas. Immunophenotypic, virologic, and cytogenetic findings of three patients without immune defects. Cancer 73:455–463

Alizadeh AA, EisenMB DRE et al (2000) Distinct types of diffuse large B-cell lymphoma identified by gene expression profiling. Nature 403:503–511

Rosenwald A, Wright G, Chan WC et al (2002) The use of molecular profiling to predict survival after chemotherapy for diffuse large B-cell lymphoma. N EnglJ Med 346:1937–1947
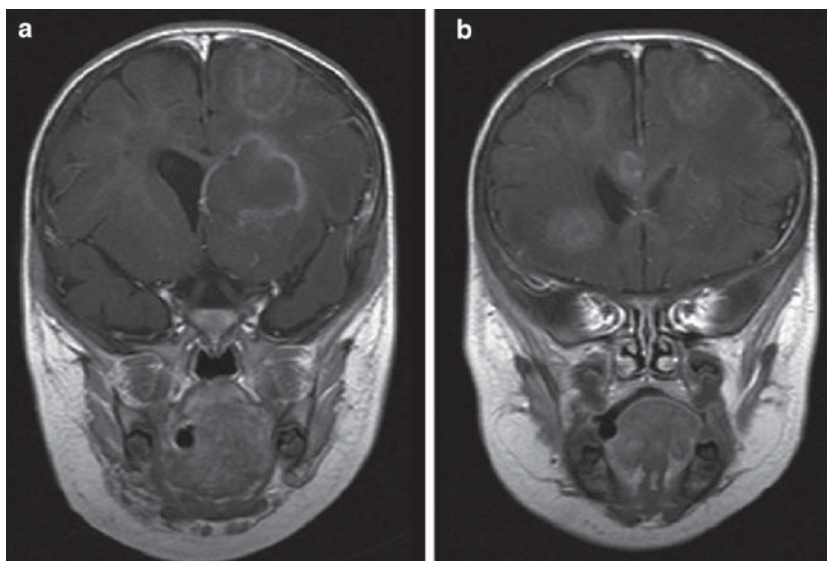
Fig. 35.1. (**a**) and (**b**) represent coronal T1-w post contrast images showing multiple enhancing lesions in a patient who is immunosuppressed post bone marrow transplant for Hurler's syndrome. Ring enhancement is seen in (**a**).
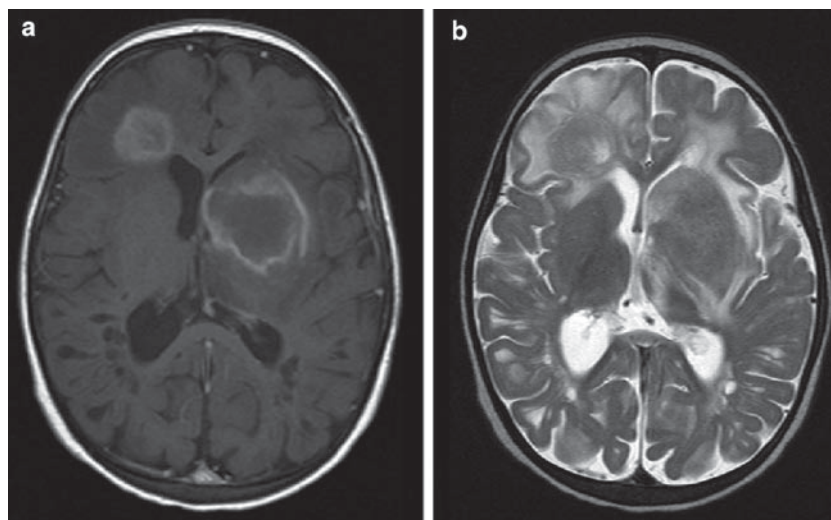
Fig. 35.2. (**a**) Axial T1-w post contrast image showing heterogenous and ring enhancement while (**b**) axial T2-w post contrast image shows less intense tumor enhancement and peritumoral hyperintensity due to severe peritumoral edema.
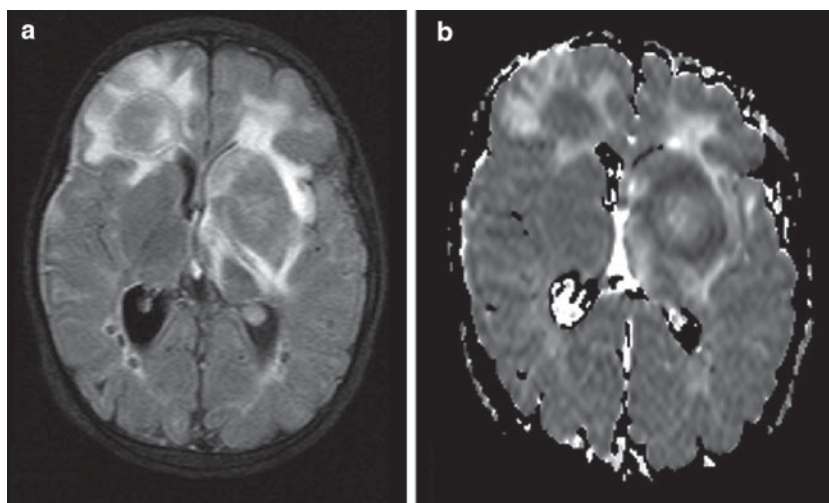
Fig. 35.3. Same patient as Fig. 35.2 with (**a**) axial FLAIR post contrast image showing similar changes to Fig. 35.2b above and (**b**) ADC map showing heterogeneous diffusion pattern with regions of restricted diffusion in solid parts of tumor and increased diffusion in areas of peripheral edema.
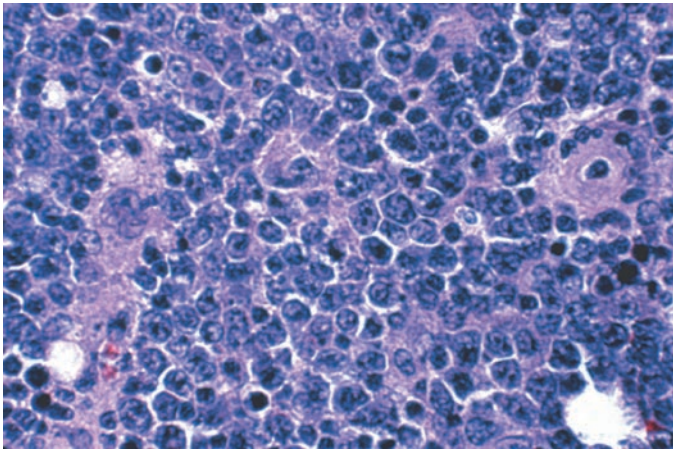
Fig. 35.4. Diffuse large cell lymphoma. This tumor shows immunopositivity for CD20 consistent with a B-cell phenotype.
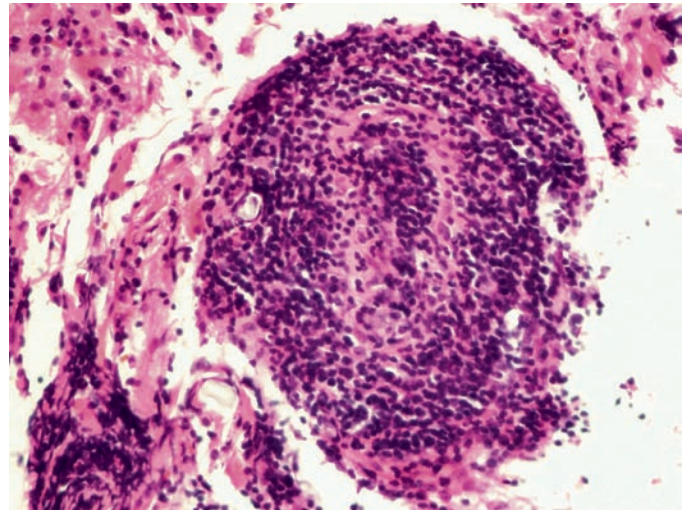
Fig. 35.5. Perivascular arrangement of cells represents a characteristic histologic feature of PCNSL.
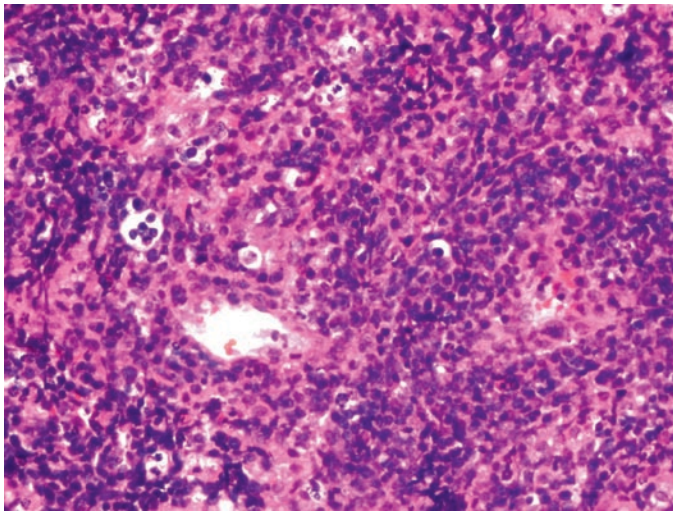
Fig. 35.6. Diffuse neoplastic lymphoid infiltrate in a 5-year-old boy.
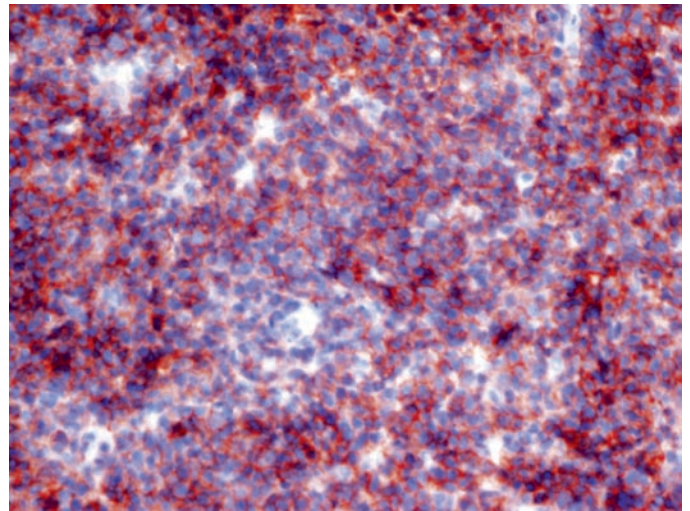
Fig. 35.7. Tumor from patient in Fig. 35.6 demonstrating membranous positivity for LCA.
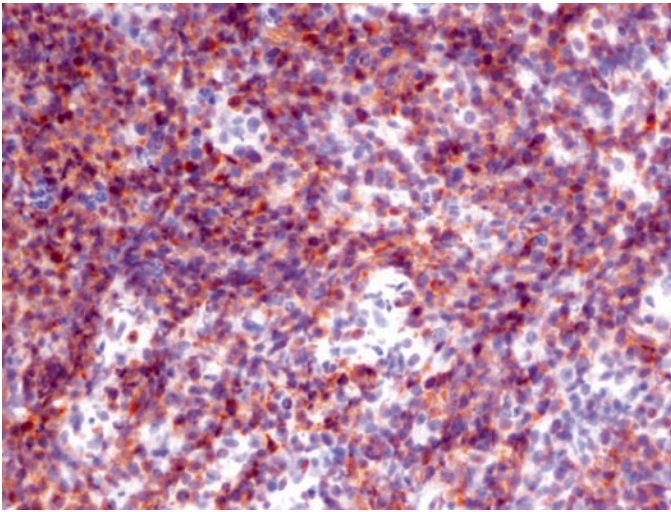
Fig. 35.8. Same tumor as in Fig. 35.6 demonstrating diffuse immunopositivity for CD3 consistent with a T-cell phenotype. Analysis for CD20 expression was negative.
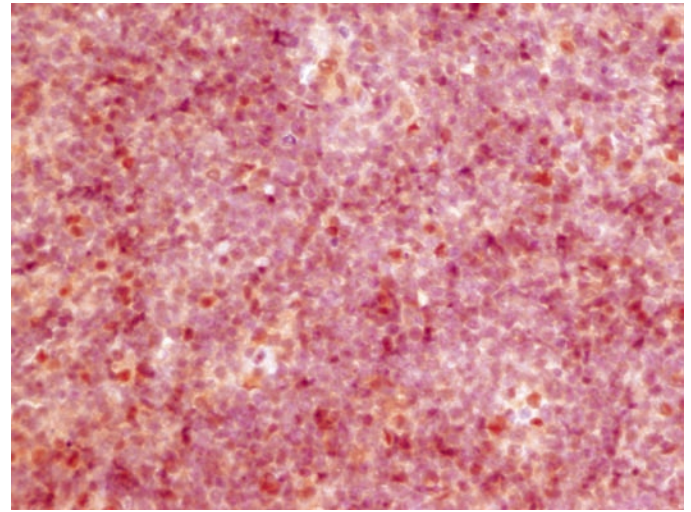
Fig. 35.9. Same tumor as in Fig. 35.6 demonstrating immunopositivity for terminal deoxynucleotide transferase (Tdt) consistent with a precursor T-cell lymphoblastic lymphoma.
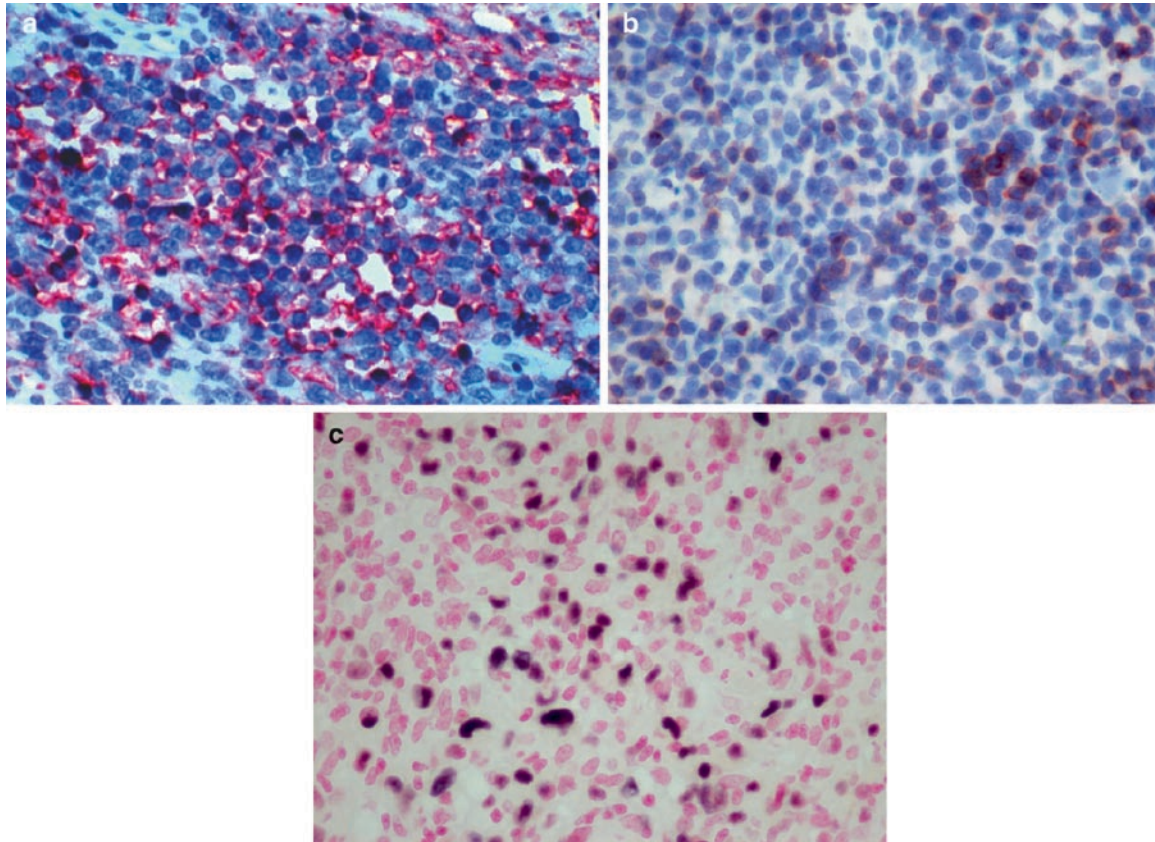
Fig. 35.10. (**a**) CD20 immunopositivity in a diffuse large B-cell lymphoma. (**b**) infiltrating T cells (CD3 positive) represent a minor component of another example of diffuse large B-cell lymphoma, and (**c**) in situ hybridization demonstrating *EBV* genome in the viable region of the same diffuse large B-cell lymphoma.

Histiocytic Tumors

A. Mukherjee and A.M. Adesina

Keywords Langerhans cell histiocytosis; Rosai-Dorfman disease; Erdheim-Chester disease; Hemophagocytic lymphohistiocytosis; Juvenile Xanthogranuloma; CD1a; S-100 protein; Birbeck granule

36.1 OVERVIEW

- Represents a heterogeneous group of tumors and tumor-like masses commonly associated with histologically identical extracranial lesions.
  - Broadly classified into two groups: Langerhans cell histiocytosis (LCH) and non-Langerhans cell histiocytosis (non-LCH).
- LCH results from clonal proliferation of dendritic cells with Langerhans cell characteristics;
  - Previously known as Histiocytosis X that included entities such as eosinophilic granuloma, Hand-Schüller-Christian disease and Letterer-Siwe disease.
  - LCH as currently defined may present as unifocal, multifocal (usually polyostotic), or disseminated disease.
- The estimated annual incidence of LCH ranges from 0.5 to 5.4 cases per million persons per year with a male-to-female ratio of 2:1.
- The etiology of LCH is unknown.
  - Putative triggers of the clonal proliferation include viral infections, a defect in intercellular communication (T cell–macrophage interaction) and/or a cytokine-driven process mediated by tumor necrosis factor, interleukin 11 and leukemia inhibitory factor.
- Non-LCH associated lesions have cells with features of macrophage differentiation and encompass a varied group.
  - Most common examples are Rosai-Dorfman disease (RDD), hemophagocytic lymphohistiocytosis, Erdheim-Chester disease, and Juvenile Xanthogranuloma.
- RDD has an estimated annual incidence of approximately 100 cases per year in the United States.
  - CNS involvement accounts for less than 5% of cases of RDD.
- True histiocytic malignant tumors of the CNS are extremely rare and include histiocytic sarcoma and follicular dendritic cell sarcoma.
  - Rare examples of primary CNS histiocytic sarcoma and intracranial follicular dendritic cell sarcoma have been described.

36.2 CLINICAL FEATURES

- LCH typically occurs in children with a mean age of onset of 12 years.

- Diabetes insipidus with or without associated signs of hypothalamic dysfunction including obesity, hypogonadism, and growth retardation is the usual clinical presentation.
  - Signs of increased intracranial pressure, cranial nerve palsies, seizures, visual disturbances, and ataxia also occur.
- RDD in the CNS shows a predilection for males and typically presents during the fourth to fifth decade.
  - In contrast, nodal-based RDD has a mean age of presentation of 20.6 years.
  - CNS forms usually present as intracranial space-occupying mass.
  - Cervical lymphadenopathy and systemic symptoms may be absent.
- Juvenile Xanthogranuloma occurs in young children, primarily as cutaneous nodules.
  - Dural and parenchymal lesions can occur with or without skin lesions.
  - Xanthoma disseminatum occurs in young adults, typically involving hypothalamus, pituitary gland, and dura in addition to extracranial involvement.
- Erdheim-Chester disease typically affects adults. Systemic involvement of bone, viscera, and adipose tissue is usual, but may not be evident.
  - CNS involvement usually affects cerebellum, spinal cord, pituitary, meninges or orbit.
- Hemophagocytic lymphohistiocytosis is a rare autosomal recessive multisystem disease of early infancy.
  - Clinical symptoms are fever, hepatosplenomegaly, and cytopenias.
  - Diffuse leptomeningeal and multifocal parenchymal brain involvement is seen in almost all cases.

36.3 NEUROIMAGING

- MRI lesions in LCH often include craniofacial bone and skull base lesions in 56% (Fig. 36.1a–e), hypothalamic-pituitary region lesions in 29%, choroid plexus lesions in 6%, intra-axial grey and white matter lesions in 36%, and cerebral atrophy in 8%.
  - With diabetes insipidus, there is loss of the posterior pituitary bright spot.
- The MRI lesions in LCH can range from sharply demarcated tumor-like lesions to punctate lesions in the cerebral parenchyma.
  - MR T1-weighted hyperintensities in the cerebellar dentate nucleus and basal ganglia may occur as well.
- MRI in Rosai-Dorfman disease usually shows solitary or multiple dural-based masses, mimicking meningioma.

- However, parenchymal and intrasellar lesions, as well as extension from an orbital/nasal/sinus lesion has been described.
  - Intramedullary spinal cord lesions have also been reported.
- Hemophagocytic lymphohistiocytosis is characterized by diffuse abnormal T2 signal intensity in the white matter.

36.4 PATHOLOGY

- LCH lesions can be yellow or white dura-based nodules or granular well-delineated or ill-defined parenchymal infiltrates.
- RDD can be single or multiple, dura-based, intracranial, or intraspinal masses.
  - The indurated lesions can be simultaneously intradural and extradural.

36.4.1 Intraoperative Cytology Smear

- Cytopreparations in LCH are cellular with a dominant population of round to oval histiocytes with ovoid to lobated, reniform nuclei containing pale chromatin and prominent longitudinal grooves or folds.
  - The cytoplasm is abundant and frequently vacuolated. The background contains a variable number of inflammatory cells, including eosinophils, lymphocytes, and neutrophils.
- Cytopreparations of RDD contain phagocytic histiocytes, admixed with small lymphocytes, transformed lymphocytes, plasmacytoid lymphocytes, and immunoblasts.
  - Phagocytic histiocytes are very large cells with macronuclei, enlarged nucleoli and abundant cytoplasm, and often contain phagocytosed lymphocytes, which are thought to traffic back and forth through the cytoplasm of these histiocytes (emperipolesis).
  - Lymphocytes should be present in the same plane of focus as the histiocytic cytoplasm, to be certain of emperipolesis.

36.4.2 Histopathology

- LCH has a polymorphic infiltrate composed of Langerhans cells, macrophages, lymphocytes, plasma cells, and a variable number of eosinophils (Fig. 36.2a and b).
  - The nuclei of Langerhans cells are typically slightly eccentric, ovoid, reniform, or convoluted with linear grooves and inconspicuous nucleoli.
  - The cytoplasm is abundant, pale to eosinophilic.
  - LCH can occasionally present with demyelination and a sparse infiltrate of Langerhans cells.
  - A paraneoplastic encephalitis-like presentation involving the cerebellum and brain stem, characterized by infiltrating CD8-reactive lymphocytes, axonal destruction and secondary demyelination, microglia activation, and gliosis is rarely associated with LCH.
- RDD shows sheets of histiocytes with vacuolated cytoplasm, admixed with lymphocytes and plasma cells.
  - Emperipolesis is pathognomonic, but may not be seen in 30% of cases presenting as leptomeningeal disease.
- Juvenile Xanthogranuloma/Xanthoma disseminatum shows histiocytes with scattered Touton giant cells, lymphocytes, and eosinophils.

- Erdheim-Chester disease shows lipid-laden histiocytes with small nuclei, Touton-like multinucleate giant cells, scant lymphocytes, and eosinophils along with fibrosis.
- Hemophagocytic lymphohistiocytosis shows diffuse infiltrations of lymphocytes and macrophages with hemophagocytosis.
- Histiocytic sarcoma shows a malignant histiocytic infiltrate.
  - Follicular dendritic cell sarcoma may show spindle cells with vesicular nuclei and whorl formation.

36.5 IMMUNOHISTOCHEMISTRY

- Immunohistochemistry is critical in defining these often histologically similar lesions.
- In LCH:
  - Langerhans cells express S-100 protein, vimentin, CD1a (Fig. 36.3), langerin (CD207) and HLA-DR.
  - They almost never express CD45, CD15 and lysozyme.
  - Ki67/MIB-1 proliferation indices range from 4 to 16%.
- Histiocytes in Rosai-Dorfman disease are S-100 protein+, CD1a−, CD11c+, CD68+, MAC387+, lysozyme −/+.
- Histiocytes in Juvenile Xanthogranuloma/Xanthoma disseminatum are CD1a−, CD 11c+, CD68+, factor XIIIa+, MAC387 −/+, lysozyme−, and S-100 protein−.
- Histiocytes in Erdheim-Chester disease are CD1a−, CD68+, and S-100 protein−.
- Macrophages in Hemophagocytic lymphohistiocytosis are CD11c+, CD68+, CD1a −/+, and S-100 protein−/+.
- Histiocytic Sarcoma tumor cells are CD68+, CD11c+, lysozyme+ and CD14+.
  - Lymphoid, myeloid, and dendritic markers are negative.
- Follicular dendritic cell sarcoma may be positive for vimentin and EMA, thus mimicking meningioma, but they are also positive for dendritic cell markers such as CD21, CD23, and CD35.

36.6 ELECTRON MICROSCOPY

- The ultrastructural hallmark of Langerhans cells are Birbeck granules, which are 34 nm rod-shaped or "tennis racket-shaped" intracytoplasmic pentalaminar structures with cross striation and a zipper-like central core (Fig. 36.4).

36.7 DIFFERENTIAL DIAGNOSIS

- A major diagnostic dilemma is distinguishing LCH from non-LCH lesions.
  - Appropriate panel, including immunostains for CD1a and Langerin or electron microscopy to determine the presence of Birbeck granules, allows an unequivocal diagnosis of LCH.
- LCH and non-LCH lesions must be distinguished from granulomas induced by infectious organisms.
  - Parasitic infections may be associated with granulomas having a prominent eosinophilic infiltrate.
  - Excluding an infection is critical in ensuring accurate diagnosis and appropriate management.

36.8 MOLECULAR PATHOLOGY

- LCH is a monoclonal proliferation.
  - Karyotype analysis, array-based comparative genomic hybridization (array CGH) and single nucleotide polymorphism arrays have failed to demonstrate genomic aberrations in Langerhans cell histiocytosis.
  - p53 positivity has been noted in the Langerhans cell nuclei, but mutations of the p53 gene have yet to be documented.
- Molecular studies using polymorphic regions of human androgen receptor locus have demonstrated that RDD is a polyclonal disorder.
  - Etiology of RDD is unknown, but molecular and immunophenotypic studies suggest derivation from activated macrophages, shown to produce interleukin-1β and TNFα.
- Hemophagocytic lymphohistiocytosis is a rare autosomal recessive multisystem disease of early infancy.
  - Associated genetic defect is currently unknown.

36.9 PROGNOSIS

- The overall survival of LCH at 5, 15, and 20 years are 88%, 88%, and 77%, respectively.
  - Spontaneous recovery may be seen in unifocal LCH.
  - Poorer prognosis with mortality rate reaching up to 20% has been observed in multifocal, multisystem LCH with organ dysfunction.
  - No prognostic significance has been associated with cytologic atypia and mitotic activity in LCH.
- RDD has excellent prognosis with no evidence of disease progression following surgery.
- Hemophagocytic lymphohistiocytosis is lethal without bone marrow transplantation.

SUGGESTED READING

Louis DN, Ohgaki H, Wiestler OD, Cavenee WK (ed) (2007) WHO Classification of Tumors of the central Nervous system, pp 193–196

Da Costa CE, Szuhai K, Van Ejik R, Hoogeboom M et al (2009) No genomic aberrations in Langerhans cell histiocytosis as assessed by diverse molecular technologies: Genes chromosomes. Cancer 48(3):239–249

Grois N, Prayer D, Prosch H, Lassmann H (2005) Neuropathology of CNS disease in Langerhans cell histiocytosis. Brain 128(4):829–838

Weintraub M, Bhatia KG, Chandra RS, Magrath IT, Ladisch S (1998) p53 expression in Langerhans cell histiocytosis. J Pediatr Hematol Oncol 20(1):7–12

Beverly PC, Egeler RM, Arceci RR, Pritchard J (2005) The Nikolas Symphosia and histiocytosis. Natl Rev Cancer 5:488–494

Prayer D, Grois N, ProschH GH, Barkoviich AJ (2004) MR imaging presentation of intracranial disease associated with Langerhans cell histiocytosis. AJNR Am J Neuroradiol 25:880–891

Willis B, Abin A, Weinberg V, Zoger S, Wara WM, Matthay KK (1996) Disease course and late sequelae of Langerhans cell histiocytosis: 25 year experience at University of California, San Francisco. J Clin Oncol 14:2073–2082

Andriko JA, Morrison A, Colegial CH, Davis BJ, Jones RV (2001) Rosai-Dorfman disease isolated to the central Nervous system: A report of 11 cases. Mod Pathol 14(3):172–178

Paulli M, Bergamaschi G, Tonon L, Viglio A, Rosso R, Facchetti F, Geerts ML (1995) Evidence of polyclonal nature of the cell infiltrate in sinus histiocytosis with massive lymphadenopathy (Rosai-Dorfman disease). Br J Hematol 91(2):415–418

Weidauuer S, Stuckrad-Barre S, Dettmann E, Zanella FE, Lanfermann H (2003) Cerebral Erdheim-Chester disease: Case report and review of literature. Neuroradiology 45:241–245

Shinoda J, Murase S, Takenaka K, Sakai N (2005) Isolated central nervous system hemophagocytic lymphohistiocytosis: Case report. Neurosurgery 56:187

Lesniak MS, Viglione MP, Weingart J (2002) Multicentric parenchymal Xanthogranuloma in a child: case report and review of literature. Neurosurgery 51:1493–1498

Sun W, Nordberg ML, Fowler MR (2003) Histiocytic sarcoma involving the central nervous system: clinical, immunohistochemical and molecular genetic studies of a case with review of literature. Am J Surg Pathol 27(3):258–265

Hasselblatt M, Sepeehrnia A, Von Falkenhoausen M, Paulus W (2003) Intracranial follicular dendritic cell sarcoma: Case report. J Neurosurg 99:1089–1090
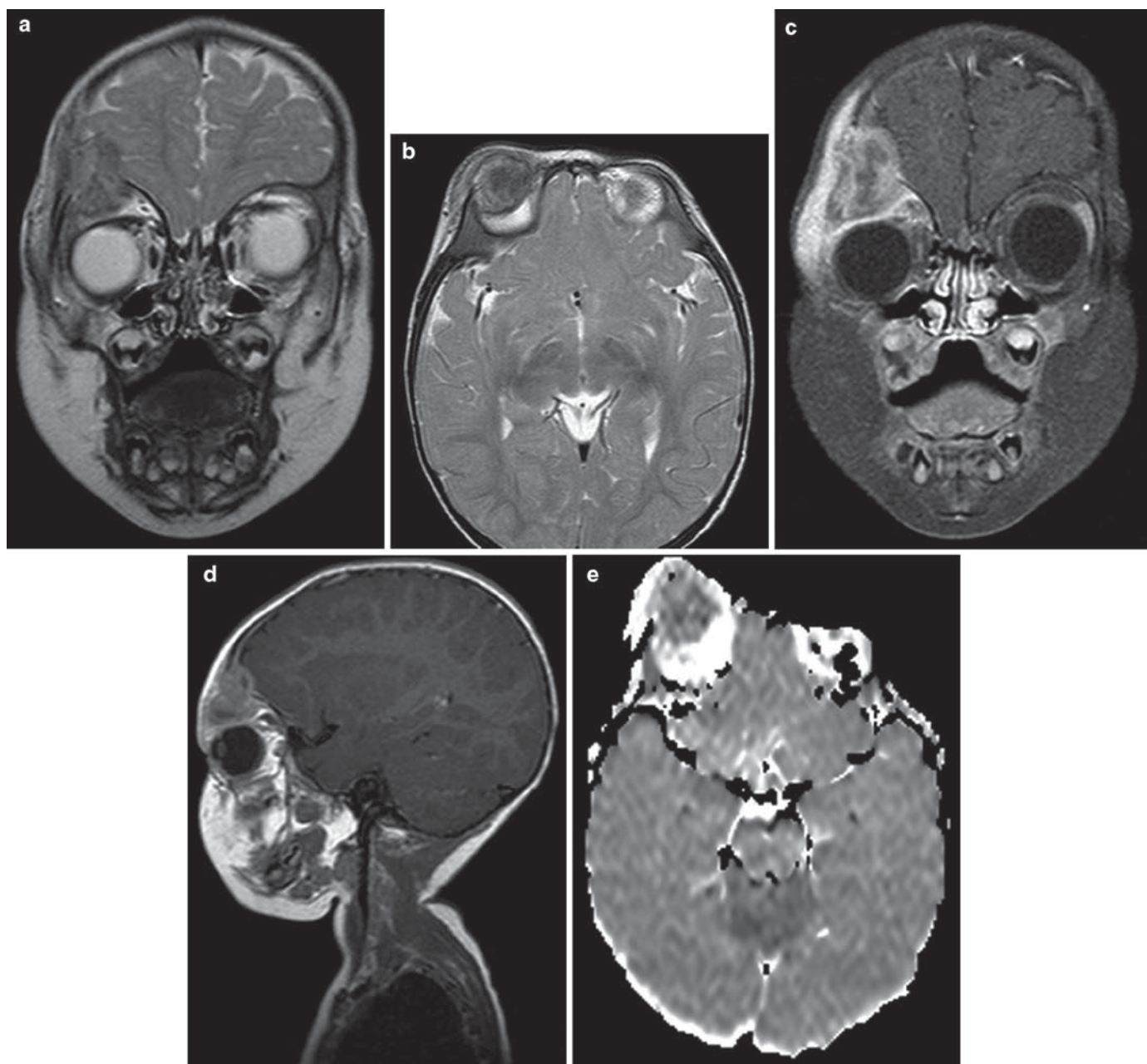
Fig. 36.1. Orbital MRI showing (**a**) coronal and (**b**) axial T2-weighted images with an orbital mass extending into the anterior cranial fossa and having heterogeneous signal intensity. (**c**) Coronal and (**d**) sagittal T1-weighted post contrast images show heterogeneous moderate enhancement, while (**e**) ADC map shows increased diffusion.
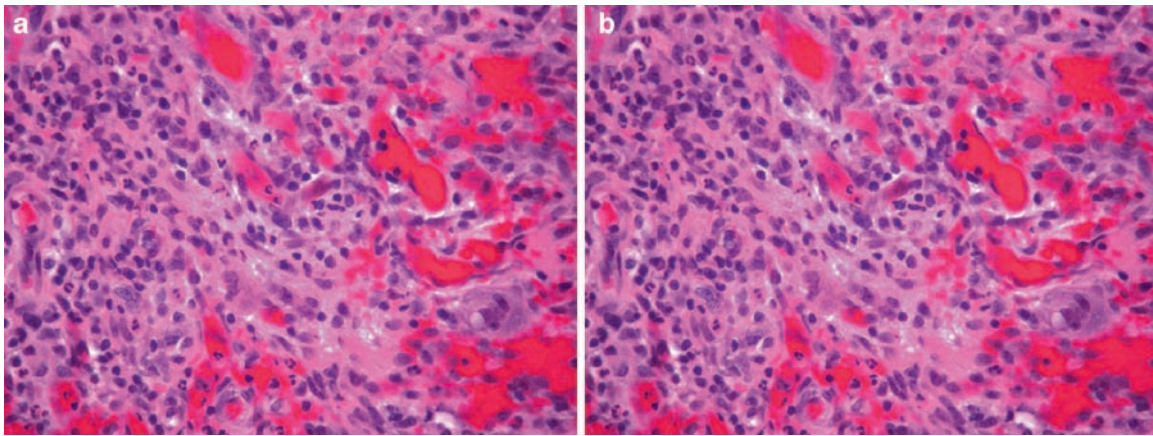
Fig. 36.2. Histology of LCH histiocytosis showing (**a**) a heterogeneous inflammatory infiltrate, including histiocytes, eosinophils, lymphocytes, and plasma cells, and (**b**) with a variable amount of multinucleated giant cells.
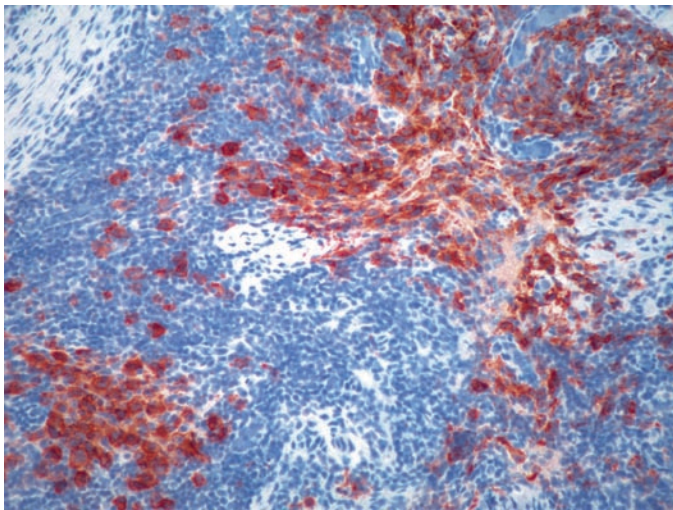
Fig. 36.3. CD1a immunopositivity is seen in the proliferating dendritic cells of LCH.
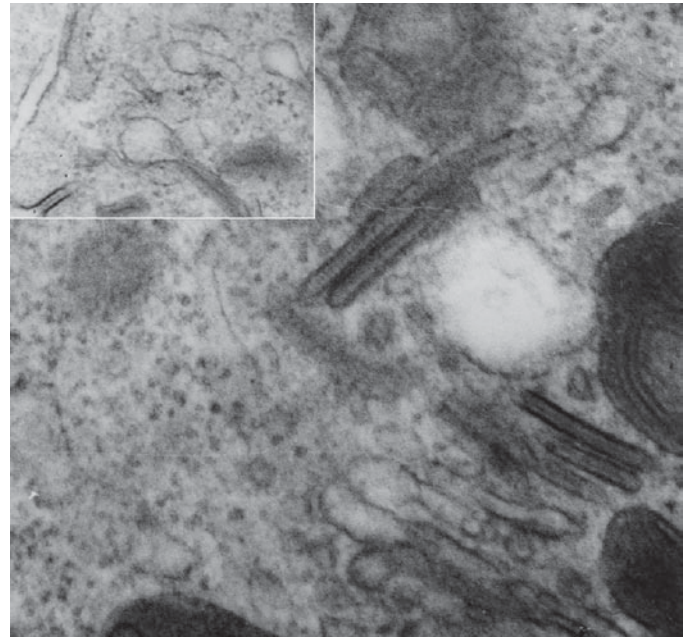
Fig. 36.4. Classic ultrastructural diagnostic feature of LCH is the Birbeck granule, which is a rod-shaped or "tennis racket-shaped" intra-cytoplasmic pentalaminar structure with cross striation and a zipper-like central core.

Section M: Interesting/Challenging Cases and Exercises in Pattern Recognition

Christine E. Fuller and Adekunle M. Adesina

Abstract This chapter represents the most educational of all the chapters in this book. It was prepared with the intention of providing ten interesting and sometimes challenging cases to the reader who is interested in sharpening his/her diagnostic skills.

Case Studies

Adekunle M. Adesina, Christine E. Fuller and Lucy Rocke-Adams

37.1 CASE STUDY – A

History Summary
- A 2½ year old girl presented with signs/symptoms of increased intracranial pressure.
- MRI studies disclosed a large, partially cystic mass involving the right cerebellar hemisphere/right cerebellopontine angle with hydrocephalus. The lesion was isointense on T1-w images and showed heterogeneous contrast enhancement.
- Additional imaging studies revealed multiple drop metastases along the spinal cord.

Pathology Findings
- Figures 37.1–37.3 are of different areas from the tumor tissue retrieved at the time of surgical debulking. Representative images of some immunohistochemical studies are provided here, including EMA (Fig. 37.4), smooth muscle actin (SMA – Fig. 37.5), and BAF-47/INI1 (Fig. 37.6).
- What is the diagnosis?

37.2 CASE STUDY – B

History Summary
- An 8-year-old boy presented with headache, vomiting, and decreased visual acuity.
- MRI studies disclosed a large solid intracerebral lesion involving the right temporoparietal region. The lesion had a minor cystic component, focal necrosis, was isointense to grey matter on both T1 and T2-w images, and enhanced post contrast. There were some peritumoral edema and mass effect. The lesion was not in close proximity to the ventricular system.

Pathology Findings
- Figures 37.7 and 37.8 are representative photomicrographs of routine H & E stained sections of tumor from partial surgical excision, while immunohistochemical studies for GFAP and EMA are depicted in Figs. 37.9 and 37.10, respectively.
- What is the diagnosis?

37.3 CASE STUDY – C

History Summary
- A 10 year old boy presented with headaches and "clumsiness." According to his parents, these symptoms have been slowly progressive over the course of a year.
- MRI studies revealed a large posterior fossa lesion; a representative T1-w postcontrast image is given in Fig. 37.11.

Pathology Findings
- Figures 37.12–37.15 are representative photomicrographs of routine H & E stained sections from tissue obtained at

gross total resection of this lesion. No additional stains were performed.
- What is the diagnosis?

37.4 CASE STUDY – D

History Summary
- A 16 year old boy presented with headaches, nausea, and vomiting.
- A large right posterior parasagittal lesion was detected on MR imaging studies. A representative T1-postcontrast image is given in Fig. 37.16. Of note, a smaller lesion was present more anteriorly (not shown); this lesion was also parasagittal and was solid with diffuse contrast enhancement.

Pathology Findings
- Figures 37.17–37.19 are representative photomicrographs of routine H & E stained sections from tissue obtained at gross total resection of this lesion. The features depicted in Figs. 37.17 and 37.18 made up the majority of the lesion, while the findings in Fig. 37.19 were seen only focally.
- Examples of EMA and INI1 are shown in Figs. 37.20 and 37.21, respectively.
- What is the diagnosis?

37.5 CASE STUDY – E

History Summary
- A 16 year old male presented with headache and blurred vision.
- MRI shows a slightly heterogeneous but predominantly T1 hypointense (Fig. 37.22a) and T2 hyperintense (Fig. 37.22b) mass eccentrically placed to the right of midline and occupying the suprasellar cistern and apparently arising from the region of the sella.
- Following the administration of gadolinium, there is enhancement of the more solid appearing superior aspect of the tumor with more heterogeneous enhancement of the right-sided suprasellar mass.
- There is evidence for a left-to-right downward sloping of the pituitary fossa.
- There is increased diffusion (Fig. 37.22c).
- Patient underwent a biopsy and partial resection of tumor.

Pathology
- Intraoperative smear shows a hypocellular myxoid lesion (Fig. 37.23a).
- Additional microscopic images show a chondroid lesion with variable cellularity (Fig. 37.23b–d) and surrounding reactive bone changes (Fig. 37.23e).

- Immunostains include S-100+(Fig. 37.24a), EMA (Fig. 37.24b) and Ki67 (Fig. 37.24c).
- What is the diagnosis?

37.6 CASE STUDY – F

History Summary
- A 15 year old male presented with headache and blurred vision.
- MRI and CT scans showed the presence of a clival mass.
- Patient had surgery for biopsy and partial resection.

Pathology
- Microscopy shows a moderately cellular and pleomorphic tumor with variably vacuolated cells in a myxoid matrix (Fig. 37.25a–e).
- There are frequent mitoses, as well as diffuse positivity for S-100 (not shown) and cytokeratin (Fig. 37.26).
- What is the diagnosis?

37.7 CASE STUDY – G

History Summary
- A 17 year old girl presented with upper extremity weakness.
- MRI/CT studies show the presence of an extra-axial, dura-attached mass in the right posterior frontal lobe.
- Patient underwent a gross total surgical resection.

Pathology
- Microscopy sections show a highly cellular, small blue cell tumor (Figs. 37.27 and 37.28) with a prominent myxoid component (Fig. 37.29), chondroid differentiation (Fig. 37.30), and regional spindle cells (Fig. 37.31) sometimes arranged in a herring-bone pattern (Figs. 37.31 and 37.32).
- Tumor cells show a diffuse membranous immunopositivity for CD99 and focal positivity for S-100 in the chondroid regions. EMA, synaptophysin, cytokeratin, desmin, myogenin, and myoD are negative (not shown).
- What is the diagnosis?

37.8 CASE STUDY – H

History Summary
- A 4 year, old boy presented with multiple cranial nerve deficits, dysarthria, and motor weakness, more severe on the left than right side.
- MRI/CT studies disclosed a tumor in the brainstem. A biopsy was not done.

Treatment
- The child was radiated.
- Treated with Thiotepa.
- Had an autologous bone marrow transplant.
- In spite of these, there was inexorable growth of tumor, and he died 18 months later.

Autopsy
- Postmortem examination disclosed a hemorrhagic tumor extending from the right cerebral peduncle in the midbrain caudally into the most caudal portion of the pons.
  - It was the largest at the level of the locus ceruleus Fig. 37.33.
  - In addition, multiple metastases were found in leptomeninges at all levels, along with parenchymal, hemorrhagic tumor in temporal lobe Figs. 37.34 and 37.35.
  - Microscopic images – (Fig. 37.36a and b).
- What is the diagnosis?

37.9 CASE STUDY – I

History Summary
- A 9 year old boy presented with recent onset of seizures and headache.
- MRI studies disclosed a left hemispheric mass isointense on T1-weighted image (Fig. 37.37a) and hyperintense on T2-weighted image (Fig. 37.37b).
  - There is slight enhancement postcontrast (Fig. 37.37c and d).
- Patient underwent a near gross total resection.
- Postsurgery, the patient is alive 10 years postresection.

Histology
- Tumor is composed of oval to spindle cells in a fibrillary matrix (Fig. 37.38a and b).
- There is a distinct perivascular pseudorosette-like arrangement of tumor cells, which is florid in some regions (Fig. 37.38c), and less florid at the infiltrative edge (Fig. 37.38d).
- There is associated diffuse immunopositivity for GFAP (Fig. 37.39a).
- Immunostain for Ki67 shows a low proliferation index (Fig. 37.39b).
- What is the diagnosis?

37.10 CASE STUDY – J

History Summary
- A 5 month old boy presented with vomiting and altered sensorium.
- MRI studies reveal a left hemispheric mass heterogeneous on T1-weighted image (Fig. 37.40a), and hyperintense on T2-weighted image (Fig. 37.40b), associated with extensive peritumoral edema.
  - There are marked contrast enhancement (Fig. 37.40c) and associated diffusion restriction on ADC map (Fig. 37.40d).
- Patient underwent biopsy followed by a limited resection.

Pathology
- Intraoperative smears and frozen sections are shown in Fig. 37.41a–e.
- Microscopic images from the permanent sections are shown in Fig. 37.42a and b.
- Immunostains include, GFAP (Fig. 37.43a), p53 (Fig. 37.43b), and Ki67 (Fig. 37.43c).
- Synaptophysin and neurofilament immunostains are negative.
- What is the diagnosis?

37.11 ANSWERS

37.12 CASE STUDY – A

Diagnosis
- Atypical teratoid/rhabdoid tumor.

Other findings: additional immunohistochemical stains that were positive include GFAP, pancytokeratin (in the epithelial islands and rare individual cells), synaptophysin, and CD99.

Comment

This case teaches several lessons:
- Not all cerebellar tumors with a predominance of small blue cells are medulloblastomas. AT/RT should be suspected in

cases occurring in the very young (under age 3 years) and in cases with cells/components divergent from the typical "small blue cell" appearance.

- Judicious utilization of multiple immunohistochemical stains, to include especially EMA and SMA together with neuronal and glial markers, is essential in the assessment of polyphenotypia characteristic of AT/RT.
- Immunohistochemical assessment for INI1 status (BAF47 stain-note the tumor cells have lost expression for this marker in the current case) is confirmatory of AT/RT status and is helpful in differentiating this tumor from other lesions that may contain cells with a rhabdoid morphology (glioblastoma, choroid plexus tumors, meningioma). In the latter tumors, nuclear positivity for BAF47/INI1 would be retained.

37.13 CASE STUDY – B

Diagnosis
- Clear cell ependymoma.

Comment
This case teaches several lessons:
- Not all ependymomas arise in association with the ventricles; they may be intraparenchymal as well.
- The presence of perivascular pseudorosettes (Fig. 37.8) should always raise the suspicion for ependymoma, particularly in the setting of a clear cell tumor.
- Clear cell ependymoma may closely mimic a variety of other clear cell tumors, including oligodendroglioma, neurocytoma, hemangioblastoma, meningioma, and metastatic renal cell carcinoma. As noted above, the finding of perivascular pseudorosettes is an important clue; GFAP positivity and a dot-like pattern by EMA effectively rule out the other listed possibilities. Ultrastructural analysis may be needed only in rare cases.

37.14 CASE STUDY – CS

Diagnosis
- Pilocytic astrocytoma.

Comment
This case teaches several lessons:
- Review of available radioimaging studies is critical in the pathologic workup of tumors of the CNS and often provides very helpful clues to diagnosis in cases where tissue is limited or unusual/uncommon histologic patterns of otherwise readily-recognizable tumors are detected. In the current case, the enhancing cyst with mural nodule configuration found in this child's cerebellum should alert the pathologist to be on the lookout for features of low grade tumors, especially pilocytic astrocytoma.
- Pilocytic astrocytoma represents a "great mimicker" among the pediatric CNS tumors, as it may exhibit a wide array of histologic features, including areas that look like oligodendroglioma (Fig. 37.12) or perivascular pseudorosettes (as in ependymoma; Fig. 37.13), amongst others. In the context of more typical features of pilocytic astrocytoma as seen in the current case, including biphasic loose and compact architecture and numerous eosinophilic granular bodies (Fig. 37.14 and 15), the diagnosis of pilocytic astrocytoma is more readily apparent.
- Pleomorphism does not always connote malignancy; degenerative nuclear atypia is not uncommonly found in slow-growing low grade tumors. Often these bizarre nuclei may have intranuclear cytoplasmic invaginations instead of prominent nucleoli. It is the features in the tissue surrounding these pleomorphic nuclei where diagnostic features of malignancy or benignity are found.

37.15 CASE STUDY – D

Diagnosis
- Anaplastic meningioma with papillary and rhabdoid components.

Comment
This case teaches several lessons:
- Parasagittal lesions that appear to have dural attachment/involvement, be they solid or with a cystic component, should raise a suspicion for dural-based tumors, most commonly meningioma. The finding of a dural tail is particularly helpful in confirming the dural-based nature of a lesion.
- WHO grade II and grade III meningioma variants are more frequent in children. Lesions exhibiting a prominent papillary architecture with/without concomitant rhabdoid cells are features (Fig. 37.17 and 18) that should prompt a careful search for more classic features of meningioma, including a more spindle cell morphology as seen in Fig. 37.19. Unfortunately, well-formed whorl arrangements are infrequent in high grade meningiomas, necessitating application of immunohistochemical stains. EMA staining is characteristic of meningiomas, while choroid plexus carcinomas should be positive for pancytokeratin. Nuclear positivity for INI1/BAF47 should be retained in rhabdoid meningiomas, while this is not true of AT/RT.
- The finding of multiple meningiomas should prompt workup for NF2.

37.16 CASE STUDY – E

Diagnosis
- Chondrosarcoma, intermediate grade.

Comment
- Chondrosarcoma mimicking a pituitary adenoma is unusual.
- Tumor probably arising from bone of skull base.
- Important differential diagnosis is chondroid chordoma.

37.17 CASE STUDY – F

Diagnosis
- Chordoma with malignant transformation.

Comment
- Malignant transformation is infrequent in chordoma.
- The presence of malignant transformation portends a poor prognosis.
- An important differential diagnosis is chondrosarcoma.

37.18 CASE STUDY – G

Diagnosis
- Extraskeletal mesenchymal chondrosarcoma.

Comment
- Rare tumor in the CNS.

- H & E histologic features as illustrated are characteristic.
- Presence of chondroid differentiation is a major distinguishing feature from hemangiopericytoma.
- Small biopsies without a distinct chondroid component may be problematic.

37.19 CASE STUDY – H

Diagnosis
- Medulloepithelioma.
  - The neoplastic cells did not express any antigen except for a few fields showing histological features of glial differentiation.

Comment

This case teaches several lessons:
(1) All brainstem tumors are not astrocytomas.
(2) Although the majority of medulloepitheliomas arise in the cerebrum, they occur in other CNS sites as well.
(3) Antigen expression may be inconsistent.

37.20 CASE STUDY – I

Diagnosis
- Angiocentric glioma.

Comment
  - Perivascular pseudorosette-like arrangements though characteristic for ependymoma may occur in tumors other than ependymomas.

37.21 CASE STUDY – J

Diagnosis
- Congenital glioblastoma.

Comment
- Congenital glioblastoma is uncommon.
- In this infant, clinical and neuroradiologic profile would suggest a differential diagnoses that include supratentorial primitive neuroectodermal tumor, medulloepithelioma, atypical teratoid rhabdoid tumor, choroid plexus carcinoma, and anaplastic ependymoma.
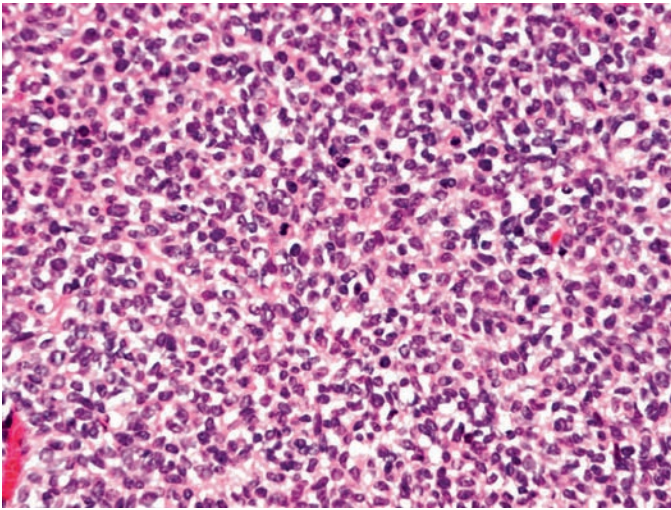
Fig. 37.1. Case A - Sheet of poorly differentiated cells.
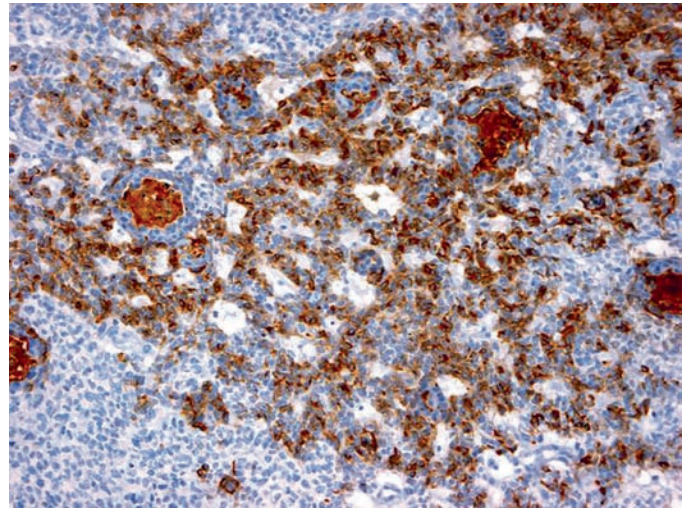
Fig. 37.4. Case A - Immunostain for EMA.
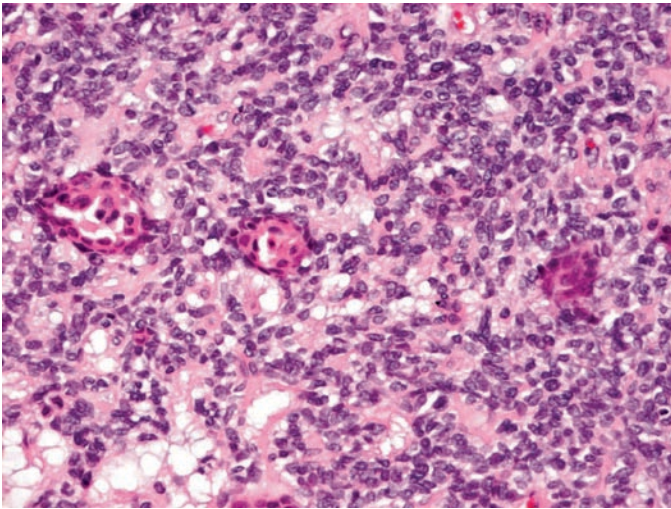
Fig. 37.2. Case A - Epithelioid islands are prominent regionally.
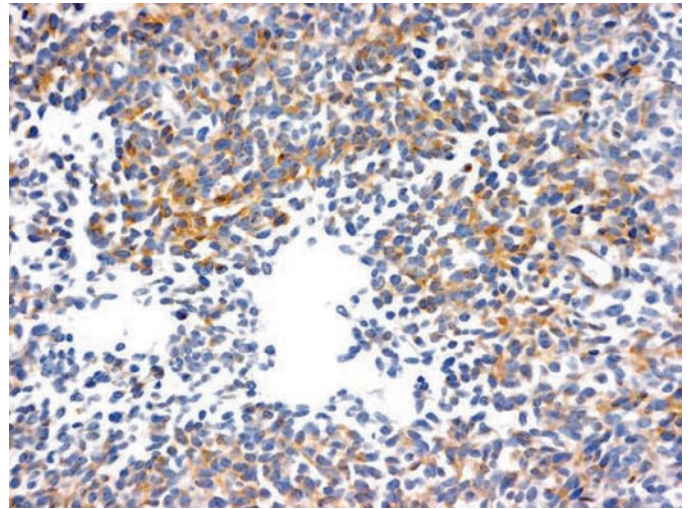
Fig. 37.5. Case A - Immunostain for smooth muscle actin.
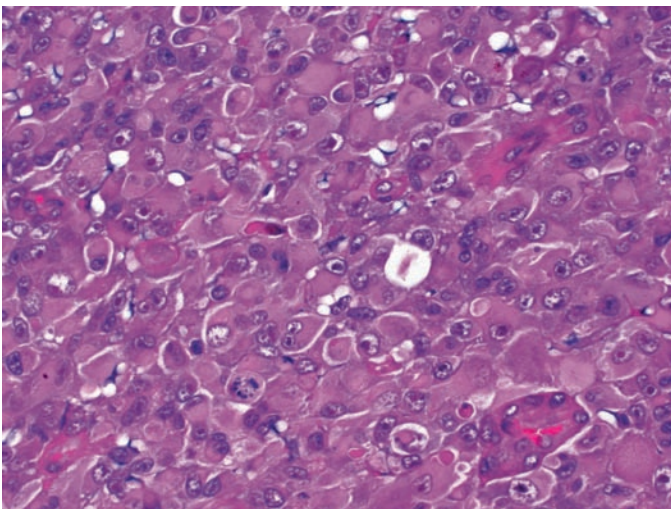
Fig. 37.3. Case A - Region of tumor with epithelioid cells having eccentric nuclei and eosinophilic cytoplasm.
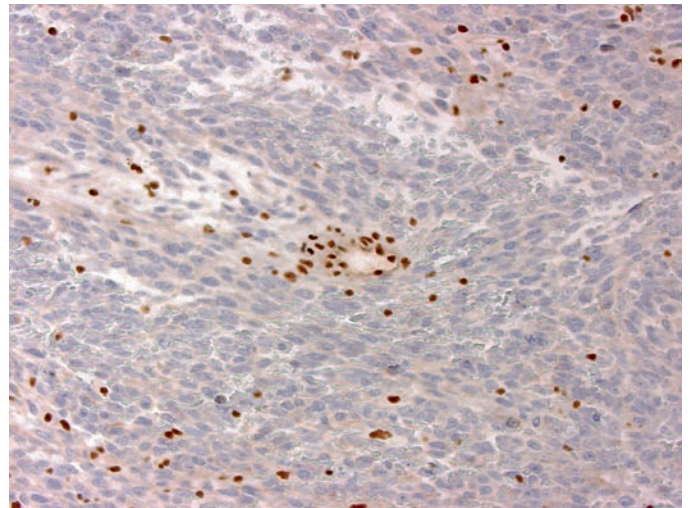
Fig. 37.6. Case A - Immunostain for INI1 (BAF-47 antibody).
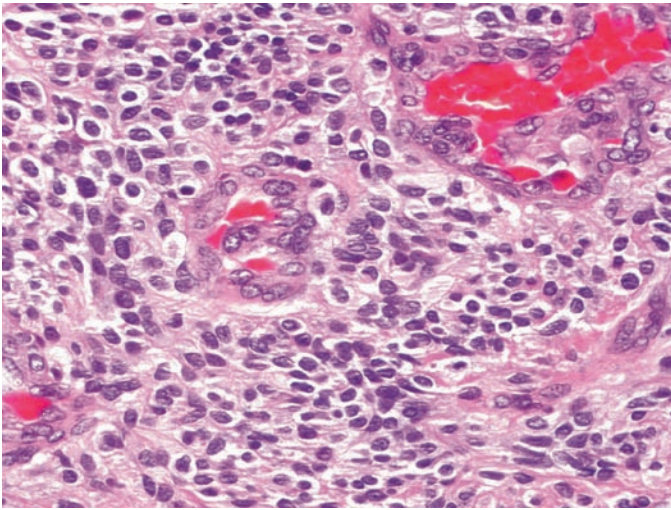
Fig. 37.7. Case B - Monomorphic cells with clear cytoplasm and endothelial proliferation.

Fig. 37.8. Case B - Monomorphic clear cells.
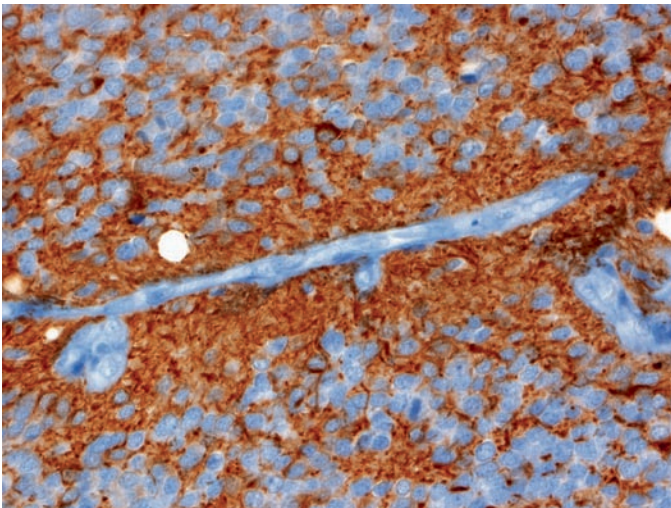
Fig. 37.9. Case B - Immunostain for GFAP.

Fig. 37.10. Case B - Immunostain for EMA.
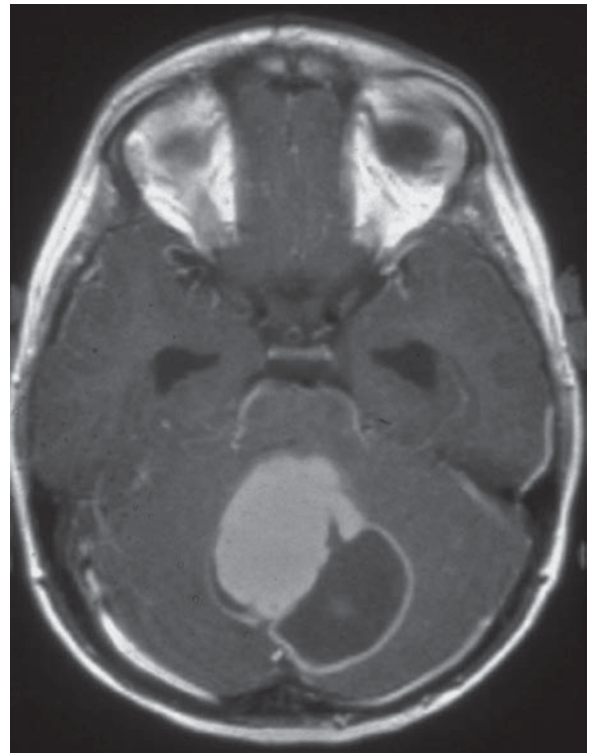
Fig. 37.11. Case C - T1-w post contrast MR image.
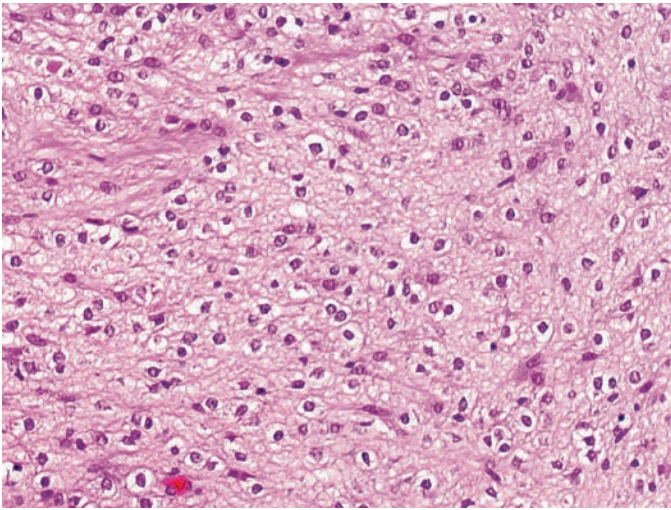
Fig. 37.12. Case C - H & E stained section.
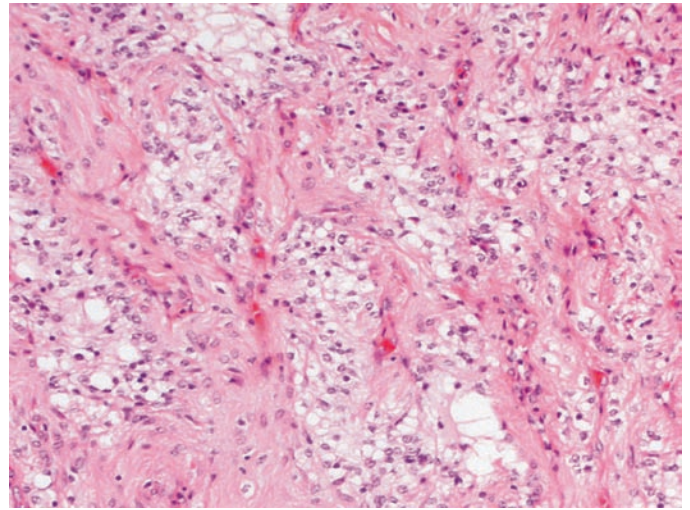
Fig. 37.14. Case C - H & E stained section.
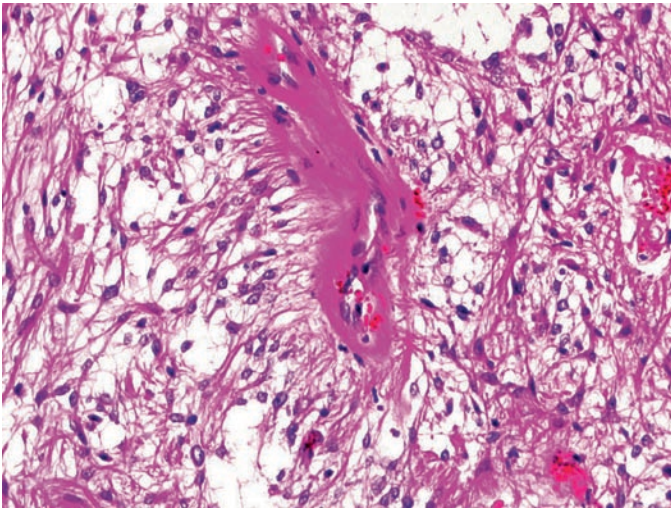
Fig. 37.13. Case C - H & E stained section.
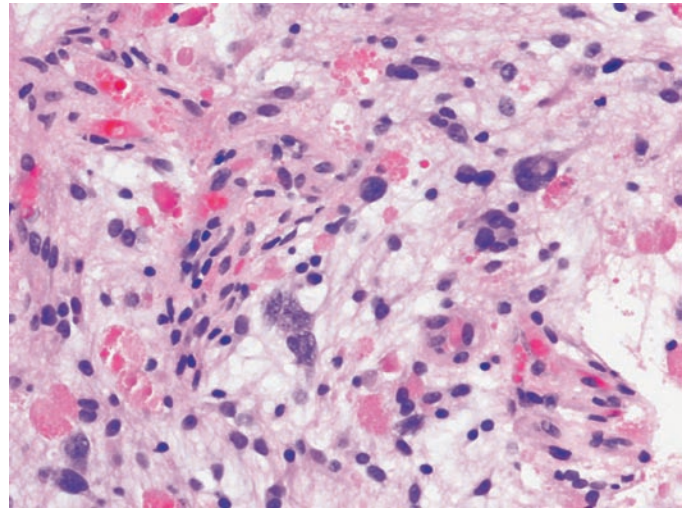
Fig. 37.15. Case C - H & E stained section.
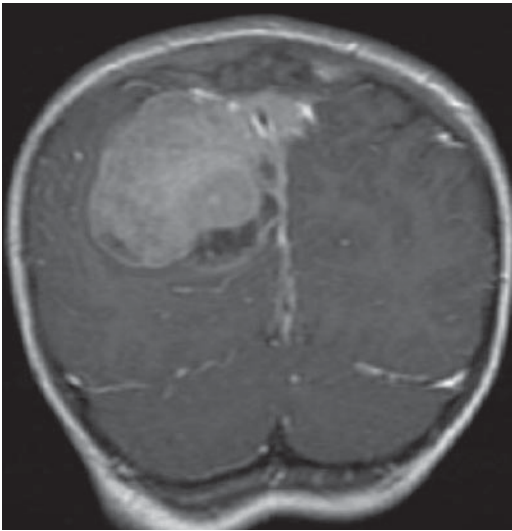
Fig. 37.16. Case D - T1-w post contrast MR image.
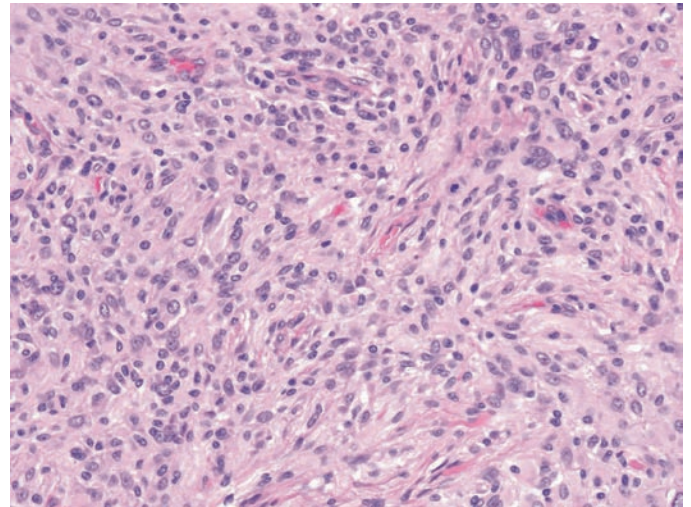
Fig. 37.19. Case D - H & E stained section.
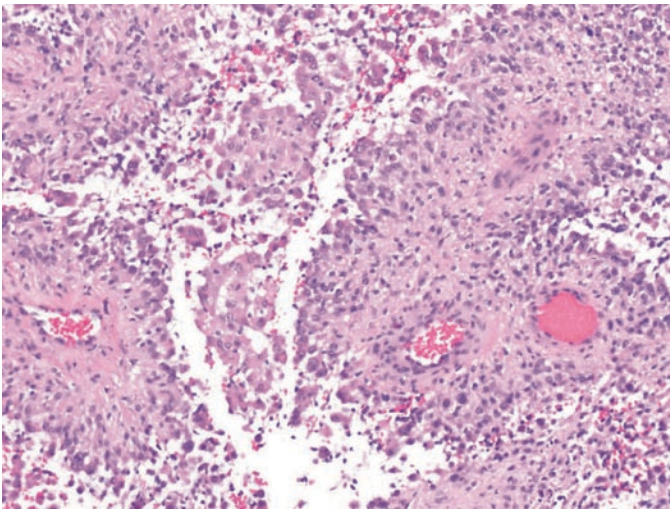
Fig. 37.17. Case D - H& E stained section.
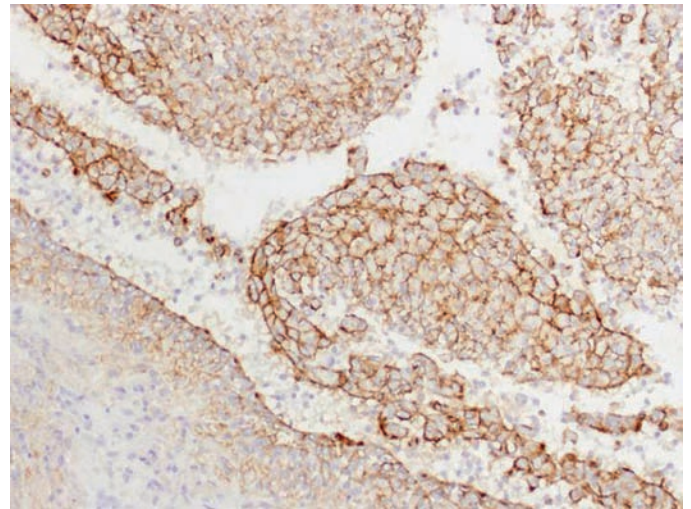
Fig. 37.20. Case D - Immunostain for EMA.
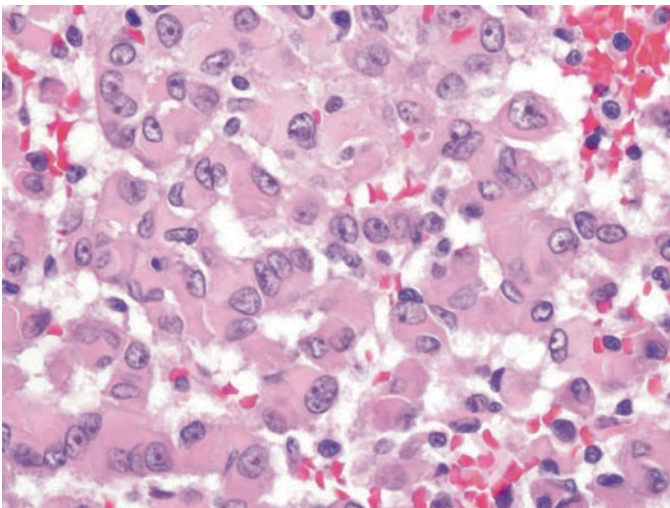
Fig. 37.18. Case D - H & E stained section.
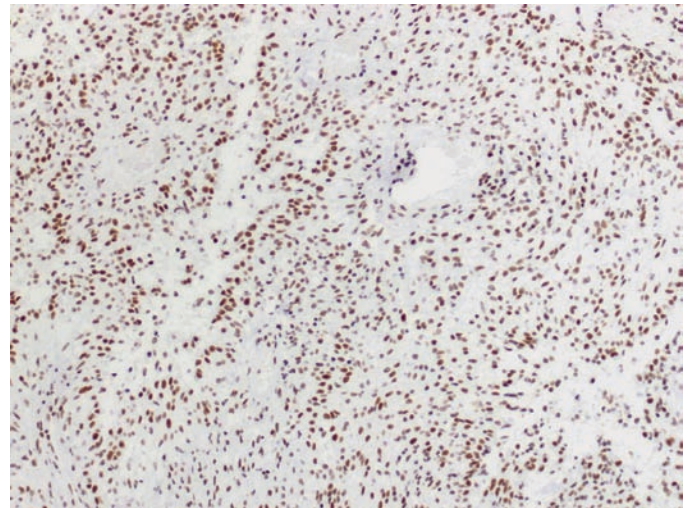
Fig. 37.21. Case D - Immunostain for INI1 (BAF-47 antibody).
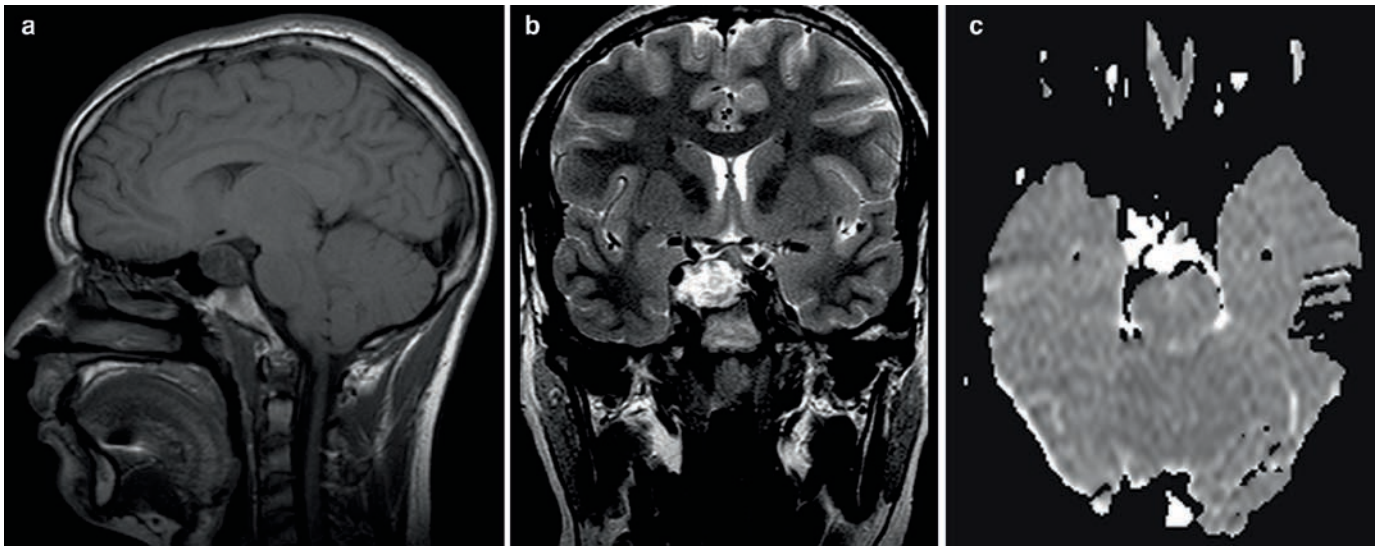
Fig. 37.22. Case E - (**a**) T1 hypointense (**b**) T2 hyperintense (**c**) ADC map.
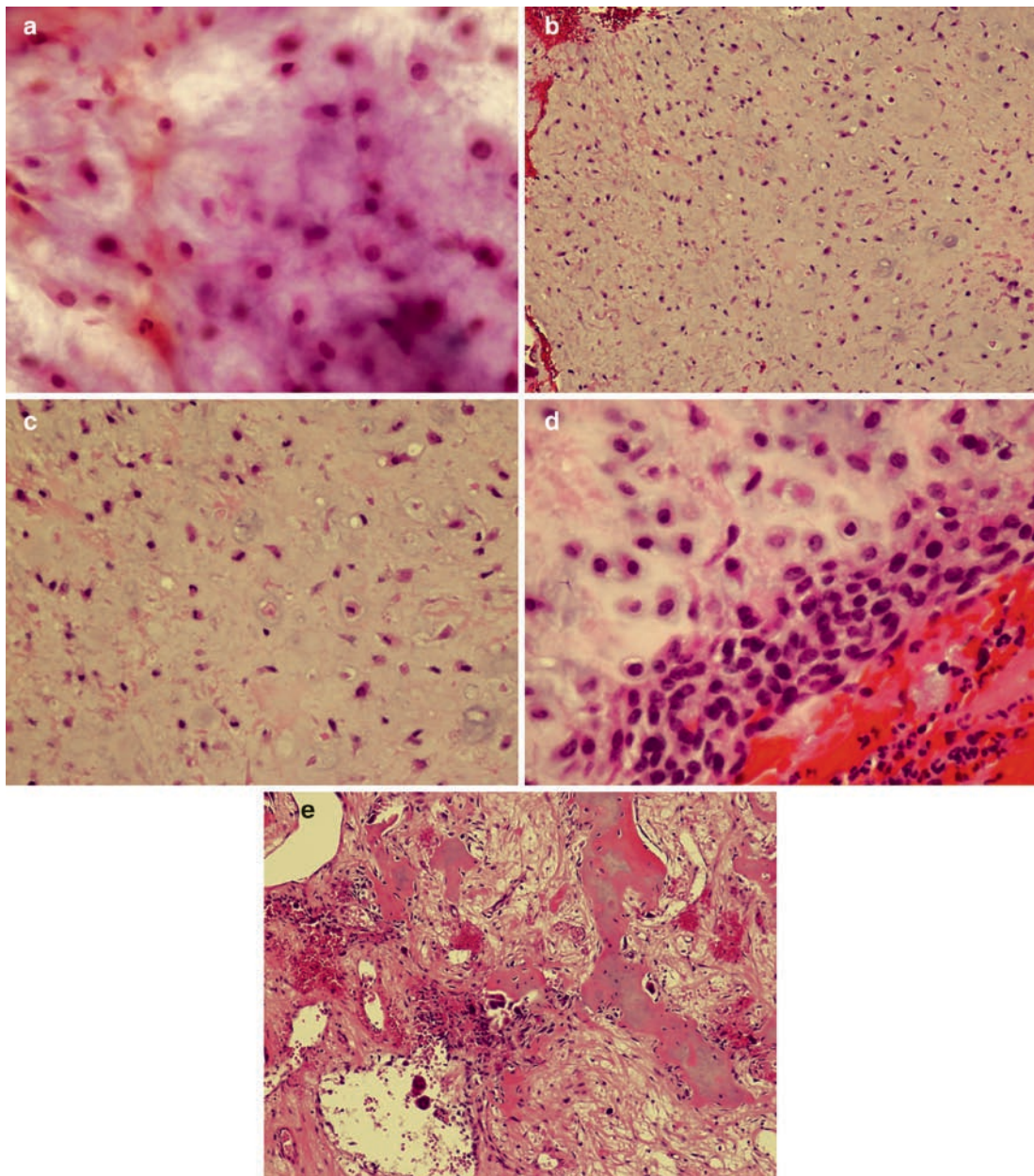
Fig. 37.23. Case E - (**a**) intraoperative smear preparation (**b-e**) H & E stained sections.
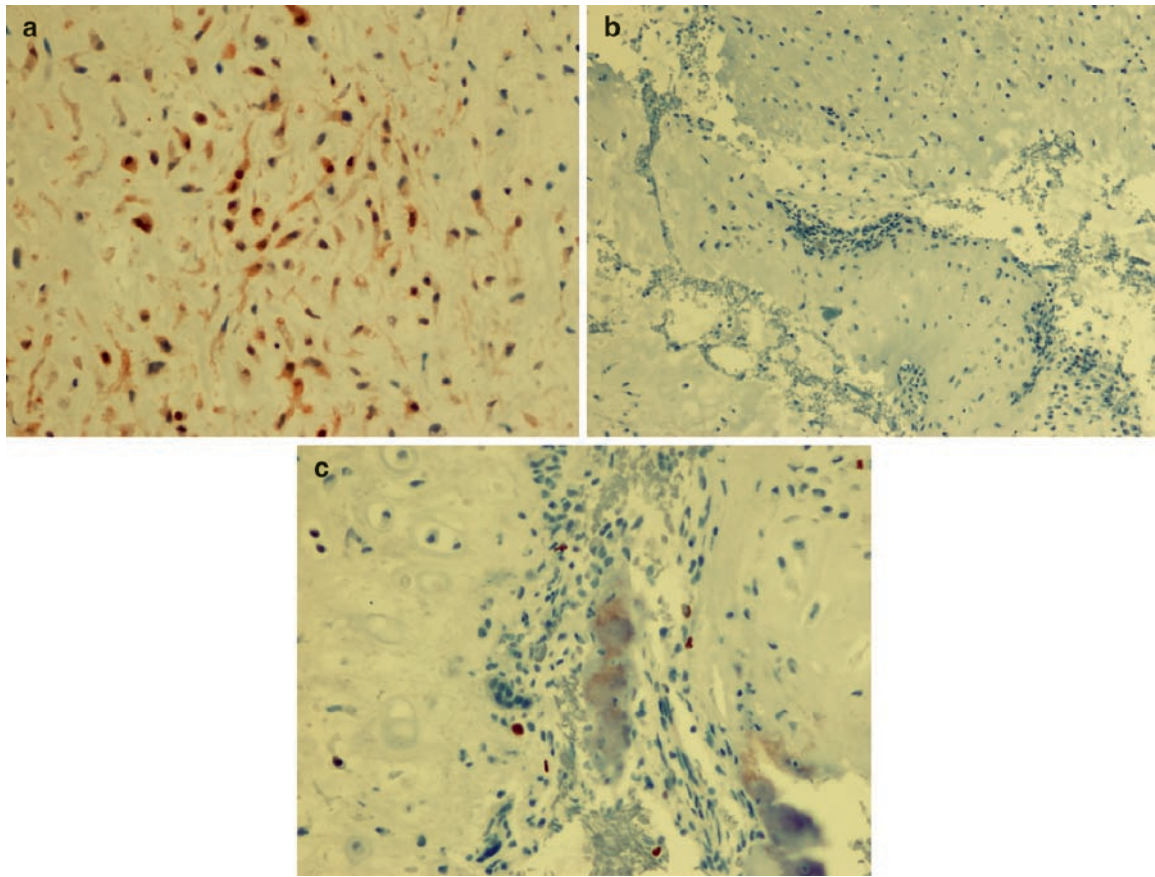
Fig. 37.24. Case E - Immunostains for (**a**) S-100 (**b**) EMA (**c**) Ki67.
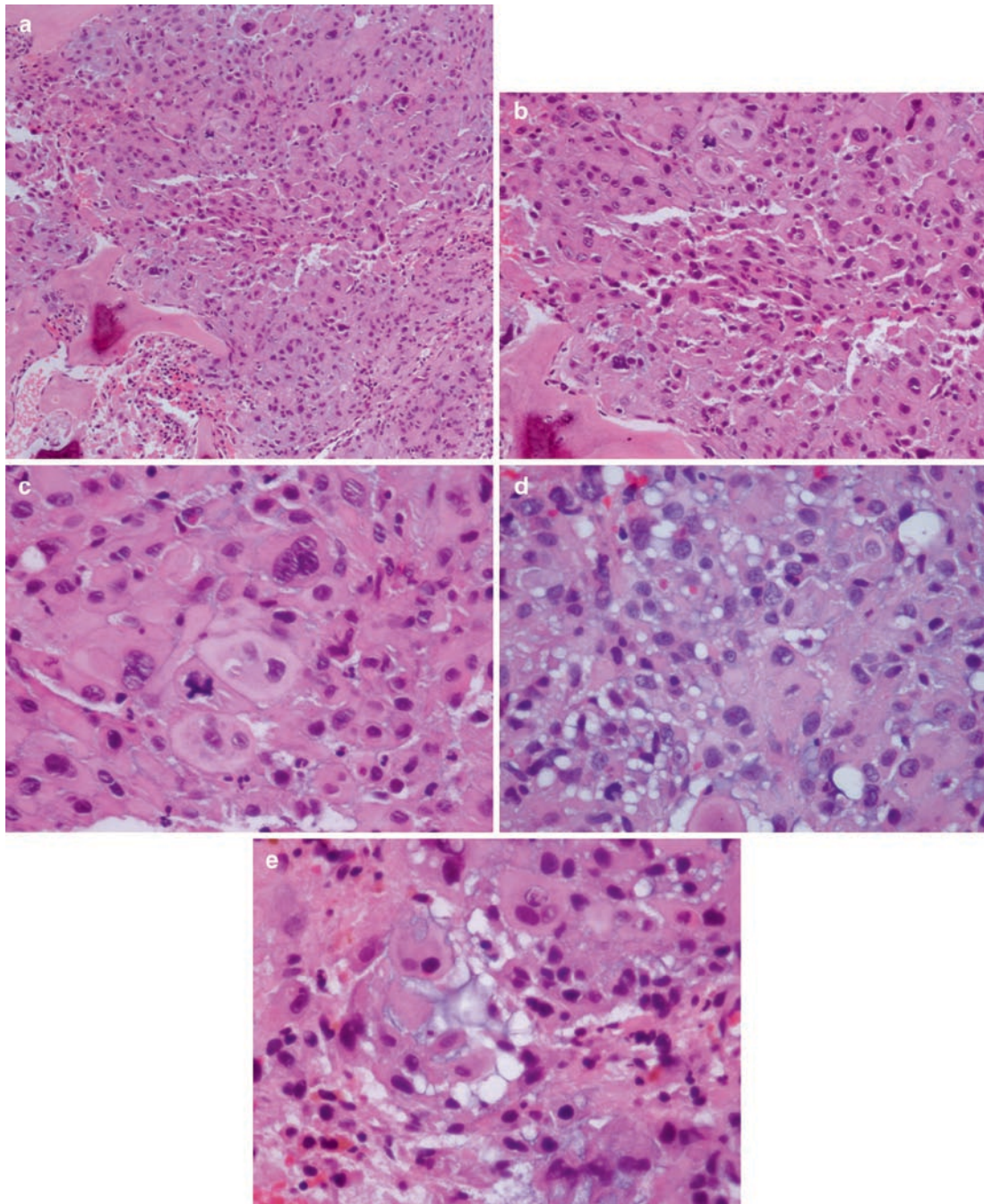
Fig. 37.25. Case F - (**a-e**) H & E stained sections.
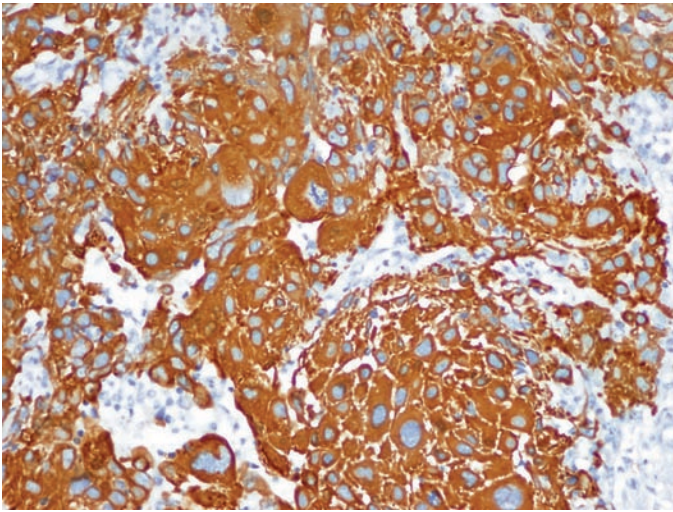
Fig. 37.26. Case F - Immunostain for Cytokeratin.
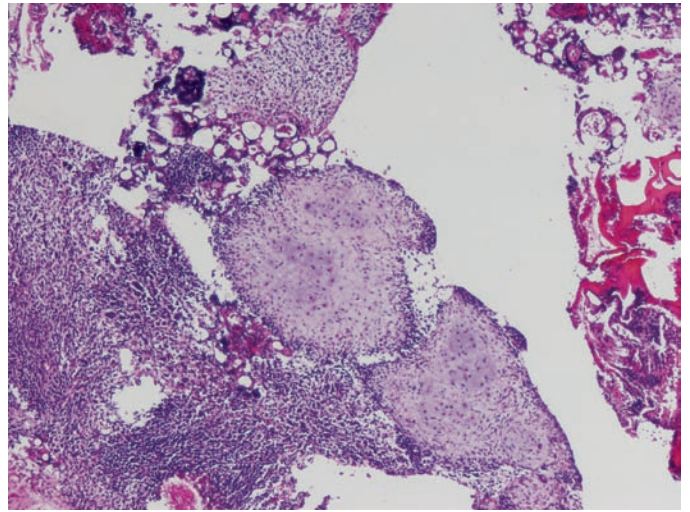
Fig. 37.27. Case G - H & E stained section.
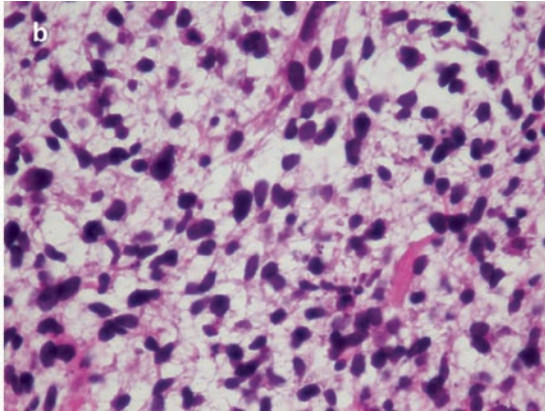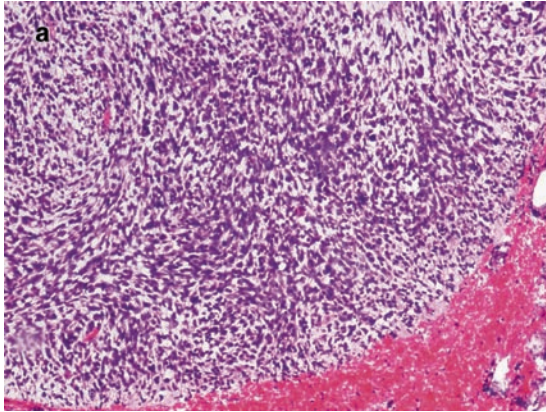
Fig. 37.28. Case G - H & E stained sections.
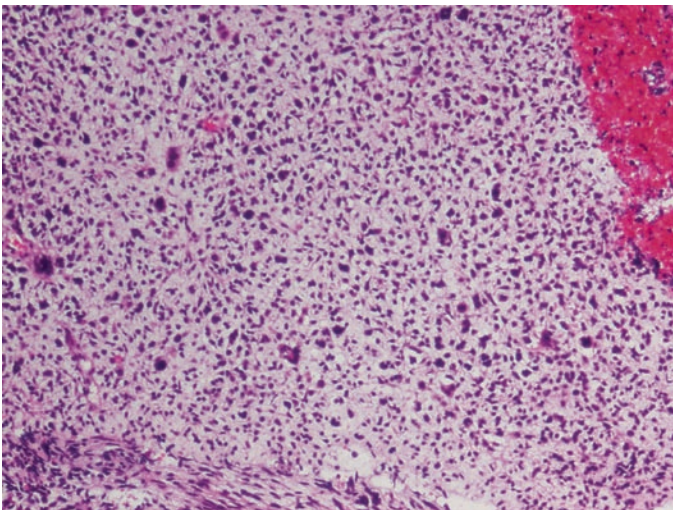
Fig. 37.29. Case G - H & E stained section.
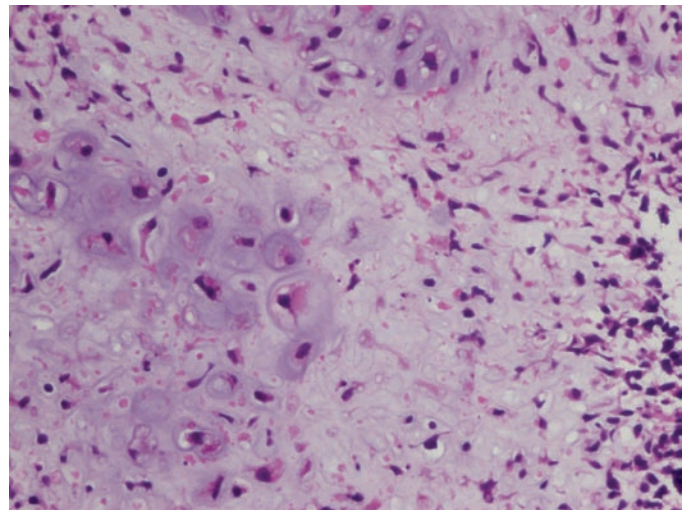
Fig. 37.30. Case G - H & E stained section.
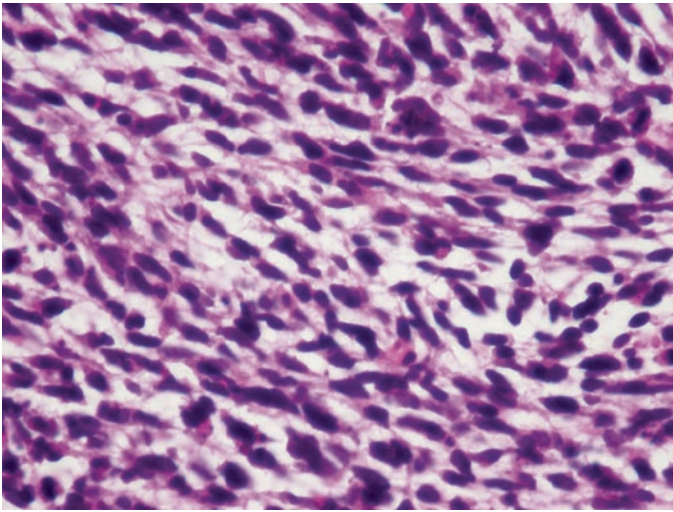
Fig. 37.31. Case G - H & E stained section.

Fig. 37.34. Case H.
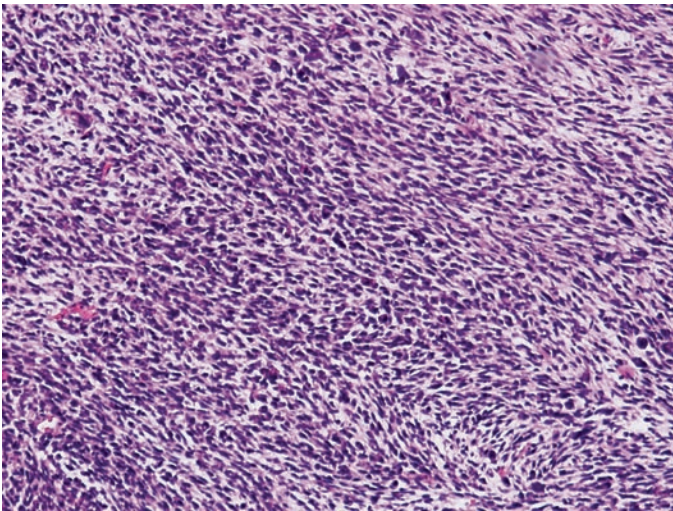
Fig. 37.32. Case G - H & E stained section.

Fig. 37.33. Case H.

Fig. 37.35. Case H.
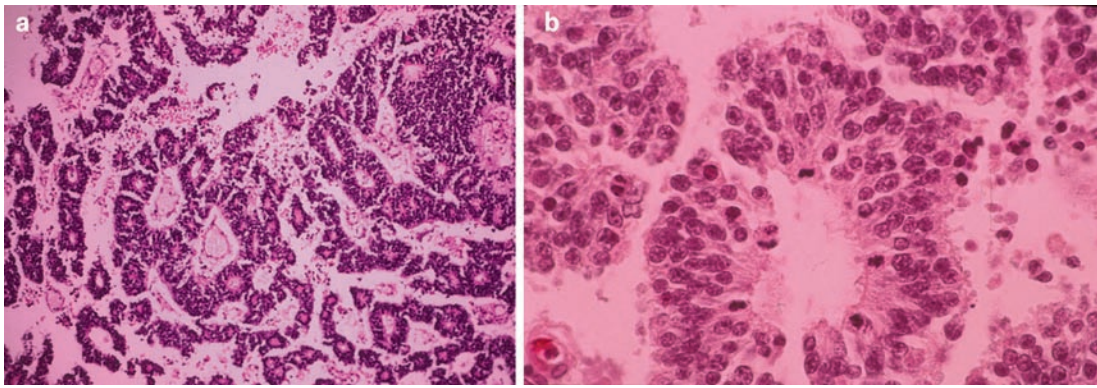
Fig. 37.36. Case H - H & E stained sections.
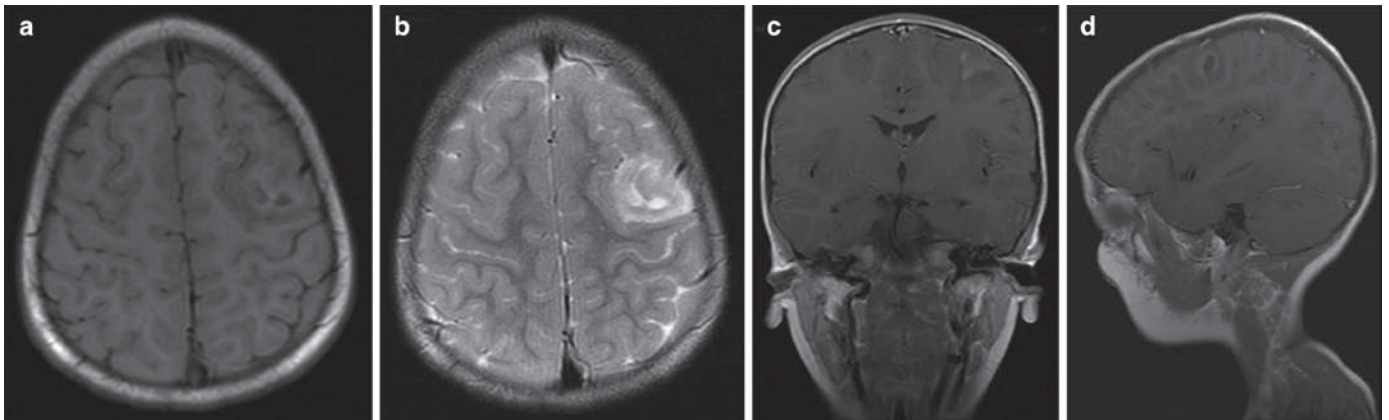
Fig. 37.37. Case I - (**a**) T1-weighted image (**b**) T2-weighted image (**c** and **d**) post contrast MR images.
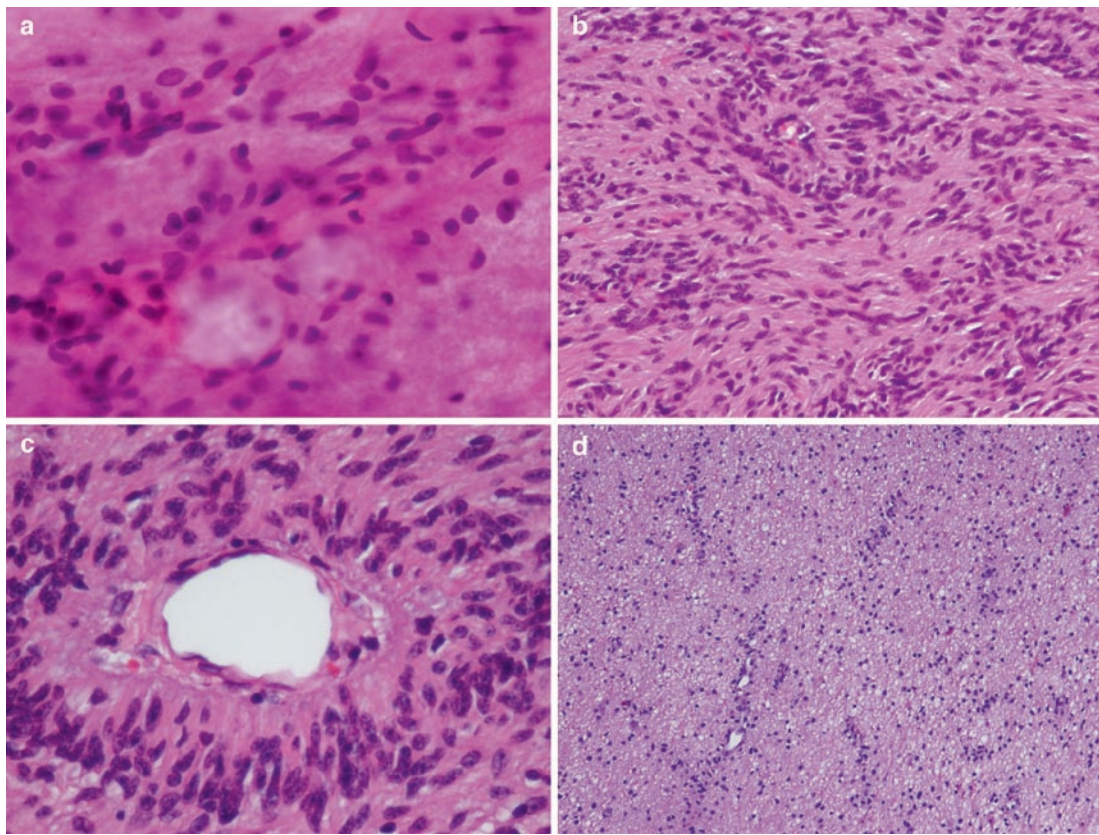
Fig. 37.38. Case I - (**a**) smear preparation (**b-d**) H & E stained sections.
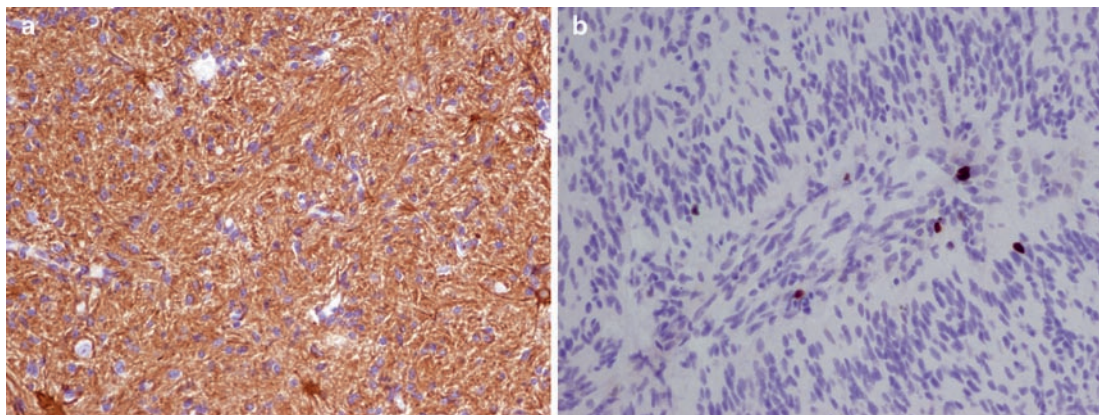
Fig. 37.39. Case I - Immunostains for (**a**) GFAP and (**b**) Ki67.
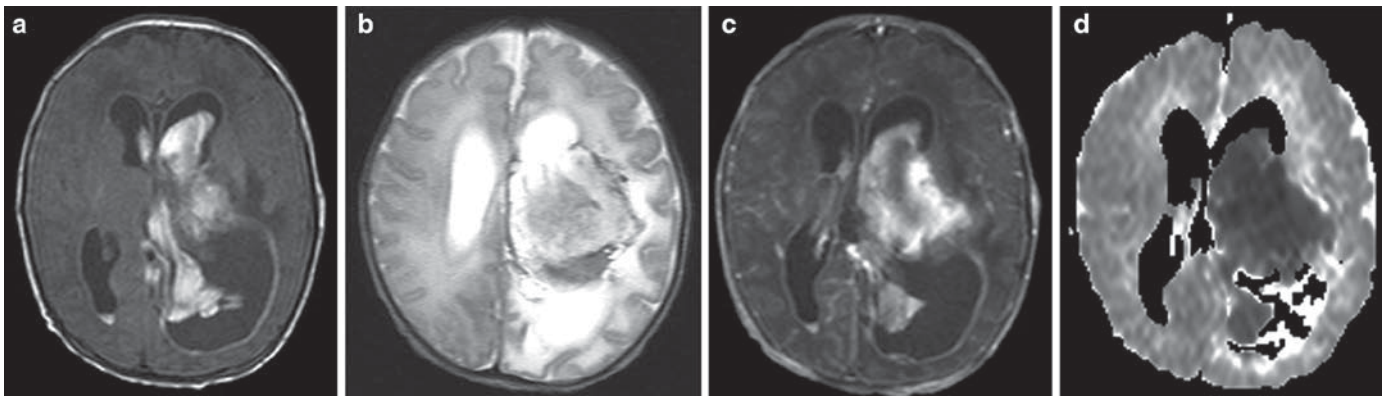
Fig. 37.40. Case J - (**a**) T1-w (**b**) T2-w (**c**) T1-w post contrast MR images and (**d**) ADC map.
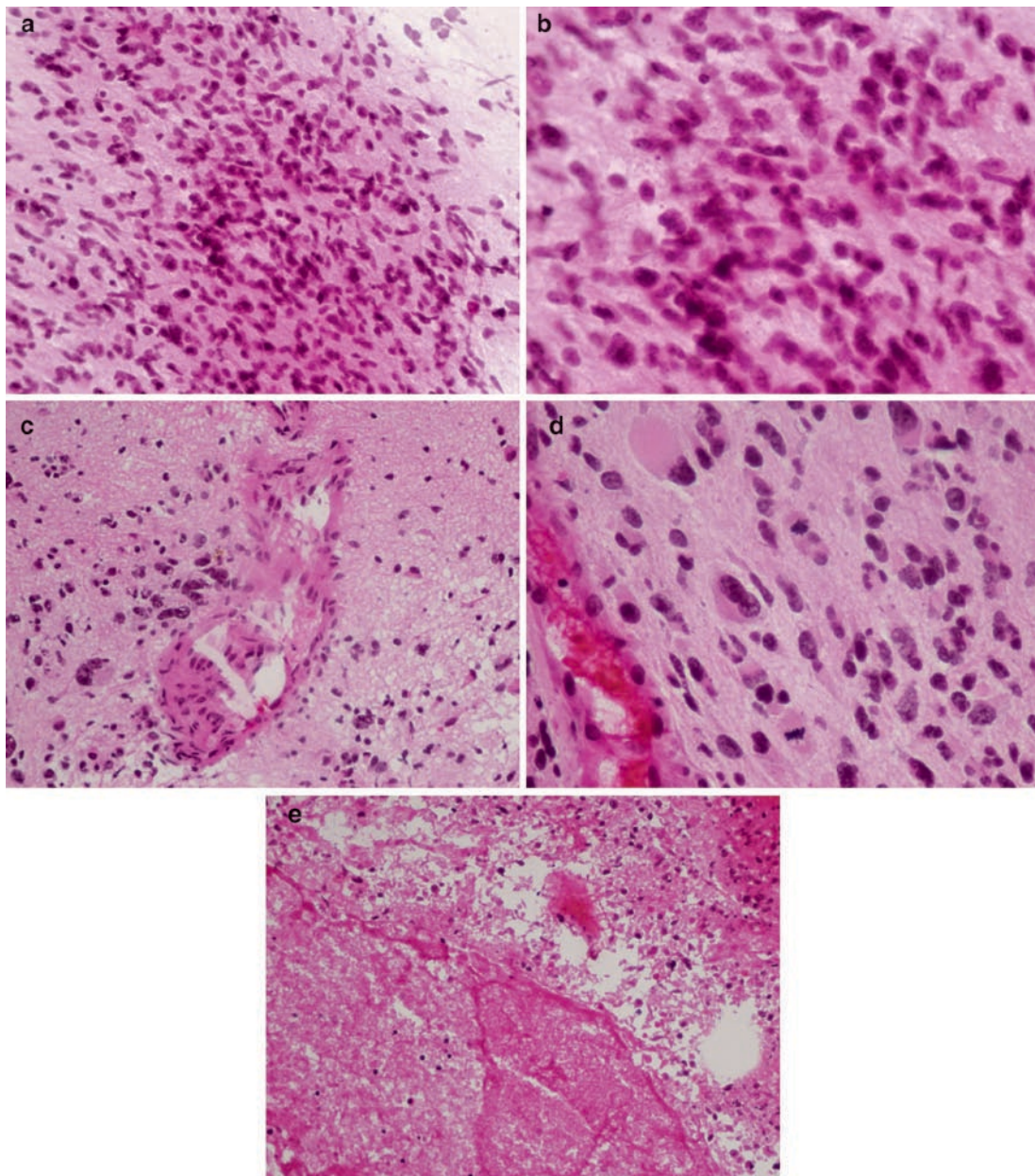
Fig. 37.41. Case J (**a** and **b**) - Intraoperative smears (**c-d**) H & E stained frozen sections.
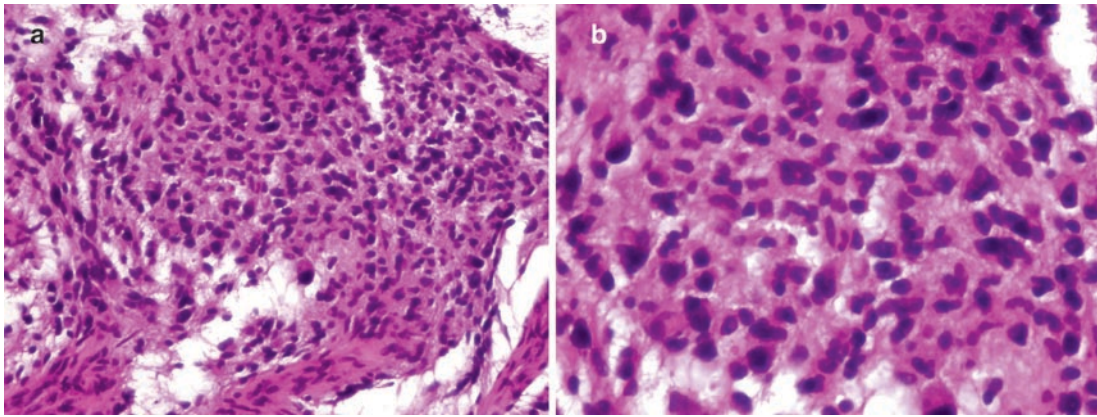
Fig. 37.42. Case J - H & E stained paraffin embedded sections.
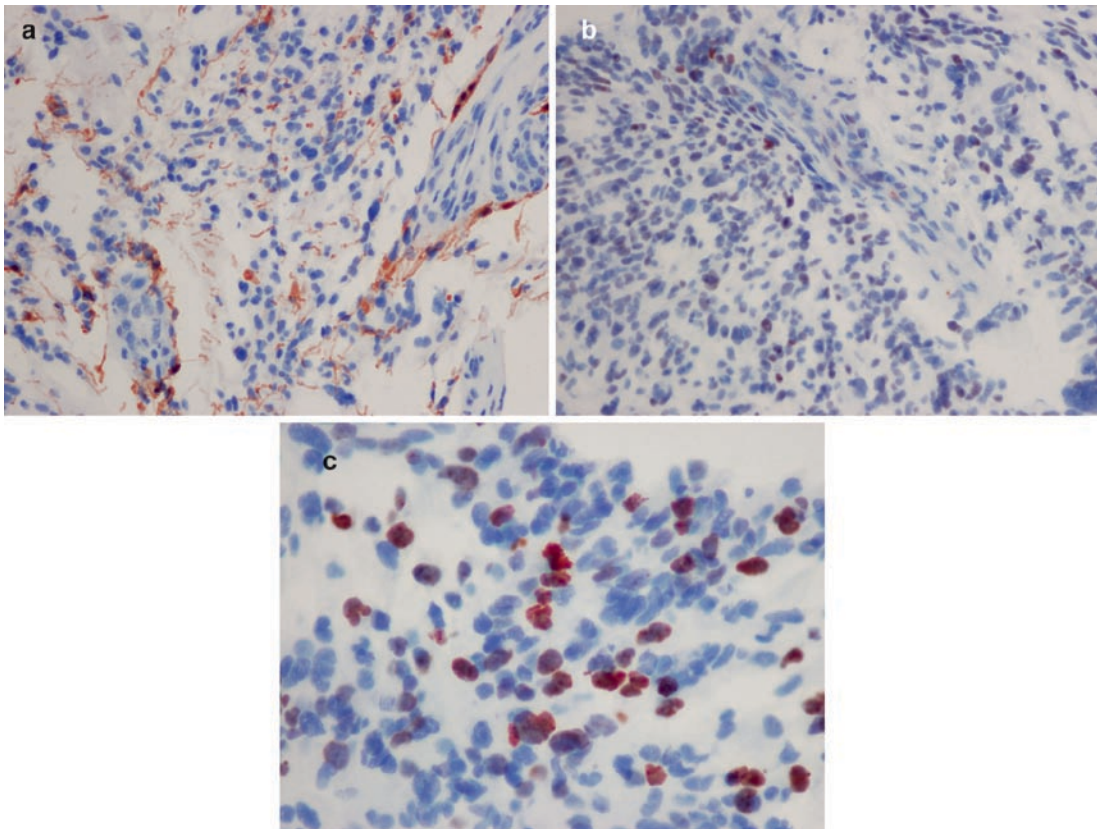
Fig. 37.43. Case I - Immunostains for (**a**) GFAP (**b**) P53 and (**c**) Ki67.

Index